Applications of Lewis Acid Gold(I) Catalysis in the Synthesis of Polycyclic Carbocycles and the Total Synthesis of (±)-Salvinorin A

Huy Minh Tran

A thesis submitted in partial fulfillment of the

requirements for the Doctorate in Philosophy degree in Chemistry

Department of Chemistry and Biomolecular Science

Faculty of Science

University of Ottawa

© Huy Minh Tran, Ottawa, Canada, 2022

Abstract

For most of human history, precious metals such as gold, silver, and platinum were used as currency and jeweler. Beginning in the 20th century, with the onset of transition metal catalysis, chemists developed new methods to support industrial chemical synthesis. There are many notable examples, one is the Ziegler-Natta catalysts to perform olefin polymerization using titanium/aluminum-based systems. Another is the Fisher-Tropsch process to convert synthesis gas (CO/H_2) into liquid hydrocarbons typically using cobalt, ruthenium, and iron. Also, the Haber-Bosch process where nitrogen and hydrogen gases are reacted in the presence of an iron catalyst to generate ammonia is a critically important process for the production of agricultural fertilizer worldwide. For precious transition metals such as gold, the first report of the metal being used in homogenous catalysis was in 1986. In this thesis, the application of gold homogenous into the synthesis of polycyclic carbocycles is being reported. This method was designed as a three-step one-pot sequence where an initial Diels-Alder reaction forms the first carbocycle with an embedded silyl enol ether moiety reactive to homogenous gold(I) catalysis. By selecting specific catalyst ligand and solvent conditions, selectivity between tri or steroid-like tetracycles was achieved via gold then Prins cyclizations or gold then Diels-Alder cyclizations. A combined total of 31 examples across 3 scopes was demonstrated using this divergent and modular strategy. This methodology aims to be applied in medicinal chemistry research in the synthesis of libraries of structurally related compounds baring resemblance to bioactive natural products.

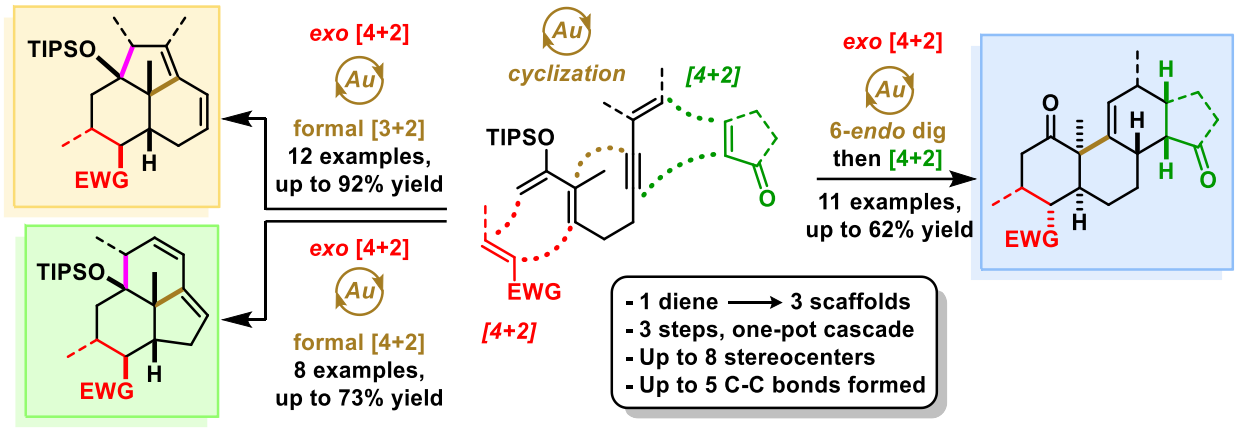

A related synthetic strategy was also used by our group in the total synthesis of salvinorin A. Initially isolated from Salvia divinorum in 1972, salvinorin A is trans neo-clerodane diterpene and was found to be a selective agonist of the kappa opioid receptor (κOR). This is unique compared to traditional morphine type opioids which are substrates of mu (μOR) and delta (δOR) opioid receptors. And as such, extensive work in medicinal chemistry has been published on utilizing salvinorin A as starting point towards the development of new analgesics.

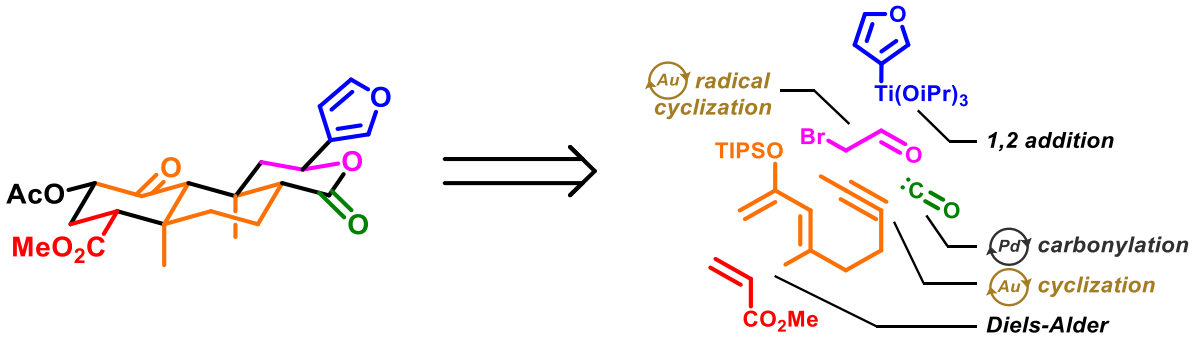

Our approach to synthesize salvinorin A centered around using a Diels-Alder reaction then gold cyclization to form the AB rings. The remaining C ring was formed via gold photoredox catalyzed radical cyclization, 1,2-addition of a furanyl organotitanium, and palladium catalyzed carbonylation. The formal synthesis of salvinorin A was completed in

21 steps by intercepting an intermediate in Hagiwara's reported synthesis, and addition 3 steps would complete the total synthesis.

Acknowledgements

My journey into the organic chemistry lab began in the summer nine years in the Barriault lab. For that I thank my thesis supervisor, Prof. Louis Barriault. Your mentorship, advising, and guidance allowed my adventures in total synthesis and gold chemistry a reality. And your decision to allow me to join your lab was the springboard to let me take my career in chemistry to where it is today.

I thank my parents, Hung and Bic, and my sister, Thanh for their decade long support in obtaining the first PhD in our family, giving me a home to come to, and for building our lives in Canada where my success is possible. I thank my oldest friends, Fares, Nathan, Ryan, Brock, Shivam, and Liz for sticking around in countless gaming nights, adventures, and keeping me grounded throughout my studies.

Within my own research group, I have had the pleasure of working with so many talented scientists whose presence only elevates my own abilities. I thank foremost Mathieu for being the first to mentor and train my skills as an organic chemist, as well as an avid snow sport buddy. You were an encyclopedia of knowledge and laid the foundation for me to becoming a chemist. I thank Terry as well for your mentorship and advising in my honors project and my early years as a graduate student, for being my roommate for several years, and a steadfast conference buddy over the years. I thank Phil as my former lab office buddy for imparting knowledge in gold chemistry to allow me to achieve success in my research. I thank Gab for your knowledge and help during my honors project, and for the board game nights with the lab. I acknowledge Julie as my preeminent coffee buddy, thank you for your company and mutual appreciation of Diels-Alder reactions. I thank Andre for our stimulating conversations on total synthesis,

business, and investing. I wish you great success in the future. I thank Marina for hosting parties and hangouts, as well as keeping me grounded during tough times in grad school. Samantha, thank you being a part so many conference, party and travel adventures, and also general lab antics. Those years were a blast with you around. Montse, I thank you for your organizational work in the lab, taking IR's, knowledge in Mexican cuisine, company in hangouts, mutual appreciation for expensive things, excellent baked goods, and conversations on photochemistry. Tegan and Avery, I concomitantly express thanks for our late-night lab antics and conversations on chemistry, life, games, etc. Research life during COVID would have been tougher without y'all on the night crew, when exploring chemistry after dark! I thank Martin and Victor for our engaging conversations in total synthesis and congratulate you both on recent successes. I thank Alyson for collaborating and working with me on the gold project. It was a long and challenging project, and it would have been tougher without you. I thank Dom and David for their company in hangouts and knowledge in chemistry. I acknowledge Kiara's defensive prowess during volleyball matches. Rowan, Lea, Chad, Lucas, Jason, Steph, Amandine, Mike, Anika, Tom, Spencer, Amanda, I'm glad we crossed paths.

For my time as the president of the CBGSA, Maddy, I thank you for your work as VP in organizing events with famous guests. I also thank both Ryans for their role as former VP and GSEAD rep respectively, Josh as treasurer and problem set co-host, Roxana as secretary, and beforementioned Barriault lab members who joined to form the Barriault lab government! I thank my committee members, Prof. Fabien Gagosz and Prof. Andre Beauchemin for their advice, guidance, and evaluation in the comprehensive exam, research proposal, and thesis. I thank Prof. Jim Gleason in evaluating this thesis

as external examiner. I would also like to thank Prof. Bill Ogilvie and Prof. Chris Boddy for teaching me the fundamentals in class and introducing me to the field. I thank Sharon Curtis (MS), Peter Pallister (NMR), and Jeff Ovens (X-RAY) for their work. I thank my past supervisors in industry: Jeff Warrington and Gary Brandt for their mentorship, their influence on my career, and for imparting invaluable knowledge in medicinal chemistry. Lastly, thank the University of Ottawa for their financial support.

Abbreviations

Ac: acetyl

Ad: adamantyl

AIBN: 2,2′-Azobis(2-methylpropionitrile)

BBN: borabicyclo[3.3.1]nonane

BINOL: 1,1′-Binaphthalene-2,2′-diol

Bn: benzyl

Bz: benzoyl

Boc: tert-butyloxycarbonyl

BOX: bis(oxazoline)

Cy: cyclohexyl

CNS: central nervous system

CSA: camphorsulfonic acid

DCM: dichloromethane

DCE: 1,2-dichloroethane

DAIB: (diacetoxyiodo)benzene

DBU: 1,8-diazabicyclo[5.4.0]undec-7-ene

DIPEA: N,N-diisopropylethylamine

DMAP: 4-(dimethylamino)pyridine

DMF: dimethylformamide

DMP: Dess-Martin periodinane

DMPU: N,N′-Dimethylpropyleneurea

DMS: dimethyl sulfide

DMSO: dimethyl sulfoxide

δOR: delta opioid receptor

dppm: bis(diphenylphosphino)methane

Et: ethyl

HMDS: hexamethyldisilazane

HWE: Horner-Wadsworth-Emmons

IMDA: intramolecular Diels-Alder

iPr: isopropyl

κOR: kappa opioid receptor

L: ligand

LDA: lithium diisopropylamide

LED: light-emitting diode

LLS: longest linear sequence

LUMO: lowest occupied molecular orbital

Me: methyl

μOR: mu opioid receptor

MS: molecular sieves

MVK: methyl vinyl ketone

NBS: N-bromosuccinimide

NHC: N-heterocyclic carbene

NMR: nuclear magnetic resonance

NPM: N-phenyl maleimide

Nu: nucleophile

OTf: trifluoromethanesulfonate

PPAP: polycyclic polyprenylated acylphloroglucinols

PCC: pyridinium chlorochromate

Ph: phenyl

PTAD: 4-phenyl-1,2,4-triazole-3,5-dione

PyBOX: pyridyl-bis(oxazoline)

RDS: rate determining step

SAR: structure activity relationships

SCXRD: single crystal X-ray diffraction

SET: single electron transfer

t-Bu: tert-butyl

TCNE: tetracyanoethylene

TES: triethylsilyl

TEMPO: 2,2,6,6-Tetramethylpiperidine 1-oxyl

TBAF: tetrabutylammonium fluoride

TFA: trifluoroacetic acid

THF: tetrahydrofuran

TMS: trimethylsilyl

TIPS: triisopropylsilyl

OTs: p-toluenesulfonate

TS: transition state

UVA: ultraviolet A

Table of Contents

List of Schemes

List of Figures

List of Tables

1. *INTRODUCTION TO GOLD CATALYSIS*

Gold is considered among the most valuable elements throughout human history.[1] From ancient civilizations of Egypt, Minoa, Assyria, and Etruria, gold was used in various forms of workmanship owing to its lustrous appearance and malleability. Many of these artifacts are still in perfect condition in the present day due to elemental gold's resistance to atmospheric oxidation, and thus does not tarnish or corrode. In its pure form, gold is a soft metal, and therefore is typically alloyed with silver, copper, and zinc to improve its hardness. The purity is commonly expressed in karats, where one karat equals 1/24 purity. Outside of jewelry, some of gold's uses in the present day include applications in electronics for its high electrical conductivity, infrared shielding, and use as a reserve currency. Organogold complexes have been used as treatments for rheumatoid arthritis[2] (ex. Auranofin, aurothioglucose, or sodium aurothiomaleate), though more relevant to this thesis is its catalytic application in organic synthesis. Structurally, Au(I) is typically bicoordinate with a linear geometry.[3] An experimental implication of this is that for a neutral Au(I) complex to possess catalytic activity, the abstraction of a ligand is necessary in order for it to become the reactive cationic Au(I) species.

1.1 Relativistic Effect of Gold

The soft Lewis acidic activity of gold can be attributed to relativistic effects,[4] i.e. because of quantum mechanics and special relativity, the velocity of an atom's electrons relative to the speed of light (*c*) must be considered to account for such effects. According to the theory of special relativity, as a body's velocity increases towards *c*, the body's mass increases towards infinity. This increase in mass only realistically applies to bodies moving at speeds nearing *c*. The mass increase due to special relativity of a car moving

at 100 km/h is negligible for example. Electrons on the other hand, do move at velocities approaching *c*. The average radial velocity of an electron in gold's 1s orbital can be calculated to be 0.58*c* or 58% of *c*, thus the mass increase of the electron is significant, accounting for the relativistic effects of gold. The most relevant of these effects is due to the fact that the Bohr radius of an electron orbiting a nucleus decreases as its mass increases, I.e., the mass increase of an electron due to special relativity will cause it to have a smaller Bohr radius. This results in the contraction of the s and p orbitals. The contraction of the s and p orbitals in turn allows its electrons to shield electrons occupying the d and f orbitals. As a result, the d and f orbital electrons exhibit a weaker nuclear attraction and therefore expands. Within Au(I) catalysis, the contraction specifically of the 6s orbital and expansion of the 5d orbital are attributed to the catalyst's relativistic effects. One consequence of such effects is the increased bond strength of Au-ligand bonds. Another is the tendency of Au(I) to form an interaction with another Au(I) atom, with bond strengths on the order of hydrogen bonds. The expanded 5d orbitals also possess electrons that are less affected by electron/electron repulsion and thus are held within the orbital greater energy compared with the 3d electrons of copper.[5] This phenomenon makes gold less nucleophilic, and therefore less easily to underdo oxidative addition reactions compared to copper. Au(I) is typically not affected by oxygen, which can be attributed to gold's redox stability between Au(I) and Au(III). This gives reactions utilizing Au(I) practical advantages such as the ease of performing such reactions, and also in methodology development: the ability to generally avoid oxidative addition/reductive

elimination pathways seen with metals like palladium and copper for example, in favor of different reactivity such as Lewis acid activity.

1.2 π-Bond Lewis Acid Activation

Au(I) catalysts have been extensively reported in the activation of various π-systems,[4] such as allenes, alkenes, but especially alkynes. This π-Lewis acidity (or "soft" Lewis acidity) is attributed to the relativistic effects arising from the contraction of the valence s or p orbitals, which correspond to a low-lying lowest unoccupied molecular orbital (LUMO). Meanwhile, the expanded and more diffuse valence d orbital allows the stabilization of positive charges via back bonding as a result for its more delocalized electrons (Scheme 1.2.1).

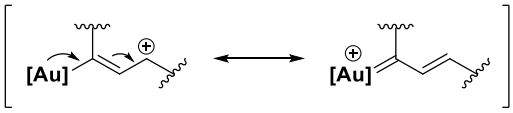

Scheme 1.2.1 – Stabilization of a cationic charge via Au(I) back-bonding

Mechanistically (Scheme 1.2.2), the typical Lewis acid Au(I) catalytic cycle begins with the coordination of cationic Au(I) catalyst **1.2.2** to a π-system, exemplified by alkyne **1.2.1**. This forms complex **1.2.3,** then a nucleophilic attack occurs onto the now electron-deficient alkyne which is polarized by the Au(I) catalyst through transition state **1.2.4**. The nucleophilic attacks then occurs across the triple bond in a trans fashion to generate vinyl gold intermediate **1.2.5**. At this point, protodeauration occurs in the presence of a proton source, to give final product **1.2.6** as well as regenerating the catalyst.

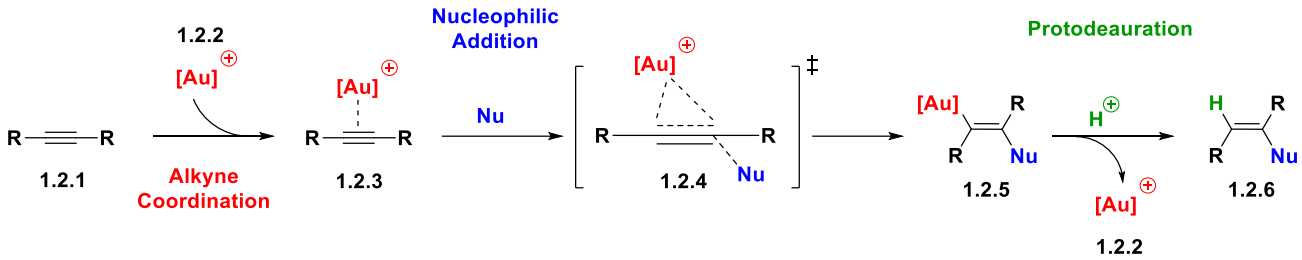

Scheme 1.2.2 – Generic Lewis acid Au(I) catalytic cycle

1.3 Additions of Oxygen and Nitrogen Functional Groups

Some of the earliest reported uses of gold catalysis were in the hydration of alkynes (Scheme 1.3.1), typically using Au(III) salts. In 1991, the use of $NaAuCl_4$ was described[6] by Utimoto *et al.* in the addition of methanol to alkyne substrates to generate the corresponding methyl enol ether, which then converts to the final ketone or methyl ketal. The use of Au(I) in the same reactivity was later reported[7] in a seminal publication by Teles *et al.* in 1998. The catalyst in this case was a cationic gold(I) phosphine complex. These methodologies carried much interest as less toxic alternatives for the traditional mercury(II) enabled alcohol addition to alkynes[8] using a catalytic mixture of BF_3 in MeOH, and mercury(II) oxide.

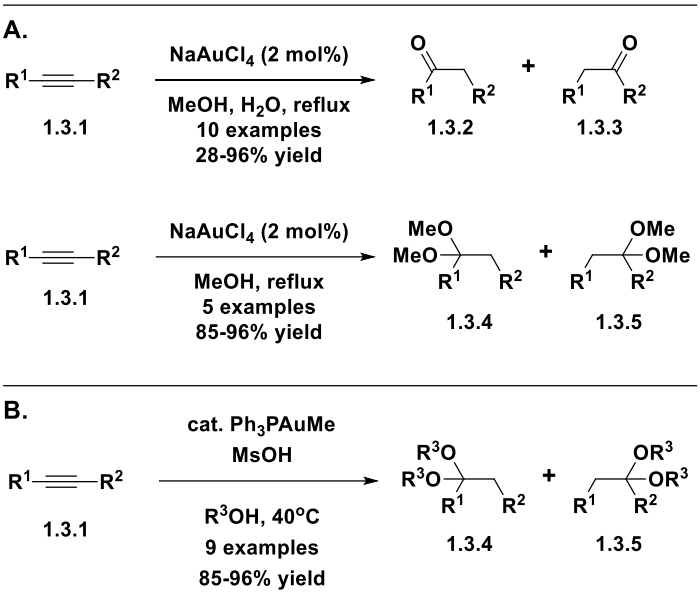

Scheme 1.3.1 – Seminal publications in Au catalyzed hydration of alkynes

Analogous reactivities were also published with amines, first in 1987 by Utimoto *et al.* for the addition of an amine to an alkyne through an intramolecular hydroamination to generate the corresponding enamine which tautomerizes to the cyclic imine.[9] This was accomplished with $NaAuCl_4$. In 2003, the intermolecular hydroamination of alkynes was reported using Au(I)[10] by Hayashi and Tanaka *et al.*

1.4 Conia-Ene Reaction

The Conia-Ene reaction was originally reported in 1965 by Jean-Marie Conia,[11] as a method to synthesize 5-membered carbocycles from linear keto-alkenes under intensely thermal conditions (Scheme 1.4.1). Later, the methodology was further applied in constructing 3, 4, 6, and 9- membered carbocycles.

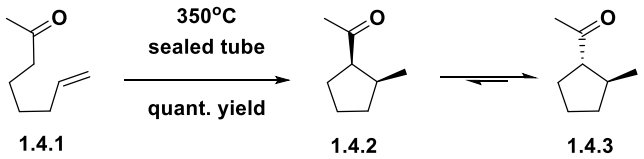

Scheme 1.4.1 – Thermal Conia-ene reaction

Deuterium experiments were also performed to determine the mechanism of the thermal Conia-ene reaction (Scheme 1.4.2). Using deuterated keto-olefin **1.4.4**, deuteration of the olefin was observed with the isolation of ketone **1.4.6**. It was proposed that this occurred first via the tautomerization of **1.4.4** into deuterated enol **1.4.5**, which then cyclized into **1.4.6** via an ene-type mechanism.

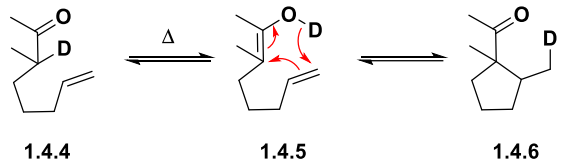

Scheme 1.4.2 – Proposed mechanism of the Conia-ene reaction

Several decades later in 2004, Toste *et al.* reported the application of a Au(I) catalyst in then Conia-ene type reaction of β-ketoesters onto alkynes[12] (Scheme 1.4.3). In the representative example, β-ketoester **1.4.7** was transformed into carbocycle **1.4.8** in the presence of a Au(I) catalyst under mild conditions. This reaction was proposed to occur first through the tautomerization of **1.4.7** into enol **1.4.9**, which then cyclized into **1.4.10** or **1.4.11** via an alkyne Au(I)-activated transition state (**TS1**) or an alkyne+enol Au(I)-activated transition state (**TS2**) respectively. Both vinyl gold species can then undergo protodeauration to form **1.4.8**.

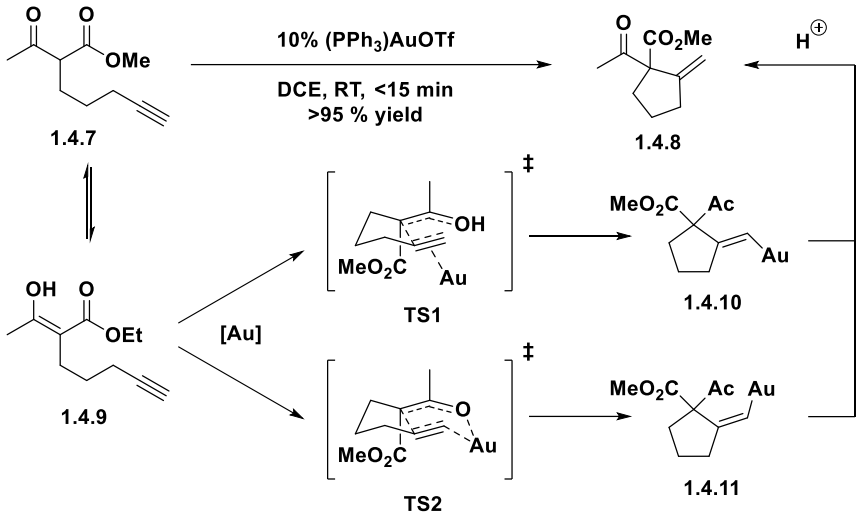

Scheme 1.4.3 – Au(I) catalyzed Conia-ene type reaction

Later examples of Au(I) catalyzed Conia-ene type reactions would be reported directly using enols[13] rather its carbonyl tautomer. This concept was extended, where Toste *et al.* reported the use of silyl enol ethers as "frozen enol" substrates in Au(I) catalyzed 5-*exo*-*dig* cyclizations and its application in the total synthesis of (+)-lycopladine A[14] (Scheme 1.4.4).

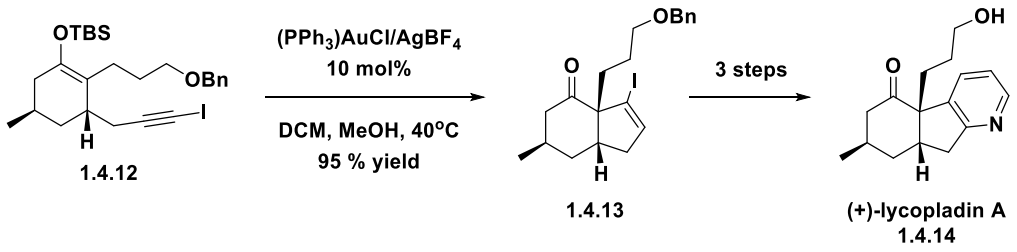

Scheme 1.4.4 – Total synthesis of (+)-lycopladine A via Au(I) catalysis

An analogous 6-*exo*-*dig* version of the reaction[15] was later published by Lee *et al.,* and the more challenging 6-*endo*-*dig* Au(I) cyclization was published in 2011 by our own group[16] and will act as an important foundation for work within this thesis and will be discussed in later chapters.

1.5 Effects of Ligand, Counterion, and Additives

Although the earliest examples of gold catalysis were using Au(I) and Au(III) as their chloride salts, much work has been published on the topic of ligand, counteranion, as well as additive effects for Au(I) catalysis.[17] Examples of gold catalysts are typically reported in the form of complexes, such as gold phosphines. Additionally, the chloride counteranion acting as the X-ligand is typically replaced with more dissociated counteranions (ex. SbF_6^-, NTf_2^-, OTf^-, BF_4^-, $BArF^-$), as the more strongly coordinating a counteranion is, the less catalytic activity the Au(I) complex will have. Previous reports by Echavarren,[18] Zhdanko and Maier,[19] as well as Hammond and Xu[20] most recently in 2017, described similar reactivity trends when varying the Au(I) counteranion. As the affinity a counteranion has towards the Au(I) atom decreases, the catalytic activity of the Au(I) complex increases. This can be attributed to the lower energetic barrier required to overcome the Coulombic energy of the Au-X bond and disassociate the counteranion (X) from the Au(I) atom to achieve charge separation required for the cationic Au(I) to proceed towards the binding of a reaction substrate. Halide counteranions with concentrated negative charge had the strongest gold affinity, while counteranions with more dispersed negative charge such as SbF_6^-, had the weakest gold affinity (Figure 1.5.1).

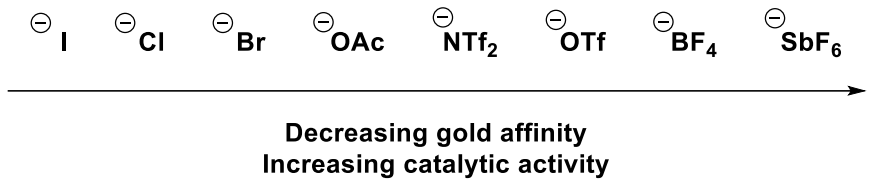

Figure 1.5.1 – Counteranion reactivity trend for Au(I) complexes

In addition to trends in counteranion reactivity, Hammond and Xu also reported significant work in reactivity trends with respect to the L ligands (most commonly phosphines) complexed to Au(I).[17] In the context of their generic Au(I) catalytic cycle, the

authors describe 3 stages within the Au(I) catalytic cycle that are of significance with respect to the L ligand (Ln) present (Scheme 1.5.1). Stage 1 is the electrophilic activation of the substrate where the cationic Au(I) catalyst binds to the alkyne. Ligands that were electron-poor were found to promote this step. Thus, if the particular Au(I) reaction has stage 1 as the rate determining step (RDS), an increase in reaction rate would be observed. In stage 2, protodeauration of the vinyl gold intermediate occurs, where electron-rich ligands were found to promote. Thus conversely, in a Au(I) reaction which has stage 2 as the rate determining step (RDS), an increase in reaction rate would be observed. Lastly in stage 3, cationic Au(I) gradually degrades by reduction to Au(0) which can occur in the presence of a reductive substrate (ex. Alkynes). This process can be visually observed as gold precipitates or gold mirroring of the reaction vessel. Also degradation can occur via the formation of an Ln_2Au^+ species, which is no longer catalytically active as the linear bicoordinate complex has no free coordination site for the substrate. Both electron-poor and electron-rich ligands, relative to triphenylphosphine, were found to accelerate catalyst degradation.

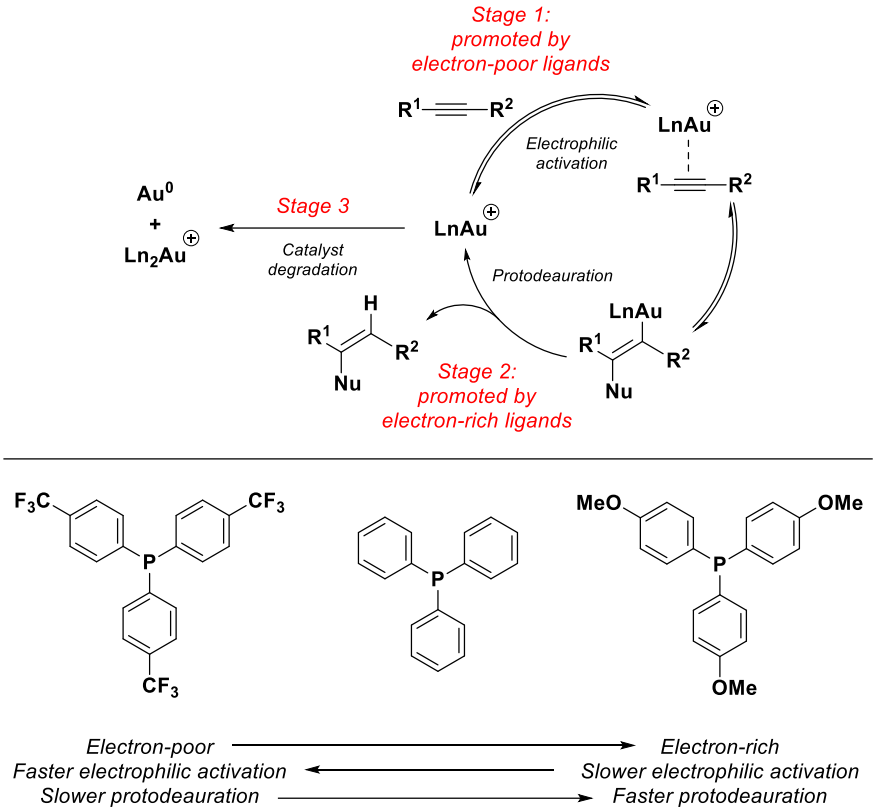

Scheme 1.5.1 - Stages in the Au(I) catalytic cycle affected by ligand

1.6 Photoredox Catalysis

Within the past decade, a reemergence of the interest in radical chemistry occurred in the scientific literature with a particular focus on its initiation using photoredox catalysis.[21] The main advantage was the absence of the toxic organostannane and explosive azobisisobutyronitrile (AIBN) initiator typically needed for radical chemistry. After a seminal publication of Yoon *et al.* on the formal [2+2] cycloaddition catalyzed by tris(2,2′-bipyridine)ruthenium(II),[22] many other photoredox catalysts have been reported, such has ones based of iridium, tungsten,[23] or acridinium organo-photocatalysts.[24] Gold(I) complexes[25] have also been reported as a photoredox catalyst, with extensive work in photoredox methodology using dimeric gold complexes reported by Barriault *et al*. The instigating publication[26] was on the 5-*exo*-*trig* radical cyclization of unactivated alkyl

bromides using the dimeric gold $Au_2[dppm]_2Cl_2$ complex as the photoredox catalyst under sunlight (Scheme 1.6.1).

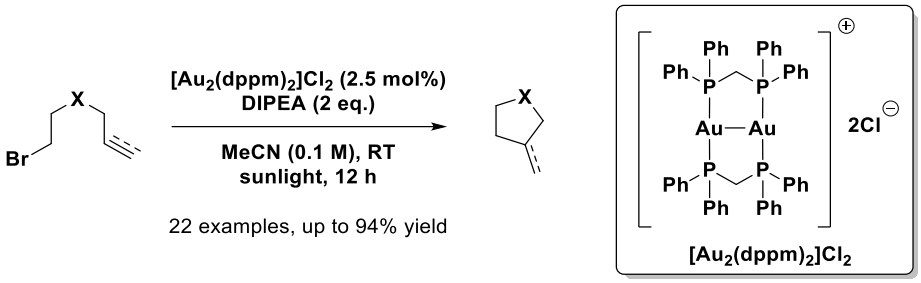

Scheme 1.6.1 - 5-*exo-trig* radical cyclization using $Au_2[dppm]_2Cl_2$

The reaction mechanism for the generation of radicals[27] (Scheme 1.6.2) within the $[Au_2(dppm)_2]Cl_2$ photocatalytic system begins when an electron is promoted (denoted by asterisk) from the singlet state to the triplet state by UVA irradiation. At this point, two chemical reaction pathways are possible. The first is oxidative quenching of the excited catalyst where it donates an electron to the reaction substrate via SET to cleave the carbon-halogen bond (C-Br in this example) to produce a reactive carbon centered radical and halide anion, while the catalyst is oxidized from a 2+ complex to a 3+ complex. Then a tertiary amine base (DIPEA in this example) regenerates the catalyst by reducing the gold complex back to 2+, producing an amino radical cation. The second possible mechanistic pathway after catalyst photoexcitation is reductive quenching of the excited catalyst, where a tertiary amine base first reduces the gold complex from 2+ to 1+. Then the 1+ complex donates an electron via SET and cleaves the carbon-halogen bond to produce the reactive carbon centered radical and halide anion. In this process the gold complex is oxidized and regenerated from a 1+ complex to a 2+ complex.

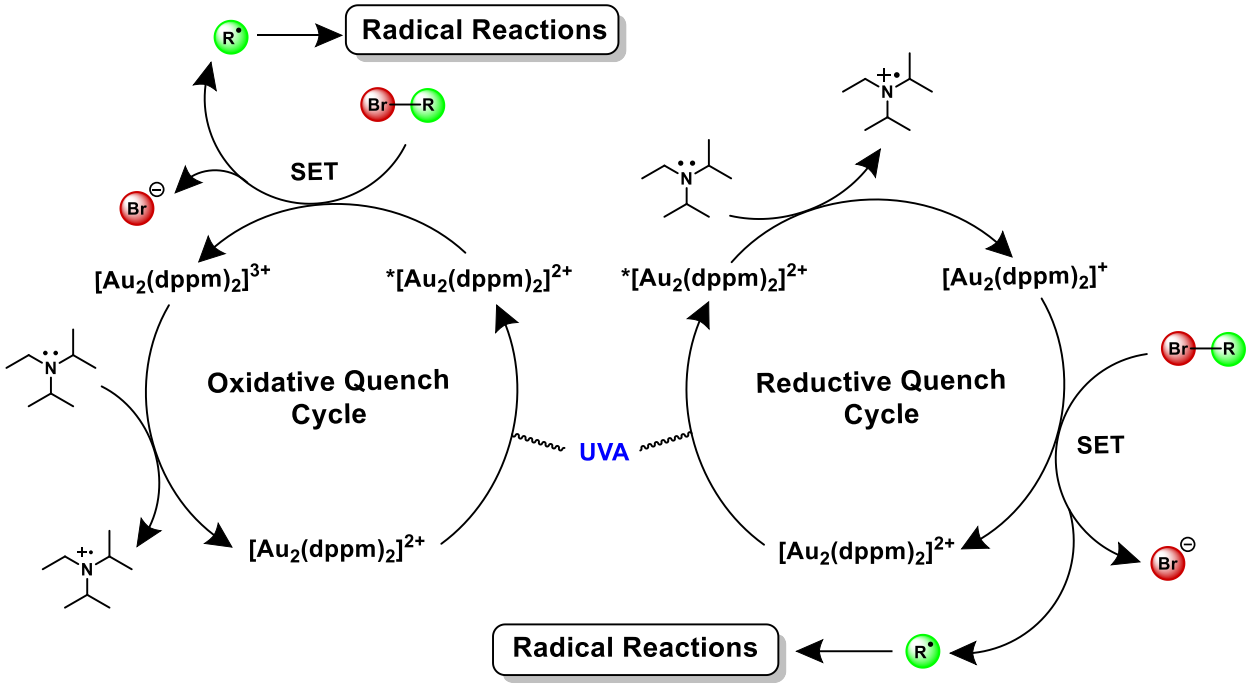

Scheme 1.6.2 – Possible mechanisms for the $[Au_2(dppm)_2]Cl_2$ photocatalytic system.

Some examples of later methodologies by Barriault *et al.* using $Au_2[dppm]_2Cl_2$ included homocoupling of iodoarenes[28] (Table 1.6.1, *a*.), intramolecular cyclization with an aryl radical[29] (Table 1.6.1, *b*.), alkylation of N-heterocycles[30] (Table 1.6.1, *c*. and *d.*), and addition to isocyanides[31] (Table 1.6.1, *e*.).

Table 1.6.1 – Selected examples of methodologies by Barriault *et al.* using $Au_2[dppm]_2Cl_2$

a.

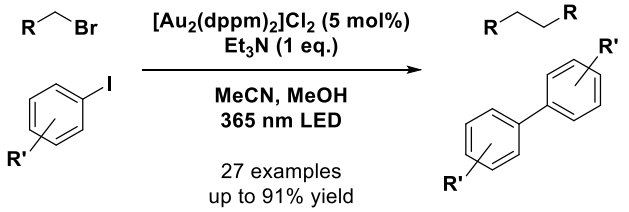

b.

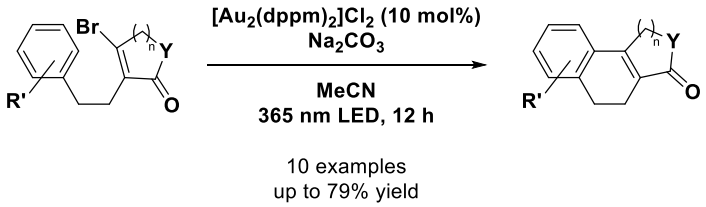

c.

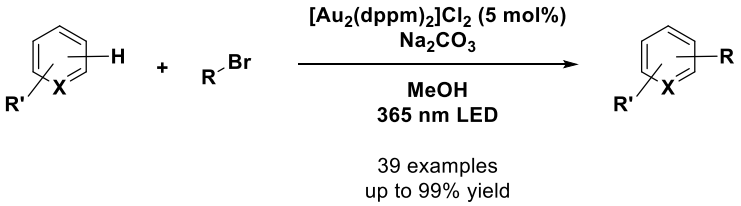

d.

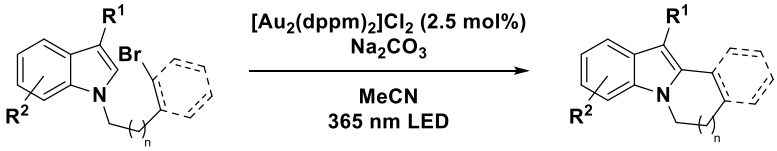

e.

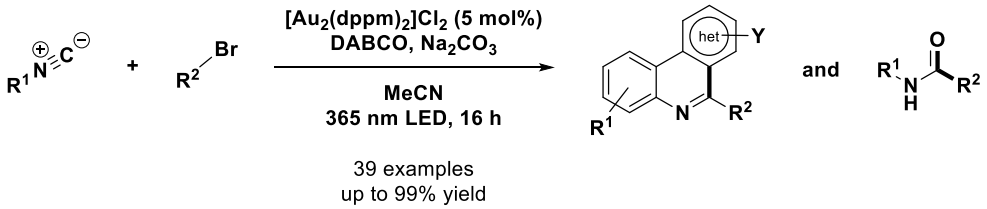

1.7 Gold in Total Synthesis

Gold(I) catalysis have been applied extensively in the reported literature in natural product synthesis, often as key steps in the construction of core scaffolds.[32] Multiple examples have been published from our group[33] harnessing both soft Lewis acid activity of monomeric gold complexes as well as photoredox reactivity with dimeric Au(I) catalysis. The first example[34] was an application of a Au(I) Lewis acid in the benzoannulation of alkynyl alcohols (Scheme 1.7.1), where alkyne **1.7.1** was transformed into tetrahydronaphalene **1.7.2**. This product was then used in the total synthesis of (+)-isofregenedol (**1.7.3**) in an additional 9 steps.

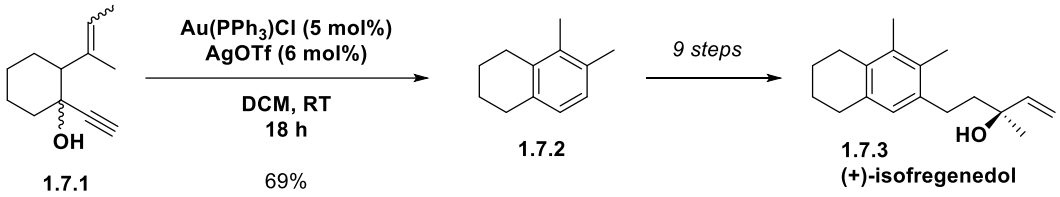

Scheme 1.7.1 – Key Au(I) catalyzed step in the total synthesis of (+)-isofregenedol

In 2014, the total synthesis of five polycyclic polyprenylated acylphloroglucinols (PPAP)[35] were accomplished via catalysis using a Buchwald phosphine - Au(I) complex (Scheme 1.7.2). Using alkyne **1.7.4**, a 6-*endo*-*dig* cyclization, using JohnPhosAu(NCMe)SbF_6, was performed to generate the [3.3.1] bridged bicycle **1.7.5**. Then depending on the substituents, **1.7.5** was functionalized pupuaforin A-C (**1.7.6, 1.7.7, 1.7.8)**, hyperforin (**1.7.9**), or nemorosone (**1.7.10**) in 9-11 steps.

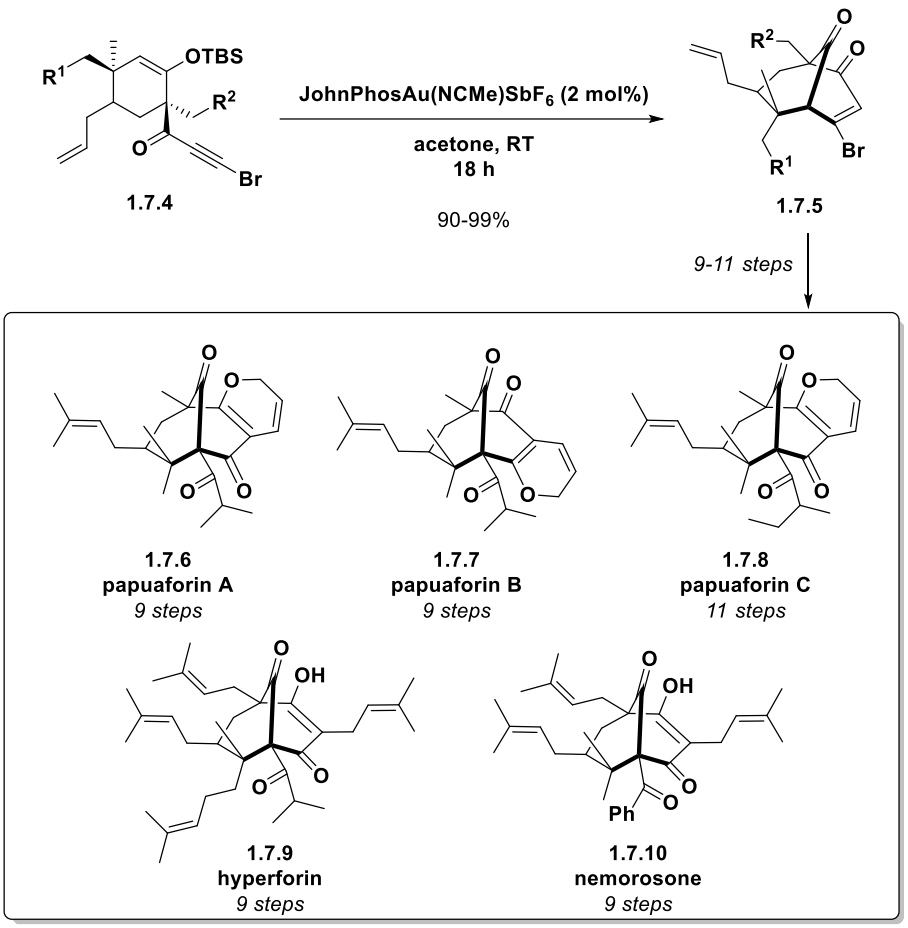

Scheme 1.7.2 – Key Au(I) catalyzed step in the total synthesis of PPAPs

Later, the application of a similar Au(I) catalyst: JackiePhosAu(NCMe)SbF_6 was reported in the total synthesis of magellanine[36] (Scheme 1.7.3). In this example a Au(I) catalyzed dehydro-Diels-Alder reaction was performed on alkyne **1.7.11** followed by treatment with camphorsulfonic acid (CSA) to generate **1.7.12** featuring an angular core. After an additional 6 steps, magellanine (**1.7.13**) was synthesized.

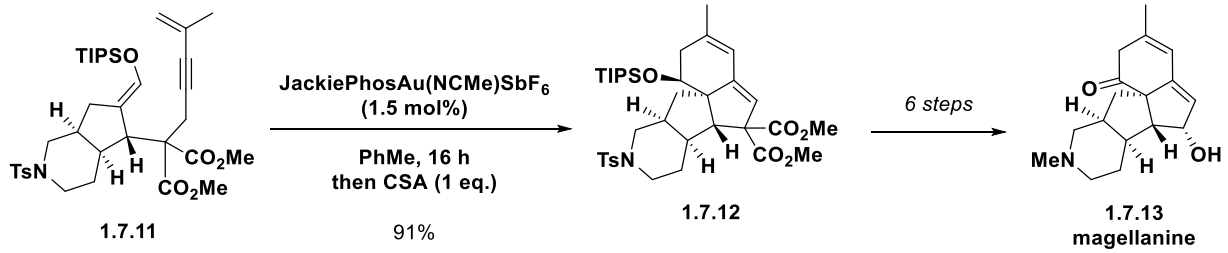

Scheme 1.7.3 – Key Au(I) catalyzed step in the total synthesis of magellanine

An example of an Au(I) catalyzed Conia-ene reaction from outside the group is in the synthesis of daphenylline (**1.7.16**) by Li *et al.* in 2003 (Scheme 1.7.4).[37] In the key step, silyl enol ether **1.7.14** underwent a Lewis acid Au(I) catalyzed 6-*exo*-*dig* cyclization to form bridged bicycle **1.7.15** in 70% yield. The final product was synthesized in an additional 16 steps.

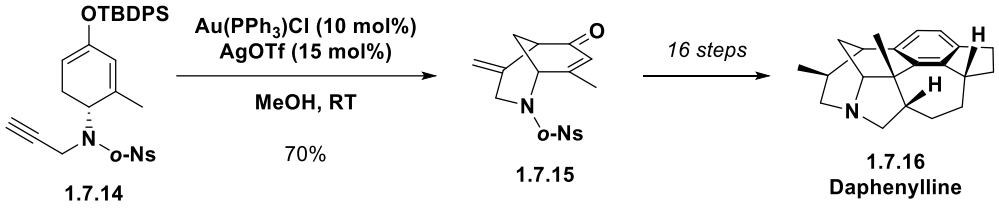

Scheme 1.7.4 - Key Au(I) catalyzed step in the synthesis of daphenylline

The most recent application of Au(I) catalysis in total synthesis by Barriault *et al.* was a photoredox enabled radical cyclization towards the formal synthesis of triptolide (Scheme 1.7.5).[29] Vinyl bromide **1.7.17** was converted into tetracycle **1.7.18** via two successive 6-*endo*-*trig* radical cyclizations starting from a vinyl radical formed from the dimeric Au(I) photoredox conditions under UVA irradiation.

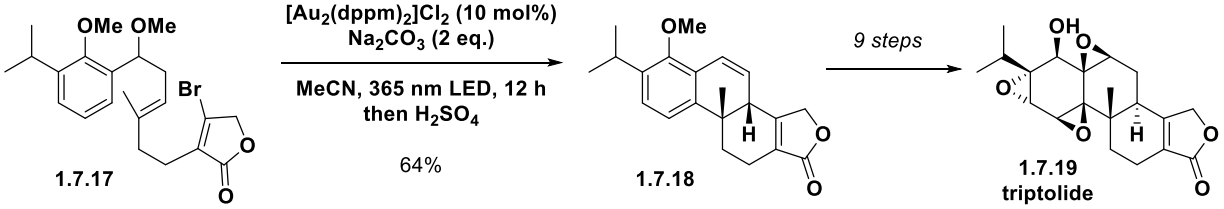

Scheme 1.7.5 - Key photoredox Au(I) catalyzed step in the synthesis of triptolide

A well executed application of Au(I) photoredox catalysis was the highly divergent total synthesis of seven natural products from the pyrroloazocine indole alkaloid family by Echavarren *et al.* (Table 1.7.1).[38] The advanced indole intermediate **1.7.20** was synthesized in 11 steps (LLS.) in both racemic and enantiopure forms. A photoredox Au(I)-catalyzed 6-*exo*-*trig* radical cyclization was performed to produce indoline **1.7.21** in

excellent yield, whereas when $[Ru(bpy)_3]Cl_2$ was employed, full conversion of starting material was not observed. From this point, the synthesis diverges to eventually produce seven pyrroloazocine indole alkaloids (**1.7.22** to **1.7.28**) in an additional 3-10 steps.

Table 1.7.1 - Total synthesis of pyrroloazocine indole alkaloids

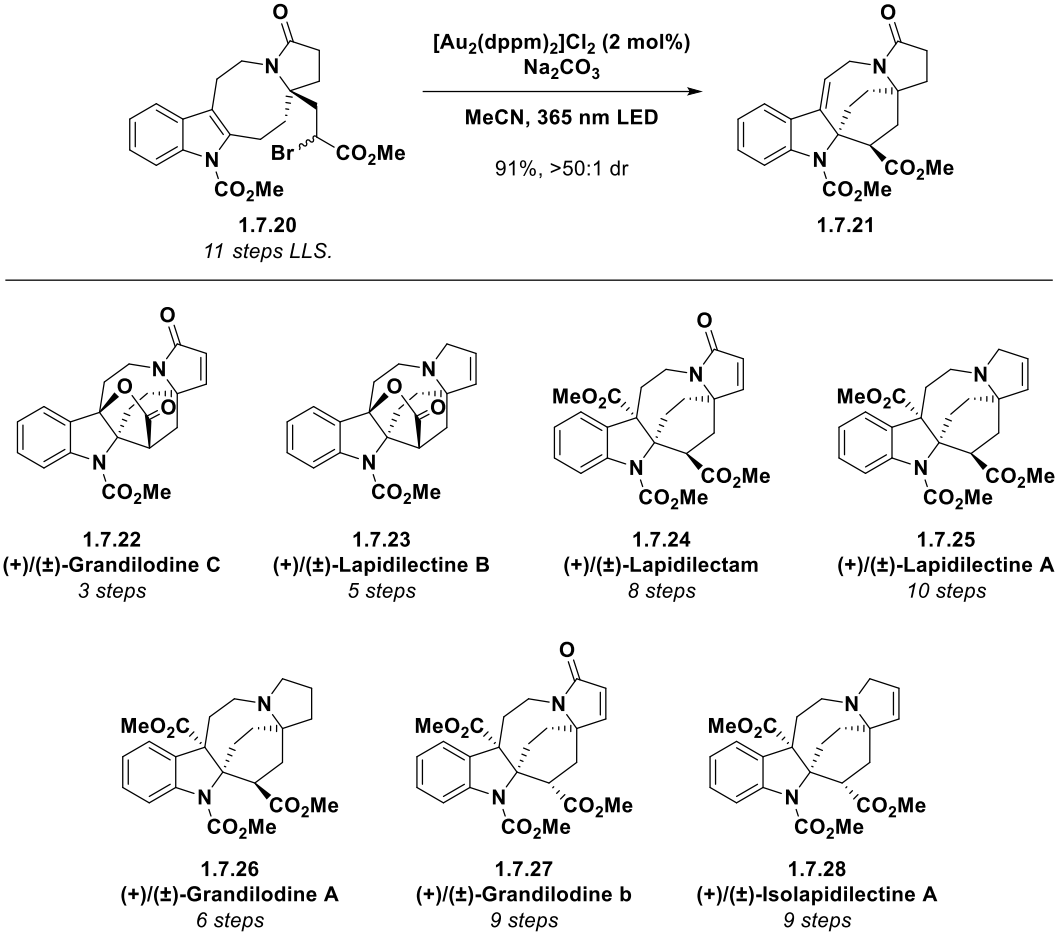

An example of a Au(I) catalyzed nucleophilic addition of an alcohol to an alkyne in total synthesis is in the formal synthesis of polycavernoside A (**1.7.31**) by Fürstner *et al.* (Scheme 1.7.6).[39] Alkyne **1.7.29** was submitted to Lewis acid Au(I) conditions that were anhydrous with the use of 4Å molecular sieves (MS) to give cyclic enol ether **1.7.30** via a 6-*endo-dig* cyclization in 84% yield. This reaction intercepted an advanced intermediate by Woo and Lee, where **1.7.31** was synthesized in an additional 8 steps.[40]

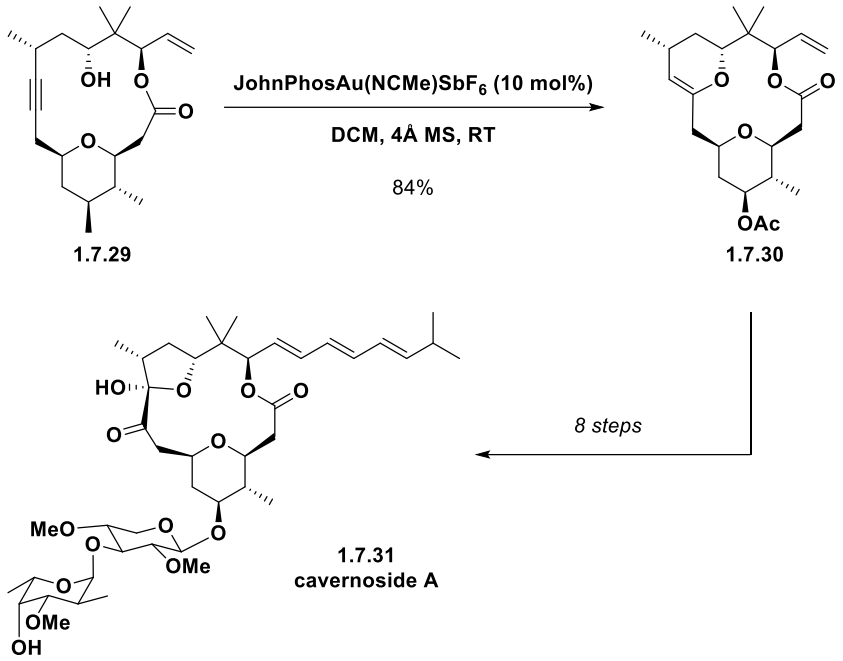

Scheme 1.7.6 - Key Au(I) catalyzed step in the formal synthesis of polycavernoside A

1.8 Conclusion

Given the great synthetic applicability of gold catalysis, particularly Au(I) catalysis, its reactivity will be harnessed within this thesis in the cascade methodology in the synthesis of polycyclic carbocycles (Chapter 2) where it is hypothesized that a method involving a Lewis acid catalyzed Diels-Alder reaction followed by a Au(I) catalyzed cyclization followed by a second Diels-Alder reaction can be developed with catalysts that are chemically compatible with one another. This will be followed by a double application of Au(I) catalysis in the total synthesis of salvinorin A (Chapter 3) where a novel synthetic approach to the molecule is performed with the intention of showcasing Au(I) methodology developed by Barriault *et al.* as well as producing the shortest synthesis route.

1.9 Bibliography

1. Britannica, T. E. o. E., Gold. In *Encyclopedia Britannica*, 2022.
2. Berners-Price, S. J., Gold-Based Therapeutic Agents: A New Perspective. *Bioorg. Med. Chem.* **2011**, 197-222.
3. Carvajal, M. A.; Novoa, J. J.; Alvarez, S., Choice of Coordination Number in d10 Complexes of Group 11 Metals. *J. Am. Chem. Soc.* **2004,** *126* (5), 1465-1477.
4. Gorin, D. J.; Toste, F. D., Relativistic effects in homogeneous gold catalysis. *Nature* **2007,** *446* (7134), 395-403.
5. Nakanishi, W.; Yamanaka, M.; Nakamura, E., Reactivity and Stability of Organocopper(I), Silver(I), and Gold(I) Ate Compounds and Their Trivalent Derivatives. *J. Am. Chem. Soc.* **2005,** *127* (5), 1446-1453.
6. Fukuda, Y.; Utimoto, K., Effective transformation of unactivated alkynes into ketones or acetals with a gold(III) catalyst. *J. Org. Chem.* **1991,** *56* (11), 3729-3731.
7. Teles, J. H.; Brode, S.; Chabanas, M., Cationic Gold(I) Complexes: Highly Efficient Catalysts for the Addition of Alcohols to Alkynes. *Angew. Chem. Int. Ed.* **1998,** *37* (10), 1415-1418.
8. Hinton, H. D.; Nieuwland, J. A., A NEW METHOD OF PREPARING ACETALS. II. ACETALS OF MONOHYDRIC ALCOHOLS. *J. Am. Chem. Soc.* **1930,** *52* (7), 2892-2896.
9. (a) Fukuda, Y.; Utimoto, K., Preparation of 2,3,4,5-Tetrahydropyridines from 5-Alkynylamines Under the Catalytic Action of Gold(III) Salts. *Synthesis* **1991,** *1991* (11), 975-978; (b) Fukuda, Y.; Utimoto, K.; Nozaki, H., Preparation of 2,3,4,5-tetrahydropyridines from 5-Alkynylamines under the Catalytic Action of Au(III). *Hetrocycles* **1987,** *25* (1), 297-300.
10. Mizushima, E.; Hayashi, T.; Tanaka, M., Au(I)-Catalyzed Highly Efficient Intermolecular Hydroamination of Alkynes. *Org. Lett.* **2003,** *5* (18), 3349-3352.
11. (a) Rouessac, F.; Beslin, P.; Conia, J.-M., La cyclisation thermique des cetones cycliques εζ-ethyleniques. Voie d'acces aux cetones polycycliques. *Tetrahedron Lett.* **1965,** *6* (37), 3319-3323; (b) Conia, J. M.; Le Perchec, P., The Thermal Cyclisation of Unsaturated Carbonyl Compounds. *Synthesis* **1975,** *1975* (01), 1-19.
12. Kennedy-Smith, J. J.; Staben, S. T.; Toste, F. D., Gold(I)-Catalyzed Conia-Ene Reaction of β-Ketoesters with Alkynes. *J. Am. Chem. Soc.* **2004,** *126* (14), 4526-4527.
13. (a) Nevado, C.; Cárdenas, D. J.; Echavarren, A. M., Reaction of Enol Ethers with Alkynes Catalyzed by Transition Metals: 5exo-dig versus 6endo-dig Cyclizations via Cyclopropyl Platinum or Gold Carbene Complexes. *Chem. Eur. J.* **2003,** *9* (11), 2627-2635; (b) Sherry, B. D.; Maus, L.; Laforteza, B. N.; Toste, F. D., Gold(I)-Catalyzed Synthesis of Dihydropyrans. *J. Am. Chem. Soc.* **2006,** *128* (25), 8132-8133; (c) Suhre, M. H.; Reif, M.; Kirsch, S. F., Gold(I)-Catalyzed Synthesis of Highly Substituted Furans. *Org. Lett.* **2005,** *7* (18), 3925-3927.
14. Staben, S. T.; Kennedy-Smith, J. J.; Huang, D.; Corkey, B. K.; LaLonde, R. L.; Toste, F. D., Gold(I)-Catalyzed Cyclizations of Silyl Enol Ethers: Application to the Synthesis of (+)-Lycopladine A. *Angew. Chem. Int. Ed.* **2006,** *45* (36), 5991-5994.
15. Lee, K.; Lee, P. H., Gold-Catalyzed 5- and 6-exo-dig Selective Cyclizations of Alkynyl Silyl Enol Ethers: Efficient Method for [3+2] and [4+2] Annulations onto α,β-Enones. *Adv. Synth. Catal.* **2007,** *349* (13), 2092-2096.

16. Barabé, F.; Levesque, P.; Korobkov, I.; Barriault, L., Synthesis of Fused Carbocycles via a Selective 6-Endo Dig Gold(I)-Catalyzed Carbocyclization. *Org. Lett.* **2011,** *13* (20), 5580-5583.
17. Wang, W.; Hammond, G. B.; Xu, B., Ligand Effects and Ligand Design in Homogeneous Gold(I) Catalysis. *J. Am. Chem. Soc.* **2012,** *134* (12), 5697-5705.
18. Homs, A.; Obradors, C.; Lebœuf, D.; Echavarren, A. M., Dissecting Anion Effects in Gold(I)-Catalyzed Intermolecular Cycloadditions. *Adv. Synth. Catal.* **2014,** *356* (1), 221-228.
19. Zhdanko, A.; Maier, M. E., Explanation of Counterion Effects in Gold(I)-Catalyzed Hydroalkoxylation of Alkynes. *ACS Catal.* **2014,** *4* (8), 2770-2775.
20. Lu, Z.; Han, J.; Okoromoba, O. E.; Shimizu, N.; Amii, H.; Tormena, C. F.; Hammond, G. B.; Xu, B., Predicting Counterion Effects Using a Gold Affinity Index and a Hydrogen Bonding Basicity Index. *Org. Lett.* **2017,** *19* (21), 5848-5851.
21. Prier, C. K.; Rankic, D. A.; MacMillan, D. W. C., Visible Light Photoredox Catalysis with Transition Metal Complexes: Applications in Organic Synthesis. *Chem. Rev.* **2013,** *113* (7), 5322-5363.
22. Ischay, M. A.; Anzovino, M. E.; Du, J.; Yoon, T. P., Efficient Visible Light Photocatalysis of [2+2] Enone Cycloadditions. *J. Am. Chem. Soc.* **2008,** *130* (39), 12886-12887.
23. (a) Tzirakis, M. D.; Lykakis, I. N.; Orfanopoulos, M., Decatungstate as an efficient photocatalyst in organic chemistry. *Chem. Soc. Rev.* **2009,** *38* (9), 2609-2621; (b) Ravelli, D.; Protti, S.; Fagnoni, M., Decatungstate Anion for Photocatalyzed "Window Ledge" Reactions. *Acc. Chem. Res.* **2016,** *49* (10), 2232-2242.
24. Romero, N. A.; Nicewicz, D. A., Organic Photoredox Catalysis. *Chem. Rev.* **2016,** *116* (17), 10075-10166.
25. (a) Zidan, M.; Rohe, S.; McCallum, T.; Barriault, L., Recent advances in mono and binuclear gold photoredox catalysis. *Catal. Sci. Technol.* **2018,** *8* (23), 6019-6028; (b) Witzel, S.; Hashmi, A. S. K.; Xie, J., Light in Gold Catalysis. *Chem. Rev.* **2021,** *121* (14), 8868-8925.
26. Revol, G.; McCallum, T.; Morin, M.; Gagosz, F.; Barriault, L., Photoredox Transformations with Dimeric Gold Complexes. *Angew. Chem. Int. Ed.* **2013,** *52* (50), 13342-13345.
27. McTiernan, C. D.; Morin, M.; McCallum, T.; Scaiano, J. C.; Barriault, L., Polynuclear gold(i) complexes in photoredox catalysis: understanding their reactivity through characterization and kinetic analysis. *Catal. Sci. Technol.* **2016,** *6* (1), 201-207.
28. Tran, H.; McCallum, T.; Morin, M.; Barriault, L., Homocoupling of Iodoarenes and Bromoalkanes Using Photoredox Gold Catalysis: A Light Enabled Au(III) Reductive Elimination. *Org. Lett.* **2016,** *18* (17), 4308-4311.
29. Cannillo, A.; Schwantje, T. R.; Bégin, M.; Barabé, F.; Barriault, L., Gold-Catalyzed Photoredox C(sp2) Cyclization: Formal Synthesis of (±)-Triptolide. *Org. Lett.* **2016,** *18* (11), 2592-2595.
30. (a) McCallum, T.; Barriault, L., Direct alkylation of heteroarenes with unactivated bromoalkanes using photoredox gold catalysis. *Chem. Sci.* **2016,** *7* (7), 4754-4758; (b) Kaldas, S. J.; Cannillo, A.; McCallum, T.; Barriault, L., Indole Functionalization via Photoredox Gold Catalysis. *Org. Lett.* **2015,** *17* (11), 2864-2866.

31. Rohe, S.; McCallum, T.; Morris, A. O.; Barriault, L., Transformations of Isonitriles with Bromoalkanes Using Photoredox Gold Catalysis. *J. Org. Chem.* **2018,** *83* (17), 10015-10024.
32. (a) Pflästerer, D.; Hashmi, A. S. K., Gold catalysis in total synthesis – recent achievements. *Chem. Soc. Rev.* **2016,** *45* (5), 1331-1367; (b) Dorel, R.; Echavarren, A. M., Gold(I)-Catalyzed Activation of Alkynes for the Construction of Molecular Complexity. *Chem. Rev.* **2015,** *115* (17), 9028-9072.
33. Philippe, M.; Julie, B.; Louis, B., Development of New Gold (I)-Catalyzed Carbocyclizations and their Applications in the Synthesis of Natural Products. *Isr. J. Chem.* **2017,** *57*, 1-11.
34. Riou, M.; Barriault, L., De Novo Synthesis of (+)-Isofregenedol. *J. Org. Chem.* **2008,** *73* (18), 7436-7439.
35. (a) Bellavance, G.; Barriault, L., Total Syntheses of Hyperforin and Papuaforins A–C, and Formal Synthesis of Nemorosone through a Gold(I)-Catalyzed Carbocyclization. *Angew. Chem. Int. Ed.* **2014,** *53* (26), 6701-6704; (b) Bellavance, G.; Barriault, L., Modular Total Syntheses of Hyperforin, Papuaforins A, B, and C via Gold(I)-Catalyzed Carbocyclization. *J. Org. Chem.* **2018,** *83* (13), 7215-7230.
36. McGee, P.; Bétournay, G.; Barabé, F.; Barriault, L., A 11-Steps Total Synthesis of Magellanine through a Gold(I)-Catalyzed Dehydro Diels–Alder Reaction. *Angew. Chem. Int. Ed.* **2017,** *56* (22), 6280-6283.
37. Lu, Z.; Li, Y.; Deng, J.; Li, A., Total synthesis of the Daphniphyllum alkaloid daphenylline. *Nat. Chem.* **2013,** *5* (8), 679-684.
38. Miloserdov, F. M.; Kirillova, M. S.; Muratore, M. E.; Echavarren, A. M., Unified Total Synthesis of Pyrroloazocine Indole Alkaloids Sheds Light on Their Biosynthetic Relationship. *J. Am. Chem. Soc.* **2018,** *140* (16), 5393-5400.
39. Brewitz, L.; Llaveria, J.; Yada, A.; Fürstner, A., Formal Total Synthesis of the Algal Toxin (−)-Polycavernoside A. *Chem. Eur. J.* **2013,** *19* (14), 4532-4537.
40. Woo, S. K.; Lee, E., Polycavernoside A: The Prins Macrocyclization Approach. *J. Am. Chem. Soc.* **2010,** *132* (13), 4564-4565.

2. *GOLD(I) CATALYSIS IN THE SYNTHESIS OF POLYCYCLIC CARBOCYCLES*

2.1 INTRODUCTION

Within the fields of pharmaceutical science, synthetic organic chemistry and chemical biology, efficient strategies to build collections of natural product-like frameworks exhibiting a great degree of molecular diversity and complexity from commercially available starting materials are in high demand. Thus, efforts have been made to develop a divergent one-pot process for the generation of analogues of natural or biologically active products.[41] Au(I/III) complexes have found widespread synthetic applications in organic chemistry in recent decades, notably in the Lewis acid activation of C-C π-moieties, particularly alkynes.[42] This reactivity has been extensively leveraged in total synthesis campaigns[32a, 33, 43] and methodologies to synthesize natural product cores.[32b]

By harnessing previous methodology by Toste *et al.*[12, 14] on the cyclization of silyl enol ethers catalyzed by Au(I), we reported the synthesis of fused carbocycles, showing that by changing the ancillary ligand on the Au(I) catalyst, the regioselectivity of the carbocyclization of silyl enol ether **2.1.0.1** with a substituted enyne can be controlled via a 6-*endo*-*dig* or 5-*exo* cyclization to give **2.1.0.2** or **2.1.0.3** respectively (Scheme 2.1.1).[16]

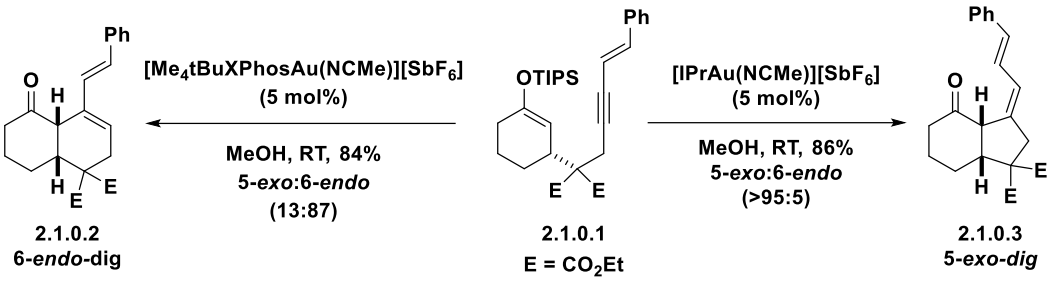

Scheme 2.1.1 – Previous in-group work on regioselective Au(I) cyclization

For example, when a σ-donor ligand such as IPr[44] ligand was used, silyl enol ether **2.1.0.1** cyclized in a 5-*exo-dig* fashion to furnish diene **2.1.0.3**. In contrast, when a bulky phosphine ligand such as Me$_4$*t*BuXPhos (**L1**, Table 2.6.1) was used, the regioselectivity of the carbocyclization shifted to the 6-*endo-dig* pathway to afford synthetically relevant diene **2.1.0.2**.

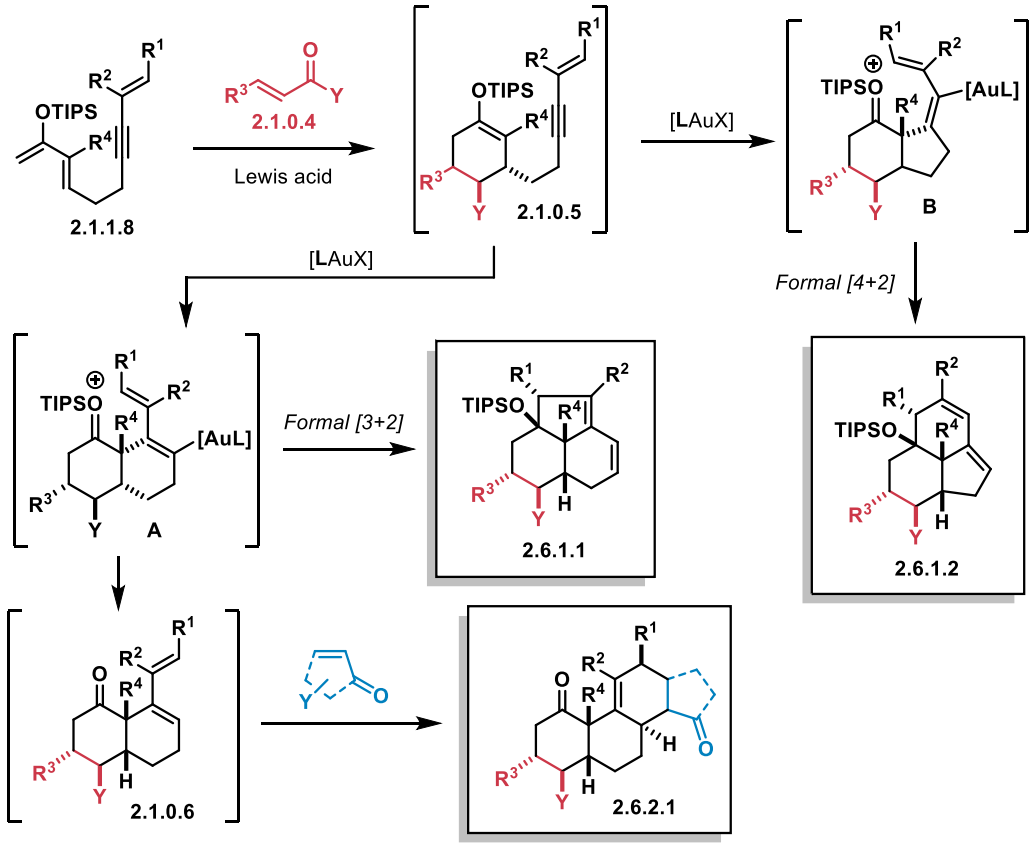

Scheme 2.1.2 – Overview of discussed current work

In light of this ligand effect, we envisioned using cyclic silyl enol ether **2.1.0.5** as a pivotal intermediate to generate molecular diversity (Scheme 2.1.2).[45] At the outset, enol **2.1.0.5** could be readily accessed from diene **2.1.1.8** and dienophile **2.1.0.4** via an intermolecular Diels-Alder (DA) reaction. By modulating the ancillary ligand, enol **2.1.0.5** could be directly converted to compounds **2.6.1.1** and **2.6.1.2** via formal [3+2] and [4+2] Au(I)-catalyzed cyclizations,[36, 46] via intermediates **A** and **B** respectively.[47] On the other hand, one can imagine that intermediate **A** could undergo a protodeauration that would unmask a diene **2.1.0.6**, which in the presence of a dienophile would give tetracycle **2.6.2.1**. The Diels-Alder reaction adds modularity and functionality, while the Au(I) catalytic system enhances the diversity of the framework, where divergent mechanistic pathways are exploited to selectively produce prevalent terpenoid scaffolds embedded in diverse natural products (Scheme 2.1.3), in a single one-pot operation.

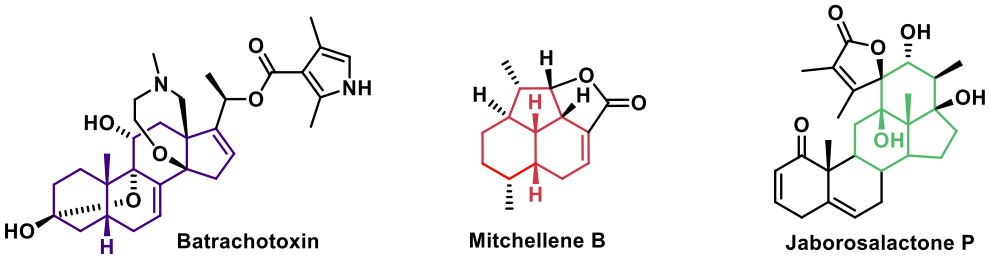

Scheme 2.1.3 – Selected potential natural product targets

Thus the overall goal of the project within this chapter was to develop methodological routes towards all three envisioned cores in Scheme 2.1.2 via one-pot cascade reactions. The longer term objective with the established methodology would then be to apply it in total synthesis of natural products such as those proposed in Scheme 2.1.3.

2.1.1 Substrate Synthesis

The key dienes **2.1.1.8** were synthesized (Scheme 2.1.4) in 5 steps from commercially available diethyl ethylphosphonate **2.1.1.1** via deprotonation with *n*-butyllithium followed by acylation with methyl acetate to give keto-phosphonate **2.1.1.2**. A Horner-Wadsworth-Emmons (HWE) reaction was performed between **2.1.1.2** and aldehyde **2.1.1.3** which was synthesized via PCC oxidation of commercially available alcohol **2.1.1.4**. The HWE reaction yielded enone **2.1.1.5**, which was converted into enynes **2.1.1.7** by a Sonogashira coupling reaction with vinyl bromides **2.1.1.6** in low to good yields. Then dienes **2.1.1.8** were synthesized from **2.1.1.7** via silyl enol ether formation using TIPSOTf under basic conditions from moderate to excellent yields.

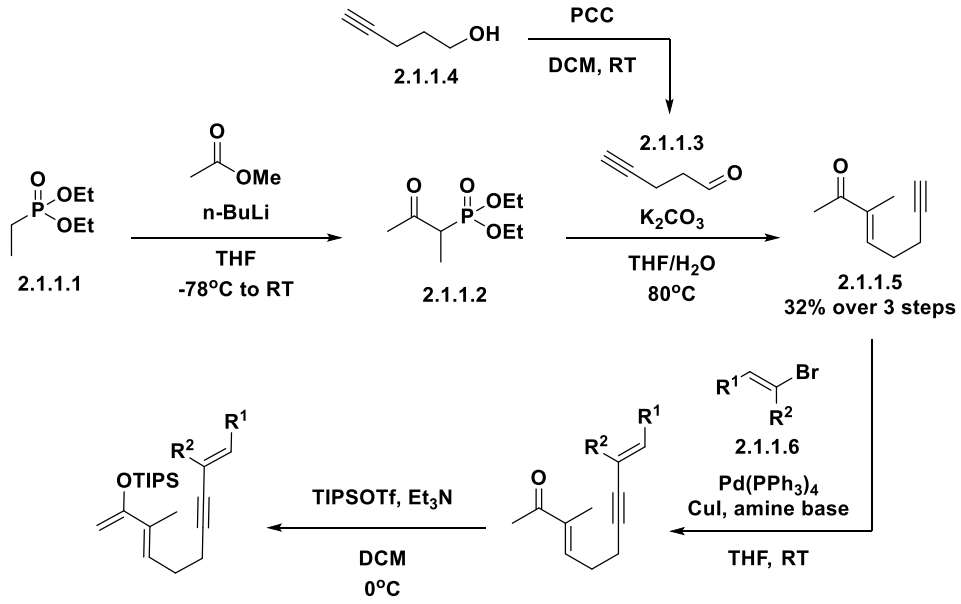

Scheme 2.1.4 – Synthesis of key diene substrate for cascade methodology

2.2 INTRINSIC REACTIVITY STUDIES

The first series of experiments (Scheme 2.2.1) revolved around gaining an understanding of the reactivity of each of the individual three steps (I.e. first DA reaction, gold cyclization, and then second DA reaction) to identify challenges, variables to optimize, as well as potential reactivity trends that can be exploited. How such trends can be addressed or harnessed is summarized and discussed later in the chapter.

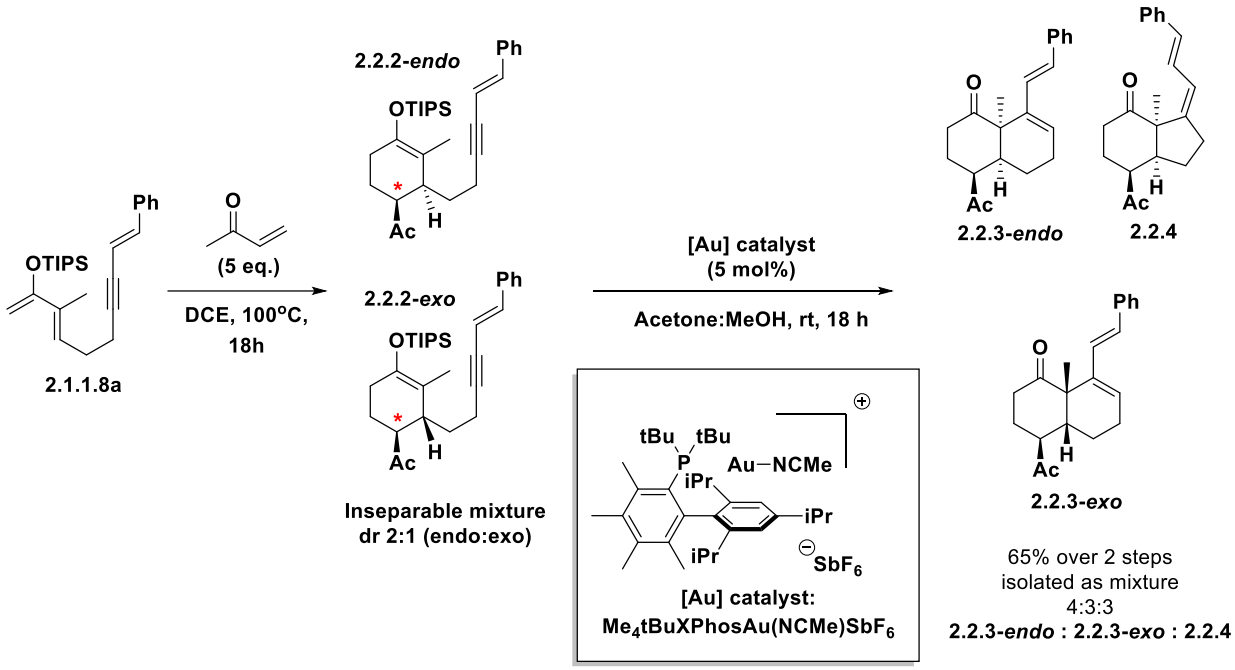

Scheme 2.2.1 – Intrinsic reactivity for the 1st Diels-Alder and gold cyclization steps.

In the first [4+2] cycloaddition step, diene **2.1.1.8a** was used as a model substrate, where under thermal conditions was reacted with methyl vinyl ketone (MVK) to form an inseparable mixture of *endo* and *exo* DA adducts: **2.2.2-*endo*** and **2.2.2-*exo*** respectively. This result was expected and represented the first parameter (i.e., diastereomeric ratio) to be optimized within the developed cascade methodology. This mixture of **2.2.2-endo** and **2.2.2-exo** was then submitted to the 2nd step: Lewis acid gold(I) catalyzed carbocyclization under conditions intended to favor the formation of the 6-*endo*-dig

regioisomer: decalins **2.2.3-*exo*** and **2.2.3-*endo***.[16] This experiment was performed to determine if the substrates possessed any intrinsic regioselectivity. The Au(I)-catalyzed cyclization using Me_4tBuXPhos as the ancillary ligand and a 10:1 acetone:MeOH led to the formation of three products: **2.2.3-endo** and **2.2.3-exo** arising from 6-*endo*-dig cyclizations, as well as **2.2.4** arising from a 5-*exo*-dig cyclization. From these reactions, several pieces of information were obtained. First, after separation by normal phase preparatory HPLC and NMR characterization with stereochemical assignment of the three gold cyclization products, **2.2.3-endo** and **2.2.4** have been found to originate from **2.2.2-endo** through stereochemical inference:, representing 70% of the isolated mixture. The remaining 30% comprises of **2.2.3-exo**, found to have originated from **2.2.2-exo** again through stereochemical inference. Since most of the isolated mixture originated from **2.2.2-endo**, this suggests that the major diastereomer formed in the first DA reaction step is in fact the *endo* product as expected. The second finding was the fact that the only regioisomer formed from **2.2.2-exo** was the 6-*endo*-dig product: **2.2.3-exo**, with no 5-*exo*-dig product observed. This would indicate that the *exo* DA adduct has a propensity to selectively undergo a 6-*endo*-dig cyclization under gold catalytic conditions, presenting a potential trend in reactivity that can be exploited.

The next reaction that was examined was the 2nd DA reaction to form the final polycyclic carbocycle (Scheme 2.2.2). When diene **2.2.3-endo** was submitted to thermal DA conditions with N-phenyl maleimide (NPM) as the dienophile (Scheme 2.2.2 A), steroid-like tetracycle **2.2.5** was formed as the sole diastereomer. This was considered an example of an intrinsic reactivity trend that could be exploited in a diastereoselective DA reaction with substrates similar to **2.2.3-endo**.

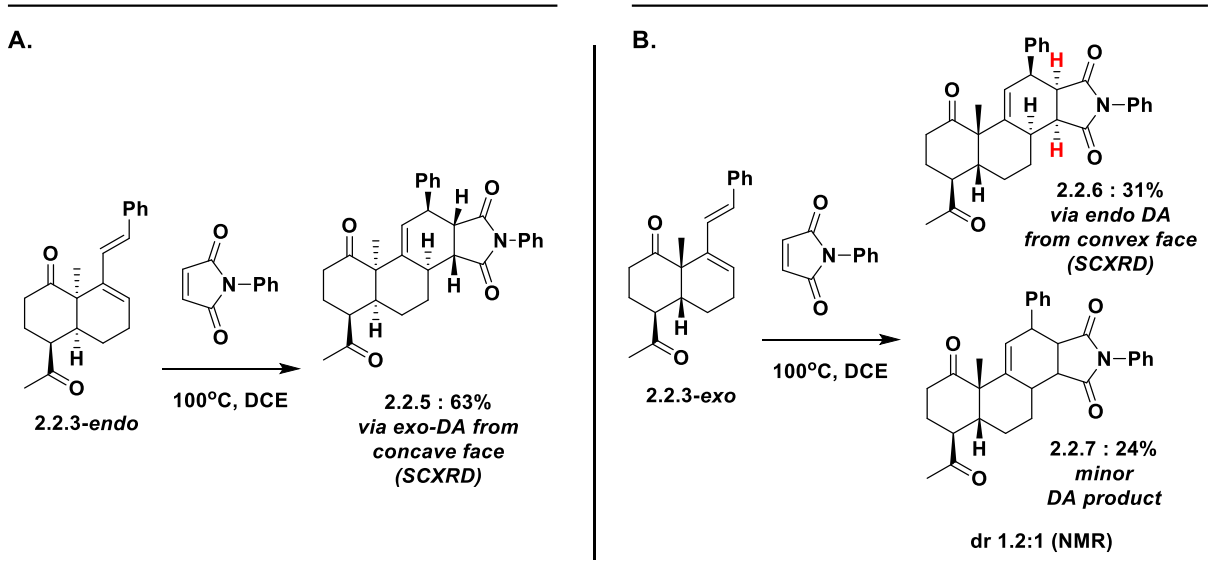

Scheme 2.2.2 – Intrinsic reactivity in the final Diels-Alder reaction

The stereochemistry was established using data from single crystal X-ray diffraction (SCXRD). At first glance, the high diastereoselectivity of the cycloaddition is somewhat surprising as four possible diastereomer can be formed. If one assumes that the reaction is not reversible, the formation of compound **2.2.5** proceeds by an *exo*-DA transition state of the concave face (Scheme 2.2.3).

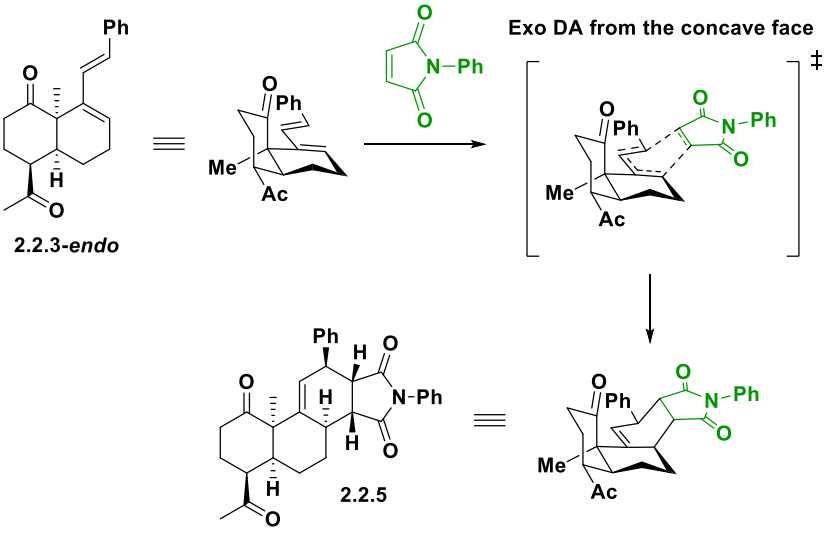

Scheme 2.2.3 – Proposed TS for the formation of tetracycle **2.2.5**

When compound **2.2.3-exo** was subjected to the same DA reaction conditions (Scheme 2.2.2 B), a mixture of two diastereomers were observed: **2.2.6** and **2.2.7** with a 1.2:1 ratio respectively (NMR). The former being produced via an *endo*-DA transition state (Scheme 2.2.4) from the convex face with confirmation by SCXRD analysis. This observation was somewhat unexpected as the *cis*-junction methyl group was thought to have been blocking the approach of the dienophile from the convex face. An *exo*-DA transition state from the concave face in similar fashion in the formation **2.2.5** was predicted.

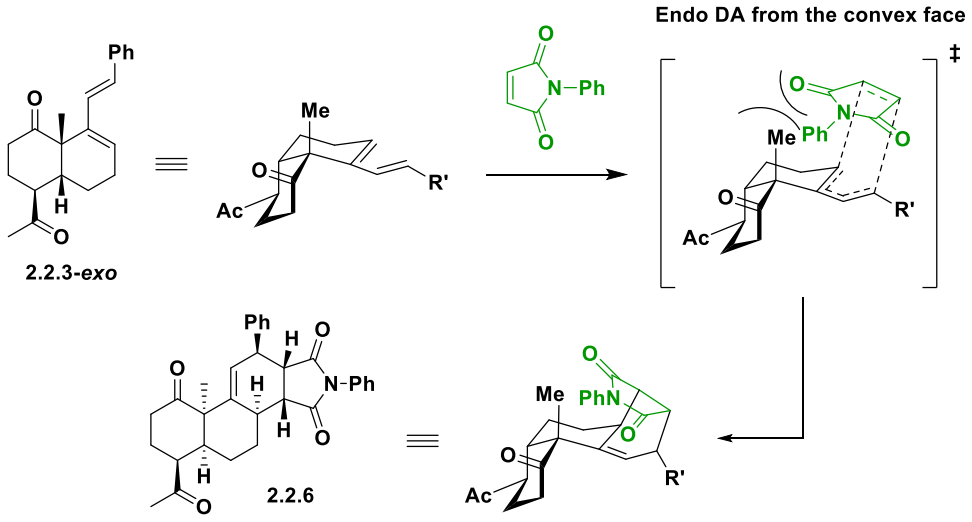

Scheme 2.2.4 - Proposed TS for the formation of tetracycle **2.2.6**

Unfortunately, the stereochemistry of **2.2.7** was not successfully determined due to failed recrystallizations preventing SCXRD analysis, and key signals on ^{1}H NMR overlapping, preventing stereochemical assignment by NOESY analysis. Lastly, an analogous DA reaction was carried out on **2.2.4** (Scheme 2.2.5). No conversion into **2.2.8** was observed, most likely due to the much higher energy associated with the reactive *s-cis* conformation of **2.2.4** compared to the *s-trans* conformation, as well as highly hindered transition states associated with the *s-cis* conformer with the cis-junction methyl group blocking the convex-face approach of a dienophile.

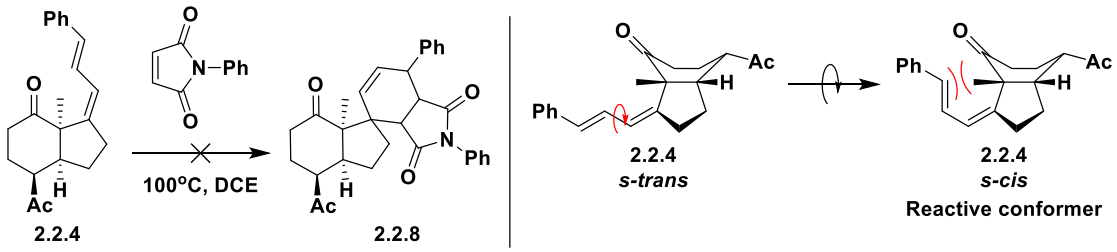

Scheme 2.2.5 – Attempted Diels-Alder reaction of bicycle **2.2.4**

2.3 EPIMERIZATION STUDIES

Further experiments were carried out to determine the possibility of the epimerization of the C1 carbon on **2.2.2**, represented as the interconversion between **2.2.2-endo** and **2.2.2-exo** (Scheme 2.3.1). Such reactivity, if found to be occurring, would suggest the DA reaction to generate **2.2.2** is thermodynamically driven giving the unimpressive diastereomeric ratio of 2:1, rather than simply being one driven by reaction kinetics

First, using **2.2.2** as a diastereomeric mixture, a trans-DA reaction was attempted with NPM as a dienophile (Scheme 2.3.1 A.). The reasoning was that if DA adduct **2.3.1** was observed, a retro-DA reaction was occurring to reform diene **2.1.1.8a** followed by a DA reaction with NPM to form **2.3.1**. This would indicate the DA performed in the creation of **2.2.2** was reversible which would be one reason for C1 epimerization. Since no conversion of **2.2.2** was observed (crude NMR) in the reaction after heating, it was concluded that a trans-DA reaction does not occur in this reaction, therefore providing no evidence for an epimerization of **2.2.2**.

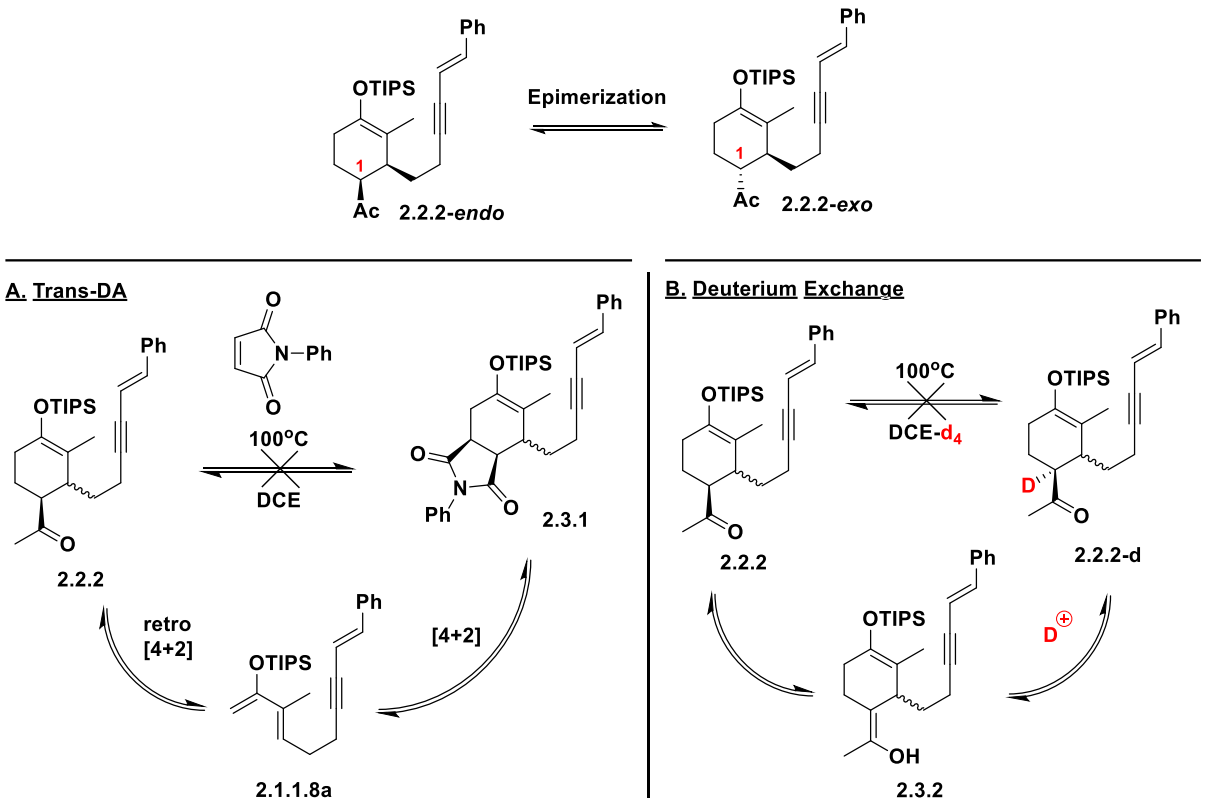

Scheme 2.3.1 – Epimerization experiments for the first Diels-Alder reaction step of the cascade.

The second experiment (Scheme 2.3.1 B.) was to determine if epimerization was occurring as a result of the solvent. This would happen via tautomerization of **2.2.2** into enolate **2.3.2,** followed tautomerization again in the presence of deuterium cation, hypothesized to come from DCE-d_4, to generate **2.2.2-d**. Using a deuterated solvent in this experiment would provide evidence that epimerization of **2.2.2** is occurring if deuterium incorporation was observed. However, no **2.2.2-d** was observed (crude NMR) with no conversion of **2.2.2**. Therefore, this result provides no evidence that epimerization of **2.2.2** occurs. Further experiments could be performed using acetone-d_6 as the solvent, as acetone would be a far more likely cause of epimerization because of its similar pK_a to the C1 epimerizable proton.

When moving on to the Au(I) cyclization, as second step of the cascade, the possibility of the epimerization of the C1 carbon during this step was also probed (Scheme 2.3.2) since Au(I) is a Lewis acid, albeit a soft rather than hard Lewis acid, and methanol is present as a proton source. This experiment (Scheme 2.3.2 A.) was done by re-submitting pure Au(I) cyclization product **2.2.3-exo** to the same conditions that it was synthesized by. If epimerization of the C1 position was occurring under the catalytic conditions, a mixture of both **2.2.3-exo** and **2.2.3-endo** would be observed. This was not the case however, as no conversion of **2.2.3-exo** was observed by crude NMR. The analogous experiment (Scheme 2.3.2 B.) was also carried out on **2.2.3-endo**, with no epimerization observed.

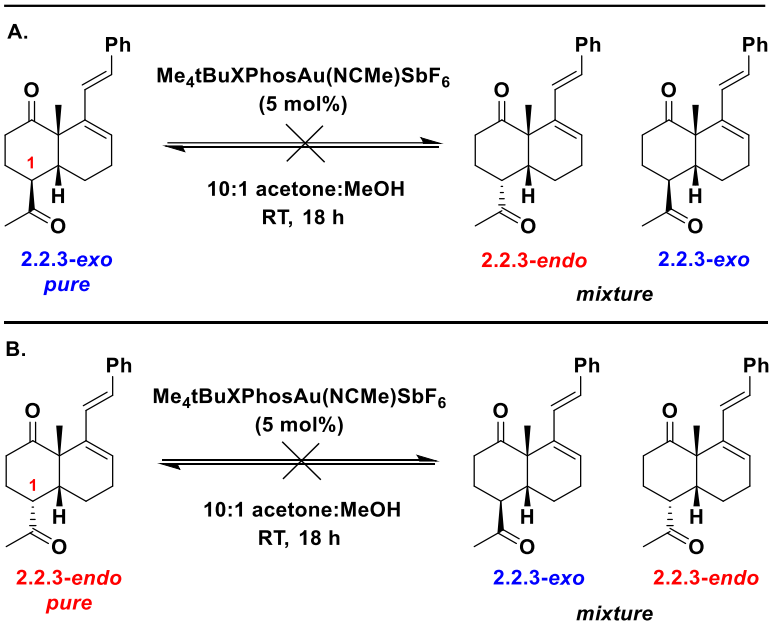

Scheme 2.3.2 - Epimerization experiments for the Au(I) cyclization of the cascade.

The last and most definitive experiment (Scheme 2.3.3) that was performed was the Au(I) cyclization of a substrate deuterated at the C1 position. Using deuterated silyl enol ether **2.3.1** as an inseparable 2:1 mixture of *exo* and *endo*-DA adducts, made via DA reaction with **2.1.1.1** and methyl acrylate-d_6, a Au(I) cyclization with undeuterated MeOH

gave deuterated products **2.3.2-*endo***, **2.3.2-*exo***, and **2.3.3**. All products remained deuterated at the C1 position, further indicating that epimerization does not occur during the Au(I) cyclization.

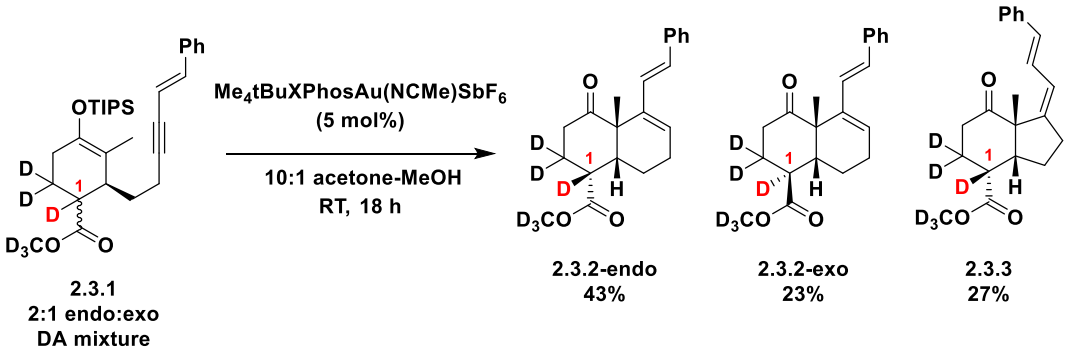

Scheme 2.3.3 – Epimerization experiments using deuterated substrate **2.3.1**

2.4 PLANNED METHODOLOGY OBJECTIVES

With all of the accumulated experimental observations on the intrinsic reactivity of the cascade reactions and the tests on epimerization, two paths on how to develop the methodology were proposed: Routes A and B (Scheme 2.4.1). Considering that the first DA reaction step generates two diastereomers: **2.2.2-exo** and **2.2.2-endo** from **2.1.1.8a**, this is the initial point of divergence in the cascade and therefore the stereoselectivity must be controlled if the project objective of developing a selective methodology is to be achieved. An unselective first DA reaction step would result in three tetracyclic diastereomers: **2.2.5**, **2.2.6**, and **2.2.7**, as well as bicycle **2.2.4** which fails to react in the second DA reaction. If the selective formation of *exo*-DA adduct **2.2.2-exo** can be achieved, Route A (red) would be followed where the propensity of **2.2.2-exo** to undergo only 6-*endo*-*dig* Au(I) cyclization to form **2.2.3-exo** can be taken advantage of. Though

once at the 2nd DA step, the formation of two diastereomers: **2.2.6** and **2.2.7** would have to be accepted, unless the diastereoselectivity can be controlled.

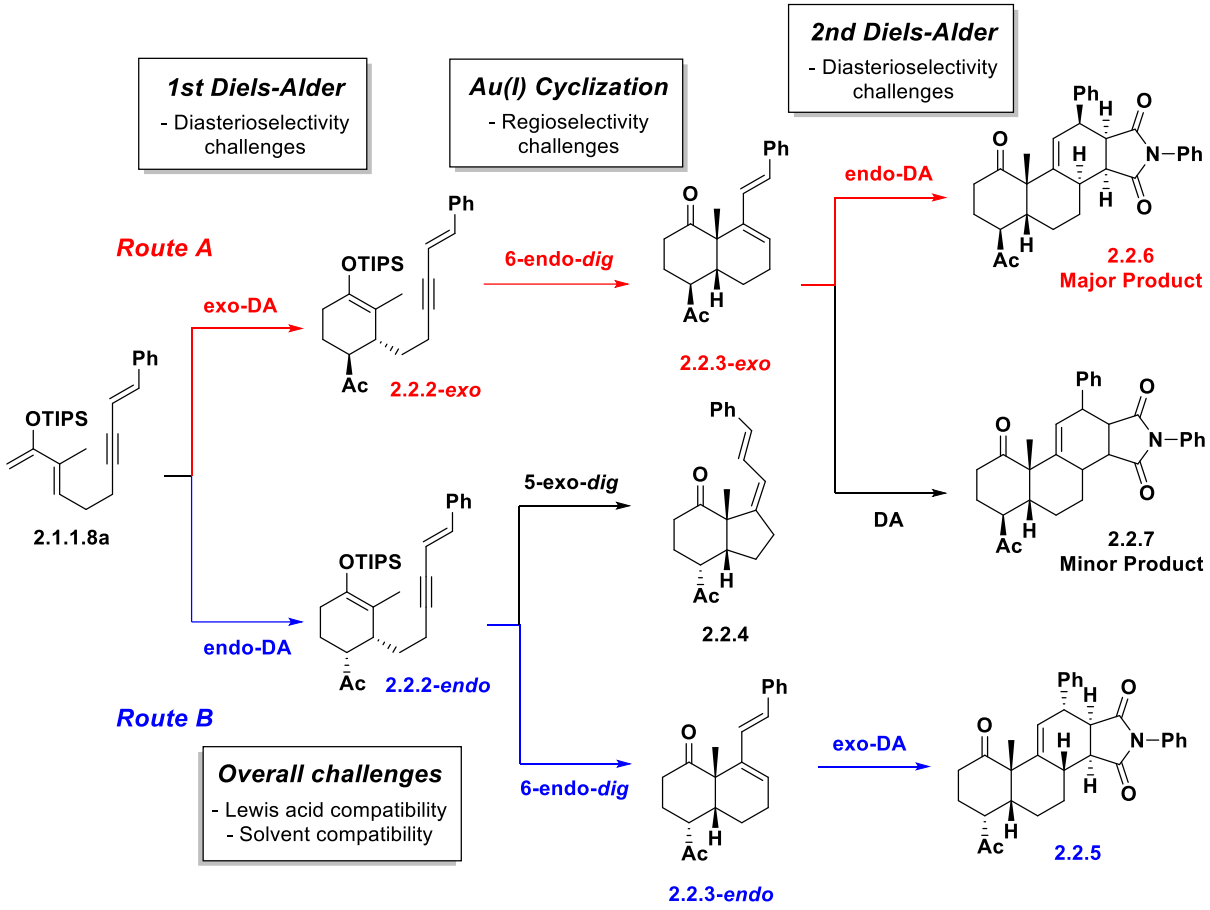

Scheme 2.4.1 – Possible routes for the planned methodology development

On the other hand, if *endo*-DA adduct **2.2.2-endo** is formed during the first DA reaction step, then Route B (blue) is followed where the Au(I) cyclization gives both 5-*exo* and 6-*endo-dig* regioisomers. This lack of intrinsic selectivity of the Au(I) cyclization compared to Route A is a downside to Route B since **2.2.4** cannot be telescoped to the end of the cascade as it is unreactive under our standard thermal DA conditions (DCE, 100°C). The upside to Route B was the intrinsic selectivity of **2.2.3-endo** to form **2.2.5** via *exo*-DA transition state, meaning Route B yielded a single tetracyclic end-product with >20:1 selectivity, which is very appealing for methodology development.

A project plan was devised where Route B was to be targeted, because it was predicted that optimization of the first DA reaction step to form the kinetically favored *endo*-DA adduct would be easier, rather than optimizing to form the *exo*-DA adduct. The use of LUMO-lowering Lewis acids was planned for this purpose. This also gave an opportunity to explore the use of chiral Lewis acids to catalyze an enantioselective DA reaction. However, it is important to then note that any reagent or catalyst used in the first DA reaction step must be compatible with the Au(I) catalyst of the second step if the sequence is be performed as a one-pot cascade. And finally, the solvent choice must also be compatible and useful for all three steps. This is especially challenging considering both the enantioselectivity of the first DA reaction step and the regioselectivity of the Au(I) cyclization is heavily influenced by solvent choice. For example, a Lewis acid used for the first DA reaction step would generally not be compatible with Lewis basic solvents. In the model example (Scheme 2.1.4), Lewis basic acetone is the optimal solvent for the Au(I) cyclization.

2.5 OPTIMIZATION OF THE 1ST STEP – ENANTIOSELECTIVE DIELS-ALDER REACTION

The first attempts to optimize the first DA reaction step were done concurrently with the search for conditions to perform enantio- and diastereoselective cycloadditions. Two methods were explored predominantly: Cu(II)- bis(oxazoline) (BOX) catalytic systems,[48] as well as Co(III)[49] and Cr(III)[50] SALEN and SALEN-type catalysts by Evans and Rawal respectively.

2.5.1 Cu(II)-BOX Catalyzed Enantioselective Diels-Alder Reaction

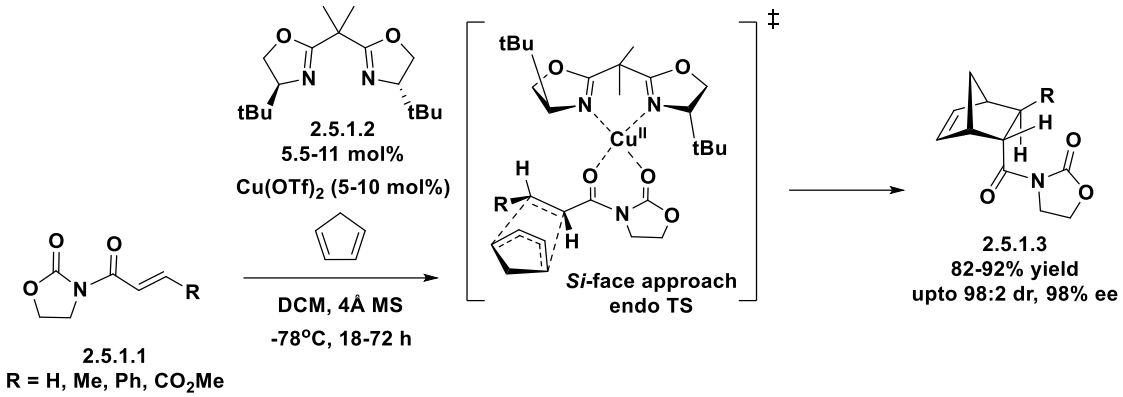

Scheme 2.5.1– Seminal work on Cu(II)-BOX catalyzed enantioselective Diels-Alder reaction

In 1993, Evans *et al.* reported a method[48a, 48b] (Scheme 2.5.1) of using a C2-symmetric chiral Cu(II)-BOX complex as chiral Lewis acid for enantioselective DA reactions using cyclopentadiene and oxazolidinone acrylate **2.5.1.1** as a dienophile. These reactions occurred first via the preformation of the chiral Cu(II)-BOX complex from Cu(II)OTf and BOX ligand **2.5.1.2**. This complex then binds with **2.5.1.1** to form a chiral catalyst-substrate complex with a square-planar geometry. Cyclopentadiene then approaches from the *Si*-face via an *endo* transition state, giving bicycle **2.5.1.3** in excellent yields, as well as diastereo and enantioselectivity. This method provided the starting point for the initial attempts (Table 2.5.1) at inducing enantioselectivity in the first DA reaction step. Diene **2.1.1.8a** and dienophile **2.5.1.1a** were chosen as model substrates.

Table 2.5.1 – Optimization of copper(II)-BOX catalyzed enantioselective Diels-Alder reaction

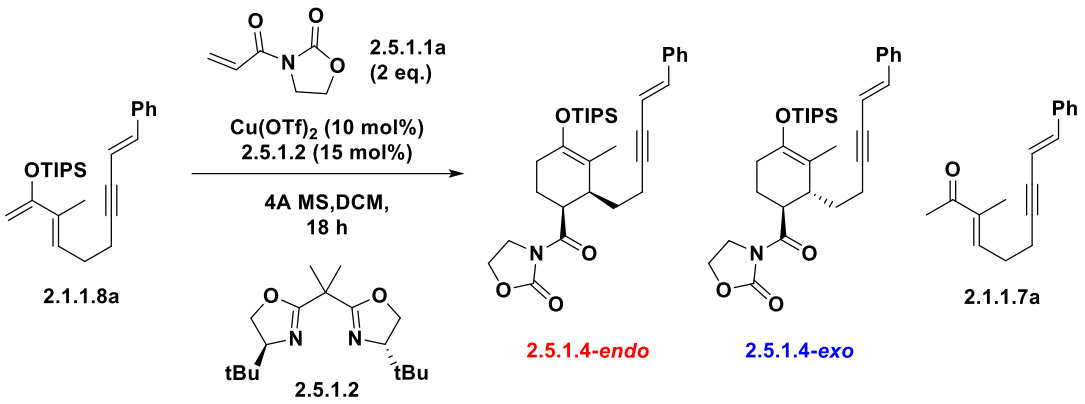

	NMR Yield (%)[a]					
Entry	**Temperature (˚C)**	**2.5.1.4-exo + 2.5.1.4-endo**	**2.1.1.7a**	**SM**	**dr[d] *exo*:*endo***	**% ee[c] (*exo*)**
1	-78	0	0	75	n.d	n.d
2	25	66 (60)	7	0	4:1	72
3	0	15	4	60	n.d	n.d
4[b]	100	(59)	0	0	1:1.5	n.d

[a]NMR yields determined using mesitylene standard. Isolated yields are in brackets. [b]Reaction performed at 100°C in DCE with no catalyst or 4Å MS. [c]Enantiomeric excess determined by chiral HPLC. n.d = not determined. [d]Diastereomeric ratio determined by 1H NMR analysis.

The first attempt (Entry 1) at -78°C for 18 h gave no desired product and low conversion. Raising the temperature to ambient temperature (Entry 2) gave full conversion, yielding **2.5.1.4-*endo*** and **2.5.1.4-*exo*** with a surprising diastereomeric ratio of 4:1 in favor of the *exo*-DA product, as well as trace **2.1.1.7a** via desilylation of starting material diene. The enantiomeric excess of **2.5.1.4-exo** was determined to be moderate. The reaction was lowered to 0°C (Entry 3) with the intent on improving enantioselectivity, however full conversion was not observed with a low combined yield of **2.5.1.4**. A thermal DA (Entry 4) was also performed as a comparison reaction giving a mixture of **2.5.1.4** favoring **2.5.1.4-endo** with poor diastereoselectivity. This experiment suggested that the

Cu(II)-BOX catalytic system was responsible for the selectivity observed for **2.5.1.4-exo**, as well as the degradation of starting diene **2.1.1.8a** into ketone **2.1.1.7a**.

Table 2.5.2 – Time trial experiments of copper(II)-BOX catalyzed enantioselective DA

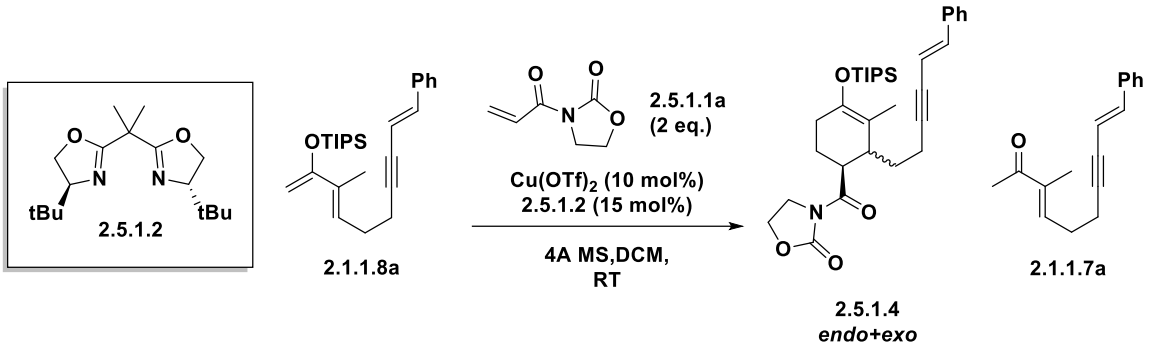

Entry	Time elapsed (h)	NMR Yield (%)[a]		
		2.5.1.4 *exo* +*endo*	2.1.1.7a	SM
1	3	22	6	51
2	6	53	10	16
3	12	61	5	5
4	18	66	7	0

[a]NMR yields determined using mesitylene standard.

A time trial experiment (Table 2.5.2) was carried out to gain insight into the apparent slow reaction rate of copper(II)-BOX catalyzed enantioselective DA. Parallel reactions were performed and then quenched at the 3, 6, 12, and 18 hour marks. Analysis by quantitative NMR with mesitylene internal standard gave the yields, which was then plotted (Figure 2.5.1) over reaction time elapsed.

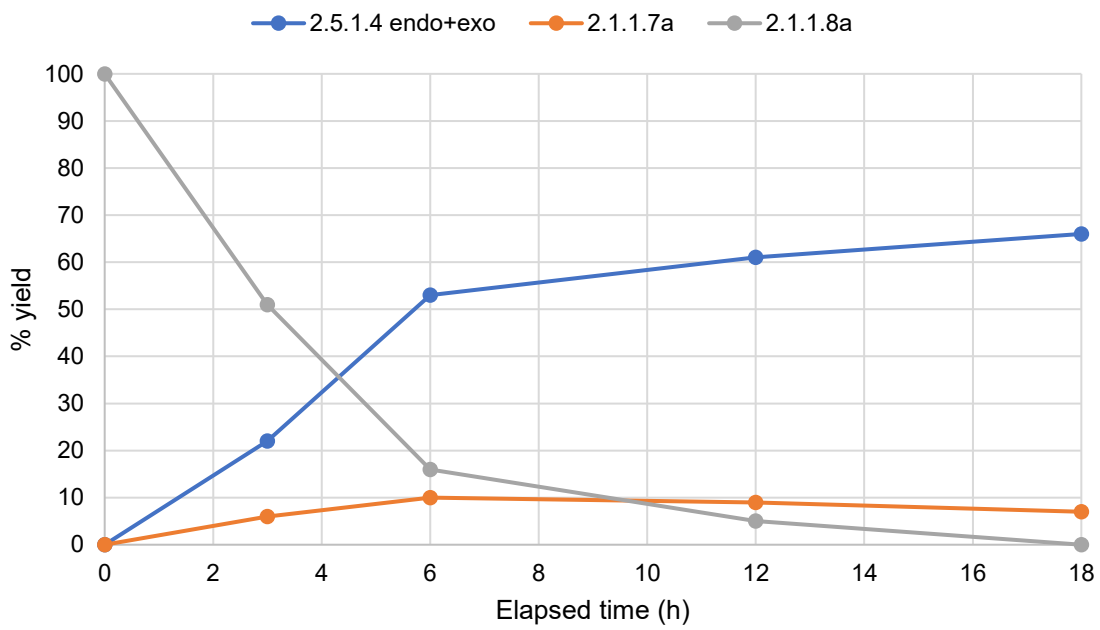

Figure 2.5.1 – Reaction progress of Cu(II)-BOX catalyzed Diels-Alder reaction

No drop off in desired products **2.5.1.4** ***endo+exo*** were observed over reaction progression, thus no obvious evidence of product degradation was found. However, mass balance was not found, where the combined yields of **2.5.1.4** ***endo+exo*** and known degradation product **2.1.1.8a** was only 73% after full reaction conversion. There are likely further degradation products that have yet to be found, which possibly could be forming concurrently with the known products. Both **2.5.1.4** ***endo+exo*** diastereomers were observed to form simultaneously, with no erosion in diastereomeric ratio being observed. Another important finding was that full conversion required 18 h at ambient temperature. As a result, running the reaction to completion at cryogenic temperatures with the intention of improving enantioselectivity would not be practical.

The catalyst loading for the copper(II)-BOX catalyzed enantioselective DA was also optimized (Table 2.5.3). In comparison to a 10 mol% catalyst loading, lowering it by

half (Entry 2) reduced the yield for **2.5.1.4 *endo+exo***, while doubling the catalyst loading (Entry 3) made a negligible difference in yield.

Table 2.5.3 – Catalyst loading experiments of copper(II)-BOX Diels-Alder reaction

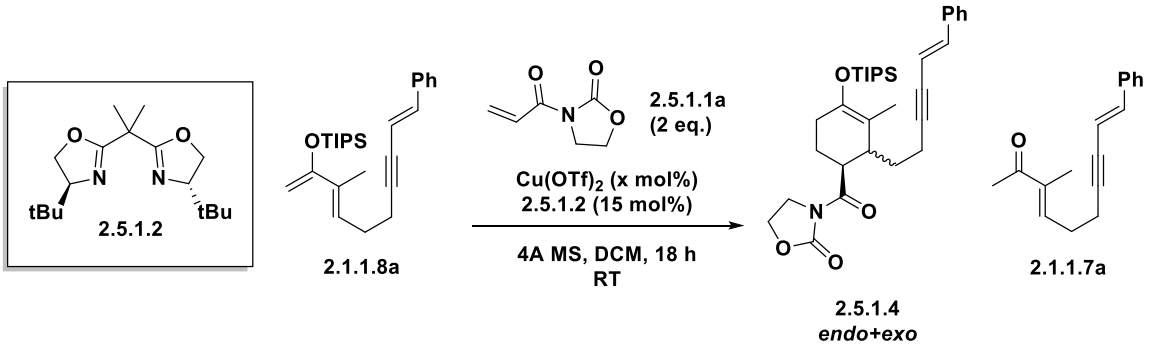

Entry	Catalyst loading (mol %)	NMR Yield (%)[a]		
		2.5.1.4 *exo* +*endo*	2.1.1.7a	SM
1	10	66	7	0
2	5	54	7	8
3	20	64	5	0

[a]NMR yields determined using mesitylene standard.

Although, the potential of the Cu(II)-BOX catalytic system by Evans *et al.* in inducing an enantioselective DA reaction was demonstrated with the substrates within this project. Only moderate enantioselectivity, diastereoselectivity, and yield were observed. Also, the lower reactivity of dienes such as **2.1.1.8a**, meant that the reaction temperature could not be lowered to improve enantioselectivity while having a practically feasible reaction time. Experiments with the Cu(II)-BOX catalytic system were generally not pursued any further. However, future work should investigate the use of less coordinating counterions with Cu(II)-BOX, such as SbF_6^-.

2.5.2 Rare-Earth Metal Lewis-Acid Catalyzed Diels-Alder Reaction

Further screening of Lewis acidic metals (Table 2.5.4) was then performed in comparison with the best enantioselective conditions at the time (Entry 1) using $Cu(OTf)_2$ where it was substituted for a variety of Lewis acids (primarily metal triflates). Initial attempts (Entry 2-5) using Pd, Mg, In, Zn salts were largely unsuccessful. Full conversion was not observed for any of these examples, and yields for **2.5.1.4 *endo+exo*** were very low except for $Zn(OTf)_2$ (Entry 5), which gave a moderate yield and diastereoselectivity. When $Fe(OTf)_3$ (Entry 6) was used, full conversion, and a moderate yield and diastereoselectivity were observed. Enantioselectivity of entries 2-6 were not determined due to the insufficient yields or diastereoselectivity not warranting further investigation. Afterwards, $Sc(OTf)_3$ was tried (Entry 7), which gave **2.5.1.4 *endo+exo*** in good yields and diastereoselectivity, though with significant degradation of the starting material into ketone **2.1.1.7a** was found. Enantioselectivity was determined to be minimal unfortunately.

Eventually when experiments using a slew of lanthanide triflates were performed (Entry 8-12), quantitative yields (NMR yields) of **2.5.1.4 *endo+exo*** were observed with excellent diastereoselectivity for **2.5.1.4-exo**. Though no enantioselectivity was observed for any of these reactions except for $Er(OTf)_3$ (Entry 10), which gave low enantioselectivity for the opposite enantiomer that was observed for $Cu(OTf)_2$ (Entry 1). Ultimately, $Gd(OTf)_3$ (Entry 11) was found to be the most successful Lewis acid with an isolated yield of 88%. The lack of enantioselectivity with Yb, Eu, and Gd triflates indicated that the formation of the metal-chiral BOX ligand complex was not likely the reactive species

involved in catalyzing the DA reaction. A similar methodology has been developed by Evans

Table 2.5.4 – Metal center optimization for the Lewis-acid-BOX Diels-Alder reaction

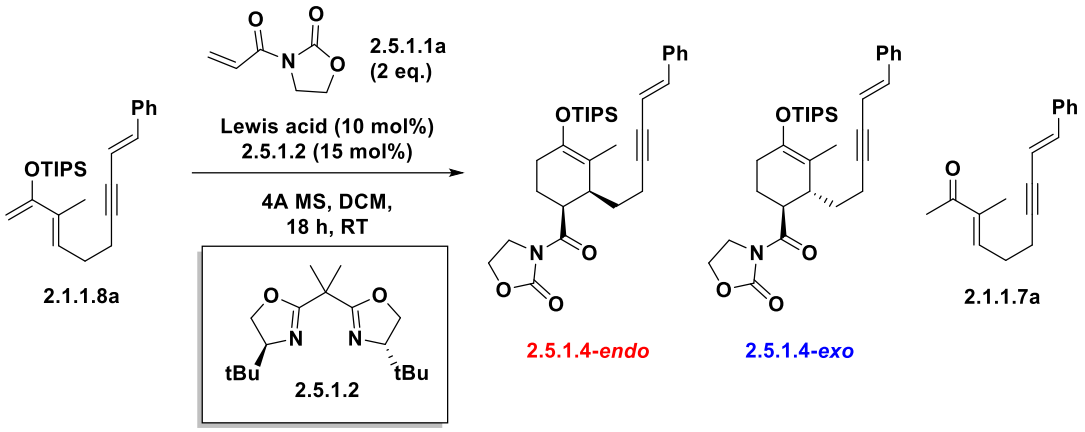

Entry	Lewis acid	NMR Yield (%)[a] 2.5.1.4 *exo* +*endo*	2.1.1.7a	SM	dr[d] *exo* :*endo*	% ee[b] (*exo*)
1	$Cu(OTf)_2$	66 (60)	7	0	4:1	72
2	$Pd(TFA)_2$	8	36	38	n.d	n.d
3	$Mg(OTf)_2$	10	3	77	n.d	n.d
4	$In(OTf)_3$	20	41	31	n.d	n.d
5	$Zn(OTf)_2$	46	6	35	5.3:1	n.d
6	$Fe(OTf)_3$	60	34	0	5.6:1	n.d
7	$Sc(OTf)_3$	70	18	0	10:1	8
8	$Yb(OTf)_3$	95 (81)	trace	0	13:1	0
9	$Eu(OTf)_3$	>95 (82)	trace	0	13:1	0
10	$Er(OTf)_3$	94 (83)	trace	0	13:1	-10
11	$Gd(OTf)_3$	>95 (88)	trace	0	13:1	0
12[c]	$Gd(OTf)_3$	(>95)	0	0	>20:1	N/A

[a]NMR yields determined using mesitylene standard. Isolated yields are in brackets. [b]Enantiomeric excess determined by chiral HPLC. [c]Reaction performed at 3.0 mmol scale without ligand 2.5.1.2. n.d = not determined. N/A = not applicable. [d]Diastereomeric ratio determined by 1H NMR analysis.

One possibility could be the displacement of BOX ligand **2.5.1.2** by oxazolidinone dienophile **2.5.1.1a** off of the metal center since it is in a ~13:1 stoichiometric excess

relative to the ligand. Lanthanide metals are also known to be capable of forming octahedral complexes,[51] thus 1 molecule of $Gd(OTf)_3$ may be binding up to 3 molecules of oxazolidinone dienophile **2.5.1.1a**. When the same DA reaction with $Gd(OTf)_3$ was performed (Entry 12) on larger scale and without BOX ligand **2.5.1.2**, a quantitative isolated yield for **2.5.1.4-exo** exclusively was observed. Though a pre-aging step was required where $Gd(OTf)_3$, oxazolidinone dienophile **2.5.1.1a**, and 4Å molecular sieves (MS) were stirred together in DCM for 3 hours. This was followed by addition of diene **2.1.1.8a** initializing the actual DA reaction. If the pre-aging step was not performed (I.e. all reagents were added at once), the reaction failed, yielding only ketone **2.1.1.7a** as a degradation product. This requirement for pre-aging and the non-requirement of chiral BOX ligand **2.5.1.2** for a successful DA reaction supports the hypothesis that the active reactive species is a $Gd(OTf)_3$-oxazolidinone dienophile complex. This $Gd(OTf)_3$ catalyzed *exo*-DA was then chosen as the optimal DA method moving forward, though it would be an racemic method.

Attention was then turned towards the solvent optimization of the $Gd(OTf)_3$ catalyzed *exo*-DA (Table 2.5.5). At this stage, diene **2.1.1.8c** was chosen as the model diene since the absence of a phenyl substituent would make the method more applicable towards natural product synthesis. Also, chiral BOX ligand **2.5.1.2** was still used as the ligand as it was believed at the time that it was necessary for the DA reaction despite it not inducing any enantioselectivity. The first several experiments (Entry 1-5) gave **2.5.2.1 *exo+endo*** in all in low yield and low conversion. When nitromethane was used (Entry 1), full conversion was observed but mostly towards ketone degradation product **2.1.1.7c** in good yield, **2.5.2.1 *exo+endo*** was found in low yield. Better results were found with

chlorinated solvents. DCE (Entry 7) gave incomplete conversion with moderate diastereoselectivity and yield for **2.5.2.1** ***exo+endo***. Chloroform (Entry 8) gave almost complete conversion with high diastereoselectivity and yield of **2.5.2.1** ***exo+endo***. A DA reaction with acetone (Entry 9) over 5 days gave complete conversion with moderate diastereoselectivity and excellent yield of **2.5.2.1** ***exo+endo***. DCM (Entry 10) however, was still found to be the optimal solvent giving excellent diastereoselectivity and yield of **2.5.2.1** ***exo+endo***.

Table 2.5.5 – Solvent optimization of $Gd(OTf)_3$ catalyzed *exo*-Diels-Alder reaction

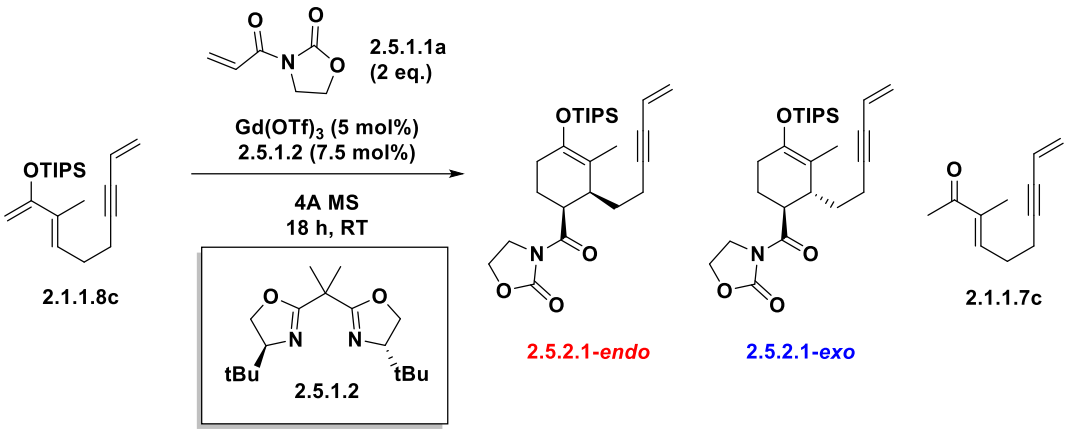

		NMR Yield (%)[a]			
Entry	**Solvent**	**2.5.2.1 *exo* +*endo***	**2.1.1.7c**	**SM**	**dr[c] *exo* :*endo***
1	toluene	19	21	63	n.d
2	THF	22	0	74	n.d
3	MeCN	24	18	44	n.d
4	DMF	26	0	68	n.d
5	benzene	26	8	68	n.d
6	$MeNO_2$	15	77	0	n.d
7	DCE	52	14	27	4:1
8	chloroform	86	0	9	16:1
9	acetone[b]	92	4	0	9:1
10	DCM	92	0	0	19:1

[a]NMR yields determined using mesitylene standard. Isolated yields are in brackets. [b]Reaction was run for 5 days. n.d = not determined. [c]Diastereomeric ratio determined by 1H NMR analysis.

Further investigation into the use of $Gd(OTf)_3$ and $Sc(OTf)_3$ in enantioselective DA reactions were briefly carried out with pyridyl-bis(oxazoline) (PyBOX) ligands. Literature precedence[52] (Scheme 2.5.2) was found in work by Evans *et al.* where an enantioselective DA was performed using Sm(III)/Gd(III) – chiral PyBOX complexes with unactivated dienes and highly electron-poor quinoline dienophiles with bidentate binding sites. This work notably differs in the fact that the *endo* DA adduct is formed selectively, and not the *exo* DA adduct.

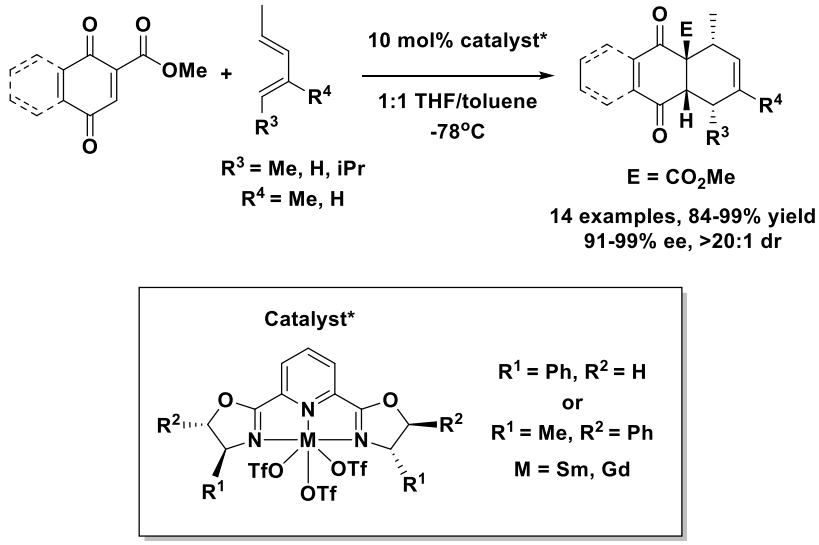

Scheme 2.5.2 – Enantioselective Diels-Alder reaction catalyzed by La(III) PyBOX complexes

Our experiments (Table 2.5.6) used $Gd(OTf)_3$ and $Sc(OTf)_3$ and chiral PyBOX ligand **2.5.1.5**, and were performed in comparison with yields when using chiral BOX ligand **2.5.1.2**. Diene **2.1.1.8a** and oxazolidinone dienophile **2.5.1.1a** were used as model substrates. For $Gd(OTf)_3$, the use of PyBOX ligand **2.5.1.5** (Entry 1) did not improve diastereoselectivity when compared to the same reaction but with BOX ligand **2.5.1.2**

(Entry 2) and still no enantioselectivity was observed, and the isolated yield was diminished.

Table 2.5.6 – Examination of PyBOX ligands in an enantioselective Diels-Alder reaction reaction

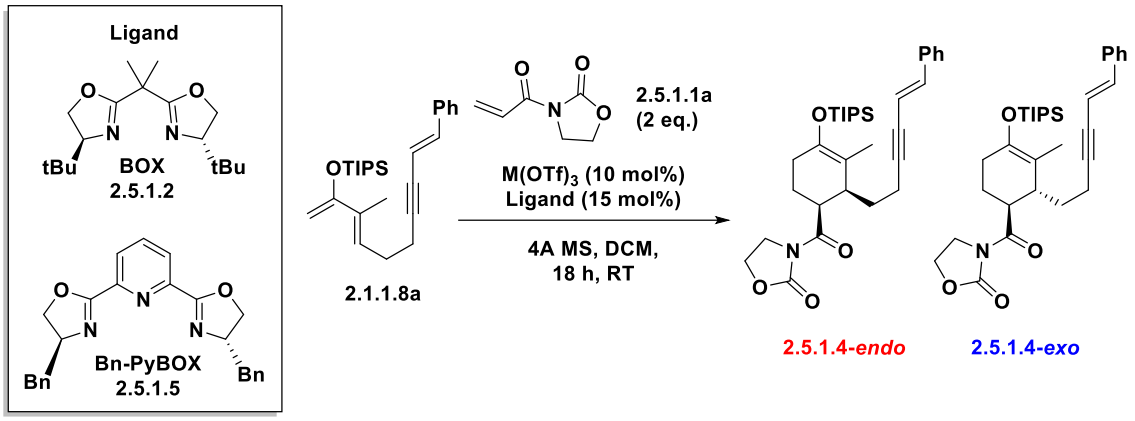

Entry	M	Ligand	2.5.1.4[a] *exo* +*endo*	dr[c] *exo* :*endo*	% ee[b] (*exo*)
1	Gd^{3+}	2.5.1.3	(67)	13:1	0
2	Gd^{3+}	2.5.1.2	>95 (88)	13:1	0
3	Sc^{3+}	2.5.1.3	(59)	7:1	40
4	Sc^{3+}	2.5.1.2	70	10:1	8

[a]NMR yields determined using mesitylene standard. Isolated yields are in brackets. [b]Enantiomeric excess determined by chiral HPLC. [c]Diastereomeric ratio determined by 1H NMR analysis.

However, when $Sc(OTf)_3$ was used, improved enantioselectivity was observed when using **2.5.1.5** (Entry 3) compared to **2.5.1.2** (Entry 4) though with slightly diminished diastereoselectivity. No further investigations were carried out to optimize enantioselectivity with PyBOX ligands. Future work can be done optimizing the solvent, though the solvent choice would be limited given it also needs to be an optimal solvent for the subsequent Au(I) cyclization for the one-pot cascade to work. Different temperature conditions should also be investigated, specifically lowering the temperature to possibly enhance enantioselectivity.

2.5.3 Cobalt(III) Catalyzed Enantioselective Diels-Alder Reaction

An exploration was done into harnessing methods for enantioselective DA reactions catalyzed by Co(III)-SALEN complexes. In 2002, Rawal *et al.* (Scheme 2.5.3) reported a method[49] for a highly effective enantioselective DA reaction between a Rawal diene and acrolein-type dienophiles using a TMS substituted Co(III)-SALEN catalyst. High yields, diastereoselectivity, and enantioselectivity were achieved. The ability for the reaction to be ran in air atmosphere without sieves is also noteworthy.

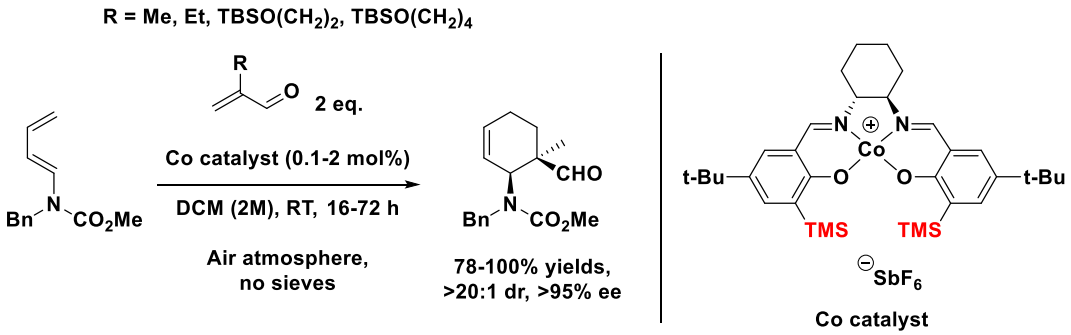

Scheme 2.5.3 - Cobalt(III)-SALEN catalyzed enantioselective Diels-Alder reaction

This became the main methodology that was used in the optimization (Table 2.5.7) with our own substrates: diene **2.1.1.8c** reacting with methacrolein to generate *endo*-DA adduct **2.5.3.2**. The catalysts used were silane and alkyl substituted Co(III)-SALEN complexes **2.5.3.1**. The solvent was kept consistent using DCM, and the reactions were set-up in air atmosphere but ran in sealed vials without molecular sieves. All reactions (Entry 1-8) except for a trial using catalyst **2.5.3.1-Ad** (Entry 9) gave high to excellent diastereoselectivity for the *endo*-DA product. Though when starting with the model catalyst **2.5.3.1-TMS** (Entry 1) from Rawal's methodology from Scheme 2.5.3, high yields for desired product **2.5.3.2** was observed but surprisingly no enantioselectivity was found. Enlarging the silyl substituent on the Co(III)-SALEN catalyst (Entry 2-4) gave interesting results where **2.5.3.1-TBS** (Entry 2) was found to have the optimal alkyl bulk where the

highest yield, enantioselectivity, and diastereoselectivity for desired product **2.5.3.2** was found. When the alkyl bulk was increased to TIPS (Entry 3) then TBDPS (Entry 4), catalysts **2.5.3.1-TIPS** and **2.5.3.1-TBDPS** both gave low yields for **2.5.3.2** and very low enantioselectivity. Diastereoselectivity was excellent both catalysts, however. Afterwards, trials were ran with **2.5.3.1-TBS** with lower temperatures. When the reaction temperature was lowered to 0°C (Entry 5), a moderate yield for **2.5.3.2**, high diastereoselectivity, and the highest enantioselectivity in this series were obtained. Though oddly, when the reaction temperature was lowered to -20°C (Entry 6), enantioselectivity and diastereoselectivity were diminished when compared to 0°C (Entry 5). Alkyl substituted SALEN ligands were then used. Catalyst **2.5.3.1-tBu** (Entry 7) gave moderate yields, high diastereoselectivity, but low enantioselectivity of **2.5.3.2**. When a much larger adamantyl substituent was used in catalyst **2.5.3.1-Ad**, only starting material degradation was observed. Lastly, catalyst **2.5.3.1-CrtBu** (Entry 9) with a Cr(III) metal center,[50] gave good yields, high diastereoselectivity, and low enantioselectivity again for **2.5.3.2**.

Table 2.5.7 – Optimization of the Co(III)-SALEN catalyzed Diels-Alder reaction

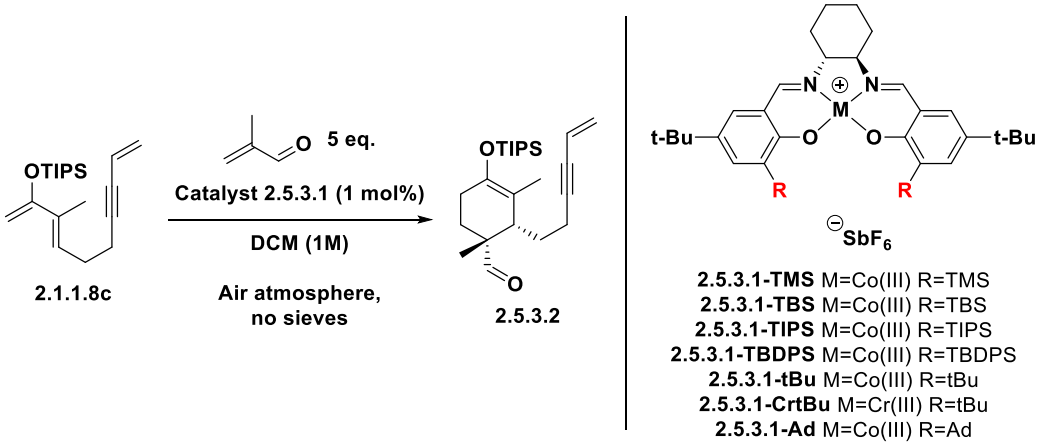

Entry	M	R	Temperature (°C)	Isolated Yield 2.5.3.2 (%)	dr[b]	% ee[a] (*endo*)
1	Co(III)	TMS	25	79	13:1	0

2	Co(III)	TBS	25	90	16:1	27
3	Co(III)	TIPS	25	19	16:1	6
4	Co(III)	TBDPS	25	19	13:1	6
5	Co(III)	TBS	0	46	16:1	41
6	Co(III)	TBS	-20	56	9:1	22
7	Co(III)	tBu	25	62	10:1	35
8	Co(III)	Ad	25	degradation	n.d	n.d
9	Cr(III)	tBu	25	78	16:1	30

[a]Enantiomeric excess determined by chiral HPLC after Au(I)-Prins cyclization, $NaBH_4$ reduction, and TIPS deprotection. n.d = not determined. [b]Diastereomeric ratio determined by 1H NMR analysis.

A short scope exploring the reactivity of cobalt(III)-SALEN catalyzed DA reaction using **2.5.3.1-TBS** was performed (Table 2.5.8). Since enantioselectivity was low thus far with this catalyst, only yield and diastereoselectivity were examined. When diene **2.1.1.8a** and methacrolein (Entry 1) were used, high yields and diastereoselectivity for **2.5.3.3** were obtained. When the less substituted diene **2.1.1.8f** (Entry 2) was used, both the yield and diastereoselectivity for adduct **2.5.3.4** were diminished. Heating the same reaction at 40°C (Entry 3) did not change the yield but unsurprisingly decreased the diastereoselectivity even further. Methyl vinyl ketone (MVK), a less reactive ketone dienophile, was then reacted with diene **2.1.1.8a**, to give DA product **2.5.3.5** in low yields and moderate diastereoselectivity. When diene **2.1.1.8f** was used instead, slightly higher yields of **2.5.3.6** where obtained with very little diastereoselectivity. These unsuccessful attempts of Co(III)-SALEN catalyzed DA reactions with MVK (Entry 4-5) indicates that this catalytic system is limited to aldehyde dienophiles.

Table 2.5.8 – Short scope of Co(III)-SALEN catalyzed Diels-Alder reaction

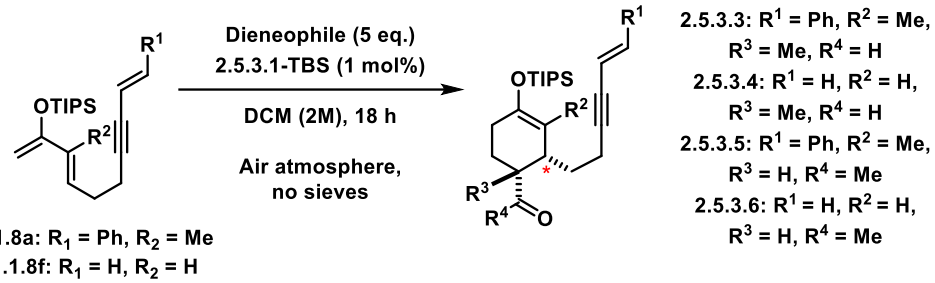

Entry	Diene	Dienophile	Product	Isolated Yield (%)	dr[b]
1	2.1.1.8a	methacrolein	2.5.3.3	81	16:1
2	2.1.1.8f	methacrolein	2.5.3.4	62	7:1
3[a]	2.1.1.8f	methacrolein	2.5.3.4	62	5:1
4	2.1.1.8a	MVK	2.5.3.5	15	5:1
5	2.1.1.8f	MVK	2.5.3.6	21	1.6:1

MVK = methyl vinyl ketone. n.d = not determined. [a]Reaction was heated at 40°C. [b]Diastereomeric ratio determined by 1H NMR analysis.

In light of the gathered results regarding Co(III)-SALEN catalyzed DA reactions, the optimization for an enantioselective reaction was not continued after this point. However, the high yield and diastereoselectivity for **2.5.1.2** when using catalyst **2.5.3.1-TBS** means that the catalytic system can have some applicability in performing an *endo*-DA reaction in an efficient manner.

2.6 OPTIMIZATION OF THE SECOND STEP – GOLD(I) CYCLIZATION

After significant efforts in searching for an efficient catalytic system for the first DA reaction step, attention was turned towards optimizing the second Au(I) cyclization step. With the catalytic conditions utilizing $Gd(OTf)_3$ to perform an *exo*-selective DA reaction (Scheme 2.6.1, Route A), exemplified by the formation of **2.5.1.4-exo** from **2.1.1.8a**, the possibility for **Route A** was then opened. This allowed for the exploitation of intrinsic reactivity of the *exo*-DA product to selectively under 6-*endo*-*dig* cyclization under Au(I)

Lewis acidic conditions. This trend was also expected to be true for DA adduct **2.5.1.4-exo**, generating the target 6-*endo-dig* product **2.6.0.1**. On the other hand, when Co(III)SALEN catalyst **2.5.3.1-TBS** was used (Route B), an *endo* selective DA catalytic system was identified, exemplified by the formation of **2.5.3.2** from **2.1.1.8c.** However, the lack of adequate enantioselectivity despite the use of a chiral catalyst, and low substrate scope potential rendered **Route B** less desirable. From this point forward, **Route A** became the main focus moving forward into Au(I) cyclization optimization.

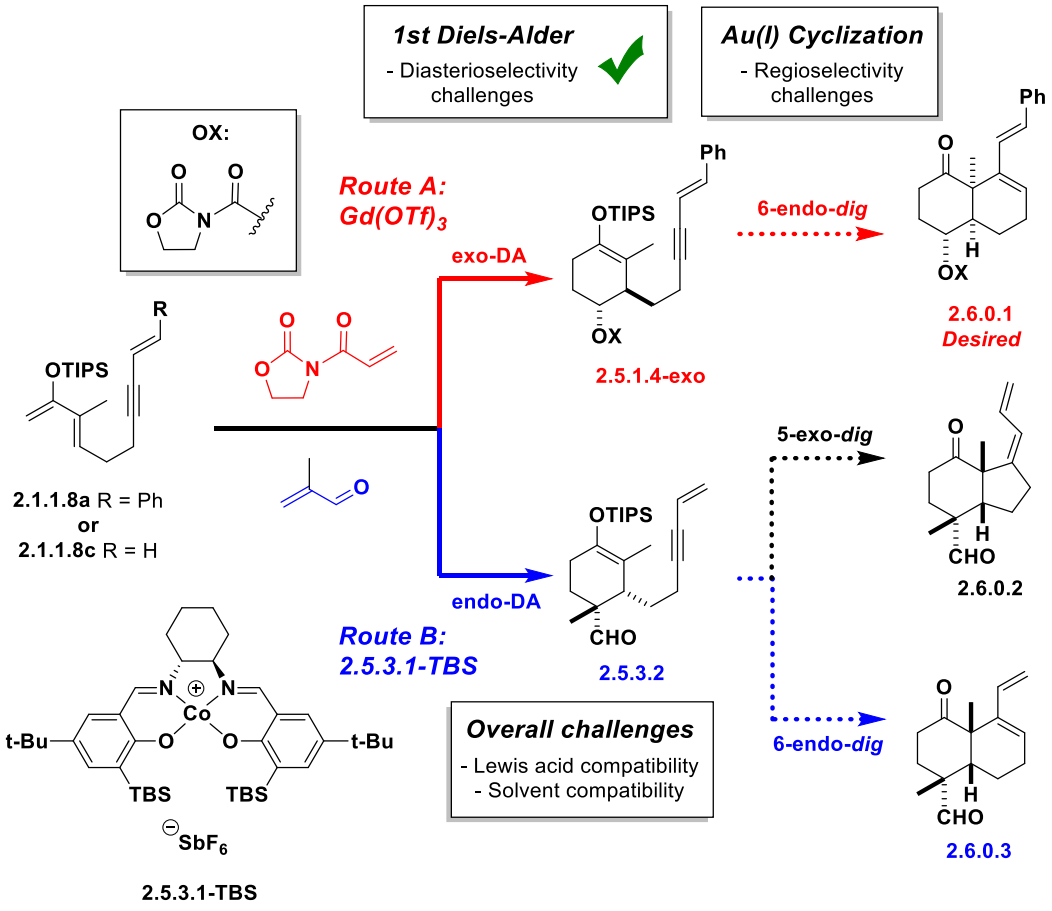

Scheme 2.6.1 – Review of the state of the methodology development

2.6.1 Ligand Optimization

Literature precedence in previous work by our group[16] (Scheme 2.6.2) were used to give the initial starting conditions, where the selective 5-*exo-dig* or 6-*endo-dig*

cyclization of silyl enol ether **2.6.1.1** was demonstrated to give **2.6.1.3** and **2.6.1.2** bicyclic carbocycles. The regioselectivity was determined by ligand selection and solvent choice predominantly. Specifically, Me_4tBuXPhos and iPr were the optimal ligand choices for a 5-*exo*-*dig* or 6-*endo*-*dig* cyclization respectively. Both conditions used methanol as solvent.

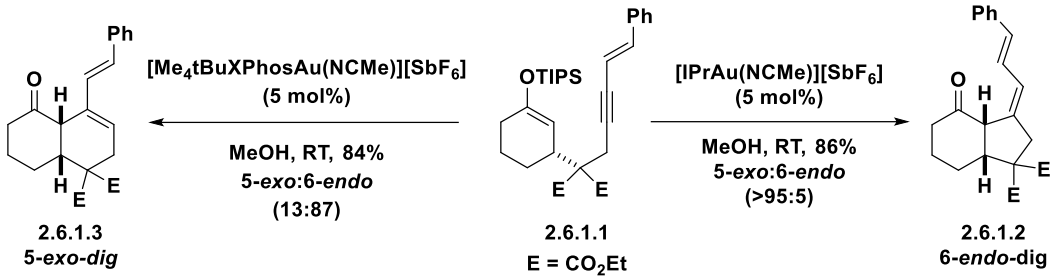

Scheme 2.6.2 – Previous in-group work on regioselective Au(I) cyclization

In the to be described series of ligand optimizations, *exo*-DA adduct **2.5.1.4-exo** was used as the model substrate to generate **2.6.0.1**, **2.6.1.1aa**, **2.6.1.2aa**, or **2.6.1.3.** Compounds **2.6.0.1**, **2.6.1.1aa**, and **2.6.1.2aa** will be targeted separately in three different ligand optimizations. Tricyclic products **2.6.1.1aa** and **2.6.1.2aa** form via 6-*endo*-dig and 5-*exo*-dig cyclizations respectively followed by Prins cyclization and was not previously observed in the Au(I) cyclization of **2.2.2-exo** (Scheme 2.2.1). The primary solvent that was chosen was DCM because the solvent choice is restricted to what was used in the preceding DA step in synthesizing **2.5.1.4-exo**. MeOH was used as a co-solvent and proton source in the Au(I) cyclization protodeauration step. In the first ligand optimization **2.6.0.1** was targeted (Table 2.6.1).

Table 2.6.1 – Au(I) cyclization optimization for 6-*endo-dig* product **2.6.0.1**

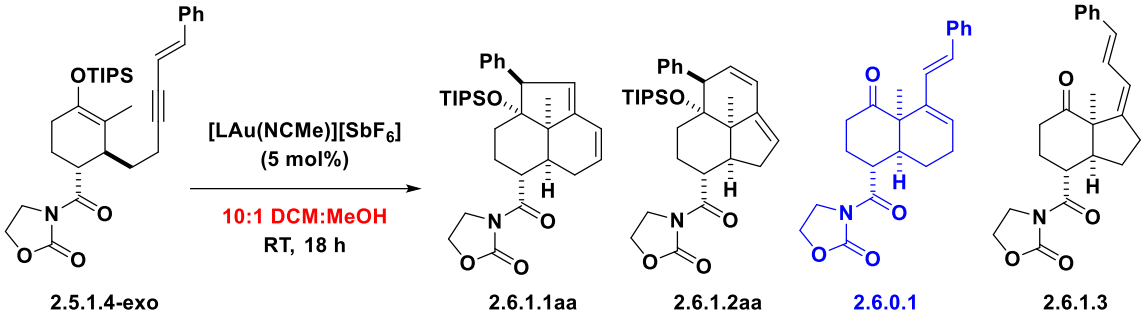

2.5.1.4-exo | 2.6.1.1aa | 2.6.1.2aa | 2.6.0.1 | 2.6.1.3

		NMR Yields (%)[a]			
Entry	**Ligand**	**2.6.1.1aa**	**2.6.1.2aa**	**2.6.0.1**	**2.6.1.3**
1	**L1** (Me_4tBuXPhos)	60	7	33	0
2	**L2** (XPhos)	13	<5	54	0
3	**L3** (JackiePhos)	<5	<5	63	<5
4	**L4** (BrettPhos)	20	7	31	<5
5	**L5** (VPhos)	9	<5	57	<5
6	**L6** (SPhos)	<5	9	35	0
7	**L7** (DavePhos)	<5	<5	66	<5
8	**L8** (Me_3(OMe)tBuXPhos)	54	7	37	0
9	**L9** (AlPhos)	55	6	35	0
10	**L10** (TrixiePhos)	6	10	60	10
11	**L11** (IPr)	<5	21	7	63

[a]NMR yields determined using mesitylene standard.

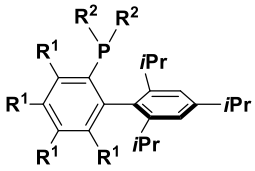

L1: R^1 = Me, R^2 = tBu
L2: R^1 = H, R^2 = Cy

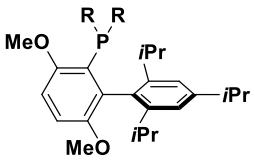

L3: R = 3,5-$(CF_3)C_6H_3$
L4: R = Cy

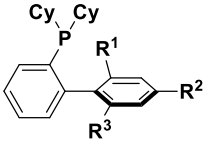

L5: R^1 = R^2 = *t*Bu, R^3 = OMe
L6: R^1 = R^3 = OMe, R^2 = H
L7: R^1 = $N(Me)_2$, R^2 = R^3 = H

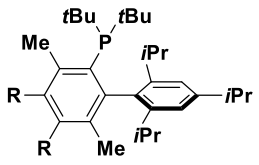

L8: R = Me (OMe)

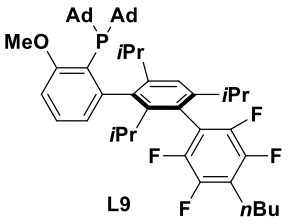

L9

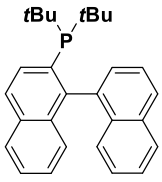

L10

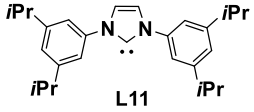

L11

When the reaction was conducted using Me_4tBuXPhos **L1** (Entry 1), which was identified as the optimal ligand to form a 6-*endo*-*dig* product, tricyclic compounds **2.6.1.1aa** (60%) and **2.6.1.2aa** (7%) were obtained, with desired 6-*endo*-*dig* product **2.6.0.1** in 33% yield. The use of XPhos **L2** (Entry 2) led to significant improvement for the formation of **2.6.0.1** in 54% yield, and even higher selectivity were achieved with JackiePhos **L3** (Entry 3) at 63%. However, BrettPhos **L4** (Entry 4) gave a lower yield for **2.6.0.1**. The use of VPhos **L5** (Entry 5) resulted in the preferential formation of **2.6.0.1**. A loss of efficiency was observed with SPhos **L6** (Entry 6), while performing the reaction with DavePhos **L7** (Entry 7) showed the highest selectivity for **2.6.0.1**. Interestingly, the gold(I)-catalyzed carbocyclization reactions using highly bulky ligands such as Me_3(OMe)tBuXPhos **L8** (Entry 8) and AlPhos **L9** (Entry 9) showed similar trends where **2.6.1.1aa** was predominantly obtained in 54% and 55% yield respectively, with **2.6.0.1** being observed as the minor product. The use of TrixiePhos **L10** (Entry 10) did not lead to any improvement on the reaction selectivity. And as expected, switching to a carbene ligand such as IPr (**L11)** (Entry 11) favored the formation of the 5-*exo* products **2.6.1.2aa/2.6.1.3** over the 6-*endo* products **2.6.1.1aa**/**2.6.0.1**, with **2.6.1.3** being the major product.

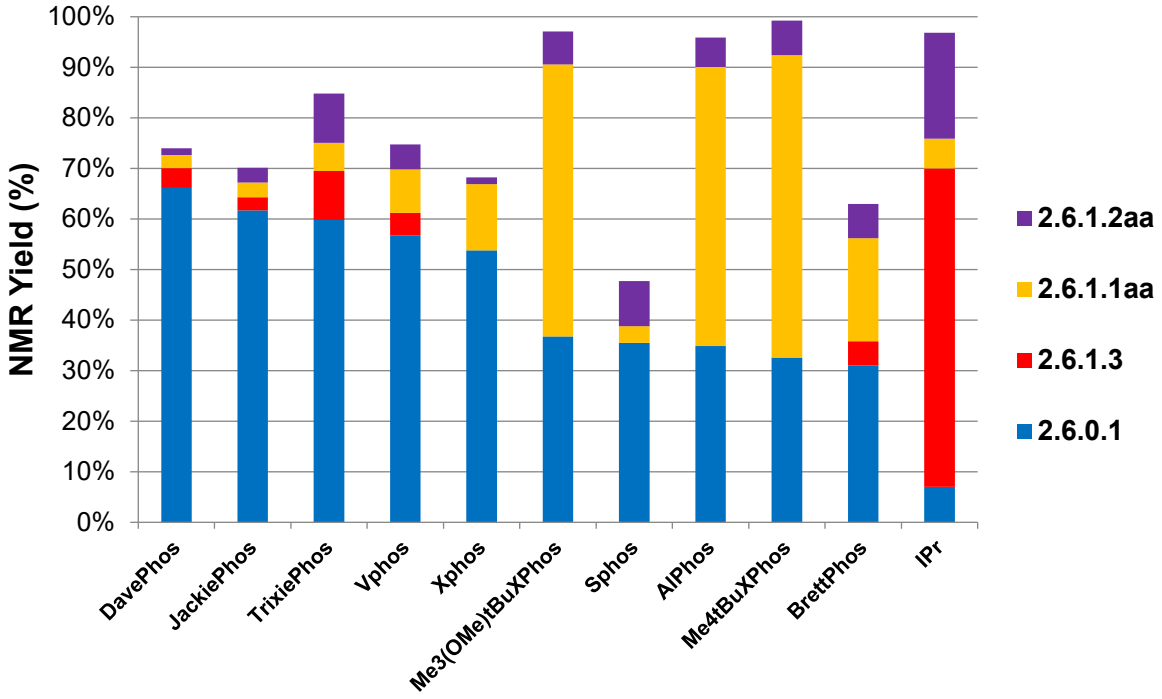

Figure 2.6.1 – Bar graph representation of the ligand screening (Table 2.6.1)

With these results, DavePhos **L7** was found the be the optimal ligand for the selective formation of **2.6.0.1**, with JackiePhos **L3**, TrixiePhos **L10**, and VPhos **L5** as the next three best ligands. These best four ligands would be then tested in the one-pot method involving the $GdOTf_3$ catalyzed DA reaction followed by Au(I) catalyzed cyclization.

2.6.2 One-Pot Methodology

Although the regioselectivity of Au(I)-catalyzed cyclizations can be modulated by both the ligands and the stereochemistry on enol ether **2.5.1.4-exo**, the challenges of telescoping a multi-step synthesis into a one-pot reaction must be addressed. A small selection of the most efficient gold catalysts from the ligand screening (Table 2.6.1) were chosen and tested in a one-pot sequence (

Table 2.6.2) starting from diene **2.1.1.8a** to selectively generate 6-*endo*-*dig* product **2.6.0.1** via **2.5.1.4-exo** as an in-*situ* intermediate. Thankfully, Au(I) catalysts were found to be compatible with the Lewis acid for the DA reaction, $Gd(OTf)_3$. Only **L10** failed to produce **2.6.0.1** in good yield. Meanwhile **L3, L5, L7** all performed similarly well to generate **2.6.0.1** in moderate yields (64-66%). Though the key differentiator in performance for these ligands would be the time required to complete the reaction. Reaction completion using VPhos **L5** (Entry 1) was the fastest at 6 hours. DavePhos **L7** gave reaction completion with reasonable time at 24 hours, but JackiePhos **L3** was very slow where reaction completion was not observed even after 72 hours. As a result [**L5**Au(NCMe)][SbF_6] was chosen as the ideal catalyst moving forward.

Table 2.6.2 – Ligand selection for the one-pot *exo*-Diels-Alder then Au(I) cyclization

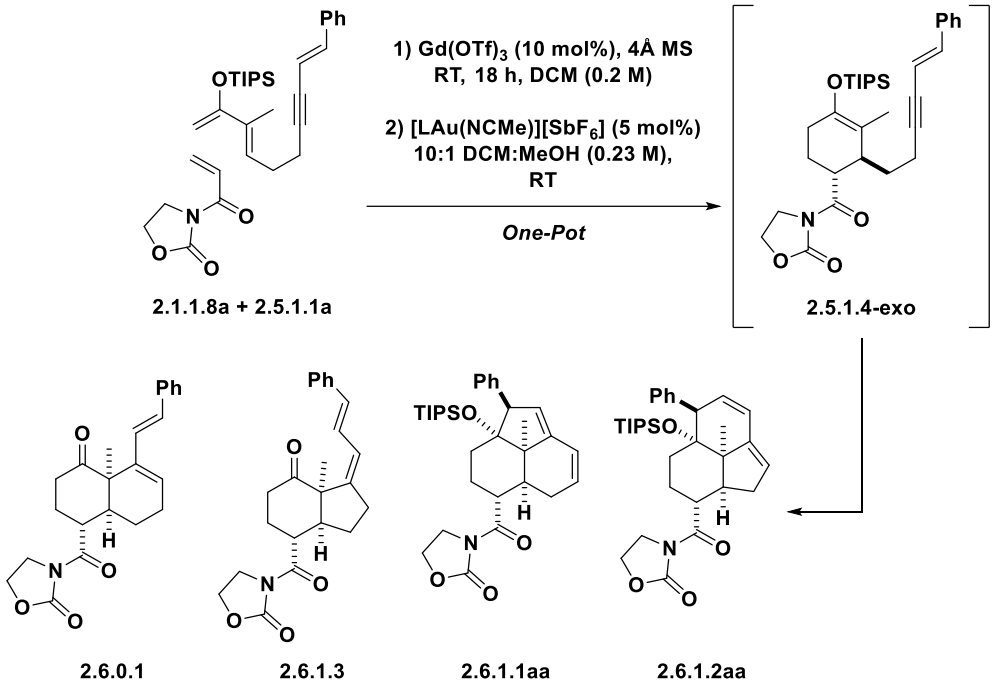

			NMR Yields (%)[a]				
Entry	**Ligand**	**Rxn time (h)**	**2.6.0.1**	**2.6.1.3**	**2.6.1.1aa**	**2.6.1.2aa**	**2.5.1.4-exo**
1	**L5** (VPhos)	6	64	0	6	2	0
2	**L7** (DavePhos)	24	65	0	5	3	0
3	**L3** (JackiePhos)	72	66	0	3	0	16
4	**L10** (TrixiePhos)	6	36	0	5	0	0

[a]NMR yields determined using mesitylene standard.

Our attention was finally turned towards the third step of the one-pot cascade: another DA reaction to produce a tricyclic or tetracyclic carbocycle as the final product of the cascade (Table 2.6.3). Using model diene **2.6.0.1** a short scope was performed to explore its reactivity in the context of a DA reaction. When using N-methylmaleimide as a dienophile (Entry 1), tetracycle **2.6.2.1aaa** was formed in high yield and moderate diastereoselectivity. The formation of two diastereomers was expected as the same trend was previously observed with diene **2.2.3-exo** (Scheme 2.2.2). When tetracyanoethylene

(TCNE) was used (Entry 2), good yields of **2.6.2.1aab** was obtained as a single diastereomer. With 4-phenyl-1,2,4-triazole-3,5-dione (PTAD) (Entry 3), exclusive diastereoselectivity for **2.6.2.1aac** was obtained but with lower yields, which was possibly due to degradation at the higher reaction temperature that the reaction was performed at. Lastly, when 1,4-benzoquinone (Entry 4) was unsuccessfully applied in a DA reaction, where no DA products were obtained.

Table 2.6.3 - Short scope of the final Diels-Alder reaction step within the cascade

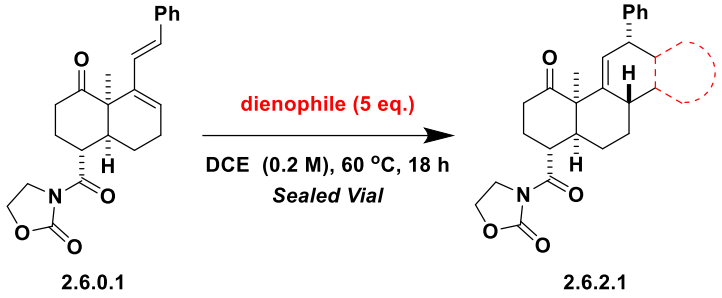

2.6.0.1 2.6.2.1

Entry	Dienophile	Product	Isolated Yield (%)[a]	dr[c]
1	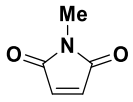	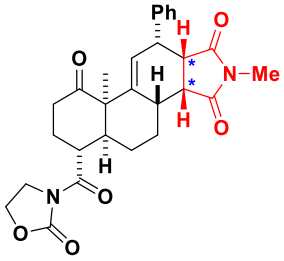 **2.6.2.1aaa**	81	2.9:1
2	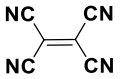	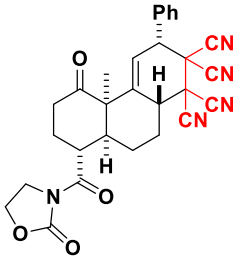 **2.6.2.1aab (SCXRD)**	77	>20:1

3[b]	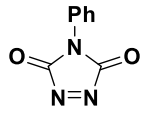	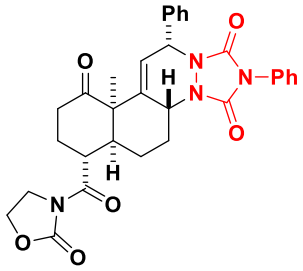 **2.6.2.1aac (SCXRD)**	40	>20:1
4	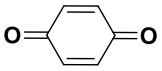	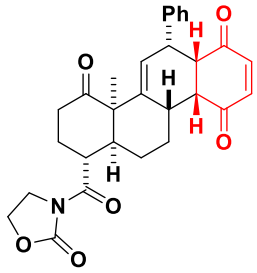 **2.6.2.1aad**	n.r	n.d

n.r = no reaction. n.d = not determined. [a]combined yield of diastereomers. [b]Reaction was heated at 100°C. [c]Diastereomeric ratio determined by ^{1}H NMR analysis.

These results gave evidence that diene **2.6.0.1** is least reactive to very electron poor dienophiles under mild thermal conditions (60°C), meaning that the use of DCM (bp = 40°C) for the complete three-step DA-Au(I) cyclization-DA one-pot sequence was feasible with the use of a sealed vial. An attempt was made at performing the complete sequence (Scheme 2.6.3) with diene **2.1.1.8a**, oxazolidinone dienophile **2.5.1.1a**, and TCNE as the second dienophile where tricycle **2.6.2.1aab** was obtained as the sole diastereomer in low yield. It is noteworthy that this sequence was carried out entirely at ambient temperature, and was not set-up using air-free techniques. Also, even though a low yield of 26% was obtained, this equals an average yield of 64% per step where 5 stereocenters and 5 C-C bonds were formed at the end. Afterwards, application of a chiral oxazolidinone dienophile **2.5.1.1b** was attempted successfully in the same sequence, allowing for the synthesis of enantiopure product **2.6.2.1abb** as the sole diastereomer in moderate yield.

Absolute stereochemistry for **2.6.2.1abb** was determined by SCXRD and via inference from chiral oxazolidinone **2.5.1.1b**.

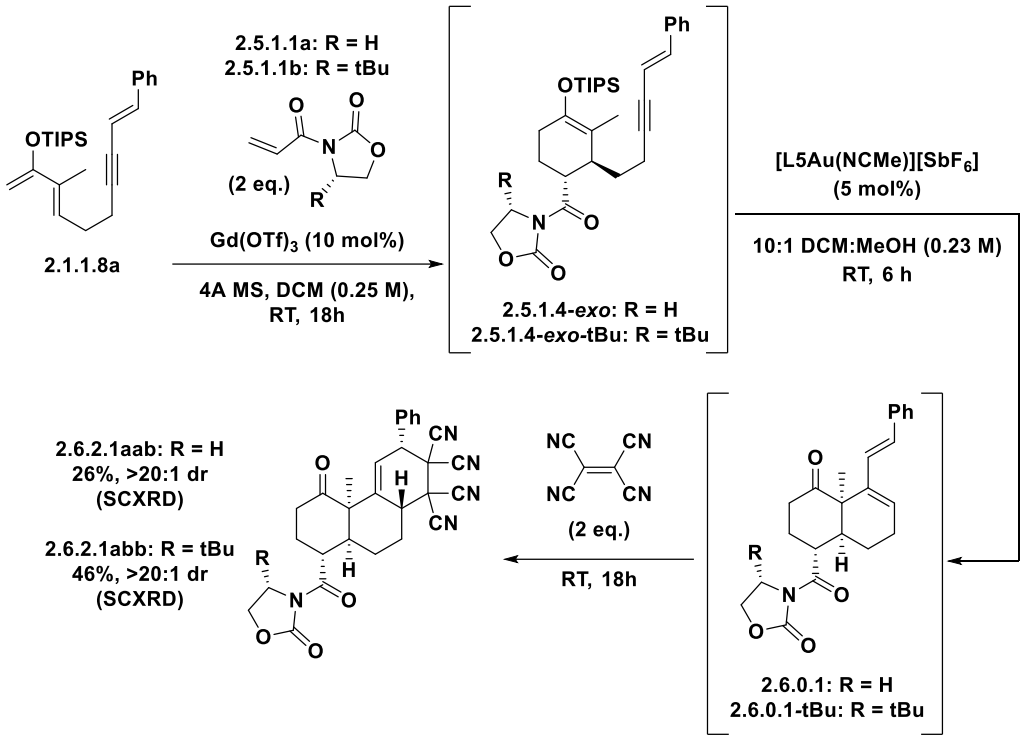

Scheme 2.6.3 – First example of the Diels-Alder-Au(I) cyclization-Diels-Alder one-pot sequence

With the success in carrying out the complete DA-Au(I) cyclization-DA one-pot sequence, a scope was performed (Table 2.6.4) demonstrating an additional ten examples of tri and tetracycles made using this method. And since this method is modular, requiring three starting material substrates: the diene, an oxazolidinone dienophile, and a regular dienophile, a library of related compounds can be synthesized as the number of possible combinations are multiplicative. Using dienophiles **2.5.1.1a** (R^3 = R^4 = H) and PTAD under the standard conditions, enyne diene **2.1.1.8a** (R^1 = Ph, R^2 = H) was directly converted to tetracycle **2.6.2.1aac** in 62% yield as the sole diastereomer. High diastereoselectivity was also observed with dienophile **2.5.1.1b** (R^3 = H, R^4 = *t*-Bu) to

provide **2.6.2.1abc** in 52% yield as a single diastereomer. Enyne diene **2.1.1.8b** (R^1 = CH_2OBn, R^2 = H) was converted to the corresponding tetracycle **2.6.2.1bbc** in 39% yield and **2.1.1.8c** (R^1 and R^2= H) led to **2.6.2.1cbc** in 33% yield.

Table 2.6.4 - Reaction scope of the Diels-Alder-Au(I) cyclization-Diels-Alder one-pot sequence [a]

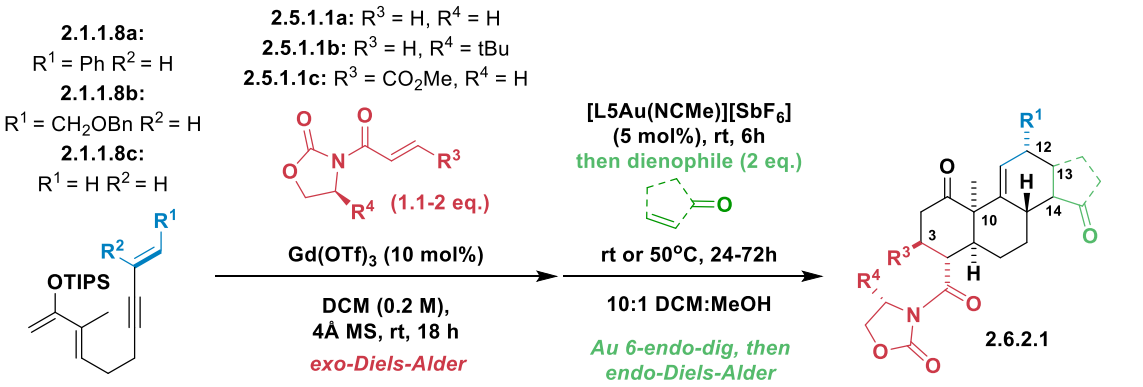

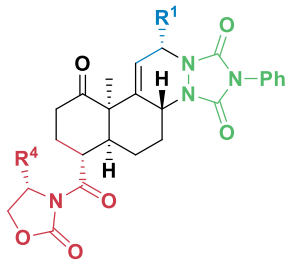

2.6.2.1aac: R^1=Ph, R^4=H, 62%, >20:1 dr (SCXRD)
2.6.2.1abc: R^1=Ph, R^4=tBu, 52%[b], >20:1 dr (SCXRD)
2.6.2.1bbc: R^1=CH_2OBn, R^4=tBu, 39%[b], >20:1 dr
2.6.2.1cbc: R^1=H, R^4=tBu, 33%[b], >20:1 dr (SCXRD)

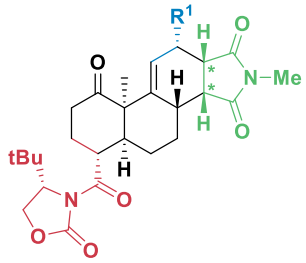

2.6.2.1aba: R^1=Ph, 40%[b], 7:1 dr (SCXRD)
2.6.2.1bba: R^1=CH_2OBn, 52%[b], 8:1 dr
2.6.2.1cba: R^1=H, 43%[b], 5:1 dr

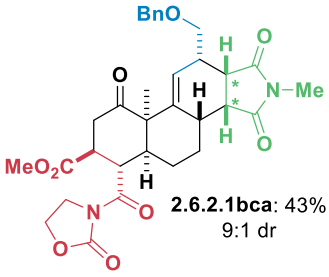

2.6.2.1bca: 43%
9:1 dr

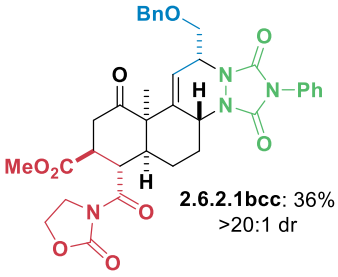

2.6.2.1bcc: 36%
>20:1 dr

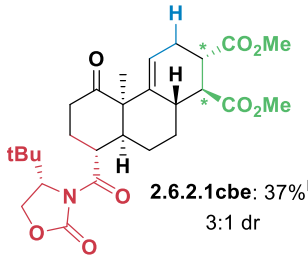

2.6.2.1cbe: 37%[b]
3:1 dr

[a] Percentages represent combined isolated yields, diastereomeric ratios were determined by ^{1}H NMR. [b] Enantiopure product.

Remarkably in all cases, the second [4+2] cycloaddition proceeded selectively *syn* to the angular methyl at C10. The use of *N*-methylmaleimide provided the desired tetracycles **2.6.2.1aba**, **2.6.2.1bba** and **2.6.2.1cba** in 40%, 52% and 43% yields respectively with diastereomeric ratios between 5:1 and 7:1 favoring the *endo* [4+2] product (C13 and C14). The use of dimethyl fumarate afforded compound **2.6.2.1cbe** in 37% yield as a separable mixture of *endo/exo* cycloaddition products (3:1). Introduction of the dienophile **2.5.1.1c** (R^3 = CO_2Me, R^4 = H) into the gold(I)-catalyzed process led to the formation of tetracyclic products **2.6.2.1bca** (43%) and **2.6.2.1bcc** (36%) with high diastereoselectivity where up to 8 stereogenic centers were generated in a single operation.

2.6.3 *Exo*-Diels-Alder-Au(I)-Prins Cyclization Methodology

After the success of the DA-Au(I) cyclization-DA cascade, results from the Au(I) cyclization optimization was reviewed (Figure 2.6.2) with a particular interest on the ligands that showed selectivity for 6-*endo* and 5-*exo* Au(I)-cyclization followed by Prins cyclization represented by tricycles **2.6.1.1aa** and **2.6.1.2aa** respectively. It was found that at least several ligands (**L8, L9, L1**) could be chosen for the formation of **2.6.1.1aa**. Though only **L11** showed some ability at forming **2.6.1.2aa** as the minor product.

Figure 2.6.2 – Ligands selective for the formation of **2.6.1.1aa** and **2.6.1.2aa**

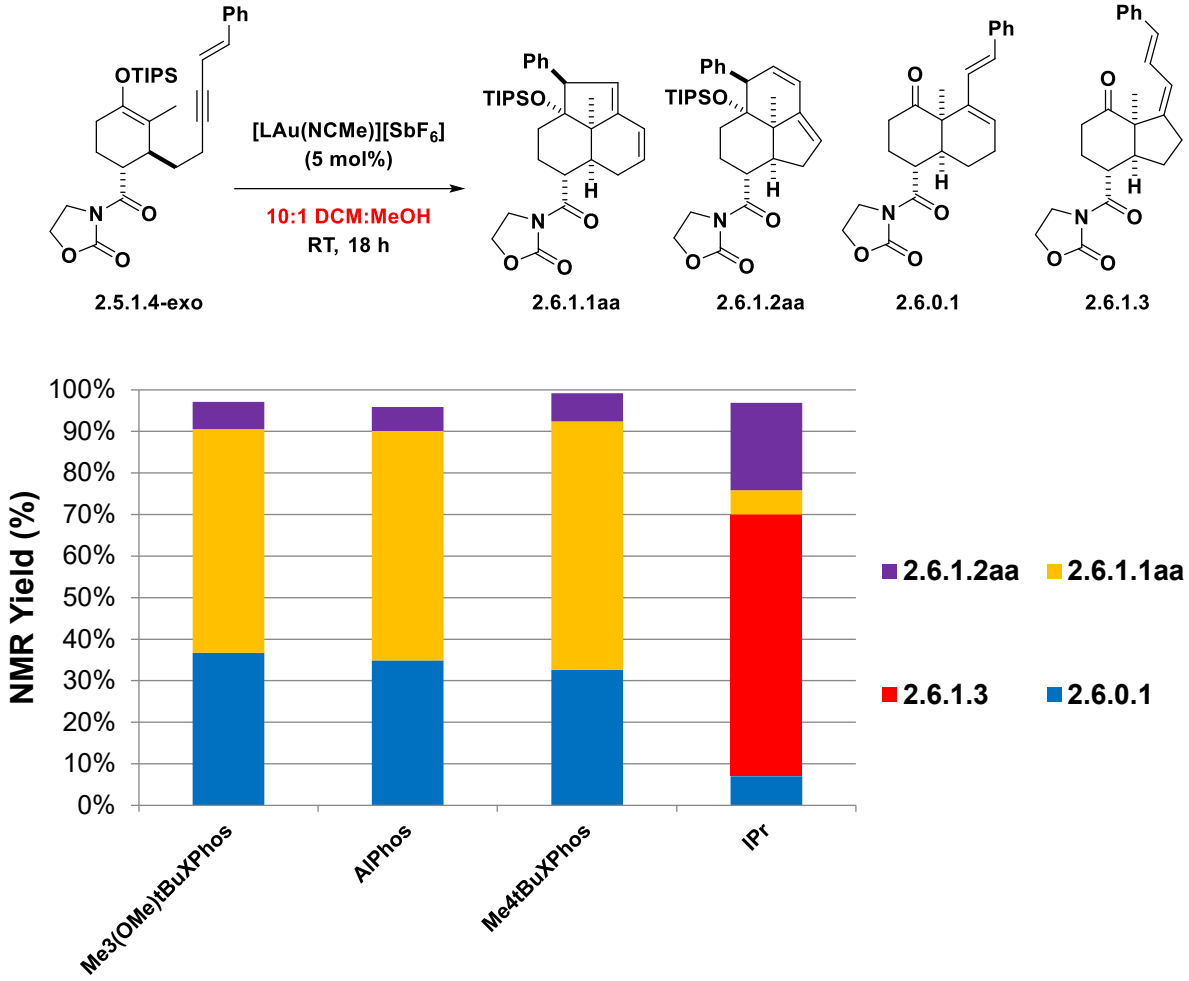

A ligand optimization to determine the best ligands to form **2.6.1.1aa** and **2.6.1.2aa** selectively was then performed. Silyl enol ether **2.5.1.4-exo** was used again as the model substrate, and DCM was again chosen as the solvent, keeping consistent with the planned cascade sequence. The MeOH co-solvent was removed however, as having such a large excess of a proton donor will invariably accelerate the rate-determining protodeauration step in the catalytic cycle, allowing for the formation of non-Prins products **2.6.0.1** and **2.6.1.3**. With the slowing of the protodeauration step via the removal of MeOH, it was found that **2.6.1.1aa** and **2.6.1.2aa** could be formed selectively. The mechanistic details are later discussed.

Table 2.6.5 - Au(I) cyclization optimization for 6-*endo-dig*-Prins product **2.6.1.1aa**

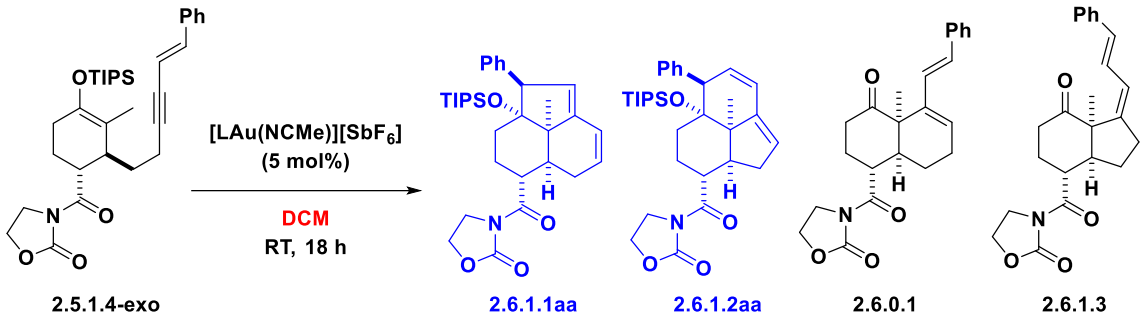

		NMR Yields (%)[a]			
Entry	**Ligand**	**2.6.1.1aa**	**2.6.1.2aa**	**2.6.0.1**	**2.6.1.3**
1	**L1** (Me_4tBuXPhos)	66	<5	0	0
2	**L2** (XPhos)	62	6	<5	0
3	**L3** (JackiePhos)	51	<5	0	0
4	**L4** (BrettPhos)	62	9	<5	0
5	**L5** (VPhos)	56	<5	0	0
6	**L6** (SPhos)	37	<5	0	0
7	**L7** (DavePhos)	47	8	14	0
8	**L8** (Me_3(OMe)tBuXPhos)	68	<5	<5	0
9	**L9** (AlPhos)	73	<5	<5	0
10	**L10** (TrixiePhos)	43	<5	0	0
11	**L11** (IPr)	7	<5	0	0

[a]NMR yields determined using mesitylene standard.

When the reaction was conducted using **L1**, tricyclic compounds **2.6.1.1aa** was obtained in 66% yield as the major product (Entry 1). The use of XPhos **L2,** JackiePhos **L3,** BrettPhos **L4,** or VPhos **L5** led to no improvement for the formation of **2.6.1.1aa** (Entry 2-5) giving similar yields and selectivity. A loss of efficiency was observed with SPhos **L6** (Entry 6), while performing the reaction with DavePhos **L7** (Entry 7) gave some non-Prins product **2.6.0.1** as a minor product. Interestingly, the gold(I)-catalyzed carbocyclization

reactions using highly bulky ligands such as **L8** and AlPhos **L9** showed similar trends where compound **2.6.1.1aa** was obtained in 68% and 73% yield respectively (Entries 8-9). The use of TrixiePhos **L10** did not lead to any improvement on the reaction selectivity (Entry 10). Surprisingly, mainly degradation of starting material **2.5.1.4-exo** was observed (Entry 11). Of the ligands attempted AlPhos **L9** was chosen as the optimal ligand for the selective formation of 6-*endo*-Prins product for its superior yield which remained consistent in a one-pot process as well. Unfortunately, none of ligands thus far demonstrated efficient synthesis of 5-*exo*-Prins product **2.6.1.2aa**. The issue was found to be because the model starting material **2.5.1.4-exo** was a poor substrate to form the 5-*exo*-Prins. As a result, the less substituted silyl enol ether **2.5.2.1-*exo*** with a terminal enyne, was chosen as a more suitable substrate where the synthesis of **2.6.1.2ca** was observed (Scheme 2.6.4) in moderate yield and selectivity using IPr **L11**. These conditions were chosen for the scope to make 5-*exo*-Prins tricycles **2.6.1.2**

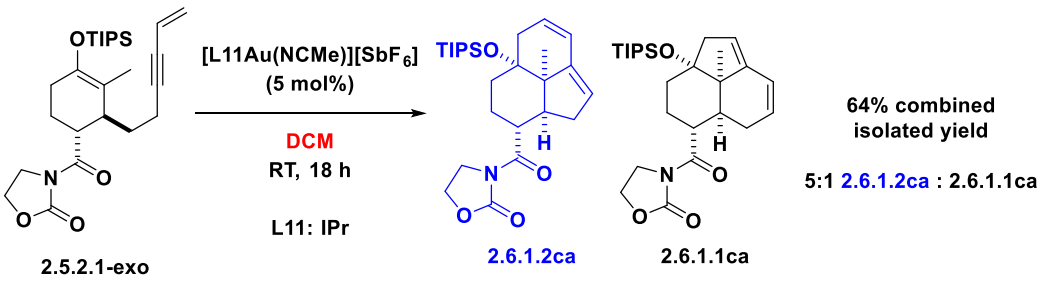

Scheme 2.6.4 – Selective formation of 5-*exo*-Prins product **2.6.1.1ca** using IPr (**L11**)

As shown in Table 2.6.6, a variety of dienes **2.1.1.8** and dienophiles **2.5.1.1** were found to be effective in selectively forming tricycles **2.6.1.1**. The presence of an additional electron withdrawing substituent (R^3) on the dienophile **2.5.1.1** such as methyl ester **2.5.1.1c**, trifluoromethyl **2.5.1.1d**, or acetyl **2.5.1.1d** was tolerated leading to the formation of the corresponding tricyclic products **2.6.1.1ac**, **2.6.1.1ad**, and **2.6.1.1ae** in good yields

(58 – 76%) with high diastereo- and regioselectivity (**2.6.1.1/2.6.1.2**). It was observed that the substituents at R^1 and R^2 on the enyne part of **2.1.1.8** has an impact on the regioselectivity of the formal gold-catalyzed [3+2] reaction step. While the carbocyclization of **2.1.1.8b** (R^1 = CH_2OBn, R^2 = H) produced **2.6.1.1ba** and **2.6.1.1bc** in 55% yields in moderate to good regioselectivity (7/8), lower selectivity was observed with **2.1.1.8c** (R^1= R^2 = H). The one-pot process using **2.5.1.1a** gave tricycles **2.6.1.1ca** and **2.6.1.2ca** in 83% yield in a ratio of 2.3:1 whereas **2.5.1.1c** led to the formation of **2.6.1.1cc** and **2.6.1.2cc** (92%) in 1.5:1 ratio. Higher regioselectivities (>20:1) were obtained with 4d (R^1 = R^2 = Me) and 4e (R^1 = H, R^2 = Me), with the corresponding tricycles (**2.6.1.1da**, **2.6.1.1ea**, **2.6.1.1ec**) being obtained in yields ranging from 39% to 54%.

Table 2.6.6 - Reaction scope of the Diels-Alder-Au(I) 6-*endo*-Prins one-pot sequence

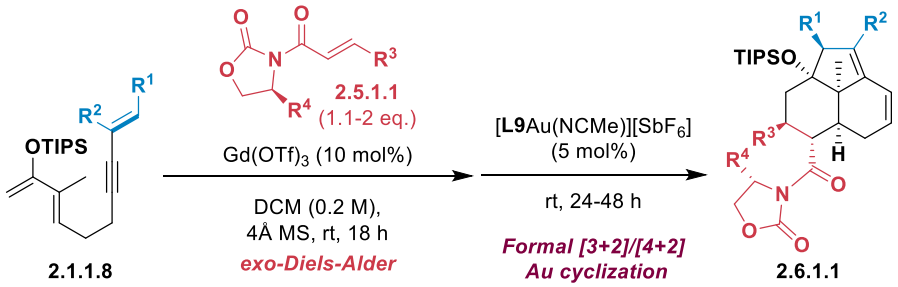

2.1.1.8a: R^1 = Ph R^2 = H
2.1.1.8b: R^1 = CH_2OBn R^2 = H
2.1.1.8c: R^1 = H R^2 = H
2.1.1.8d: R^1 = Me R^2 = Me
2.1.1.8e: R^1 = H R^2 = Me

2.5.1.1a: R^3, R^4 = H
2.5.1.1b: R^3 = H, R^4 = tBu
2.5.1.1c: R^3 = CO_2Me, R^4 = H
2.5.1.1d: R^3 = CF_3, R^4 = H
2.5.1.1e: R^3 = Ac, R^4 = H

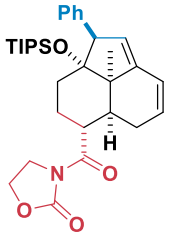

2.6.1.1aa: 48%
>95:5 dr, >20:1[f]

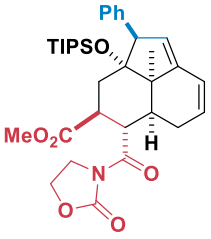

2.6.1.1ac: 75%
>95:5 dr, 11:1[f]

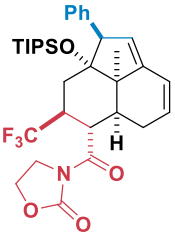

2.6.1.1ad: 58%
>95:5 dr, >20:1[f]

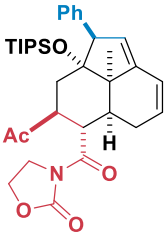

2.6.1.1ae: 76%
9:1 dr, 9:1[f]

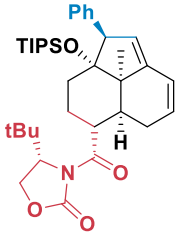

2.6.1.1ab: 54%[b]
>95:5 dr, >20:1[f]

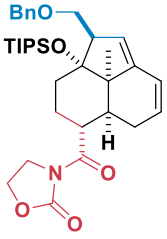

2.6.1.1ba: 55%
>95:5 dr, 2:1[f]

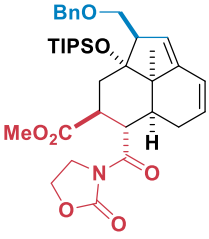

2.6.1.1bc: 55%[c]
>95:5 dr, 8:1[f]

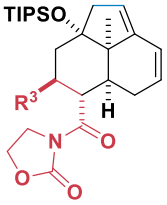

2.6.1.1ca: R^3=H, 83%
>95:5 dr, 2.3:1[f]
2.6.1.1cc: R^3=CO_2Me, 92%
>95:5 dr, 1.5:1[f]

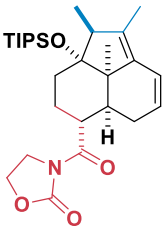

2.6.1.1da: 39%[c]
>95:5 dr, >20:1[f]

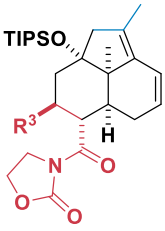

2.6.1.1ea: R^3=H, 39%[e]
>95:5 dr, >20:1[f]
2.6.1.1ec: R^3=CO_2Me, 54%[d]
>95:5 dr, >20:1[f]

[a] Percentages represent combined isolated yields, diastereomeric ratios were determined by ^{1}H NMR. [b] Enantiopure product. [c] [**L1**PhosAu(NCMe)][SbF_6] was used. [d] [**L11**Au(NCMe)][SbF_6] was used. [e] [JohnPhosAu(NCMe)][SbF_6] was used. [f] Selectivity for regioisomer shown as determined by ^{1}H NMR. Minor regioisomer is **2.6.1.2**.

Table 2.6.7 - Reaction scope of the Diels-Alder-Au(I) 5-*exo*-Prins one-pot sequence

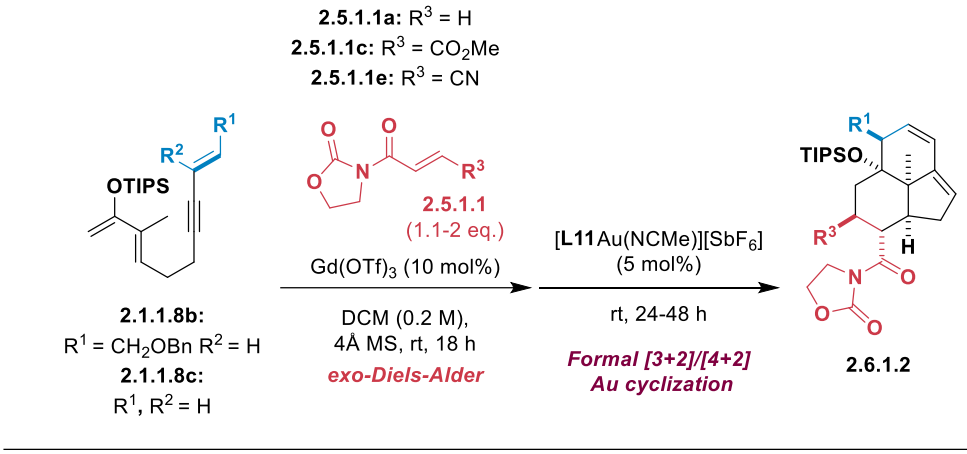

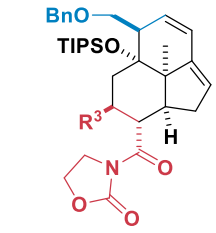

2.6.1.2ba: R^3=H, 73%
>95:5 dr, 13:1[b]
2.6.1.2bc: R^3=CO_2Me, 27%
>95:5 dr, 13:1[b]

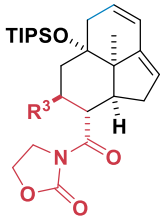

2.6.1.2ca: R^3=H, 64%, >95:5 dr, 5:1[b]
2.6.1.2cc: R^3=CO_2Me, 35%, >95:5 dr, 11:1[b]
2.6.1.2ce: R^3=CN, 42%, >95:5 dr, 5:1[b]

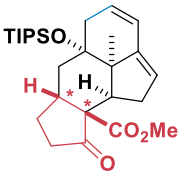

2.6.1.2cf: 33%
1.3:1 dr, >20:1[b]
(SCXRD)

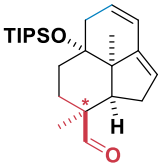

2.6.1.2cg: 53%[c]
12:1 dr, >20:1[b]

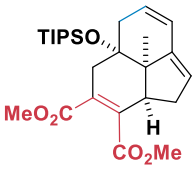

2.6.1.2ch: 51%[d]
>95:5 dr, >20:1[b]

[a] Percentages represent combined isolated yields, diastereomeric ratios were determined by ^{1}H NMR. [b] Selectivity for regioisomer shown as determined by ^{1}H NMR. Minor regioisomer is **2.6.1.1**. [c] 5 eq. dienophile, DCE at 100˚C, then [JohnPhosAu(NCMe)][SbF_6] (5 mol%). [d] 5 eq. dienophile, 1:1 acetone/DCE at 100˚C, then [JohnPhosAu(NCMe)][SbF_6] (5 mol%).

When forming **2.6.1.2** (Table 2.6.7) via a Diels-Alder reaction then gold(I) catalyzed formal dehydro-[4+2] cyclization, all examples employing an oxazolidinone-based dienophile (**2.6.1.2ba, 2.6.1.2bc, 2.6.1.2ca, 2.6.1.2cc, 2.6.1.2ce**) gave high diastereoselectivity. However, the use of dienes **2.1.1.8** was more limited. When diene **2.1.1.8a**, **2.1.1.8d**, or **2.1.1.8e** was utilized, the result was substrate degradation during the gold cyclization

step. The applicability of non-oxazolidinone dienophiles was demonstrated as well. Tetracycle **2.6.1.2cf** was regioselectivity synthesized from the corresponding cyclopentenone methyl ester. Tricycles **2.6.1.2cg** and **2.6.1.2ch** were formed utilizing a thermal Diels-Alder reaction followed by the gold(I) catalyzed formal dehydro-[4+2] cyclization, where **2.6.1.2cg** was formed from methacrolein via an *endo*-DA as the initial step, and **2.6.1.2ch** was generated via a dehydro-Diels-Alder reaction utilizing dimethyl acetylenedicarboxylate (DMAD).

2.7 MECHANISTIC STUDIES

A proposed mechanism is depicted in Scheme 2.7.1 using **2.5.1.4-exo** as a typical example. Upon activation of the alkyne (**2.7.1**), the attack of the silyl enol ether leads to the formation of the oxo species **2.7.2** and **2.7.3**.[53] Previous work from our group demonstrated the bulkiness and the electronic properties of the ligand play a role in the first bond formation of the carbocyclization.[16] As shown in Table 2.6.1 and Table 2.6.5, bulky phosphine ligands **L1**-**L10** favor the formation of compounds **2.6.0.1/2.6.1.1aa** over **2.6.1.2aa/2.6.1.3**. Taking into consideration that the P-Au-Cl angle is bent (<180°),[54] one could consider that the steric environment on the phosphine ligand would cause the C-Au-P bond angle to be distorted at the transition state, leading to a reduction in the Au-dp→C-pp overlap.[55] This could promote a cationic process where the formation of a partial positive charge is developed at C1 at the transition state promoting a *6-endo* dig cyclization. On the other hand, σ-donating ligands such as a NHC **L11** favor the formation of the vinyl gold intermediate **2.7.3**, which under protic condition A, undergoes protodeauration to give bicycle **2.6.1.3.** Similarly, under the same condition, intermediate

2.7.3 is converted to **2.6.1.2aa** via **2.7.4**. However, under aprotic condition B with a bulky phosphine ligand, vinyl gold intermediate **2.7.2** would undergo a cationic cyclization to generate tricycle **2.6.1.1aa**. According to this proposed mechanism, the carbene intermediate **2.7.5** would undergo a subsequent 1,2-hydrogen migration to give the desired tricycle **2.6.1.1aa**.[13,16]

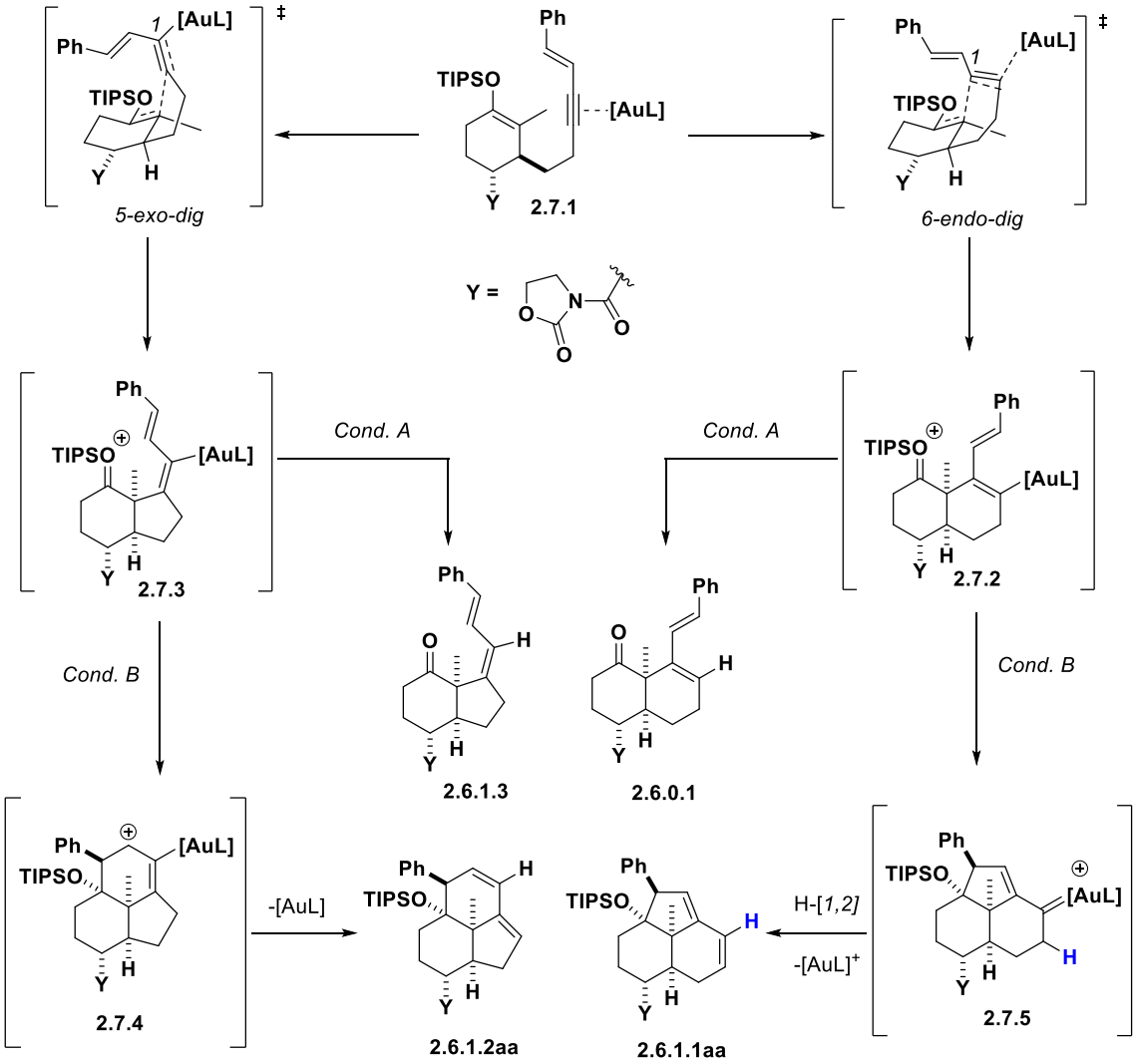

Scheme 2.7.1 - Proposed Mechanism for the carbocyclization.

To probe the proposed mechanism, deuterium labelling experiments were performed (Scheme 2.7.2). Carbocyclization of **2.5.1.4-exo** using [**L11**AuNCMe][SbF_6] in

DCM/CD_3OD gave deuterated adducts **2.6.1.2aa-*d*** (90%-D) and **2.6.1.3-*d*** (91%-D) (eq. 2), while using [**L1**AuNCMe][SbF_6] provided **2.6.1.1aa-*d*** and **2.6.0.1-*d*** with deuteration incorporation of 46% and 85%, respectively (eq. 3). Interestingly, in the case of **2.6.1.1aa-*d***, partial deuteration at C8 was observed. One could consider that two mechanisms are at play suggesting that the protodeauration step following the cyclization competes with the hydrogen [1,2]-migration process. These results support the proposed mechanism.

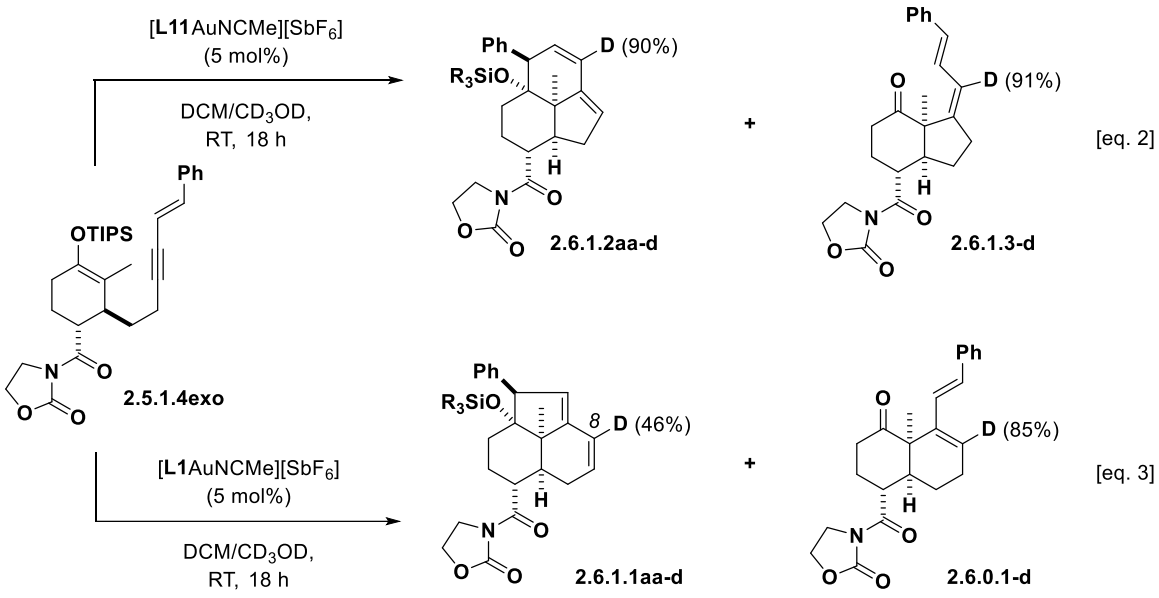

Scheme 2.7.2 - Deuterium labelling experiments

2.8 CONCLUSION

In summary, a powerful methodology exploiting the inherent mechanistic divergence of a gold(I)-catalyzed cyclization to generate three different molecular scaffolds is reported, where a broad applicability for the formation of steroid-like and tricyclic carbocycles was found. The modularity and the complexity generated by the one-pot reaction through the number of C-C bonds and rings formed is a demonstration of the synthetic utility of both Diels-Alder cyclizations and Lewis acid gold(I) catalysis. Investigations into the application

of this methodology for the synthesis of natural products are currently underway and will be reported in due course. Upon the completion of this chapter's project, attention was then turned to the completion of the total synthesis of salvinorin A, taking over the project instigated by Phillipe McGee. Although the synthesis does not utilize the methodology developed in this chapter, it still does feature similar synthetic strategies including a DA followed by 6-*endo*-dig Au(I)-cyclization.

2.9 BIBLIOGRAPHY

12. Kennedy-Smith, J. J.; Staben, S. T.; Toste, F. D., Gold(I)-Catalyzed Conia-Ene Reaction of β-Ketoesters with Alkynes. *J. Am. Chem. Soc.* **2004,** *126* (14), 4526-4527.
14. Staben, S. T.; Kennedy-Smith, J. J.; Huang, D.; Corkey, B. K.; LaLonde, R. L.; Toste, F. D., Gold(I)-Catalyzed Cyclizations of Silyl Enol Ethers: Application to the Synthesis of (+)-Lycopladine A. *Angew. Chem. Int. Ed.* **2006,** *45* (36), 5991-5994.
16. Barabé, F.; Levesque, P.; Korobkov, I.; Barriault, L., Synthesis of Fused Carbocycles via a Selective 6-Endo Dig Gold(I)-Catalyzed Carbocyclization. *Org. Lett.* **2011,** *13* (20), 5580-5583.
32. (a) Pflästerer, D.; Hashmi, A. S. K., Gold catalysis in total synthesis – recent achievements. *Chem. Soc. Rev.* **2016,** *45* (5), 1331-1367; (b) Dorel, R.; Echavarren, A. M., Gold(I)-Catalyzed Activation of Alkynes for the Construction of Molecular Complexity. *Chem. Rev.* **2015,** *115* (17), 9028-9072.
33. Philippe, M.; Julie, B.; Louis, B., Development of New Gold (I)-Catalyzed Carbocyclizations and their Applications in the Synthesis of Natural Products. *Isr. J. Chem.* **2017,** *57*, 1-11.
36. McGee, P.; Bétournay, G.; Barabé, F.; Barriault, L., A 11-Steps Total Synthesis of Magellanine through a Gold(I)-Catalyzed Dehydro Diels–Alder Reaction. *Angew. Chem. Int. Ed.* **2017,** *56* (22), 6280-6283.
41. (a) Hong, B.-C.; Raja, A.; Sheth, V. M., Asymmetric Synthesis of Natural Products and Medicinal Drugs through One-Pot-Reaction Strategies. *Synthesis* **2015,** *47* (21), 3257-3285; (b) Transition Metal-Catalyzed Domino Reactions: Section 6.1. In *Domino Reactions in Organic Synthesis*, 2006; pp 359-422; (c) Poulin, J.; Grisé-Bard, C. M.; Barriault, L., Pericyclic domino reactions: concise approaches to natural carbocyclic frameworks. *Chem. Soc. Rev.* **2009,** *38* (11), 3092-3101; (d) Padwa, A., Domino reactions of rhodium(ii) carbenoids for alkaloid synthesis. *Chem. Soc. Rev.* **2009,** *38* (11), 3072-3081.
42. (a) Campeau, D.; León Rayo, D. F.; Mansour, A.; Muratov, K.; Gagosz, F., Gold-Catalyzed Reactions of Specially Activated Alkynes, Allenes, and Alkenes. *Chem. Rev.* **2021,** *121* (14), 8756-8867; (b) Shahzad, S. A.; Sajid, M. A.; Khan, Z. A.; Canseco-Gonzalez, D., Gold catalysis in organic transformations: A review. *Synth. Commun.* **2017,** *47* (8), 735-755; (c) Hashmi, A. S. K., Gold-Catalyzed Organic Reactions. In *Inventing Reactions*, Gooßen, L., Ed. Springer: Berlin, Heidelberg, 2013; pp 143-164;

(d) Braun, I.; Asiri, A. M.; Hashmi, A. S. K., Gold Catalysis 2.0. *ACS Catal.* **2013,** *3* (8), 1902-1907.
43. Hashmi, A. S. K.; Rudolph, M., Gold catalysis in total synthesis. *Chem. Soc. Rev.* **2008,** *37* (9), 1766-1775.
44. (a) de Frémont, P.; Marion, N.; Nolan, S. P., Cationic NHC–gold(I) complexes: Synthesis, isolation, and catalytic activity. *J. Organomet. Chem.* **2009,** *694* (4), 551-560; (b) Nolan, S. P., The Development and Catalytic Uses of N-Heterocyclic Carbene Gold Complexes. *Acc. Chem. Res.* **2011,** *44* (2), 91-100.
45. (a) Gorin, D. J.; Sherry, B. D.; Toste, F. D., Ligand Effects in Homogeneous Au Catalysis. *Chem. Rev.* **2008,** *108* (8), 3351-3378; (b) Chintawar, C. C.; Yadav, A. K.; Kumar, A.; Sancheti, S. P.; Patil, N. T., Divergent Gold Catalysis: Unlocking Molecular Diversity through Catalyst Control. *Chem. Rev.* **2021**; (c) Wei, Y.; Shi, M., Divergent Synthesis of Carbo- and Heterocycles via Gold-Catalyzed Reactions. *ACS Catal.* **2016,** *6* (4), 2515-2524.
46. (a) Mascareñas, J. L.; Varela, I.; López, F., Allenes and Derivatives in Gold(I)- and Platinum(II)-Catalyzed Formal Cycloadditions. *Acc. Chem. Res.* **2019,** *52* (2), 465-479; (b) Lopez, F.; Mascareñas, J. L., Recent developments in gold-catalyzed cycloaddition reactions. *Beilstein J. Org. Chem.* **2011,** *7*, 1075–1094.
47. Nieto-Oberhuber, C.; López, S.; Echavarren, A. M., Intramolecular [4 + 2] Cycloadditions of 1,3-Enynes or Arylalkynes with Alkenes with Highly Reactive Cationic Phosphine Au(I) Complexes. *J. Am. Chem. Soc.* **2005,** *127* (17), 6178-6179.
48. (a) Evans, D. A.; Lectka, T.; Miller, S. J., Bis(imine)-copper(II) complexes as chiral lewis acid catalysts for the Diels-Alder reaction. *Tetrahedron Lett.* **1993,** *34* (44), 7027-7030; (b) Evans, D. A.; Miller, S. J.; Lectka, T., Bis(oxazoline)copper(II) complexes as chiral catalysts for the enantioselective Diels-Alder reaction. *J. Am. Chem. Soc.* **1993,** *115* (14), 6460-6461; (c) Evans, D. A.; Miller, S. J.; Lectka, T.; von Matt, P., Chiral Bis(oxazoline)copper(II) Complexes as Lewis Acid Catalysts for the Enantioselective Diels−Alder Reaction. *J. Am. Chem. Soc.* **1999,** *121* (33), 7559-7573.
49. Huang, Y.; Iwama, T.; Rawal, V. H., Design and Development of Highly Effective Lewis Acid Catalysts for Enantioselective Diels−Alder Reactions. *J. Am. Chem. Soc.* **2002,** *124* (21), 5950-5951.
50. Huang, Y.; Iwama, T.; Rawal, V. H., Highly Enantioselective Diels−Alder Reactions of 1-Amino-3-siloxy-dienes Catalyzed by Cr(III)-Salen Complexes. *J. Am. Chem. Soc.* **2000,** *122* (32), 7843-7844.
51. Ward, B. D.; Gade, L. H., Rare earth metal oxazoline complexes in asymmetric catalysis. *Chem. Commun.* **2012,** *48* (86), 10587-10599.
52. Evans, D. A.; Wu, J., Enantioselective Rare-Earth Catalyzed Quinone Diels−Alder Reactions. *J. Am. Chem. Soc.* **2003,** *125* (34), 10162-10163.
53. Brazeau, J.-F.; Zhang, S.; Colomer, I.; Corkey, B. K.; Toste, F. D., Enantioselective Cyclizations of Silyloxyenynes Catalyzed by Cationic Metal Phosphine Complexes. *J. Am. Chem. Soc.* **2012,** *134* (5), 2742-2749.
54. Herrero-Gómez, E.; Nieto-Oberhuber, C.; López, S.; Benet-Buchholz, J.; Echavarren, A. M., Cationic η1/η2-Gold(I) Complexes of Simple Arenes. *Angew. Chem. Int. Ed.* **2006,** *45* (33), 5455-5459.

55. Benitez, D.; Tkatchouk, E.; Gonzalez, A. Z.; Goddard, W. A.; Toste, F. D., On the Impact of Steric and Electronic Properties of Ligands on Gold(I)-Catalyzed Cycloaddition Reactions. *Org. Lett.* **2009,** *11* (21), 4798-4801.

2.10 CONTRIBUTION STATEMENT

2.10.1 Claims to Original Research

- Intrinsic reactivity studies for the DA-Au(I) cyclization-DA cascade
- Epimerization studies for the DA-Au(I) cyclization-DA cascade
- Optimization of the enantioselective DA reaction using Cu(II) and rare-earth Lewis acids
- Optimization of the enantioselective DA reaction using Co(III) in collaboration with Alyson Poyser
- Ligand optimization for the Au(I) cyclization in the cascade methodology
- Completion of DA-Au(I) cyclization-DA cascade scope in collaboration with Alyson Poyser
- Completion of DA-Au(I) cyclization-Prins cascade scope in collaboration with Alyson Poyser

2.10.2 Publications From This Work

- Tran, H.; Revol, G.; Poyser, A.; Barriault, L., Divergent and Modular Synthesis of Terpenoid Scaffolds via a Au(I) Catalyzed One-Pot Cascade. *Angew. Chem. Int. Ed.* **2022,** *61* (1), e202110575.

2.10.3 Oral Presentations

- *Gold(I) Catalysis in the Synthesis of Polycyclic Carbocycles*. Tran, H; Poyser, A.; Barriault, L., Canadian Chemistry Conference & Exhibition (CCCE) 2018.
- *Gold(I) Catalysis in the Synthesis of Polycyclic Carbocycles.* Tran, H; Poyser, A.; Barriault, L., CCCE 2019.

2.11 Poster Presentations

- *Gold(I) Catalysis in the Synthesis of Polycyclic Carbocycles.* Tran, H; Poyser, A.; Barriault, L., QOMSBOC 2017.
- *Gold(I) Catalysis in the Synthesis of Polycyclic Carbocycles.* Tran, H; Poyser, A.; Barriault, L., QOMSBOC 2018.
- *Gold(I) Catalysis in the Synthesis of Polycyclic Carbocycles.* Tran, H; Poyser, A.; Barriault, L., QOMSBOC 2019.

3. *TOTAL SYNTHESIS OF SALVINORIN A*

3.1 INTRODUCTION

Salvinorin A (**3.1.0.1**) is trans neo-clerodane diterpene belonging to the labdane-related superfamily of terpenoid natural products.[56] It is the bioactive component of *Salvia divinorum*, a plant within the same genus as sage and rosemary herbs. The earliest preparations of this *S. divinorum* were made by the Mazatec people of Oaxaca, Mexico for medicinal applications[57] such as the treatment of diarrhea, headaches and joint pain. It is also notably known for its use in shamanic-guided rituals by Mazatecs who believe it possesses divinatory properties, hence the name: *divinorum*. It has been used in such rituals for identifying illnesses and even determining a person's guilt in a robbery. The discovery of *S. divinorum* by researchers was by Gómez-Pompa[56] in 1957, who during a visit to the village of Huautla de Jiménez in Oaxaca to search for hallucinogenic mushrooms was informed about a stimulant plant called Ŝka Pastora (meaning Shepherdess's Leaves). After the collection of the unknown plant, Gómez-Pompa classified it within the *Salvia* genus, but the lack of flower sample preventing the classification of species. Later in 1962, Wassen and Epling[58] were able to obtain enough plant material to classify *S. divinorum*. Isolation and characterization[59] of **3.1.0.1** from *S. divinorum* was achieved in 1972 by Ortega *et al.*, and the attribution[60] of **3.1.0.1** to the psychoactive nature of *S. divinorum* was reported by Valdés *et al.*

Structurally, **3.1.0.1** (Figure 3.1.1) can be described as a highly oxygenated bicarbocycle (Rings A,B) with a fused lactone (Ring C) and 5 stereogenic centers. A noteworthy structural feature of **3.1.0.1**, are the C19 and C20 methyl groups which exhibit an unfavorable 1,3-diaxial interaction.

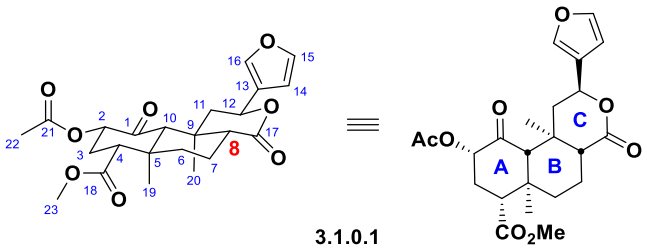

Figure 3.1.1 – Structure of salvinorin-A with numbering and lettering

A consequence of this repulsive interaction is particularly apparent in the epimerization at the C8 stereocenter (Table 3.1.1), which has been reported to occur in a variety of salvinorin A derivatives under basic, acidic, and thermal conditions.[61]

Table 3.1.1 – List of conditions known in literature to epimerize C8

Conditions	Ratio non-*epi*-C8 to *epi*-c8
NH_3, MeOH, 0°C	1:1
Na_2CO_3, MeOH, 0°C	1:1
$NaHCO_3$, DMPU or DMF, 150°C nr	nr
K_2CO_3, MeOH, RT nr	nr
alkylamide oxime, EDCI, HOBt, DCM, 23°C; PhMe, 110°C nr	nr
CCl_4, PPh_3, PhH, 80°C	4.4:1
NaH, DMF, -40°C	2.3:1 to 1:3.2
LiI, pyridine, 120°C	1:1
RSO_2NH_2, AcOH, 95°C	1.5:1 to 1.2:1
$RB(OH)_2$, $Pd_2(dba)_3$, SPhos, K_3PO_4, PhMe, 100°C	12:1
LiOH	nr
NaOH, MeOH/H2O; 1 M HCl; Ac_2O, pyridine	4:6
Neat, 248°C	nr

nr: not reported

As a result, total synthesis of **3.1.0.1** in the late stage has been known to be perilous once C8 possesses an epimerizable proton. Furthermore, potency[62] of **3.1.0.1** after epimerization to **Error! Reference source not found.** drops significantly (18 nM to 3 07±92 nM).

3.1.1 Biological Properties and Structure Activity Relationships

Pharmacological studies[63] by Roth *et al.* found **3.1.0.1** to be a selective agonist of the kappa opioid receptor (κOR). This is unique compared to traditional morphine type opioids which are substrates of mu (μOR) and delta (δOR) opioid receptors.[62] The duration of effect of **3.1.0.1** is fairly short at about 30 minutes. This is attributed to the ease of **3.1.0.1** in crossing the blood-brain barrier as well as its metabolic susceptibility.[56] Pharmacokinetic studies in resus primates showed a peak concentration in the brain 40 seconds after intravenous administration, a rate faster than cocaine.[64]

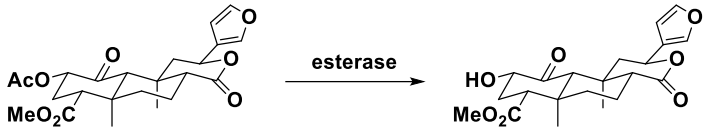

Salvinorin A
3.1.0.1
18 nM

Salvinorin B
3.1.1.1
>10000nM

Scheme 3.1.1 – Metabolism of salvinorin A

The rapid metabolism (Scheme 3.1.1) is attributed to the ease of conversion of **3.1.0.1** into salvinorin B (**3.1.1.1**), where the C2 acetoxy group is hydrolyzed into a hydroxy group by esterases.[65] This is evidenced by the accumulation of **3.1.1.1** as the major metabolite *ex vivo*.

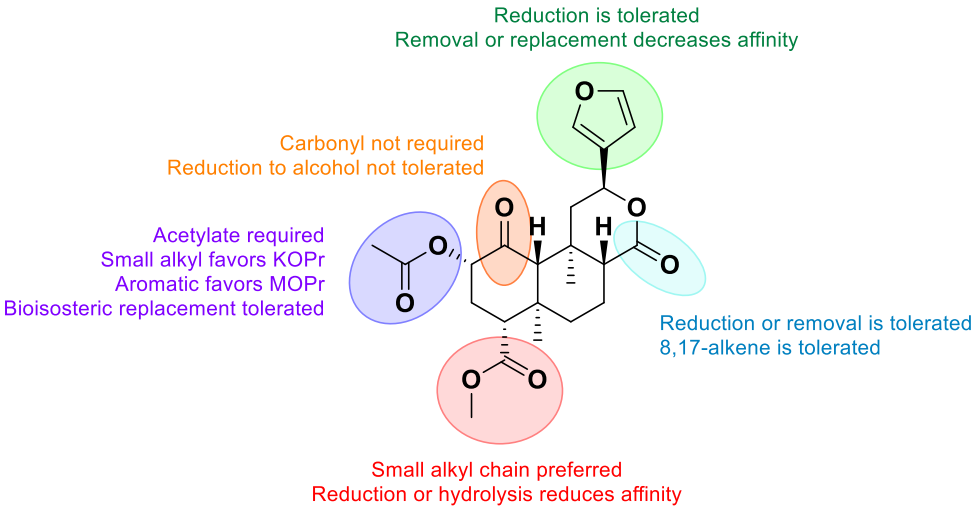

Figure 3.1.2 – SAR trends for **3.1.0.1**.

Extensive work in medicinal chemistry has been published on synthesized analogues and structure activity relationships of **3.1.0.1**. There are several key trends in the SAR which were summarized[61-62] in a review by Rothman *et al.* and Shenvi *et al.* (Figure 3.1.2). First, at the C2 position, the ester group was found to be critical to the bioactivity of **3.1.0.1**, where removal was not tolerated, and it was found that having a small alkyl ester favored the κOR while an aromatic ester favored the μOR. Also, bioisosteric replacement of the ester to amides for example, was tolerated. For the C1 ketone, the presence of the ketone was not required, but reducing it to an alcohol was not tolerated. At C4, an ester with a small alkyl chain was preferred, but reduction or hydrolysis of the ester reduced affinity. For the C12 furan ring, reduction of the ring was tolerated, but removal or replacing it with another aromatic group was not tolerated. Lastly, the reduction or removal of the C17 carbonyl is tolerated, as well as the conversion of lactone into an enol ether with an alkene at C8-C17.

Research into the nature of the binding model of **3.1.0.1** within κOR has been reported by Ferguson *et al.* via the use of site-directed mutagenesis, chimeric opioid

receptors, and molecular-modelling techniques.[66] Traditional opiates bind to κOR via a key salt-link interaction between the opiate's protonated amine moiety, and the aspartate (D138) and glutamate (E297) residues within the transmembrane (TM) III and TM VI domains respectively. Unsurprisingly, evidence of **3.1.0.1** binding via such a salt-link has not been found since it lacks a protonatable amine moiety needed for the interaction with D138 or E297. Instead, **3.1.0.1** has been shown to bind in a vertical orientation to the helical face of TM VII, and through key interactions in TM II with tyrosine (Y119, Y313, Y320), glutamine (Q115), and isoleucine (I316) residues (Figure 3.1.3).

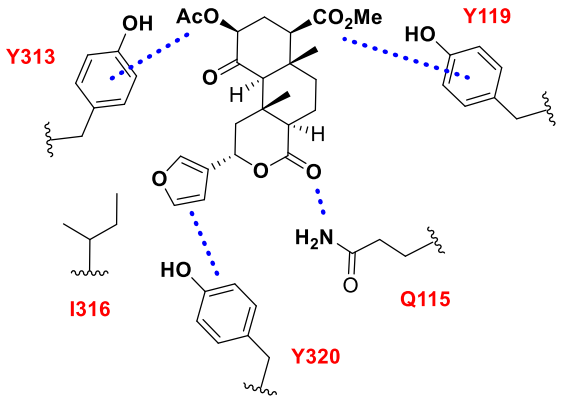

Figure 3.1.3 – Proposed binding model of **3.1.0.1** to κOR

The hydrophobic interaction of **3.1.0.1** with I316 bares particular interest as the removal of this residue completely abolishes any interaction with **3.1.0.1**, reinforcing the general hypothesis that hydrophobic interactions (rather than salt-links) drive the binding and selectivity of **3.1.0.1** to κOR.

3.1.2 Previous Synthesis

The potential of **3.1.0.1** as a scaffold for the development of new analgesics has thus spurred efforts in total synthesis by multiple groups. The first synthesis[67] (Scheme 3.1.2)

was reported by Evans *et al.* utilizing an intramolecular Michael cascade triggered upon treatment with mild base.

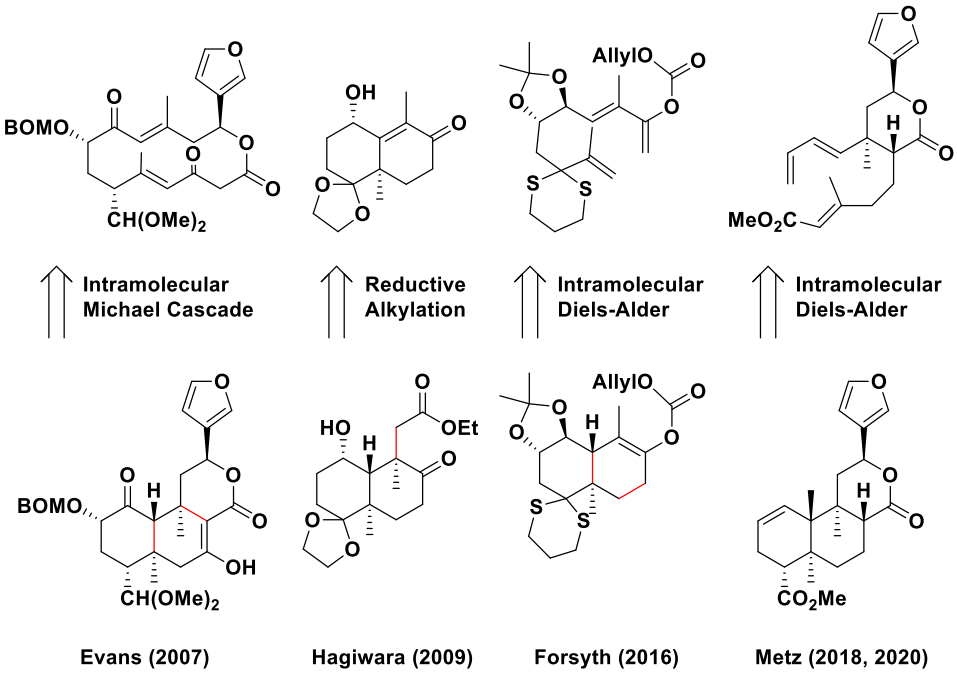

Scheme 3.1.2 – Past synthesis of salvinorin A

Hagiwara *et al.* completed their initial synthesis[68] of **3.1.0.1** via a reductive alkylation via dissolving metal reaction, and later published a 2nd generation synthesis.[69] Then Forsyth *et al.* reported their strategy in synthesizing **3.1.0.1** via an intramolecular Diels-Alder (IMDA) reaction.[70] Most recently Metz *et al.* published a synthesis of (±)-**3.1.0.1**,[71] and then later an enantioselective 2nd generation synthesis.[72] Both utilized an IMDA as the key strategy. A fifth synthesis is now being proposed in this chapter. By harnessing methodology in Au(I) catalysis developed by Barriault *et al.*, the intention of this synthesis is to showcase the applicability and robustness of the methodologies, as well as developing the shortest synthetic route to **3.1.0.1**.

3.1.3 Retrosynthetic Analysis

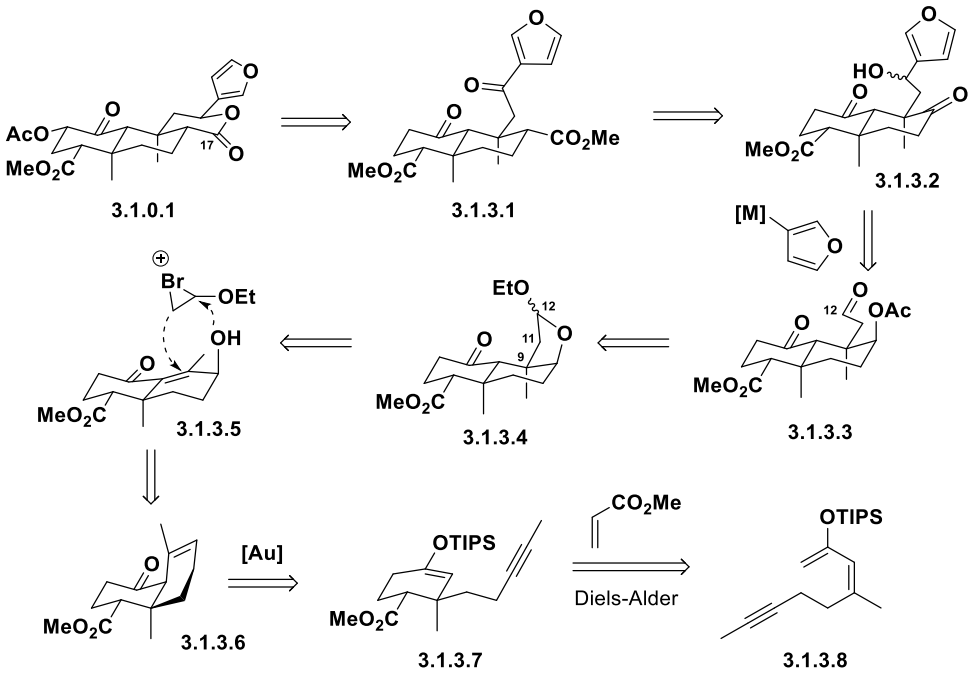

Scheme 3.1.3 - Retrosynthetic analysis of Salvinorin A.

Our strategy (Scheme 3.1.3) is a multi-stage sequence where we envisioned **3.1.0.1** could be made by α-acetoxylation and ketone reduction of **3.1.3.1**, which in turn produced from **3.1.3.2** via installation of C17 ester. The pendant furan moiety was planned to be added via 1,2-addition of a carbon furanyl nucleophile onto the C12 aldehyde of **3.1.3.3**, which was unmasked from cyclic acetal **3.1.3.4**. The disconnective strategy at this point involving installing the C11-12 carbons as well as the formation of a challenging quaternary carbon stereocenter at C9. This would be accomplished though nucleophilic addition of **3.1.3.5** onto an alkyl bromonium species, followed by a radical cyclization with the enone moiety. The C8 axial hydroxy group in effect acts as a directing group to diastereoselectively form the C9 quaternary center. Enone **3.1.3.5** would in turn be synthesized via oxidation of cis-decalin **3.1.3.6**, which can be rapidly constructed from

acyclic diene **3.1.3.8** via Diels-Alder reaction followed by Au(I) catalyzed 6-*endo*-dig cyclization of **3.1.3.7**. It is noteworthy that at multiple points during the synthesis, opportunities exist to potentially create analogues of **3.1.0.1** via a divergent synthetic strategy. An example is during the DA reaction of **3.1.3.8** into **3.1.3.7**, different dienophiles can be used to form analogues of **3.1.3.7**, which can be carried through the synthetic route. Another example is the 1,2-addition of a carbon nucleophile onto **3.1.3.1** to generate **3.1.3.2**, where different organotitaniums, organolithiums, or Grignard reagents can be used.

3.2 FORWARD SYNTHESIS

3.2.1 A-Ring Synthesis

The construction of the A-ring (Scheme 3.2.1) was spearheaded by Philippe McGee.[73] The synthesis started from commercially available vinyl iodide **3.2.1.1**, where **3.2.1.2** was synthesized by Negishi coupling on decagram scale, which was then converted to methyl ketone **3.2.1.3** by treatment with in *situ* formed lithium dimethylcuprate.[74] Silyl enol ether diene **3.1.3.8** was formed from **3.2.1.3** using triisopropylsilyl triflate and base to set the stage for the A-ring synthesis via Diels-Alder (DA) cyclization. Diethylaluminium chloride was used as the stoichiometric Lewis acid and methyl acrylate as the dienophile to generate the *endo*-DA adduct **3.1.3.7** as the sole diastereomer as well as forming the appropriate silyl enol ether moiety needed in the subsequent Lewis acid Au(I) catalyzed cyclization to construct the B-ring.

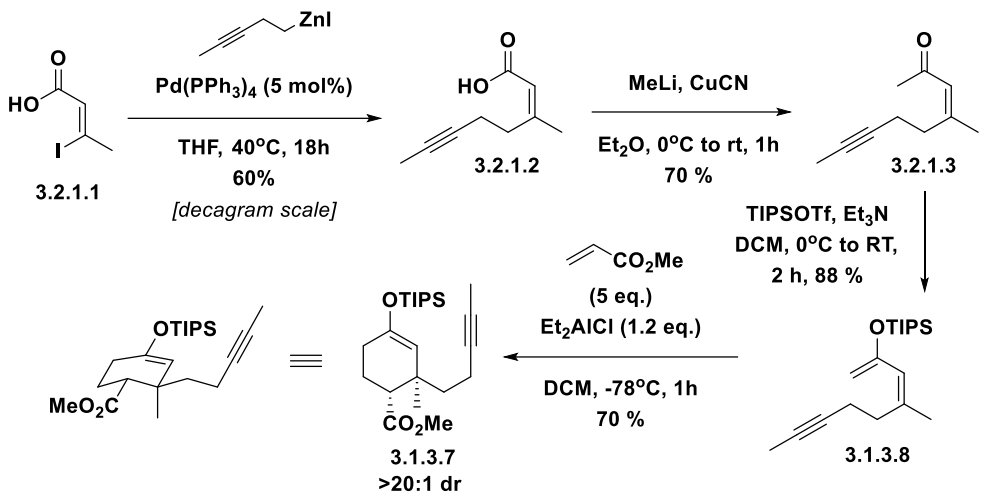

Scheme 3.2.1 - Synthesis of Ring-A from vinyl iodide **3.2.1.1**.

3.2.2 6-*Endo*-*dig* Au(I)-Cyclization Optimization

Table 3.2.1 - Optimization of Lewis acid gold(I) catalyzed 6-*endo*-dig cyclization.

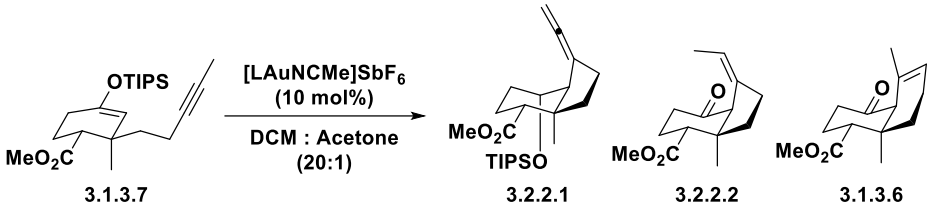

Entry	Ligand	Conversion	**3.2.2.1**[a]	**3.2.2.2**[a]	**3.1.3.6**[a]
1	**L11 (IPr)**	>99%	0	45	55
2	**L3 (JackiePhos)**	79%	0	33	57
3	**L1 (Me4tBuXPhos)**	>99%	19	14	67
4	**L4 (BrettPhos)**	>99%	5	30	65
5	**L12 (tBuXPhos)**	>99%	5	27	68
6	**L13 (MorDalPhos)**	>99%	9	20	69
7	**L14**	39%	0	27	73
8	**L15 (JohnPhos)**	>99% (76%)[b]	2	18	80

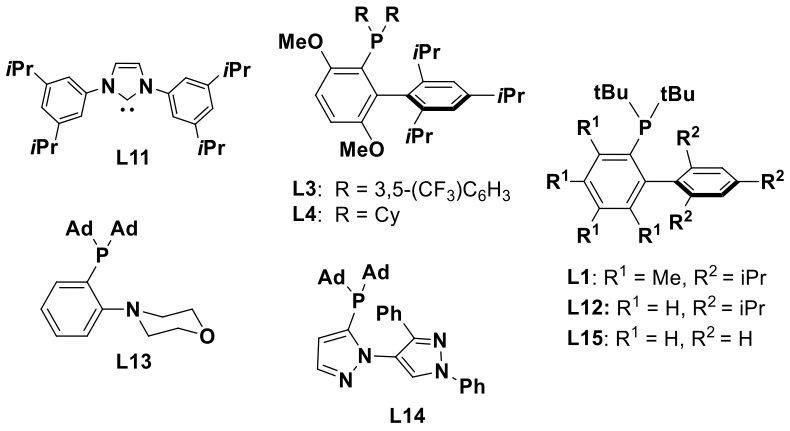

[a] Percent ratio determined by ^{1}H NMR. [b] Isolated yield of **3.1.3.6**

Through the optimization of solvent condition and catalyst ligand (Table 3.2.1) done by Philippe McGee,[73] the selective formation of desired decalin **3.1.3.6** via 6-*endo*-dig cyclization was achieved while minimizing side products **3.2.2.1** and **3.2.2.2,** which are proposed to arise from a 5-*exo*-dig cyclization followed by 1,5-hydride shift for **3.2.2.1** or protodeauration for **3.2.2.2**. A 20:1 solvent mixture of DCM:acetone was found to be optimal, while a number of phosphine and NHC ligands were screened. When IPr **L11** (Entry 1) was used, a near equal mixture of regioisomers **3.2.2.2/3.1.3.6** was observed. JackiePhos **L3** (Entry 2) did not yield full reaction conversion but gave higher selectivity for **3c**. **L1, L4, L12, L13** (Entry 3-6) all gave similar selectivity for **3.1.3.6** as well as allene **3.2.2.1** in trace to low yields. **L14** (Entry 7) gave good selectivity for **3.1.3.6** but with low reaction conversion. The optimal ligand was determined to be JohnPhos **L15** (Entry 8), with good selectivity for **3.1.3.6**, with full reaction conversion and an isolated yield of 76%.

3.2.3 B-Ring Functionalization

The next phase of the synthesis (Scheme 3.2.2), also carried out by Philippe McGee,[73] was the functionalization of decalin **3.1.3.6** to form the challenging 1,3-diaxial dimethyl moiety where it was first converted to epoxide **3.2.3.1** using in-*situ* generated

performic acid.[75] The stereoselectivity observed in this transformation is notably on the more hindered concave face. This could be explained with the nearby ring-A ketone acting as a directing group for the epoxidation involving the performic acid reagent, possibly via hydrogen bonding.[76] After addition of 1,8-diazabicyclo[5.4.0]undec-7-ene (DBU), γ-alcohol **3.1.3.5** was formed via E1cB elimination.

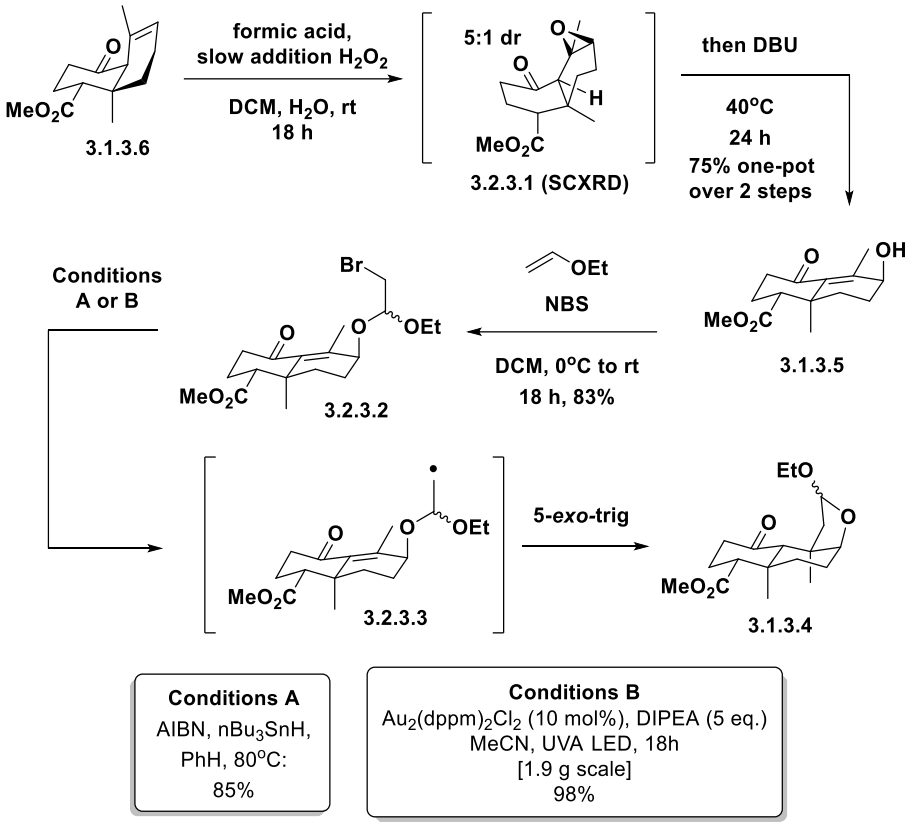

Scheme 3.2.2 - Synthesis towards the C-ring via radical cyclization.

Then **3.2.3.2** was generated by treating **3.1.3.5** to bromo-alkylation conditions using N-bromosuccinimide (NBS) and ethyl vinyl ether. This set the stage for the subsequent 5-*exo*-trig radical cyclization, where an initial trial (Conditions A) with AIBN/nBu_3SnH yielding desired cyclic acetal **3.1.3.4** in high yield via radical intermediate **3.2.3.3**. However, using Au(I) photoredox conditions (Conditions B)[26] previously developed by our

group gave **3.1.3.4** in stoichiometric yields on multi-gram scale, forming the challenging 1,3-diaxial dimethyl moiety diastereoselectively. This method was chosen as it bypassed the use of explosive AIBN and toxic organotin reagents.

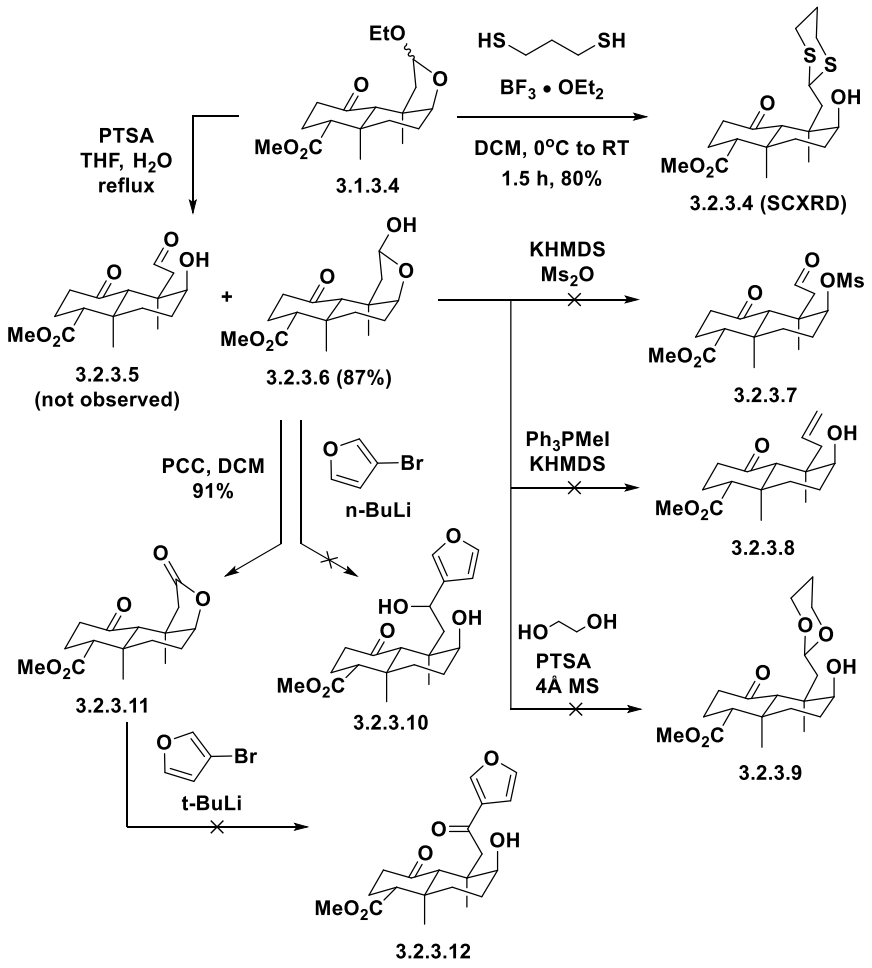

Scheme 3.2.3 - Attempted strategies in opening and functionalizing cyclic acetal

With **3.1.3.4** in hand, many attempts at opening and functionalizing the cyclic acetal ring were attempted by Phillipe McGee (Scheme 3.2.3). Initially, treating **3.1.3.4** to aqueous acid failed to generate desired free aldehyde **3.2.3.5**, instead only giving the more thermodynamically favored[77] lactol **3.2.3.6** in high yield. Many trials at this point to functionalize **3.2.3.6** via its free aldehyde **3.2.3.5** were met with failures. This included

mesylation (**3.2.3.7**), Wittig olefination (**3.2.3.8**), transacetalization (**3.2.3.9**), and 1,2-addition of an organolithium (**3.2.3.10**). However, lactol **3.2.3.6** was successfully oxidized into lactone **3.2.3.11**, but an attempt at a 1,2-addition of an furanyl-organolithiate at this stage also failed to yield ketone **3.2.3.12**. Finally, transacetalization of **3.1.3.4** into thioacetal **3.2.3.4** was carried out successfully under Lewis acidic conditions in high yield to reveal the free alcohol.

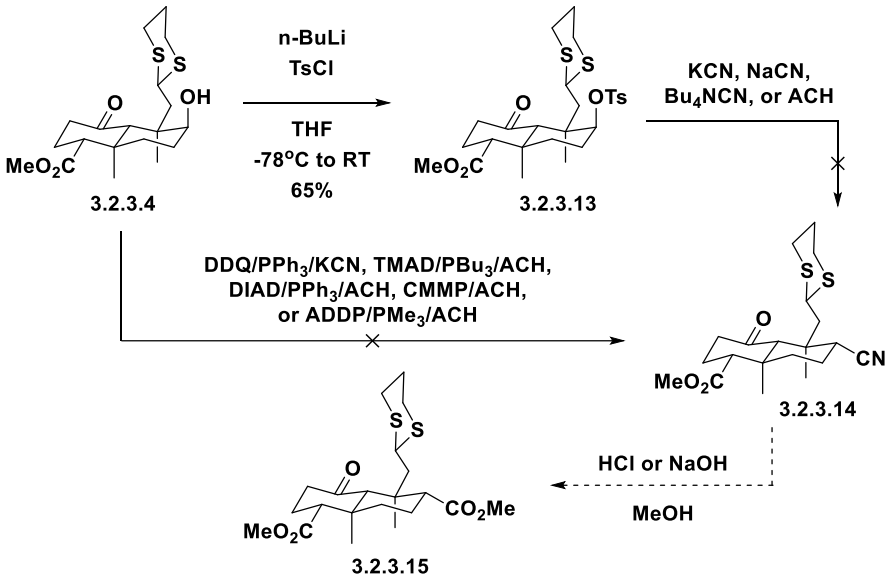

Scheme 3.2.4 - Attempted strategies towards ester **3.2.3.15**.

The strategy at this point (Scheme 3.2.4) was aimed at the installation of the C17 ester through the conversion of alcohol **3.2.3.4** into nitrile **3.2.3.14** then into ester **3.2.3.15**. This was attempted entirely by Phillipe McGee. First, **3.2.3.4** was converted to corresponding tosylate **3.2.3.13**, then was treated unsuccessfully with a variety of cyanide sources (ex. KCN, NaCN, Bu_4NCN, acetone cyanohydrin) in attempts to generate **3.2.3.14**. Direct cyanation of **3.2.3.4** was also attempted unsuccessfully with a variety of Mitsunobu-type conditions.[78]

3.2.4 Other B-Ring Functionalization Attempts

Other experiments at attempting to functionalize the B-ring by Philippe McGee from **3.1.3.5** were also performed, particularly in the installation of the C-17 ester as previously discussed but starting from an earlier intermediate (Scheme 3.2.5). First, γ-alcohol **3.1.3.5** was successfully brominated to form γ-bromide **3.2.4.1**, which was isolated as a 2:1 diastereomeric mixture. This bromide was then displaced using sodium cyanide to form vinyl cyanide **3.2.4.2** as the sole diastereomer, indicating that the vinyl cyanide was the thermodynamically favored tautomer over the enone.

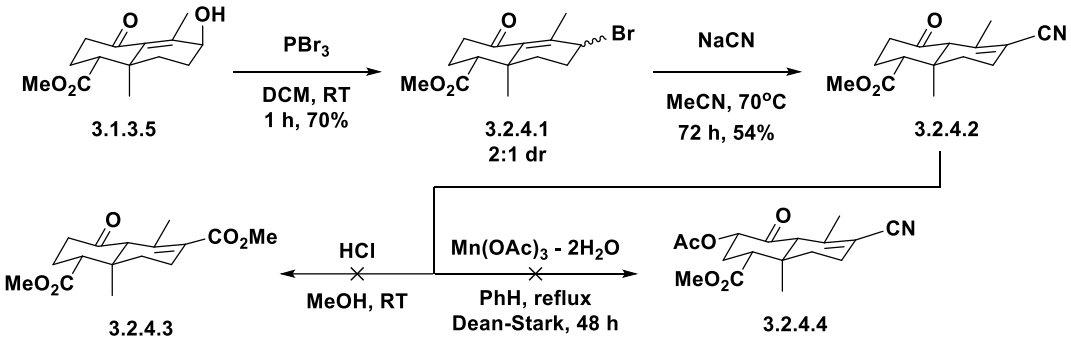

Scheme 3.2.5- Attempted strategies towards ester **3.2.4.3**

With **3.2.4.2** in hand, an attempt was made to convert the nitrile functional group to a methyl ester, which unfortunately did not yield any desired ester **3.2.4.3**. An alpha-acetoxylation of **3.2.4.2** was also attempted unsuccessfully where no oxidized product **3.2.4.4** was observed.

3.2.5 C-12 Furan Ring Installation

The synthetic approach (Scheme 3.2.6) then shifted towards installing the pendant furan moiety first then the C17 ester at a later point. Alcohol **3.2.3.4** was first acetyl protected to form **3.2.5.1**. The thioacetal was deprotected to reveal the free aldehyde **3.1.3.3**. A chemoselective 1,2-addition of an organotitanate onto an aldehyde was then

performed to give cyclic hemiacetal **3.2.5.2** in 63% as the sole diastereomer.[79] This reaction was done first by converting 3-bromofuran **3.2.5.4** to its corresponding organolithium **3.2.5.5** via lithium-halogen exchange, which was then reacted with triisopropyltitanium(IV) chloride[79b] to form furanyl organotitanium – LiCl suspension **3.2.5.6**. Two equivalents of **3.2.5.6** were added to aldehyde **3.1.3.3** which generated hemiacetal **3.2.5.2** presumably via titanium alkoxide **3.2.5.3** as an intermediate. Hemiacetal **3.2.5.2** was the only 1,2-addition product isolated and was confirmed to possess the incorrect stereochemistry at the C12 position by X-ray crystallography.

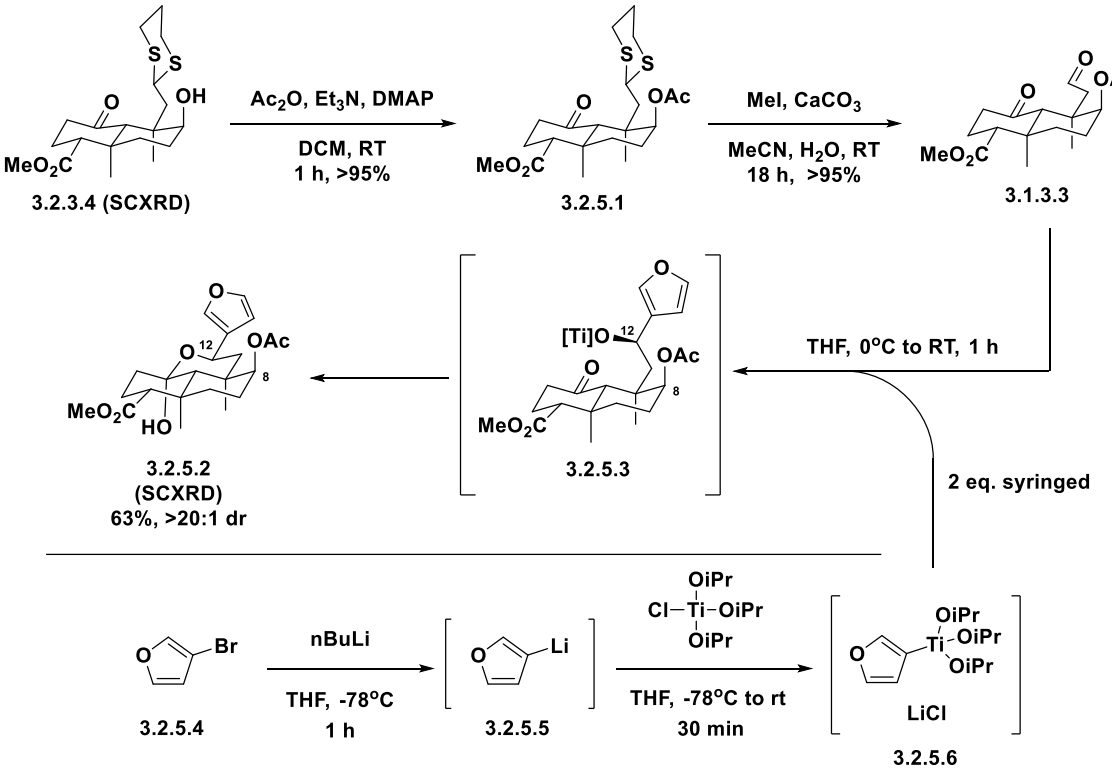

Scheme 3.2.6 – Sequence towards the installation of the C-12 furan moiety

The high diastereoselectivity (Scheme 3.2.7) of the furanyl titanate 1,2-addition was surprising, the hypothesis was that since the aldehyde carbon of **3.1.3.3** is two carbons away from the nearest stereocenter, low or no diastereoselectivity would be observed. The high diastereoselectivity could potentially be a result of the C8 acetoxy moiety acting

as a directing group[80] where furanyl titanate **3.2.5.6** is proposed to bind **3.1.3.3** in a bidentate fashion at the C8 acetoxyl and C12 aldehyde groups. Addition of the furan ring then occurs on the top face in the depicted conformer to give titanium alkoxide **3.2.5.3**, which finally cyclizes to form hemiacetal **3.2.5.2**. This hypothesis, however, would involve a questionable 7-membered ring transition state.

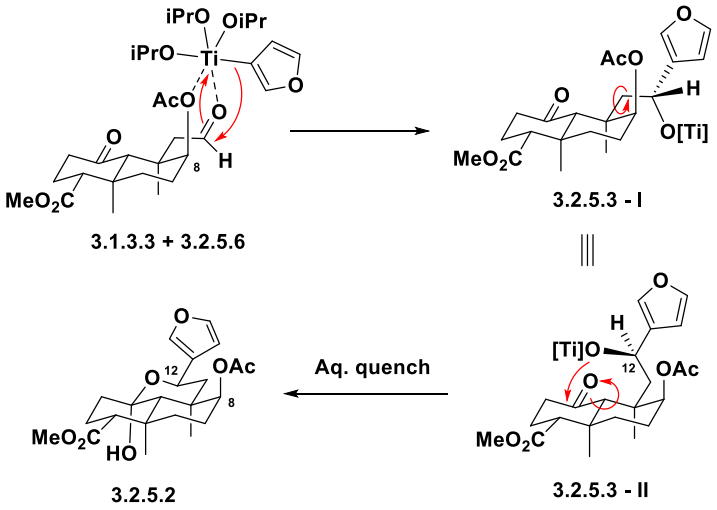

Scheme 3.2.7 – Proposed model for diastereoselective organotitanate addition

In light of this undesired result, some efforts in exploring the reactivity was done (Table 3.2.2). First (Entry 2), the usage of the chiral (R)-BINOL ligand[70] was experimented with the intention with inducing some stereoselectivity for the opposite C12 diastereomer. This was unsuccessful, where only **3.2.5.2** was observed and no desired diastereomer **3.2.5.7** found. The equivalents of **3.2.5.6** was reduced to 1.5 (Entry 3). This gave lower yields of **3.2.5.2** and did not affect the diastereoselectivity, indicating that the superstoichiometric amount of **3.2.5.2** did not reduce yield or diastereoselectivity.

Table 3.2.2 – Experimentation on organotitanate addition reactivity

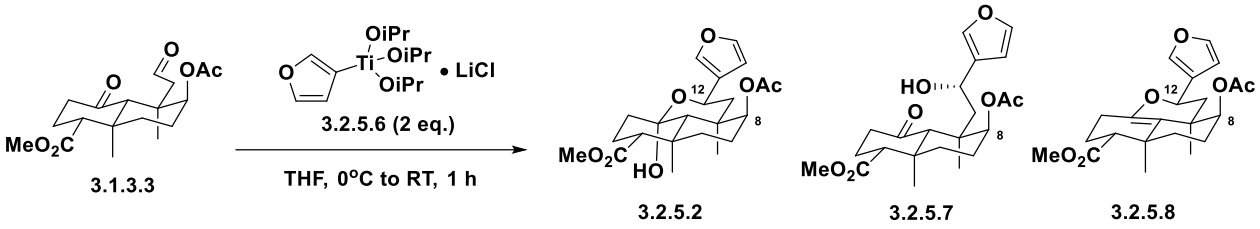

Entry	Modification to method	**3.2.5.2**[a]	**3.2.5.7**[a]	**3.2.5.8**[a]	**dr**[c]
1	none	(63)[b]	0	0	>20:1
2	Add (R)-BINOL (5 mol%)	51	0	0	>20:1
3	1.5 eq. **3.2.5.6**	30	0	0	>20:1
4	Add TESOTf (3 eq.)	0	0	(70)[b]	9:1

[a] Percent ratio determined by 1H NMR. [b] Isolated yield. [c] dr with respect to C12

Lastly (Entry 4), a one-pot sequence consisting of an organotitanate addition followed by hemiacetal TES protection was attempted, where 3 eq. of TESOTf was added to the reaction mixture before aqueous quench. This reaction interestingly only gave enol ether **3.2.5.8** in good yield and diastereoselectivity. The formation of **3.2.5.8** is the result of a dehydration reaction of hemiacetal **3.2.5.2** (Scheme 3.2.8), which maybe explained by the amount of triflic acid that is likely present in the TESOTf reagent as a result of exposure to moisture. The protonated hemiacetal **3.2.5.9** is proposed to undergo elimination of water to form oxonium **3.2.5.10**, which then tautomerizes to enol ether **3.2.5.8** while triflic acid is regenerated.

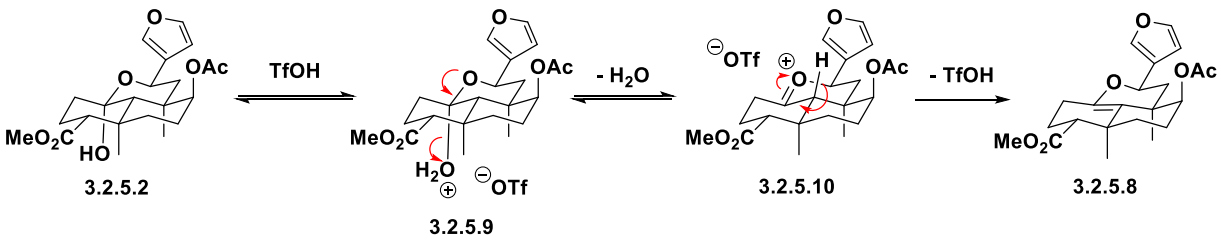

Scheme 3.2.8 – Proposed mechanism for dehydration of **3.2.5.2**

Initially, enol ether **3.2.5.8** was planned to be carried forward in the synthesis since the formation of an enol ether presented an opportunity to have the C1 ketone in a masked protected from which would have been reverted back into hemiacetal **3.2.5.2** under acidic conditions. Several experiments were performed to test this approach (Scheme 3.2.9). First, enol ether **3.2.5.8** was heated in Bronsted acidic conditions using HCl, but no desired hemiacetal **3.2.5.2** was observed with no conversion of starting material. Attempts to oxidize **3.2.5.8** into diketone **3.2.5.11** presumably via **3.2.5.2** which was thought to have existed in equilibrium with **3.2.5.8**. DMP alone, or with water or trifluoroacetic acid (TFA)[81] additive were tried unsuccessfully where no **3.2.6.11** was observed. Lastly, an opening of the enol ether ring of **3.2.5.8** to form vinyl furan **3.2.5.12** was attempted with a variety of conditions[82].

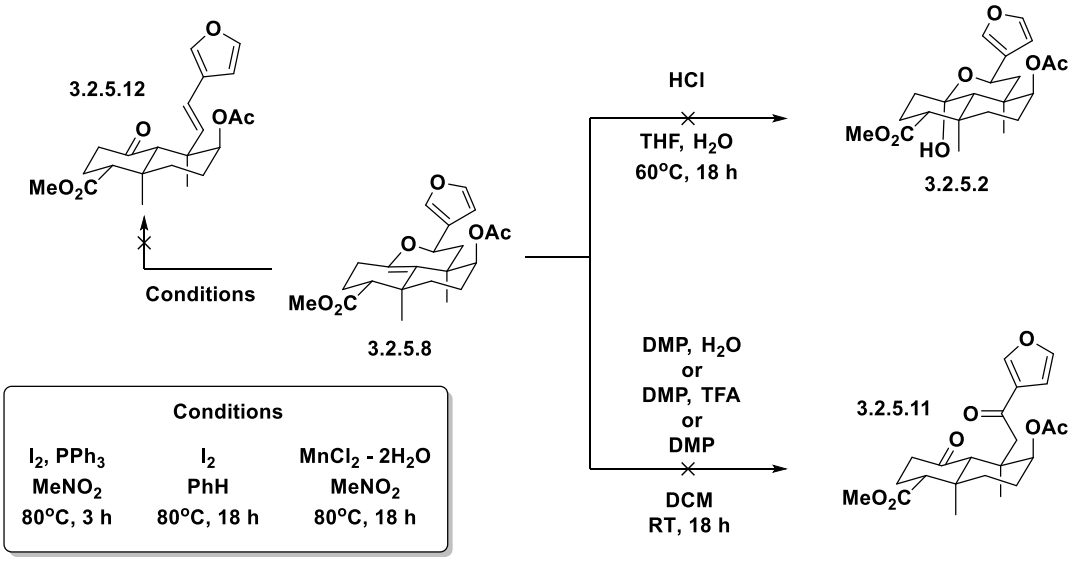

Scheme 3.2.9 – Attempted functionalization of enol ether **3.2.5.8**

The usage of iodine/PPh_3, or iodine alone under heating did not produce any desired vinyl furan **3.2.5.12**. Lewis acidic conditions using manganese(II) chloride with heating also did not yield **3.2.5.12**. With these results, the concept of using enol ether **3.2.5.8** as a masked

ketone advanced intermediate in the synthesis was abandoned, and hemiacetal **3.2.5.2** was carried forward instead. It is noteworthy, that proceeding with hemiacetal **3.2.5.2** in the synthesis still presents an opportunity to have the C1 ketone in a "masked hemiacetal" form, where after capping the hemiacetal with a protecting group would prevent side reactivity with the C1 ketone if it was unprotected in later synthetic steps.

3.2.6 Installation of the C-17 Methyl Ester

With the success of installing the C-12 furan moiety, albeit with the incorrect stereochemistry, attention was then turned to installing the key C-17 methyl ester group (Scheme 3.2.10). After silyl protection of the anomeric hydroxyl group of **3.2.5.2** to form silyl ether **3.2.6.1**, and then deprotection of the C8 acetyl protected alcohol, **3.2.6.2** was generated. This was then oxidized into the ketone **3.2.6.3** via Dess-Martin oxidation. My contribution towards new synthetic route steps begins with this oxidation.

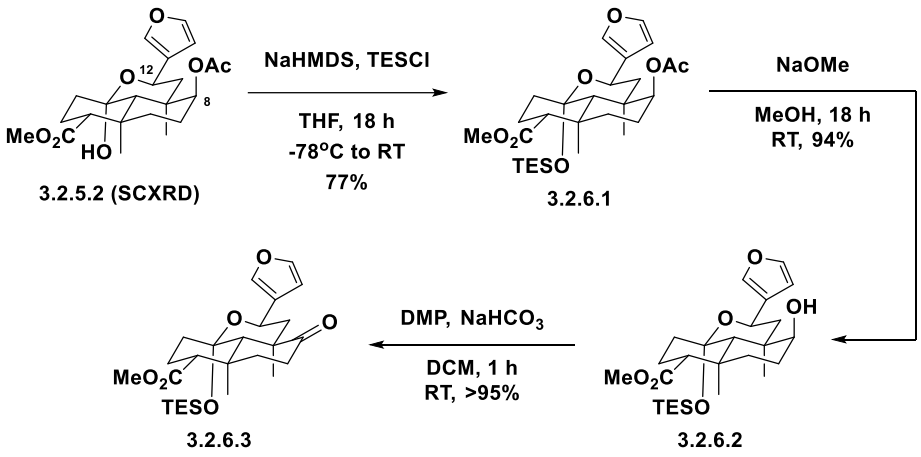

Scheme 3.2.10 – Sequence towards advanced ketone intermediate **3.2.6.3**

The initial strategy (Scheme 3.2.11) attempted involved accessing the desired ester **3.2.6.7** through installing the C-17 carbon through a Wittig olefination of ketone **3.2.6.3** to form *exo*-cyclic olefin **3.2.6.4**. A hydroboration using the bulky 9-borabicyclo[3.3.1]nonane

(9-BBN) reagent to synthesize primary alcohol **3.2.6.5** in a moderately stereoselective fashion. This forms the key C8 chiral center with a diastereomeric ratio of 8:1. At this point oxidations were attempted to convert the primary alcohol into a methyl ester. A direct conversion of alcohol **3.2.6.5** into ester **3.2.6.7** was tried using conditions[83] by Milovanović *et al.* using tert-butyl hypochlorite and pyridine but failed to produce any desired ester. The crude NMR spectrum did not show any aromatic signals associated with the furan moiety, suggesting over-oxidation of the furan ring. A mild oxidation of **3.2.6.5** into carboxylic acid **3.2.6.6** under aerobic conditions[84] by Ma *et al.* using catalytic iron(III) nitrate, TEMPO, and KCl was carried out successfully. Carboxylic acid **3.2.6.6** was purified only by silica plug and was then carried forward in a methylation using methyl iodide to give methyl ester **3.2.6.7** in a low yield over 2 steps

When the Fe(III)/TEMPO catalyzed oxidation was scaled up to 135 mg from 25 mg, the results were unfortunately not reproducible. The heterogeneous nature of the reaction likely contributed to its difficulty in scale-up. Lastly an attempt at oxidizing alcohol **3.2.6.5** into diketo aldehyde **3.2.6.9** was performed by first deprotecting the TES group on **3.2.6.5** to form hemiacetal **3.2.6.8**. This was done successfully but was only purified by silica plug then immediately submitted to the subsequent double oxidation due to the unstable nature of **3.2.6.8**. The double oxidation was performed using DMP but did not yield any desired **3.2.6.9**.

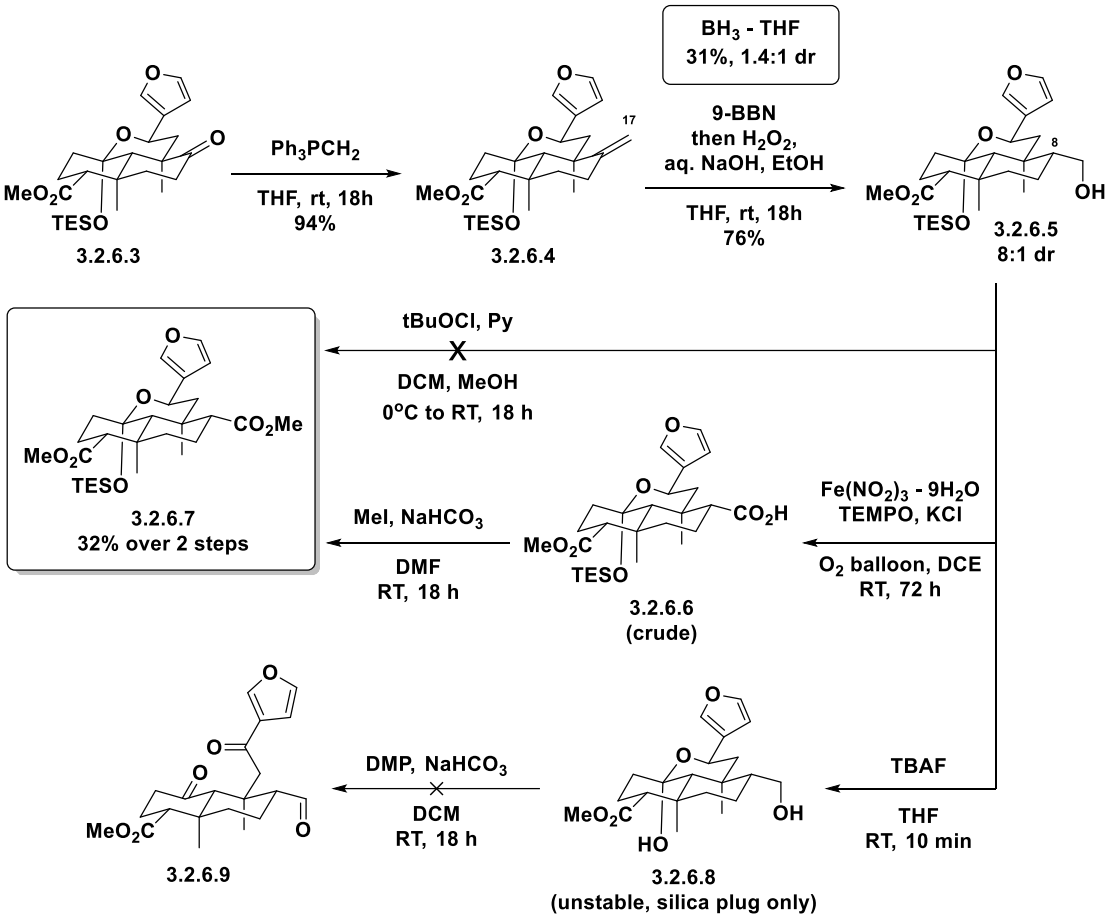

Scheme 3.2.11 – Initial route to key C17 ester **3.2.6.7**

Considering the difficulty encountered in the scale-up of the Fe(III)/TEMPO catalyzed oxidation of **3.2.6.5**, another synthetic path[70] inspired by Forsyth *et al.* to ester **3.2.6.7** was explored using a palladium catalyzed carbonylation (Scheme 3.2.12). First, ketone **3.2.6.3** was converted to corresponding vinyl triflate **3.2.6.10** in quantitative yield, which was then subjected to Pd catalytic conditions under carbon monoxide atmosphere in the presence of methanol. This generated α,β-unsaturated methyl ester **3.2.6.11**, which was reduced into saturated ester **3.2.6.7** via treatment with samarium diiodide in moderate yield and stereoselectivity for the key C8 diastereomer. This reaction was carried out under strict exclusion of air and using a fresh bottle of samarium diiodide solution gave superior yields and diastereoselectivity. Also, scale up of this reaction

sequence was successfully carried out from 25 mg test reactions to 250 mg, 420 mg, and 200 mg for the triflation, Pd-carbonylation, and samarium reduction respectively. Conditions by Evans *et al.* on the conjugate reduction[67] of α,β-unsaturated methyl ester **3.2.6.11** using L-Selectride/tBuOH was also attempted unsuccessfully, with no desired product observed.

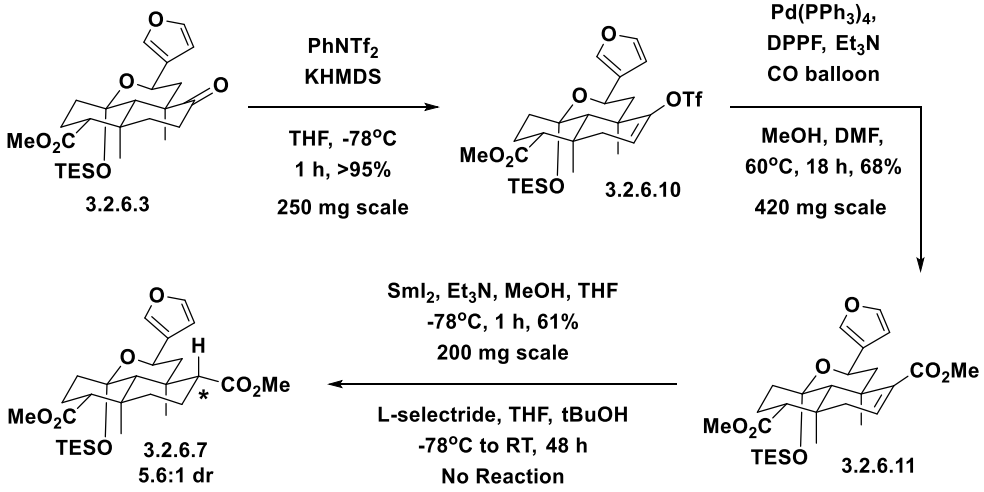

Scheme 3.2.12 - Synthesis of key C-17 ester **3.2.6.7** via Pd-catalyzed carbonylation

Considering the successful scale-up of the Pd-catalyzed carbonylation sequence (Scheme 3.2.12) and lower step count (1 step shorter) to ester **3.2.6.7** compared to the initial sequence (Scheme 3.2.11) via 9-BBN hydroboration, this was the selected pathway towards the end to the total synthesis.

3.2.7 Final C-Ring Formation and Formal Synthesis of (±)-Salvinorin A

Work at this point then focused on the formation of the final C-ring (Scheme 3.2.13) of **3.1.0.1**. First a silyl deprotection of ester **3.2.6.7** gave cyclic hemiacetal **3.2.7.1**, which was found to be unstable under ambient conditions similar to hemiacetal **3.2.6.8**, and therefore was immediately oxidized with Dess-Martin periodane to form desired diketone **3.1.3.1.** This reaction represents an important step in the synthesis, where the incorrect

C12 stereocenter was reconverted into a non-chiral center. Enol ether **3.2.7.2** was also produced as a side product in this reaction from the dehydration of **3.2.7.1**. Then a hydride reduction[69] inspired by Hagiwara *at al.* of the C12 ketone using K-Selectride/tert-butanol was performed to produce in *situ* presumptive intermediate alcohols **3.2.7.3** and **3.2.7.4** as diastereomers. Alcohol diastereomer **3.2.7.3** was proposed to then cyclize into hemiacetal **3.2.7.1**, whose inherent instability induced its dehydration to form enol ether **3.2.7.2** as a minor isolated side product.

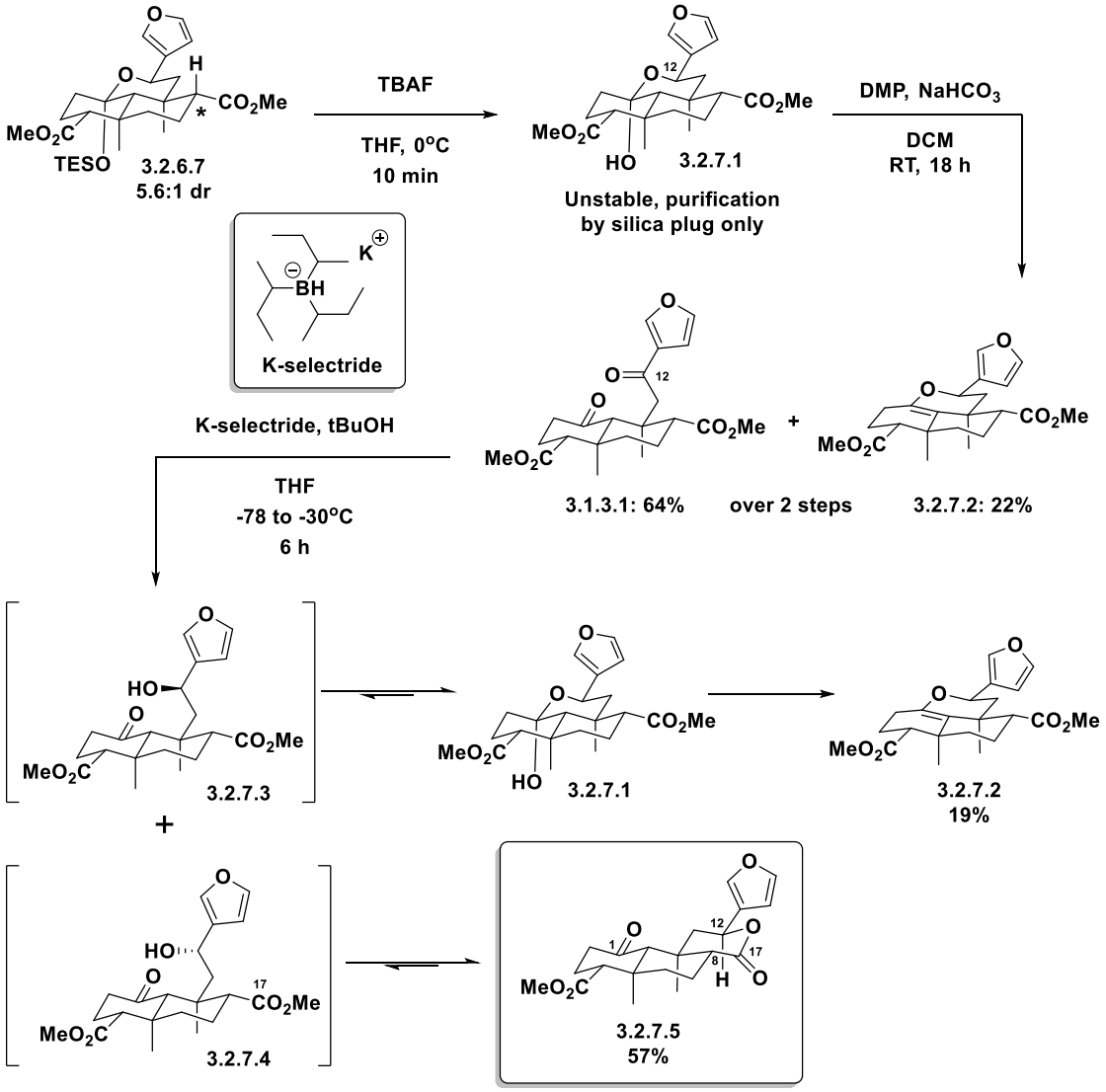

Scheme 3.2.13 – Formal synthesis of salvinorin A

The desired alcohol diastereomer **3.2.7.4** was proposed on the other hand to lactonize onto the nearby C17 methyl ester to form the Hagiwara[68] advanced intermediate **3.2.7.5** as the major product in moderate yield, thus concluding the formal synthesis of (±)-**3.1.0.1**.It is noteworthy that this reduction was performed chemoselectively, with no reduction of the C1 ketone and no epimerization of the C8 proton. The latter is a known key problem in past late-stage synthesis of **3.1.0.1**.

The finals steps to **3.1.0.1** (Scheme 3.2.14) were previously reported[68] by Hagiwara *et al.* First tricyclic lactone **3.2.7.5** was converted to the corresponding silyl enol ether **3.2.7.6**, which was then submitted to Rubottom oxidative conditions to give *epi*-salvinorin B **3.2.7.7** as the sole diastereomer with the undesired stereoconfiguration at C2. Then lastly, a Mitsunobu inversion of the C2 hydroxyl group was performed with acetic acid as the nucleophile to install the C2 acetoxy group, finishing the total synthesis of **3.1.0.1**. These final steps have not been performed by Barriault *et al.*

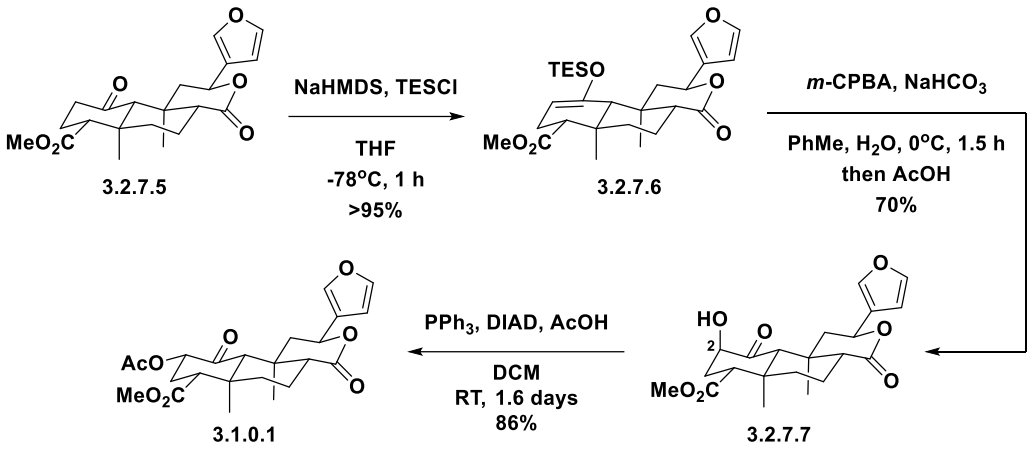

Scheme 3.2.14 – Final steps towards salvinorin A **3.1.0.1** by Hagiwara *et al.*

3.3 CONCLUSION

The formal synthesis of (±)-**3.1.0.1** has been reported. Our synthesis uniquely utilizing a DA then Au(I) catalyzed cyclization to synthesize the AB rings of **3.1.3.6**, then

later a Au(I) photoredox catalyst initiated radical cyclization to stereoselectively form a key quaternary carbon in **3.1.3.4**. During the synthesis of **3.2.5.2** via an aldehyde selective 1,2-addition of an organotitanium, the incorrect diastereomer was disappointingly obtained, however this set-back was harnessed into an advantage and unique approach in our synthesis, where it allowed for the facile protection of the C1 ketone in the form of a TES capped hemiacetal represented by **3.2.6.1**. In the final sequence towards Hagiwara intermediate **3.2.7.5**, we were able to form the correct stereoconfiguration at C8 in **3.2.6.7** in a samarium(II) iodide reduction and preserve the stereoconfiguration without epimerization through the end of the formal synthesis, which has not been accomplished in previous syntheses.

3.4 BIBLIOGRAPHY

26. Revol, G.; McCallum, T.; Morin, M.; Gagosz, F.; Barriault, L., Photoredox Transformations with Dimeric Gold Complexes. *Angew. Chem. Int. Ed.* **2013,** *52* (50), 13342-13345.
56. Hernández-Alvarado, R. B.; Madariaga-Mazón, A.; Ortega, A.; Martinez-Mayorga, K., DARK Classics in Chemical Neuroscience: Salvinorin A. *ACS Chem. Neurosci.* **2020,** *11* (23), 3979-3992.
57. Vortherms, T. A.; Roth, B. L., Salvinorin A From Natural Product to Human Therapeutics. *Mol. Interv.* **2006,** *6* (5), 257-256.
58. (a) Wasson, R. G., A new Mexican psychotropic drug from the mint family. *Bot. Mus. leaf., Harv. Univ.* **1962,** *20* (3), 77-84; (b) Epling, C.; Jativa-M, C. D., A new species of salvia from Mexico. *Bot. Mus. leaf., Harv. Univ.* **1962,** *20* (3), 75-76.
59. Ortega, A.; Blount, J. F.; Manchand, P. S., Salvinorin, a new trans-neoclerodane diterpene from Salvia divinorum(Labiatae). *J. Chem. Soc., Perkin Trans. 1* **1982,** (0), 2505-2508.
60. Valdes, L. J.; Butler, W. M.; Hatfield, G. M.; Paul, A. G.; Koreeda, M., Divinorin A, a psychotropic terpenoid, and divinorin B from the hallucinogenic Mexican mint, Salvia divinorum. *J. Org. Chem.* **1984,** *49* (24), 4716-4720.
61. Roach, J. J.; Shenvi, R. A., A review of salvinorin analogs and their kappa-opioid receptor activity. *Bioorg. Med. Chem. Lett.* **2018,** *28* (9), 1436-1445.
62. Prisinzano, T. E.; Rothman, R. B., Salvinorin A Analogs as Probes in Opioid Pharmacology. *Chem. Rev.* **2008,** *108* (5), 1732-1743.
63. Roth, B. L.; Baner, K.; Westkaemper, R.; Siebert, D.; Rice, K. C.; Steinberg, S.; Ernsberger, P.; Rothman, R. B., Salvinorin A: A potent naturally occurring

nonnitrogenous κ opioid selective agonist. *Proc. Natl. Acad. Sci. U.S.A.* **2002,** *99* (18), 11934-11939.
64. Hooker, J. M.; Xu, Y.; Schiffer, W.; Shea, C.; Carter, P.; Fowler, J. S., Pharmacokinetics of the potent hallucinogen, salvinorin A in primates parallels the rapid onset and short duration of effects in humans. *NeuroImage* **2008,** *41* (3), 1044-1050.
65. Schmidt, M. D.; Schmidt, M. S.; Butelman, E. R.; Harding, W. W.; Tidgewell, K.; Murry, D. J.; Kreek, M. J.; Prisinzano, T. E., Pharmacokinetics of the plant-derived κ-opioid hallucinogen salvinorin A in nonhuman primates. *Synapse* **2005,** *58* (3), 208-210.
66. Kane, B. E.; McCurdy, C. R.; Ferguson, D. M., Toward a Structure-Based Model of Salvinorin A Recognition of the κ-Opioid Receptor. *J. Med. Chem.* **2008,** *51* (6), 1824-1830.
67. Scheerer, J. R.; Lawrence, J. F.; Wang, G. C.; Evans, D. A., Asymmetric Synthesis of Salvinorin A, A Potent κ Opioid Receptor Agonist. *J. Am. Chem. Soc.* **2007,** *129* (29), 8968-8969.
68. Nozawa, M.; Suka, Y.; Hoshi, T.; Suzuki, T.; Hagiwara, H., Total Synthesis of the Hallucinogenic Neoclerodane Diterpenoid Salvinorin A. *Org. Lett.* **2008,** *10* (7), 1365-1368.
69. Hagiwara, H.; Suka, Y.; Nojima, T.; Hoshi, T.; Suzuki, T., Second-generation synthesis of salvinorin A. *Tetrahedron* **2009,** *65* (25), 4820-4825.
70. Line, N. J.; Burns, A. C.; Butler, S. C.; Casbohm, J.; Forsyth, C. J., Total Synthesis of (−)-Salvinorin A. *Chem. Eur. J.* **2016,** *22* (50), 17983-17986.
71. Wang, Y.; Metz, P., Total Synthesis of the Neoclerodane Diterpene Salvinorin A via an Intramolecular Diels–Alder Strategy. *Org. Lett.* **2018,** *20* (11), 3418-3421.
72. Zimdars, P.; Wang, Y.; Metz, P., A Protecting-Group-Free Synthesis of (−)-Salvinorin A. *Chem. Eur. J.* **2021,** *27* (29), 7968-7973.
73. McGee, P. Application of Gold(I) Catalysis in the Synthesis of Bridged Carbocycles, (±)-Magellanine and (±)-Salvinorin A. Université d'Ottawa / University of Ottawa, Ottawa, 2018.
74. Genna, D. T.; Posner, G. H., Cyanocuprates Convert Carboxylic Acids Directly into Ketones. *Org. Lett.* **2011,** *13* (19), 5358-5361.
75. Swern, D., Organic Peracids. *Chem. Rev.* **1949,** *45* (1), 1-68.
76. (a) Armstrong, A.; Barsanti, P. A.; Clarke, P. A.; Wood, A., Ketone-directed peracid epoxidation. *Tetrahedron Lett.* **1994,** *35* (33), 6155-6158; (b) Armstrong, A.; Barsanti, P. A.; Clarke, P. A.; Wood, A., Ketone-directed peracid epoxidation of cyclic alkenes. *J. Chem. Soc., Perkin Trans. 1* **1996,** (12), 1373-1380.
77. (a) Hurd, C. D.; Saunders Jr, W. H., Ring-chain tautomerism of hydroxy aldehydes. *J. Am. Chem. Soc.* **1952,** *74* (21), 5324-5329; (b) Endo, K.; Takahashi, H.; Aihara, M., Neighboring Assistance of a Hydroxyl Group on Manganese Dioxide Oxidation of Benzyl Alcohols to Lactones. *Heterocycles* **1996,** *42* (2), 589-596.
78. (a) Davis, R.; Untch, K. G., Direct one-step conversion of alcohols into nitriles. *J. Org. Chem.* **1981,** *46* (14), 2985-2987; (b) Tsunoda, T.; Uemoto, K.; Nagino, C.; Kawamura, M.; Kaku, H.; Itô, S., A facile one-pot cyanation of primary and secondary alcohols. Application of some new Mitsunobu reagents. *Tetrahedron Lett.* **1999,** *40* (41), 7355-7358; (c) Iranpoor, N.; Firouzabadi, H.; Akhlaghinia, B.; Nowrouzi, N., Conversion of Alcohols, Thiols, and Trimethysilyl Ethers to Alkyl Cyanides Using

Triphenylphosphine/2,3-Dichloro-5,6-dicyanobenzoquinone/n-Bu4NCN. *J. Org. Chem.* **2004,** *69* (7), 2562-2564.
79. (a) Sibi, M. P.; He, L., Application of Enantioselective Radical Reactions: Synthesis of (+)-Ricciocarpins A and B. *Org. Lett.* **2004,** *6* (11), 1749-1752; (b) Reetz, M. T.; Westermann, J.; Steinbach, R.; Wenderoth, B.; Peter, R.; Ostarek, R.; Maus, S., Chemoselective addition of organotitanium reagents to carbonyl compounds. *Chem. Ber.* **1985,** *118* (4), 1421-1440.
80. Reetz, M. T., Stereoselectivity in the Addition of Organotitanium Reagents to Carbonyl Compounds. In *Organotitanium Reagents in Organic Synthesis*, Reetz, M. T., Ed. Springer Berlin Heidelberg: Berlin, Heidelberg, 1986; pp 123-193.
81. Skiles, J. W.; Miao, C.; Sorcek, R.; Jacober, S.; Mui, P. W.; Chow, G.; Weldon, S. M.; Possanza, G.; Skoog, M., Inhibition of human leukocyte elastase by N-substituted peptides containing .alpha.,.alpha.-difluorostatone residues at P1. *J. Med. Chem.* **1992,** *35* (26), 4795-4808.
82. Liu, C.; Pan, B.; Gu, Y., Lewis base-assisted Lewis acid-catalyzed selective alkene formation via alcohol dehydration and synthesis of 2-cinnamyl-1,3-dicarbonyl compounds from 2-aryl-3,4-dihydropyrans. *Chinese J. Catal.* **2016,** *37* (6), 979-986.
83. Milovanović, J. N.; Vasojević, M.; Gojković, S., Oxidation of primary alcohols to methyl esters using tert-butyl hypochlorite, pyridine and methyl alcohol. *J. Chem. Soc., Perkin trans. II* **1991,** (8), 1231-1233.
84. Jiang, X.; Zhang, J.; Ma, S., Iron Catalysis for Room-Temperature Aerobic Oxidation of Alcohols to Carboxylic Acids. *J. Am. Chem. Soc.* **2016,** *138* (27), 8344-8347.

3.5 CONTRIBUTION STATEMENT

3.5.1 Claims to Original Research

- Completion of the formal synthesis of salvinorin A from **3.2.6.2** to Hagiwara's intermediate **3.2.7.5**.
- Modification and/or optimization of Phillipe McGee's procedures for Negishi coupling of **3.2.1.1**, methylation of **3.2.1.2**, bromination-alkylation of 3.1.3.5, radical cyclization of **3.2.3.2**, TES protection of **3.2.5.2**, deacetylation of **3.2.6.1**.
- In-depth investigation into furan-organotitanium 1,2-addition to **3.1.3.3**, initially performed by Phillipe McGee**.** Determination of relative stereoconfiguration of **3.2.5.2** by SCXRD, and attempted functionalization of enol ether **3.2.5.8** in Scheme 3.2.9.
- Development of DMP oxidation of **3.2.6.2**, as well as all successful and attempted reactions in Scheme 3.2.11, Scheme 3.2.12, and Scheme 3.2.13.
- Resynthesis of synthesis route intermediates previously accessed by Phillipe McGee: **3.2.1.1, 3.2.1.2, 3.2.1.3, 3.1.3.8, 3.1.3.7, 3.2.2.1, 3.1.3.6, 3.1.3.5, 3.2.3.2, 3.1.3.4, 3.2.3.4, 3.2.5.1, 3.1.3.3, 3.2.5.2, 3.2.6.1,** and **3.2.6.2.**

3.5.2 Oral Presentations

- *Towards the Synthesis of Salvinorin A.* Tran, H.; McGee, P.; Barriault, L., CCCE 2021.

3.5.3 Poster Presentations

- *Towards the Synthesis of Salvinorin A.* Tran, H.; McGee, P.; Barriault, L., QOMSBOC 2021

4. CONCLUSION

From the initial discoveries on the applications of gold catalysis in the hydration and hydroamination of alkynes, chemists have continued to harness the potential of gold in organic synthesis. For our group and especially in this thesis, the Au(I) catalyzed Conia-ene type reaction was of the greatest interest. With the seminal reports, particularly by Echavarren *et al.*, on the use of silyl enol ethers as a carbon nucleophile in Au(I) 5-*exo*-*dig* cyclization, our group contributed to the literature with a report of a Au(I) catalyzed 6-*endo*-*dig* cyclization.

This work served as the foundation for the work described in chapter 2 in the synthesis of polycyclic carbocycles via a three step one-pot cascade comprising of an unconventional *exo* Diels-Alder catalyzed by $Gd(OTf)_3$, then Au(I) 6-*endo*-*dig* cyclization then Diels-Alder again. A scope of 12 examples was achieved. This work was further extended in the synthesis of fused tricycles via an *exo* Diels-Alder then Au(I) 6-*endo*-*dig*/5-*exo*-*dig* cyclization then Prins cyclization. This produced two scopes of 11 and 8 examples respectively. The use of this methodology is proposed for the total synthesis of cardenolide natural products such as digitoxigenin and batrachotoxin. The objectives of this project were mostly achieved, but could benefit by future work in pushing the methodology development towards making the initial DA reaction enantioselective.

In chapter 3, the completion of the formal synthesis of salvinorin A is reported. Foundational work was performed by former Ph.D. student Philippe McGee, where the construction of the A and B rings were executed in two steps via an *endo* Diels-Alder reaction followed by another application of Au(I) catalysis in a 6-*endo*-*dig* cyclization. The C-ring was constructed first via a 5-*exo*-*trig* radical cyclization using a dimeric Au(I)

photoredox catalyst creating a challenging quaternary stereocenter. The pendant furan ring was installed via its 1,2-addition onto an aldehyde as an organotitanium species. The incorrect stereochemistry was unfortunately obtained, but harnessed into an advantage where the C1 ketone was essentially protected as a hemiacetal. The incorrect stereocenter was later corrected in the final step inspired by Hagiwara and co-worker's synthesis of salvinorin A, where a ketone reduction followed by lactonization using K-Selectride performed to intercept a Hagiwara intermediate in 21 steps, constituting a formal synthesis. The additional 3 steps to make salvinorin A have been established by Hagiwara *et al.*, where an acetoxyl group is installed at the C2 position. The final step count would therefore be 24 steps. Although this synthesis failed to materialize as the shortest in literature, this route still effectively showcases Au(I) methodology previously developed by Barriault *et al.*, as well as giving a unique synthetic approach to salvinorin A with the ability to divergently synthesize analogues of salvinorin A. Future work with the synthesis of salvinorin A should involve shortening the synthesis, developing an enantioselective synthesis using an enantioselective DA reaction to construct the A-ring, and exploring the potential of creating a library of Salvinorin A analogues.

5. *EXPERIMENTAL PROCEDURES*

5.1 GENERAL INFORMATION

All reactions were performed in Pyrex glassware equipped with a magnetic stir bar, capped with a screw cap or septum, unless otherwise indicated. All commercial reagents were purchased from Sigma-Aldrich, Alfa-Aesar, Oakwood Chemicals, Strem or Combi-Blocks and were used without further purification, unless otherwise noted. DCM for scope reactions (GP1-3) was dried over 3Å molecular sieves. 4Å molecular sieves were dried under vacuum overnight at 180°C and stored in a glovebox. Gadolinium(III) triflate was stored in a glovebox. Reactions were monitored by thin layer chromatography (TLC) analysis. TLC plates were viewed under UV light and stained with potassium permanganate or p-anisaldehyde staining solution. Yields refer to products isolated after purification, unless otherwise stated. NMR samples were dissolved in $CDCl_3$ (unless specified otherwise) and chemical shifts are reported in ppm referenced to residual nondeuterated solvent. Proton nuclear magnetic resonance (^{1}H NMR) spectra were recorded on a Bruker Avance II 400 or Bruker Avance III HD 600 equipped with autotuning cryoprobe. Carbon nuclear magnetic resonance (^{13}C NMR) spectra were recorded on Bruker Avance II 400 (101 MHz) or Bruker Avance III HD 600 (151 MHz) equipped with autotuning cryoprobe. Phosphorous nuclear magnetic resonance (^{31}P NMR) spectra were recorded on a Bruker Avance 300. Fluorine nuclear magnetic resonance (^{19}F NMR) spectra were recorded on a Bruker Avance 300. IR spectra were recorded with an Agilent Technologies Cary 630 IR Spectrometer equipped with a diamond ATR module. EI HRMS were obtained on a Kratos Analytical Concept instrument, ESI+ HRMS were obtained on a Waters QTOF Global instrument (University of Ottawa Mass Spectrometry Facility),

ESI- HRMS were obtained on a Sciex QStar XL QTOF instrument (Carleton Mass Spectrometry Centre). Optical rotations were obtained on an Anton Paar MCP 500 polarimeter. X-RAY crystal structures were obtained on a Bruker SMART APPEX II diffractometer.

5.2 CHAPTER 2 SUPPORTING INFORMATION (GOLD CASCADE)

5.2.1 Scope General Procedures

General Procedure GP1 (Diels-Alder/Au 6-endo-dig/Diels-Alder)

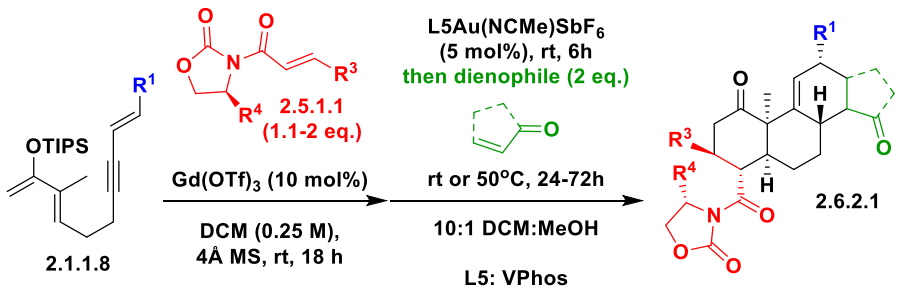

To a capped 4 mL oven dried reaction vial was added oxazolidinone dienophile **2.5.1.1** (1.1- 2 eq.), gadolinium(III) trifluoromethanesulfonate (9 mg, 0.015 mmol, 10 mol%), DCM (0.750 ml, 0.200M), and 4Å MS (38mg, 250mg/mmol). The mixture was stirred for 3 h at rt. Then, the diene **2.1.1.8** (0.150 mmol) was added. The mixture was stirred at rt for 18 h. Then, to the mixture was added MeOH (0.075 ml), and **L5**Au(NCMe)SbF_6 (7 mg, 8 µmol, 5 mol%). The mixture was stirred at rt for 6 h. Then, the 2nd dienophile (0.300 mmol, 2 eq.) was added. The mixture was stirred at rt or 50°C for 18–48 h. The mixture was dry-packed in silica, evaporated, and separated by flash chromatography, yielding **2.6.2.1.**

General Procedure GP2 (Diels-Alder/Au 6-endo-dig/Prins)

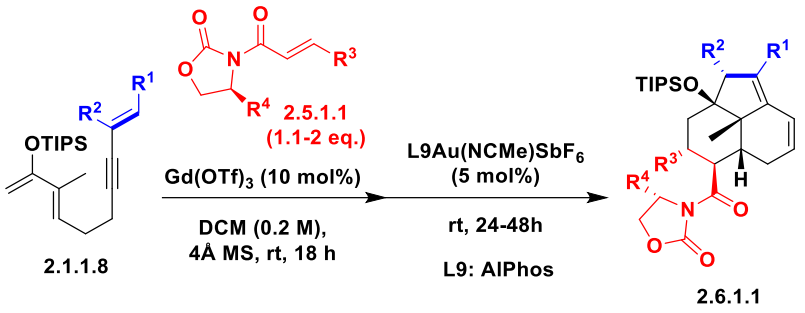

To a capped 4 mL oven dried reaction vial was added oxazolidinone dienophile **2.5.1.1** (1.1- 2 eq.), gadolinium(III) trifluoromethanesulfonate (9 mg, 0.015 mmol, 10 mol%), DCM (0.750 ml, 0.200M), and 4Å MS (38mg, 250mg/mmol). The mixture was stirred for 3 h at rt. Then, the diene **2.1.1.8** (0.150 mmol) was added. The mixture was stirred at room temperature for 18 h.

Then, to the mixture was added **L9**Au(NCMe)SbF_6 (9 mg, 8 µmol, 5 mol%). The mixture was stirred at rt for 24–48 h. The mixture was dry-packed in silica, evaporated and separated by flash chromatography, yielding a mixture of regioisomers with **2.6.1.1** as the major product**.**

General Procedure GP3 (Diels-Alder/Au 5-exo -dig/Prins)

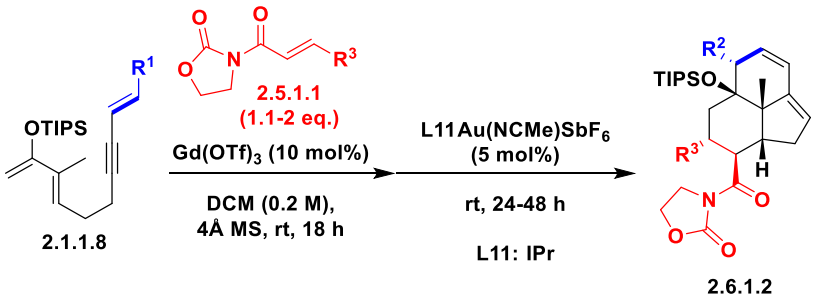

To a capped 4 mL oven dried reaction vial was added oxazolidinone dienophile **2.5.1.1** (0.165 mmol, 1.1 eq.), gadolinium(III) trifluoromethanesulfonate (9 mg, 0.015 mmol, 10 mol%), DCM (0.750 ml, 0.200M), and 4Å MS (38mg, 250mg/mmol). The mixture was

stirred for 3 h at rt. Then, the diene **2.1.1.8** (0.150 mmol) was added. The mixture was stirred at room temperature for 18 h.

Then, to the mixture was added **L11**Au(NCMe)SbF_6 (7 mg, 8 μmol, 5 mol%). The mixture was stirred at rt for 24–48 h. The mixture was dry-packed in silica, evaporated and separated by flash chromatography, yielding a mixture of regioisomers with **2.6.1.2** as the major product**.**

5.2.2 Diels-Alder/Au 6-*endo*-dig/*Diels-Alder* Scope Characterization

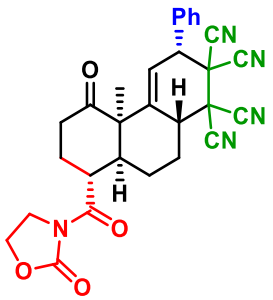

Tricycle 2.6.2.1aab

Characterization data obtained from literature (Alyson Poyser's Master's thesis).[85]

In a capped 4 mL oven dried reaction vial, tetracyanoethylene (2 equiv.) was added to diene **2.6.0.1** in DCE (0.2M). The mixture was stirred at 60˚C overnight and purified by flash chromatography. Tricycle **2.6.2.1aab** was formed in 73% yield (0.054 g).

1H NMR (400 MHz, $CDCl_3$) δ 7.58–7.36 (m, 5H), 5.73 (t, *J* = 1.9 Hz, 1H), 4.54 (td, *J* = 8.8, 2.5 Hz, 2H), 4.40 (t, *J* = 2.1 Hz, 1H), 4.25–4.14 (m, 1H), 4.03 (ddd, *J* = 11.1, 8.3, 6.4 Hz, 1H), 3.70–3.62 (m, 1H), 3.26–3.03 (m, 2H), 2.48–2.30 (m, 5H), 2.27–2.13 (m, 2H), 1.82–1.65 (m, 1H), 1.45 (s, 3H).

13C NMR (101 MHz, $CDCl_3$) δ 211.6, 176.1, 153.3, 140.6, 133.8, 130.2, 129.6, 129.4, 120.1, 111.3, 111.0, 110.1, 62.3, 56.4, 49.1, 46.8, 43.7, 43.1, 42.8, 42.1, 42.0, 35.6, 31.7, 29.8, 23.1, 22.0.

IR (neat, cm^{-1}): 2968, 2921, 2854, 2364, 2360, 1774, 1698.

HRMS (ESI): m/z calc'd for $C_{29}H_{25}N_5O_4Na$ [M+Na] = 530.1804, found [M+Na] = 530.1792.

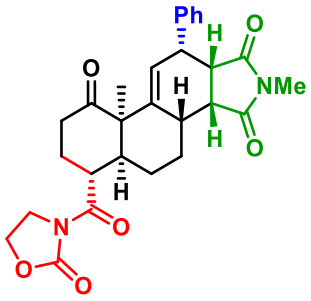

Tetracycle 2.6.2.1aaa

Characterization data obtained from literature (Alyson Poyser's Master's thesis).[85]

In a capped 4 mL oven dried reaction vial, *N*-methylmaleimide (2 equiv.) was added to diene **2.6.0.1** in DCE (0.2M). The mixture was stirred at 60˚C overnight and purified by flash chromatography. Tetracycle **2.6.2.1aaa** was formed in 79% yield (0.056 g).

1H NMR (400 MHz, $CDCl_3$) δ = 7.40 – 7.27 (m, 3H), 7.25 – 7.19 (m, 2H), 5.75 (t, *J* = 3.4 Hz, 1H), 4.46 (ddd, *J* = 8.7, 7.4, 2.6 Hz, 2H), 4.25 (td, *J* = 11.2, 3.4 Hz, 1H), 4.15 – 4.00 (m, 2H), 3.60 (ddd, *J* = 6.3, 4.2, 1.5 Hz, 1H), 3.26 (dd, *J* = 8.4, 6.5 Hz, 1H), 3.15 (dd, *J* = 8.4, 6.2 Hz, 1H), 2.86 (s, 1H), 2.82 (s, 3H), 2.69 (td, *J* = 14.0, 6.0 Hz, 1H), 2.53 (ddd, *J* = 12.4, 8.2, 3.9 Hz, 1H), 2.31 (tt, *J* = 15.6, 3.6 Hz, 2H), 2.20 – 2.05 (m, 3H), 1.79 (tdd, *J* = 13.3, 11.4, 4.1 Hz, 1H), 1.50 (dt, *J* = 7.6, 3.7 Hz, 1H), 1.20 (s, 3H).

13C NMR (101 MHz, $CDCl_3$) δ = 210.0, 178.1, 176.0, 174.9, 153.6, 142.8, 138.8, 128.9, 128.4, 127.3, 126.5, 62.1, 53.2, 46.4, 46.4, 43.8, 42.9, 42.4, 41.9, 37.4, 32.4, 29.5, 25.0, 24.6, 22.2, 19.9.

IR (neat, cm^{-1}): 2949, 2365, 1774, 1698.

HRMS (ESI): m/z calc'd for $C_{28}H_{30}N_2O_6$ $[M]^+$ = 490.2104, found $[M]^+$ = 490.2096.

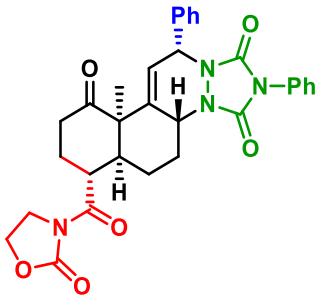

Tricycle (2.6.2.1aac)

Synthesized according to GP1, reacting at ambient temperature for 18 h for the final DA step, using oxazolidinone dienophile **2.5.1.1a** (2 eq.)**,** diene **2.1.1.8a**, and 4-phenyl-1,2,4-triazoline-3,5-dione as the second dienophile**,** yielding **2.6.2.1aac** in 62% yield as the sole diastereomer as a white foam**.**

^{1}H NMR (600 MHz, $CDCl_3$) δ 7.45 – 7.27 (m, 10H), 5.71 (d, *J* = 4.5 Hz, 1H), 5.54 (dd, *J* = 4.6, 2.2 Hz, 1H), 4.54 – 4.44 (m, 2H), 4.45 – 4.40 (m, 1H), 4.18 (q, *J* = 9.6 Hz, 1H), 3.99 (ddd, *J* = 11.1, 8.8, 5.6 Hz, 1H), 3.69 – 3.64 (m, 1H), 3.17 (ddd, *J* = 15.1, 12.2, 6.9 Hz, 1H), 3.00 (dq, *J* = 12.1, 3.6 Hz, 1H), 2.45 – 2.36 (m, 3H), 2.29 – 2.17 (m, 2H), 1.81 (qd, *J* = 13.2, 3.7 Hz, 1H), 1.76 – 1.67 (m, 1H), 1.41 (s, 3H).

^{13}C NMR (151 MHz, $CDCl_3$) δ 211.98, 176.54, 153.38, 152.42, 150.65, 137.96, 137.02, 131.17, 128.96, 128.89, 128.70, 128.09, 127.90, 125.44, 120.24, 62.27, 57.32, 55.52, 55.03, 49.22, 43.14, 42.26, 35.60, 31.76, 29.24, 22.89, 22.28.

IR (neat, cm^{-1}): 1756, 1670, 1422, 1220.

HRMS (ESI) m/z calc'd for $C_{31}H_{30}N_4O_6$ [M+] 554.2165, found [M+] 554.2155.

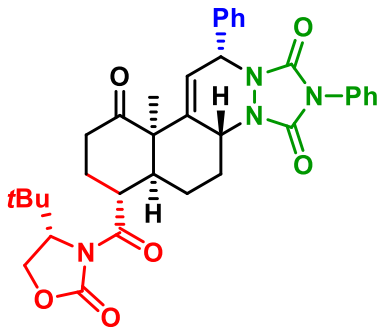

Tetracycle (**2.6.2.1abc)**

Synthesized according to GP1, reacting at ambient temperature for 18 h for the final DA step, using oxazolidinone dienophile **2.5.1.1b** (2 eq.)**,** diene **2.1.1.8a**, and 4-phenyl-1,2,4-triazoline-3,5-dione as the second dienophile**,** yielding **2.6.2.1abc** in 52% yield as a white foam as the sole diastereomer**.**

^{1}H NMR (400 MHz, $CDCl_3$) δ 7.48 – 7.25 (m, 10H), 5.81 – 5.66 (m, 1H), 5.60 – 5.47 (m, 1H), 4.54 – 4.38 (m, 2H), 4.37 – 4.22 (m, 2H), 3.59 – 3.48 (m, 1H), 3.15 (ddd, *J* = 15.8, 11.1, 5.6 Hz, 1H), 3.08 – 2.97 (m, 1H), 2.60 – 2.46 (m, 1H), 2.45 – 2.10 (m, 4H), 1.84 – 1.66 (m, 2H), 1.48 (s, 3H), 0.96 (s, 9H).

^{13}C NMR (101 MHz, $CDCl_3$) δ 212.15, 176.35, 154.96, 152.70, 150.66, 138.18, 137.04, 131.28, 129.01, 128.94, 128.79, 128.27, 127.95, 125.52, 120.25, 65.84, 61.85, 57.35, 55.40, 55.36, 49.10, 42.48, 35.91, 35.80, 31.47, 29.13, 25.96, 23.84, 23.79.

IR (neat, cm^{-1}): 2973, 1776, 1711, 1418.

HRMS (EI) calculated for $C_{35}H_{38}N_4O_6$ $[M]^+$: 610.2791, found $[M]^+$: 610.2818.

Optical Rotation: $[\alpha]_d^{24}$ = -32° (c 0.5, DCM)

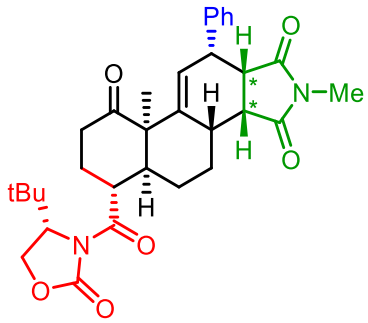

Tetracycle (2.6.2.1aba)

Synthesized according to GP1, reacting at 50°C for 48 h for the final DA step, using oxazolidinone dienophile **2.5.1.1b** (2 eq.)**,** diene **2.1.1.8a**, and N-methylmaleimide as the second dienophile**,** yielding **2.6.2.1aba** in 40% yield as a 7:1 mixture of diastereomers as a white foam**.**

^{1}H NMR (400 MHz, $CDCl_3$) δ 7.41 – 7.20 (m, 5H), 5.77 (t, *J* = 3.5 Hz, 1H), 4.49 (dd, *J* = 7.6, 1.5 Hz, 1H), 4.37 (td, *J* = 11.4, 3.3 Hz, 1H), 4.33 (dd, *J* = 9.3, 1.4 Hz, 1H), 4.24 (dd, *J* = 9.3, 7.6 Hz, 1H), 3.65 – 3.58 (m, 1H), 3.27 (dd, *J* = 8.4, 6.4 Hz, 1H), 3.17 (dd, *J* = 8.4, 6.1 Hz, 1H), 2.98 – 2.91 (m, 1H), 2.84 (s, 3H), 2.72 – 2.55 (m, 2H), 2.35 – 2.17 (m, 3H), 2.16 – 2.01 (m, 2H), 1.82 – 1.71 (m, 1H), 1.64 (ddt, *J* = 14.6, 6.7, 3.3 Hz, 1H), 1.21 (s, 3H), 0.98 (s, 9H).

^{13}C NMR (101 MHz, $CDCl_3$) δ 209.91, 178.13, 175.98, 174.56, 154.82, 142.84, 138.76, 128.90, 128.33, 127.24, 126.64, 65.29, 61.42, 53.33, 46.52, 46.39, 44.17, 42.39, 41.74, 37.49, 35.85, 32.16, 29.71, 25.92, 24.95, 24.56, 21.96, 19.71.

IR (neat, cm^{-1}): 2963, 2926, 2864, 1777, 1702.

HRMS (EI) calculated for $C_{32}H_{38}N_2O_6$ $[M]^+$: 546.2730, found $[M]^+$: 546.2701.

Optical Rotation: $[\alpha]_d^{24}$ = -38° (c 0.27, DCM)

MP: 273-276°C

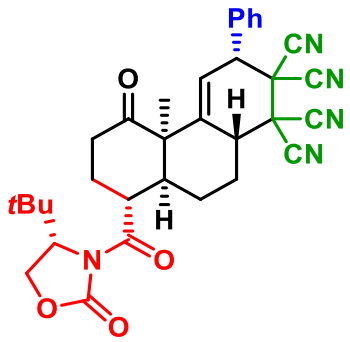

Tricycle (2.6.2.1abd)

Synthesized according to GP1, reacting at ambient temperature for 18 h for the final DA step, using oxazolidinone dienophile **2.5.1.1b** (2 eq.)**,** diene **2.1.1.8a**, and tetracyanoethylene as the second dienophile**,** yielding **2.6.2.1abd** in 46% yield as an off-white solid as the sole diastereomer**.**

^{1}H NMR (400 MHz, $CDCl_3$) δ 7.56 – 7.38 (m, 5H), 5.79 – 5.69 (m, 1H), 4.53 (dd, *J* = 7.7, 1.6 Hz, 1H), 4.44 – 4.35 (m, 2H), 4.31 (dd, *J* = 9.4, 7.7 Hz, 1H), 3.61 – 3.51 (m, 1H), 3.29 – 3.11 (m, 2H), 2.63 – 2.52 (m, 1H), 2.47 – 2.29 (m, 4H), 2.31 – 2.10 (m, 2H), 1.79 – 1.66 (m, 1H), 1.53 (s, 3H), 1.03 (s, 9H).

^{13}C NMR (101 MHz, $CDCl_3$) δ 211.81, 176.03, 154.86, 140.85, 133.86, 130.31, 129.68, 129.51, 120.23, 111.37, 111.18, 110.23, 110.19, 65.91, 61.92, 56.38, 49.18, 46.94, 43.75, 42.91, 42.16, 42.14, 35.95, 35.83, 31.37, 29.57, 26.05, 24.88, 24.05, 23.49.

IR (neat, cm^{-1}): 2926, 2362, 2340, 1774, 1708.

LRMS (APCI-) calculated for $C_{33}H_{32}N_5O_4$ $[M-H]^+$: 562.2, found $[M-H]^+$: 562.3.

Optical Rotation: $[\alpha]_d^{24}$ = +139° (c 0.2, DCM)

MP: decomposition at ~250°C

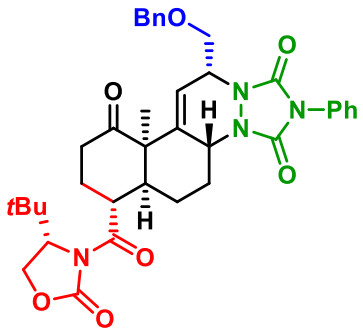

Tetracycle (**2.6.2.1bbc)**

Synthesized according to GP1, reacting at ambient temperature for 18 h for the final DA step, using oxazolidinone dienophile **2.5.1.1b** (2 eq.)**,** diene **2.1.1.8b**, and 4-phenyl-1,2,4-triazoline-3,5-dione as the second dienophile**,** yielding **2.6.2.1bbc** in 39% yield as a white foam as the sole diastereomer**.**

^{1}H NMR (400 MHz, $CDCl_3$) δ 7.52 – 7.41 (m, 4H), 7.39 – 7.23 (m, 6H), 5.81 – 5.75 (m, 1H), 4.77 – 4.69 (m, 1H), 4.

63 – 4.49 (m, 3H), 4.39 – 4.24 (m, 3H), 3.92 (dd, *J* = 9.8, 5.0 Hz, 1H), 3.79 (dd, *J* = 9.8, 6.0 Hz, 1H), 3.53 – 3.47 (m, 1H), 3.24 – 3.11 (m, 1H), 2.73 (dq, *J* = 12.0, 3.8 Hz, 1H), 2.53 – 2.43 (m,f 1H), 2.42 – 2.29 (m, 2H), 2.28 – 2.11 (m, 2H), 1.80 – 1.64 (m, 1H), 1.62 – 1.47 (m, 1H), 1.52 (s, 3H), 1.00 (s, 9H).

^{13}C NMR (101 MHz, $CDCl_3$) δ 212.32, 176.48, 154.88, 151.73, 151.09, 139.54, 137.92, 131.48, 129.17, 128.59, 128.07, 127.92, 127.61, 125.74, 118.16, 73.39, 69.90, 65.83, 61.86, 55.71, 54.65, 53.35, 49.45, 42.35, 35.96, 35.77, 31.58, 29.67, 26.03, 23.77, 23.58.

IR (neat, cm^{-1}): 2962, 2859, 2360, 1777, 1709.

HRMS (EI) calculated for $C_{37}H_{43}N_4O_7$ $[M]^+$: 654.3053, found $[M]^+$: 654.3075.

Optical Rotation: $[\alpha]_d^{24}$ = +11° (c 0.4, DCM)

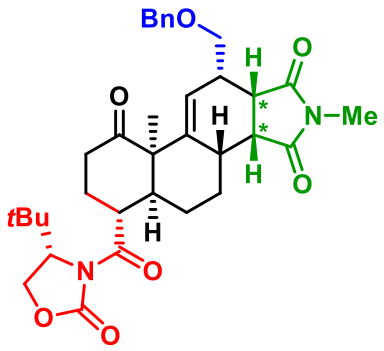

Tetracycle (2.6.2.1bba)

Synthesized according to GP1, reacting at 50°C for 48 h for the final DA step, using oxazolidinone dienophile **2.5.1.1b** (2 eq.)**,** diene **2.1.1.8b**, and N-methylmaleimide as the second dienophile**,** yielding **2.6.2.1bba** in 52% yield as 8:1 mixture of diastereomers as a white foam**.**

^{1}H NMR (400 MHz ,$CDCl_3$) δ 7.38 – 7.32 (m, 4H), 7.32 – 7.28 (m, 1H), 5.24 – 5.19 (m, 1H), 4.59 (q, *J* = 11.8 Hz, 2H), 4.47 (dd, *J* = 1.4, 7.5 Hz, 1H), 4.36 – 4.27 (m, 2H), 4.26 – 4.19 (m, 1H), 4.02 (dd, *J* = 7.6, 9.1 Hz, 1H), 3.76 (dd, *J* = 7.7, 9.1 Hz, 1H), 3.22 (dd, *J* = 6.0, 8.4 Hz, 1H), 3.07 (dd, *J* = 6.6, 8.4 Hz, 1H), 2.86 (s, 3H), 2.80 – 2.66 (m, 2H), 2.63 – 2.54 (m, 1H), 2.54 - 2.45 (m, 1H), 2.33 - 2.23 (m, 2H), 2.23 - 2.10 (m, 1H), 2.09 - 1.94 (m, 2H), 1.82 - 1.68 (m, 1H), 1.63 - 1.53 (m, 1H), 1.08 (s, 3H), 0.95 (s, 9H).

^{13}C NMR (101 MHz ,$CDCl_3$) δ 209.98, 178.64, 177.29, 174.63, 154.68, 142.14, 138.37, 128.54, 127.98, 127.79, 126.59, 73.56, 70.14, 65.25, 61.39, 53.04, 46.42, 44.12, 41.58, 41.55, 37.82, 37.41, 35.84, 32.05, 29.63, 25.93, 25.08, 24.89, 24.60, 21.98, 19.49.

IR (neat, cm^{-1}): 2926, 2873, 1775, 1698.

HRMS (EI) m/z calc'd for $C_{27}H_{35}N_2O_7$ $[M\text{-}Bn]^+$: 499.2444, found $[M\text{-}Bn]^+$: 499.2452.

Optical Rotation: $[\alpha]_d^{24}$ = +21° (c 0.38, DCM)

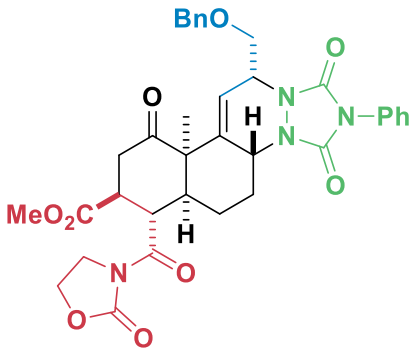

Tetracycle (2.6.2.1bcc)

Synthesized according to GP1, reacting at ambient temperature for 18 h for the final DA step, using oxazolidinone dienophile **2.5.1.1c** (1.1 eq.), diene **2.1.1.8b**, and 4-phenyl-1,2,4-triazoline-3,5-dione as the second dienophile, yielding **2.6.2.1bcc** in 36% yield as a white foam as the sole diastereomer.

^{1}H NMR (400 MHz, $CDCl_3$) δ 7.52 – 7.40 (m, 4H), 7.38 – 7.27 (m, 6H), 5.83 (dd, *J* = 4.3, 1.4 Hz, 1H), 4.77 – 4.68 (m, 1H), 4.61 – 4.52 (m, 2H), 4.54 – 4.40 (m, 2H), 4.31 (dd, *J* = 9.0, 2.0 Hz, 1H), 4.20 – 4.10 (m, 2H), 4.09 – 3.94 (m, 2H), 3.93 (dd, *J* = 10.0, 4.8 Hz, 1H), 3.78 (dd, *J* = 9.9, 6.1 Hz, 1H), 3.72 (s, 3H), 3.05 (dd, *J* = 18.0, 5.6 Hz, 1H), 2.79 – 2.66 (m, 2H), 2.57 – 2.46 (m, 1H), 2.01 (ddd, *J* = 12.2, 4.7, 2.0 Hz, 1H), 1.64 – 1.51 (m, 1H), 1.51 – 1.41 (m, 1H), 1.40 (s, 3H).

^{13}C NMR (101 MHz, $CDCl_3$) δ 209.33, 174.69, 173.15, 153.30, 151.73, 151.02, 138.88, 137.90, 131.40, 129.18, 128.58, 128.14, 127.97, 127.69, 125.70, 118.89, 73.49, 69.92, 62.25, 54.83, 54.33, 53.27, 52.85, 46.61, 43.97, 43.47, 38.53, 37.63, 31.44, 30.62, 22.14.

IR (neat, cm^{-1}): 2972, 2891, 2359, 1773, 1709.

HRMS (ESI) m/z calc'd for $C_{35}H_{36}N_4O_9Na$ [M+Na]: 679.2380, found [M+Na]: 679.2357.

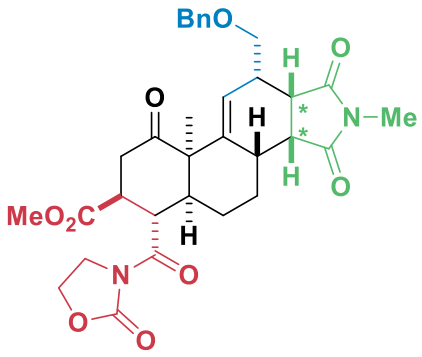

Tetracycle (2.6.2.1bca)

Synthesized according to GP1, reacting at 50°C for 48 h for the final DA step, using oxazolidinone dienophile **2.5.1.1c** (1.1 eq.)**,** diene **2.1.1.8b**, and N-methylmaleimide as the second dienophile**,** yielding **2.6.2.1cba** in 43% yield as 9:1 mixture of diastereomers as a white foam**.**

^{1}H NMR (400 MHz, $CDCl_3$) δ 7.34 (d, *J* = 3.4 Hz, 4H), 7.31 – 7.27 (m, 1H), 5.19 (t, *J* = 3.3 Hz, 1H), 4.64 – 4.38 (m, 5H), 4.15 – 4.03 (m, 2H), 3.99 (dd, *J* = 9.2, 7.2 Hz, 1H), 3.73 (dd, *J* = 9.2, 7.9 Hz, 1H), 3.63 (s, 3H), 3.19 (dd, *J* = 8.5, 6.1 Hz, 1H), 3.15 – 3.07 (m, 1H), 3.09 – 3.00 (m, 1H), 2.86 (t, *J* = 14.1 Hz, 1H), 2.84 (s, 3H), 2.79 – 2.72 (m, 1H), 2.68 (dd, *J* = 14.2, 4.3 Hz, 1H), 2.60 – 2.45 (m, 2H), 2.21 – 2.10 (m, 2H), 2.04 – 1.94 (m, 1H), 1.49 – 1.38 (m, 1H), 1.06 (s, 3H).

^{13}C NMR (101 MHz, $CDCl_3$) δ 207.94, 178.70, 177.19, 175.24, 172.20, 153.93, 141.53, 138.35, 128.57, 128.00, 127.82, 126.67, 73.56, 70.10, 62.00, 52.78, 52.56, 46.46, 46.17, 44.56, 43.19, 42.65, 41.55, 39.10, 37.76, 31.60, 24.60, 24.17, 21.24, 18.72.

IR (neat, cm^{-1}): 2928, 1777, 1697, 1385.

HRMS (ESI) m/z calc'd for $C_{32}H_{36}N_2O_9Na$ [M+Na]: 615.2318, found [M+Na]: 615.2329.

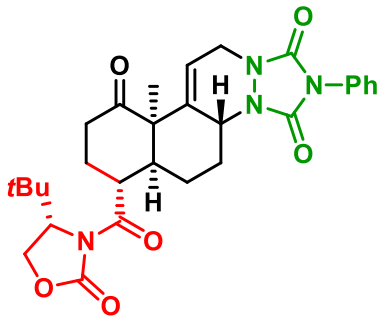

Tetracycle (2.6.2.1cbc)

Synthesized according to GP1, reacting at ambient temperature for 18 h for the final DA step, using oxazolidinone dienophile **2.5.1.1b** (2 eq.)**,** diene **2.1.1.8c**, and 4-phenyl-1,2,4-triazoline-3,5-dione as the second dienophile**,** yielding **2.6.2.1cbc** in 33% yield as an off-white solid as the sole diastereomer**.**

^{1}H NMR (400 MHz, $CDCl_3$) δ 7.57 – 7.47 (m, 2H), 7.52 – 7.41 (m, 2H), 7.39 – 7.33 (m, 1H), 5.77 – 5.68 (m, 1H), 4.53 (dd, *J* = 7.7, 1.7 Hz, 1H), 4.48 – 4.40 (m, 1H), 4.39 – 4.33 (m, 1H), 4.32 – 4.25 (m, 2H), 4.20 – 4.08 (m, 1H), 3.52 – 3.45 (m, 1H), 3.25 – 3.12 (m, 1H), 2.53 – 2.34 (m, 4H), 2.33 – 2.24 (m, 1H), 2.23 – 2.13 (m, 1H), 1.74 (qd, *J* = 13.3, 4.0 Hz, 1H), 1.64 – 1.52 (m, 1H), 1.52 (s, 3H), 1.01 (s, 9H).

^{13}C NMR (101 MHz, $CDCl_3$) δ 211.45, 175.45, 153.84, 151.92, 150.18, 138.24, 130.42, 128.23, 127.13, 124.58, 114.17, 64.82, 60.80, 55.03, 52.91, 48.66, 42.72, 41.15, 34.97, 34.71, 29.16, 28.88, 25.01, 22.51, 22.26.

IR (neat, cm^{-1}): 2962, 2928, 2857, 1779, 1703.

HRMS (EI) calculated for $C_{29}H_{34}N_4O_6$ $[M]^+$: 534.2478, found $[M]^+$: 534.2478.

Optical Rotation: $[\alpha]_d^{24}$ = -19° (c 0.2, DCM)

XRAY: CCDD 1967540

MP: 276-278°C

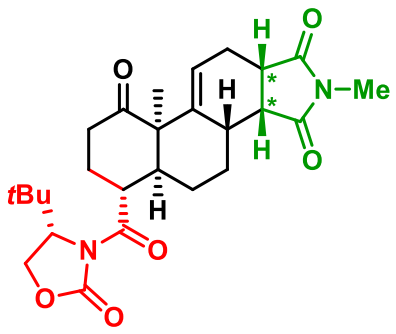

Tetracycle (2.6.2.1cba)

Synthesized according to GP1, reacting at 50°C for 18 h for the final DA step, using oxazolidinone dienophile **2.5.1.1b** (2 eq.)**,** diene **2.1.1.8c**, and N-methylmaleimide as the second dienophile**,** yielding **2.6.2.1cba** in 43% yield as 5:1 mixture of diastereomers as a white foam**.**

^{1}H NMR (400 MHz, $CDCl_3$) δ 5.40 – 5.31 (m, 1H), 4.48 (dd, *J* = 7.6, 1.5 Hz, 1H), 4.37 – 4.25 (m, 2H), 4.23 (dd, *J* = 9.3, 7.6 Hz, 1H), 3.09 – 3.02 (m, 2H), 2.p 3H), 2.78 – 2.67 (m, 2H), 2.65 (dd, *J* = 14.1, 5.9 Hz, 1H), 2.54 – 2.41 (m, 1H), 2.35 – 2.21 (m, 2H), 2.24 – 1.97 (m, 4H), 1.82 – 1.66 (m, 1H), 1.62 – 1.53 (m, 1H), 1.10 (s, 3H), 1.00 – 0.94 (m, 9H).

^{13}C NMR (101 MHz, $CDCl_3$) δ 210.02, 179.54, 179.11, 174.65, 154.81, 142.92, 123.81, 65.30, 61.41, 53.26, 46.37, 44.19, 41.78, 40.12, 37.45, 35.87, 31.43, 29.73, 25.94, 25.03, 24.91, 24.78, 22.06, 20.06.

IR (neat, cm^{-1}): 2967, 2875, 1774, 1698.

HRMS (ESI) m/z calc'd for $C_{26}H_{34}N_2O_6Na$ [M+Na]: 493.2315, found [M+Na]: 493.2326.

Optical Rotation: $[\alpha]_d^{24}$ = +56° (c 0.12, DCM)

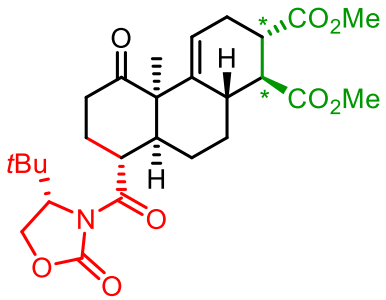

Tricycle (2.6.2.1cbe)

Synthesized according to GP1, reacting at 50°C for 48 h for the final DA step, using oxazolidinone dienophile **2.5.1.1b** (2 eq.)**,** diene **2.1.1.8c**, and dimethyl fumarate as the second dienophile**,** yielding **2.6.2.1cbe** in 37% yield as 3:1 mixture of diastereomers as a white foam**.**

^{1}H NMR (400 MHz, $CDCl_3$) δ 5.45 (dt, *J* = 5.2, 2.2 Hz, 1H), 4.48 (dd, *J* = 7.6, 1.6 Hz, 1H), 4.32 (dd, *J* = 9.3, 1.6 Hz, 1H), 4.24 (dd, *J* = 9.3, 7.6 Hz, 1H), 3.91 (q, *J* = 6.6 Hz, 1H), 3.70 (s, 3H), 3.66 (s, 3H), 2.99 (td, *J* = 11.7, 5.4 Hz, 1H), 2.72 – 2.60 (m, 2H), 2.55 – 2.41 (m, 2H), 2.40 (dd, *J* = 11.7, 10.1 Hz, 1H), 2.35 – 2.28 (m, 1H), 2.19 (dddd, *J* = 17.9, 11.7, 4.0, 2.3 Hz, 1H), 2.13 – 1.98 (m, 2H), 1.98 – 1.86 (m, 1H), 1.49 (ddt, *J* = 13.7, 10.7, 6.7 Hz, 1H), 1.37 (s, 3H), 1.36 – 1.23 (m, 2H), 0.97 (s, 9H).

^{13}C NMR (101 MHz, $CDCl_3$) δ 211.46, 176.09, 174.91, 174.82, 154.64, 139.90, 121.31, 65.50, 61.74, 54.21, 52.06, 51.97, 50.08, 45.89, 44.08, 41.89, 37.00, 36.55, 35.96, 28.74, 27.89, 27.00, 26.33, 26.02, 25.07.

IR (neat, cm^{-1}): 2956, 2875, 1779, 1736, 1702.

HRMS (ESI) m/z calc'd for $C_{27}H_{37}NO_8Na$ [M+Na]: 526.2417, found [M+Na]: 526.2437.

Optical Rotation: $[\alpha]_d^{24}$ = +19° (c 0.17, DCM)

5.2.3 Diels-Alder/Au 6-*endo*-dig/Prins Scope Characterization

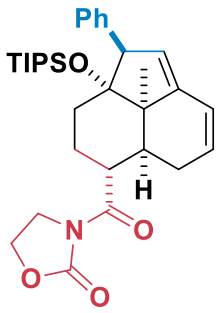

Tricycle (2.6.1.1aa)

Synthesized according to GP2 using oxazolidinone dienophile **2.5.1.1a** (2 eq.) and diene **2.1.1.8a,** reacting for 24 h for the gold cyclization, yielding **2.6.1.1aa** in 48% yield as a white foam as the sole diastereomer**.**

^{1}H NMR (400 MHz, $CDCl_3$) δ 7.32 – 7.18 (m, 5H), 6.22 (dd, *J* = 9.9, 2.8 Hz, 1H), 5.70 – 5.62 (m, 1H), 5.49 – 5.43 (m, 1H), 4.39 (t, *J* = 8.3 Hz, 2H), 4.26 – 4.22 (m, 1H), 4.10 – 3.94 (m, 2H), 3.59 (td, *J* = 11.6, 3.3 Hz, 1H), 2.62 – 2.49 (m, 1H), 2.34 (dd, *J* = 11.7, 5.9 Hz, 1H), 2.00 (td, *J* = 14.1, 3.9 Hz, 1H), 1.81 (dd, *J* = 19.4, 5.9 Hz, 1H), 1.68 – 1.51 (m, 2H), 1.30 (s, 3H), 1.15 – 1.08 (m, 1H), 1.05 – 0.95 (m, 21H).

^{13}C NMR (101 MHz, $CDCl_3$) δ 176.47, 153.13, 144.31, 139.32, 130.50, 127.90, 126.93, 126.90, 126.07, 123.33, 87.76, 61.93, 59.08, 50.64, 43.32, 42.89, 36.51, 31.88, 28.11, 25.73, 19.86, 18.78, 14.27.

IR (neat, cm^{-1}): 2967, 2945, 2867, 1778, 1698.

HRMS (EI) calculated for $C_{32}H_{45}NO_4Si$ $[M]^+$: 535.3118, found $[M]^+$: 535.3112.

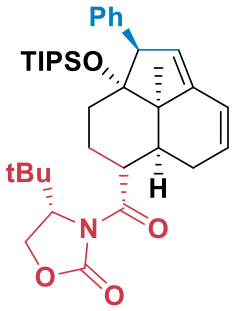

Tricycle (2.6.1.1ab)

Synthesized according to GP2 using oxazolidinone dienophile **2.5.1.1b** (2 eq.) and diene **2.1.1.8a,** reacting for 24 h for the gold cyclization, yielding **2.6.1.1ab** in 54% yield as a white foam as the sole diastereomer**.**

^{1}H NMR (400 MHz, $CDCl_3$) δ 7.37 – 7.18 (m, 5H), 6.25 (dd, *J* = 9.9, 2.9 Hz, 1H), 5.76 – 5.68 (m, 1H), 5.48 – 5.44 (m, 1H), 4.45 (dd, *J* = 7.5, 1.5 Hz, 1H), 4.27 – 4.21 (m, 2H), 4.17 (dd, *J* = 9.3, 7.5 Hz, 1H), 3.70 (td, *J* = 11.4, 3.6 Hz, 1H), 2.64 – 2.52 (m, 1H), 2.36 (dd, *J* = 11.7, 5.8 Hz, 1H), 1.98 (td, *J* = 13.6, 4.2 Hz, 1H), 1.88 (dd, *J* = 19.4, 6.0 Hz, 1H), 1.62 – 1.44 (m, 2H), 1.31 (s, 3H), 1.09 (dt, *J* = 14.6, 3.2 Hz, 1H), 1.05 – 0.90 (m, 30H).

^{13}C NMR (101 MHz, $CDCl_3$) δ 176.30, 154.44, 144.38, 139.32, 130.51, 127.90, 126.93, 126.77, 126.06, 123.48, 87.82, 65.10, 61.29, 59.07, 50.74, 43.39, 36.77, 35.79, 31.91, 28.27, 25.99, 25.92, 19.86, 18.80, 18.77, 14.25.

IR (neat, cm^{-1}): 2967, 2946, 2867, 2363, 2345, 1782, 1702.

HRMS (EI): m/z calc'd for $C_{36}H_{53}NO_4Si$ $[M]^+$= 591.3744, found $[M]^+$= 591.3732.

Optical Rotation: $[\alpha]_d^{24}$ = -213° (c 0.15, DCM)

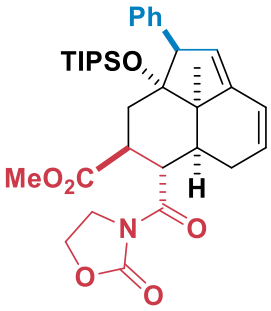

Tricycle (2.6.1.1ac)

Synthesized according to GP2 using oxazolidinone dienophile **2.5.1.1c** (2 eq.) and diene **2.1.1.8a,** reacting for 48 h for the gold cyclization, yielding a 11:1 6-*endo-dig* **(2.6.1.1ac)** : 5-*exo-dig* mixture in 75% yield as a white foam**.**

^{1}H NMR (400 MHz, $CDCl_3$) δ 7.32 – 7.18 (m, 5H), 6.22 (dd, *J* = 9.8, 2.7 Hz, 1H), 5.76 – 5.66 (m, 1H), 5.45 – 5.38 (m, 1H), 4.45 – 4.31 (m, 2H), 4.28 – 4.23 (m, 1H), 4.23 – 4.14 (m, 1H), 4.07 – 3.98 (m, 2H), 3.49 (s, 3H), 3.06 (ddd, *J* = 13.7, 11.1, 2.6 Hz, 1H), 2.56 – 2.44 (m, 1H), 2.19 (dd, *J* = 11.8, 5.8 Hz, 1H), 2.05 (t, *J* = 13.9 Hz, 1H), 1.83 (dd, *J* = 19.1, 5.9 Hz, 1H), 1.49 (dd, *J* = 14.3, 2.6 Hz, 1H), 1.26 (s, 3H), 1.17 – 1.06 (m, 3H), 1.05 – 0.97 (m, 18H).

^{13}C NMR (101 MHz, $CDCl_3$) δ 177.50, 175.08, 153.24, 143.72, 138.77, 130.48, 128.05, 127.18, 127.13, 125.92, 122.75, 87.90, 61.71, 59.08, 52.09, 50.89, 43.42, 43.07, 42.36, 39.45, 34.56, 27.25, 19.62, 18.78, 18.67, 13.93.

IR (neat, cm^{-1}): 2944, 2867, 1781, 1734, 1696.

HRMS (EI) calculated for $C_{34}H_{47}NO_6Si$ $[M]^+$: 593.3173, found [M+]: 593.3190.

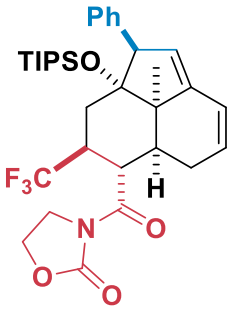

Tricycle (2.6.1.1ad)

Synthesized according to GP2 using oxazolidinone dienophile **2.5.1.1d** (2 eq.) and diene **2.1.1.8a,** reacting for 48 h for the gold cyclization, yielding **2.6.1.1ad** in 58% yield as a white foam as the sole isomer**.**

^{1}H NMR (400 MHz, $CDCl_3$) δ 7.36 – 7.20 (m, 5H), 6.32 – 6.20 (m, 1H), 5.79 – 5.67 (m, 1H), 5.51 – 5.42 (m, 1H), 4.47 – 4.34 (m, 2H), 4.31 (s, 1H), 4.23 (t, *J* = 11.4 Hz, 1H), 4.14 – 3.94 (m, 2H), 2.90 – 2.74 (m, 1H), 2.62 – 2.47 (m, 1H), 2.32 (dd, *J* = 11.6, 5.9 Hz, 1H), 2.06 (t, *J* = 13.8 Hz, 1H), 1.78 (dd, *J* = 19.2, 5.9 Hz, 1H), 1.45 – 1.36 (m, 1H), 1.30 (s, 3H), 1.11 – 0.97 (m, 21H).

^{13}C NMR (101 MHz, $CDCl_3$) δ 175.76, 152.88, 143.47, 138.38, 130.41, 128.22, 127.36, 126.93, 126.21, 122.99, 87.03, 61.81, 59.09, 50.43, 43.11, 40.92, 40.73 (q, *J* = 25.7 Hz), 39.00, 30.77, 27.35, 19.63, 18.72, 18.56, 13.88.

^{19}F NMR (282 MHz, $CDCl_3$) δ -69.89 (d, *J* = 7.8 Hz).

IR (neat, cm^{-1}): 2946, 2869, 1780, 1699, 1388, 1166, 1119.

HRMS (EI): m/z calc'd for $C_{30}H_{37}F_3NO_4Si$ $[M\text{-}iPr]^+$ = 560.2444, found $[M\text{-}iPr]^+$ = 560.2432.

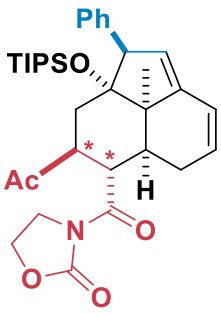

Tricycle (2.6.1.1ae)

Synthesized according to GP2 using oxazolidinone dienophile **2.5.1.1e** (2 eq.) and diene **2.1.1.8a,** reacting for 24 h for the gold cyclization, yielding a 6.2**:**1.6**:**1 6-*endo-dig* major diastereomer **(2.6.1.1ae)** : 6-*endo-dig* minor diastereomer : 5-*exo-dig* mixture in 76% yield as a white foam**.**

^{1}H NMR (400 MHz, $CDCl_3$) δ 7.34 – 7.20 (m, 5H), 6.23 (dd, *J* = 9.9, 2.8 Hz, 1H), 5.79 – 5.70 (m, 1H), 5.43 (s, 1H), 4.47 – 4.32 (m, 2H), 4.33 – 4.28 (m, 1H), 4.19 – 4.07 (m, 1H), 4.01 (t, *J* = 8.3 Hz, 2H), 3.15 (ddd, *J* = 13.6, 10.7, 2.6 Hz, 1H), 2.56 – 2.45 (m, 1H), 2.16 (dd, *J* = 11.9, 5.8 Hz, 1H), 2.00 – 1.81 (m, 2H), 1.90 (s, 3H), 1.43 (dd, *J* = 13.9, 2.7 Hz, 1H), 1.28 (s, 3H), 1.21 – 1.11 (m, 3H), 1.11 – 1.03 (m, 18H).

^{13}C NMR (101 MHz, $CDCl_3$) δ 211.05, 177.76, 153.21, 143.88, 138.67, 130.35, 128.09, 127.57, 127.26, 125.39, 122.51, 87.98, 61.67, 59.11, 50.95, 50.74, 43.05, 42.90, 39.11, 34.75, 27.95, 27.13, 19.75, 18.83, 18.63, 14.20.

IR (neat, cm^{-1}): 2943, 2866, 2357, 1777, 1706, 1685.

HRMS (EI): m/z calc'd for $C_{34}H_{47}NO_5Si$ $[M]^+$= 577.3224, found $[M]^+$= 577.3201.

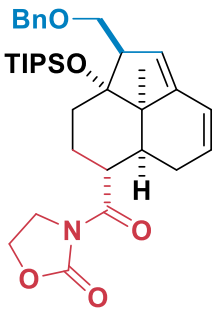

Tricycle (2.6.1.1ba)

Synthesized according to GP2 using oxazolidinone dienophile **2.5.1.1a** (2 eq.) and diene **2.1.1.8b,** reacting for 24 h for the gold cyclization, yielding a 2:1 6-*endo-dig* **(2.6.1.1ba)**: 5-*exo-dig* mixture in 55% yield as a white foam**.**

^{1}H NMR (400 MHz, $CDCl_3$) δ 7.40 – 7.24 (m, 5H), 6.15 (dd, *J* = 9.9, 2.8 Hz, 1H), 5.63 – 5.54 (m, 1H), 5.51 – 5.46 (m, 1H), 4.59 (d, *J* = 12.0 Hz, 1H), 4.45 (d, *J* = 12.1 Hz, 1H), 4.37 (t, *J* = 8.1 Hz, 2H), 4.09 – 3.92 (m, 2H), 3.70 (dd, *J* = 8.4, 3.3 Hz, 1H), 3.47 (td, *J* = 11.4, 3.3 Hz, 1H), 3.31 (dd, *J* = 10.4, 8.4 Hz, 1H), 3.21 – 3.11 (m, 1H), 2.54 – 2.42 (m, 1H), 2.24 (dd, *J* = 11.7, 5.8 Hz, 1H), 1.85 (td, *J* = 13.4, 3.8 Hz, 1H), 1.82 – 1.71 (m, 1H), 1.68 – 1.51 (m, 2H), 1.50 – 1.40 (m, 1H), 1.12 (s, 3H), 1.10 – 0.98 (m, 21H).

^{13}C NMR (101 MHz, $CDCl_3$) δ 176.37, 153.08, 143.67, 138.43, 128.52, 128.11, 127.80, 126.57, 123.69, 123.35, 84.58, 73.69, 68.85, 61.90, 52.57, 50.31, 43.13, 42.86, 36.31, 31.70, 27.93, 25.75, 20.32, 18.72, 18.66, 13.85.

IR (neat, cm^{-1}): 2945, 2867, 1778, 1698.

HRMS (EI) calculated for $C_{31}H_{42}NO_5Si$ $[M\text{-}iPr]^+$: 536.2832, found $[M\text{-}iPr]^+$: 536.2804.

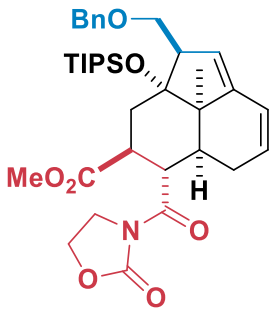

Tricycle (2.6.1.1bc)

Synthesized according to GP2 using oxazolidinone dienophile **2.5.1.1c** (1.1 eq.) and diene **2.1.1.8b,** reacting for 24 h for the gold cyclization using Me_4tBuXPhos Au(NCMe)SbF6 (7 mg, 8 μmol, 5 mol%) as the catalyst, yielding a 8:1 6-*endo-dig* **(2.6.1.1bc)** : 5-*exo-dig* mixture in 55% yield as a white foam**.**

^{1}H NMR (400 MHz, $CDCl_3$) δ 7.40 – 7.25 (m, 5H), 6.18 (dd, *J* = 9.9, 2.8 Hz, 1H), 5.71 – 5.62 (m, 1H), 5.49 – 5.44 (m, 1H), 4.60 (d, *J* = 12.1 Hz, 1H), 4.46 (d, *J* = 12.1 Hz, 1H), 4.46 – 4.31 (m, 2H), 4.15 – 4.04 (m, 1H), 4.03 (t, *J* = 8.1 Hz, 2H), 3.74 (dd, *J* = 8.4, 3.3 Hz, 1H), 3.58 (s, 3H), 3.32 (dd, *J* = 10.1, 8.4 Hz, 1H), 3.23 – 3.17 (m, 1H), 3.06 (ddd, *J* = 12.7, 11.1, 3.4 Hz, 1H), 2.52 – 2.37 (m, 1H), 2.11 (dd, *J* = 11.7, 5.8 Hz, 1H), 1.95 – 1.74 (m, 3H), 1.13 – 1.02 (m, 24H).

^{13}C NMR (101 MHz, $CDCl_3$) δ 174.92, 153.22, 143.20, 138.38, 128.54, 128.05, 127.84, 126.90, 123.38, 122.82, 84.79, 73.68, 68.62, 61.70, 52.53, 52.07, 50.41, 43.15, 43.07, 42.19, 39.22, 34.34, 27.14, 20.09, 18.67, 18.63, 13.81.

IR (neat, cm^{-1}): 2964, 2867, 2363, 2339, 1781, 1734, 1697.

HRMS (EI) calculated for $C_{33}H_{44}NO_7Si$ $[M\text{-}iPr]^+$: 594.2887, found $[M\text{-}iPr]^+$: 594.2884.

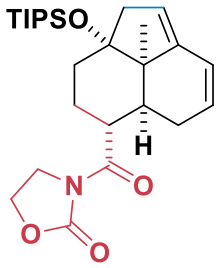

Tricycle (2.6.1.1ca)

Synthesized according to GP2 using oxazolidinone dienophile **2.5.1.1a** (2 eq.) and diene **2.1.1.8c,** reacting for 24 h for the gold cyclization, yielding a 2.3:1 6-*endo-dig* **(2.6.1.1ca)** : 5-*exo-dig* mixture in 83% yield as a white foam**.**

^{1}H NMR (400 MHz, $CDCl_3$) δ 6.15 (dd, *J* = 9.9, 2.9 Hz, 1H), 5.63 – 5.53 (m, 1H), 5.40 – 5.33 (m, 1H), 4.38 (t, *J* = 8.1 Hz, 2H), 4.10 – 3.93 (m, 2H), 3.58 – 3.44 (m, 1H), 2.74 – 2.64 (m, 1H), 2.54 – 2.42 (m, 1H), 2.24 (dd, *J* = 11.7, 5.9 Hz, 1H), 2.14 (dd, *J* = 15.6, 3.6 Hz, 1H), 1.97 – 1.85 (m, 1H), 1.83 – 1.74 (m, 2H), 1.67 – 1.59 (m, 2H), 1.13 – 1.05 (m, 24H).

^{13}C NMR (101 MHz, $CDCl_3$) δ 176.60, 153.10, 144.63, 126.40, 123.43, 121.39, 82.47, 61.89, 49.43, 44.58, 43.20, 42.89, 36.54, 36.44, 27.96, 26.07, 20.80, 18.60, 18.53, 13.62.

IR (neat, cm^{-1}): 2945, 2867, 1778, 1698.

HRMS (EI) calculated for $C_{23}H_{34}NO_4Si$ $[M\text{-}iPr]^+$: 416.2257, found $[M\text{-}iPr]^+$: 416.2282.

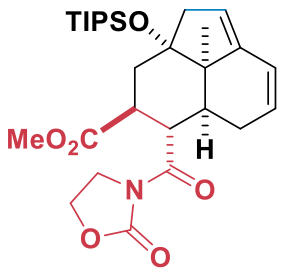

Tricycle (2.6.1.1cc)

Synthesized according to GP2 using oxazolidinone dienophile **2.5.1.1c** (2 eq.) and diene **2.1.1.8c,** reacting for 24 h for the gold cyclization, yielding a 1.5:1 6-*endo-dig* **(2.6.1.1cc)** : 5-*exo-dig* mixture in 92% yield as a white foam**.**

^{1}H NMR (400 MHz, $CDCl_3$) δ 6.18 (dd, *J* = 9.9, 2.8 Hz, 1H), 5.70 – 5.62 (m, 1H), 5.38 – 5.33 (m, 1H), 4.39 (td, *J* = 8.0, 5.9 Hz, 2H), 4.04 (t, *J* = 8.1 Hz, 2H), 3.59 (s, 3H), 3.12 (ddd, *J* = 13.8, 11.2, 3.0 Hz, 1H), 2.74 (d, *J* = 15.7 Hz, 1H), 2.51 – 2.39 (m, 1H), 2.23 – 2.09 (m, 3H), 1.95 (t, *J* = 13.7 Hz, 1H), 1.81 (dd, *J* = 19.1, 5.8 Hz, 1H), 1.73 – 1.57 (m, 1H), 1.16 – 1.10 (m, 21H), 1.09 (s, 3H).

^{13}C NMR (151 MHz, $CDCl_3$) δ 177.52, 175.06, 153.24, 144.17, 126.76, 122.90, 120.97, 82.63, 61.68, 52.05, 49.53, 44.27, 43.07, 42.38, 39.37, 38.81, 27.15, 20.53, 18.61, 18.51, 13.54, 13.54.

IR (neat, cm^{-1}): 2943, 2867, 2359, 2342, 1782, 1732, 1692.

HRMS (EI) calculated for $C_{25}H_{36}NO_6Si$ $[M\text{-}iPr]^+$: 474.2312, found $[M\text{-}iPr]^+$: 474.2317.

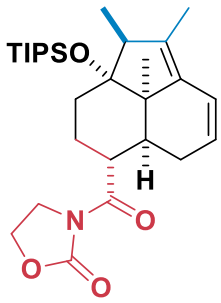

Tricycle (2.6.1.1da)

Synthesized according to GP2 using oxazolidinone dienophile **2.5.1.1a** (1.1 eq.) and diene **2.1.1.8d,** reacting for 24 h for the gold cyclization using Me_4tBuXPhos Au(NCMe)SbF6 (7 mg, 8 μmol, 5 mol%) as the catalyst, yielding **2.6.1.1da** in 39% yield as a white foam as the sole isomer**.**

^{1}H NMR (400 MHz, $CDCl_3$) δ 6.24 (dd, *J* = 10.0, 2.8 Hz, 1H), 5.57 – 5.46 (m, 1H), 4.38 (t, *J* = 8.1 Hz, 2H), 4.10 – 3.94 (m, 2H), 3.50 – 3.38 (m, 1H), 2.97 – 2.87 (m, 1H), 2.55 – 2.42 (m, 1H), 2.24 (dd, *J* = 11.7, 6.0 Hz, 1H), 1.76 (dd, *J* = 19.3, 5.9 Hz, 1H), 1.72 – 1.52 (m, 4H), 1.61 (s, 3H), 1.15 – 1.05 (m, 21H), 1.06 (s, 3H), 1.00 (d, *J* = 7.3 Hz, 3H).

^{13}C NMR (101 MHz, $CDCl_3$) δ 176.74, 153.13, 135.34, 132.54, 124.35, 120.92, 84.41, 61.90, 49.54, 49.13, 43.28, 42.90, 36.46, 31.46, 28.03, 26.03, 20.09, 18.83, 18.79, 14.03, 11.72, 10.49.

IR (neat, cm^{-1}): 2967, 2945, 2867, 1777, 1698.

HRMS (EI) calculated for $C_{28}H_{45}NO_4Si$ $[M]^+$: 487.3118, found $[M]^+$: 487.3092.

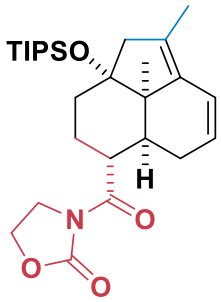

Tricycle (2.6.1.1ea)

Synthesized according to GP2 using oxazolidinone dienophile **2.5.1.1a** (1.1 eq.)**,** diene **2.1.1.8e,** JohnPhosAu(NCMe)SbF_6 (6 mg, 8 μmol, 5 mol%) as the gold catalyst, reacting for 24 h for the gold cyclization, to yield **2.6.1.1ea** in 39% yield as a white foam as the sole diastereomer**.**

^{1}H NMR (400 MHz, $CDCl_3$) δ 6.25 (dd, *J* = 9.9, 2.8 Hz, 1H), 5.56 – 5.47 (m, 1H), 4.37 (t, *J* = 8.1 Hz, 2H), 4.10 – 3.93 (m, 2H), 3.53 – 3.41 (m, 1H), 2.73 (d, *J* = 15.2 Hz, 1H), 2.52 – 2.40 (m, 1H), 2.20 (dd, *J* = 11.7, 6.0 Hz, 1H), 1.97 (d, *J* = 15.2 Hz, 1H), 1.86 – 1.70 (m, 3H), 1.67 (s, 3H), 1.66 – 1.55 (m, 2H), 1.12 – 1.07 (m, 21H), 1.06 (s, 3H).

^{13}C NMR (101 MHz, $CDCl_3$) δ 176.70, 153.10, 136.17, 129.95, 124.45, 120.78, 81.13, 61.88, 50.18, 50.05, 43.22, 42.90, 36.64, 36.47, 27.82, 26.05, 20.93, 18.61, 18.53, 14.34, 13.60.

IR (neat, cm^{-1}): 2942, 2868, 2361, 2340, 1782, 1698.

HRMS (EI) calculated for $C_{24}H_{36}NO_4Si$ $[M\text{-}iPr]^+$: 430.2414, found $[M\text{-}iPr]^+$: 430.2427.

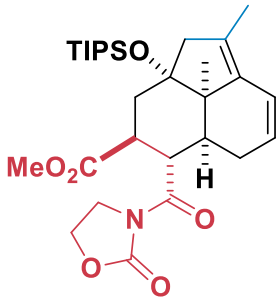

Tricycle (2.6.1.1ec)

Synthesized according to GP2 using oxazolidinone dienophile **2.5.1.1c** (1.1 eq.) and diene **2.1.1.8e,** reacting for 24 h for the gold cyclization, and IPrAu(NCMe)SbF_6 as the gold catalyst, yielding **2.6.1.1ec** in 54% yield as a white foam as the sole isomer**.**

^{1}H NMR (400 MHz

, $CDCl_3$) δ 6.27 (dd, *J* = 10.0, 2.8 Hz, 1Hp), 5.64 – 5.55 (m, 1H), 4.46 – 4.31 (m, 2H), 4.11 – 3.99 (m, 3H), 3.58 (s, 3H), 3.11 (ddd, *J* = 13.9, 11.1, 3.0 Hz, 1H), 2.77 (d, *J* = 15.3 Hz, 1H), 2.49 – 2.36 (m, 1H), 2.14 (dd, *J* = 13.9, 3.0 Hz, 1H), 2.08 (dd, *J* = 11.6, 5.9 Hz, 1H), 2.01 (d, *J* = 15.5 Hz, 1H), 1.89 – 1.73 (m, 2H), 1.66 (s, 3H), 1.15 – 1.11 (m, 21H), 1.04 (s, 3H).

^{13}C NMR (101 MHz, $CDCl_3$) δ 177.57, 175.11, 153.22, 135.80, 129.65, 124.79, 120.34, 81.36, 61.67, 51.99, 50.28, 49.73, 43.08, 42.38, 39.42, 38.95, 27.02, 20.66, 18.61, 18.51, 14.27, 13.54.

IR (neat, cm^{-1}): 2945, 2867, 1778, 1730, 1693.

HRMS (EI): m/z calc'd for $C_{26}H_{38}NO_6Si$ [M-iPr]$^+$ = 488.2468, found [M-iPr]$^+$= 488.2481.

5.2.4 Diels-Alder/Au 5-*exo* -dig/Prins Scope Characterization

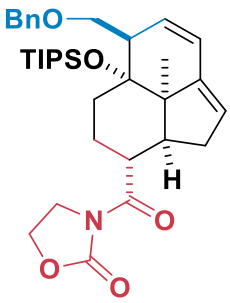

Tricycle (2.6.1.2ba)

Synthesized according to GP3 using oxazolidinone dienophile **2.5.1.1a** and diene **2.1.1.8b,** reacting for 24 h for the gold cyclization, yielding a 13:1 5-*exo-dig* **(2.6.1.2ba)** : 6-*endo-dig* mixture in 73% yield as a white foam**.**

^{1}H NMR (400 MHz, $CDCl_3$) δ 7.38 – 7.26 (m, 5H), 6.20 (dd, *J* = 9.7, 2.8 Hz, 1H), 5.84 – 5.78 (m, 1H), 5.41 – 5.35 (m, 1H), 4.59 (d, *J* = 11.8 Hz, 1H), 4.47 (d, *J* = 11.8 Hz, 1H), 4.37 (t, *J* = 8.1 Hz, 2H), 4.08 – 3.94 (m, 2H), 3.78 (dd, *J* = 8.0, 3.1 Hz, 1H), 3.46 (ddd, *J* = 12.4, 10.3, 3.8 Hz, 1H), 3.24 (dd, *J* = 10.4, 8.1 Hz, 1H), 2.86 – 2.78 (m, 1H), 2.75 – 2.59 (m, 2H), 1.81 – 1.55 (m, 3H), 1.47 (td, *J* = 13.1, 3.1 Hz, 1H), 1.40 (dt, *J* = 13.6, 3.5 Hz, 1H), 1.11 – 1.01 (m, 24H).

^{13}C NMR (101 MHz, $CDCl_3$) δ 176.27, 153.13, 147.84, 138.28, 130.29, 128.52, 128.23, 127.86, 122.01, 121.95, 77.43, 73.91, 69.97, 61.89, 53.07, 45.67, 44.58, 43.80, 43.06, 37.71, 30.53, 23.19, 19.61, 19.04, 18.97, 14.37.

IR (neat, cm^{-1}): 2944, 2866, 2862, 1779, 1694.

HRMS (EI): m/z calc'd for $C_{31}H_{42}NO_5Si$ [M-iPr]$^+$ = 536.2832, found [M-iPr]$^+$= 536.2847.

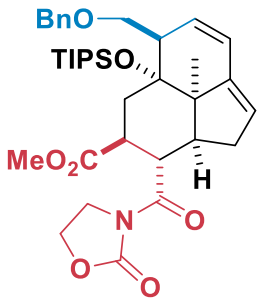

Tricycle (2.6.1.2bc)

Synthesized according to GP3 using oxazolidinone dienophile **2.5.1.1c** and diene **2.1.1.8b,** reacting for 24 h for the gold cyclization, yielding a 13:1 5-*exo-dig* **(2.6.1.2cb)** : 6-*endo-dig* mixture in 27% yield as a white foam**.**

^{1}H NMR (400 MHz, $CDCl_3$) δ 7.41 – 7.25 (m, 5H), 6.20 (dd, *J* = 9.8, 2.8 Hz, 1H), 5.85 – 5.75 (m, 1H), 5.51 – 5.45 (m, 1H), 4.61 (d, *J* = 11.8 Hz, 1H), 4.48 (d, *J* = 11.8 Hz, 1H), 4.44 – 4.32 (m, 2H), 4.09 – 4.00 (m, 3H), 3.84 (dd, *J* = 8.1, 3.0 Hz, 1H), 3.57 (s, 3H), 3.36 – 3.22 (m, 2H), 2.88 – 2.80 (m, 1H), 2.62 – 2.51 (m, 1H), 2.43 (dd, *J* = 10.4, 5.0 Hz, 1H), 2.01 (dd, *J* = 16.7, 3.4 Hz, 1H), 1.82 (dd, *J* = 13.6, 2.8 Hz, 1H), 1.50 (d, *J* = 13.3 Hz, 1H), 1.17 – 1.03 (m, 24H).

^{13}C NMR (101 MHz, $CDCl_3$) δ 177.54, 175.06, 153.59, 146.79, 138.26, 130.02, 128.55, 128.17, 127.90, 122.73, 121.96, 77.85, 73.96, 69.88, 61.70, 53.42, 52.04, 47.40, 45.48, 43.33, 43.26, 40.13, 35.84, 33.04, 19.12, 18.99, 18.93, 14.35.

IR (neat, cm^{-1}): 2944, 2867, 1780, 1731, 1694.

HRMS (EI): m/z calc'd for $C_{33}H_{44}NO_7Si$ $[M\text{-}iPr]^+$ = 594.2887, found $[M\text{-}iPr]^+$= 594.2917.

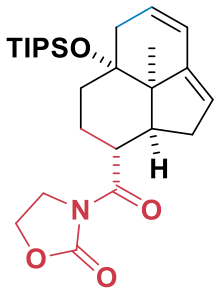

Tricycle (2.6.1.2ca)

Synthesized according to GP3 using oxazolidinone dienophile **2.5.1.1a** and diene **2.1.1.8c,** reacting for 24 h for the gold cyclization, yielding a 5:1 5-*exo-dig* **(2.6.1.2ca)** : 6-*endo-dig* mixture in 64% yield as a white foam**.**

^{1}H NMR (400 MHz, $CDCl_3$) δ 6.19 – 6.11 (m, 1H), 5.68 – 5.59 (m, 1H), 5.42 – 5.36 (m, 1H), 4.42 – 4.32 (m, 2H), 4.09 – 3.94 (m, 2H), 3.54 – 3.42 (m, 1H), 2.70 – 2.56 (m, 3H), 2.09 (dd, *J* = 17.6, 5.9 Hz, 1H), 1.87 – 1.46 (m, 5H), 1.14 – 1.02 (m, 24H).

^{13}C NMR (101 MHz, $CDCl_3$) δ 176.44, 153.18, 147.74, 127.24, 122.57, 74.34, 61.90, 52.60, 45.15, 44.01, 43.11, 39.20, 37.55, 34.85, 23.37, 19.94, 18.73, 18.66, 13.92.

HRMS (EI): m/z calc'd for $C_{23}H_{34}NO_4Si$ $[M\text{-}iPr]^+$ = 416.2257, found $[M\text{-}iPr]^+$= 416.2230.

IR (neat, cm^{-1}): 2943, 2867, 1778, 1699.

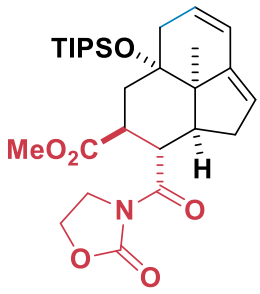

Tricycle (2.6.1.2cc)

Synthesized according to GP3 using oxazolidinone dienophile **2.5.1.1c** and diene **2.1.1.8c,** reacting for 24 h for the gold cyclization, yielding a 11:1 5-*exo-dig* **(2.6.1.2cc)** : 6-*endo-dig* mixture in 35% yield as a white foam**.**

^{1}H NMR (400 MHz, $CDCl_3$) δ 6.16 (dd, *J* = 9.7, 2.9 Hz, 1H), 5.67 – 5.58 (m, 1H), 5.53 – 5.47 (m, 1H), 4.46 – 4.31 (m, 2H), 4.11 – 4.00 (m, 3H), 3.57 (s, 3H), 3.40 – 3.28 (m, 1H), 2.72 – 2.62 (m, 1H), 2.62 – 2.52 (m, 1H), 2.39 (dd, *J* = 10.3, 5.0 Hz, 1H), 2.18 (dd, *J* = 17.4, 6.1 Hz, 1H), 2.02 (dd, *J* = 16.8, 3.3 Hz, 1H), 1.93 (dd, *J* = 13.7, 2.9 Hz, 1H), 1.75 (t, *J* = 13.3 Hz, 1H), 1.17 – 1.10 (m, 21H), 1.06 (s, 3H).

^{13}C NMR (101 MHz, $CDCl_3$) δ 177.66, 175.20, 153.62, 146.69, 126.78, 123.29, 122.61, 74.74, 61.69, 52.97, 52.00, 47.79, 43.78, 43.35, 40.21, 38.91, 36.92, 35.68, 19.39, 18.73, 18.65, 13.90.

IR (neat, cm^{-1}): 2943, 2866, 2362, 2334, 1778, 1731, 1697.

HRMS (EI): m/z calc'd for $C_{25}H_{36}NO_6Si$ $[M\text{-}iPr]^+$ = 474.2312, found $[M\text{-}iPr]^+$= 474.2325.

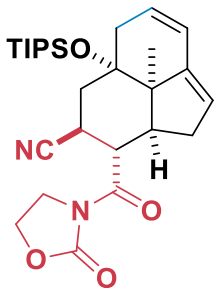

Tricycle (2.6.1.2ce)

Synthesized according to GP3 using oxazolidinone dienophile **2.5.1.1e** and diene **2.1.1.8c**, reacting for 24 h for the gold cyclization, yielding a 5:1 5-*exo-dig* (**2.6.1.2ce**) : 6-*endo-dig* mixture in 42% yield as a white foam.

^{1}H NMR (400 MHz, $CDCl_3$) δ 6.20 (dd, *J* = 9.7, 2.9 Hz, 1H), 5.70 – 5.61 (m, 1H), 5.54 – 5.51 (m, 1H), 4.49 – 4.37 (m, 2H), 4.23 (dd, *J* = 11.9, 10.2 Hz, 1H), 4.17 – 4.02 (m, 2H),

3.32 (td, *J* = 12.4, 2.6 Hz, 1H), 2.71 – 2.56 (m, 2H), 2.51 (dd, *J* = 10.3, 5.0 Hz, 1H), 2.16 (dd, *J* = 17.5, 5.9 Hz, 1H), 2.05 – 1.94 (m, 1H), 1.92 (dd, *J* = 16.7, 3.2 Hz, 1H), 1.82 (dd, *J* = 13.6, 2.7 Hz, 1H), 1.17 – 1.09 (m, 21H), 1.06 (s, 3H).

^{13}C NMR (101 MHz, $CDCl_3$) δ 174.49, 153.31, 146.38, 126.60, 123.29, 122.66, 120.78, 73.82, 61.99, 52.68, 46.13, 45.00, 43.18, 38.34, 37.88, 36.20, 26.37, 19.28, 18.67, 18.61, 13.85.

IR (neat, cm^{-1}): 2944, 2868, 2363, 2343, 1780, 1695.

HRMS (ESI): m/z calc'd for $C_{27}H_{40}N_2O_4SiNa$ $[M+Na]^+$ = 507.2655, found $[M+Na]^+$= 507.2682.

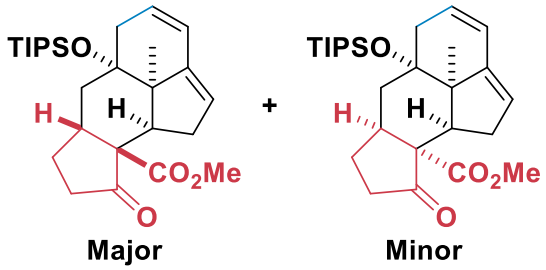

Tetracycle (2.6.1.2cf)

Synthesized according to GP3 (0.300 mmol scale) using methyl 5-oxocyclopent-1-ene-1-carboxylate as the dienophile and diene **2.1.1.8c,** reacting for 48 h for the gold cyclization, yielding a 5:4 mixture of diastereomers of 5-*exo-dig* products **(2.6.1.2cb major + minor)** in 33% yield as a white foam**.**

Major Diastereomer: ^{1}H NMR (400 MHz, $CDCl_3$) δ 6.15 (dd, *J* = 9.6, 2.9 Hz, 1H), 5.66 – 5.57 (m, 1H), 5.40 – 5.35 (m, 1H), 3.63 (s, 3H), 2.91 – 2.83 (m, 1H), 2.83 – 2.73 (m, 2H), 2.61 – 2.52 (m, 1H), 2.52 – 2.41 (m, 1H), 2.29 (dd, *J* = 15.1, 9.9 Hz, 1H), 2.26 – 2.12 (m, 2H), 2.11 – 2.03 (m, 1H), 2.03 – 1.92 (m, 1H), 1.86 – 1.77 (m, 1H), 1.36 (dd, *J* = 15.4, 4.2 Hz, 1H), 1.17 – 1.09 (m, 24H).

^{13}C NMR (101 MHz, $CDCl_3$) δ 213.42, 172.94, 144.93, 127.35, 125.80, 122.62, 74.26, 61.25, 52.86, 52.81, 49.58, 39.22, 37.13, 36.55, 36.17, 31.53, 24.54, 19.90, 18.73, 18.66, 13.95.

IR (neat, cm^{-1}): 2945, 2868, 1759, 1729.

HRMS (EI): m/z calc'd for $C_{24}H_{35}O_4Si$ $[M\text{-}iPr]^+$ =415.2305, found $[M\text{-}iPr]^+$=415.2315.

XRAY: CCDC 1967646

MP: 116-119°C

Minor Diastereomer: ^{1}H NMR (400 MHz, $CDCl_3$) δ 6.08 (dd, *J* = 9.6, 3.0 Hz, 1H), 5.58 – 5.48 (m, 2H), 3.70 (s, 3H), 3.39 (dd, *J* = 17.0, 3.4 Hz, 1H), 3.09 (dt, *J* = 11.8, 6.1 Hz, 1H), 2.70 – 2.60 (m, 2H), 2.58 – 2.47 (m, 1H), 2.30 – 2.07 (m, 3H), 1.91 (dddd, *J* = 13.0, 10.9, 9.7, 6.2 Hz, 1H), 1.52 – 1.45 (m, 1H), 1.44 – 1.40 (m, 2H), 1.16 – 1.09 (m, 21H), 1.07 (s, 3H).

^{13}C NMR (101 MHz, $CDCl_3$) δ 213.17, 172.68, 144.67, 127.10, 125.54, 122.37, 74.01, 60.99, 52.61, 52.56, 49.33, 38.96, 36.87, 36.29, 35.92, 31.28, 24.28, 19.65, 18.48, 18.41, 13.70.

IR (neat, cm^{-1}): 2941.9, 2865.9, 2359.4, 1754.3, 1729.1, 1463.1, 1220.6, 1104.4, 1057.2, 672.4.

HRMS (EI): m/z calc'd for $C_{24}H_{35}O_4Si$ $[M\text{-}iPr]^+$ =415.2305, found $[M\text{-}iPr]^+$=415.2321.

MP: 92-94°C

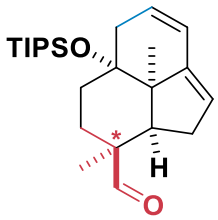

Tricycle (2.6.1.2cg)

To a capped 4 mL oven dried reaction vial was added diene **2.1.1.8c** (0.150 mmol, 0.048 g) methacrolein (0.750 mmol, 0.062 mL), and DCE (0.750 ml, 0.200M). The mixture was heated at 100°C for 18 h. Then to the mixture added JohnPhos Au(NCMe)SbF_6 (5.8 mg, 7.50 µmol, 5 mol%). The mixture was stirred at rt for 24 h then purified according to GP3, yielding **2.6.1.2cg** as a 12:1 mixture of diastereomers of 5-*exo*-*dig* products in 53% yield as a colourless oil**.**

^{1}H NMR (400 MHz, $CDCl_3$) δ 9.48 (s, 1H), 6.12 (dd, *J* = 9.7, 3.0 Hz, 1H), 5.72 – 5.63 (m, 1H), 5.41 – 5.35 (m, 1H), 2.68 – 2.56 (m, 2H), 2.34 (dd, *J* = 17.3, 3.1 Hz, 1H), 2.18 – 2.06 (m, 2H), 1.84 – 1.75 (m, 2H), 1.58 – 1.49 (m, 1H), 1.47 – 1.38 (m, 1H), 1.14 – 1.07 (m, 21H), 1.07 (s, 3H), 0.99 (s, 3H).

^{13}C NMR (101 MHz, $CDCl_3$) δ 205.46, 149.60, 128.66, 123.65, 122.15, 74.65, 54.70, 52.78, 46.21, 39.36, 31.81, 31.75, 27.05, 25.02, 19.63, 18.74, 18.66, 13.89.

IR (neat, cm^{-1}): 2942, 2865, 1713, 1450.

HRMS (EI): m/z calc'd for $C_{24}H_{40}O_2Si$ $[M]^+$ =388.2798, found $[M]^+$=388.2816.

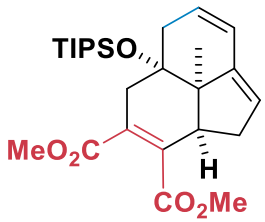

Tricycle (2.6.1.2ch)

To a capped 4 mL oven dried reaction vial was added diene **2.1.1.8c** (0.150 mmol, 0.048 g) dimethyl acetylenedicarboxylate (0.375 mmol, 0.046 mL), and 1:1 DCE:acetone (1.00 ml, 0.200M). The mixture was heated at 100°C for 18 h. Then to the mixture added JohnPhos Au(NCMe)SbF_6 (5.8 mg, 7.50 µmol, 5 mol%). The mixture was heated at 60°C

for 18 h then purified according to GP3, yielding **2.6.1.2ch** in 53% yield as the sole diastereomer and regioisomer as a colourless oil**.**

^{1}H NMR (400 MHz, $CDCl_3$) δ 6.13 (dd, *J* = 9.7, 2.8 Hz, 1H), 5.71 – 5.61 (m, 1H), 5.38 – 5.32 (m, 1H), 3.76 (s, 3H), 3.69 (s, 3H), 2.94 (dd, *J* = 7.9, 3.1 Hz, 1H), 2.83 (dd, *J* = 17.8, 7.6 Hz, 1H), 2.62 (d, *J* = 17.2 Hz, 1H), 2.51 (dd, *J* = 17.7, 3.2 Hz, 1H), 2.35 (dd, *J* = 17.7, 3.3 Hz, 1H), 2.29 (dd, *J* = 17.7, 1.1 Hz, 1H), 2.27 (dd, *J* = 17.8, 5.7 Hz, 1H), 1.12 (s, 3H), 1.09 – 0.99 (m, 21H).

^{13}C NMR (101 MHz, $CDCl_3$) δ 169.29, 168.31, 146.39, 139.75, 129.68, 127.59, 122.59, 122.56, 73.20, 52.43, 52.15, 52.03, 45.73, 38.69, 35.67, 35.37, 18.97, 18.53, 18.47, 13.62.

IR (neat, cm^{-1}): 2944, 2866, 1724, 1255.

HRMS (ESI): m/z calc'd for $C_{26}H_{40}O_5SiNa$ $[M+Na]^+$ =483.2543, found $[M]^+$=483.2518

5.2.5 Model Cascade and Optimizations

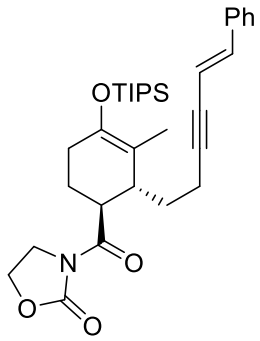

Enyne (**2.5.1.4-exo**)

To oven dried reaction vial was added gadolinium (III) triflate (92 mg, 0.152 mmol), DCM (7.6 ml), 4Å MS (380 mg, 250mg/1mmol), and oxazolidinone dienophile **2.5.1.1a** (0.429 g, 3.04 mmol). The mixture was stirred for 3h at room temperature. Then diene **2.1.1.8a** (0.600 g, 1.52 mmol) was added. The mixture was then stirred at room temperature for

18h then filtered through celite and evaporated. The crude product was purified by flash chromatography (10-20% EtOAc in hexanes), yielding **2.5.1.4-exo** in 98% yield as the sole diastereomer, as a white foam.

^{1}H NMR (400 MHz, $CDCl_3$) δ 7.37 – 7.18 (m, 5H), 6.83 (d, *J* = 16.2 Hz, 1H), 6.12 (dt, *J* = 16.2, 2.3 Hz, 1H), 4.40 – 4.28 (m, 2H), 4.08 – 3.91 (m, 2H), 3.74 (ddd, *J* = 9.2, 7.6, 3.3 Hz, 1H), 2.78 – 2.68 (m, 1H), 2.35 – 2.18 (m, 3H), 2.14 – 2.03 (m, 1H), 2.03 – 1.92 (m, 1H), 1.79 – 1.65 (m, 3H), 1.66 (s, 3H), 1.18 – 1.01 (m, 21H).

^{13}C NMR (101 MHz, $CDCl_3$) δ 175.64, 153.29, 144.82, 140.17, 136.65, 128.78, 128.37, 126.16, 111.27, 108.93, 93.25, 79.91, 61.95, 43.03, 41.65, 39.83, 31.14, 29.46, 25.72, 18.21, 16.13, 14.19, 13.29.

IR (neat, cm^{-1}): 2944, 2865, 2209, 1775, 1698.

HRMS (EI): m/z calc'd for $C_{32}H_{45}NO_4Si$ $[M]^+$ =535.3118, found $[M]^+$=535.3088.

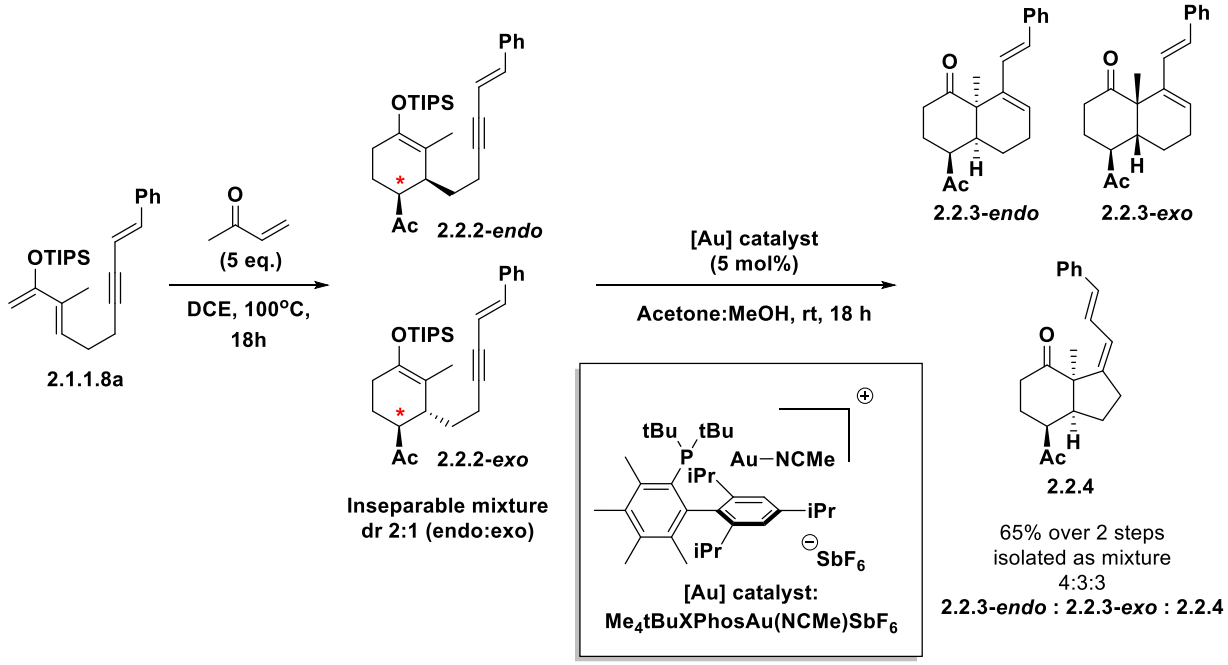

Bicycles (**2.2.3-endo, 2.2.3-exo, 2.2.4**)

To a flame dried high pressure reaction tube under inert atmosphere was added **2.1.1.8a** (0.447 g, 1.133 mmol), DCE (11 ml), and methyl vinyl ketone (0.510 ml, 5.66 mmol). The mixture was heated at 100°C for 18 h, then cooled to rt where the solvent was evaporated in vacuo to yield a crude residue, which was purified by flash chromatography, yielding **2.2.2** as a 2:1 mixture of *endo*:*exo* Diels-Alder adducts. Then, to a flame dried reaction vial under argon was added **2.2.2**, acetone (3.24 ml), MeOH (0.324 ml), and [**L1**Au(NCMe)][SbF_6] (0.039 g, 0.041 mmol). The mixture was then stirred for 18 h at rt and the solvent was evaporated in vacuo to yield a crude residue, which was separated by flash chromatography, yielding a 4:3:3 **2.2.3-endo**:**2.2.3-exo**:**2.2.4** mixture of isomers in 65% yield over two steps as colorless residues.

Bicycle (**2.2.3-exo)**

^{1}H NMR (600 MHz, $CDCl_3$) δ 7.35 – 7.31 (m, 2H), 7.30 – 7.26 (m, 2H), 7.22 – 7.18 (m, 1H), 6.52 (d, *J* = 16.3 Hz, 1H), 6.40 (dd, *J* = 16.3, 1.1 Hz, 1H), 6.08 – 6.05 (m, 1H), 3.07 (td, *J* = 12.2, 3.9 Hz, 1H), 2.52 (ddd, *J* = 14.4, 12.3, 5.3 Hz, 1H), 2.43 – 2.25 (m, 3H), 2.21 (s, 3H), 2.19 – 2.12 (m, 2H), 1.93 – 1.85 (m, 1H), 1.72 (dtd, *J* = 14.5, 12.9, 3.7 Hz, 1H), 1.52 – 1.46 (m, 1H), 1.42 (s, 3H).

^{13}C NMR (151 MHz, $CDCl_3$) δ 214.18, 210.93, 137.51, 137.33, 128.71, 128.20, 128.12, 127.64, 127.01, 126.46, 52.28, 49.94, 45.11, 39.11, 30.36, 29.11, 23.02, 21.93, 20.66.

IR (neat, cm^{-1}): 2944, 2868, 1780, 1694.

HRMS (EI): m/z calc'd for $C_{21}H_{24}O_2$ $[M]^+$ = 308.1776, found $[M]^+$=308.1802.

Bicycle (**2.2.3-endo)**

^{1}H NMR (600 MHz, $CDCl_3$) δ 7.40 – 7.37 (m, 2H), 7.31 – 7.27 (m, 2H), 7.22 – 7.18 (m, 1H), 6.70 (d, *J* = 16.0 Hz, 1H), 6.59 (d, *J* = 15.9 Hz, 1H), 6.13 (dd, *J* = 5.7, 2.3 Hz, 1H), 3.34 – 3.27 (m, 1H), 2.68 (td, *J* = 13.7, 8.0 Hz, 1H), 2.41 – 2.34 (m, 2H), 2.30 – 2.22 (m, 1H), 2.22 (s, 3H), 2.15 – 2.03 (m, 3H), 1.54 (s, 3H), 1.39 – 1.27 (m, 2H).

^{13}C NMR (151 MHz, $CDCl_3$) δ 213.41, 209.41, 139.73, 137.79, 130.38, 128.62, 128.60, 127.27, 126.50, 125.46, 52.56, 49.38, 46.44, 36.63, 28.47, 25.81, 23.60, 23.40, 21.18.

IR (neat, cm^{-1}): 2930, 1705.

HRMS (EI): m/z calc'd for $C_{21}H_{24}O_2$ $[M]^+$ = 308.1776, found $[M]^+$=308.1794.

Bicycle (**2.2.4)**

^{1}H NMR (600 MHz, $CDCl_3$) δ 7.35 (d, *J* = 7.8 Hz, 2H), 7.28 (q, *J* = 7.4 Hz, 2H), 7.22 – 7.17 (m, 1H), 6.92 (dd, *J* = 15.3, 11.5 Hz, 1H), 6.40 (d, *J* = 15.4 Hz, 1H), 6.26 (d, *J* = 11.3 Hz, 1H), 2.93 (dt, *J* = 12.0, 4.3 Hz, 1H), 2.65 – 2.53 (m, 4H), 2.47 – 2.38 (m, 1H), 2.26 –

2.14 (m, 1H), 2.20 (s, 3H), 2.04 – 1.96 (m, 1H), 1.74 – 1.66 (m, 1H), 1.57 (s, 3H), 1.57 – 1.47 (m, 1H).

^{13}C NMR (151 MHz, $CDCl_3$) δ 212.23, 208.92, 146.00, 137.71, 132.39, 128.67, 127.45, 126.50, 126.01, 125.22, 58.67, 53.27, 48.17, 36.40, 34.57, 28.65, 25.67, 24.13, 22.22.

IR (neat, cm^{-1}): 2964, 1707.

HRMS (EI): m/z calc'd for $C_{21}H_{24}O_2$ $[M]^+$ = 308.1776, found $[M]^+$=308.1789.

General Procedure GP4 (Thermal Diels-Alder Reaction)

To an oven-dried high pressure tube was added bicyclic diene **9** (1 eq.), DCE (0.1 M), and N-phenylmaleimide (2 eq.). The mixture was heated at 60°C for 48 h and evaporated. The crude product was purified by flash chromatography, yielding tetracycle **10**.

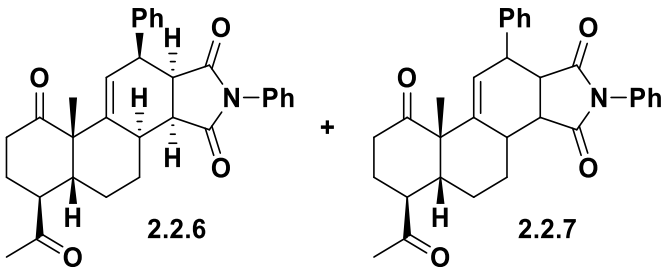

Tetracycles (**2.2.6+2.2.7**)

Synthesized according to GP4 with bicyclic diene **2.2.3-exo** (0.184 mmol, 0.0567 g)**,** yielding a 1.2:1 **2.2.6** : **2.2.7** mixture of diastereomers in 55% yield, as an off-white solid and colourless residue respectively.

Tetracycle **(2.2.6)**

^{1}H NMR (400 MHz, $CDCl_3$) δ 7.43 – 7.21 (m, 8H), 7.07 (dd, *J* = 7.1, 1.6 Hz, 2H), 5.90 – 5.83 (m, 1H), 3.73 – 3.65 (m, 1H), 3.44 (dd, *J* = 8.7, 6.9 Hz, 1H), 3.36 (dd, *J* = 8.7, 6.2 Hz, 1H), 2.92 – 2.85 (m, 1H), 2.82 (td, *J* = 10.8, 3.7 Hz, 1H), 2.61 – 2.50 (m, 2H), 2.38

(dt, *J* = 14.4, 4.2 Hz, 1H), 2.21 (s, 3H), 2.32 – 2.02 (m, 4H), 1.83 (tdd, *J* = 13.0, 11.0, 4.4 Hz, 1H), 1.49 (ddt, *J* = 15.0, 6.2, 4.5 Hz, 1H), 1.33 (s, 3H).

^{13}C NMR (101 MHz, $CDCl_3$) δ 210.39, 210.14, 176.87, 174.89, 143.05, 138.60, 131.71, 129.19, 129.04, 128.68, 128.48, 127.39, 126.52, 126.41, 53.43, 52.88, 46.22, 46.10, 43.88, 42.64, 37.33, 32.75, 28.23, 27.97, 25.45, 23.24, 20.58.

IR (neat, cm^{-1}): 2930, 1703.

HRMS (EI): m/z calc'd for $C_{31}H_{31}NO_4$ $[M]^+$ =481.2253, found $[M]^+$=481.2284.

MP: 253-258°C

Tetracycle (**2.2.7**)

^{1}H NMR (400 MHz, $CDCl_3$) δ 7.50 – 7.45 (m, 2H), 7.42 – 7.32 (m, 5H), 7.30 – 7.24 (m, 3H), 5.65 (dd, *J* = 4.2, 2.1 Hz, 1H), 3.98 (p, *J* = 4.5, 2.4 Hz, 1H), 3.18 (dd, *J* = 8.7, 4.8 Hz, 1H), 2.81 (dd, *J* = 8.7, 6.5 Hz, 1H), 2.66 (ddd, *J* = 14.9, 8.7, 5.9 Hz, 1H), 2.60 – 2.47 (m, 3H), 2.46 – 2.33 (m, 2H), 2.29 (s, 3H), 2.30 – 2.18 (m, 1H), 2.12 – 2.03 (m, 1H), 2.02 – 1.91 (m, 1H), 1.72 – 1.61 (m, 2H), 1.33 (s, 3H).

^{13}C NMR (151 MHz, $CDCl_3$) δ 211.59, 210.24, 177.98, 176.86, 143.72, 140.82, 132.03, 129.30, 129.05, 128.68, 128.01, 127.24, 126.66, 124.83, 55.36, 53.74, 46.21, 45.50, 44.89, 39.66, 36.22, 34.60, 31.79, 29.88, 28.61, 24.00, 23.71.

IR (neat, cm^{-1}): 2930, 2361, 2341, 1713.

HRMS (EI): m/z calc'd for $C_{31}H_{31}NO_4$ $[M]^+$ =481.2253, found $[M]^+$=481.2279.

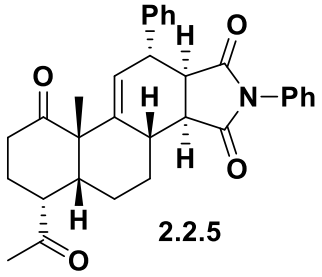

2.2.5

Tetracycle (**2.2.5**)

Synthesized according to GP4 with bicyclic diene **2.2.3-endo** (0.198 mmol, 0.0611 g)**,** yielding **10aaac** as the sole diastereomer in 63% yield**,** as an off-white solid.

^{1}H NMR (400 MHz, $CDCl_3$) δ 7.48 – 7.24 (m, 10H), 5.89 (t, *J* = 2.9 Hz, 1H), 3.46 (ddd, *J* = 9.5, 3.0, 1.6 Hz, 1H), 3.28 (t, *J* = 9.5 Hz, 1H), 3.25 – 3.18 (m, 1H), 2.93 (dd, *J* = 10.7, 9.5 Hz, 1H), 2.66 – 2.46 (m, 3H), 2.36 (dq, *J* = 13.7, 4.3 Hz, 1H), 2.20 (s, 3H), 2.29 – 2.09 (m, 3H), 1.60 – 1.52 (m, 2H), 1.47 (s, 3H), 1.42 – 1.29 (m, 1H).

^{13}C NMR (101 MHz, $CDCl_3$) δ 212.66, 209.07, 176.97, 176.81, 143.99, 143.05, 131.86, 130.52, 129.08, 128.82, 128.66, 128.47, 127.12, 126.50, 52.84, 50.28, 48.58, 45.91, 43.23, 41.14, 38.23, 36.80, 28.30, 24.88, 22.85, 22.80, 21.89.

IR (neat, cm^{-1}): 2971, 2820, 1715, 1699.

HRMS (EI): m/z calc'd for $C_{31}H_{31}NO_4$ $[M]^+$ =481.2253, found $[M]^+$=481.2267.

MP: 106-108°C

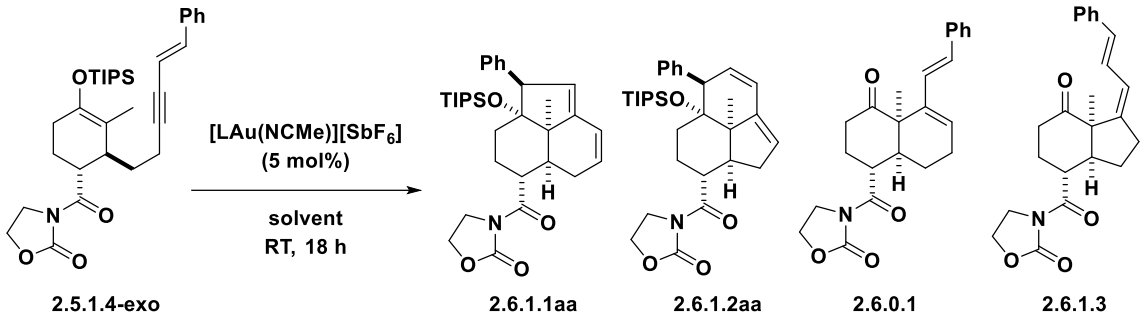

Au(I) Catalyst Ligand Optimization

To a reaction vial was added **2.5.1.4-exo** (25 mg, 0.047 mmol), solvent (0.23 M), and the [LAu(NCMe)][SbF_6] (5 mol%). The reaction was stirred at room temperature for 18 h, then evaporated. The crude residue was analyzed by NMR with mesitylene standard to determine the NMR yield. The products were purified by flash chromatography (20-30-45% EtOAc in hexanes).

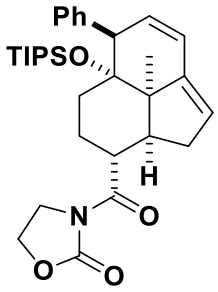

Tricycle **(2.6.1.2aa)**

Isolated and characterized as an inseparable mixture (81% purity, NMR).

^{1}H NMR (600 MHz, $CDCl_3$) δ 7.28 – 7.26 (m, 4H), 7.24 – 7.21 (m, 1H), 6.22 (dd, *J* = 9.9, 2.8 Hz, 1H), 5.69 – 5.62 (m, 1H), 5.48 – 5.44 (m, 1H), 4.41 – 4.36 (m, 2H), 4.24 (d, *J* = 2.2 Hz, 1H), 4.07 – 3.96 (m, 2H), 3.59 (td, *J* = 11.7, 3.1 Hz, 1H), 2.55 (dtd, *J* = 19.4, 4.4, 3.4, 1.7 Hz, 1H), 2.34 (dd, *J* = 11.8, 6.0 Hz, 1H), 2.00 (td, *J* = 14.1, 3.7 Hz, 1H), 1.85 – 1.77 (m, 1H), 1.66 – 1.59 (m, 1H), 1.59 – 1.48 (m, 1H), 1.30 (s, 3H), 1.11 (ddd, *J* = 14.5, 4.0, 2.6 Hz, 1H), 1.03 – 0.96 (m, 21H).

^{13}C NMR (151 MHz, $CDCl_3$) δ 176.46, 153.13, 144.30, 139.31, 130.50, 127.90, 126.93, 126.06, 123.32, 87.75, 61.93, 59.08, 50.64, 43.32, 42.90, 36.49, 31.87, 28.11, 25.73, 19.86, 18.80, 18.78, 14.26.

IR (neat, cm^{-1}): 2867, 1777, 1701, 1388.

HRMS (EI): m/z calc'd for $C_{32}H_{45}NO_4Si$ $[M]^+$ = 535.3118, found $[M]^+$= 535.3112

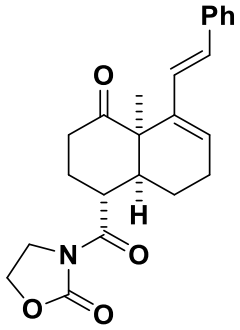

Bicycle **(2.6.0.1)**

^{1}H NMR (600 MHz, $CDCl_3$) δ 7.34 – 7.31 (m, 2H), 7.29 – 7.25 (m, 2H), 7.21 – 7.17 (m, 1H), 6.52 (d, *J* = 16.4 Hz, 1H), 6.41 (dd, *J* = 16.5, 0.8 Hz, 1H), 6.07 (dd, *J* = 5.1, 3.0 Hz, 1H), 4.45 – 4.41 (m, 2H), 4.36 (td, *J* = 11.8, 3.9 Hz, 1H), 4.11 – 3.99 (m, 2H), 2.63 (ddd, *J* = 14.3, 12.2, 5.3 Hz, 1H), 2.43 – 2.20 (m, 5H), 1.90 (ddt, *J* = 18.8, 11.9, 3.6 Hz, 1H), 1.74 (dtd, *J* = 14.5, 12.3, 3.5 Hz, 1H), 1.52 – 1.47 (m, 1H), 1.43 (s, 3H).

^{13}C NMR (151 MHz, $CDCl_3$) δ 214.21, 175.08, 153.31, 137.40, 137.20, 128.29, 128.03, 127.51, 127.22, 126.43, 62.00, 52.19, 45.08, 42.93, 39.96, 39.00, 31.17, 23.08, 22.12, 20.94.

IR (neat, cm^{-1}): 2968, 2927, 1772, 1699.

HRMS (EI): m/z calc'd for $C_{23}H_{25}NO_4$ $[M]^+$ = 379.1784, found $[M]^+$= 379.1778

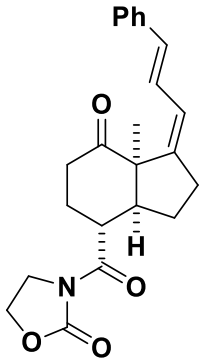

Bicycle **(2.6.1.3)**

^{1}H NMR (600 MHz, $CDCl_3$) δ 7.30 (dt, *J* = 15.5, 8.1 Hz, 4H), 7.22 – 7.16 (m, 1H), 6.77 (dd, *J* = 15.3, 11.5 Hz, 1H), 6.35 (d, *J* = 15.3 Hz, 1H), 6.13 (d, *J* = 11.5 Hz, 1H), 4.49 – 4.39 (m, 2H), 4.12 – 3.99 (m, 3H), 2.89 (dt, *J* = 19.9, 10.2 Hz, 1H), 2.73 – 2.64 (m, 2H), 2.62 (dd, *J* = 18.5, 9.1 Hz, 1H), 2.40 (dt, *J* = 13.1, 3.5 Hz, 1H), 2.23 (ddt, *J* = 12.4, 5.0, 3.5 Hz, 1H), 2.02 (dddd, *J* = 13.2, 11.2, 9.2, 5.9 Hz, 1H), 1.78 (dtd, *J* = 14.1, 12.8, 3.4 Hz, 1H), 1.45 (dd, *J* = 13.3, 8.0 Hz, 1H), 1.34 (s, 3H).

^{13}C NMR (151 MHz, $CDCl_3$) δ 214.02, 174.84, 153.37, 147.29, 137.50, 132.69, 128.72, 127.55, 126.48, 124.85, 123.65, 62.07, 59.18, 54.82, 43.02, 42.57, 38.84, 31.83, 30.23, 28.87, 22.44.

IR (neat, cm^{-1}): 2370, 2346, 1777, 1697.

HRMS (EI): m/z calc'd for $C_{23}H_{25}NO_4$ $[M]^+$ = 379.1784, found $[M]^+$=379.1794.

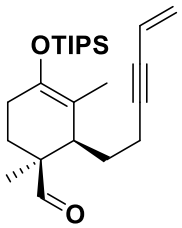

Silyl enol ether 2.5.3.2

Characterization data obtained from literature (Alyson Poyser's Master's thesis).[85]

To an oven dried reaction tube was added diene **2.1.1.8c** (0.15 mmol), methacrolein (0.75 mmol), Co(III) catalyst **2.5.3.1-TBS** (1 mol%) and DCM (2M). The reaction mixture was stirred overnight at room temperature and the solvent evaporated in vacuo. The crude product was purified by flash chromatography to yield **2.5.3.2** in 62% yield (0.036 g).

1H NMR (400 MHz, $CDCl_3$) δ 9.62 (s, 1H), 5.76 (ddt, *J* = 17.5, 11.0, 2.1 Hz, 1H), 5.55 (dd, *J* = 17.5, 2.2 Hz, 1H), 5.38 (dd, *J* = 11.0, 2.3 Hz, 1H), 2.30 (qd, *J* = 7.4, 2.2 Hz, 2H), 2.17–2.09 (m, 3H), 1.88 (dt, *J* = 13.8, 9.2 Hz, 1H), 1.72 (t, *J* = 1.9 Hz, 3H), 1.62–1.48 (m, 3H), 1.18–1.02 (m, 24H)

13C NMR (101 MHz, CDCl3) δ 206.2, 143.4, 126.0, 117.6, 111.5, 90.5, 80.3, 48.7, 45.0, 32.2, 26.6, 24.1, 19.4, 19.3, 18.2, 18.2, 16.8, 13.3.

IR (neat, cm^{-1}): 2942, 2896, 2866, 1724, 1677.

HRMS (EI): m/z calc'd for $C_{24}H_{40}O_2Si$ $[M]^+$ = 388.2798, found mass = 388.2773.

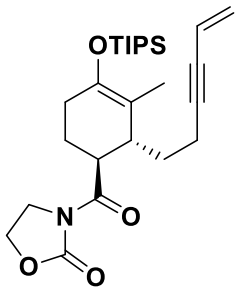

Silyl enol ether 2.5.2.1-exo

Characterization data obtained from literature (Alyson Poyser's Master's thesis).[85]

To oven dried reaction tube was added gadolinium(III) triflate (0.015 mmol), DCM (0.450 ml), 4A MS (32 mg, 250mg/1mmol) and oxazolidinone dienophile **2.5.1.1a** (0.30 mmol). The mixture was stirred for 3h at room temperature. Then, a solution of diene **2.1.1.8c** (0.15 mmol) in DCM (0.15 ml) was added via syringe. The mixture was then

stirred at room temperature for 18 h. The mixture was filtered through celite and evaporated. The crude residue was purified by flash chromatography, yielding **2.5.2.1-exo** in 93% yield (0.064 g) as a 95:5 *exo*:*endo* mixture.

1H NMR (400 MHz, CDCl3) δ 5.76 (ddt, *J* = 17.6, 11.0, 2.1 Hz, 1H), 5.53 (dd, *J* = 17.5, 2.3 Hz, 1H), 5.36 (dd, *J* = 11.0, 2.3 Hz, 1H), 4.41 (t, *J* = 8.1 Hz, 2H), 4.09 – 3.95 (m, 2H), 3.72 (ddd, *J* = 9.3, 7.6, 3.4 Hz, 1H), 2.71 (s, 1H), 2.31 – 2.17 (m, 3H), 2.09 (dtt, *J* = 16.3, 5.0, 1.4 Hz, 2H), 1.97 (dtd, *J* = 12.6, 5.3, 3.4 Hz, 1H), 1.71 (m, 2H), 1.65 (s, 3H), 1.15 – 1.03 (m, 21H).

13C NMR (101 MHz, CDCl3) δ 175.6, 153.3, 144.8, 125.7, 117.7, 111.3, 91.4, 79.5, 62.0, 43.0, 41.6, 39.8, 31.1, 29.4, 25.7, 18.2, 15.7, 14.2, 13.3.

IR (neat, cm^{-1}): 2944, 2866, 1775, 1698.

HRMS (EI) m/z calculated for $C_{26}H_{41}NO_4Si$ $[M]^+$ = 459.2805, found $[M]^+$ = 459.2787.

5.2.6 Deuteration Experiments

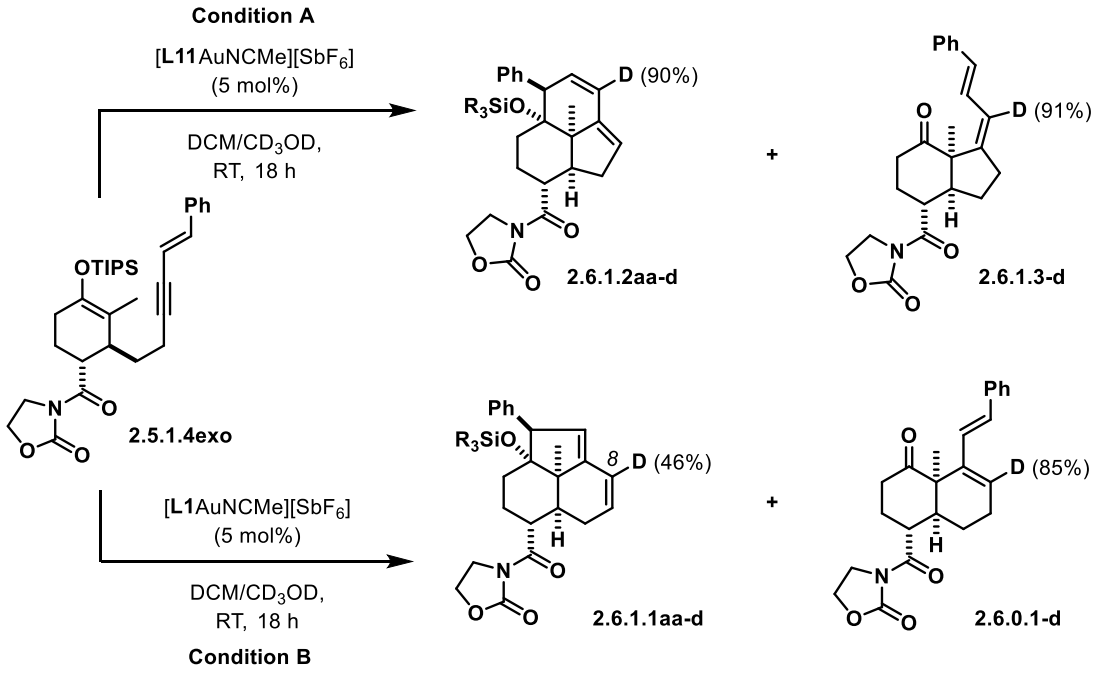

Condition A

To a flame-dried reaction vial under argon was added a solution of **2.5.1.4-exo** (0.060 g, 0.112 mmol) in anhydrous DCM (0.443 ml), and a solution of **L1**Au(NCMe)SbF_6 (10.69 mg, 0.011 mmol) in methanol-d4 (0.044 ml) was added via syringe. The mixture was stirred at RT for 18 h, then evaporated. The crude residue was then analyzed by NMR to determine percentage of deuterium incorporation via comparison with non-deuterated spectra of **2.6.1.1aa** and **2.6.0.1**.

Condition B

To a flame-dried reaction vial under argon was added a solution of **2.5.1.4-exo** (0.060 g, 0.112 mmol) in anhydrous DCM (0.443 ml), and a solution of **L11**Au(NCMe)SbF_6 (10.69 mg, 0.011 mmol) in methanol-d4 (0.044 ml) was added via syringe. The mixture was stirred at RT for 18 h, then evaporated. The crude residue was then analyzed by NMR to

determine percentage of deuterium incorporation via comparison with non-deuterated spectra of **2.6.1.2aa** and **2.6.1.3**.

5.2.7 Substrate Synthesis and Characterization

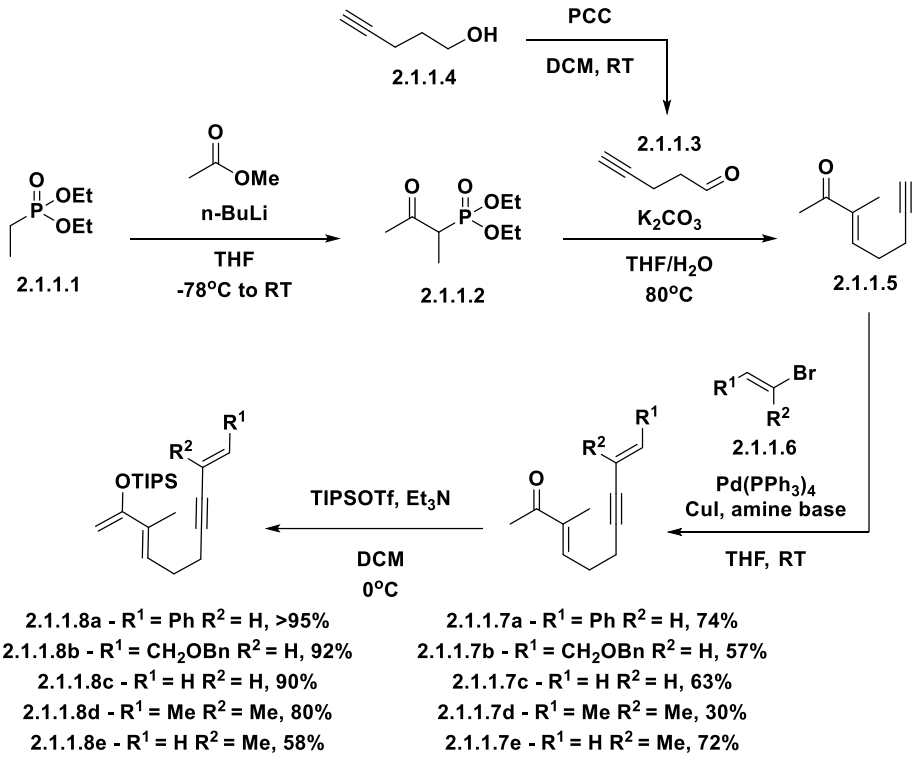

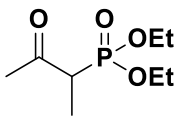

diethyl (3-oxobutan-2-yl)phosphonate (2.1.1.2)

To a flame-dried round-bottom flask under argon was added diethyl ethylphosphonate (37.2 ml, 229 mmol) and THF (230 ml). The mixture was cooled to -78 °C then 11M n-BuLi in hexane (25 ml, 275 mmol) was added via cannulation. The mixture was stirred for 3 h at -78 °C. Methyl acetate (91 ml, 1146 mmol) in THF (46.0 ml) was then added. The mixture was stirred for 1 h while warming to rt, then was quenched with sat. NH_4Cl. The mixture was extracted with EtOAc (3 x 100 mL). The combined organic layers were

washed with brine, dried (Na_2SO4), filtered, and evaporated, yielding **2.1.1.2** as a crude amber oil which was carried forward without further purification.

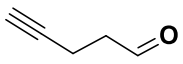

pent-4-ynal (2.1.1.3)

To a flame-dried round-bottom flask under argon was added PCC (29.1 g, 135 mmol), 1 PCC mass equivalent of silica gel (29 g), and DCM (400 ml). Then pent-4-yn-1-ol (**2.1.1.4**) (8.37 ml, 90 mmol) in DCM (200 ml) was added via addition funnel over 30 min. The mixture was stirred at rt for 1h. The reaction mixture was filtered through a silica plug (~200mL) and was eluded with DCM. The filtrate was collected and carefully rotary evaporated (low bath temperature at ~35°C), yielding **2.1.1.3** as a crude clear oil which was carried forward without further purification.

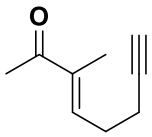

(E)-3-methyloct-3-en-7-yn-2-one (2.1.1.5)

Adopted from literature procedure[86]. To a solution of crude phosphonate **2.1.1.2** in THF (115 ml) in a round-bottom flask was added a solution of potassium carbonate (22.0 g, 160 mmol) in water (57 ml), and crude aldehyde **2.1.1.3** . The mixture was then heated at 80°C overnight with vigorous stirring. The product was extracted with ethyl acetate (3 x 50 mL), and the combined organic layers were dried over sodium sulfate and evaporated. The crude product was diluted with DMF (250 mL) and added to an extraction funnel. Then, aq. sat. sodium bisulfite (250 mL) was added and shaken for 30 s. Water (250 mL) was added then the mixture was extracted with hexanes (250 mL x 3). The

combined organic layers were dried with sodium sulfate, filtered, and concentrated in vacuo to give a crude liquid which was separated via flash chromatography (5-10% EtOAc in hexanes) to give ketone **2.1.1.5** (4.91 g, 36.0 mmol, 32 % yield over 3 steps). Characterized according to reported literature.[87]

General Procedure GP5 (Sonogoshira coupling)

A flame-dried round-bottom flask under argon was added ketone **2.1.1.5** (1 eq.) in THF (0.1M) followed by copper(I) iodide (10 mol%) and an amine base (5 eq.). The solution was degassed with argon (sparge), then vinyl bromide **2.1.1.6** (2-3 eq.) and $Pd(PPh_3)_4$ (2.5-5 mol%) were added. The mixture was stirred overnight at room temperature. The reaction mixture was filtered through celite and evaporated. Then, the residue was diluted with hexanes where the precipitates were filtered off and the mother liquor was evaporated to yield a crude oil, which was then purified by flash chromatography yielding ketone **2.1.1.7**. In some cases, a second purification by flash chromatography (eluding with DCM) was needed to remove the phosphine oxide by-product.

General Procedure GP6 (Silyl Enol Ether Diene synthesis)

To a flame dried round-bottom flask under argon was added ketone **2.1.1.7** (1 eq.), DCM (0.2M), and triethylamine (2 eq.). Then triisopropylsilyl trifluoromethanesulfonate (1 eq.) was added at 0 °C. The mixture was stirred at 0 °C for 1h, then quenched with sat. $NaHCO_3$. The layers were separated and the organic phase was collected. The aq. layer was back-extracted with DCM (2 x 10 mL). The combined organic layers were dried with sodium sulfate, filtered and concentrated. The crude product was added to a basicified

silica gel column (TEA) and was eluted with 1% triethylamine in hexanes, yielding diene **2.1.1.8**.

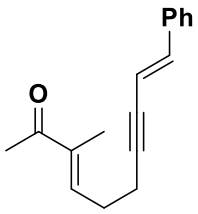

Ketone 2.1.1.7a

Synthesized according to GP4 using ketone **2.1.1.5** (1.50g, 11.0 mmol), diisopropylamine (6.17 mL, 44.1 mmol), 2-bromovinylbenzene (4.74 g, 25.9 mmol), and $Pd(PPh_3)_4$ (0.318 g, 2.5 mol%) yielding **2.1.1.7a** in 74% yield as an orange oil**.**

^{1}H NMR (400 MHz, $CDCl_3$) δ 7.40 – 7.20 (m, 5H), 6.87 (d, *J* = 16.2 Hz, 1H), 6.73 – 6.63 (m, 1H), 6.14 (dt, *J* = 16.3, 2.0 Hz, 1H), 2.59 – 2.45 (m, 4H), 2.33 (s, 3H), 1.83 – 1.77 (m, 3H).

^{13}C NMR (101 MHz, $CDCl_3$) δ 199.70, 141.10, 140.66, 138.74, 136.35, 128.71, 128.46, 126.13, 108.39, 91.09, 80.68, 28.38, 25.54, 19.06, 11.37.

IR (neat, cm^{-1}): 3027, 2962, 2925, 1665.

HRMS (EI): m/z calc'd for $C_{17}H_{18}O$ $[M]^+$ = 238.1358, found $[M]^+$ = 238.1325.

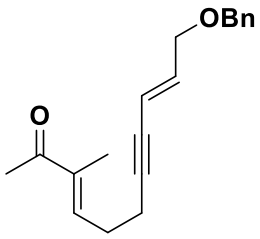

Ketone 2.1.1.7b

Synthesized according to GP4 using ketone **2.1.1.5** (0.219 g, 1.61 mmol), diisopropylamine (1.12 mL, 44.1 mmol), (E)-(((3-bromoallyl)oxy)methyl)benzene[88] (0.729 g, 3.21 mmol), and $Pd(PPh_3)_4$ (0.093 g, 2.5 mol%) yielding **2.1.1.7b** (0.260 g, 57%) as a colourless oil**.**

^{1}H NMR (400 MHz, $CDCl_3$) δ 7.40 – 7.25 (m, 5H), 6.69 – 6.63 (m, 1H), 6.14 (dt, *J* = 15.9, 5.6 Hz, 1H), 5.78 – 5.71 (m, 1H), 4.52 (s, 2H), 4.05 (dd, *J* = 5.6, 1.7 Hz, 2H), 2.53 – 2.45 (m, 4H), 2.32 (s, 3H), 1.83 – 1.77 (m, 3H).

^{13}C NMR (101 MHz, $CDCl_3$) δ 199.87, 141.17, 138.85, 138.73, 138.15, 128.56, 127.84, 127.83, 112.13, 89.50, 79.47, 72.42, 69.95, 28.41, 25.64, 18.92, 11.46.

IR (neat, cm^{-1}): 2927, 2927, 2361, 2341, 1667.

HRMS (ESI): m/z calc'd for $C_{19}H_{22}O_2Na$ $[M+Na]^+$ = 305.1517, found $[M+Na]^+$ = 305.1519.

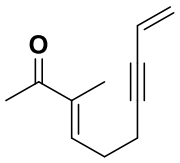

Ketone 2.1.1.7c

Synthesized according to GP4 using ketone **2.1.1.5** (0.300 g, 2.20 mmol), diisopropylamine (1.54 mL, 11.0 mmol), vinyl bromide 1M in THF (6.61 mL, 6.61 mmol), and $Pd(PPh_3)_4$ (0.064 g, 2.5 mol%) yielding **2.1.1.7c** (0.226 g, 63%) as an orange oil**.**

^{1}H NMR (400 MHz, $CDCl_3$) δ 6.71 – 6.61 (m, 1H), 5.77 (ddt, *J* = 17.5, 11.0, 2.1 Hz, 1H), 5.56 (dd, *J* = 17.5, 2.2 Hz, 1H), 5.41 (dd, *J* = 11.0, 2.2 Hz, 1H), 2.53 – 2.44 (m, 4H), 2.32 (s, 3H), 1.79 (d, *J* = 1.2 Hz, 3H).

^{13}C NMR (101 MHz, $CDCl_3$) δ 199.87, 141.13, 138.86, 126.33, 117.39, 89.42, 80.34, 28.36, 25.63, 18.85, 11.44.

IR (neat, cm^{-1}): 2924, 1666.

HRMS (EI): m/z calc'd for $C_{11}H_{13}O$ $[M-H]^+$= 161.0966, found $[M-H]^+$ = 161.0968.

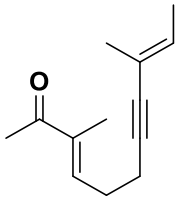

Ketone 2.1.1.7d

Synthesized according to GP4 using ketone **2.1.1.5** (0.150 g, 1.10 mmol), diethylamine (0.570 mL, 5.50 mmol), (E)-2-Bromo-2-butene (0.340 mL, 3.30 mmol), and $Pd(PPh_3)_4$ (0.064 g, 5 mol%) yielding **2.1.1.7d** (0.063 g, 30%) as an orange oil**.**

^{1}H NMR (400 MHz, $CDCl_3$) δ 6.69 – 6.59 (m, 1H), 5.78 (qq, *J* = 7.1, 1.6 Hz, 1H), 2.49 – 2.38 (m, 4H), 2.28 (s, 3H), 1.79 – 1.72 (m, 3H), 1.74 – 1.68 (m, 3H), 1.62 (dq, *J* = 7.0, 1.1 Hz, 3H).

^{13}C NMR (101 MHz, $CDCl_3$) δ 199.74, 141.48, 138.58, 131.44, 118.54, 84.59, 84.54, 28.56, 25.48, 18.67, 17.13, 13.97, 11.31.

IR (neat, cm^{-1}): 2921, 2859, 1667, 1644.

HRMS (EI): m/z calc'd for $C_{12}H_{15}O$ $[M-Me]^+$= 175.1123, found $[M-Me]^+$ = 175.1108

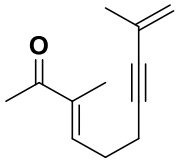

Ketone 2.1.1.7e

Synthesized according to GP4 using ketone **2.1.1.5** (0.300 g, 2.20 mmol), diethylamine (1.14 mL, 11.0 mmol), (E)-2-Bromo-2-butene (0.587 mL, 6.61 mmol), and $Pd(PPh_3)_4$ (0.127 g, 5 mol%) yielding **2.1.1.7e** (0.278 g, 72%) yield as a colourless oil**.**

^{1}H NMR (400 MHz, $CDCl_3$) δ 6.72 – 6.61 (m, 1H), 5.23 – 5.17 (m, 1H), 5.17 – 5.13 (m, 1H), 2.52 – 2.44 (m, 4H), 2.32 (s, 3H), 1.87 – 1.83 (m, 3H), 1.81 – 1.76 (m, 3H).

^{13}C NMR (101 MHz, $CDCl_3$) δ 199.86, 141.26, 138.79, 127.05, 121.09, 87.70, 82.91, 28.41, 25.59, 23.83, 18.77, 11.43.

IR (neat, cm^{-1}): 2942, 2865, 1665, 1369.

HRMS (EI): m/z calc'd for $C_{12}H_{16}O$ $[M]^+$= 176.1201, found $[M]^+$ = 176.1218.

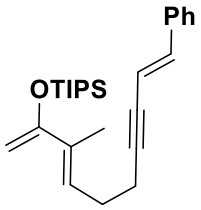

Silyl enol ether 2.1.1.8a

Synthesized according to GP5 using ketone **2.1.1.7a** (0.6775 g, 2.84 mmol), yielding **2.1.1.8a** (1.173 g, >95 % yield).

^{1}H NMR (400 MHz, $CDCl_3$) δ 7.39 – 7.21 (m, 5H), 6.85 (d, *J* = 16.3 Hz, 1H), 6.19 (t, *J* = 6.6 Hz, 1H), 6.13 (dt, *J* = 16.2, 2.0 Hz, 1H), 4.41 (d, *J* = 1.4 Hz, 1H), 4.30 – 4.25 (m, 1H), 2.51 – 2.35 (m, 4H), 1.80 – 1.77 (m, 3H), 1.30 – 1.19 (m, 3H), 1.11 (d, *J* = 7.1 Hz, 18H).

^{13}C NMR (101 MHz, $CDCl_3$) δ 157.57, 140.24, 136.75, 132.24, 128.79, 128.36, 126.49, 126.19, 108.97, 92.49, 90.63, 80.15, 27.92, 20.02, 18.28, 13.58, 13.01

IR (neat, cm^{-1}): 2946, 2866, 2364, 2342, 1712, 1668.

HRMS (EI): m/z calc'd for $C_{26}H_{38}OSi$ $[M^+]$ = 394.2692, found mass = 394.2698.

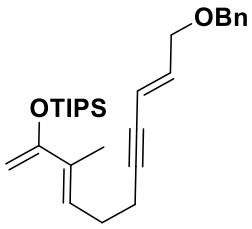

Silyl enol ether 2.1.1.8b

Synthesized according to GP5 using ketone **2.1.1.7b** (0.283 g, 1.00 mmol), yielding **2.1.1.8b** (0.404 g, 92 % yield).

^{1}H NMR (400 MHz, $CDCl_3$) δ 7.40 – 7.24 (m, 5H), 6.20 – 6.05 (m, 2H), 5.78 – 5.66 (m, 1H), 4.51 (s, 2H), 4.40 (d, *J* = 1.4 Hz, 1H), 4.27 (d, *J* = 1.3 Hz, 1H), 4.05 (dd, *J* = 5.7, 1.7 Hz, 2H), 2.44 – 2.32 (m, 4H), 1.78 (d, *J* = 1.2 Hz, 3H), 1.33 – 1.17 (m, 3H), 1.14 – 1.06 (m, 18H).

^{13}C NMR (101 MHz, $CDCl_3$) δ 157.53, 138.25, 138.09, 132.20, 128.54, 127.82, 127.79, 126.46, 112.67, 90.80, 90.62, 78.78, 72.20, 70.05, 27.86, 19.77, 18.26, 13.56, 12.98.

IR (neat, cm^{-1}): 2945, 2864.

HRMS (EI): m/z calc'd for $C_{28}H_{42}O_2Si$ [M^+] = 438.2954, found mass = 438.2961.

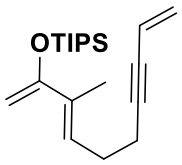

Silyl enol ether 2.1.1.8c

Synthesized according to GP5 using ketone **2.1.1.7c** (0.226 g, 1.39 mmol), yielding **2.1.1.8c** (0.402 g, 90 % yield).

^{1}H NMR (400 MHz, $CDCl_3$) δ 6.20 – 6.11 (m, 1H), 5.82 – 5.69 (m, 1H), 5.53 (dd, *J* = 17.5, 2.3 Hz, 1H), 5.37 (dd, *J* = 11.0, 2.3 Hz, 1H), 4.39 (d, *J* = 1.4 Hz, 1H), 4.27 (d, *J* = 1.4 Hz, 1H), 2.41 – 2.33 (m, 4H), 1.80 – 1.75 (m, 3H), 1.31 – 1.16 (m, 3H), 1.14 – 1.06 (m, 18H).

^{13}C NMR (101 MHz, $CDCl_3$) δ 157.57, 132.22, 126.47, 125.68, 117.74, 90.67, 90.61, 79.71, 27.82, 19.71, 18.26, 13.55, 13.00.

IR (neat, cm^{-1}): 2945, 2867.

HRMS (EI): m/z calc'd for $C_{20}H_{34}OSi$ [M^+] = 318.2379, found mass = 318.2380.

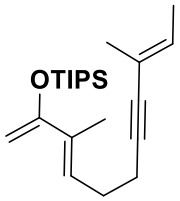

Silyl enol ether 2.1.1.8d

Synthesized according to GP5 using ketone **2.1.1.7d** (0.257 g, 1.35 mmol), yielding **2.1.1.8d** (0.376 g, 80 % yield).

^{1}H NMR (400 MHz, $CDCl_3$) δ 6.19 – 6.08 (m, 1H), 5.81 (qq, *J* = 7.0, 1.5 Hz, 1H), 4.39 (d, *J* = 1.4 Hz, 1H), 4.26 (s, 1H), 2.41 – 2.30 (m, 4H), 1.77 (d, *J* = 1.2 Hz, 3H), 1.75 – 1.72 (m, 3H), 1.65 (dq, *J* = 7.1, 1.2 Hz, 3H), 1.31 – 1.17 (m, 3H), 1.13 – 1.06 (m, 18H).

^{13}C NMR (101 MHz, $CDCl_3$) δ 157.65, 132.07, 131.03, 126.74, 118.89, 90.50, 85.81, 83.90, 28.22, 19.63, 18.26, 17.26, 14.05, 13.56, 13.00.

IR (neat, cm^{-1}): 2945, 2870.

HRMS (EI): m/z calc'd for $C_{22}H_{38}OSi$ [M^+] = 346.2692, found [M^+] = 346.2701.

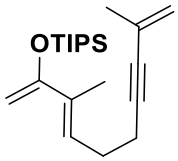

Silyl enol ether 2.1.1.8e

Synthesized according to GP5 using ketone **2.1.1.7e** (0.069 g, 0.39 mmol), yielding **2.1.1.8e** (0.075 g, 58% yield).

^{1}H NMR (400 MHz, $CDCl_3$) δ 6.19 – 6.09 (m, 1H), 5.21 – 5.15 (m, 1H), 5.13 (p, *J* = 1.7 Hz, 1H), 4.39 (d, *J* = 1.4 Hz, 1H), 4.29 – 4.24 (m, 1H), 2.43 – 2.31 (m, 4H), 1.88 – 1.82 (m, 3H), 1.78 (d, *J* = 1.1 Hz, 3H), 1.31 – 1.16 (m, 3H), 1.13 – 1.07 (m, 18H).

^{13}C NMR (101 MHz, $CDCl_3$) δ 157.59, 132.21, 127.39, 126.53, 120.58, 90.58, 88.95, 82.13, 27.97, 23.92, 19.65, 18.26, 13.56, 12.99.

IR (neat, cm^{-1}): 2953, 2863.

HRMS (EI): m/z calc'd for $C_{21}H_{36}OSi$ [M^+] = 332.2535, found [M^+] = 332.2521.

5.2.8 Dienophile Synthesis

General Procedure GP7 (Oxazolidinone dienophile synthesis)

Synthesized via modified literature procedure.[89]

To a round-bottom flask was added the acrylic acid (1 eq.), DCM (0.4M), 2-chloro-1-methylpyridin-1-ium iodide (1.2 eq.), oxazolidin-2-one (1.1 eq.) and triethylamine (2.4 eq.). The mixture was stirred at rt for 48-72 h. The solvent was evaporated, then the crude product was diluted with EtOAc and the resulting precipitates were filtered off, washing with EtOAc (30 mL). The mother liquor was evaporated and the crude product was added to a silica gel column, eluted with Hex/EtOAc to yield oxazolidinone dienophile **2.5.1.1.**

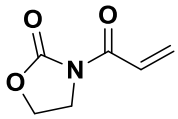

Oxazolidinone dienophile 2.5.1.1a

Synthesized and characterized according to reported literature.[90]

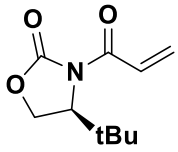

Oxazolidinone dienophile 2.5.1.1b

Synthesized and characterized according to reported literature.[91]

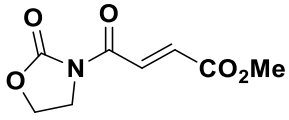

Oxazolidinone dienophile 2.5.1.1c

Synthesized according to GP7 using mono-methyl fumarate (2.00 g, 15.4 mmol), reacting for 48 h, yielding **2.5.1.1c** (2.76 g, 90% yield). Characterized according to reported literature.[89]

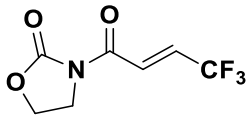

Oxazolidinone dienophile 2.5.1.1d

Synthesized according to GP7 using (E)-4,4,4-trifluorobut-2-enoic acid[92] (0.200 g, 1.43 mmol), reacting for 72 h, yielding **2.5.1.1d** (0.228 g, 76% yield). Characterized according to reported literature.[92]

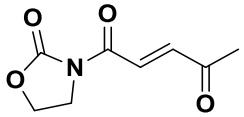

Oxazolidinone dienophile 2.5.1.1e

Synthesized according to GP7 using (E)-4-oxopent-2-enoic acid[92] (0.200 g, 1.75 mmol), reacting for 48 h, yielding **2.5.1.1e** (0.131 g, 41% yield). Characterized according to reported literature.[92]

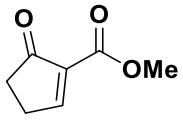

Dienophile 2.5.1.1f

Synthesized and characterized according to reported literature.[93]

5.2.9 Catalyst Synthesis and Characterization

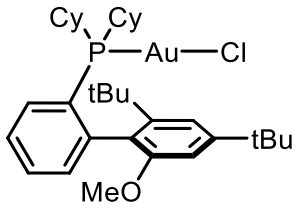

L5AuCl (L5 = VPhos)

To a solution of VPhos (0.254 g, 0.515 mmol) in DCM (6.61 ml) in a flame-dried reaction vial under argon was added gold(I) chloride dimethyl sulfide complex (0.152 g, 0.515 mmol). The mixture was stirred at rt for 3 h, then filtered through a short silica plug and eluding with DCM, and evaporated in vacuo to yield **L5**AuCl (0.390 g, 0.538 mmol, >95% yield), as a white solid.

^{1}H NMR (400 MHz, $CDCl_3$) δ 7.54 – 7.38 (m, 3H), 7.35 (d, *J* = 1.7 Hz, 1H), 7.34 – 7.29 (m, 1H), 6.77 (d, *J* = 1.7 Hz, 1H), 3.61 (s, 3H), 2.48 – 2.33 (m, 1H), 2.16 – 1.93 (m, 4H), 1.91 – 1.61 (m, 8H), 1.43 (s, 9H), 1.43 – 1.23 (m, 6H), 1.21 – 1.06 (m, 12H).

^{13}C NMR (101 MHz, $CDCl_3$) δ 156.31, 152.52, 147.84, 146.65, 146.52, 134.32, 134.24, 131.42, 131.39, 130.07, 130.05, 128.99, 128.45, 126.90, 126.83, 125.78, 125.71, 119.37, 104.98, 55.11, 53.56, 38.36, 38.04, 37.46, 35.35, 34.18, 34.12, 33.85, 33.68, 31.76, 31.40, 31.34, 29.99, 29.98, 28.05, 27.89, 27.65, 27.54, 27.14, 27.10, 26.85, 26.72, 26.51, 26.36, 26.12, 26.11, 25.71, 25.70. (The observed complexity is due to the P–C splitting.)

^{31}P NMR (121 MHz, $CDCl_3$) δ 34.43.

IR (neat, cm^{-1}): 2929, 2854, 2361, 2342.

HRMS (ESI+): m/z calc'd for $C_{33}H_{49}AuOP$ $[M\text{-}Cl]^+$ = 689.3206, found $[M\text{-}Cl]^+$ = 689.3187.

HRMS (ESI-): m/z calc'd for Cl $[M]^-$ = 34.9694, found $[M]^-$ = 34.9694.

XRAY: CCDC 1967543

MP: 257-259°C

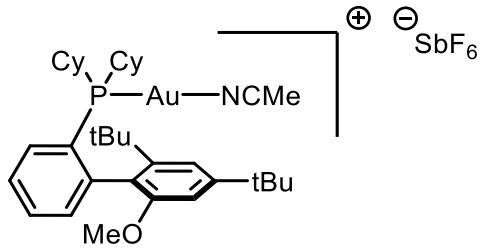

[L5Au(NCMe)][SbF$_6$] (L5 = VPhos)

To a flame-dried reaction vial under argon was added **L5**AuCl (1.6863 g, 2.325 mmol), DCM (5.00 ml), MeCN (5.00 ml), and silver(I) hexafluorostibate(V) (0.799 g, 2.325 mmol). The mixture was stirred for 4.5 h, then filtered through celite and washed with DCM. The filtrete was evaporated fully to give a white residue, which was diluted with DCM and filtered again through celite. The filtrete was evaporated fully to give a white residue, which was diluted with DCM and filtered through a short pad of silica and eluded with DCM. The eluant was evaporated to yield **L5**Au(NCMe)SbF$_6$ (1.75 g, 1.82 mmol, 78 % yield) as a white foam.

^{1}H NMR (600 MHz, $CDCl_3$) δ 7.56 – 7.48 (m, 3H), 7.33 (d, *J* = 1.7 Hz, 1H), 7.31 – 7.27 (m, 1H), 6.84 (d, *J* = 1.7 Hz, 1H), 3.65 (s, 3H), 2.54 – 2.43 (m, 1H), 2.38 (s, 3H), 2.13 – 1.97 (m, 4H), 1.97 – 1.84 (m, 3H), 1.84 – 1.76 (m, 1H), 1.76 – 1.63 (m, 3H), 1.64 – 1.52 (m, 1H), 1.49 – 1.31 (m, 14H), 1.28 – 1.13 (m, 4H), 1.11 (s, 9H).

^{13}C NMR (151 MHz, $CDCl_3$) δ 156.86, 152.74, 148.75, 145.67, 145.59, 134.22, 134.17, 131.29, 131.26, 131.00, 127.68, 127.63, 126.53, 126.13, 125.98, 125.93, 119.56, 118.57, 105.31, 55.34, 38.45, 38.22, 37.57, 35.37, 34.36, 34.33, 33.76, 33.71, 33.63, 33.48, 31.77, 31.65, 31.61, 30.41, 27.94, 27.84, 27.43, 27.36, 26.96, 26.94, 26.72, 26.63, 26.37, 26.27, 25.81, 25.47, 2.73. (The observed complexity is due to the P–C splitting.)

^{31}P NMR (121 MHz, $CDCl_3$) δ 31.60.

IR (neat, cm^{-1}): 2934, 2858, 1602.

HRMS (ESI+): m/z calc'd for $C_{35}H_{52}AuNOP$ $[M\text{-}SbF_6]^+$ = 730.3452, found $[M\text{-}SbF_6]^+$ = 730.3474.

HRMS (ESI-): m/z calc'd for SbF_6 $[M]^-$ = 234.8948, found $[M]^-$ = 234.8917.

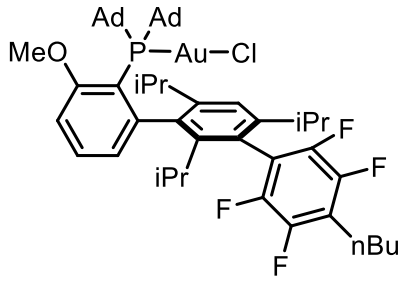

L9AuCl (L9 = AlPhos)

To a solution of AlPhos (0.100 g, 0.123 mmol) in DCM (1.57 ml) in a flame-dried reaction vial under argon was added gold(I) chloride dimethyl sulfide complex (0.036 g, 0.123 mmol). The mixture was stirred at rt for 18 h, then filtered through a short silica plug and eluding with DCM, and evaporated in vacuo to yield **L9**AuCl (0.128 g, 0.122 mmol, >95% yield) as a white foam.

^{1}H NMR (600 MHz, $CDCl_3$) δ 7.42 (t, *J* = 7.9 Hz, 1H), 7.24 (s, 1H), 7.01 (d, *J* = 8.2 Hz, 1H), 6.84 (dd, *J* = 7.7, 3.9 Hz, 1H), 3.92 (s, 3H), 2.77 (t, *J* = 7.8 Hz, 2H), 2.65 (hept, *J* = 7.2 Hz, 1H), 2.40 (dhept, *J* = 42.1, 6.8 Hz, 2H), 2.31 – 2.22 (m, 6H), 2.22 – 2.14 (m, 6H), 2.00 – 1.91 (m, 6H), 1.73 – 1.57 (m, 14H), 1.37 (dd, *J* = 16.4, 6.9 Hz, 8H), 1.06 (d, *J* = 6.8 Hz, 3H), 0.94 (t, *J* = 7.4 Hz, 3H), 0.90 (d, *J* = 6.6 Hz, 3H), 0.80 – 0.75 (m, 6H).

^{13}C NMR (151 MHz, $CDCl_3$) δ 160.96, 151.84, 151.75, 150.08, 147.37, 145.74, 145.64, 144.81, 144.72, 144.05, 143.30, 143.22, 143.13, 139.37, 139.33, 131.48, 128.50, 128.44, 122.67, 121.75, 120.02, 119.90, 119.78, 118.74, 118.61, 118.47, 116.98, 116.76, 109.53, 109.51, 54.38, 45.81, 45.65, 45.45, 45.30, 43.07, 43.05, 43.02, 43.00, 36.52, 36.48,

31.94, 31.60, 31.21, 30.74, 29.48, 29.41, 29.29, 29.23, 25.79, 24.90, 24.58, 23.41, 22.77, 22.61, 22.60, 22.45, 21.90, 13.88. (The observed complexity is due to P-C and P-F splitting.)

^{31}P NMR (121 MHz, $CDCl_3$) δ 71.58.

^{19}F NMR (282 MHz, $CDCl_3$) δ -131.58 (dd, *J* = 24.2, 12.8 Hz), -137.70 (dd, *J* = 24.1, 12.4 Hz), -145.36 (dd, *J* = 24.2, 12.3 Hz), -146.64 (dd, *J* = 24.1, 12.8 Hz).

IR (neat, cm^{-1}): 2903, 2850, 2223.

HRMS (ESI+): m/z calc'd for $C_{52}H_{67}AuClF_4OP$ $[M+H]^+$ = 1047.4292, found $[M+H]^+$ = 1047.4275.

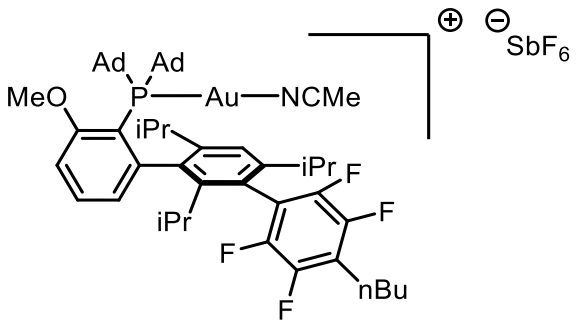

[L9Au(NCMe)][SbF_6] (L9 = AlPhos)

To a solution of **L9**AuCl (0.111 g, 0.106 mmol) in DCM (1.06 ml) and MeCN (1.06 mL) in a flame-dried reaction vial under argon was added silver(I) hexafluorostibate(V) (0.040 g, 0.117 mmol). The mixture was stirred for 18 h, then filtered through celite and washed with DCM. The filtrete was evaporated fully to give a white residue, which was diluted with DCM and filtered again through celite. The filtrete was evaporated fully to give a white residue, which was diluted with DCM and filtered through a short pad of silica and eluded with 4:1 DCM:MeCN (100 mL). The eluant was evaporated to yield **L9**Au(NCMe)SbF_6 (0.123 g, 0.095 mmol, 90% yield) as a white foam.

^{1}H NMR (600 MHz, $CDCl_3$) δ 7.51 (dt, *J* = 24.9, 8.0 Hz, 1H), 7.37 – 7.09 (m, 2H), 6.78 (ddd, *J* = 33.8, 7.8, 4.1 Hz, 1H), 3.99 (d, *J* = 4.4 Hz, 3H), 2.79 (dt, *J* = 23.6, 7.8 Hz, 2H), 2.71 – 2.53 (m, 1H), 2.48 – 2.28 (m, 3H), 2.17 (d, *J* = 51.6 Hz, 12H), 2.09 – 1.94 (m, 6H), 1.78 – 1.59 (m, 14H), 1.46 – 1.30 (m, 4H), 1.29 – 1.07 (m, 9H), 0.99 – 0.90 (m, 6H), 0.83 – 0.64 (m, 6H).

^{13}C NMR (151 MHz, $CDCl_3$) δ 161.11, 161.00, 150.58, 150.50, 150.10, 150.01, 149.96, 149.75, 149.24, 148.47, 144.80, 144.35, 139.66, 139.61, 139.54, 139.50, 132.99, 132.63, 128.19, 128.14, 128.07, 128.02, 123.01, 121.71, 121.63, 121.21, 121.09, 120.97, 120.70, 120.57, 120.44, 119.47, 118.03, 117.90, 117.77, 117.57, 117.43, 117.30, 115.08, 114.83, 114.50, 114.23, 110.72, 110.49, 54.99, 54.90, 47.54, 47.39, 46.56, 46.41, 46.28, 46.12, 45.04, 44.89, 43.58, 43.40, 43.33, 43.05, 36.27, 32.09, 32.02, 31.77, 31.61, 31.54, 31.43, 31.35, 31.25, 30.99, 30.60, 29.80, 29.52, 29.46, 29.37, 29.30, 29.26, 29.19, 25.88, 25.83, 25.72, 24.37, 23.53, 23.33, 22.83, 22.55, 22.50, 21.97, 21.80, 13.88, 2.83. (The observed complexity is due to P-C and P-F splitting.)

^{31}P NMR (121 MHz, $CDCl_3$) δ 71.61.

^{19}F NMR (282 MHz, $CDCl_3$) δ -131.63 (dd, *J* = 24.2, 12.8 Hz), -137.64 (dd, *J* = 24.1, 12.3 Hz), -145.42 (dd, *J* = 24.3, 12.2 Hz), -146.59 (dd, *J* = 24.1, 12.6 Hz).

IR (neat, cm^{-1}): 2904, 2850.

HRMS (ESI+): m/z calc'd for $C_{52}H_{70}AuF_4NOP$ $[M\text{-}SbF_6]^+$ = 1052.4791, found $[M\text{-}SbF_6]^+$ = 1052.4787.

HRMS (ESI-): m/z calc'd for SbF_6 $[M]^-$ = 234.8948, found $[M]^-$ = 234.8947.

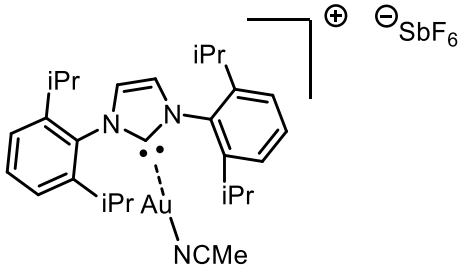

[L11Au(NCMe)][SbF_6] (L11 = IPr)

Synthesized and characterized according to reported literature.[44a]

5.3 CHAPTER 3 SUPPORTING INFORMATION (SALVINORIN A)

5.3.1 A-Ring Synthesis

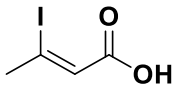

Vinyl iodide 3.2.1.1

Protocol adopted from literature procedure (Phillipe McGee's doctoral thesis)[73].

To a round-bottomed flask containing sodium iodide (14.3 g, 95 mmol) in AcOH (22 ml) was added but-2-ynoic acid (5.0 g, 59.5 mmol) and heated at 120°C for 3 hours. The reaction mixture was cooled down and H_2O (500ml) and Et_2O (500ml) was added. Sat. aq. $Na_2S_2O_3$ was added until the mixture turned pale yellow and the aqueous layer was extracted 3 times with ether. The combined organic layers were then dried over Na_2SO_4, filtered and concentrated under reduced pressure to afford **3.2.1.1** (11.98 g, 56.5 mmol, 95 % yield) as a white solid. Spectra matches reported literature.[94]

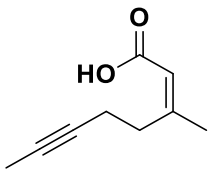

Carboxylic acid 3.2.1.2

Protocol and spectra adopted from literature procedure[95] and Phillipe McGee's doctoral thesis.[73]

In a mortar & pestle was added zinc dust (25.4 g, 389 mmol). Then 1M HCl (~10mL) was added and ground for ~1 min. The liquid was decanted. The zinc was further ground and washed sequentially in a mortar & pestle with iPrOH (3x), MeOH (1x), and ether (3x). The washed zinc was then placed into a 250 mL round-bottomed flask and flame-dried under

high vacuum, then backfilled with argon. Then THF (32.4 ml), and TMS-Cl (1.24 ml, 9.7 mmol) (Sigma-Aldrich, >99%, purified by redistillation) were added, then heated with a heat gun to reflux. The reaction mixture was cooled to RT then 1,2-dibromoethane (1.1 ml, 13 mmol) was added slowly (gas evolution observed), then heated with a heat gun to reflux. The reaction mixture was cooled to rt, then additional THF (32.4 ml) was added. Then 5-iodopent-2-yne (21.7 ml, 196 mmol) was added slowly (creeping *exo*thermic reaction is possible). The mixture was stirred under heating from it's own *exo*thermicity for 0.5 h. Then the mixture was stirred at 40°C for 48 h then allowed to settle for 4 h without stirring. The zincate solution was titrated using Knochel's method.[96]

Observed zincate conc: 3.0M

Theoretical zincate conc: 2.9M

The supernatant solution (grey-amber, translucent) was transferred via syringe (*exo*thermicity observed, do not cool with ice bath, control the *exo*thermicity by slow rate of addition) into a flame-dried 250 mL RBF under argon containing **3.2.1.1** (13.7 g, 64.8 mmol) and $Pd(Ph_3P)_4$ (3.74 g, 3.24 mmol) in THF (65 ml) (opaque orange-white emulsion) at 40°C. The mixture turned dark brown as the zincate solution was syringed in.

The mixture was stirred at 40°C for 18 h. The reaction was quenched with 1M HCl and extracted with ether (3 x 50mL). The organic layer was back extracted with 1M NaOH (3 x 150 mL). The combined NaOH aqueous layers were washed with DCM (2x) then acidified with conc. aq. HCl then extracted with EtOAc (3 x 150mL). The organic phase

was dried with sodium sulfate, filtered, and concentrated in vacuo, yielding a crude liquid. The crude product was added to a silica gel column and was eluted with 80:20 Hex/EtOAc, yielding **3.2.1.2** (5.9259 g, 38.9 mmol, 60 % yield) as a white solid.

^{1}H NMR (400 MHz, $CDCl_3$) δ ppm = 5.78 – 5.55 (m, 1H), 2.79 (t, J = 7.4 Hz, 2H), 2.33 (tq, J = 7.5, 2.6 Hz, 2H), 1.98 (d, J = 1.4 Hz, 3H), 1.76 (t, J = 2.6 Hz, 3H).

^{13}C NMR (101 MHz, $CDCl_3$) δ ppm = 171.66, 161.86, 116.58, 78.22, 76.37, 32.77, 25.92, 17.67, 3.42.

HRMS (EI) m/z calc'd for $C_9H_{12}O_2$ [M+]: 152.0837; found 152.0860.

IR (neat, cm^{-1}): 2922, 2854, 1686, 1637.

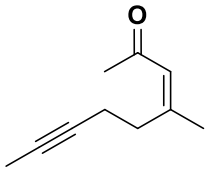

Ketone 3.2.1.3

Protocol adopted from literature procedure.[74] Spectra referenced from Phillipe McGee's doctoral thesis.[73]

To a flame-dried round-bottomed flask under argon was added copper(I) cyanide (1.79 g, 20.0 mmol) and Et_2O (33 ml). The reaction mixture was cooled to 0 °C then methyllithium 1.6M in diethyl ether (25 ml, 40 mmol) was added. The mixture was stirred at 0°C for 5 min. Then a solution of **3.2.1.2** (0.61 g, 4.0 mmol) in Et_2O (20 ml) was added dropwise. The reaction mixture was warmed to rt over 1 h. The mixture was stirred at rt for 18 h. The reaction mixture was then cannulated into an Erlenmeyer flask containing 100 mL of sat. NH_4Cl (some gas evolution) under rapid stirring. The biphasic mixture was stirred for an additional 10 min then filtered though celite. The layers were separated, and the organic phase was collected. The aq. layer was back extracted with ether (2 x 5 mL).

The combined organic layers were dried with sodium sulfate, filtered, and concentrated in vacuo to give a crude product. The crude product was purified by flash chromatography (10% EA in hexanes), yielding **3.2.1.3** (0.421 g, 2.80 mmol, 70 % yield).

^{1}H NMR (400 MHz, $CDCl_3$) δ ppm = 6.09 (s, 1H), 2.71 (t, J = 7.3 Hz, 2H), 2.30 (ddt, J = 7.4, 4.9, 2.6 Hz, 2H), 2.15 (s, 3H), 1.92 (d, J = 1.4 Hz, 3H), 1.74 (t, J = 2.6 Hz, 3H).

^{13}C NMR (101 MHz, $CDCl_3$) δ ppm = 198.09, 157.42, 124.76, 78.50, 76.06, 32.90, 31.67, 25.91, 17.60, 3.44.

HRMS (EI) m/z calc'd for $C_{10}H_{14}O$ [M+]: 150.1045; found 150.1055.

IR (neat, cm^{-1}): 2919, 2987, 1686, 1614, 1173.

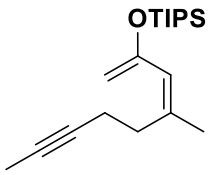

Silyl enol ether 3.1.3.8

Protocol and spectra adopted from literature procedure (Phillipe McGee's doctoral thesis).[73]

To a round-bottomed flask was added **3.2.1.3** (0.9543 g, 6.35 mmol), DCM (32 ml). The reaction mixture was cooled to 0°C. Then triisopropylsilyl trifluoromethanesulfonate (2.17 ml, 7.62 mmol) was added. The mixture was warmed to rt over 2 h, then quenched with sat. $NaHCO_3$ and the layers were separated. The aq. layer was back extracted with DCM (2 x 10 mL). The organic was dried with sodium sulfate, filtered, and concentrated in vacuo to give a crude product. The crude product was added to a Et_3N neutralized silica

gel column and was eluted with hexanes, yielding **3.1.3.8** (2.0698 g, 6.75 mmol, >95% yield) as a colourless liquid.

^{1}H NMR (400 MHz, $CDCl_3$) δ ppm = 5.61 (s, 1H), 4.27 (s, 1H), 4.19 (s, 1H), 2.60 (dd, J = 8.3, 7.4 Hz, 2H), 2.24 (ddt, J = 11.3, 7.5, 2.5 Hz, 2H), 1.77 (d, J = 1.5 Hz, 3H), 1.76 (t, J = 2.5 Hz, 3H), 1.29 – 1.17 (m, 3H), 1.15 – 1.05 (m, 18H).

^{13}C NMR (101 MHz, $CDCl_3$) δ ppm = 155.50, 138.60, 124.31, 94.10, 78.91, 75.71, 32.29, 24.25, 18.02, 17.93, 12.91, 3.45.

HRMS (EI) m/z calc'd for $C_{19}H_{34}OSi$ [M+]: 306.2379; found 306.2401.

IR (neat, cm^{-1}): 2944, 2866, 1014, 679.

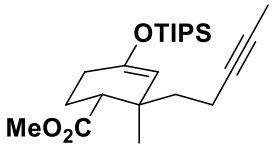

Silyl enol ether 3.1.3.7

Protocol and spectra adopted from literature procedure (Phillipe McGee's doctoral thesis).[73]

To a round-bottomed flask under air atmosphere was added **3.1.3.8** (2.0698 g, 6.75 mmol), DCM (32 ml), and methyl acrylate (3.06 ml, 33.8 mmol). The reaction mixture was cooled to -78°C then diethylaluminum chloride 1.0M in DCM (8.10 ml, 8.10 mmol) was added. The mixture was stirred at -78°C for 1 h then quenched with TEA (5 mL) and water (1mL). The reaction mixture was diluted with DCM, and washed with sat. Rochelle's salt. The aq. layer was back extracted with DCM (2 x 10 mL). The organic was dried with sodium sulfate, filtered, and concentrated in vacuo to give a crude product. The crude product was added to a silica gel column and was eluted with 98:2 Hex/EtOAc, yielding **3.1.3.7** (2.00 g, 5.09 mmol, 75 % yield) as a colourless liquid.

^{1}H NMR (400 MHz, $CDCl_3$) δ 4.54 (d, J = 1.8 Hz, 1H), 3.68 (s, 3H), 2.39 (dd, J = 12.2, 3.1 Hz, 1H), 2.30 – 1.86 (m, 6H), 1.82 (ddd, J = 7.0, 5.6, 3.7 Hz, 1H), 1.77 (t, J = 2.5 Hz, 3H), 1.51 (ddd, J = 13.6, 11.8, 4.4 Hz, 1H), 1.19 – 1.11 (m, 3H), 1.09 – 1.07 (m, 18H), 0.93 (s, 3H).

^{13}C NMR (101 MHz, $CDCl_3$) δ 174.72, 150.23, 111.66, 79.54, 75.19, 51.27, 45.49, 41.42, 37.50, 28.95, 24.87, 22.25, 17.97, 13.94, 12.60, 3.52.

HRMS (EI) m/z calc'd for $C_{23}H_{40}O_3Si$ [M+]: 392.2747; found 392.2743.

IR (neat, cm^{-1}): 2932, 2866, 1735, 1195.

5.3.2 Au(I) Cyclization Products and Characterization

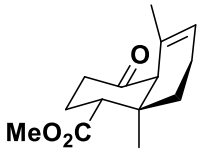

Bicycle 3.1.3.6

Protocol and spectra adopted from literature procedure (Phillipe McGee's doctoral thesis).[73]

To a reaction vial was added **3.1.3.7** (1.850 g, 4.71 mmol), DCM (20.7 ml), acetone (1.0 ml), and JohnPhosAu(NCMe)SbF_6 (0.182 g, 0.236 mmol). The mixture was stirred at rt for 18 h, then was evaporated. The crude product was added to a silica gel column and was eluted with 2-5-10% EA in hexanes, yielding **3.1.3.6** (1.019 g, 4.31 mmol, 92 % yield) as a colourless liquid.

^{1}H NMR (400 MHz, $CDCl_3$) δ 5.80 – 5.46 (m, 1H), 3.70 (s, 3H), 2.92 (dd, J = 10.6, 4.3 Hz, 1H), 2.81 – 2.69 (m, 1H), 2.53 – 2.21 (m, 3H), 2.20 – 1.95 (m, 3H), 1.63 (ddd, J = 13.6, 5.9, 3.9 Hz, 1H), 1.58 – 1.54 (m, 3H), 1.28 (ddd, J = 13.6, 9.6, 6.2 Hz, 1H), 0.99 (s, 3H).

^{13}C NMR (101 MHz, $CDCl_3$) δ 212.38, 174.27, 128.89, 123.32, 62.35, 51.51, 44.36, 38.80, 38.15, 32.74, 24.65, 22.56, 22.34, 21.73.

HRMS (EI) m/z calc'd for $C_{14}H_{20}O_3$ [M+]: 236.1412; found 236.1418.

IR (neat, cm^{-1}): 2953, 2255, 1709, 1705.

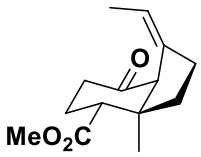

Bicycle 3.2.2.2 (Side product of Au(I) cyclization)

Spectra adopted from literature procedure (Phillipe McGee's doctoral thesis).[73]

^{1}H NMR (400 MHz, $CDCl_3$) δ 5.48 (qq, J = 6.9, 2.2 Hz, 1H), 3.65 (s, 3H), 3.02 (s, 1H), 2.64 (dd, J = 7.8, 5.9 Hz, 1H), 2.56 – 2.28 (m, 5H), 2.13 – 1.95 (m, 2H), 1.83 (ddd, J = 12.8, 8.8, 5.4 Hz, 1H), 1.44 (dq, J = 7.0, 2.0 Hz, 3H), 0.97 (s, 3H).

^{13}C NMR (101 MHz, $CDCl_3$) δ 211.14, 174.13, 138.59, 120.88, 63.28, 51.50, 49.98, 45.96, 37.79, 36.48, 29.77, 25.24, 22.16, 14.38.

HRMS (EI) m/z calc'd for $C_{14}H_{20}O_3$ [M+]: 236.1412; found 236.1373.

IR (neat, cm^{-1}): 2950, 2251, 1732, 1700.

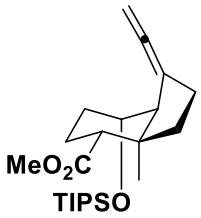

Allene 3.2.2.1 (Side product of Au(I) cyclization)

Spectra adopted from literature procedure (Phillipe McGee's doctoral thesis).[73]

^{1}H NMR (400 MHz, $CDCl_3$) δ 4.86 – 4.56 (m, 2H), 4.24 – 4.03 (m, 1H), 3.66 (s, 3H), 2.58 – 2.39 (m, 2H), 2.32 (dd, J = 12.8, 2.9 Hz, 1H), 2.25 – 2.00 (m, 2H), 1.70 – 1.41 (m, 3H), 1.41 – 1.23 (m, 2H), 1.20 (s, 3H), 1.10 – 0.99 (m, 21H).

^{13}C NMR (101 MHz, $CDCl_3$) δ 202.19, 175.23, 104.20, 77.16, 67.94, 55.62, 51.15, 44.99, 43.61, 37.16, 28.96, 26.75, 22.79, 18.93, 18.18, 12.28.

HRMS (EI) m/z calc'd for $C_{23}H_{40}O_3Si$ [M+]: 392.2747; found 392.2755.

IR (neat, cm^{-1}): 2943, 2865, 1736, 1045.

5.3.3 B-Ring Functionalization

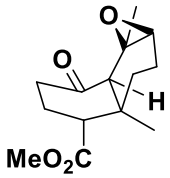

Epoxide 3.2.3.1

Protocol and spectra adopted from literature procedure (Phillipe McGee's doctoral thesis).[73]

To a solution of **3.1.3.6** (2.46 g, 10.4 mmol) and formic acid (1.74 ml, 62 mmol) in DCM (100 ml) was added 30% H_2O_2 (5.4 ml, 42 mmol) via a syringe pump over 5 hours. The mixture was then stirred overnight at room temperature and water (100 ml) was added. The aqueous layer was extracted with DCM (3x). The combined organic layer was dried over anhydrous $MgSO_4$, filtered and the solvent was evaporated under reduce pressure. The crude was purified by flash column chromatography on silica gel (10% to 20% EtOAc in hexane) to give **3.2.3.1** (2.11 g, 81%).

^{1}H NMR (400 MHz, $CDCl_3$) δ 3.65 (s, 3H), 3.55 – 3.38 (m, 1H), 3.07 (d, J = 5.6 Hz, 1H), 2.64 – 2.49 (m, 1H), 2.39 (ddt, J = 14.0, 4.0, 1.6 Hz, 1H), 2.35 – 2.17 (m, 2H), 2.09 – 1.92 (m, 3H), 1.68 – 1.57 (m, 1H), 1.21 (s, 3H), 1.11 – 0.98 (m, 1H), 0.89 (s, 3H).

^{13}C NMR (101 MHz, $CDCl_3$) δ 210.95, 174.02, 61.34, 59.08, 57.93, 51.40, 42.66, 39.23, 38.35, 32.65, 24.27, 24.01, 22.23, 20.73.

HRMS (EI) m/z calc'd for $C_{14}H_{20}O_4$ [M+Na]: 275.1262; found 275.1238.

IR (neat, cm-1): 2941, 1731, 1702, 1209.

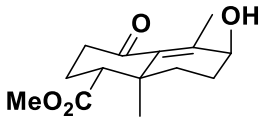

Alcohol 3.1.3.5

Protocol and spectra adopted from literature procedure (Phillipe McGee's doctoral thesis).[73]

To a round-bottomed flask was added **3.1.3.6** (0.2293 g, 0.970 mmol), DCM (9.7 ml), and formic acid (0.22 ml, 5.8 mmol). Then 30% aq. hydrogen peroxide (0.40 ml, 3.9 mmol) was added via syringe pump over 3 hours. The mixture was stirred at rt for 18 h. Then DBU (1.463 ml, 9.70 mmol) was added dropwise. The mixture was stirred at 40°C for 24 h. The reaction was quenched with sat. NH_4Cl. The layers were separated, and the organic phase was collected. The aq. layer was back extracted with DCM (2 x 5 mL). The organic phases were dried with sodium sulfate, filtered, and concentrated in vacuo to give a crude product. The crude product was added to a silica gel column and was eluted with 50:50 Hex/EtOAc, yielding **3.1.3.5** (0.1513 g, 0.600 mmol, 61.8 % yield) as a white solid.

^{1}H NMR (400 MHz, $CDCl_3$) δ 3.99 (t, J = 3.2 Hz, 1H), 3.69 (s, 3H), 2.74 (dd, J = 12.8, 3.7 Hz, 1H), 2.58 (ddd, J = 14.6, 4.7, 1.9 Hz, 1H), 2.37 (ddd, J = 14.6, 13.2, 7.1 Hz, 1H), 2.30

– 2.16 (m, 1H), 2.08 – 1.98 (m, 1H), 1.97 – 1.88 (m, 1H), 1.86 (s, 3H), 1.84 – 1.73 (m, 2H), 1.53 – 1.39 (m, 1H), 1.04 (s, 3H).

^{13}C NMR (101 MHz, $CDCl_3$) δ 205.04, 173.68, 140.92, 137.68, 67.95, 52.49, 51.54, 41.80, 40.33, 30.26, 26.97, 23.84, 18.75, 18.62.

HRMS (EI) m/z calc'd for $C_{14}H_{20}O_4$ [M+]: 252.1362; found 252.1372.

IR (neat, cm^{-1}): 3445, 2926, 1723, 1679.

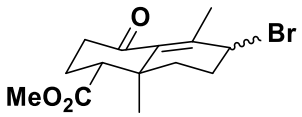

Alkyl bromide 3.2.4.1

Protocol and spectra adopted from literature procedure (Phillipe McGee's doctoral thesis).[73]

PBr_3 (0.07 ml, 0.68 mmol) was added to **3.1.3.5** (115 mg, 0.456 mmol) in DCM (2.3 ml) and stirred for 1 hour at room temperature. A saturated solution of $NaHCO_3$ was added and the aqueous layer was extracted with DCM (3x). The combined organic layer was dried over anhydrous $MgSO_4$, filtered and the solvent was evaporated under reduce pressure. The crude was purified by flash column chromatography on silica gel (10% to 30% EtOAc in hexane) to give **3.2.4.1** as mixture of diastereomer (2:1, 100 mg, 70%).

^{1}H NMR (400 MHz, $CDCl_3$) δ 4.64 – 4.55 (m, 1H), 3.71 (s, 2H), 3.69 (s, 1H), 2.99 – 2.81 (m, 0H), 2.77 (dd, *J* = 12.9, 3.7 Hz, 1H), 2.57 (ddd, *J* = 14.8, 4.9, 2.0 Hz, 1H), 2.40 (ddd, *J* = 14.8, 13.2, 7.3 Hz, 1H), 2.31 – 2.16 (m, 2H), 2.14 – 1.97 (m, 2H), 1.86 (s, 2H), 1.85 (s, 1H), 1.60 – 1.51 (m, 1H), 1.11 (s, 1H), 1.05 (d, *J* = 0.8 Hz, 2H).

^{13}C NMR (101 MHz, $CDCl_3$) δ 204.73, 204.50, 173.37, 173.19, 141.57, 140.77, 137.03, 134.03, 53.52, 53.37, 52.47, 51.67, 51.62, 49.53, 41.71 , 41.35, 40.31, 40.17, 31.26, 30.87, 28.92, 27.97, 24.05, 23.89, 21.67, 19.68, 19.35, 19.33.

HRMS (EI) m/z calc'd for $C_{14}H_{19}BrO_3$ [M^+]: 314.0518; found 314.0541.

IR (neat, cm^{-1}): 2951, 2363, 1731, 1693.

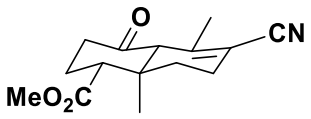

Vinyl cyanide 3.2.4.2

Protocol and spectra adopted from literature procedure (Phillipe McGee's doctoral thesis).[73]

NaCN (20 mg, 0.4 mmol) was added to **3.2.4.1** (63 mg, 0.2 mmol) in MeCN (2 ml) and heated at 70 °C for 3 days. A saturated solution of $NaHCO_3$ was added and the aqueous layer was extracted with DCM (3x). The combined organic layer was dried over anhydrous $MgSO_4$, filtered and the solvent was evaporated under reduce pressure. The crude was purified by flash column chromatography on silica gel (30% to 50% EtOAc in hexane) to give the nitrile **3.2.4.2** (28.1 mg, 54%).

^{1}H NMR (400 MHz, CHLOROFORM-*d*) δ ppm = 3.74 (s, 3H), 3.18 – 3.12 (m, 1H), 2.72 – 2.62 (m, 2H), 2.56 – 2.45 (m, 1H), 2.37 – 2.28 (m, 1H), 2.24 (dt, *J* = 14.0, 7.0 Hz, 1H), 2.11 (tdd, *J* = 7.0, 5.6, 2.0 Hz, 2H), 1.97 (td, *J* = 2.2, 0.8 Hz, 3H), 1.69 (dt, *J* = 13.5, 6.7 Hz, 1H), 1.40 – 1.30 (m, 1H), 1.01 (s, 3H).

^{13}C NMR (101 MHz, CHLOROFORM-*d*) δ ppm = 208.55, 173.75, 148.48, 118.21, 107.78, 61.06, 51.79, 46.50, 38.75, 38.16, 30.73, 24.55, 24.17, 22.30, 21.98.

HRMS (EI) m/z calcd for $C_{15}H_{19}O_3$ [M^+]: 261.1365; found 261.1392.

IR (neat, cm^{-1}): 2951, 2920, 2361, 2340, 1729, 1730.

5.3.4 C-Ring Construction

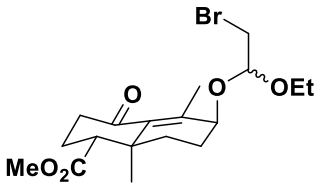

Alkyl bromide 3.2.3.2

Protocol and spectra adopted from literature procedure (Phillipe McGee's doctoral thesis).[73]

To a flame-dried round-bottomed flask under argon was added NBS (5.79 g, 32.6 mmol), and DCM (32.6 ml). Then ethyl vinyl ether (3.44 ml, 35.8 mmol) was added at 0°C. The mixture was stirred at 0 °C for 1 h. Then **3.1.3.5** (4.1068 g, 16.28 mmol) was added. The mixture was stirred at rt for 18 h then evaporated. The reaction residue was diluted with ether and washed with H2O. The aq. layer was back extracted with ether (2 x 20 mL). The combined organic layers were dried with sodium sulfate, filtered, and concentrated in vacuo to give a crude product. The crude product was added to a basified silica gel (triethylamine) column and was eluted with 80:20 Hex/EtOAc, yielding **3.2.3.2** (5.4612 g, 13.54 mmol, 83% yield) as a colourless liquid.

^{1}H NMR (400 MHz, $CDCl_3$) δ 4.77 – 4.69 (m, 2H), 3.90 (q, J = 2.2 Hz, 1H), 3.75 (t, J = 3.1 Hz, 1H), 3.73 – 3.56 (m, 10H), 3.46 – 3.37 (m, 2H), 3.41 – 3.30 (m, 2H), 2.76 (ddd, J = 12.8, 4.6, 3.8 Hz, 2H), 2.56 (ddd, J = 14.8, 5.0, 2.0 Hz, 2H), 2.38 (dddd, J = 14.7, 13.3, 7.2, 3.2 Hz, 2H), 2.21 (qd, J = 13.3, 4.9 Hz, 2H), 2.07 – 1.85 (m, 5H), 1.83 (s, 3H), 1.83 (s, 3H), 1.73 – 1.51 (m, 2H), 1.50 – 1.36 (m, 2H), 1.23 (dt, J = 7.0, 4.0 Hz, 6H), 1.06 – 1.00 (m, 6H).

^{13}C NMR (101 MHz, $CDCl_3$) δ 205.20, 205.11, 173.67, 173.62, 142.20, 141.96, 135.64, 135.52, 103.12, 100.23, 75.28, 72.58, 62.15, 62.09, 52.29, 52.28, 51.53, 51.52, 41.85, 41.81, 40.29, 40.25, 32.14, 32.01, 30.47, 30.17, 24.51, 23.95, 23.93, 22.72, 18.72, 18.63, 18.60, 18.52, 15.33, 15.13.

HRMS (ESI) m/z calc'd for $C_{18}H_{27}BrO_5$ [M+Na]: 427.0919; found 427.0942.

IR (neat, cm^{-1}): 2970, 2945, 1731, 1691.

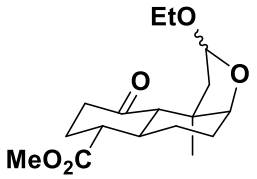

Cyclic acetal 3.1.3.4

Protocol and spectra adopted from literature procedure (Phillipe McGee's doctoral thesis).[73]

To a high-pressure tube was added **3.2.3.2** (1.92 g, 4.76 mmol), MeCN (31.7 ml), DIPEA (4.16 ml, 23.8 mmol), and $Au_2(dppm)_2Cl_2$ (0.587 g, 0.476 mmol). The mixture was degassed with argon (sparge) for 5 min. The mixture was stirred for 18 h under UVA irradiation (365 nm LED). The reaction mixture was concentrated in vacuo to give a crude product. The crude product was added to a silica gel column and was eluted with 80:20 Hex/EtOAc, yielding **3.1.3.4** (1.51 g, 4.65 mmol, 98 % yield) as a 1:1 mixture of diastereomers, as an amber liquid.

^{1}H NMR (400 MHz, $CDCl_3$) δ 5.02 – 4.94 (m, 2H), 3.81 – 3.59 (m, 9H), 3.51 (t, J = 2.8 Hz, 1H), 3.46 – 3.31 (m, 2H), 3.16 (s, 1H), 2.65 (dt, J = 12.6, 3.4 Hz, 2H), 2.40 (dddd, J = 14.7, 13.4, 5.2, 1.9 Hz, 2H), 2.33 – 2.08 (m, 7H), 2.05 – 1.90 (m, 3H), 1.89 – 1.68 (m, 5H), 1.59 (dd, J = 14.3, 4.4 Hz, 1H), 1.34 – 1.20 (m, 9H), 1.16 (dt, J = 7.1, 3.2 Hz, 6H), 1.01 (s, 6H).

^{13}C NMR (101 MHz, $CDCl_3$) δ 209.40, 208.99, 173.77, 173.58, 102.96, 102.59, 84.60, 81.18, 63.54, 63.28, 59.98, 58.37, 55.22, 54.91, 51.38, 51.36, 50.25, 49.27, 42.05, 41.59, 41.53, 40.97, 40.89, 39.31, 31.99, 31.82, 24.72, 24.64, 21.19, 20.50, 20.36, 19.80, 15.63, 15.37, 15.27.

HRMS (EI) m/z calc'd for $C_{18}H_{28}O_5$ [M+]: 324.1937; found 324.1957.

IR (neat, cm^{-1}): 2931, 1731, 1708, 995.

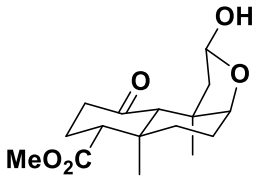

Hemiacetal 3.2.3.6

Protocol and spectra adopted from literature procedure (Phillipe McGee's doctoral thesis)[73].

In a reaction vial containing p-TSA (60 mg, 0.3 mmol) was added to **3.1.3.4** (100 mg, 0.3 mmol) in THF:H2O (1:1, 1.5 ml) and refluxed for 3 hours. The reaction mixture was quenched with saturated $NaHCO_3$ and extracted with DCM (3x). The combined organic layers were dried over anhydrous $MgSO_4$, filtered and the solvent was evaporated under reduce pressure. The crude was purified by flash column chromatography on silica gel (70% EtOAc in hexane) to give **3.2.3.6** (77 mg, 87%).

1H NMR (400 MHz, $CDCl_3$) δ 5.50 – 5.34 (m, 1H), 3.84 (d, J = 2.6 Hz, 1H), 3.66 (s, 3H), 2.96 (d, J = 3.5 Hz, 1H), 2.70 (ddd, J = 12.9, 3.5 Hz, 1H), 2.43 (ddt, J = 10.9, 5.6, 2.2 Hz, 1H), 2.36 – 2.13 (m, 3H), 2.02 – 1.91 (m, 1H), 1.89 – 1.71 (m, 3H), 1.63 – 1.54 (m, 1H), 1.34 (s, 3H), 1.31 – 1.25 (m, 1H), 1.02 (s, 3H).

13C NMR (101 MHz, $CDCl_3$) δ 208.97, 173.59, 97.12, 81.59, 59.83, 54.90, 51.50, 51.34, 42.70, 41.58, 40.98, 31.77, 24.63, 20.47, 19.87, 15.30.

HRMS (EI) m/z calc'd for $C_{16}H_{24}O_5$ [M-OH]: 279.1596; found 279.1600.

IR (neat, cm^{-1}): 3430, 2926, 1723, 1709.

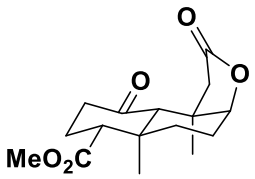

Lactone 3.2.3.11

Protocol and spectra adopted from literature procedure (Phillipe McGee's doctoral thesis).[73]

To a reaction vial containing PCC (30 mg, 0.13 mmol) was added to **3.2.3.6** (20 mg, 0.068 mmol) and SiO_2 (30 mg) in DCM (0.34 ml). The reaction mixture was stirred for 3 hours and filtrated over cotton. The residue was evaporated under reduced pressure and purified by flash column chromatography on silica gel (40% to 60% EtOAc in hexane) to give the desired **3.2.3.11** (18 mg, 91%).

1H NMR (400 MHz, $CDCl_3$) δ 4.13 (s, 1H), 3.66 (s, 3H), 2.67 (dd, J = 13.0, 3.6 Hz, 1H), 2.53 (d, J = 17.5 Hz, 1H), 2.48 – 2.40 (m, 1H), 2.39 – 2.26 (m, 2H), 2.24 – 2.10 (m, 2H), 2.09 – 1.93 (m, 2H), 1.90 – 1.69 (m, 2H), 1.42 (s, 4H), 1.06 (s, 3H).

13C NMR (101 MHz, $CDCl_3$) δ 207.62, 176.60, 173.19, 84.90, 58.39, 54.24, 51.58, 47.35, 41.09, 40.28, 40.24, 31.29, 24.34, 20.04, 19.75, 14.94.

HRMS (EI) m/z calc'd for $C_{16}H_{22}O_5$ [M+]: 294.1467; found 294.1444.

IR (neat, cm^{-1}): 2940, 1760, 1700, 1727.

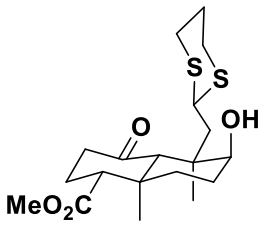

Alcohol 3.2.3.4

Protocol and spectra adopted from literature procedure (Phillipe McGee's doctoral thesis)[73].

To a round-bottomed flask was added **3.1.3.4** (1.47 g, 4.53 mmol), DCM (22.66 ml), and 1,3-propanedithiol (1.375 ml, 13.59 mmol). The reaction mixture was cooled to 0 °C. Then boron trifluoride etherate (1.723 ml, 13.59 mmol) was added. The mixture was stirred at 0 °C for 1 h. Then the mixture was stirred at rt for 20 min. The reaction was quenched with sat. NaHCO3 and stirred for 10 min. The layers were separated and the organic phase was collected. The aq. layer was back extracted with DCM (2 x 2 mL). The combined organic layers were dried with sodium sulfate, filtered, and concentrated in vacuo to give a crude product. The crude product was added to a silica gel column and was eluted with 20-30% EA in hexanes, yielding **3.2.3.4** (1.40 g, 3.62 mmol, 80 % yield) as a white amorphous solid.

^{1}H NMR (400 MHz, $CDCl_3$) δ 4.07 (dd, J = 6.4, 3.0 Hz, 1H), 3.66 (s, 3H), 3.66 – 3.63 (m, 1H), 3.00 – 2.87 (m, 2H), 2.85 – 2.73 (m, 2H), 2.70 – 2.61 (m, 2H), 2.40 – 2.32 (m, 2H), 2.24 – 1.95 (m, 5H), 1.92 – 1.79 (m, 2H), 1.75 – 1.58 (m, 2H), 1.29 (s, 3H), 1.27 – 1.18 (m, 1H), 1.06 (s, 3H).

^{13}C NMR (101 MHz, $CDCl_3$) δ 210.25, 173.62, 71.30, 58.98, 55.56, 51.38, 44.46, 42.60, 42.30, 41.39, 40.24, 31.48, 31.26, 31.19, 25.84, 25.10, 24.30, 18.66, 15.94.

HRMS (EI) m/z calc'd for $C_{19}H_{30}O_2S_2$ [M+]: 386.1586; found 386.1598.

IR (neat, cm^{-1}): 3462, 3947, 2362, 1727, 1707.

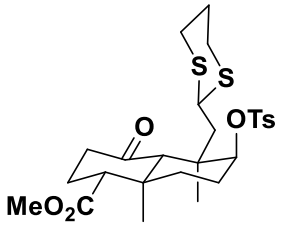

Alkyl tosylate 3.2.3.13

Protocol and spectra adopted from literature procedure (Phillipe McGee's doctoral thesis).[73]

n-BuLi (0.12 ml, 0.28 mmol) was added to **3.2.3.4** (50 mg, 0.13 mmol) in THF (0.65 ml) at -78°C and stirred for 5 minutes. TsCl (37 mg, 0.19 mmol) was added and the reaction mixture was warmed at room temperature. The reaction mixture was quenched with sat. $NaHCO_3$ and the aqueous layer was extracted with EtOAc (3x). The combined organic layers were dried over anhydrous $MgSO_4$, filtered and the solvent was evaporated under reduce pressure. The crude was purified by flash column chromatography on silica gel (20% to 30% EtOAc in hexane) to give the desired compound **3.2.3.13** (46 mg, 65%).

1H NMR (400 MHz, CHLOROFORM-d) δ ppm = 7.89 (d, J = 8.3 Hz, 2H), 7.37 (d, J = 8.0 Hz, 2H), 4.58 – 4.46 (m, 1H), 4.20 (dd, J = 7.5, 4.6 Hz, 1H), 3.66 (s, 3H), 3.08 – 2.83 (m, 1H), 2.82 – 2.63 (m, 4H), 2.46 (s, 3H), 2.30 (ddd, J = 13.4, 5.2, 1.9 Hz, 1H), 2.12 (qd, J = 13.5, 5.2 Hz, 1H), 2.02 – 1.72 (m, 6H), 1.48 (dd, J = 15.2, 4.5 Hz, 1H), 1.43 (s, 3H), 1.33 – 1.20 (m, 4H), 1.03 (s, 3H).

HRMS (EI) m/z calcd for $C_{26}H_{36}O_6S_3$ $[M^+]$: 540.1674; found 540.1674.

IR (neat, cm-1): 2953, 1735, 1711.

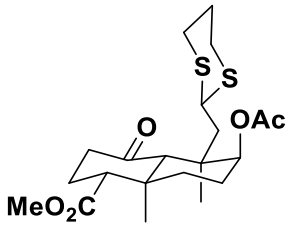

Dithiane 3.2.5.1

Protocol and spectra adopted from literature procedure (Phillipe McGee's doctoral thesis).[73]

To a round-bottomed flask under argon was added **3.2.3.4** (2.84 g, 7.35 mmol), DCM (36.7 ml), triethylamine (4.10 ml, 29.4 mmol), DMAP (0.180 g, 1.469 mmol), and acetic anhydride (2.080 ml, 22.04 mmol). The mixture was stirred at rt for 1.5 h. The reaction mixture was diluted with DCM, and washed with sat. NaHCO3. The aq. layer was back extracted with DCM (2 x 20 mL). The organic was dried with sodium sulfate, filtered, and concentrated in vacuo to give a crude product. The reaction mixture was filtered through a silica plug, eluding with 70:30 Hex/EtOAc, then evaporated, yielding **3.2.5.1** (3.10 g, 7.23 mmol, 98 % yield) as a white amorphous solid.

^{1}H NMR (400 MHz, $CDCl_3$) δ 4.72 (dd, J = 3.4, 2.2 Hz, 1H), 3.94 (t, J = 5.0 Hz, 1H), 3.65 (s, 3H), 2.86 (dddd, J = 14.5, 12.2, 4.2, 2.5 Hz, 2H), 2.77 – 2.63 (m, 2H), 2.51 (s, 1H), 2.46 – 2.29 (m, 2H), 2.23 – 2.10 (m, 1H), 2.09 (s, 3H), 2.05 – 1.91 (m, 3H), 1.86 – 1.66 (m, 4H), 1.55 (dd, J = 14.9, 4.6 Hz, 1H), 1.38 (s, 3H), 1.33 – 1.17 (m,
2H), 1.04 (s, 3H).

^{13}C NMR (101 MHz, $CDCl_3$) δ 209.24, 173.25, 170.26, 75.03, 59.81, 55.77, 51.54, 44.40, 42.47, 42.14, 41.97, 39.16, 32.03, 31.57, 31.50, 25.77, 25.13, 21.71, 21.65, 19.02, 15.88.

HRMS (EI) m/z calc'd for $C_{21}H_{32}O_5S_2$ [M+]: 428.1691; found 428.1698.

IR (neat, cm^{-1}): 2947, 2358, 1728, 1726, 1715.

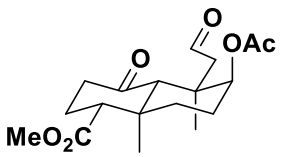

Aldehyde 3.1.3.3

Protocol and spectra adopted from literature procedure (Phillipe McGee's doctoral thesis).[73]

To a reaction vial was added **3.2.5.1** (0.8259 g, 1.927 mmol), MeCN (96 ml), Water (96 ml), calcium carbonate (3.47 g, 34.7 mmol), and iodomethane (9.64 ml, 154 mmol). The mixture was stirred at rt for 18 h, filtered through celite and extracted with EtOAc (15 mL). The aq. layer was back extracted with EtOAc (2 x 10 mL). The organic was dried with sodium sulfate, filtered, and concentrated in vacuo to give a crude product. The crude product was added to a silica gel column and was eluted with 70:30 Hex/EtOAc, yielding **3.1.3.3** (0.6442 g, 1.904 mmol, 99 % yield) as a yellow liquid.

^{1}H NMR (400 MHz, $CDCl_3$) δ 9.70 (dd, J = 3.2, 2.3 Hz, 1H), 4.69 (t, J = 2.7 Hz, 1H), 3.68 (s, 3H), 2.82 – 2.68 (m, 2H), 2.52 – 2.36 (m, 4H), 2.28 – 2.13 (m, 1H), 2.05 (s, 4H), 1.96 – 1.85 (m, 1H), 1.82 – 1.71 (m, 2H), 1.46 (s, 3H), 1.40 – 1.31 (m,

1H), 1.09 (s, 3H).

^{13}C NMR (101 MHz, $CDCl_3$) δ 209.43, 201.13, 173.17, 169.83, 76.96, 58.02, 55.54, 52.43, 51.59, 41.87, 41.83, 39.66, 32.12, 25.38, 21.74, 21.23, 20.82, 15.99.

HRMS (EI) m/z calc'd for $C_{18}H_{26}O_6$ [M-O]: 324.1937; found 324.6226.

IR (neat, cm^{-1}): 2951, 1729, 1711, 1706.

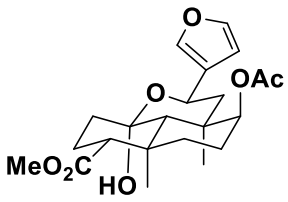

Cyclic hemiacetal 3.2.5.2

Protocol and spectra adopted from literature procedure (Phillipe McGee's doctoral thesis).[73]

To a flame-dried round-bottomed flask under argon was added distilled 3-bromofuran (1.076 ml, 11.97 mmol) (clear colourless) and THF (10.88 ml). The reaction mixture was cooled to -78 °C. Then n-butyllithium 2.5M in hexanes (4.79 ml, 11.97 mmol) was added. The mixture was stirred at -78 °C for 1 h. Then triisopropoxytitanium(IV) chloride 1.0M in hexanes (11.97 ml, 11.97 mmol) was added. The reaction mixture was warmed to rt and stirred for 0.5 h forming a brown suspension.

The mixture containing LiCl precipitate was then slowly syringed into a flame-dried round-bottomed flask under argon containing a solution of **3.1.3.3** (2.0253 g, 5.98 mmol) in THF (19.04 ml) at 0 °C. The mixture was stirred at rt for 1 h, then quenched with 5% EDTA aq. sol. (pH 9) (20 mL), and diluted with The crude product was added to a silica gel column and was eluted with 70:30 Hex/EtOAc, yielding **3.2.5.2** (1.5433 g, 3.80 mmol, 63.4 % yield) as a white solid as the sole diastereomer.

Note: The product quickly degrades via elimination of the hydroxyl group when in solution in DCM or chloroform.

^{1}H NMR (400 MHz, C_6D_6) δ 7.36 – 7.33 (m, 1H), 7.13 (t, *J* = 1.7 Hz, 1H), 6.30 (dd, *J* = 1.9, 0.8 Hz, 1H), 5.12 – 5.06 (m, 1H), 4.74 – 4.70 (m, 1H), 3.35 (s, 3H), 2.17 (dd, *J* = 12.9, 2.6 Hz, 1H), 2.06 (qd, *J* = 13.5, 3.9 Hz, 1H), 1.96 (t, *J* = 12.3 Hz, 1H), 1.91 – 1.71 (m, 3H), 1.67 – 1.58 (m, 1H), 1.60 (s, 3H), 1.58 – 1.46 (m, 2H), 1.45 – 1.36 (m, 1H), 1.39 (s, 3H), 1.34 (s, 3H), 1.29 – 1.22 (m, 2H), 1.08 (d, *J* = 2.0 Hz, 1H).

^{13}C NMR (101 MHz, C_6D_6) δ 173.58, 169.62, 143.15, 139.10, 128.50, 109.21, 97.34, 76.20, 61.97, 57.35, 50.71, 49.49, 45.35, 41.18, 37.53, 36.71, 35.98, 22.76, 22.27, 21.83, 20.69, 15.75.

HRMS (EI) m/z calc'd for $C_{22}H_{30}O_7$ [M+]: 406.1992; found 406.1982.

IR (neat, cm^{-1}): 3483, 1936, 1726, 1707.

MP: 174.5-175.5°C

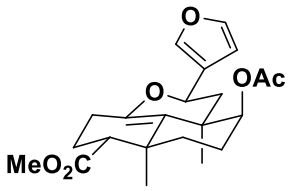

Cyclic enol ether 3.2.5.8

To a flame-dried round-bottomed flask under argon was added distilled 3-bromofuran (0.15 ml, 1.7 mmol) (clear colourless) and THF (1.5 ml). The reaction mixture was cooled to -78 °C. Then N-butyllithium 2.5M in hexanes (0.66 ml, 1.7 mmol) was added. The mixture was stirred at -78 °C for 1 h. Then triisopropoxytitanium(IV) chloride 1.0M in hexanes (1.7 ml, 1.7 mmol) was added. The reaction mixture was warmed to RT and stirred for 0.5 h forming a brown suspension. The mixture containing LiCl precipitate was then slowly syringed into a flame-dried round-bottomed flask under argon containing a solution of **3.1.3.3** (0.2801 g, 0.828 mmol) in THF (2.6 ml) at 0 °C. The mixture was stirred at RT for 1 h. Then triethylsilyl trifluoromethanesulfonate (0.56 ml, 2.5 mmol) was added to give a clear dark red solution. The mixture was stirred at RT for 18 h and quenched with sat. $NaHCO_3$ (1.5 mL). The reaction mixture was diluted with EtOAc, and washed with sat $NaHCO_3$. The layers were separated and the organic phase was collected. The aq layer was backextracted with EtOAc (2 x 5 mL). The combined organic layers were

washed with sat NaCl (1 x 20 mL). The organic was dried Na_2SO_4, filtered, and concentrated in vacuo to give a crude product. The crude product was added to a silica gel column and was eluted with 80:20 Hex/EtOAc, yielding **3.2.5.8** (0.2127g, 0.548 mmol, 66% yield) as an off-white solid.

^{1}H NMR (400 MHz, $CDCl_3$) δ 7.41 (dt, *J* = 1.6, 0.8 Hz, 1H), 7.39 (t, *J* = 1.7 Hz, 1H), 6.39 (dd, *J* = 1.8, 0.9 Hz, 1H), 5.00 (dd, *J* = 12.3, 1.6 Hz, 1H), 4.77 (dd, *J* = 3.4, 2.1 Hz, 1H), 3.67 (s, 3H), 2.45 (dd, *J* = 12.9, 2.7 Hz, 1H), 2.29 – 2.20 (m, 1H), 2.07 (s, 3H), 2.13 – 1.96 (m, 4H), 1.82 – 1.64 (m, 3H), 1.49 (dt, *J* = 13.4, 3.6 Hz, 1H), 1.41 (dd, *J* = 13.2, 2.2 Hz, 1H), 1.39 (s, 3H), 1.22 (s, 3H).

^{13}C NMR (101 MHz, $CDCl_3$) δ 175.05, 170.78, 146.77, 143.38, 139.44, 126.76, 111.93, 108.73, 74.99, 65.69, 53.46, 51.37, 40.34, 35.47, 35.29, 32.98, 29.95, 27.65, 23.47, 22.22, 21.49, 20.90.

HRMS (EI) m/z calc'd for $C_{22}H_{28}O_6$ [M+]: 388.1886; found 388.1896.

IR (neat, cm^{-1}): 2979, 2950, 2888, 2839, 1722.

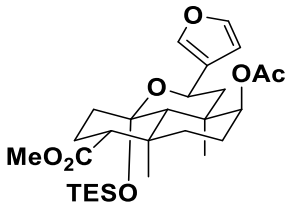

TES cyclic acetal 3.2.6.1

Protocol and spectra adopted from literature procedure (Phillipe McGee's doctoral thesis).[73]

To a flame-dried round-bottomed flask under argon was added **3.2.5.2** (1.4793 g, 3.64 mmol) and THF (31.7 ml). The reaction mixture was cooled to -78 °C then NaHMDS 1.0M in THF (4.73 ml, 4.73 mmol) was added. The mixture was stirred at -78 °C for 0.5 h then

triethylchlorosilane (1.233 ml, 7.28 mmol) was added. The mixture was left in the -78 °C bath and allowed to warm to RT overnight then quenched with sat. NaHCO3. The reaction mixture was diluted with ether and the layers were separated. The organic phase was collected. The aq. layer was back extracted with ether (2 x 50 mL). The combined organic layers were dried with sodium sulfate, filtered, and concentrated in vacuo to give a crude product. The crude product was added to a basified silica gel column and was eluted with 5-10% EA in hexanes, yielding **3.2.6.1** (1.78 g, 3.42 mmol, 94 % yield) as a white foam.

^{1}H NMR (400 MHz, $CDCl_3$) δ 7.35 (t, J = 1.7 Hz, 1H), 7.32 – 7.29 (m, 1H), 6.33 (dd, J = 1.8, 0.9 Hz, 1H), 4.96 (d, J = 11.1 Hz, 1H), 4.54 (t, J = 2.7 Hz, 1H), 3.64 (s, 3H), 2.23 (dd, J = 12.9, 2.8 Hz, 1H), 2.06 (s, 3H), 2.05 – 1.85 (m, 2H), 1.84 – 1.55 (m, 5H), 1.48 (d, J = 0.8 Hz, 3H), 1.44 – 1.35 (m, 1H), 1.35 – 1.23 (m, 2H), 1.20 (s, 3H), 0.98 (dt, J = 15.9, 7.9 Hz, 10H), 0.77 – 0.69 (m, 6H).

^{13}C NMR (101 MHz, $CDCl_3$) δ 174.17, 170.54, 142.88, 138.79, 127.43, 108.68, 99.31, 76.53, 61.69, 56.96, 51.17, 50.34, 44.24, 39.87, 37.25, 36.18, 35.52, 22.25, 21.97, 21.33, 21.31, 15.63, 6.58, 5.80.

HRMS (EI) m/z calc'd for $C_{28}H_{44}O_7Si$ [M-C_2H_5]: 491.2465; found 491.2445.

IR (neat, cm^{-1}): 2952, 1732.

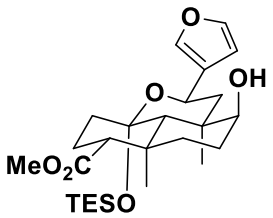

Alcohol 3.2.6.2

To a round-bottomed flask under argon containing **3.2.6.1** (1.78 g, 3.42 mmol) was added MeOH (17.09 ml). The mixture was sonicated to give a white suspension. Then sodium

methoxide 25% in MeOH (1.303 ml, 6.84 mmol) was added. The mixture was stirred at rt for 18 h. The reaction mixture was diluted with EtOAc, and washed with sat. NaHCO3. The layers were separated and the organic phase was collected. The aq. layer was back extracted with EtOAc (2 x 2 mL). The organic was dried with sodium sulfate, filtered, and concentrated in vacuo to give a crude product. The crude product was added to a silica gel column and was eluted with 80:20 Hex/EtOAc, yielding **3.2.6.2** (1.26 g, 2.63 mmol, 77 % yield) as a white foam.

Spectra adopted from literature (Phillipe McGee's doctoral thesis).[73]

^{1}H NMR (400 MHz, $CDCl_3$) δ 7.36 (s, 1H), 7.35 (s, 1H), 6.38 (t, J = 1.4 Hz, 1H), 4.97 (dd, J = 12.0, 2.1 Hz, 1H), 3.64 (s, 3H), 3.32 (t, J = 2.7 Hz, 1H), 2.24 (dd, J = 12.9, 2.9 Hz, 1H), 2.19 – 1.83 (m, 4H), 1.75 (dt, J = 13.9, 3.8 Hz, 1H), 1.69 (s, 1H), 1.67 – 1.45 (m, 3H), 1.44 – 1.38 (m, 3H), 1.39 – 1.31 (m, 1H), 1.24 (dd, J = 12.8, 2.1 Hz, 1H), 1.19 (s, 3H), 1.00 (t, J = 7.9 Hz, 9H), 0.81 – 0.65 (m, 6H).

^{13}C NMR (101 MHz, $CDCl_3$) δ 174.42, 142.83, 139.01, 127.62, 108.93, 99.44, 74.50, 61.67, 56.91, 51.11, 49.09, 44.40, 39.97, 37.37, 37.00, 34.78, 25.16, 22.01, 21.58, 15.69, 7.29, 6.34.

HRMS (EI) m/z calc'd for $C_{26}H_{42}O_6Si$ [M+]: 478.2751; found 478.2739.

IR (neat, cm^{-1}): 3500, 2952, 2361, 1731.

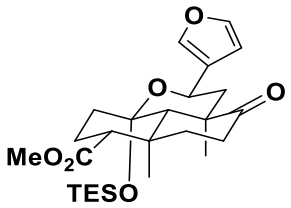

Ketone 3.2.6.3

To a reaction vial under argon containing **3.2.6.2** (1.26 g, 2.63 mmol) was added DCM (23.93 ml), sodium bicarbonate (0.663 g, 7.90 mmol) and DMP (1.675 g, 3.95 mmol). The mixture was stirred at rt for 40 min then quenched with sat. $Na_2S_2O_3$ and stirred for 5 min. The reaction mixture was diluted with DCM, and washed with sat. $NaHCO_3$. The layers were separated and the organic phase was collected. The aq. layer was back extracted with DCM (2 x 20 mL). The combined organic layers were dried with sodium sulfate, filtered, and concentrated in vacuo to give a crude product. The crude product was added to a silica gel plug and was eluted with 90:10 Hex/EtOAc, yielding **3.2.6.3** (1.2355 g, 2.59 mmol, 98 % yield) as a white solid.

^{1}H NMR (600 MHz, $CDCl_3$) δ 7.37 – 7.33 (m, 2H), 6.38 – 6.34 (m, 1H), 4.94 (dd, *J* = 12.3, 2.0 Hz, 1H), 3.65 (s, 3H), 2.85 (td, *J* = 14.7, 5.9 Hz, 1H), 2.19 (ddd, *J* = 14.7, 4.3, 2.6 Hz, 1H), 2.13 (dd, *J* = 12.9, 2.8 Hz, 1H), 2.04 (qd, *J* = 13.6, 3.5 Hz, 1H), 1.98 (ddd, *J* = 13.7, 5.9, 2.5 Hz, 1H), 1.94 (dt, *J* = 14.2, 3.4 Hz, 1H), 1.88 (dd, *J* = 13.8, 2.3 Hz, 1H), 1.81 – 1.74 (m, 1H), 1.69 – 1.61 (m, 2H), 1.60 (s, 3H), 1.56 (td, *J* = 14.0, 4.1 Hz, 1H), 1.49 (s, 1H), 1.40 (s, 3H), 1.01 (t, *J* = 8.0 Hz, 9H), 0.82 – 0.68 (m, 6H).

^{13}C NMR (151 MHz, $CDCl_3$) δ 213.99, 173.81, 143.02, 139.15, 127.05, 108.94, 99.46, 62.14, 56.59, 56.05, 51.43, 46.59, 42.61, 41.33, 39.74, 37.01, 34.00, 22.07, 20.91, 15.05, 7.31, 6.38.

HRMS (EI) m/z calc'd for $C_{24}H_{35}O_6Si$ [M-Et]: 447.2202; found 447.2197.

IR (neat, cm^{-1}): 2950, 2917, 2875, 2365, 2360, 1730, 1710.

MP: 100-103°C

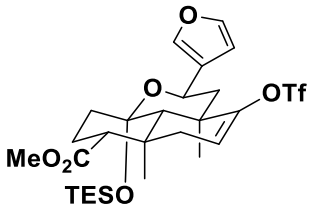

Vinyl triflate 3.2.6.10

Protocol adopted from literature procedure.[70]

To a flame-dried reaction vial under argon was added **3.2.6.3** (0.150 g, 0.315 mmol), THF (1.748 ml), and N-Phenyl-bis(trifluoromethanesulfonimide) (0.225 g, 0.629 mmol). The reaction mixture was cooled to -78 °C. Then KHMDS 0.5M in toluene (1.259 ml, 0.629 mmol) was added dropwise. The mixture was stirred at -78 °C for 1.5 h, then quenched with sat. NH_4Cl. The reaction mixture was diluted with EtOAc, and washed with sat. ammonium chloride. The layers were separated and the organic phase was collected. The aq. layer was back extracted with EtOAc (2 x 2 mL). The combined organic layers were washed with sat. NaCl (1 x 5 mL). The organic was dried with sodium sulfate, filtered, and concentrated in vacuo to give a crude product. The crude product was added to a silica gel column and was eluted with 5-10% EA in hexanes, yielding **3.2.6.10** (0.203 g, 0.333 mmol, >95% yield) as a colourless liquid.

^{1}H NMR (400 MHz, $CDCl_3$) δ 7.40 – 7.35 (m, 2H), 6.40 – 6.36 (m, 1H), 5.55 (dd, *J* = 5.7, 2.7 Hz, 1H), 5.00 (dd, *J* = 11.8, 2.3 Hz, 1H), 3.69 (s, 3H), 2.39 (dd, *J* = 18.5, 2.8 Hz, 1H), 2.31 – 2.22 (m, 2H), 2.01 – 1.90 (m, 3H), 1.77 (s, 1H), 1.71 (s, 3H), 1.76 – 1.54 (m, 3H), 1.19 (s, 3H), 1.05 – 0.97 (m, 9H), 0.82 – 0.67 (m, 6H).

^{13}C NMR (101 MHz, $CDCl_3$) δ 173.88, 153.86, 143.24, 139.26, 126.64, 118.49 (d, *J* = 319.4 Hz), 113.00, 108.90, 99.24, 62.30, 56.62, 54.27, 51.60, 44.73, 41.04, 39.76, 37.07, 35.67, 21.89, 20.20, 17.02, 7.31, 6.37.

HRMS (EI) m/z calc'd for $C_{25}H_{34}F_3O_8SSi$ [M-Et]: 579.1696, found 579.1712

IR (neat, cm^{-1}): 2953, 2878, 1731.

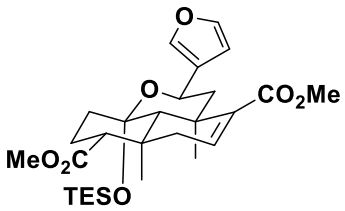

Enoate 3.2.6.11

Protocol adopted from literature procedure.[70]

To a flame-dried reaction vial under argon was added DPPF (111 mg, 0.200 mmol) and $Pd(Ph_3P)_4$ (77 mg, 0.067 mmol). The flask was evacuated and refilled with carbon monoxide (3x). Then **3.2.6.10** (203 mg, 0.333 mmol) in MeOH (5.0 mL) was added. Then DMF (1.7 mL) and triethylamine (0.14 mL, 1.0 mmol) were added. CO was bubbled through the solution for 5 min, then the mixture was stirred at 60 °C for 18 h, evaporated, then was diluted with EtOAc, and washed with sat. $NaHCO_3$. The layers were separated and the organic phase was collected. The aq. layer was back extracted with EtOAc (2 x 5 mL). The combined organic layers were washed with H2O (1 x 10 mL). The organic was dried with sodium sulfate, filtered, and concentrated in vacuo to give a crude product. The crude product was added to a silica gel column and was eluted with 10-15% EA in hexanes, yielding **3.2.6.11** (0.114 g, 0.220 mmol, 66 % yield) as a colourless residue.

^{1}H NMR (600 MHz, $CDCl_3$) δ 7.41 – 7.35 (m, 2H), 6.79 (dd, *J* = 5.4, 2.9 Hz, 1H), 6.40 (s, 1H), 5.06 (dd, *J* = 11.9, 2.3 Hz, 1H), 3.73 – 3.68 (m, 6H), 2.65 (dd, *J* = 13.0, 2.4 Hz, 1H), 2.40 (dd, *J* = 20.2, 3.0 Hz, 1H), 2.32 (dd, *J* = 20.1, 5.3 Hz, 1H), 2.26 (dd, *J* = 12.8, 3.0 Hz, 1H), 2.07 – 1.93 (m, 2H), 1.82 (s, 3H), 1.72 – 1.57 (m, 3H), 1.53 (t, *J* = 12.4 Hz, 1H), 1.18 (s, 3H), 1.03 (t, *J* = 8.0 Hz, 9H), 0.83 – 0.71 (m, 6H).

^{13}C NMR (151 MHz, $CDCl_3$) δ 174.22, 166.58, 142.94, 139.14, 137.47, 136.65, 127.38, 109.06, 99.60, 62.70, 57.30, 54.24, 51.50, 51.38, 46.28, 43.50, 40.28, 35.67, 35.40, 21.95, 21.72, 17.68, 7.35, 6.39.

HRMS (EI) m/z calc'd for $C_{22}H_{27}O_6$ [M-Et_3SiO]: 387.1808 found 387.1772.

IR (neat, cm^{-1}): 2952, 2911, 2877, 2358, 1730, 1712.

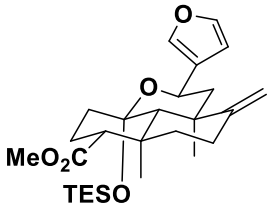

Terminal olefin 3.2.6.4

Protocol adopted from literature procedure.[97]

To a flame-dried reaction vial under argon was added methyltriphenylphosphonium iodide (0.085 g, 0.210 mmol) and THF (1.498 ml). The reaction mixture was cooled to 0 °C and n-butyllithium 2.5M in hexanes (0.078 ml, 0.194 mmol) was added. The mixture was stirred at 0 °C for 2 h then at RT for 2 h. Then **3.2.6.3** (0.025 g, 0.052 mmol) was added. The mixture was stirred at RT for 72 h then quenched with sat. NH_4Cl. The reaction mixture was diluted with DCM. The layers were separated and the organic phase was collected. The aq. layer was back extracted with DCM (2 x 2 mL). The combined organic layers were washed with sat. NaCl (1 x 5 mL). The organic was dried with sodium sulfate, filtered, and concentrated in vacuo to give a crude product. The crude product was added to a silica gel column and was eluted with 98:2 Hex/EtOAc, yielding **3.2.6.4** (0.015 g, 0.032 mmol, 60.2 % yield) as a colourless residue.

^{1}H NMR (600 MHz, $CDCl_3$) δ 7.40 – 7.38 (m, 2H), 6.42 – 6.40 (m, 1H), 5.02 (dd, *J* = 9.3, 4.7 Hz, 1H), 4.63 – 4.61 (m, 1H), 4.54 – 4.52 (m, 1H), 3.65 (s, 3H), 2.58 – 2.49 (m, 1H),

2.15 – 1.98 (m, 3H), 1.94 – 1.88 (m, 1H), 1.81 – 1.77 (m, 2H), 1.72 (ddd, *J* = 13.0, 4.3, 3.0 Hz, 1H), 1.63 – 1.53 (m, 2H), 1.52 (s, 3H), 1.36 (td, *J* = 13.8, 4.3 Hz, 1H), 1.29 (s, 3H), 1.27 (s, 1H), 1.01 (t, *J* = 7.9 Hz, 9H), 0.81 – 0.69 (m, 6H).\

^{13}C NMR (151 MHz, $CDCl_3$) δ 174.43, 157.61, 143.04, 139.11, 127.80, 109.03, 104.20, 99.51, 62.28, 57.28, 56.79, 51.28, 47.37, 43.50, 40.24, 38.54, 37.70, 29.07, 23.08, 22.16, 15.61, 7.42, 6.47.

HRMS (EI) m/z calc'd for $C_{27}H_{42}O_5Si$ [M+]: 474.2802; found 474.2773.

IR (neat, cm^{-1}): 2934, 2876, 1729, 1155.

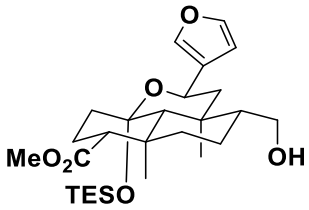

Alcohol 3.2.6.5

To a flame-dried reaction vial under argon containing **3.2.6.4** (0.010 g, 0.021 mmol) was added 9-BBN 0.5M in THF (0.17 ml, 0.086 mmol). The mixture was stirred at RT for 18 h. The reaction mixture was cooled to RT then ethanol (0.04 ml, 0.6 mmol) was added. After 5 min, sodium hydroxide 5.0m in water (0.03 ml, 0.2 mmol) and hydrogen peroxide aq. 30 wt% (0.08 ml, 0.7 mmol) were added sequentially. The mixture was stirred at RT for 18 h. The reaction mixture was diluted with EtOAc, and washed with H_2O. The layers were separated and the organic phase was collected. The aq. layer was back extracted with EtOAc (2 x 2 mL). The combined organic layers were washed with sat. NaCl (1 x 5 mL). The organic was dried with sodium sulfate, filtered, and concentrated in vacuo to give a crude product. The crude product was added to a silica gel column and was eluted

with 10-30% EA in hexanes, yielding the **3.2.6.5** (0.008 g, 0.02 mmol, 76 % yield) as a colourless residue as an inseparable 7.9:1 mixture of diastereomers.

^{1}H NMR (600 MHz, $CDCl_3$) δ 7.36 (t, *J* = 1.7 Hz, 1H), 7.34 (dt, *J* = 1.7, 0.9 Hz, 1H), 6.36 (dd, *J* = 1.8, 0.9 Hz, 1H), 4.93 – 4.88 (m, 1H), 3.76 (dd, *J* = 10.5, 3.9 Hz, 1H), 3.64 (s, 3H), 3.31 (dd, *J* = 10.6, 8.6 Hz, 1H), 2.15 (dd, *J* = 13.0, 2.8 Hz, 1H), 2.07 – 1.95 (m, 1H), 1.93 (dd, *J* = 12.9, 2.2 Hz, 1H), 1.91 – 1.87 (m, 1H), 1.76 – 1.70 (m, 1H), 1.68 (dt, *J* = 13.2, 3.3 Hz, 1H), 1.62 – 1.55 (m, 2H), 1.48 (t, *J* = 12.4 Hz, 1H), 1.45 – 1.36 (m, 1H), 1.35 – 1.28 (m, 1H), 1.32 (s, 3H), 1.22 – 1.17 (m, 2H), 1.16 (s, 3H), 0.99 (t, *J* = 7.9 Hz, 9H), 0.78 – 0.66 (m, 6H).

^{13}C NMR (151 MHz, $CDCl_3$) δ 174.51, 143.02, 139.05, 127.62, 108.92, 99.42, 62.97, 61.89, 57.59, 57.15, 52.72, 51.27, 49.42, 41.60, 40.46, 37.53, 35.43, 22.14, 21.32, 17.19, 15.77, 7.39, 6.43, 6.42.

HRMS (EI) m/z calc'd for $C_{27}H_{44}O_6Si$ [M+]: 492.2907, found 492.2903

IR (neat, cm^{-1}): 3412, 2936, 2876, 1729.

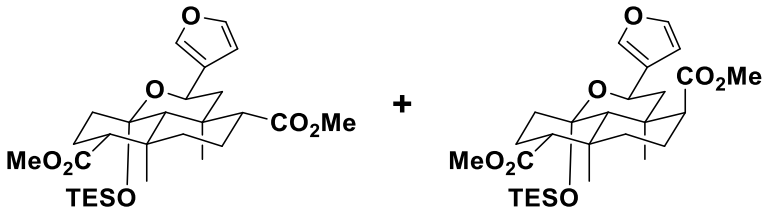

Major Minor

Methyl ester 3.2.6.7 (major) + minor diastereomer

Protocol adopted from literature procedure.[70]

To a flame-dried RBF under argon containing **3.2.6.11** (0.200 g, 0.386 mmol) in degassed (Ar sparged) THF (5.8 ml) was added degassed (Ar sparged) MeOH (0.64 ml). The reaction mixture was cooled to -78°C, then a premixed and prechilled (-78 °C) solution of

samarium(II) iodide 0.1M in THF (Acros, 31 ml, 3.1 mmol) and triethylamine (0.85 ml, 6.1 mmol) was added via cannula. The dark violet mixture was stirred at -78 °C for 1 h then quenched by exposure to air to give a white suspension. The reaction mixture was filtered through celite, washing with ether, then filtered through a silica plug, eluding with 80:20 hexanes/EtOAc, then evaporated. The crude product was added to a silica gel column and was eluted with 5-10% EtOAc in hexanes, yielding **3.2.6.7** (major diastereomer, 0.115 g, 0.221 mmol, 57 % yield) and the minor diastereomer (8.3 mg, 0.016 mmol, 4% yield) as colourless residues.

Major Isomer

^{1}H NMR (600 MHz, $CDCl_3$) δ 7.37 (t, *J* = 1.7 Hz, 1H), 7.35 (d, *J* = 0.8 Hz, 1H), 6.38 (dd, *J* = 1.9, 0.9 Hz, 1H), 4.91 (ddd, *J* = 11.9, 2.1, 0.9 Hz, 1H), 3.65 (s, 3H), 3.63 (s, 3H), 2.14 (dd, *J* = 12.9, 2.7 Hz, 1H), 2.10 (dd, *J* = 12.9, 3.2 Hz, 1H), 2.06 – 1.94 (m, 2H), 1.94 – 1.89 (m, 1H), 1.83 (dd, *J* = 13.3, 2.1 Hz, 1H), 1.69 (dt, *J* = 13.5, 3.4 Hz, 1H), 1.65 (d, *J* = 12.5 Hz, 1H), 1.63 – 1.56 (m, 3H), 1.44 (s, 3H), 1.35 – 1.28 (m, 1H), 1.26 (s, 1H), 1.19 (s, 3H), 1.00 (t, *J* = 7.9 Hz, 9H), 0.80 – 0.66 (m, 6H).

^{13}C NMR (151 MHz, $CDCl_3$) δ 174.25, 173.94, 143.02, 139.15, 127.41, 109.03, 99.19, 61.92, 57.46, 56.98, 56.11, 51.35, 51.34, 50.07, 41.03, 40.45, 37.42, 35.94, 22.07, 21.11, 17.76, 15.80, 7.38, 6.42.

HRMS (EI) m/z calc'd for $C_{28}H_{44}O_7Si$ [M+]: 520.2856; found 520.2853.

IR (neat, cm^{-1}): 2952, 2879, 1731, 1435.

Minor Isomer

^{1}H NMR (600 MHz, $CDCl_3$) δ 7.36 – 7.34 (m, 1H), 7.33 – 7.31 (m, 1H), 6.34 (dt, *J* = 1.7, 0.8 Hz, 1H), 4.97 – 4.93 (m, 1H), 3.63 (s, 3H), 3.62 (s, 3H), 2.32 (dd, *J* = 12.9, 3.1 Hz,

1H), 2.28 – 2.25 (m, 1H), 2.13 (s, 1H), 2.09 – 1.97 (m, 3H), 1.89 (dt, *J* = 13.5, 3.3 Hz, 1H), 1.71 – 1.55 (m, 4H), 1.53 (s, 3H), 1.45 (dd, *J* = 12.8, 1.9 Hz, 1H), 1.42 – 1.37 (m, 1H), 1.20 (s, 3H), 1.00 (t, *J* = 7.9 Hz, 9H), 0.78 – 0.66 (m, 6H).

^{13}C NMR (151 MHz, CDCl3) δ 173.79, 173.45, 141.76, 137.85, 126.35, 107.73, 98.41, 60.74, 55.81, 50.06, 50.02, 50.02, 48.65, 46.46, 39.03, 36.01, 35.23, 33.60, 22.42, 20.98, 19.39, 14.69, 6.24, 5.28.

HRMS (EI) m/z calc'd for $C_{28}H_{44}O_7Si$ [M+]: 520.2856; found 520.2834.

IR (neat, cm^{-1}): 2951, 2876, 1731, 1159.

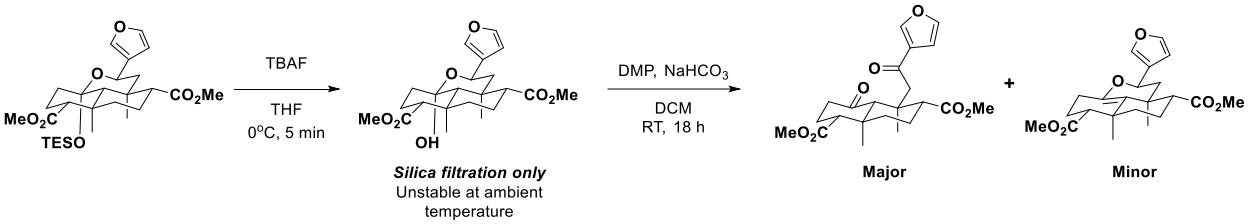

Diketone 3.1.3.1 (Major Product) and cyclic enol ether 3.2.7.2 (Minor Product)

To a reaction vial was added **3.2.6.7** (0.025 g, 0.048 mmol), and THF (1.26 ml). The reaction mixture was cooled to 0 °C, then TBAF 1.0M in THF (0.07 ml, 0.07 mmol) was added. The mixture was stirred at 0 °C for 10 min. The reaction mixture was then filtered through a silica plug, eluding with 70:30 hexanes/EtOAc, yielding crude **3.2.7.1** as a colourless residue. This product was carried forward immediately without further purification.

To the crude product in a reaction vial under argon was added sodium bicarbonate (0.012 g, 0.144 mmol), DCM (1.0 ml) and DMP (0.031 g, 0.072 mmol). The mixture was stirred at RT for 18 h then quenched with sat. $Na_2S_2O_3$ (5 drops) and stirred for 5 min. The reaction mixture was dried by filtering through celite, washing with DCM, then filtered through a silica plug, eluding with 70:30 Hex/EtOAc, then evaporated. The crude product

was added to a silica gel column and was eluted with 10-25% EtOAc in hexanes, yielding **3.1.3.3** (0.0106 g, 0.026 mmol, 55 % yield) and **3.2.7.2** (3.0 mg, 7.7 μmol, 16 % yield) as colourless residues.

Major Product

^{1}H NMR (600 MHz, $CDCl_3$) δ 7.96 (dd, *J* = 1.4, 0.8 Hz, 1H), 7.40 – 7.39 (m, 1H), 6.70 – 6.68 (m, 1H), 3.68 (s, 3H), 3.57 (s, 3H), 3.42 (d, *J* = 17.8 Hz, 1H), 3.42 (s, 1H), 3.07 (dd, *J* = 12.8, 3.2 Hz, 1H), 2.88 (d, *J* = 17.8 Hz, 1H), 2.76 (dd, *J* = 13.1, 3.7 Hz, 1H), 2.31 – 2.23 (m, 2H), 2.20 – 2.11 (m, 1H), 2.02 – 1.89 (m, 2H), 1.72 – 1.56 (m, 3H), 1.33 (s, 3H), 1.08 (s, 3H).

^{13}C NMR (151 MHz, $CDCl_3$) δ 210.43, 195.56, 174.08, 173.60, 147.50, 144.16, 128.72, 108.59, 60.05, 55.80, 51.67, 51.40, 48.58, 47.28, 42.21, 42.19, 38.27, 37.88, 25.63, 20.96, 19.58, 16.35.

HRMS (EI) m/z calc'd for $C_{22}H_{28}O_7$ [M+]: 404.1835; found 404.1807.

IR (neat, cm^{-1}): 2952, 2925, 2854, 1729, 1671.

Minor Product

^{1}H NMR (600 MHz, $CDCl_3$) δ 7.44 – 7.43 (m, 1H), 7.40 (t, *J* = 1.8 Hz, 1H), 6.43 (d, *J* = 1.8 Hz, 1H), 4.95 (dd, *J* = 12.1, 2.3 Hz, 1H), 3.67 (s, 3H), 3.65 (s, 3H), 2.37 (dd, *J* = 13.2, 2.7 Hz, 1H), 2.23 (ddd, *J* = 16.8, 12.1, 7.2 Hz, 1H), 2.20 (dd, *J* = 12.9, 3.1 Hz, 1H), 2.14 – 1.98 (m, 3H), 1.94 (dd, *J* = 13.4, 2.3 Hz, 1H), 1.88 – 1.83 (m, 1H), 1.82 (dt, *J* = 13.5, 2.9 Hz, 1H), 1.76 (ddd, *J* = 13.7, 7.0, 2.5 Hz, 1H), 1.68 (dq, *J* = 14.1, 3.5 Hz, 1H), 1.36 (qd, *J* = 13.9, 4.3 Hz, 1H), 1.34 (s, 3H), 1.21 (s, 3H).

^{13}C NMR (151 MHz, $CDCl_3$) δ 174.97, 174.63, 145.77, 143.40, 139.66, 126.72, 114.50, 108.87, 65.75, 54.10, 53.98, 51.50, 51.43, 46.18, 39.21, 35.95, 34.03, 28.09, 26.30, 23.00, 21.15, 20.96.

HRMS (EI) m/z calc'd for $C_{22}H_{28}O_6$ [M+]: 388.1886 found 388.1914.

IR (neat, cm^{-1}): 2922, 1725, 1711, 1330.

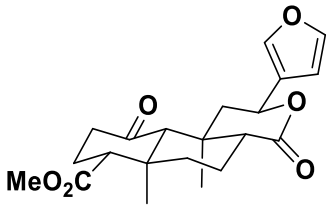

Hagiwara intermediate 3.2.7.5

Protocol adopted from literature procedure, spectra matches literature data.[69]

To a flame-dried reaction vial under argon was added **3.1.3.3** (0.018 g, 0.045 mmol) in THF (0.9 ml), and tBuOH (0.03 ml, 0.27 mmol). The reaction mixture was cooled to -78 °C then K-Selectride 1M in THF (0.05 ml, 0.05 mmol) was added slowly down the side of the vial. The reaction mixture was allowed to warm to -55 °C on its own in the cold bath (~1 h). A TLC was taken showing incomplete conversion. The reaction mixture was cooled to -78 °C, then another 6 eq. of tBuOH (0.026 ml, 0.27 mmol) and 1.2 eq. of K-Selectride 1M in THF (0.05 ml, 0.05 mmol) was added. The reaction mixture was allowed to warm to -55 °C on its own in the cold bath (~1 h). Then a TLC was taken again showing incomplete conversion. This process was repeated (2x), with warming to -55 °C. Then the process was repeated again (2x), with warming to -30 °C. The mixture was further stirred at -30 °C for an additional 0.5 h. At which point, reaction completion was observed by TLC. Reaction was quenched by addition of silica gel (0.365 g, 6.07 mmol) where gas evolution was observed, then warmed to RT. The resulting slurry was filtered through a

silica plug, eluding with 50:50 hexanes/EtOAc, then evaporated. The crude product was added to a silica gel column and was eluted with 20-30% EtOAc in hexanes, yielding **3.2.7.5** (9.6 mg, 0.026 mmol, 57% yield) as a colourless residue and **3.2.7.2** (3.3 mg, 8.5 µmol, 19 % yield) as a colourless residue.

^{1}H NMR (600 MHz, $CDCl_3$) δ 7.42 – 7.40 (m, 1H), 7.40 – 7.38 (m, 1H), 6.39 – 6.37 (m, 1H), 5.55 (dd, *J* = 11.7, 5.2 Hz, 1H), 3.70 (s, 3H), 2.70 – 2.64 (m, 2H), 2.45 (ddd, *J* = 14.4, 5.4, 1.7 Hz, 1H), 2.33 (td, *J* = 14.0, 7.4 Hz, 1H), 2.20 (qd, *J* = 13.5, 5.4 Hz, 1H), 2.14 (dq, *J* = 14.1, 3.1 Hz, 1H), 2.12 (s, 1H), 2.08 – 2.00 (m, 2H), 1.72 (dt, *J* = 13.1, 3.1 Hz, 1H), 1.69 – 1.60 (m, 1H), 1.59 – 1.50 (m, 2H), 1.42 (s, 3H), 1.13 (s, 3H).

^{13}C NMR (151 MHz, $CDCl_3$) δ 208.53, 173.14, 171.65, 143.81, 139.41, 125.68, 108.51, 72.20, 66.21, 55.83, 51.84, 51.67, 43.90, 41.74, 41.54, 38.28, 35.47, 25.25, 18.23, 16.56, 15.14.

HRMS (ESI) m/z calc'd for $C_{21}H_{26}O_6Na$ [M+Na]: 397.1627 found 397.1618.

IR (neat, cm^{-1}): 2925, 2854, 2361, 2339, 1731, 1716.

5.4 BIBLIOGRAPHY

44. (a) de Frémont, P.; Marion, N.; Nolan, S. P., Cationic NHC–gold(I) complexes: Synthesis, isolation, and catalytic activity. *J. Organomet. Chem.* **2009,** *694* (4), 551-560; (b) Nolan, S. P., The Development and Catalytic Uses of N-Heterocyclic Carbene Gold Complexes. *Acc. Chem. Res.* **2011,** *44* (2), 91-100.
69. Hagiwara, H.; Suka, Y.; Nojima, T.; Hoshi, T.; Suzuki, T., Second-generation synthesis of salvinorin A. *Tetrahedron* **2009,** *65* (25), 4820-4825.
70. Line, N. J.; Burns, A. C.; Butler, S. C.; Casbohm, J.; Forsyth, C. J., Total Synthesis of (−)-Salvinorin A. *Chem. Eur. J.* **2016,** *22* (50), 17983-17986.
73. McGee, P. Application of Gold(I) Catalysis in the Synthesis of Bridged Carbocycles, (±)-Magellanine and (±)-Salvinorin A. Université d'Ottawa / University of Ottawa, Ottawa, 2018.
74. Genna, D. T.; Posner, G. H., Cyanocuprates Convert Carboxylic Acids Directly into Ketones. *Org. Lett.* **2011,** *13* (19), 5358-5361.
85. Poyser, A. Applications of Gold Catalysis for the Synthesis of Carbocycles. University of Ottawa, Ottawa, 2020.

86. (a) Yajima, T.; Saito, C.; Nagano, H., Radical-mediated hydroxyalkylation of α,β-unsaturated esters. *Tetrahedron* **2005,** *61* (43), 10203-10215; (b) Boucher, M. M.; Furigay, M. H.; Quach, P. K.; Brindle, C. S., Liquid–Liquid Extraction Protocol for the Removal of Aldehydes and Highly Reactive Ketones from Mixtures. *Org Process Res Dev.* **2017,** *21* (9), 1394-1403.
87. Han, Y.; Zhu, L.; Gao, Y.; Lee, C.-S., A Highly Convergent Cascade Cyclization to cis-Hydrindanes with All-Carbon Quaternary Centers and Its Application in the Synthesis of the Aglycon of Dendronobiloside A. *Org. Lett.* **2011,** *13* (4), 588-591.
88. Korkis, S. E.; Burns, D. J.; Lam, H. W., Rhodium-Catalyzed Oxidative C–H Allylation of Benzamides with 1,3-Dienes by Allyl-to-Allyl 1,4-Rh(III) Migration. *J. Am. Chem. Soc.* **2016,** *138* (37), 12252-12257.
89. Knol, J.; Feringa, B. L., Direct Coupling Procedure for the Synthesis of N-Acyl-2-oxazolidinones Derived from α,β-Unsaturated Carboxylic Acids. *Synth. Commun.* **1996,** *26* (2), 261-268.
90. Ho, G.-J.; Mathre, D. J., Lithium-Initiated Imide Formation. A Simple Method for N-Acylation of 2-Oxazolidinones and Bornane-2,10-Sultam. *J. Org. Chem.* **1995,** *60* (7), 2271-2273.
91. Cannizzaro, C. E.; Ashley, J. A.; Janda, K. D.; Houk, K. N., Experimental Determination of the Absolute Enantioselectivity of an Antibody-Catalyzed Diels−Alder Reaction and Theoretical Explorations of the Origins of Stereoselectivity. *J. Am. Chem. Soc.* **2003,** *125* (9), 2489-2506.
92. Harada, S.; Morikawa, T.; Nishida, A., Chiral Holmium Complex-Catalyzed Diels–Alder Reaction of Silyloxyvinylindoles: Stereoselective Synthesis of Hydrocarbazoles. *Org. Lett.* **2013,** *15* (20), 5314-5317.
93. Lebold, T. P.; Gallego, G. M.; Marth, C. J.; Sarpong, R., Synthesis of the Bridging Framework of Phragmalin-Type Limonoids. *Org. Lett.* **2012,** *14* (8), 2110-2113.
94. Bair, J. S.; Palchaudhuri, R.; Hergenrother, P. J., Chemistry and Biology of Deoxynyboquinone, a Potent Inducer of Cancer Cell Death. *J. Am. Chem. Soc.* **2010,** *132* (15), 5469-5478.
95. Edwards, J. T.; Merchant, R. R.; McClymont, K. S.; Knouse, K. W.; Qin, T.; Malins, L. R.; Vokits, B.; Shaw, S. A.; Bao, D.-H.; Wei, F.-L.; Zhou, T.; Eastgate, M. D.; Baran, P. S., Decarboxylative alkenylation. *Nature* **2017,** *545* (7653), 213-218.
96. Krasovskiy, A.; Knochel, P., Convenient Titration Method for Organometallic Zinc, Magnesium, and Lanthanide- Reagents. *Synthesis* **2006,** *2006* (05), 0890-0891.
97. Fairweather, K. A.; Mander, L. N., A Formal Total Synthesis of the Marine Diterpenoid Diisocyanoadociane. *Org. Lett.* **2006,** *8* (15), 3395-3398.

6. *COLLECTIVE SPECTRAL DATA*

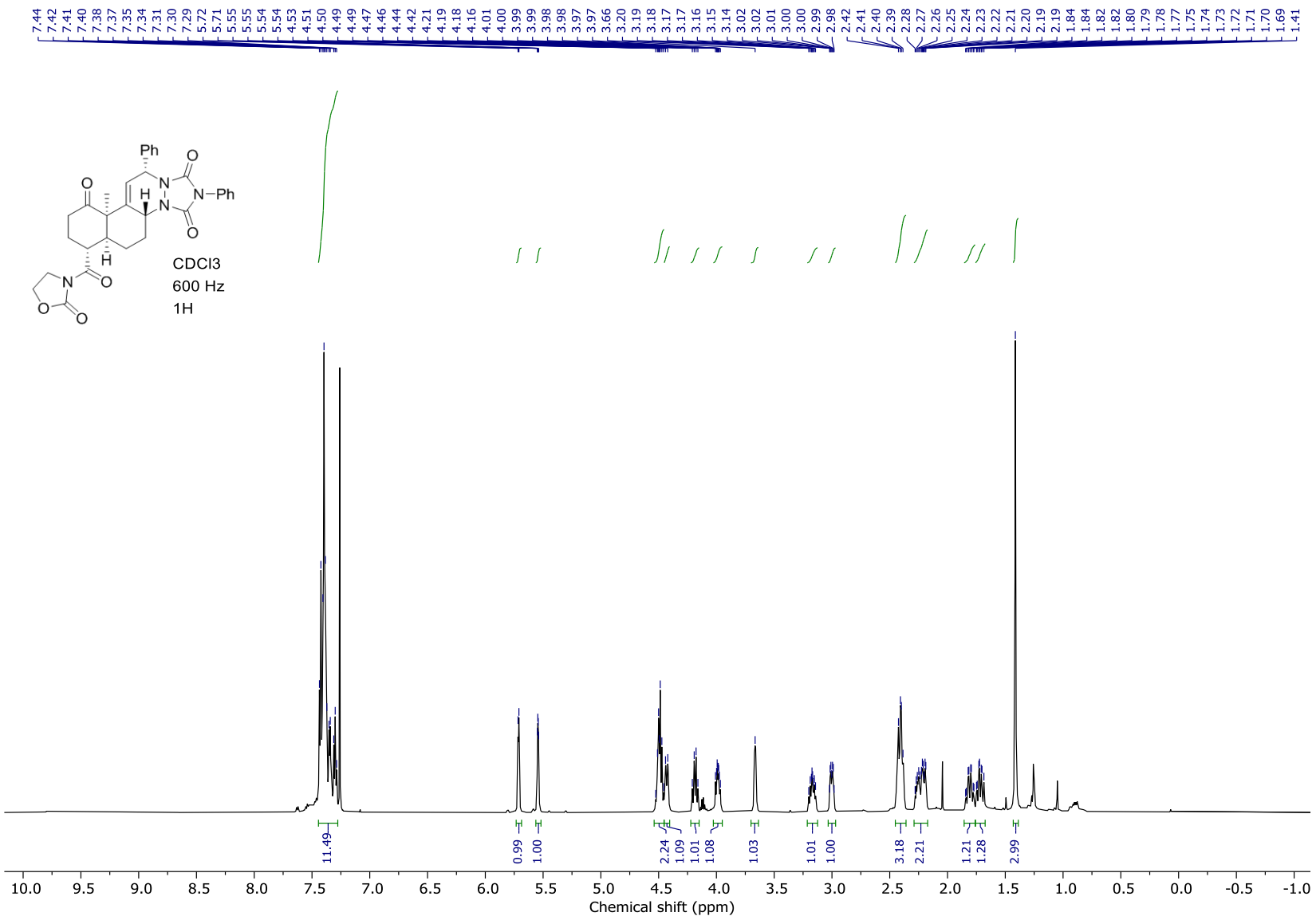
CDCl3
600 Hz
1H
Chemical shift (ppm)

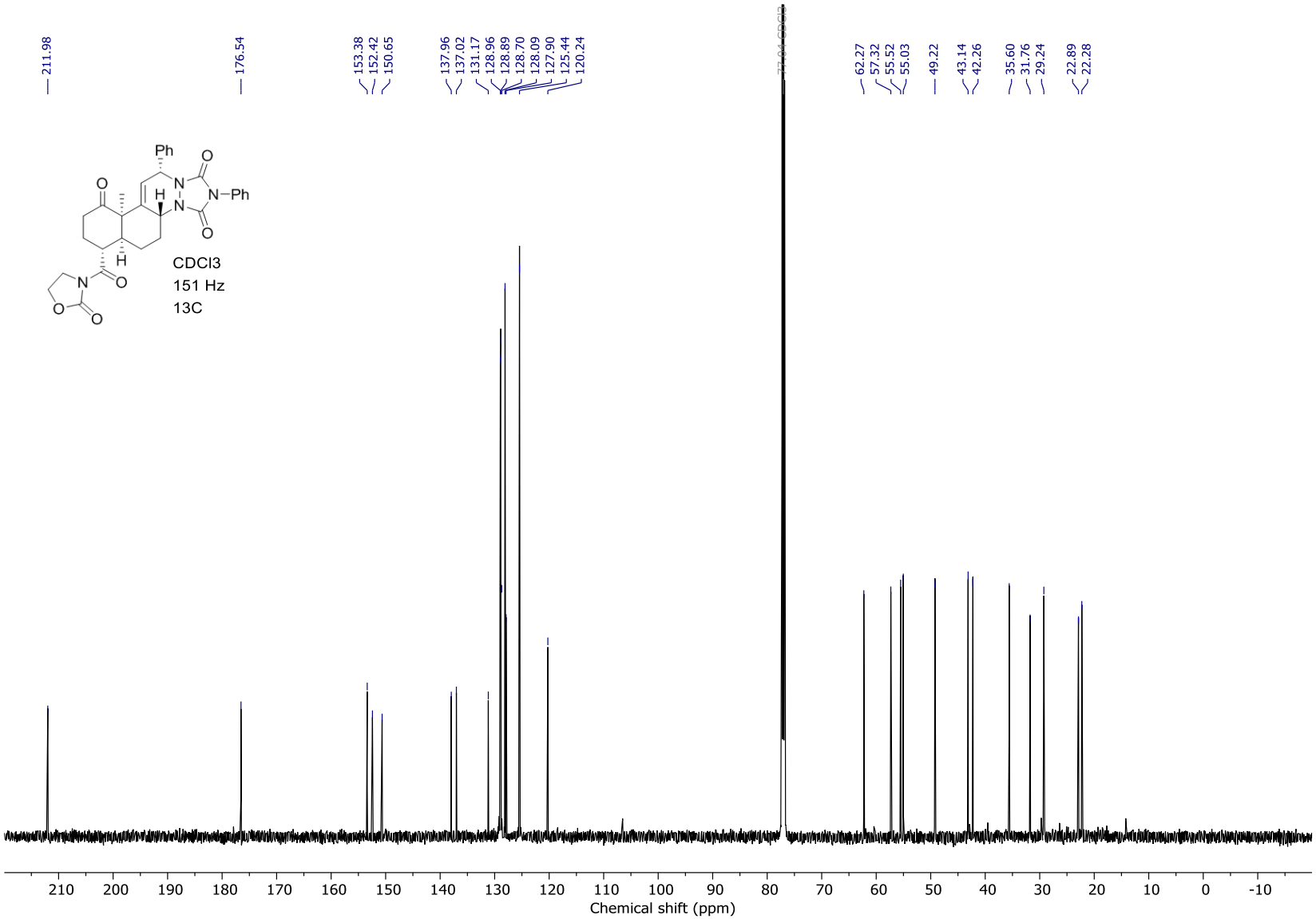
211.98
176.54
153.38
152.42
150.65
137.96
137.02
131.17
128.96
128.89
128.70
128.09
127.90
125.44
120.24
77.03
62.27
57.32
55.52
55.03
49.22
43.14
42.26
35.60
31.76
29.24
22.89
22.28
Ph
N–Ph
CDCl3
151 Hz
13C
210 200 190 180 170 160 150 140 130 120 110 100 90 80 70 60 50 40 30 20 10 0 -10
Chemical shift (ppm)

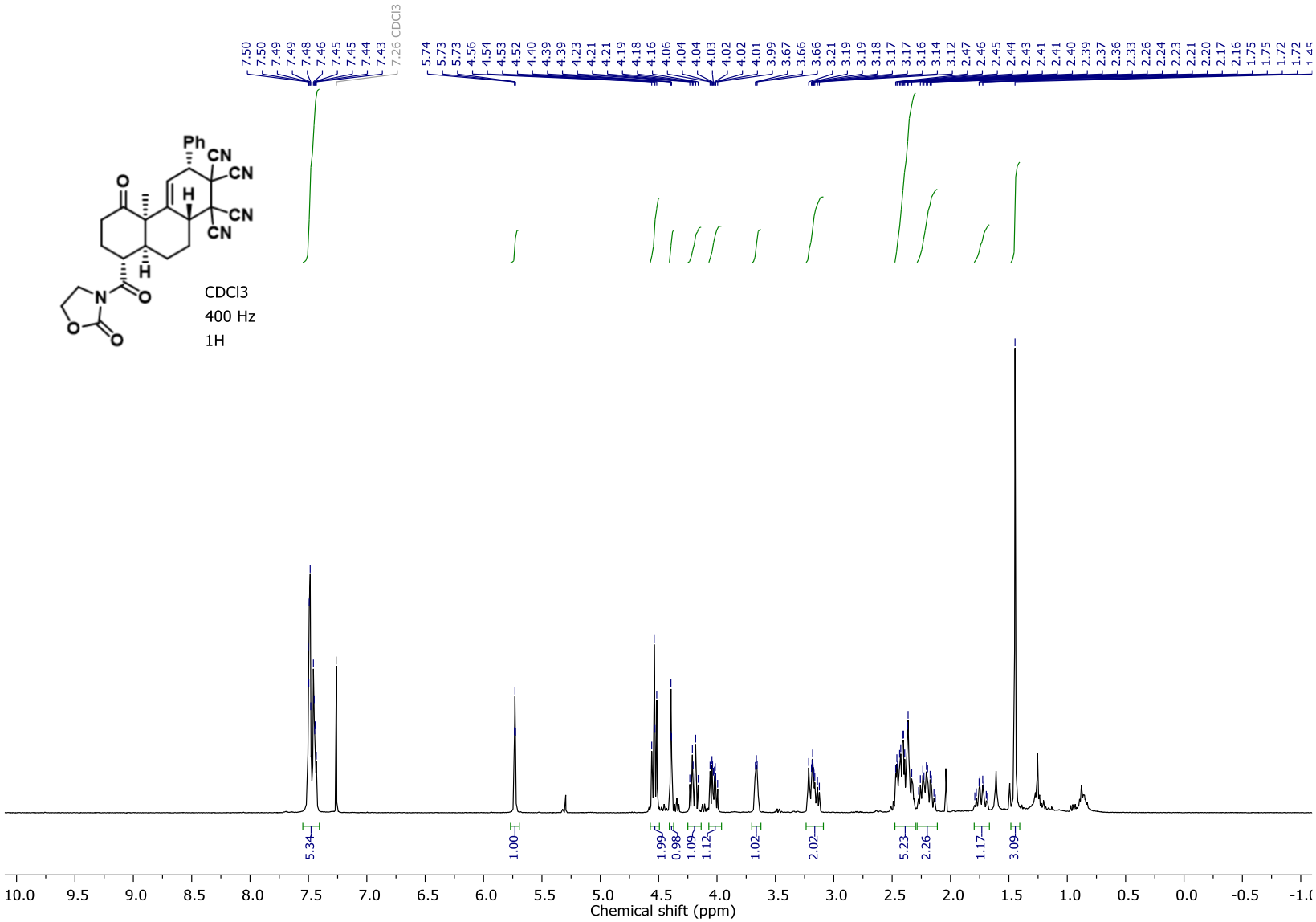

Spectra from Alyson Poyser's MSc thesis

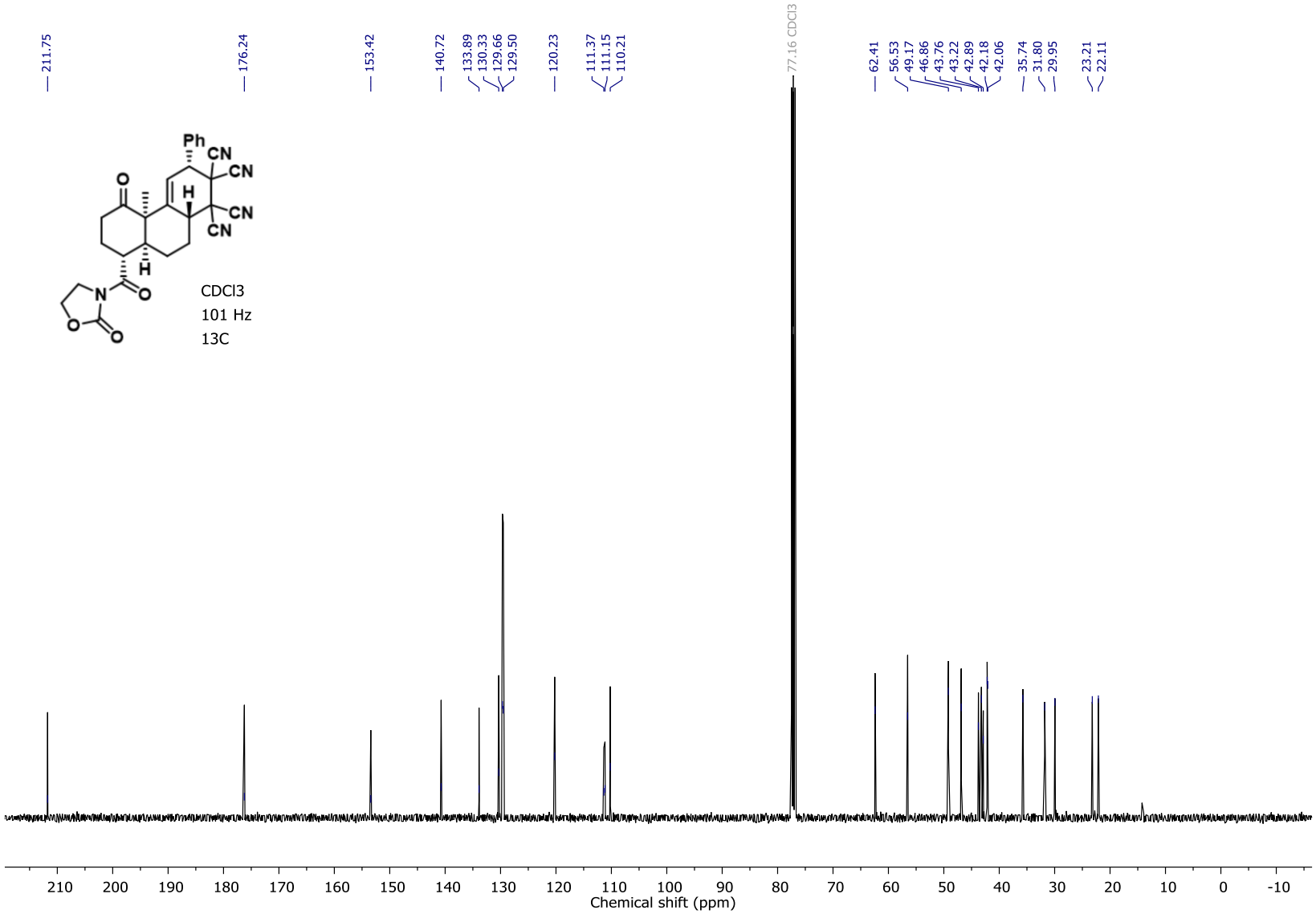

Spectra from Alyson Poyser's MSc thesis

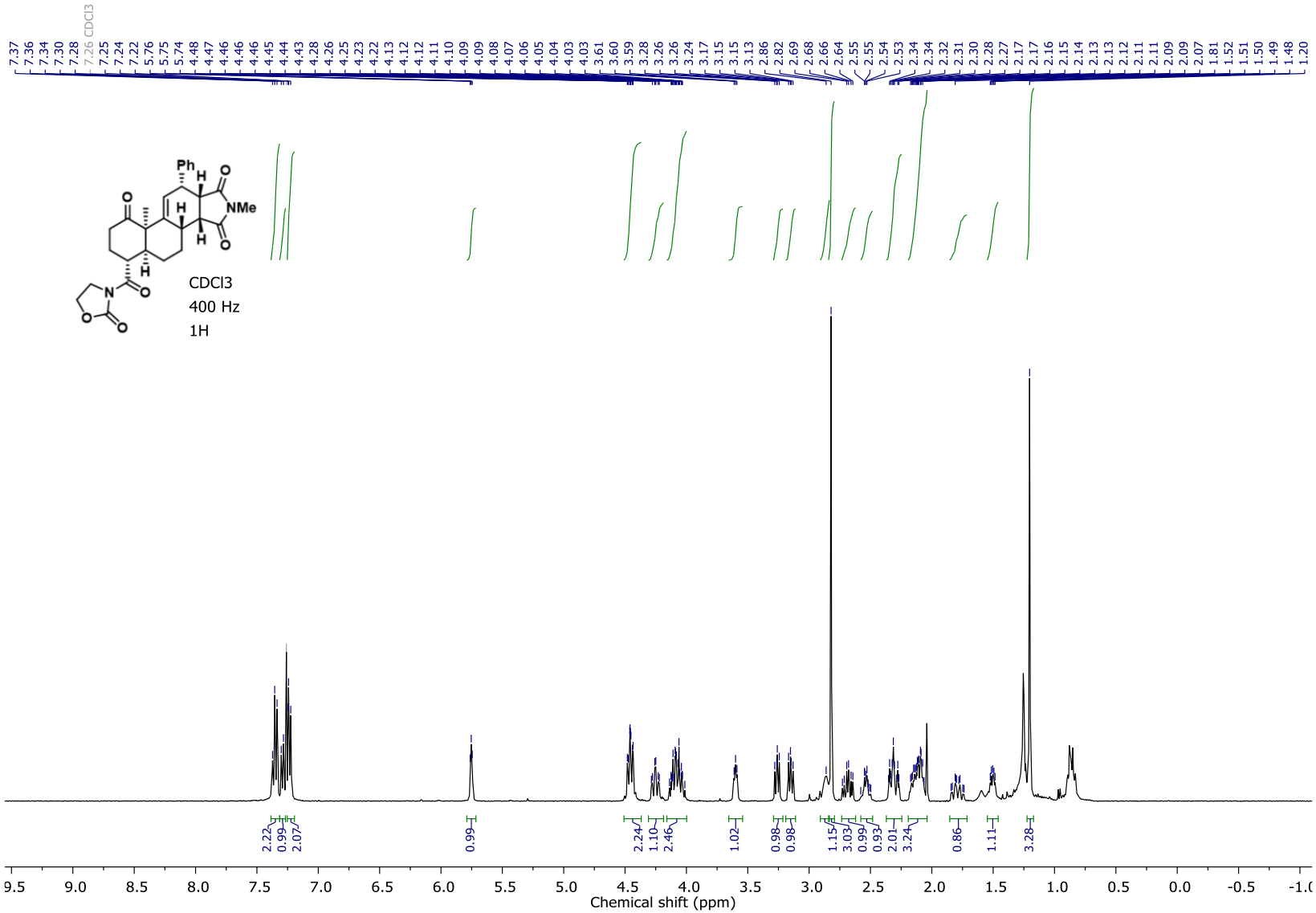

Spectra from Alyson Poyser's MSc thesis

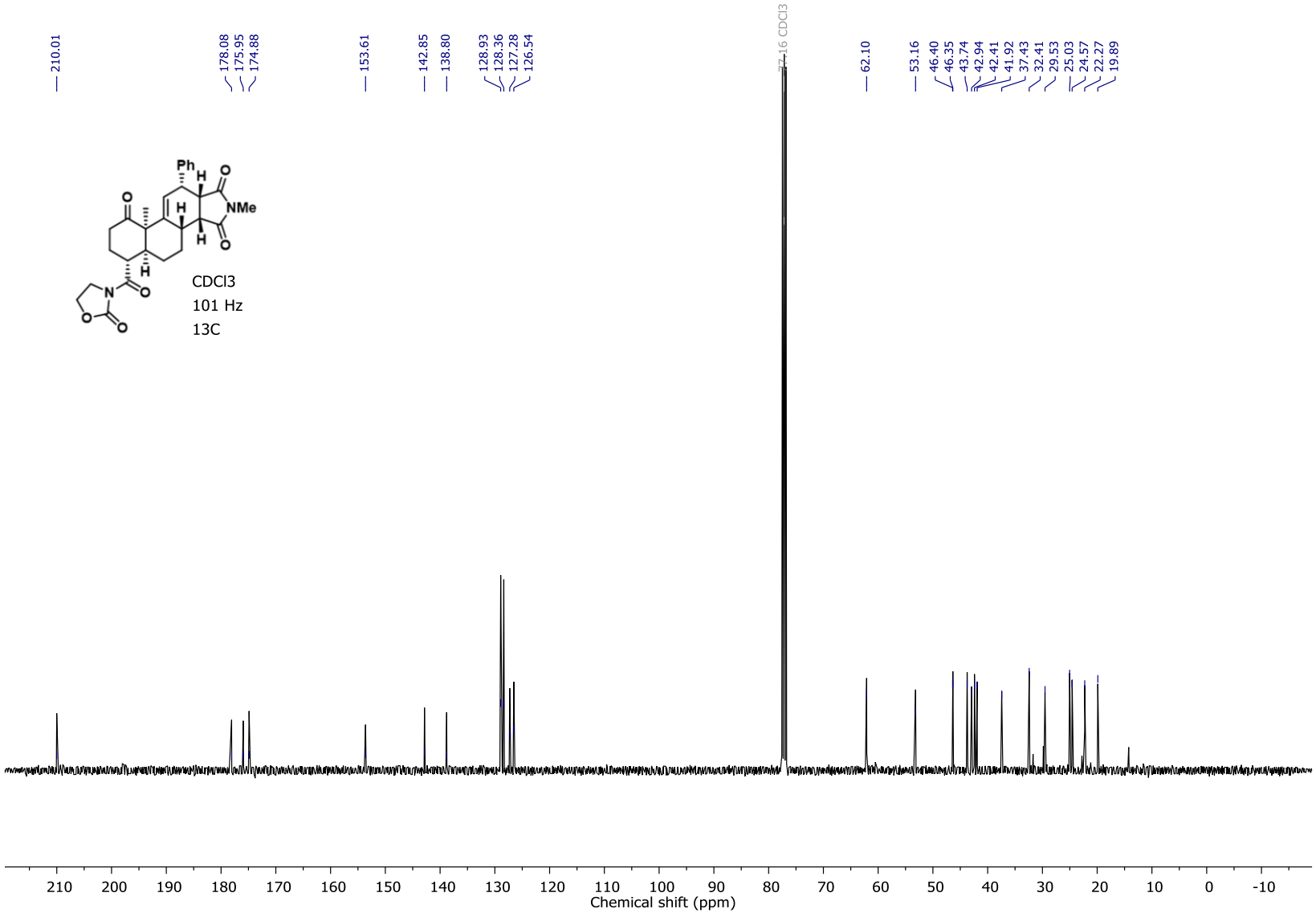

Spectra from Alyson Poyser's MSc thesis

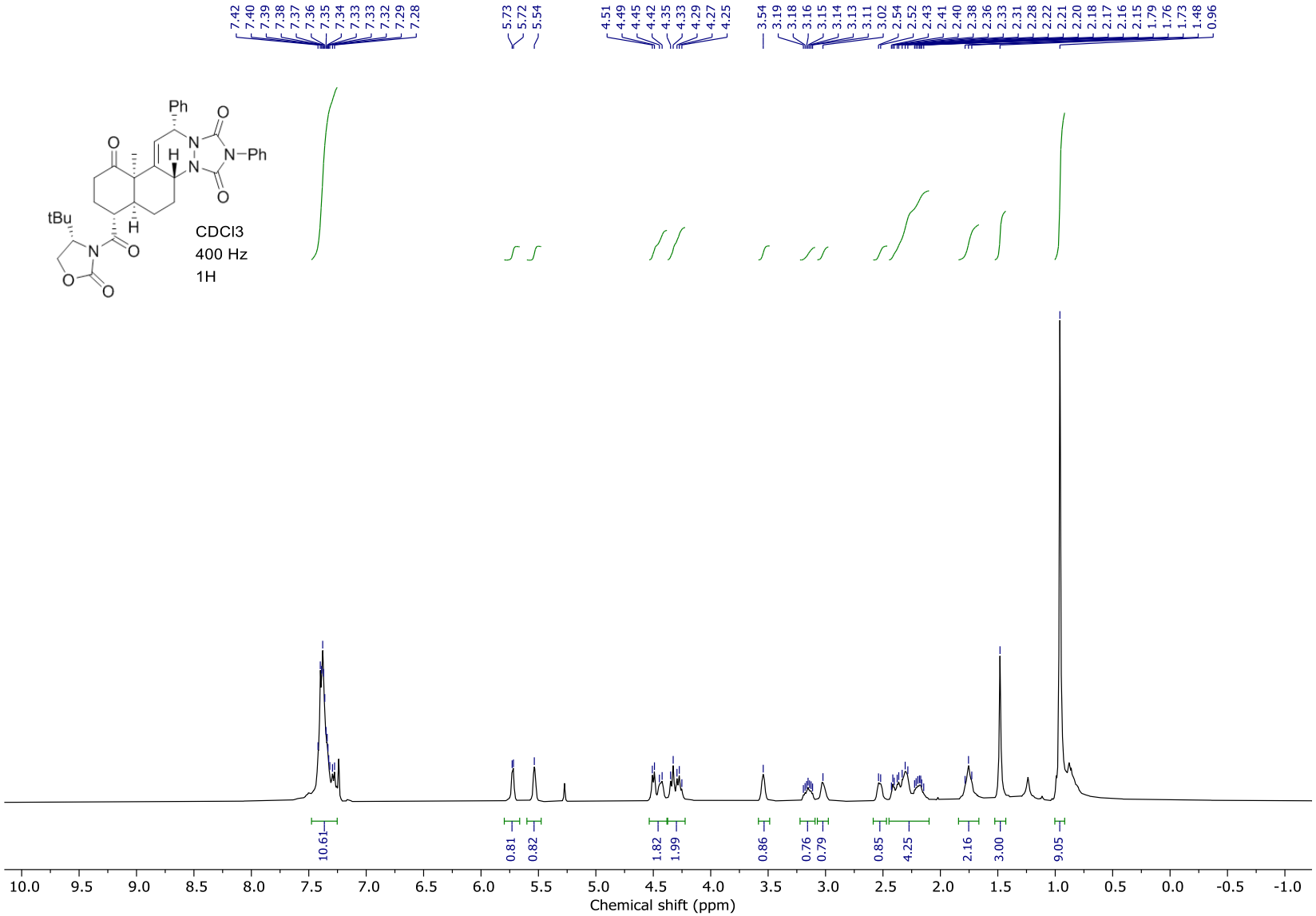
7.42 7.40 7.39 7.38 7.37 7.36 7.35 7.34 7.33 7.33 7.32 7.29 7.28
5.73 5.72 5.54
4.51 4.49 4.45 4.42 4.35 4.33 4.29 4.27 4.25
3.54 3.19 3.18 3.16 3.15 3.14 3.13 3.11 3.02 2.54 2.52 2.43 2.41 2.40 2.38 2.36 2.33 2.31 2.28 2.22 2.21 2.20 2.18 2.17 2.16 2.15 1.79 1.76 1.73 1.48 0.96
Ph
N–Ph
tBu
CDCl3
400 Hz
1H
10.61
0.81
0.82
1.82
1.99
0.86
0.76
0.79
0.85
4.25
2.16
3.00
9.05
10.0 9.5 9.0 8.5 8.0 7.5 7.0 6.5 6.0 5.5 5.0 4.5 4.0 3.5 3.0 2.5 2.0 1.5 1.0 0.5 0.0 -0.5 -1.0
Chemical shift (ppm)

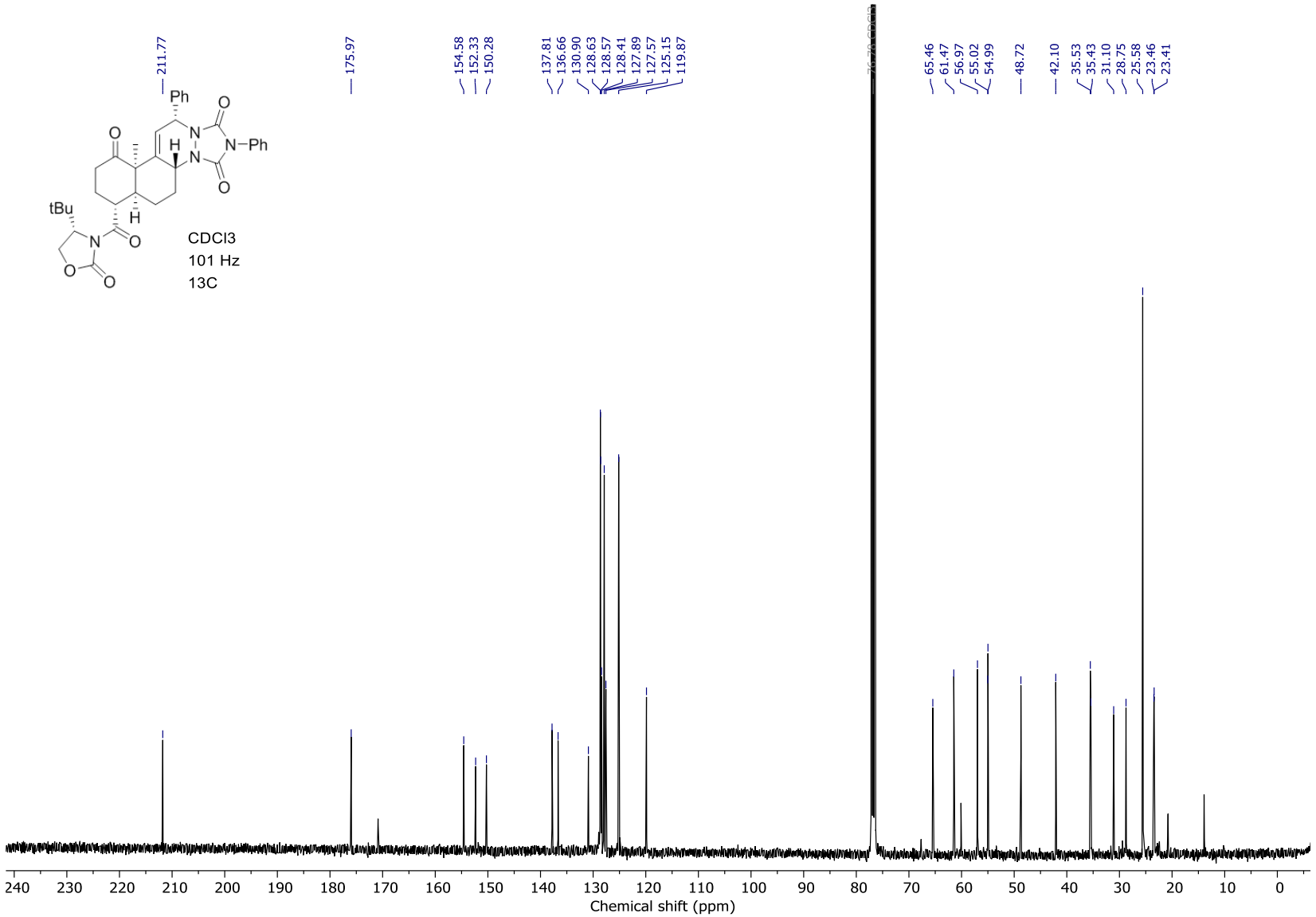
211.77
175.97
154.58
152.33
150.28
137.81
136.66
130.90
128.63
128.57
128.41
127.89
127.57
125.15
119.87
65.46
61.47
56.97
55.02
54.99
48.72
42.10
35.53
35.43
31.10
28.75
25.58
23.46
23.41
Ph
N–Ph
tBu
CDCl3
101 Hz
13C
240 230 220 210 200 190 180 170 160 150 140 130 120 110 100 90 80 70 60 50 40 30 20 10 0
Chemical shift (ppm)

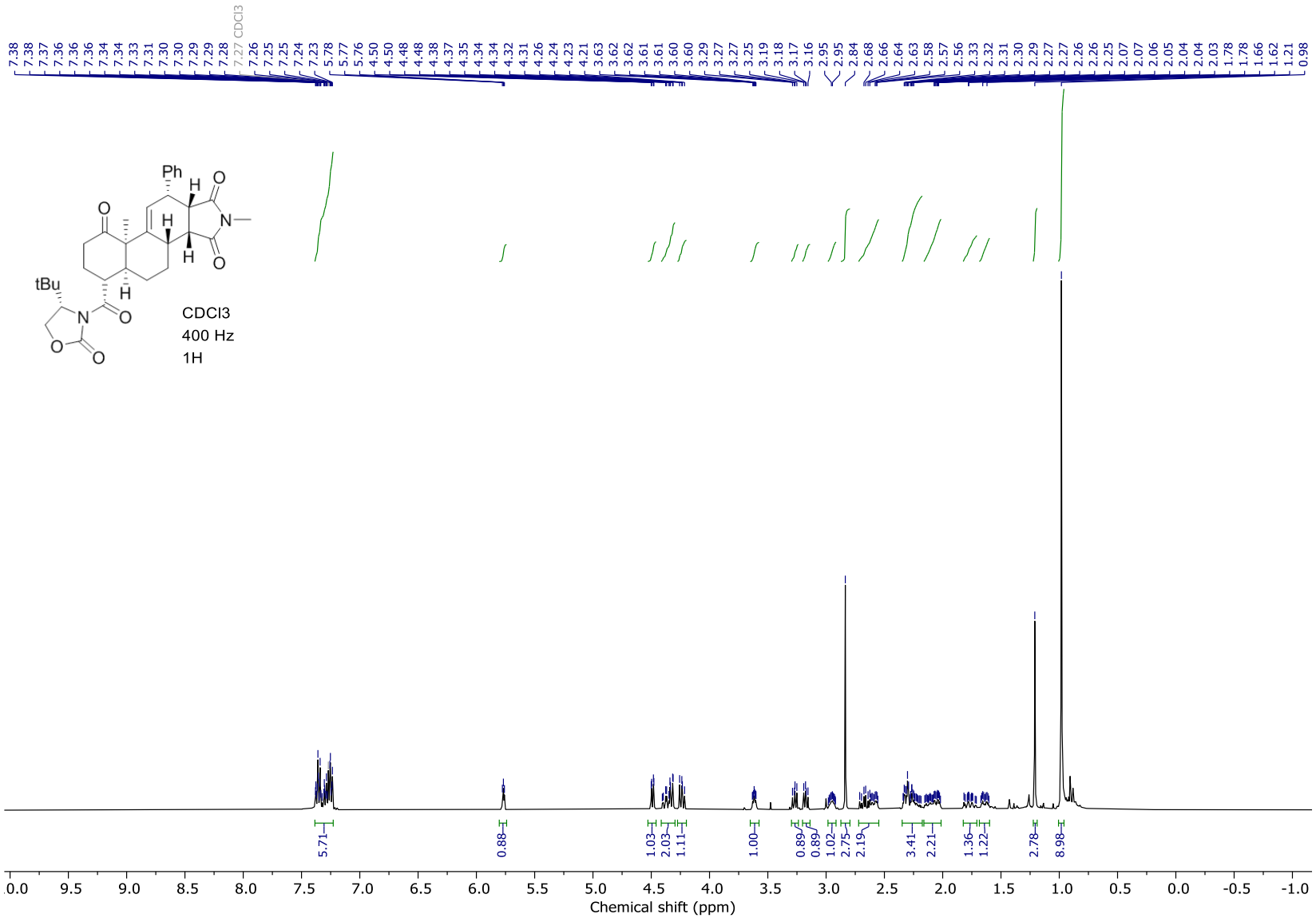
CDCl3
400 Hz
1H
Chemical shift (ppm)

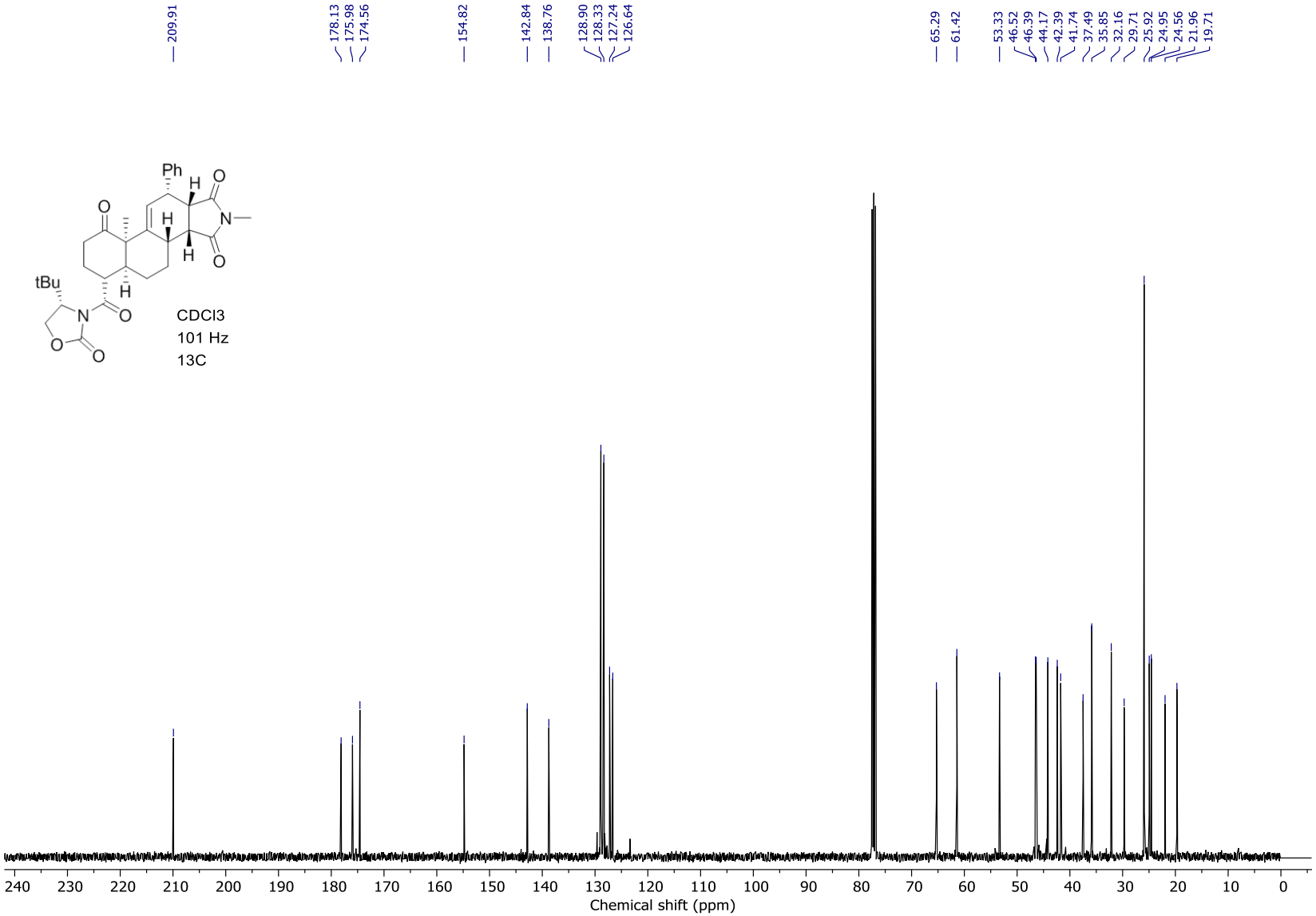
209.91
178.13
175.98
174.56
154.82
142.84
138.76
128.90
128.33
127.24
126.64
65.29
61.42
53.33
46.52
46.39
44.17
42.39
41.74
37.49
35.85
32.16
29.71
25.92
24.95
24.56
21.96
19.71
Ph
H
O
N
tBu
CDCl3
101 Hz
13C
240 230 220 210 200 190 180 170 160 150 140 130 120 110 100 90 80 70 60 50 40 30 20 10 0
Chemical shift (ppm)

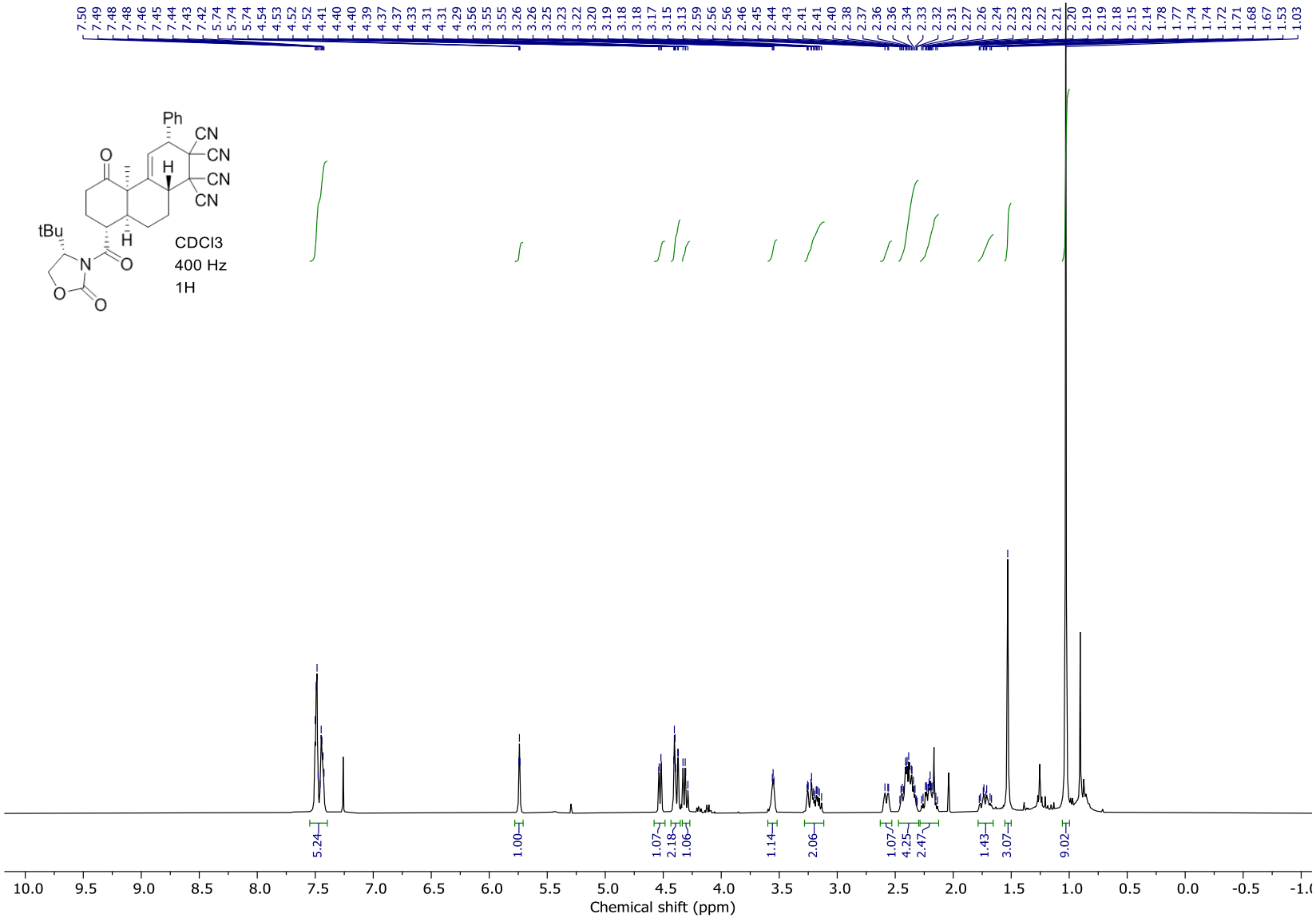
Ph
CN
CN
CN
CN
O
H
tBu
H
N
O
O
O
CDCl3
400 Hz
1H
5.24
1.00
1.07
2.18
1.06
1.14
2.06
1.07
4.25
2.47
1.43
3.07
9.02
Chemical shift (ppm)

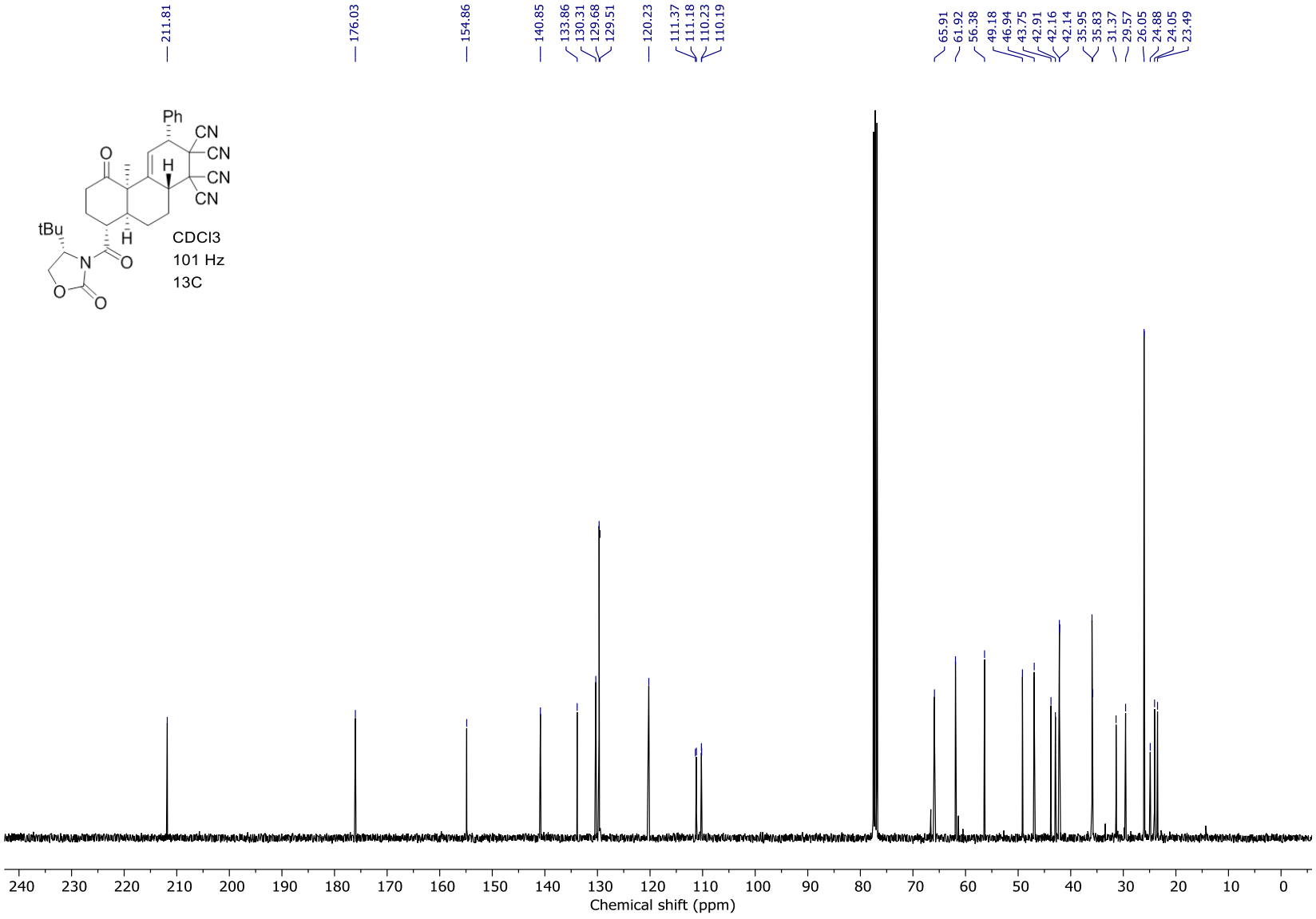
211.81
176.03
154.86
140.85
133.86
130.31
129.68
129.51
120.23
111.37
111.18
110.23
110.19
65.91
61.92
56.38
49.18
46.94
43.75
42.91
42.16
42.14
35.95
35.83
31.37
29.57
26.05
24.88
24.05
23.49
Ph
CN
CN
CN
CN
O
H
H
tBu
N
O
O
O
CDCl3
101 Hz
13C
240 230 220 210 200 190 180 170 160 150 140 130 120 110 100 90 80 70 60 50 40 30 20 10 0
Chemical shift (ppm)

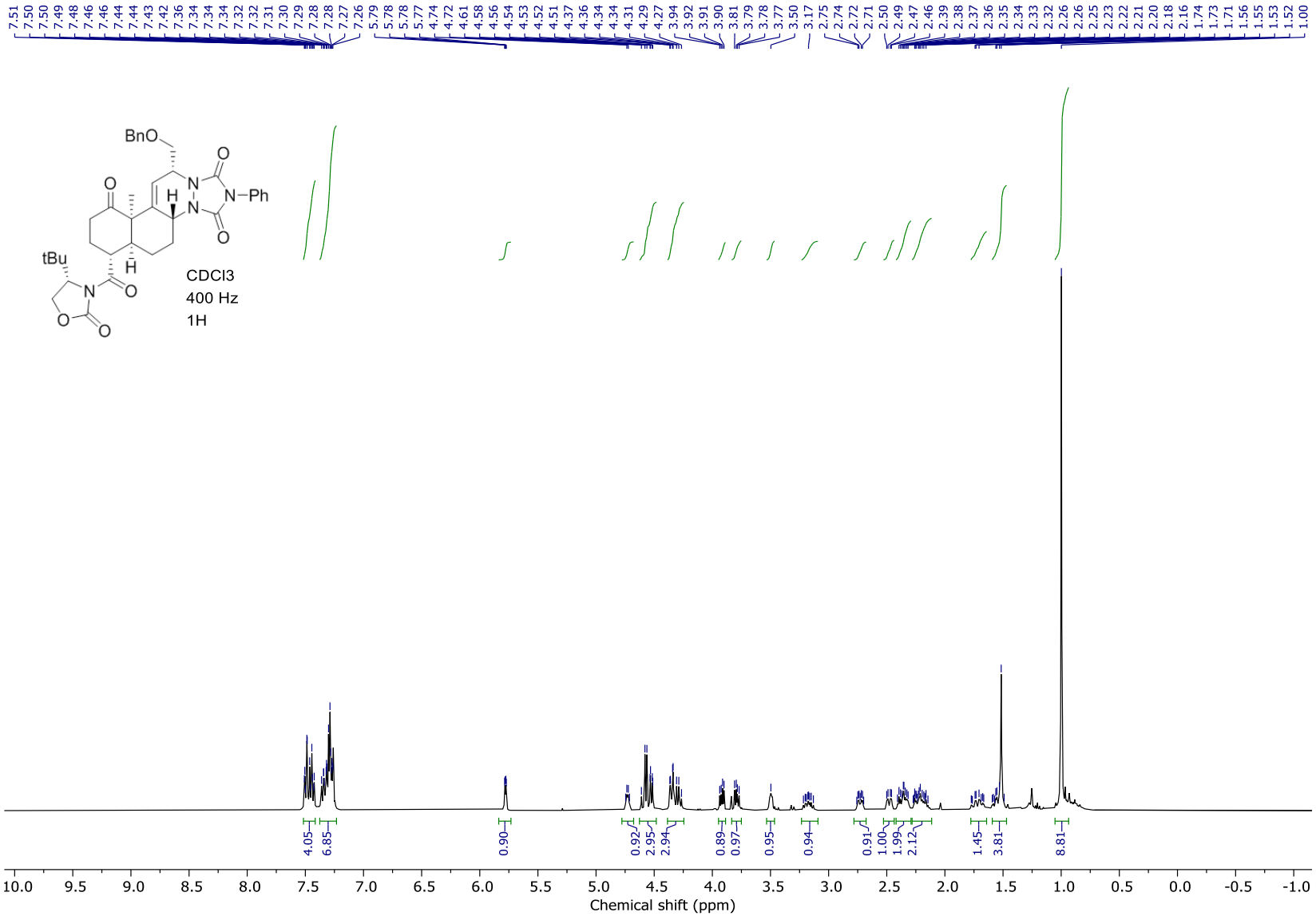
BnO
O
O
N
N
N–Ph
H
O
O
tBu
H
N
O
O
O
CDCl3
400 Hz
1H
7.51 7.50 7.50 7.49 7.48 7.46 7.46 7.44 7.44 7.43 7.42 7.36 7.34 7.34 7.34 7.32 7.32 7.31 7.30 7.29 7.28 7.28 7.27 7.26
5.79 5.78 5.78 5.77 4.74 4.72 4.61 4.58 4.56 4.54 4.53 4.52 4.51 4.37 4.36 4.34 4.34 4.31 4.29 4.27 3.94 3.92 3.91 3.90 3.81 3.79 3.78 3.77 3.50 3.17 2.75 2.74 2.72 2.71 2.50 2.49 2.47 2.46 2.39 2.38 2.37 2.36 2.35 2.34 2.33 2.32 2.26 2.26 2.25 2.23 2.22 2.21 2.20 2.18 2.16 1.74 1.73 1.71 1.56 1.55 1.53 1.52 1.00
4.05
6.85
0.90
0.92
2.95
2.94
0.89
0.97
0.95
0.94
0.91
1.00
1.99
2.12
1.45
3.81
8.81
10.0 9.5 9.0 8.5 8.0 7.5 7.0 6.5 6.0 5.5 5.0 4.5 4.0 3.5 3.0 2.5 2.0 1.5 1.0 0.5 0.0 -0.5 -1.0
Chemical shift (ppm)

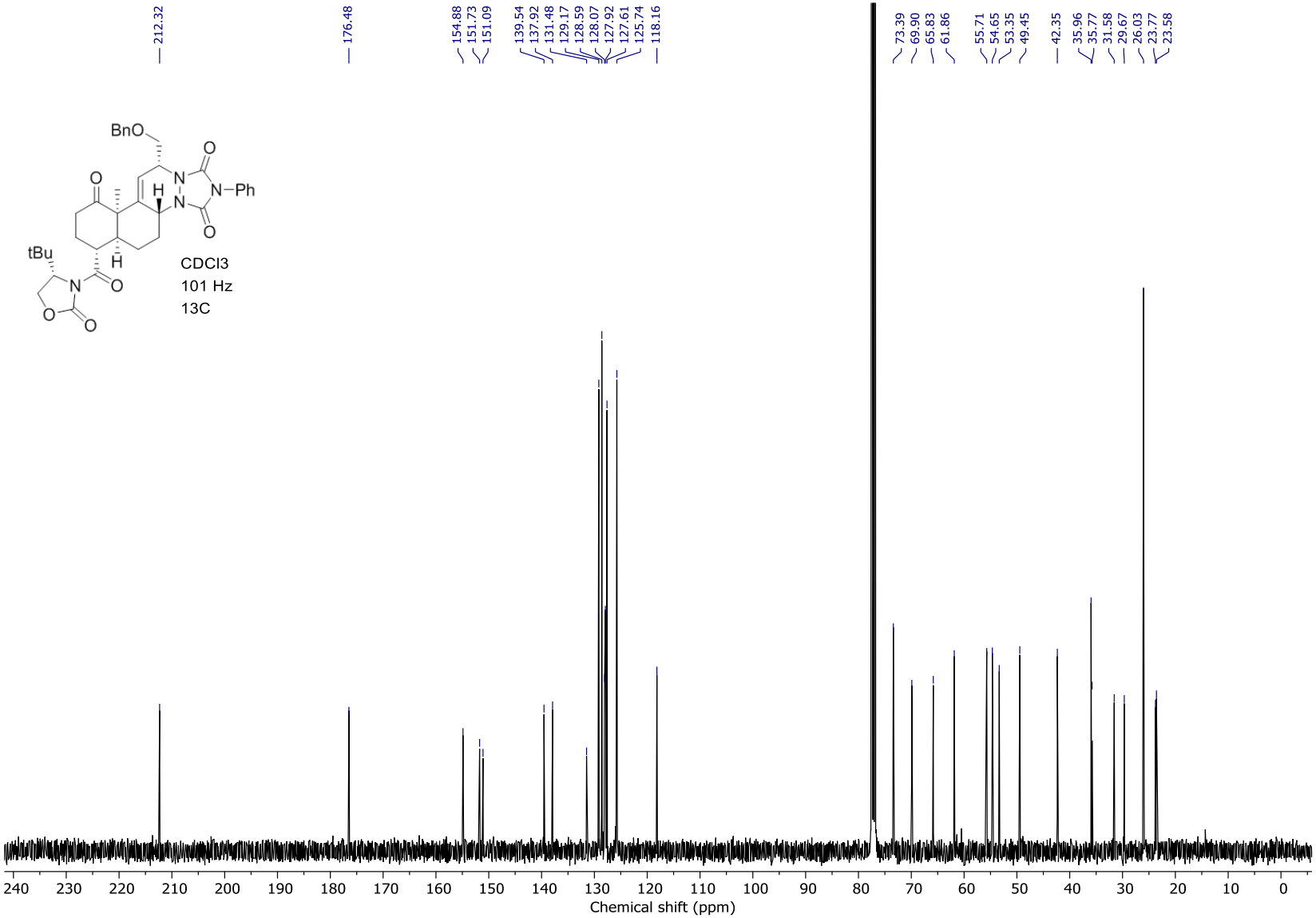
212.32
176.48
154.88
151.73
151.09
139.54
137.92
131.48
129.17
128.59
128.07
127.92
127.61
125.74
118.16
73.39
69.90
65.83
61.86
55.71
54.65
53.35
49.45
42.35
35.96
35.77
31.58
29.67
26.03
23.77
23.58
BnO
O
N
N
N–Ph
O
O
H
H
tBu
N
O
O
O
CDCl3
101 Hz
13C
240 230 220 210 200 190 180 170 160 150 140 130 120 110 100 90 80 70 60 50 40 30 20 10 0
Chemical shift (ppm)

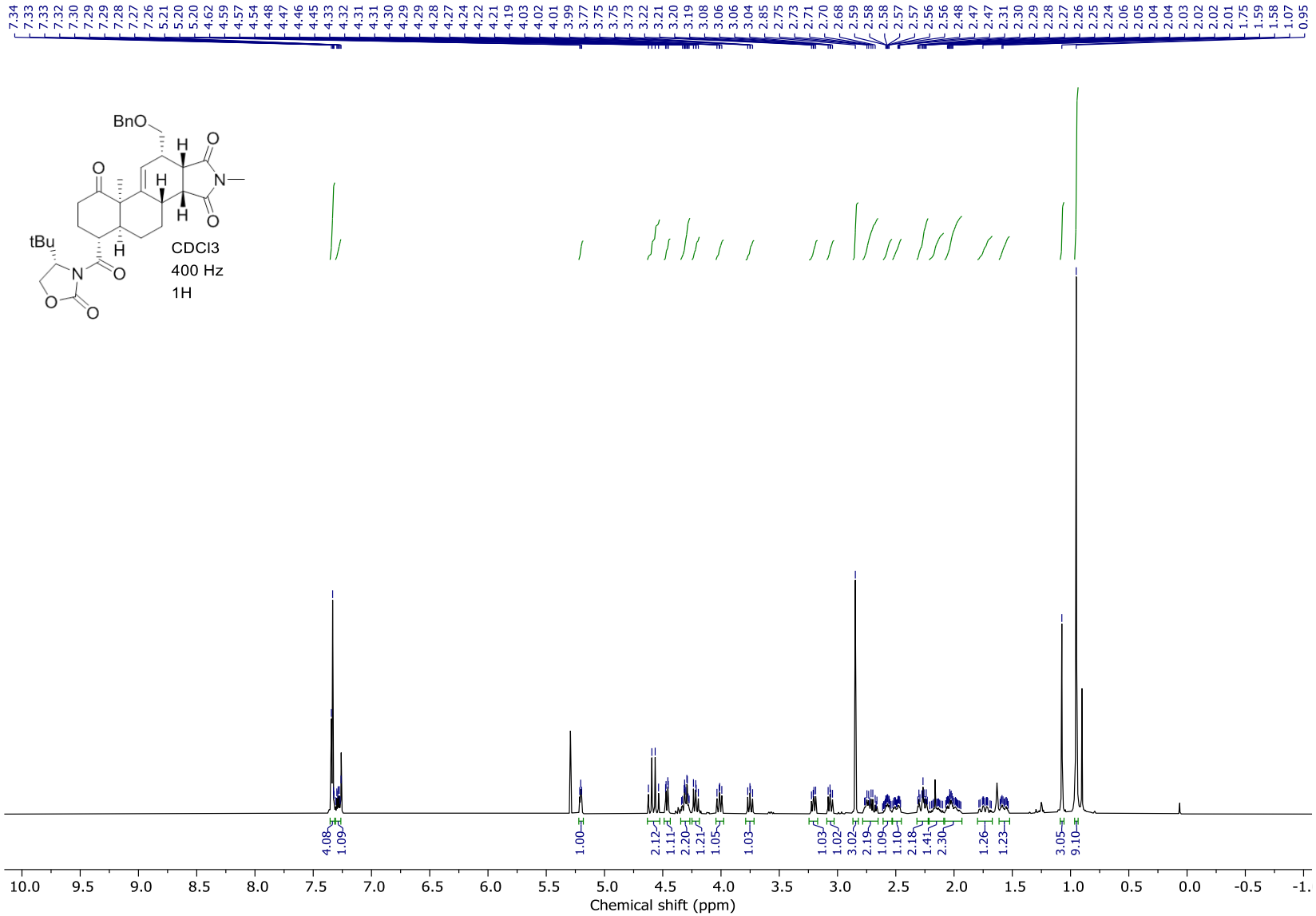
BnO
tBu
CDCl3
400 Hz
1H
Chemical shift (ppm)

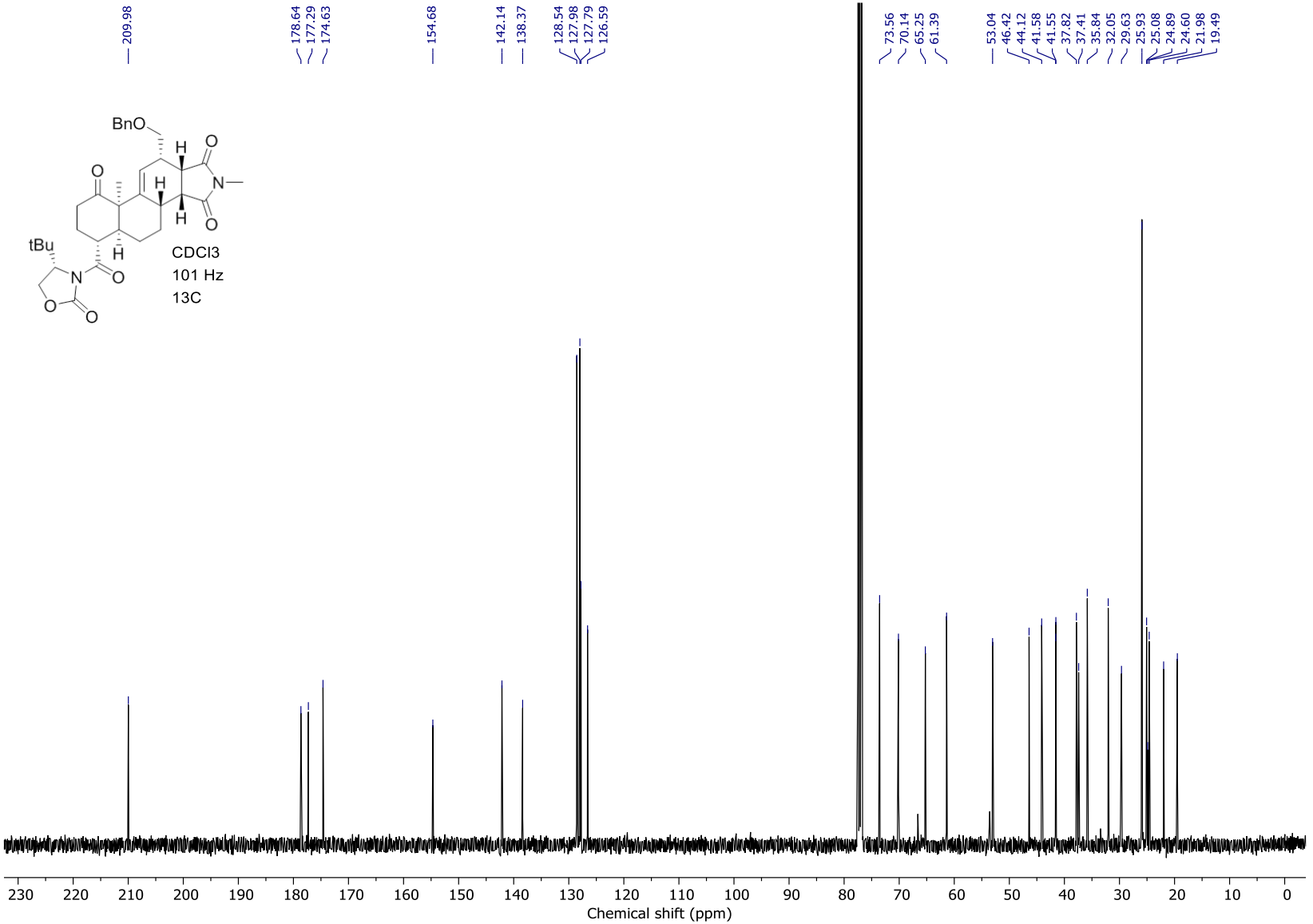
209.98
178.64
177.29
174.63
154.68
142.14
138.37
128.54
127.98
127.79
126.59
73.56
70.14
65.25
61.39
53.04
46.42
44.12
41.58
41.55
37.82
37.41
35.84
32.05
29.63
25.93
25.08
24.89
24.60
21.98
19.49
BnO
tBu
CDCl3
101 Hz
13C
Chemical shift (ppm)

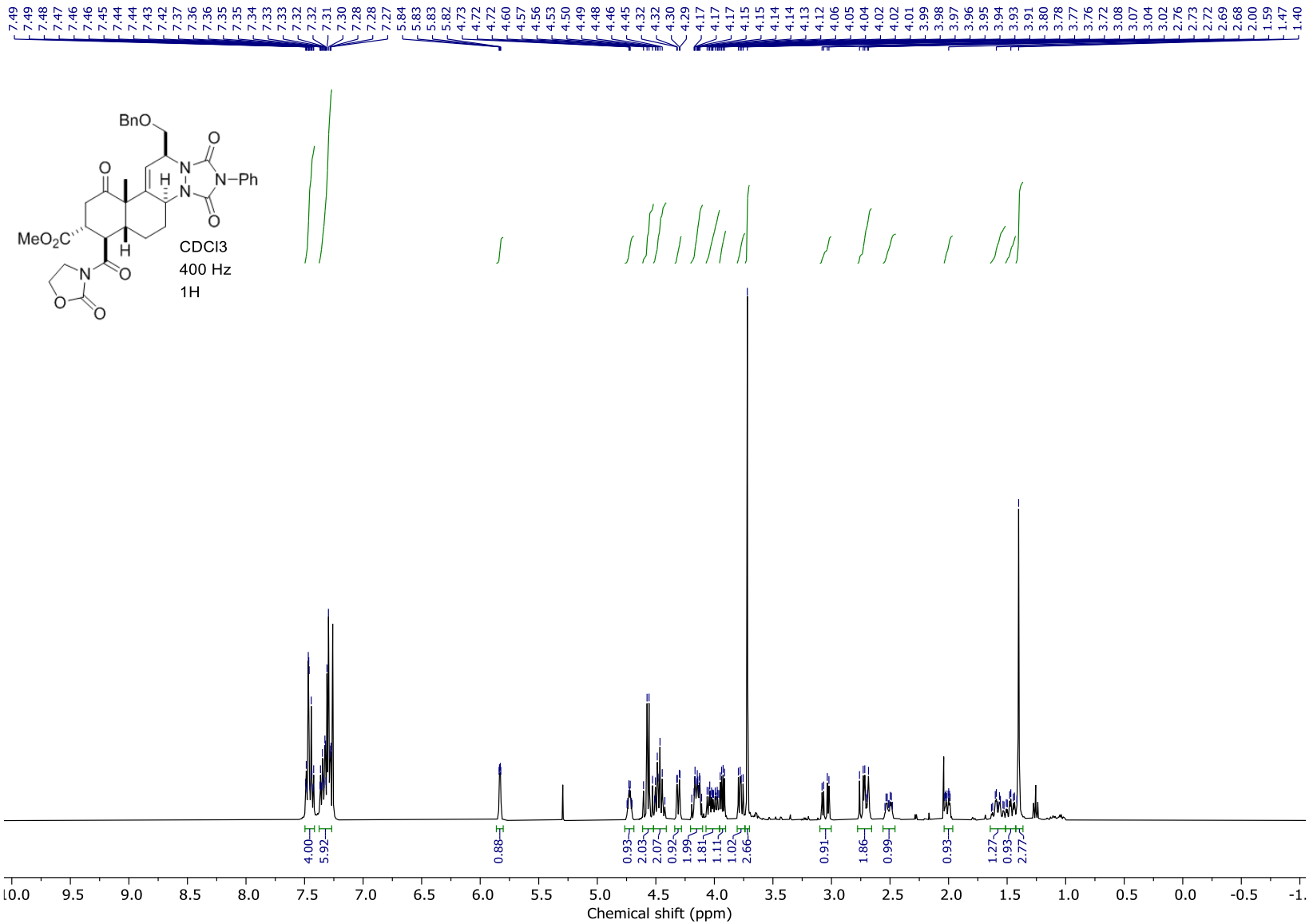
BnO
O
N
N–Ph
O
O
H
N
MeO2C
H
O
N
O
O
O
CDCl3
400 Hz
1H
4.00
5.92
0.88
0.93
2.03
2.07
0.92
1.99
1.81
1.11
1.02
2.66
0.91
1.86
0.99
0.93
1.27
0.93
2.77
10.0
9.5
9.0
8.5
8.0
7.5
7.0
6.5
6.0
5.5
5.0
4.5
4.0
3.5
3.0
2.5
2.0
1.5
1.0
0.5
0.0
-0.5
Chemical shift (ppm)

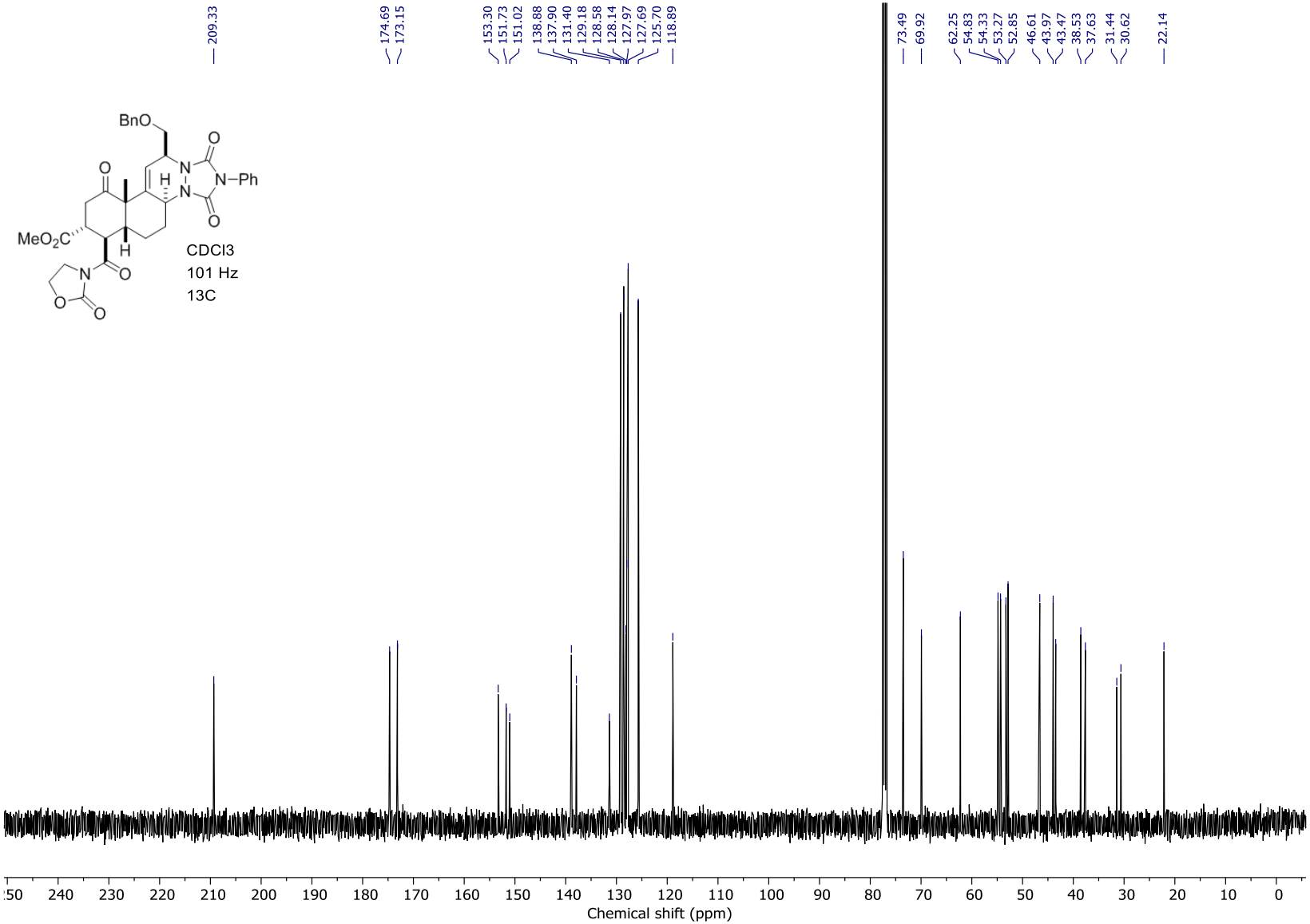
209.33
174.69
173.15
153.30
151.73
151.02
138.88
137.90
131.40
129.18
128.58
128.14
127.97
127.69
125.70
118.89
73.49
69.92
62.25
54.83
54.33
53.27
52.85
46.61
43.97
43.47
38.53
37.63
31.44
30.62
22.14
BnO
O
N
N
N–Ph
O
O
H
H
MeO2C
N
O
O
O
CDCl3
101 Hz
13C
250 240 230 220 210 200 190 180 170 160 150 140 130 120 110 100 90 80 70 60 50 40 30 20 10 0
Chemical shift (ppm)

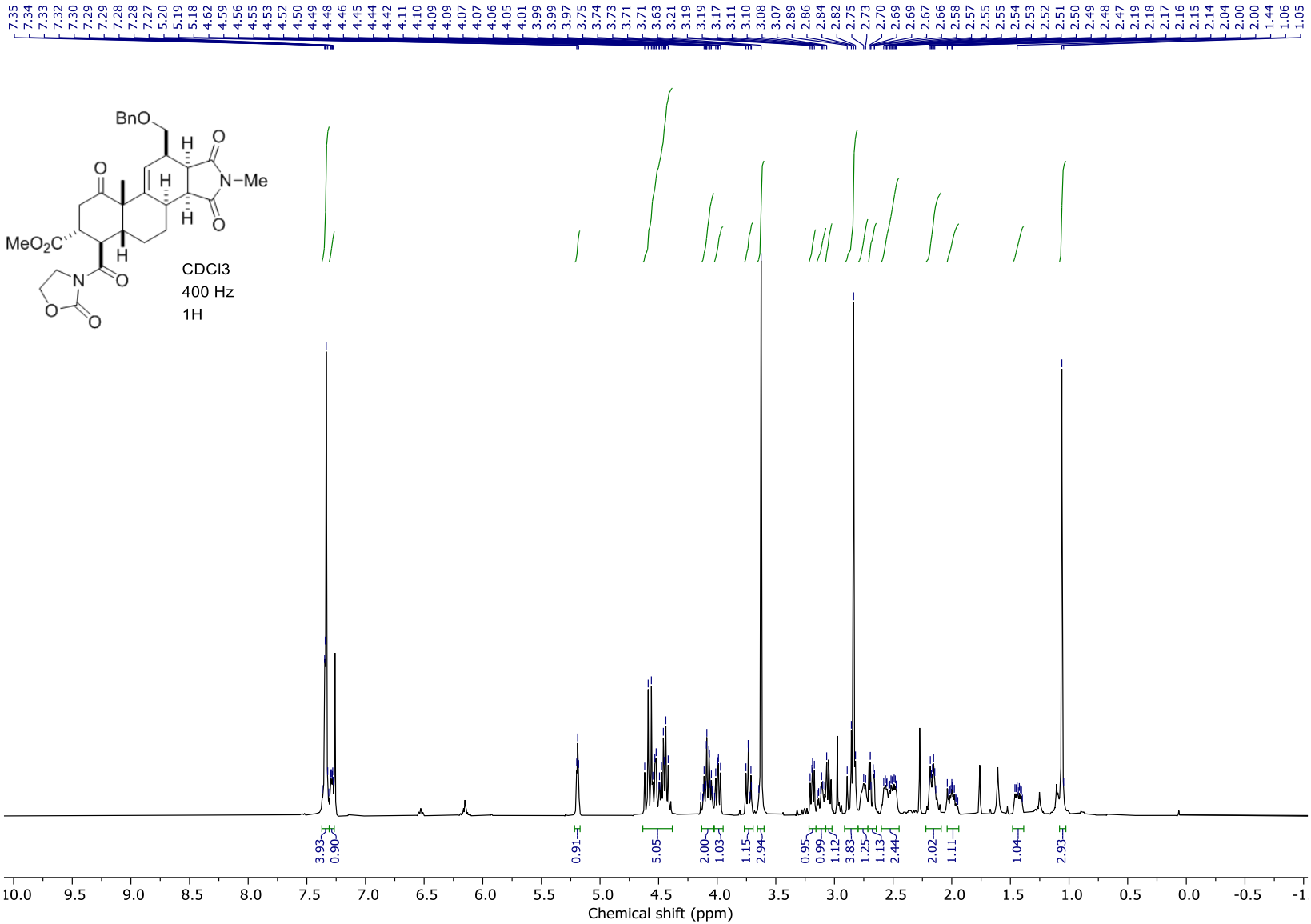
BnO
H
O
N–Me
O
H
H
O
MeO2C
H
N
O
O
O
CDCl3
400 Hz
1H
3.93
0.90
0.91
5.05
2.00
1.03
1.15
2.94
0.95
0.99
1.12
3.83
1.25
1.13
2.44
2.02
1.11
1.04
2.93
10.0
9.5
9.0
8.5
8.0
7.5
7.0
6.5
6.0
5.5
5.0
4.5
4.0
3.5
3.0
2.5
2.0
1.5
1.0
0.5
0.0
-0.5
-1
Chemical shift (ppm)

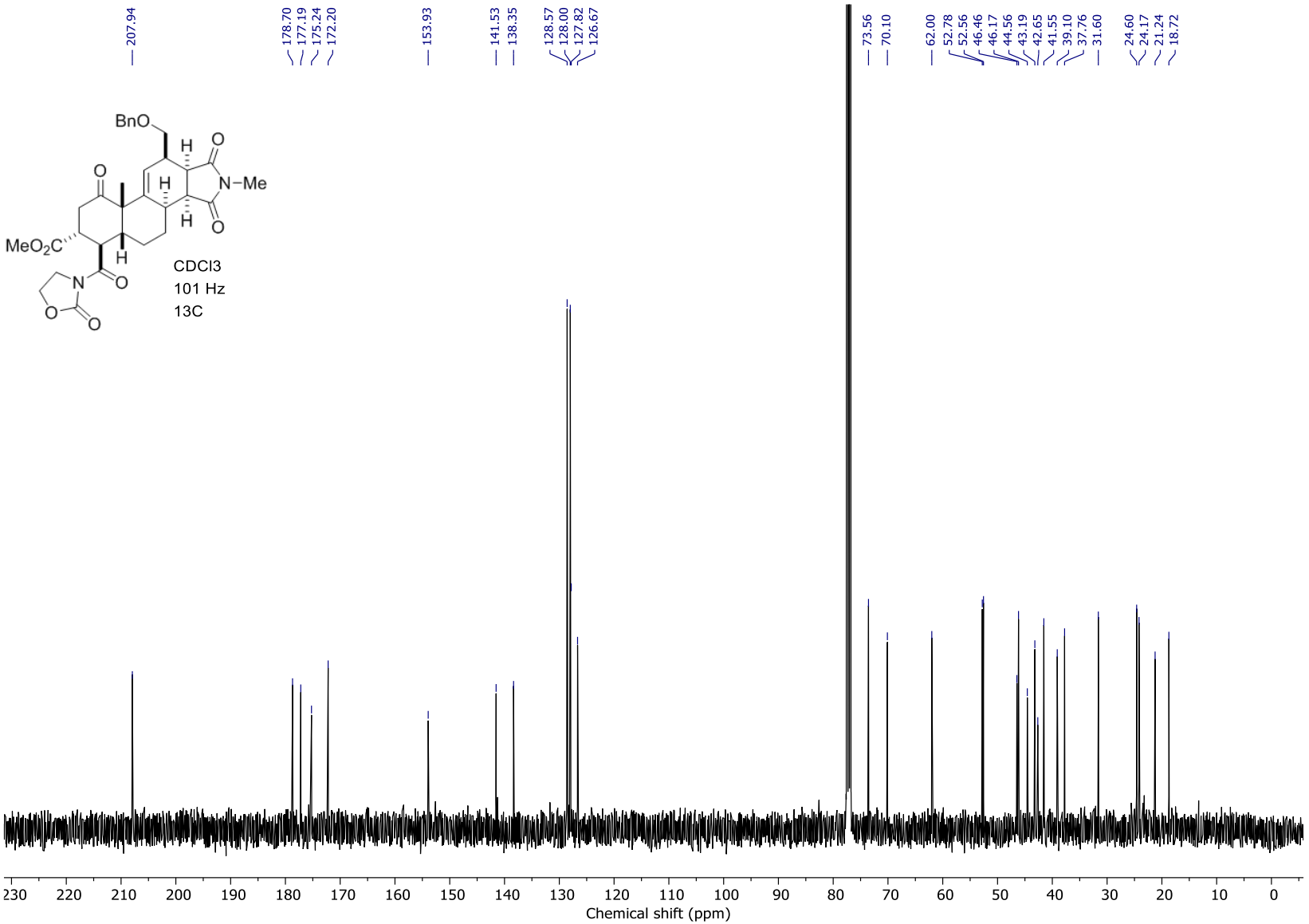
207.94
178.70
177.19
175.24
172.20
153.93
141.53
138.35
128.57
128.00
127.82
126.67
73.56
70.10
62.00
52.78
52.56
46.46
46.17
44.56
43.19
42.65
41.55
39.10
37.76
31.60
24.60
24.17
21.24
18.72
BnO
MeO2C
N–Me
CDCl3
101 Hz
13C
Chemical shift (ppm)

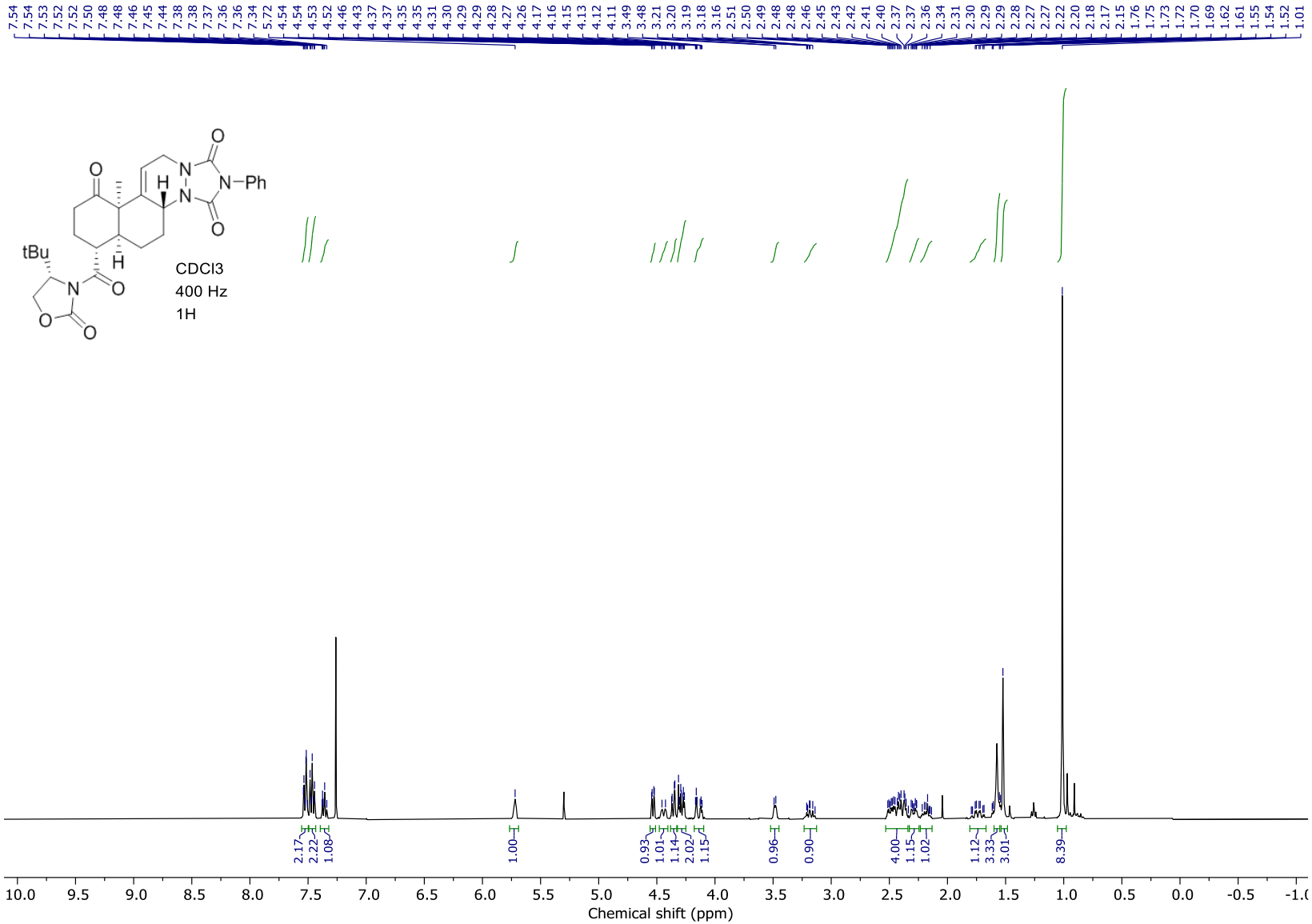
CDCl3
400 Hz
1H
tBu
N–Ph
Chemical shift (ppm)

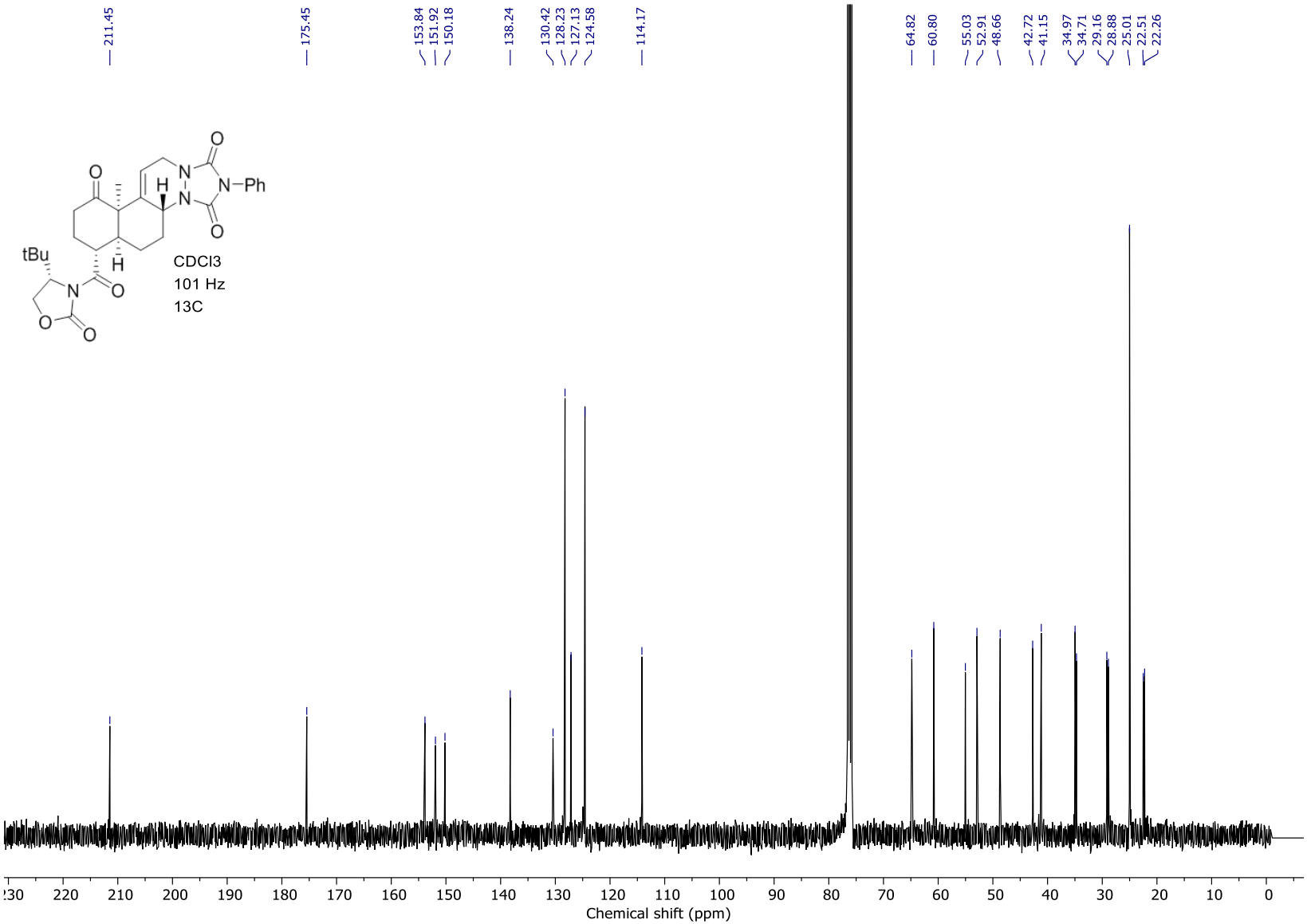
211.45
175.45
153.84
151.92
150.18
138.24
130.42
128.23
127.13
124.58
114.17
64.82
60.80
55.03
52.91
48.66
42.72
41.15
34.97
34.71
29.16
28.88
25.01
22.51
22.26
tBu
N–Ph
CDCl3
101 Hz
13C
Chemical shift (ppm)

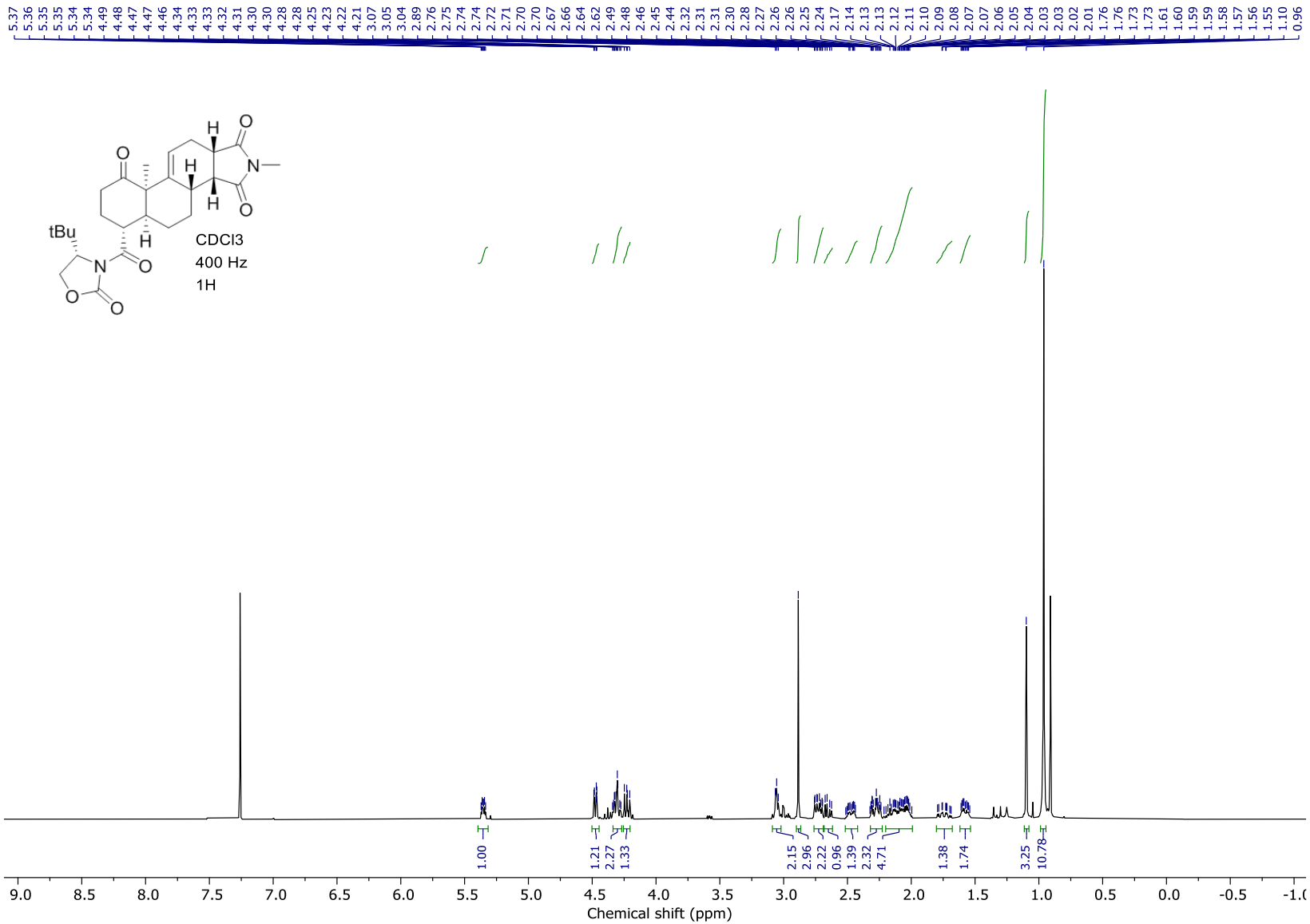
CDCl3
400 Hz
1H
Chemical shift (ppm)

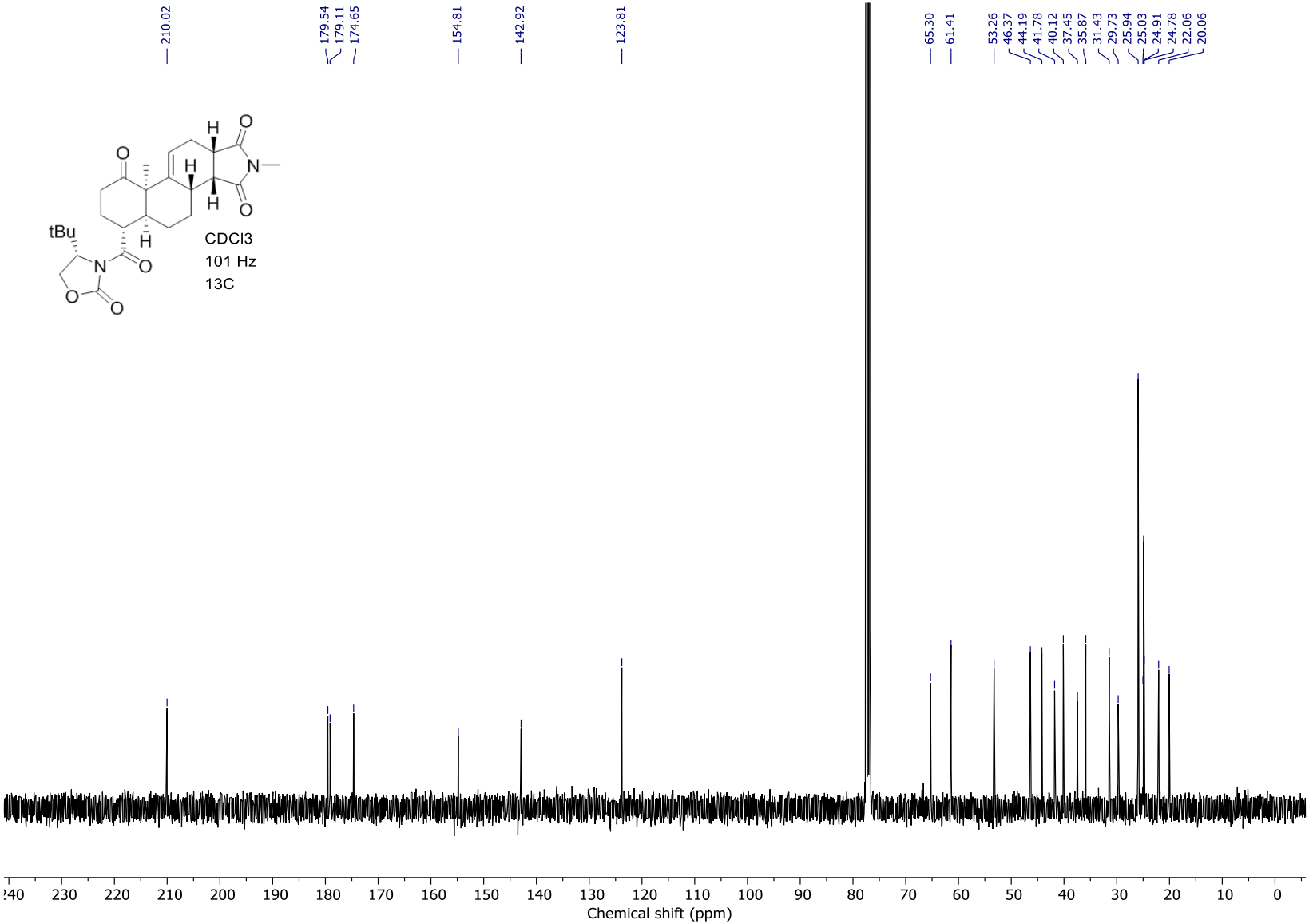
210.02
179.54
179.11
174.65
154.81
142.92
123.81
65.30
61.41
53.26
46.37
44.19
41.78
40.12
37.45
35.87
31.43
29.73
25.94
25.03
24.91
24.78
22.06
20.06
tBu
CDCl3
101 Hz
13C
240 230 220 210 200 190 180 170 160 150 140 130 120 110 100 90 80 70 60 50 40 30 20 10 0
Chemical shift (ppm)

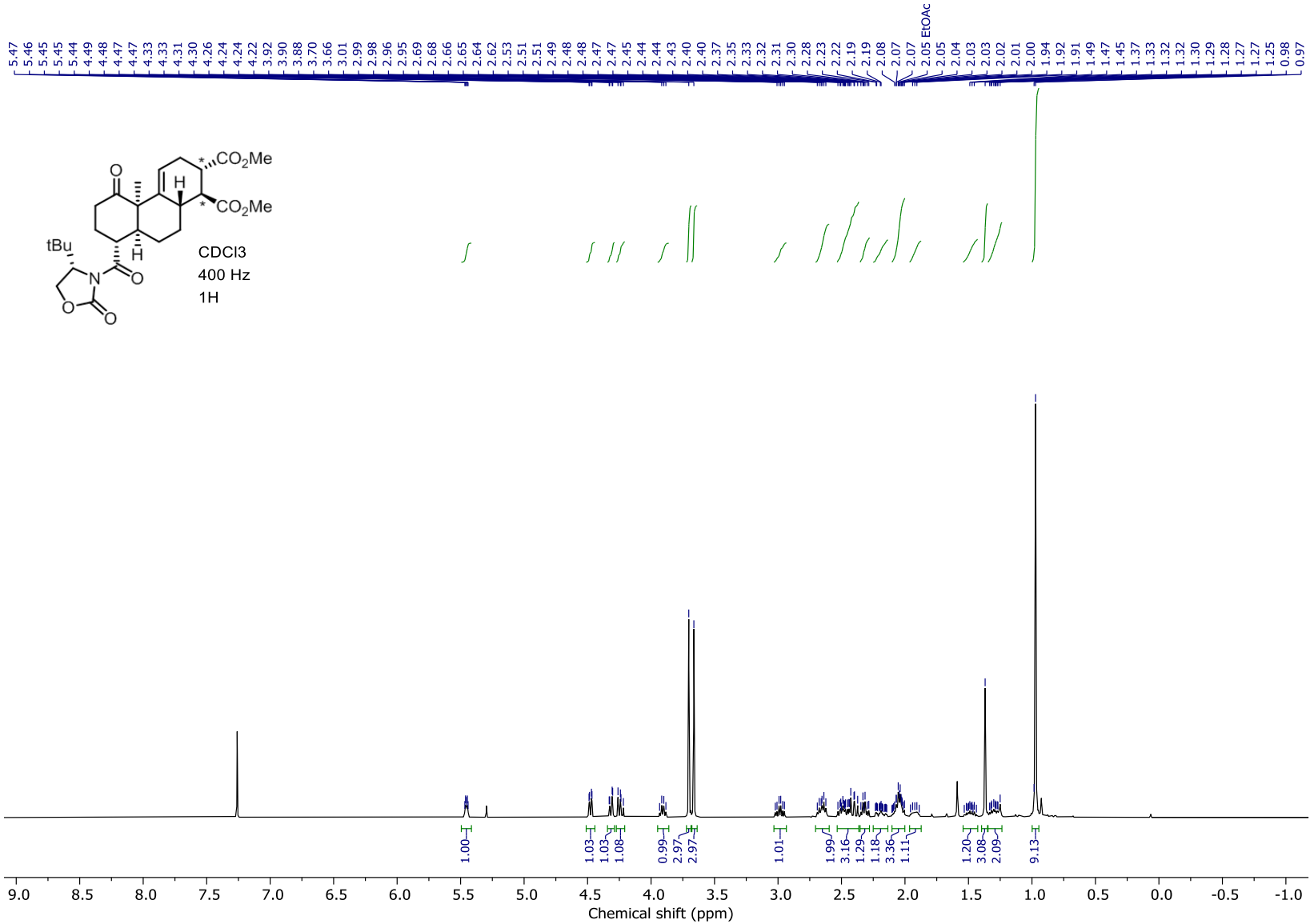
5.47 5.46 5.45 5.45 5.44 4.49 4.48 4.47 4.47 4.33 4.33 4.31 4.30 4.26 4.24 4.24 4.22 3.92 3.90 3.88 3.70 3.66 3.01 2.99 2.98 2.96 2.95 2.69 2.68 2.66 2.65 2.64 2.62 2.53 2.51 2.51 2.49 2.48 2.48 2.47 2.47 2.45 2.44 2.44 2.43 2.40 2.40 2.37 2.35 2.33 2.32 2.31 2.30 2.28 2.23 2.22 2.19 2.19 2.08 2.07 2.07 2.05 EtOAc 2.05 2.04 2.03 2.03 2.02 2.01 2.00 1.94 1.92 1.91 1.49 1.47 1.45 1.37 1.33 1.32 1.32 1.30 1.29 1.28 1.27 1.27 1.25 0.98 0.97
CO2Me
CO2Me
tBu
CDCl3
400 Hz
1H
1.00 1.03 1.03 1.08 0.99 2.97 2.97 1.01 1.99 3.16 1.29 1.18 3.36 1.11 1.20 3.08 2.09 9.13
9.0 8.5 8.0 7.5 7.0 6.5 6.0 5.5 5.0 4.5 4.0 3.5 3.0 2.5 2.0 1.5 1.0 0.5 0.0 -0.5 -1.0
Chemical shift (ppm)

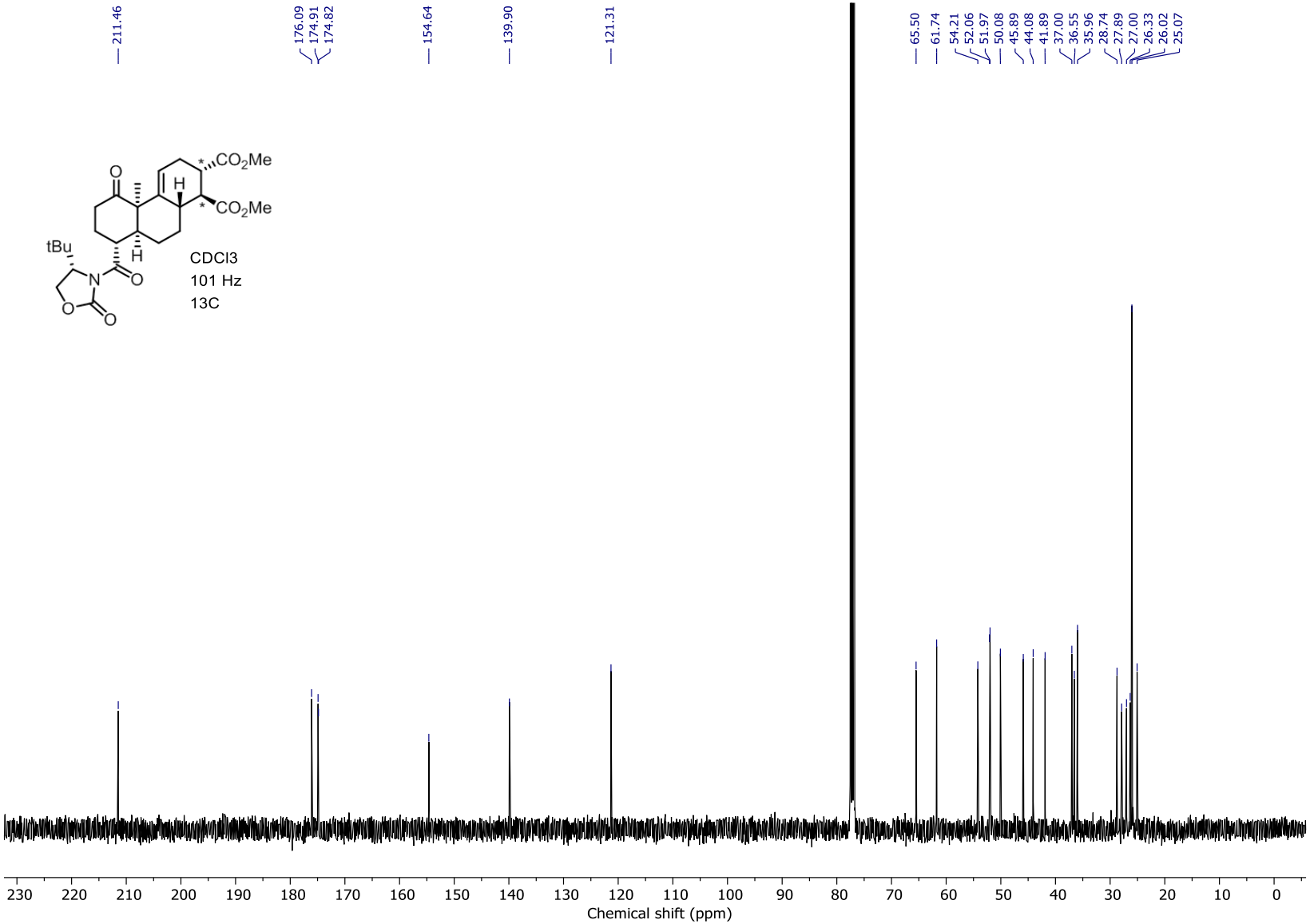
211.46
176.09
174.91
174.82
154.64
139.90
121.31
65.50
61.74
54.21
52.06
51.97
50.08
45.89
44.08
41.89
37.00
36.55
35.96
28.74
27.89
27.00
26.33
26.02
25.07
CO2Me
CO2Me
tBu
CDCl3
101 Hz
13C
230 220 210 200 190 180 170 160 150 140 130 120 110 100 90 80 70 60 50 40 30 20 10 0
Chemical shift (ppm)

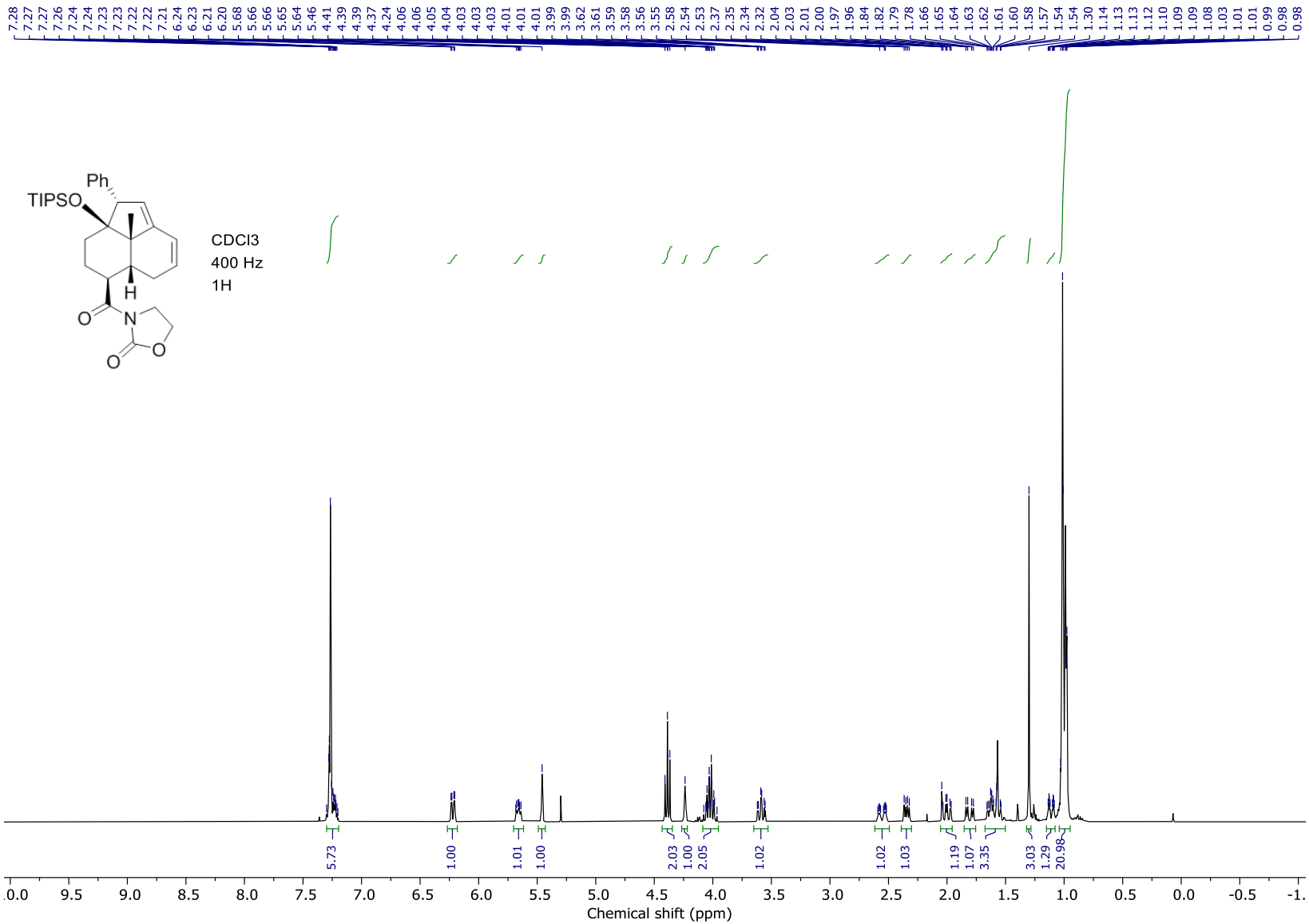
Ph
TIPSO
H
O
N
O
O
CDCl3
400 Hz
1H
5.73
1.00
1.01
1.00
2.03
1.00
2.05
1.02
1.02
1.03
1.19
1.07
3.35
3.03
1.29
20.98
Chemical shift (ppm)

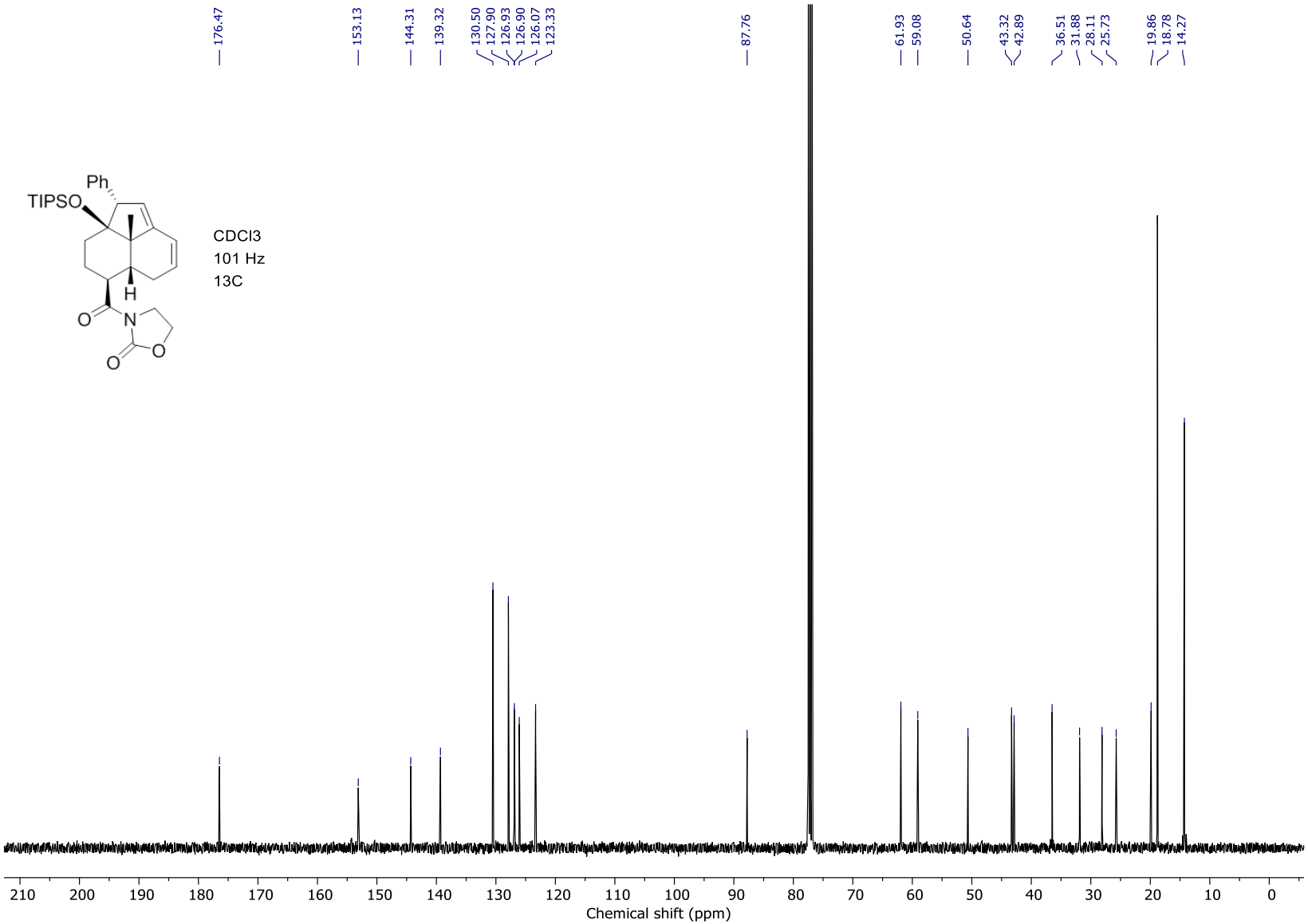
176.47
153.13
144.31
139.32
130.50
127.90
126.93
126.90
126.07
123.33
87.76
61.93
59.08
50.64
43.32
42.89
36.51
31.88
28.11
25.73
19.86
18.78
14.27
Ph
TIPSO
H
O
N
O
O
CDCl3
101 Hz
13C
210
200
190
180
170
160
150
140
130
120
110
100
90
80
70
60
50
40
30
20
10
0
Chemical shift (ppm)

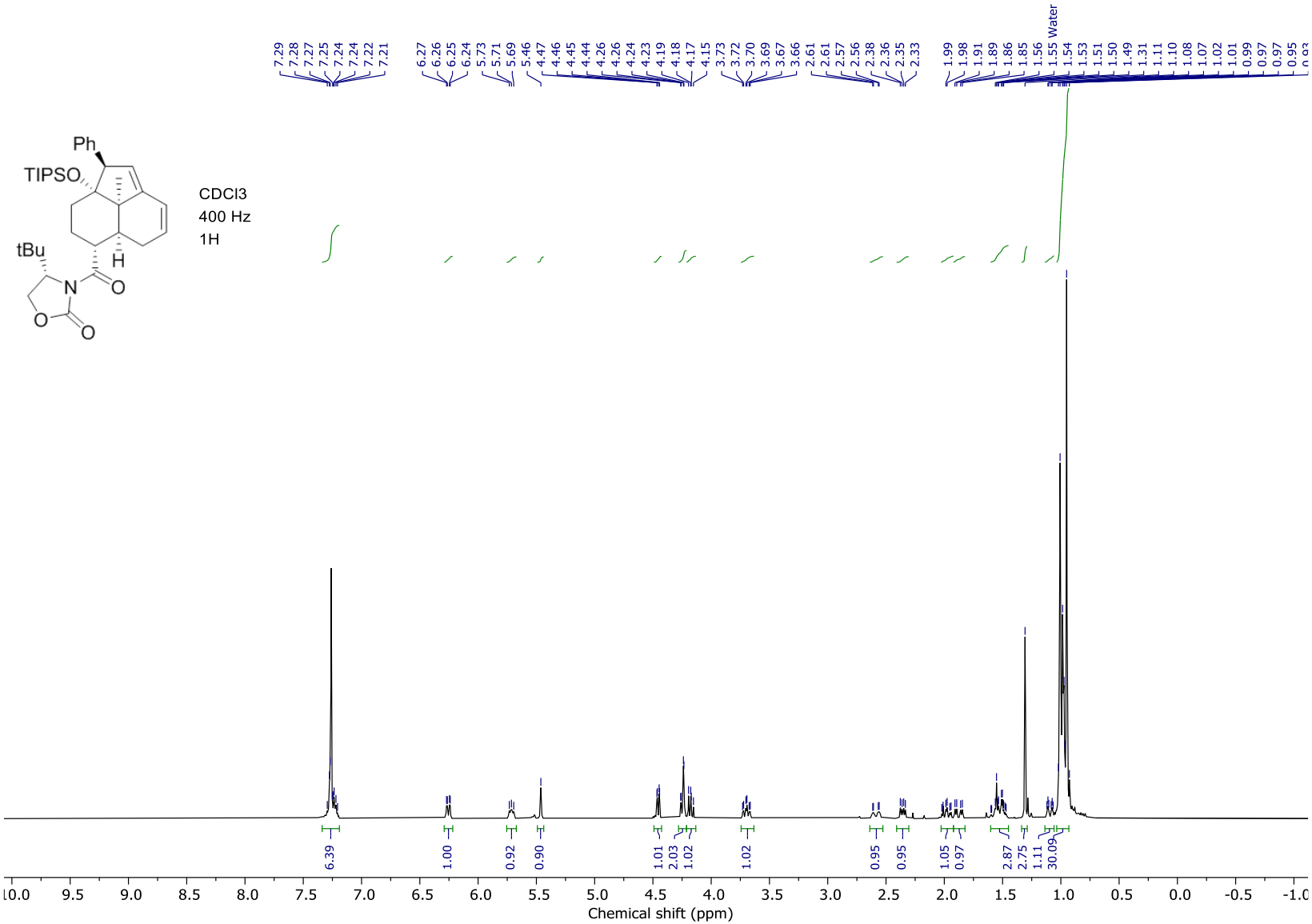
Ph
TIPSO
tBu
H
N
O
O
O
CDCl3
400 Hz
1H
Water
Chemical shift (ppm)

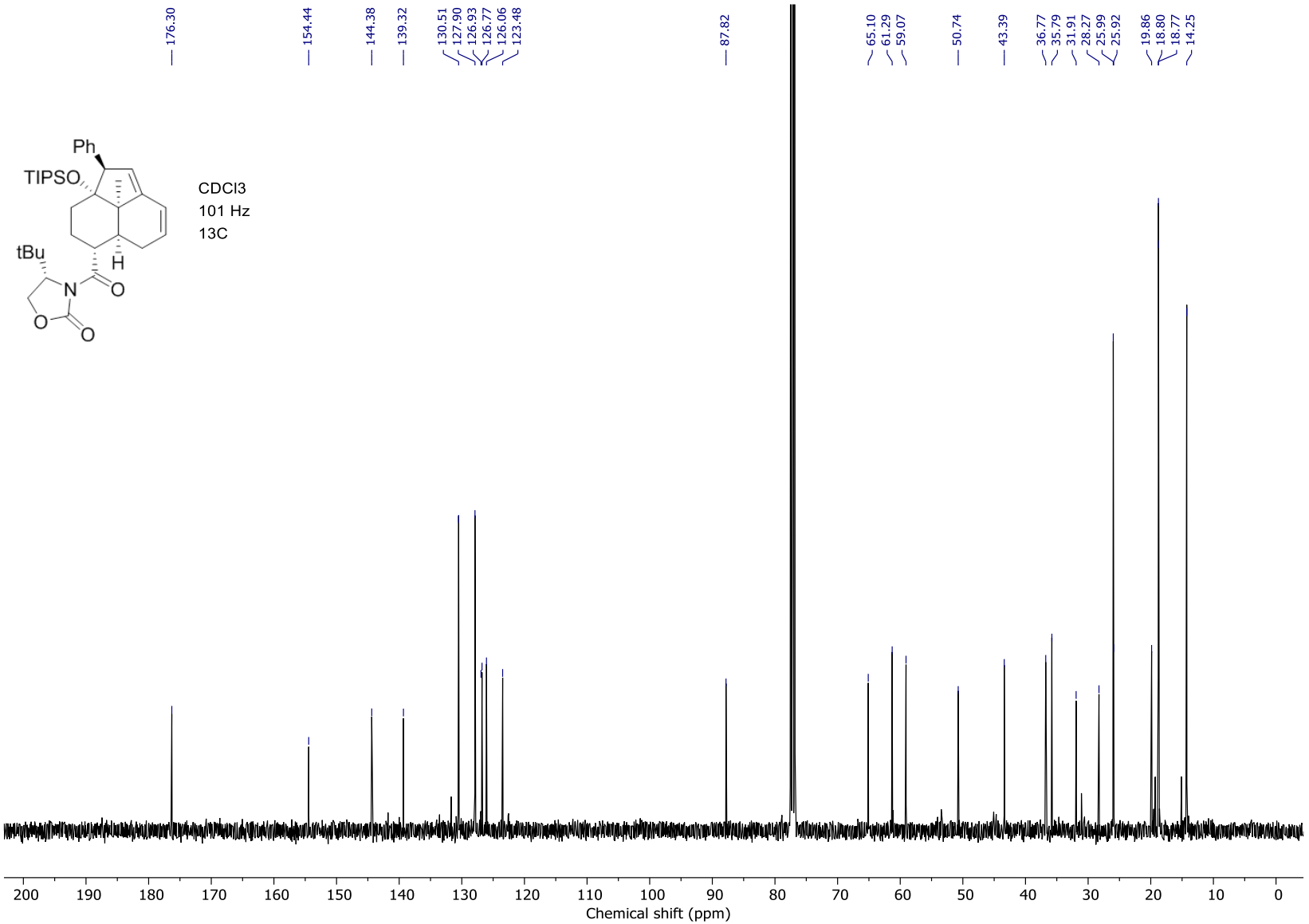
176.30
154.44
144.38
139.32
130.51
127.90
126.93
126.77
126.06
123.48
87.82
65.10
61.29
59.07
50.74
43.39
36.77
35.79
31.91
28.27
25.99
25.92
19.86
18.80
18.77
14.25
Ph
TIPSO
tBu
H
N
O
O
O
CDCl3
101 Hz
13C
200
190
180
170
160
150
140
130
120
110
100
90
80
70
60
50
40
30
20
10
0
Chemical shift (ppm)

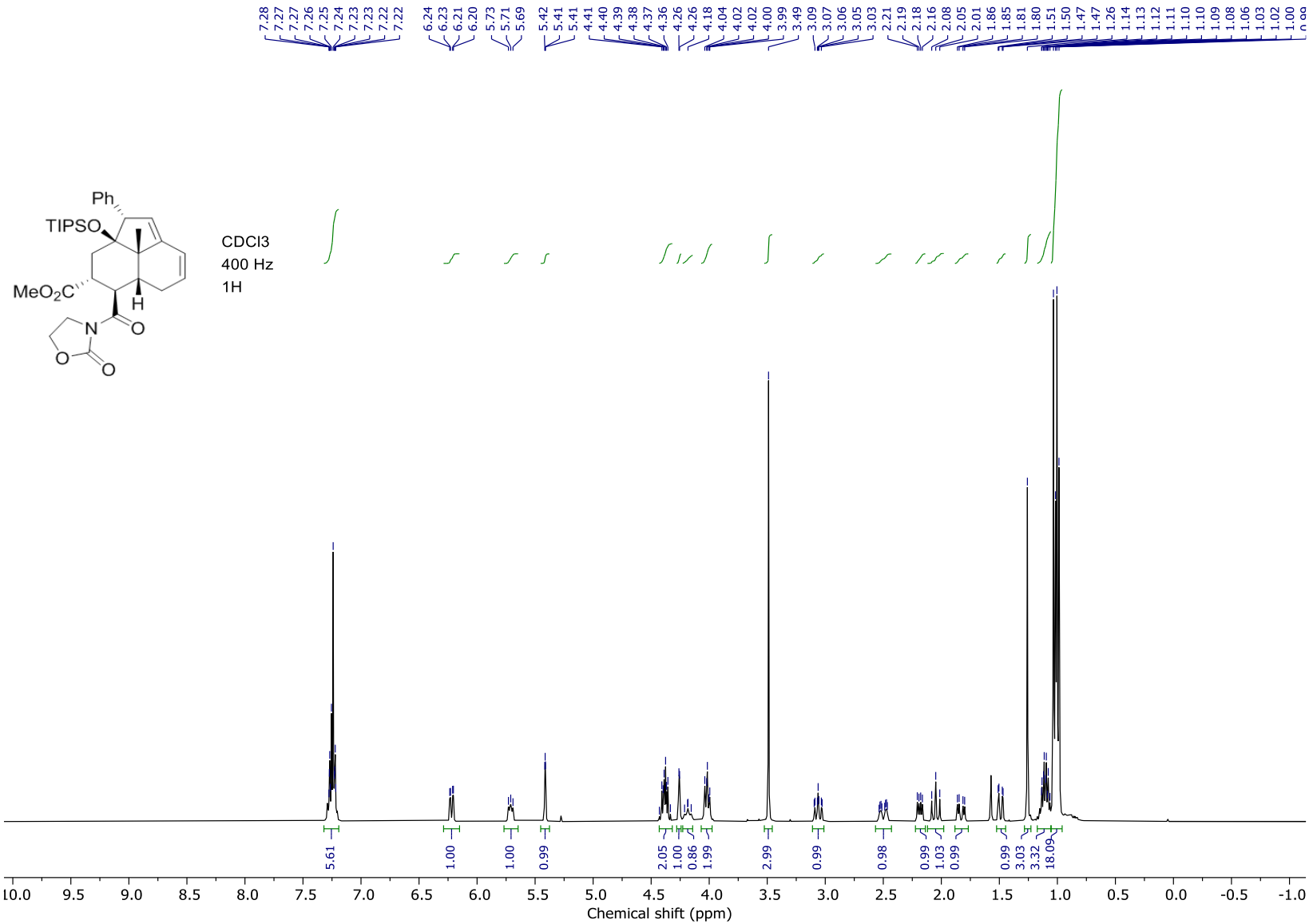
Ph
TIPSO
MeO2C
H
N
O
O
O
CDCl3
400 Hz
1H
7.28 7.27 7.27 7.26 7.25 7.24 7.23 7.23 7.22 7.22
6.24 6.23 6.21 6.20
5.73 5.71 5.69
5.42 5.41 5.41
4.41 4.40 4.39 4.38 4.37 4.36 4.26 4.26 4.18 4.04 4.02 4.02 4.00 3.99 3.49
3.09 3.07 3.06 3.05 3.03
2.21 2.19 2.18 2.16 2.08 2.05 2.01 1.86 1.85 1.81 1.80 1.51 1.50 1.47 1.47 1.26 1.14 1.13 1.12 1.11 1.10 1.10 1.09 1.08 1.06 1.03 1.02 1.00
5.61
1.00
1.00
0.99
2.05
1.00
0.86
1.99
2.99
0.99
0.98
0.99
1.03
0.99
0.99
3.03
3.32
18.09
10.0 9.5 9.0 8.5 8.0 7.5 7.0 6.5 6.0 5.5 5.0 4.5 4.0 3.5 3.0 2.5 2.0 1.5 1.0 0.5 0.0 -0.5 -1.0
Chemical shift (ppm)

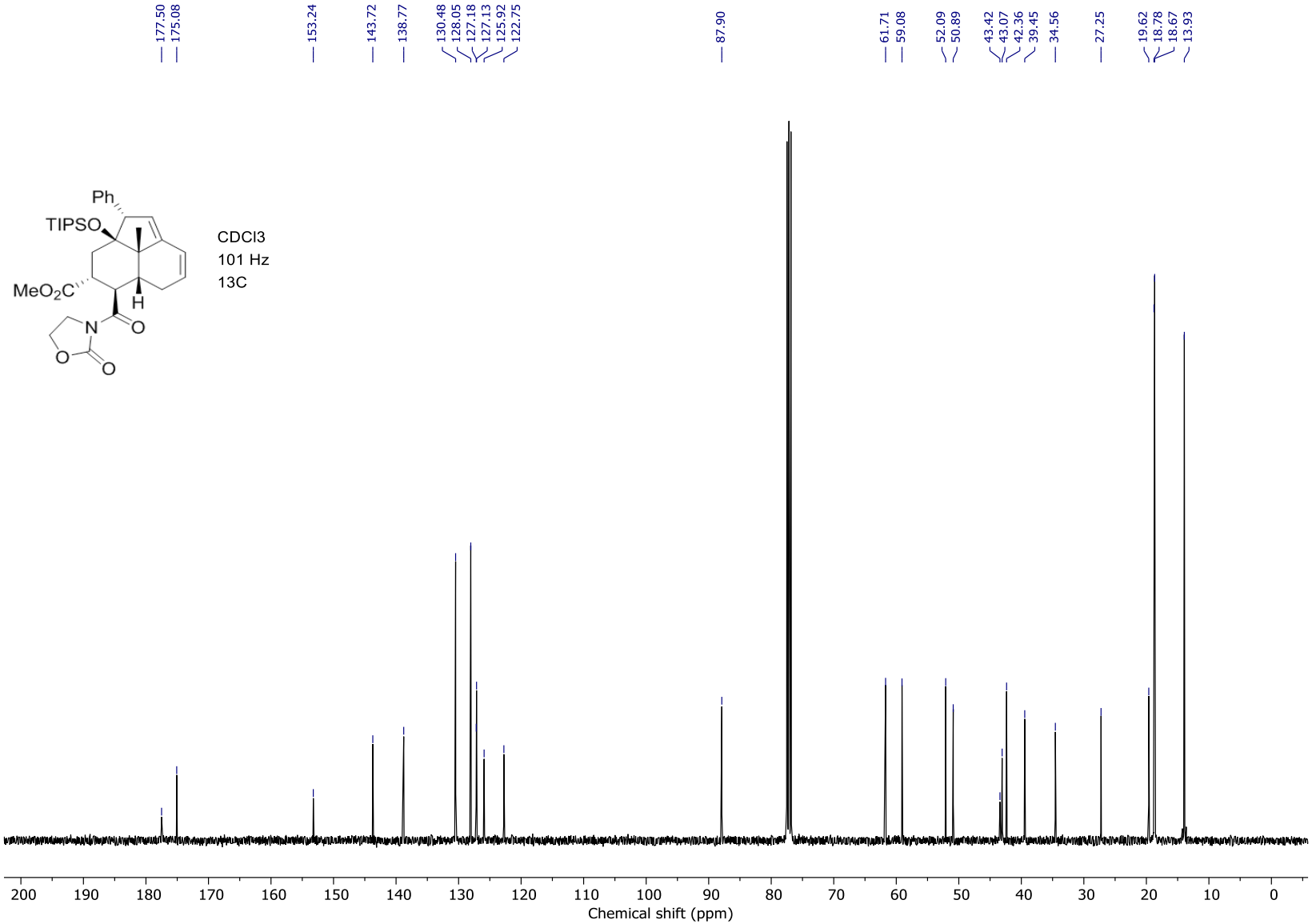
177.50
175.08
153.24
143.72
138.77
130.48
128.05
127.18
127.13
125.92
122.75
87.90
61.71
59.08
52.09
50.89
43.42
43.07
42.36
39.45
34.56
27.25
19.62
18.78
18.67
13.93
Ph
TIPSO
MeO2C
H
N
O
O
O
CDCl3
101 Hz
13C
200
190
180
170
160
150
140
130
120
110
100
90
80
70
60
50
40
30
20
10
0
Chemical shift (ppm)

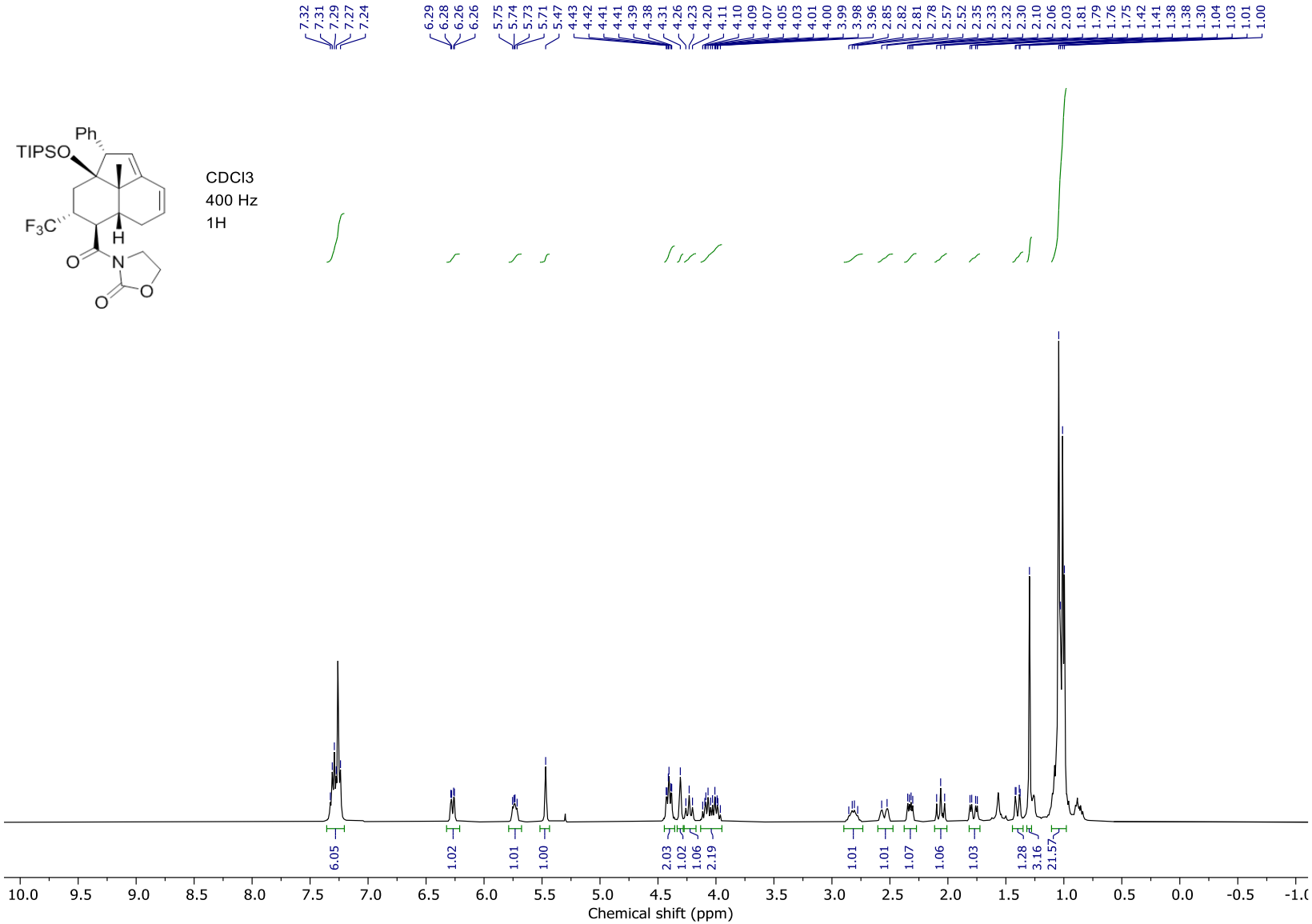
Ph
TIPSO
F3C
H
O
N
O
O
CDCl3
400 Hz
1H
7.32 7.31 7.29 7.27 7.24
6.29 6.28 6.26 6.26
5.75 5.74 5.73 5.71 5.47
4.43 4.42 4.41 4.41 4.39 4.38 4.31 4.26 4.23 4.20 4.11 4.10 4.09 4.07 4.05 4.03 4.01 4.00 3.99 3.98 3.96 2.85 2.82 2.81 2.78 2.57 2.52 2.35 2.33 2.32 2.30 2.10 2.06 2.03 1.81 1.79 1.76 1.75 1.42 1.41 1.38 1.38 1.30 1.04 1.03 1.01 1.00
6.05
1.02
1.01
1.00
2.03
1.02
1.06
2.19
1.01
1.01
1.07
1.06
1.03
1.28
3.16
21.57
10.0 9.5 9.0 8.5 8.0 7.5 7.0 6.5 6.0 5.5 5.0 4.5 4.0 3.5 3.0 2.5 2.0 1.5 1.0 0.5 0.0 -0.5
Chemical shift (ppm)

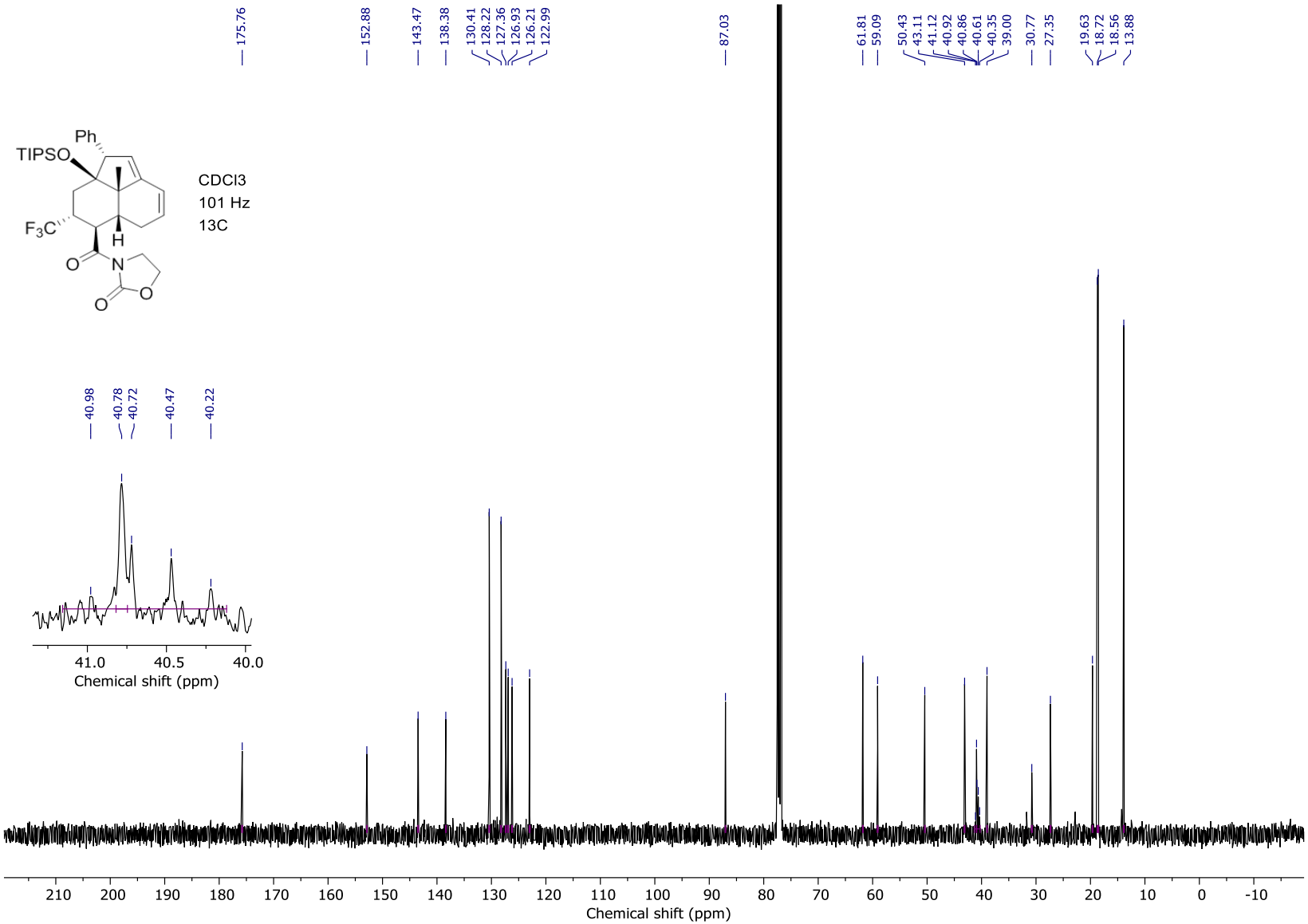
175.76
152.88
143.47
138.38
130.41
128.22
127.36
126.93
126.21
122.99
87.03
61.81
59.09
50.43
43.11
41.12
40.92
40.86
40.61
40.35
39.00
30.77
27.35
19.63
18.72
18.56
13.88
Ph
TIPSO
F3C
H
O
N
O
O
CDCl3
101 Hz
13C
40.98
40.78
40.72
40.47
40.22
41.0
40.5
40.0
Chemical shift (ppm)
210
200
190
180
170
160
150
140
130
120
110
100
90
80
70
60
50
40
30
20
10
0
-10
Chemical shift (ppm)

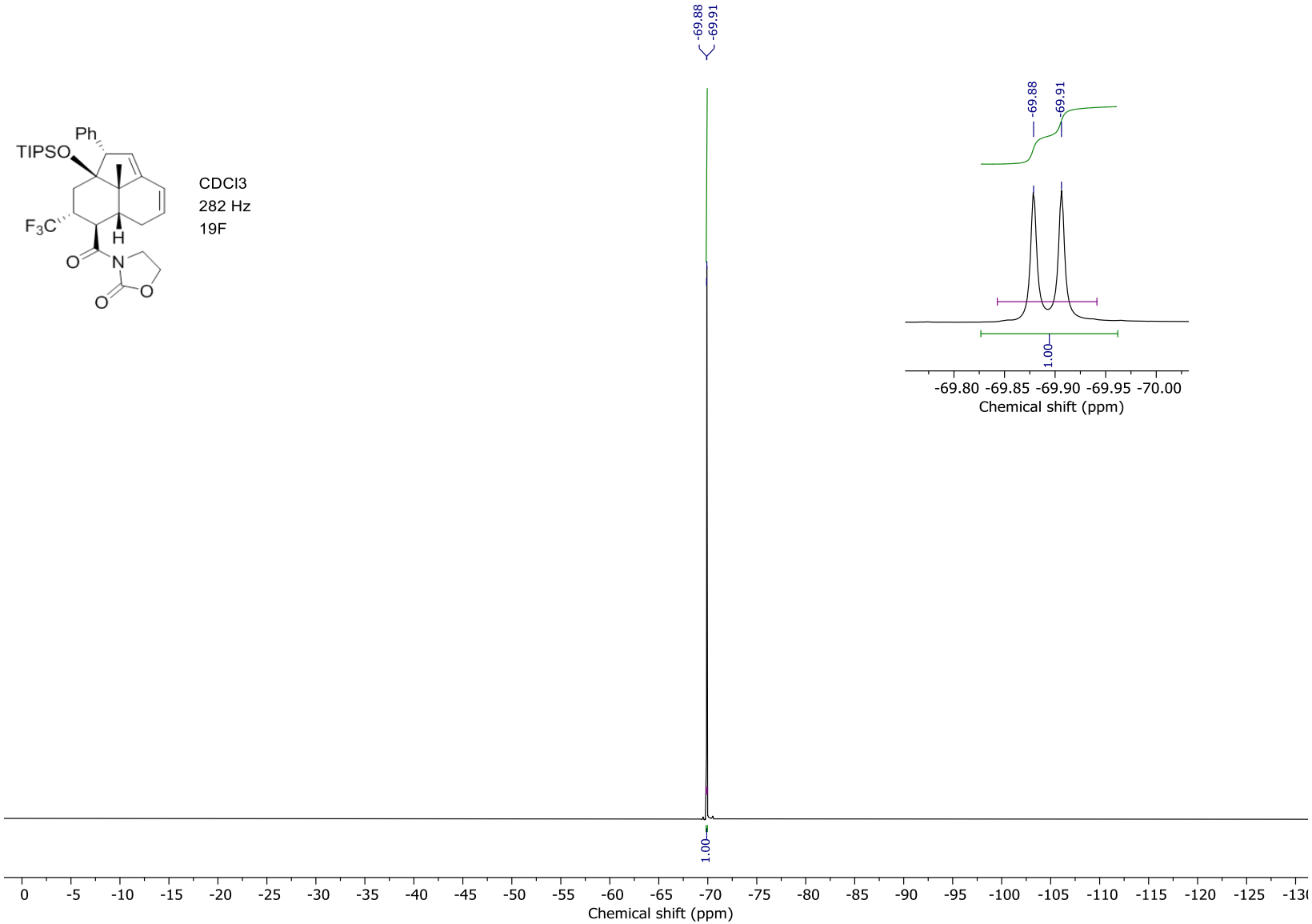
Ph
TIPSO
F3C
H
O
N
O
O
CDCl3
282 Hz
19F
-69.88
-69.91
1.00
-69.80 -69.85 -69.90 -69.95 -70.00
Chemical shift (ppm)
1.00
0 -5 -10 -15 -20 -25 -30 -35 -40 -45 -50 -55 -60 -65 -70 -75 -80 -85 -90 -95 -100 -105 -110 -115 -120 -125
Chemical shift (ppm)

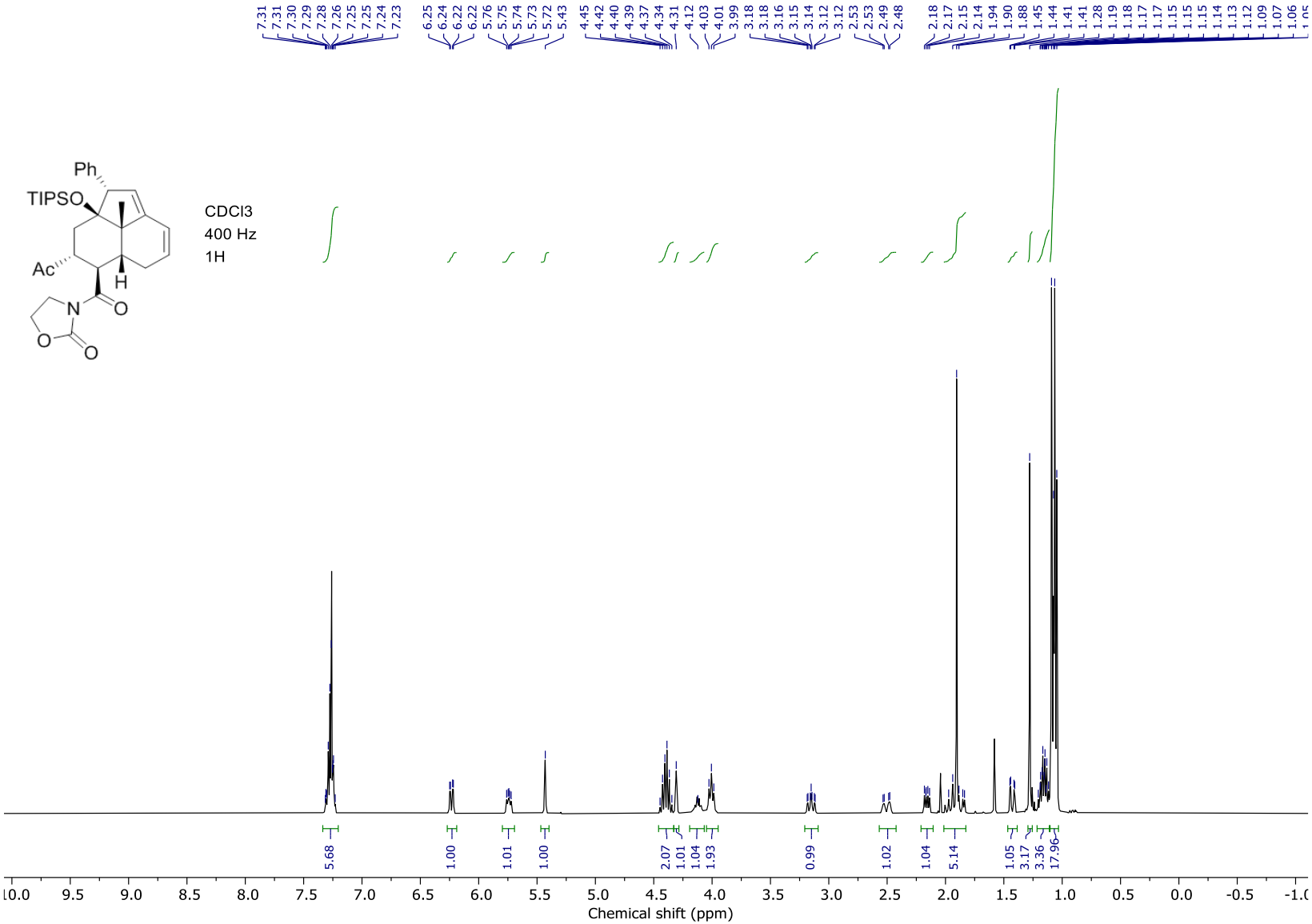
Ph
TIPSO
Ac
H
N
O
O
O
CDCl3
400 Hz
1H
7.31 7.31 7.30 7.29 7.28 7.26 7.25 7.25 7.24 7.23
6.25 6.24 6.22 6.22
5.76 5.75 5.74 5.73 5.72 5.43
4.45 4.42 4.40 4.39 4.37 4.34 4.31 4.12 4.03 4.01 3.99
3.18 3.18 3.16 3.15 3.14 3.12 3.12
2.53 2.49 2.48
2.18 2.17 2.15 2.14 1.94 1.90 1.88 1.45 1.44 1.41 1.41 1.28 1.19 1.18 1.17 1.17 1.15 1.15 1.15 1.14 1.13 1.12 1.09 1.07 1.06
5.68
1.00
1.01
1.00
2.07
1.01
1.04
1.93
0.99
1.02
1.04
5.14
1.05
3.17
3.36
17.96
10.0 9.5 9.0 8.5 8.0 7.5 7.0 6.5 6.0 5.5 5.0 4.5 4.0 3.5 3.0 2.5 2.0 1.5 1.0 0.5 0.0 -0.5 -1.0
Chemical shift (ppm)

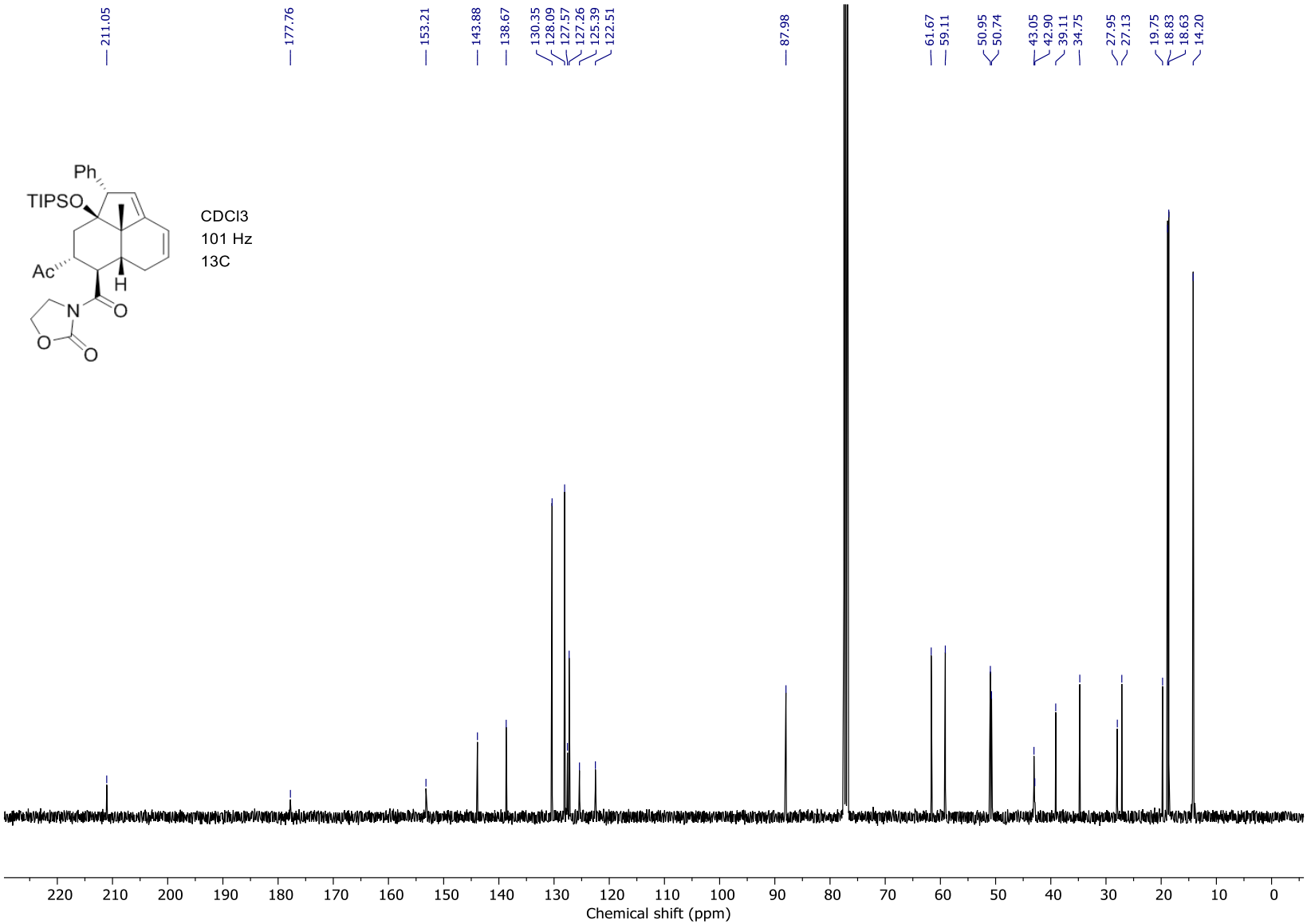
211.05
177.76
153.21
143.88
138.67
130.35
128.09
127.57
127.26
125.39
122.51
87.98
61.67
59.11
50.95
50.74
43.05
42.90
39.11
34.75
27.95
27.13
19.75
18.83
18.63
14.20
Ph
TIPSO
Ac
H
N
O
O
O
CDCl3
101 Hz
13C
220 210 200 190 180 170 160 150 140 130 120 110 100 90 80 70 60 50 40 30 20 10 0
Chemical shift (ppm)

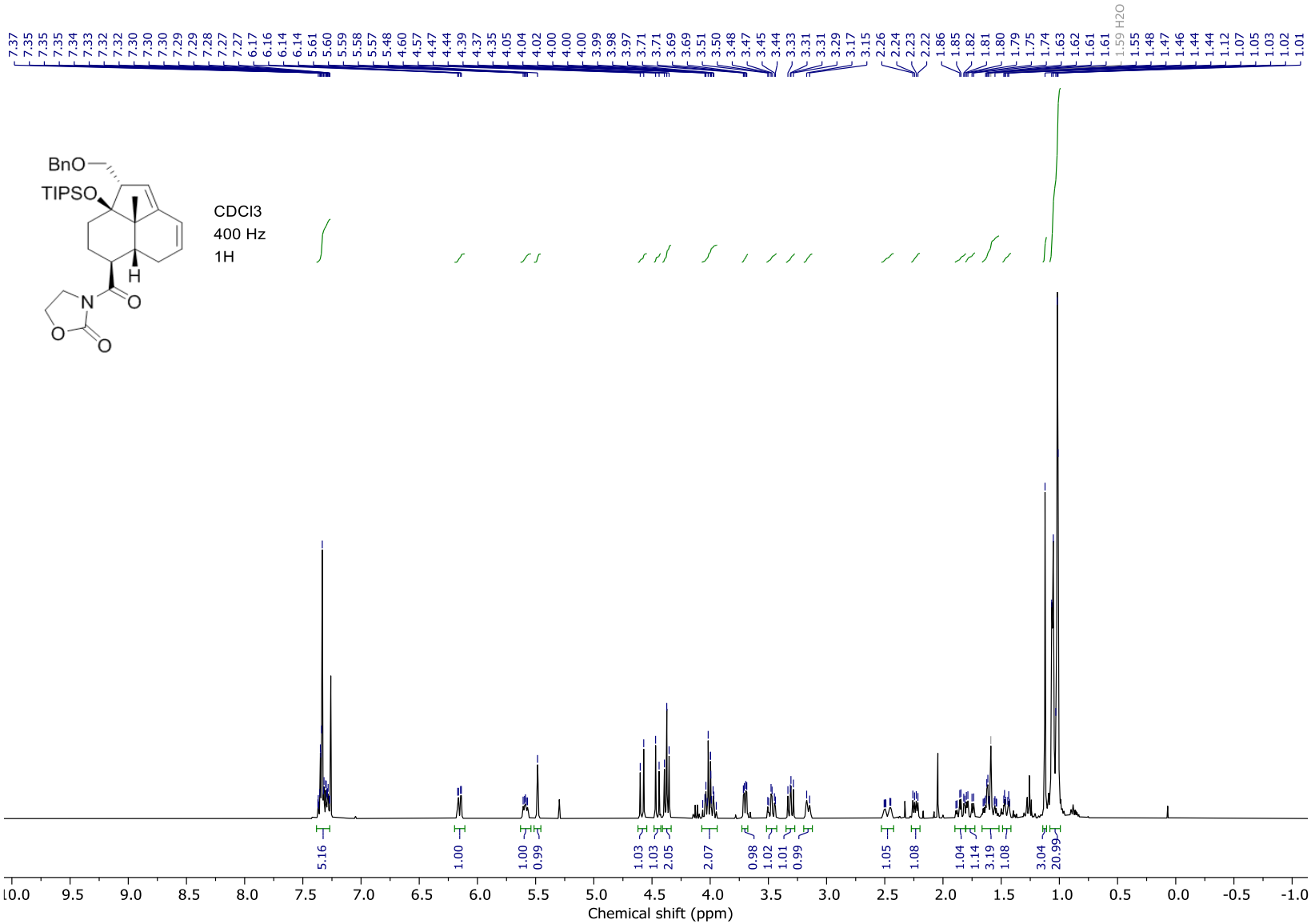
BnO
TIPSO
H
N
O
O
O
CDCl3
400 Hz
1H
H2O
5.16
1.00
1.00
0.99
1.03
1.03
2.05
2.07
0.98
1.02
1.01
0.99
1.05
1.08
1.04
1.14
3.19
1.08
3.04
20.99
Chemical shift (ppm)

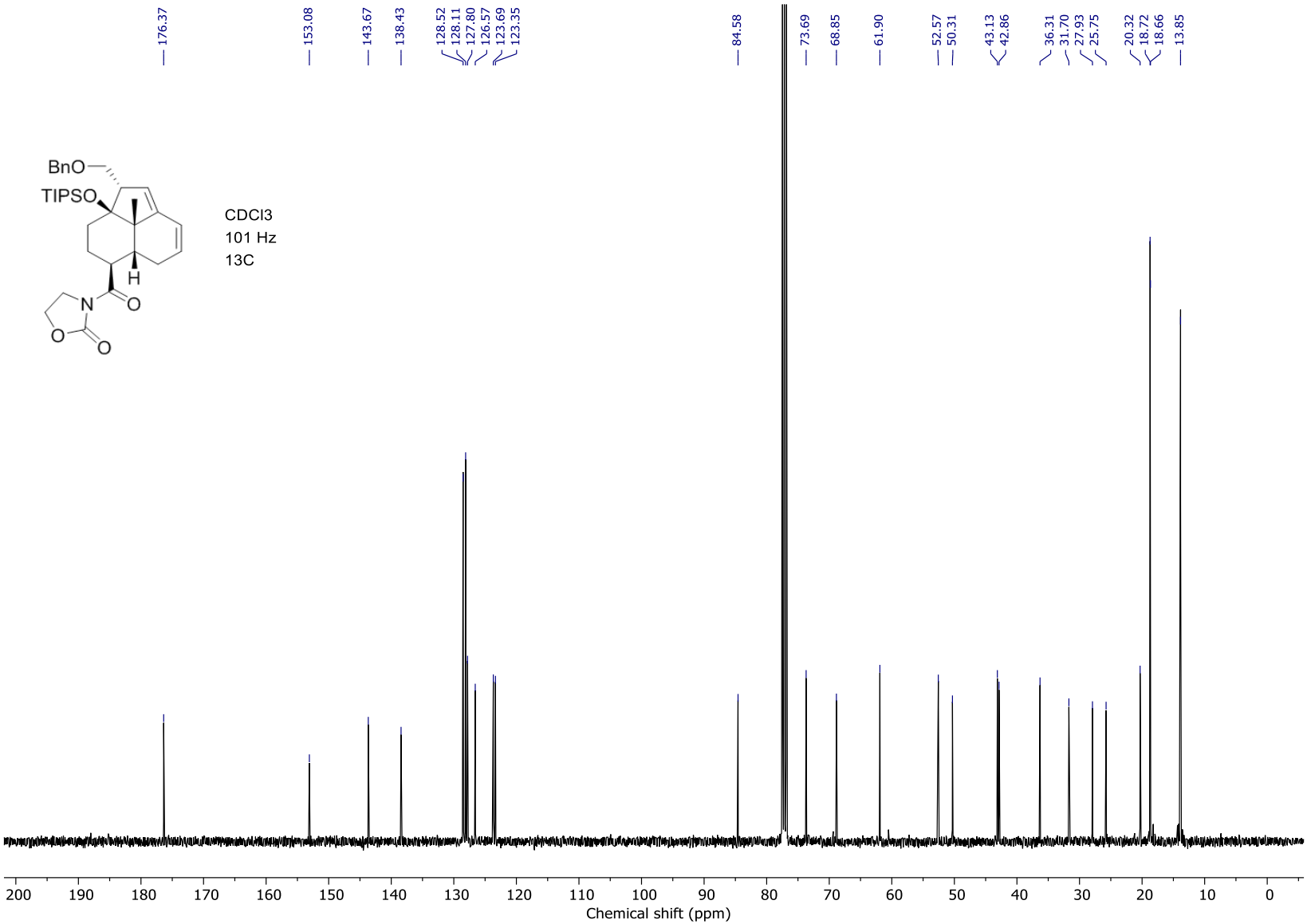
176.37
153.08
143.67
138.43
128.52
128.11
127.80
126.57
123.69
123.35
84.58
73.69
68.85
61.90
52.57
50.31
43.13
42.86
36.31
31.70
27.93
25.75
20.32
18.72
18.66
13.85
BnO
TIPSO
H
N
O
O
O
CDCl3
101 Hz
13C
200
190
180
170
160
150
140
130
120
110
100
90
80
70
60
50
40
30
20
10
0
Chemical shift (ppm)

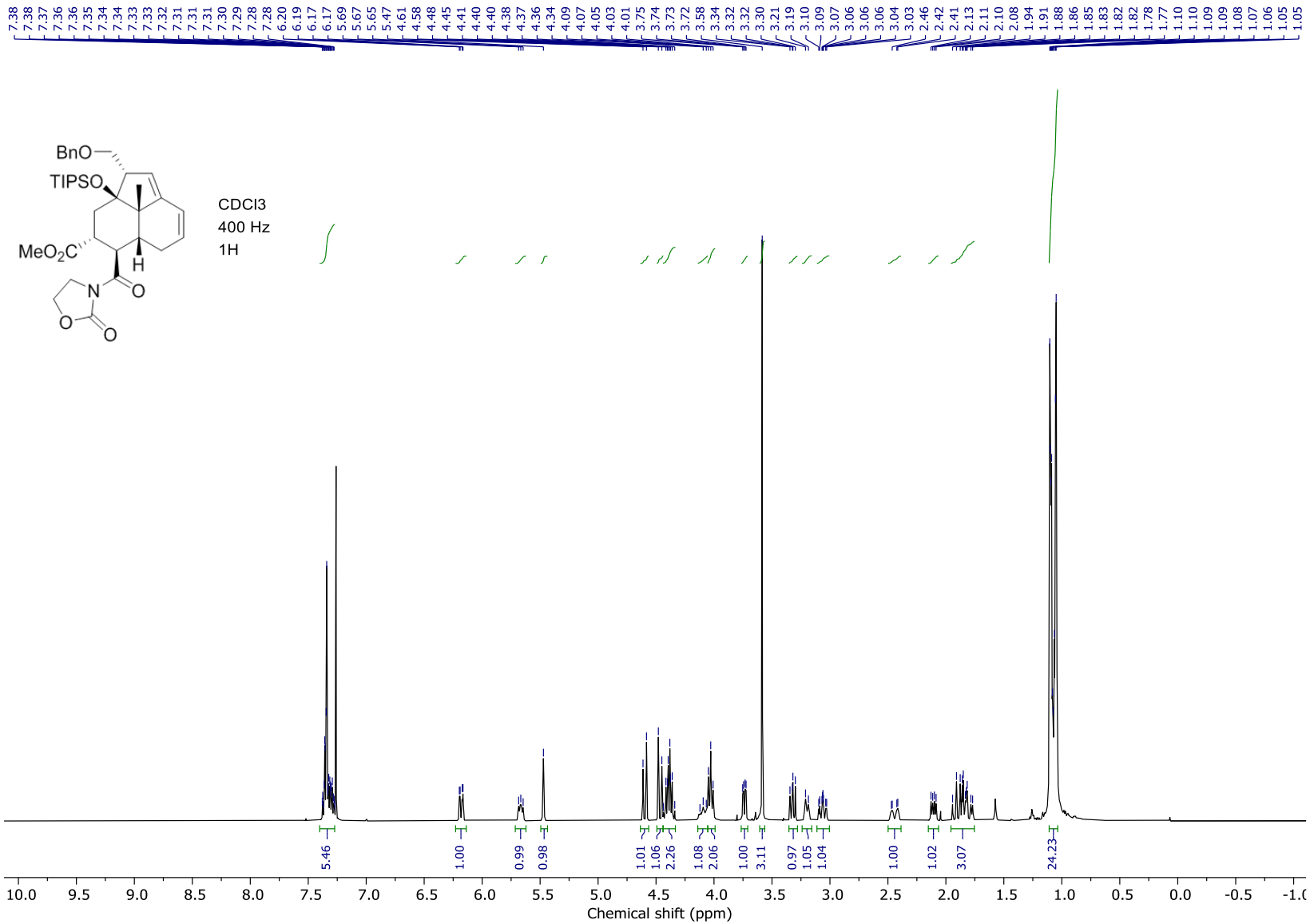
BnO
TIPSO
MeO2C
H
N
O
O
O
CDCl3
400 Hz
1H
5.46
1.00
0.99
0.98
1.01
1.06
2.26
1.08
2.06
1.00
3.11
0.97
1.05
1.04
1.00
1.02
3.07
24.23
10.0
9.5
9.0
8.5
8.0
7.5
7.0
6.5
6.0
5.5
5.0
4.5
4.0
3.5
3.0
2.5
2.0
1.5
1.0
0.5
0.0
-0.5
Chemical shift (ppm)

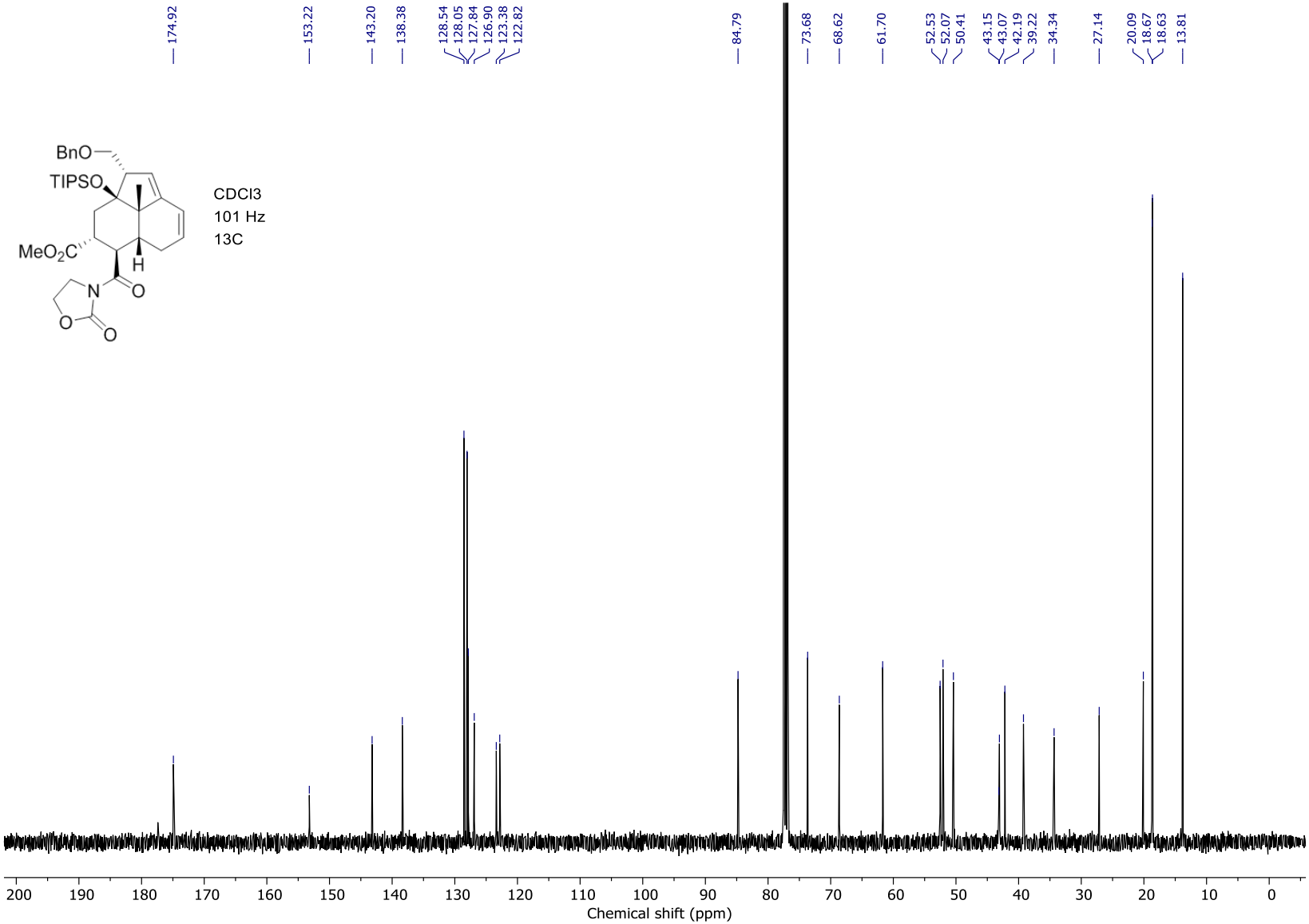
174.92
153.22
143.20
138.38
128.54
128.05
127.84
126.90
123.38
122.82
84.79
73.68
68.62
61.70
52.53
52.07
50.41
43.15
43.07
42.19
39.22
34.34
27.14
20.09
18.67
18.63
13.81
BnO
TIPSO
MeO2C
H
N
O
O
O
CDCl3
101 Hz
13C
200
190
180
170
160
150
140
130
120
110
100
90
80
70
60
50
40
30
20
10
0
Chemical shift (ppm)

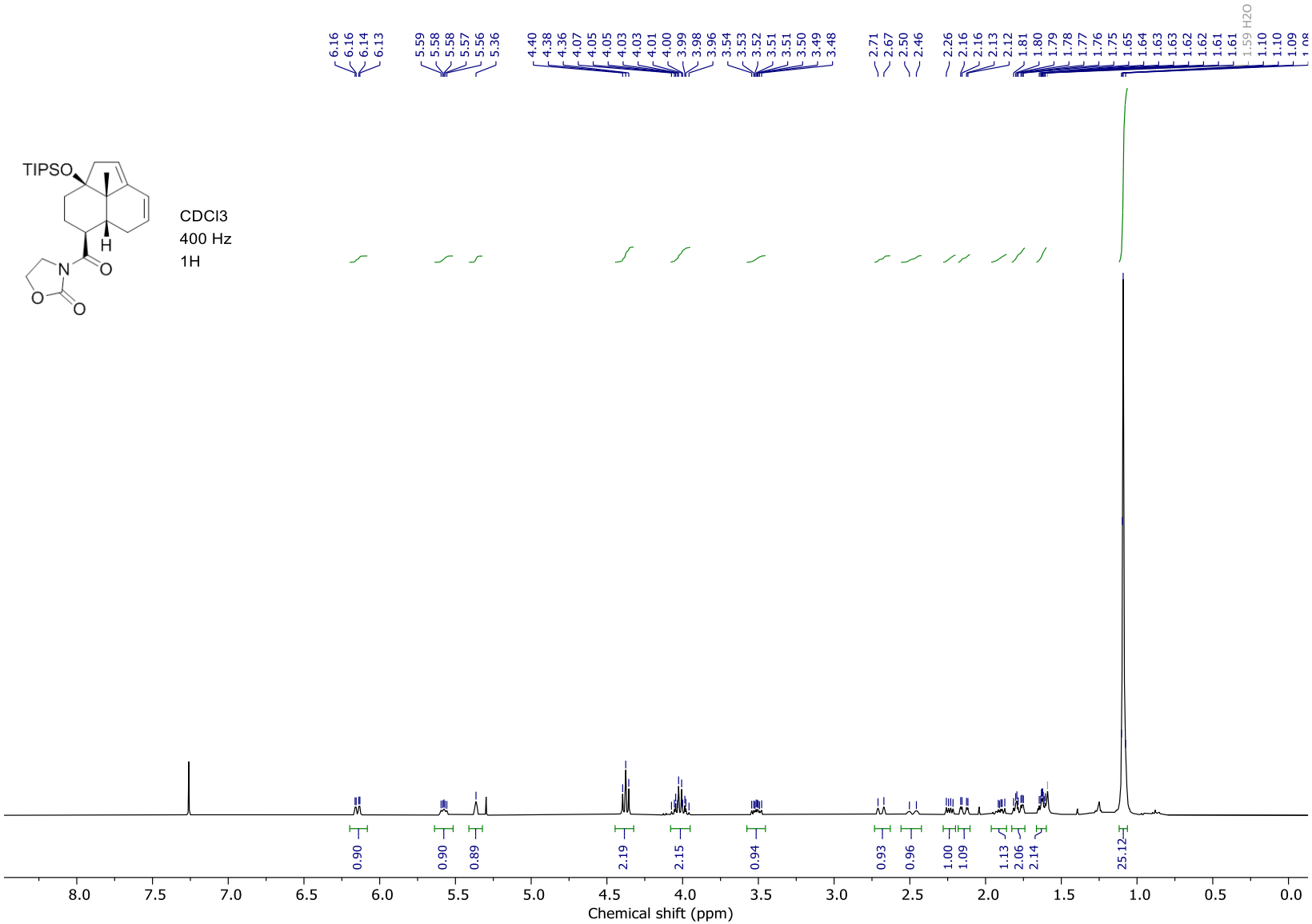
TIPSO
H
N
O
O
O
CDCl3
400 Hz
1H
6.16
6.16
6.14
6.13
5.59
5.58
5.58
5.57
5.56
5.36
4.40
4.38
4.36
4.07
4.05
4.05
4.03
4.03
4.01
4.00
3.99
3.98
3.96
3.54
3.53
3.52
3.51
3.51
3.50
3.49
3.48
2.71
2.67
2.50
2.46
2.26
2.16
2.16
2.13
2.12
1.81
1.80
1.79
1.78
1.77
1.76
1.75
1.65
1.64
1.63
1.63
1.62
1.62
1.61
1.61
1.59 H2O
1.10
1.10
1.09
0.90
0.90
0.89
2.19
2.15
0.94
0.93
0.96
1.00
1.09
1.13
2.06
2.14
25.12
8.0
7.5
7.0
6.5
6.0
5.5
5.0
4.5
4.0
3.5
3.0
2.5
2.0
1.5
1.0
0.5
0.0
Chemical shift (ppm)

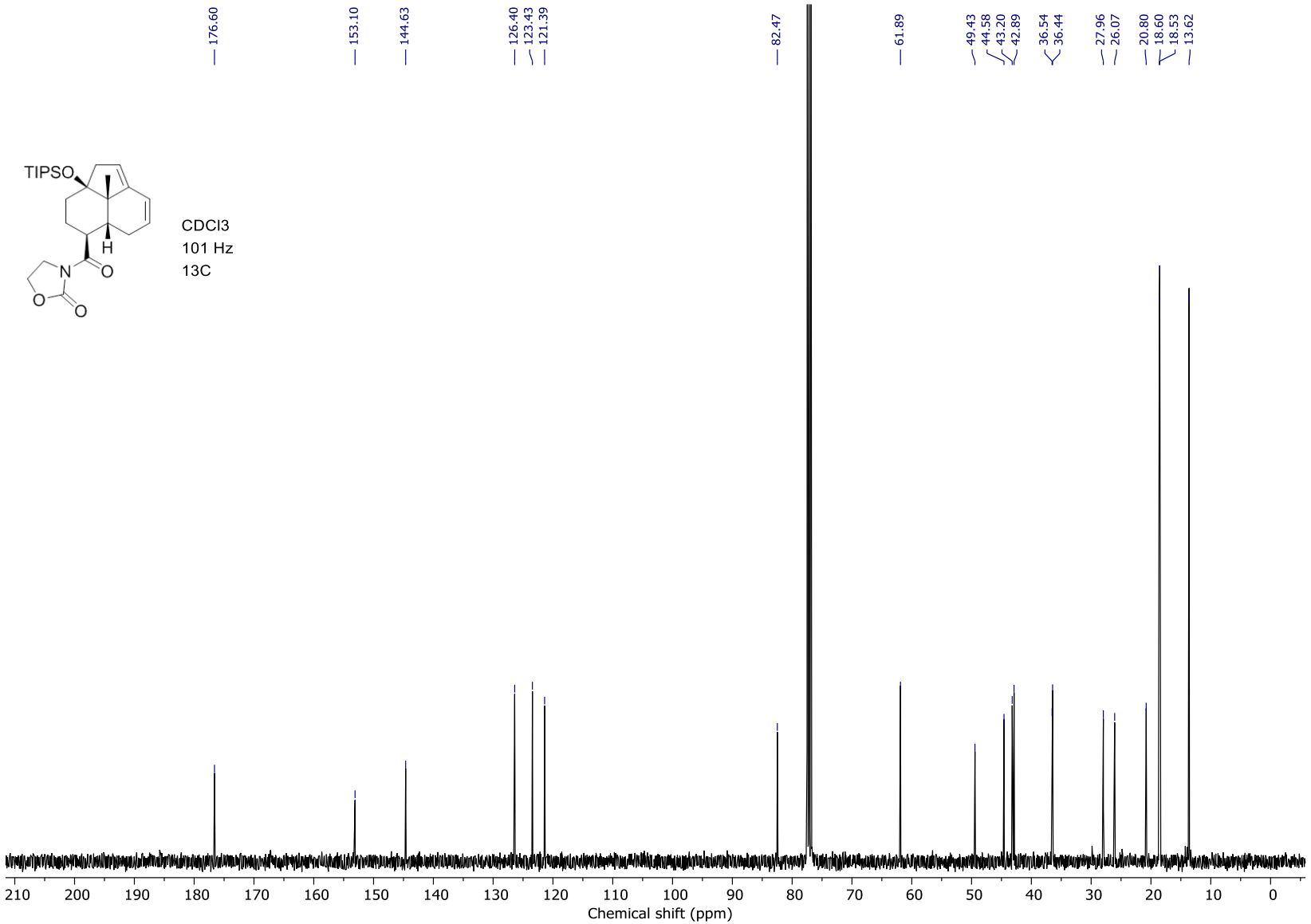
176.60
153.10
144.63
126.40
123.43
121.39
82.47
61.89
49.43
44.58
43.20
42.89
36.54
36.44
27.96
26.07
20.80
18.60
18.53
13.62
TIPSO
H
N
O
O
O
CDCl3
101 Hz
13C
210 200 190 180 170 160 150 140 130 120 110 100 90 80 70 60 50 40 30 20 10 0
Chemical shift (ppm)

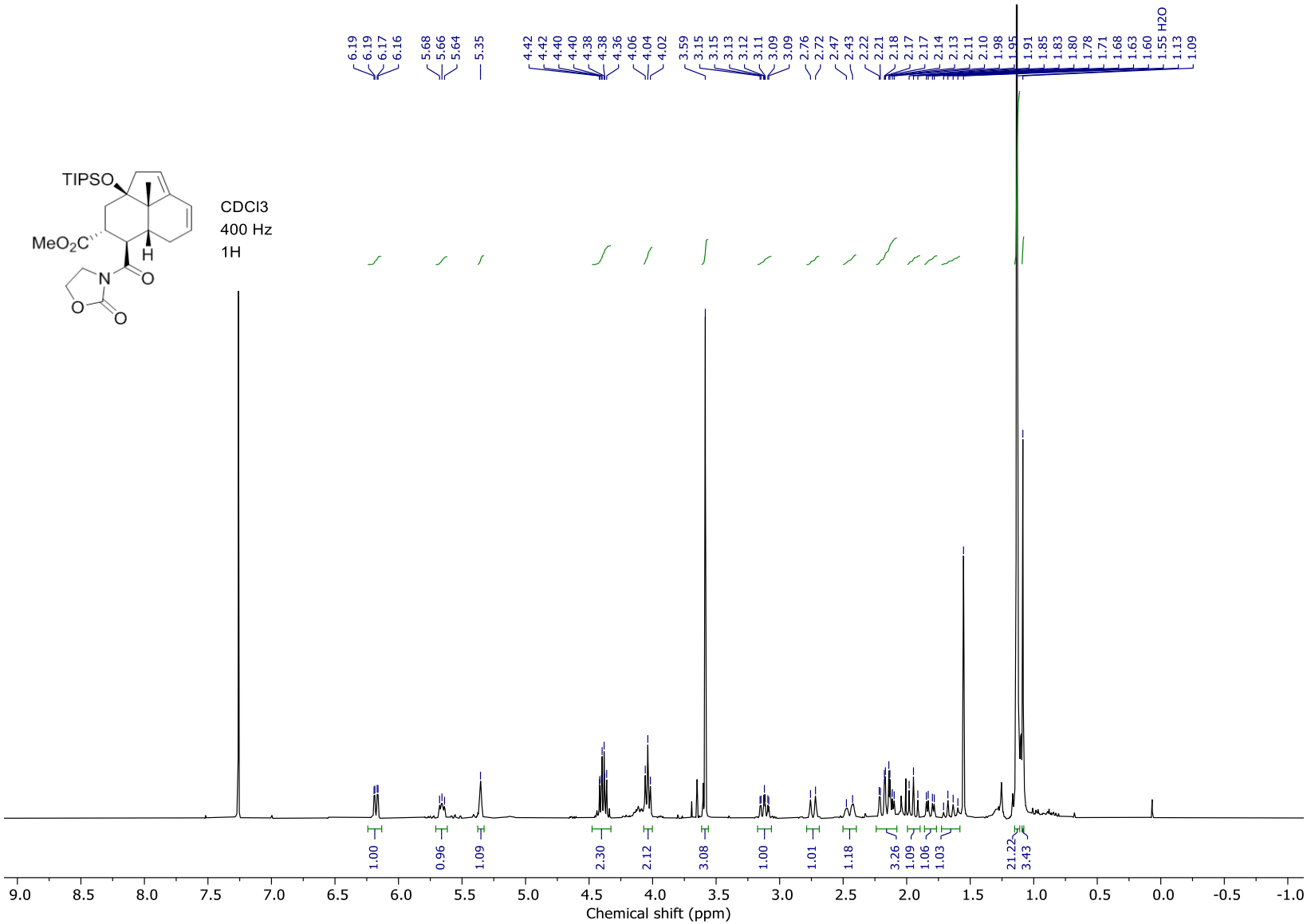
TIPSO
MeO2C
H
N
O
O
O
CDCl3
400 Hz
1H
6.19
6.19
6.17
6.16
5.68
5.66
5.64
5.35
4.42
4.42
4.40
4.40
4.38
4.38
4.36
4.06
4.04
4.02
3.59
3.15
3.15
3.13
3.12
3.11
3.09
3.09
2.76
2.72
2.47
2.43
2.22
2.21
2.18
2.17
2.17
2.14
2.13
2.11
2.10
1.98
1.95
1.91
1.85
1.83
1.80
1.78
1.71
1.68
1.63
1.60
1.55 H2O
1.13
1.09
1.00
0.96
1.09
2.30
2.12
3.08
1.00
1.01
1.18
3.26
1.09
1.06
1.03
21.22
3.43
9.0
8.5
8.0
7.5
7.0
6.5
6.0
5.5
5.0
4.5
4.0
3.5
3.0
2.5
2.0
1.5
1.0
0.5
0.0
-0.5
-1.0
Chemical shift (ppm)

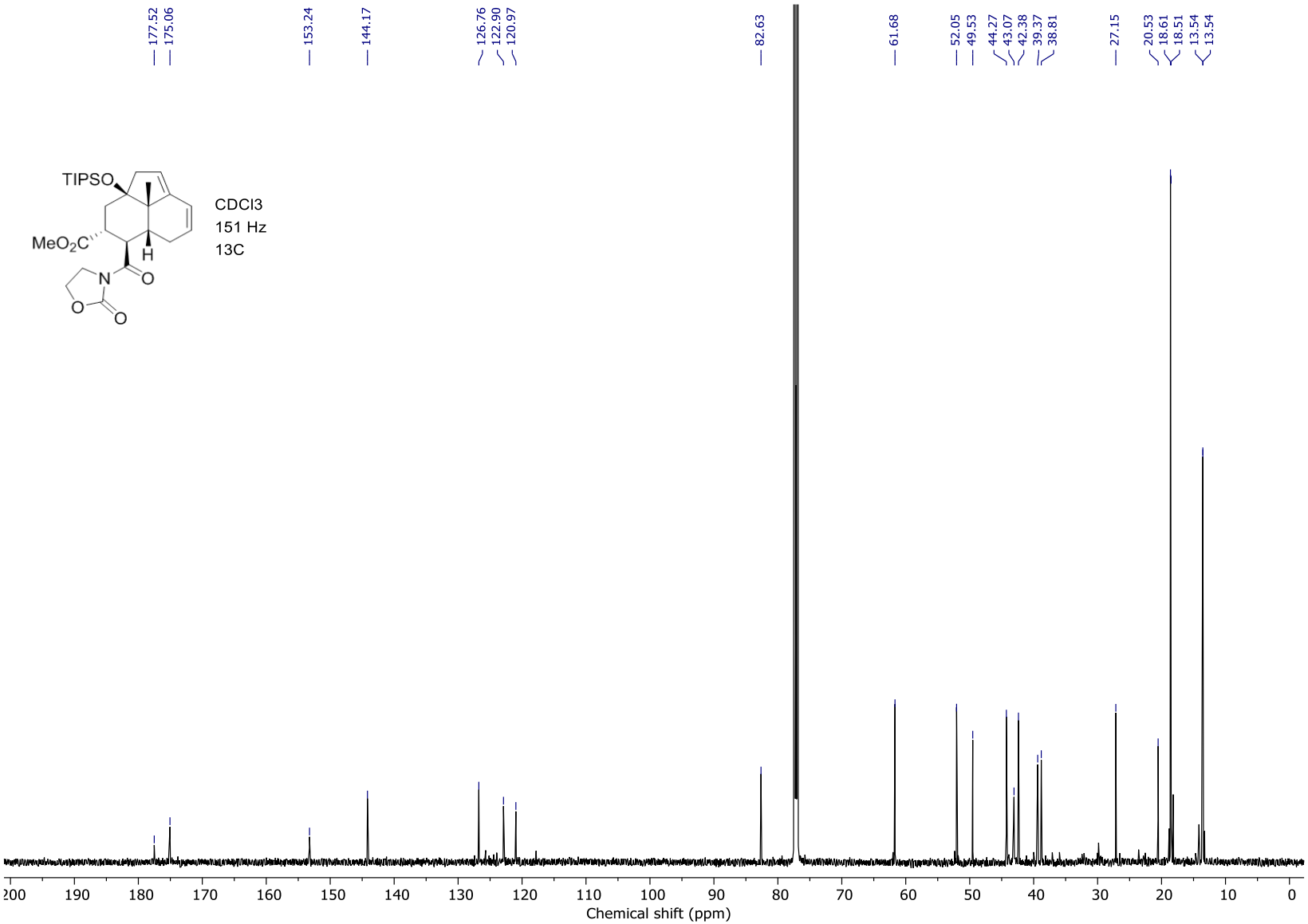
177.52
175.06
153.24
144.17
126.76
122.90
120.97
82.63
61.68
52.05
49.53
44.27
43.07
42.38
39.37
38.81
27.15
20.53
18.61
18.51
13.54
13.54
TIPSO
MeO2C
H
N
O
O
O
CDCl3
151 Hz
13C
200
190
180
170
160
150
140
130
120
110
100
90
80
70
60
50
40
30
20
10
0
Chemical shift (ppm)

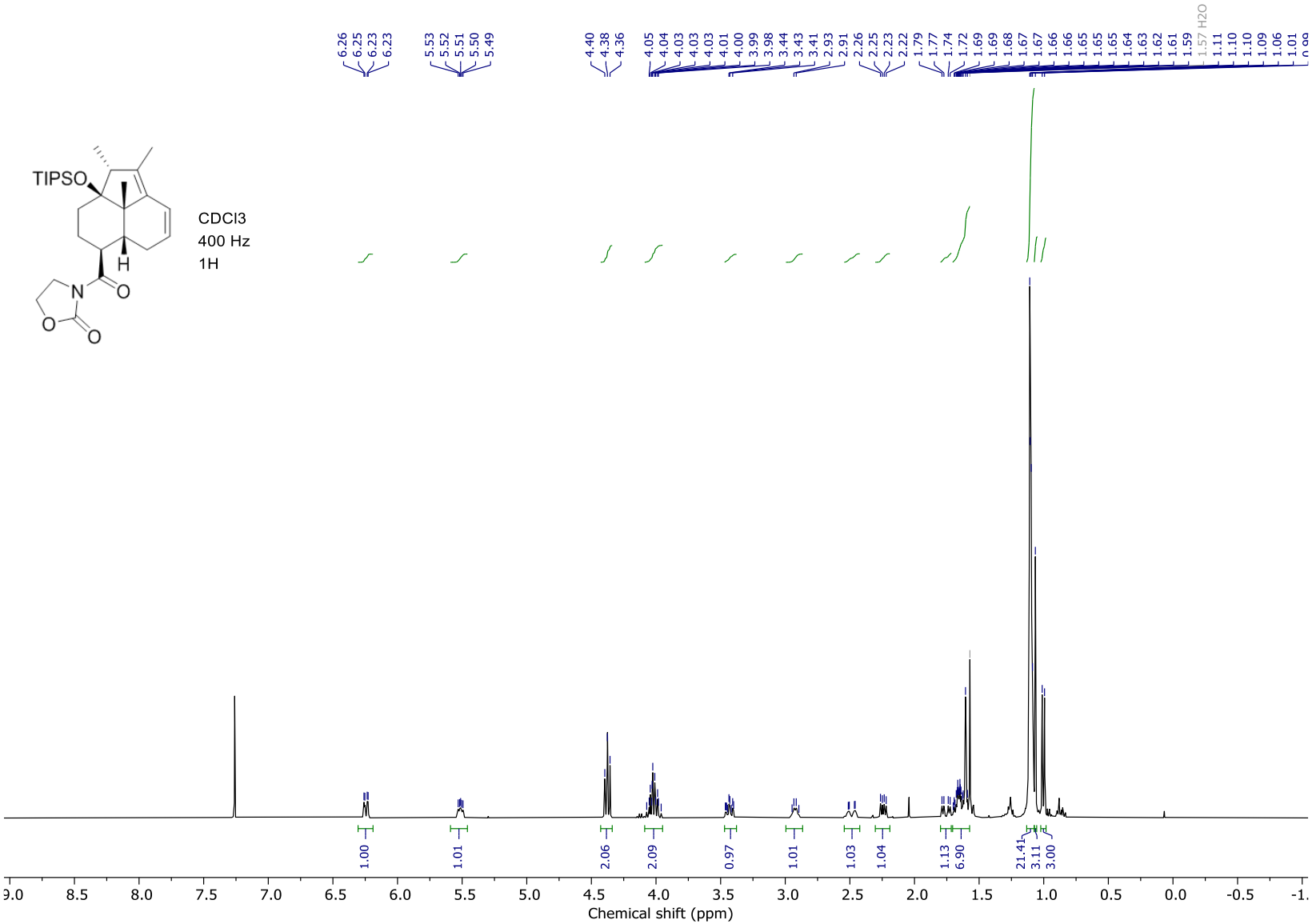
TIPSO
H
N
O
O
O
CDCl3
400 Hz
1H
6.26
6.25
6.23
6.23
5.53
5.52
5.51
5.50
5.49
4.40
4.38
4.36
4.05
4.04
4.03
4.03
4.03
4.01
4.00
3.99
3.98
3.44
3.43
3.41
2.93
2.91
2.26
2.25
2.23
2.22
1.79
1.77
1.74
1.72
1.69
1.69
1.68
1.67
1.67
1.66
1.66
1.65
1.65
1.65
1.64
1.63
1.62
1.61
1.59
1.57 H2O
1.11
1.10
1.10
1.09
1.06
1.01
1.00
1.01
2.06
2.09
0.97
1.01
1.03
1.04
1.13
6.90
21.41
3.11
3.00
9.0
8.5
8.0
7.5
7.0
6.5
6.0
5.5
5.0
4.5
4.0
3.5
3.0
2.5
2.0
1.5
1.0
0.5
0.0
-0.5
Chemical shift (ppm)

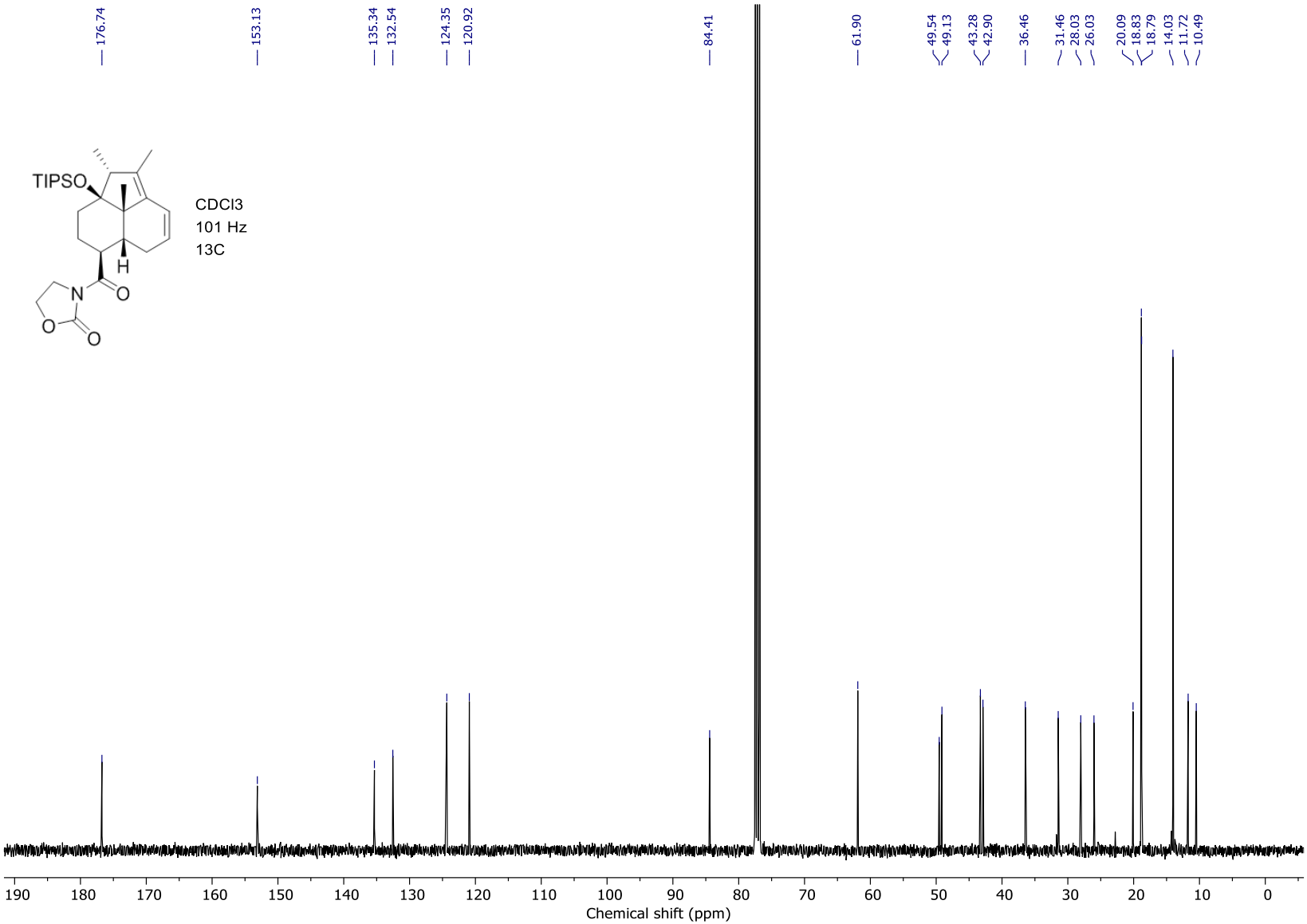
176.74
153.13
135.34
132.54
124.35
120.92
84.41
61.90
49.54
49.13
43.28
42.90
36.46
31.46
28.03
26.03
20.09
18.83
18.79
14.03
11.72
10.49
TIPSO
H
N
O
O
O
CDCl3
101 Hz
13C
190
180
170
160
150
140
130
120
110
100
90
80
70
60
50
40
30
20
10
0
Chemical shift (ppm)

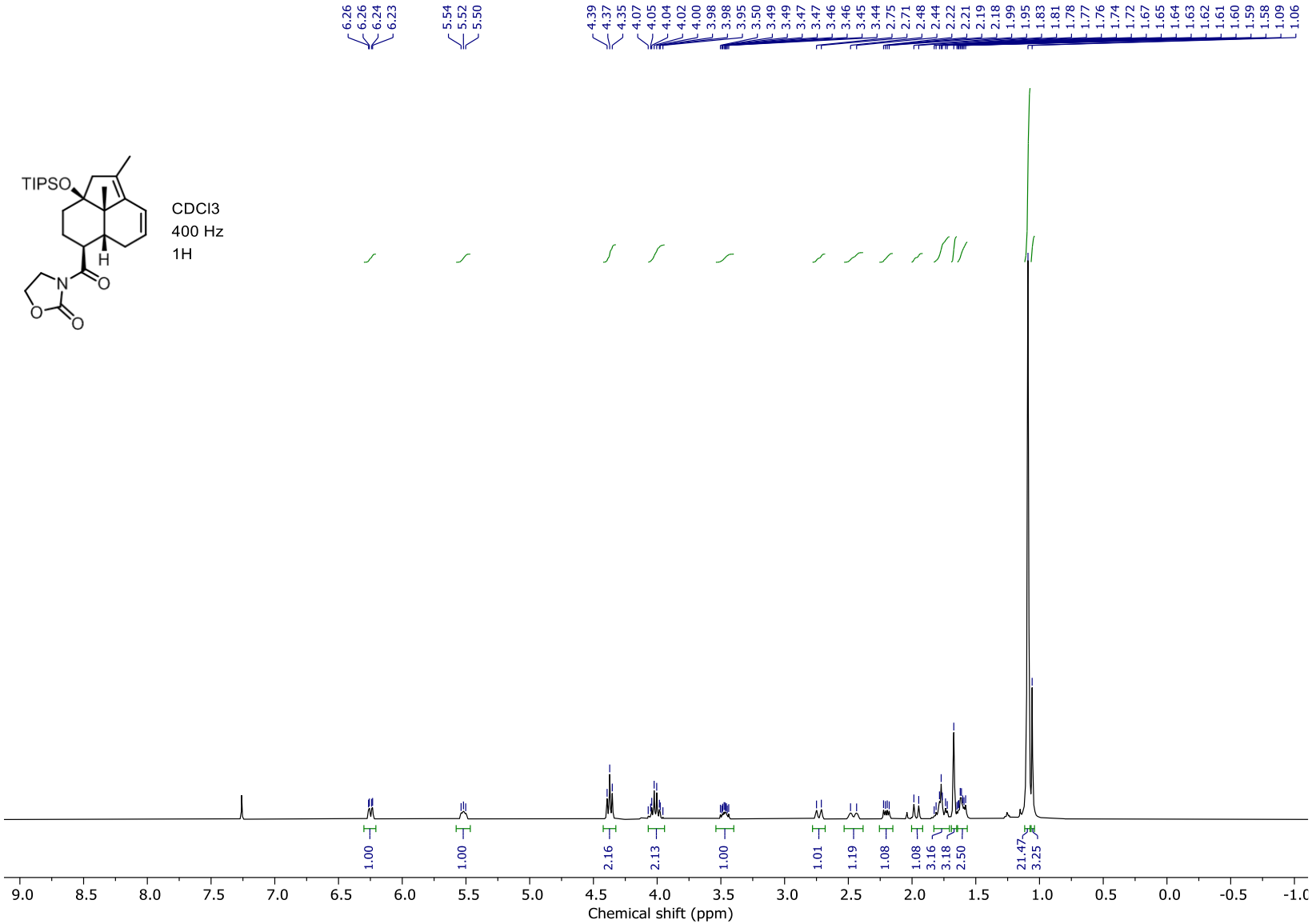
TIPSO
H
N
O
O
O
CDCl3
400 Hz
1H
6.26
6.26
6.24
6.23
5.54
5.52
5.50
4.39
4.37
4.35
4.07
4.05
4.04
4.02
4.00
3.98
3.98
3.95
3.50
3.49
3.49
3.47
3.47
3.46
3.46
3.45
3.44
2.75
2.71
2.48
2.44
2.22
2.21
2.19
2.18
1.99
1.95
1.83
1.81
1.78
1.77
1.76
1.74
1.72
1.67
1.65
1.64
1.63
1.62
1.61
1.60
1.59
1.58
1.09
1.06
1.00
1.00
2.16
2.13
1.00
1.01
1.19
1.08
1.08
3.16
3.18
2.50
21.47
3.25
9.0
8.5
8.0
7.5
7.0
6.5
6.0
5.5
5.0
4.5
4.0
3.5
3.0
2.5
2.0
1.5
1.0
0.5
0.0
-0.5
Chemical shift (ppm)

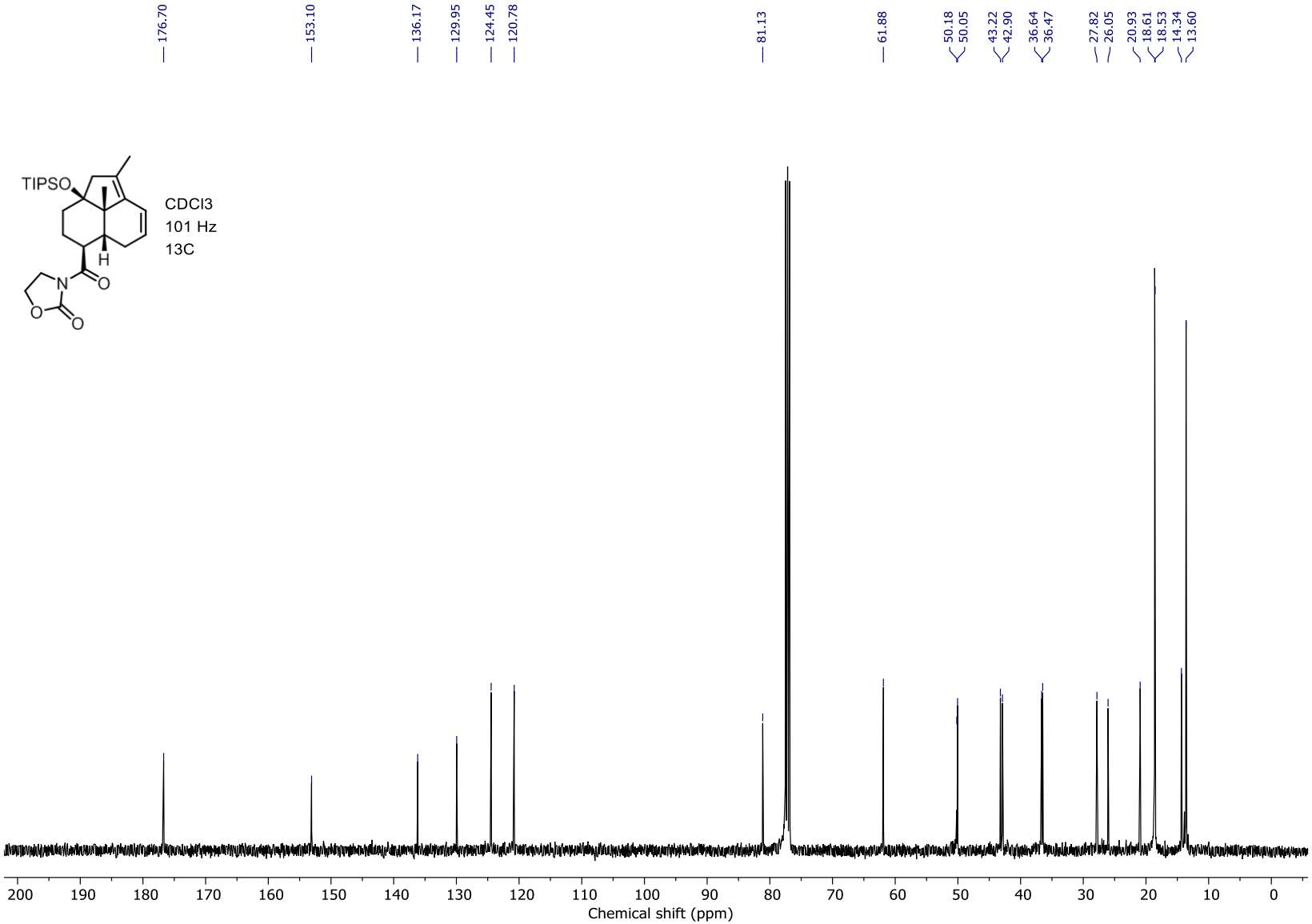
176.70
153.10
136.17
129.95
124.45
120.78
81.13
61.88
50.18
50.05
43.22
42.90
36.64
36.47
27.82
26.05
20.93
18.61
18.53
14.34
13.60
TIPSO
H
N
O
O
O
CDCl3
101 Hz
13C
200
190
180
170
160
150
140
130
120
110
100
90
80
70
60
50
40
30
20
10
0
Chemical shift (ppm)

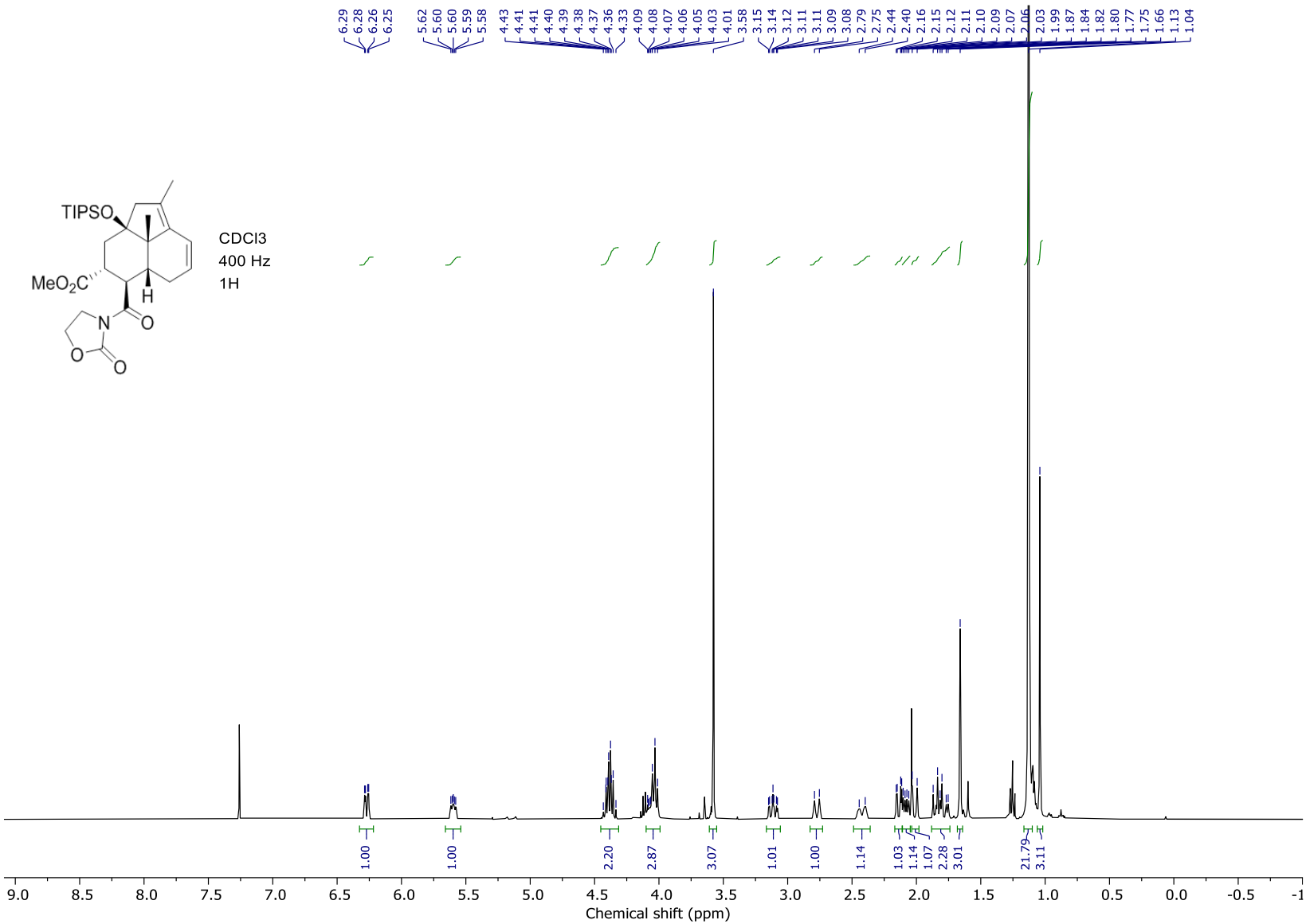
TIPSO
MeO2C
H
N
O
O
O
CDCl3
400 Hz
1H
6.29 6.28 6.26 6.25
5.62 5.60 5.60 5.59 5.58
4.43 4.41 4.41 4.40 4.39 4.38 4.37 4.36 4.33
4.09 4.08 4.07 4.06 4.05 4.03 4.01
3.58
3.15 3.14 3.12 3.11 3.11 3.09 3.08
2.79 2.75 2.44 2.40 2.16 2.15 2.12 2.11 2.10 2.09 2.07 2.06
2.03 1.99 1.87 1.84 1.82 1.80 1.77 1.75 1.66 1.13 1.04
1.00 1.00 2.20 2.87 3.07 1.01 1.00 1.14 1.03 1.14 1.07 2.28 3.01 21.79 3.11
9.0 8.5 8.0 7.5 7.0 6.5 6.0 5.5 5.0 4.5 4.0 3.5 3.0 2.5 2.0 1.5 1.0 0.5 0.0 -0.5 -1
Chemical shift (ppm)

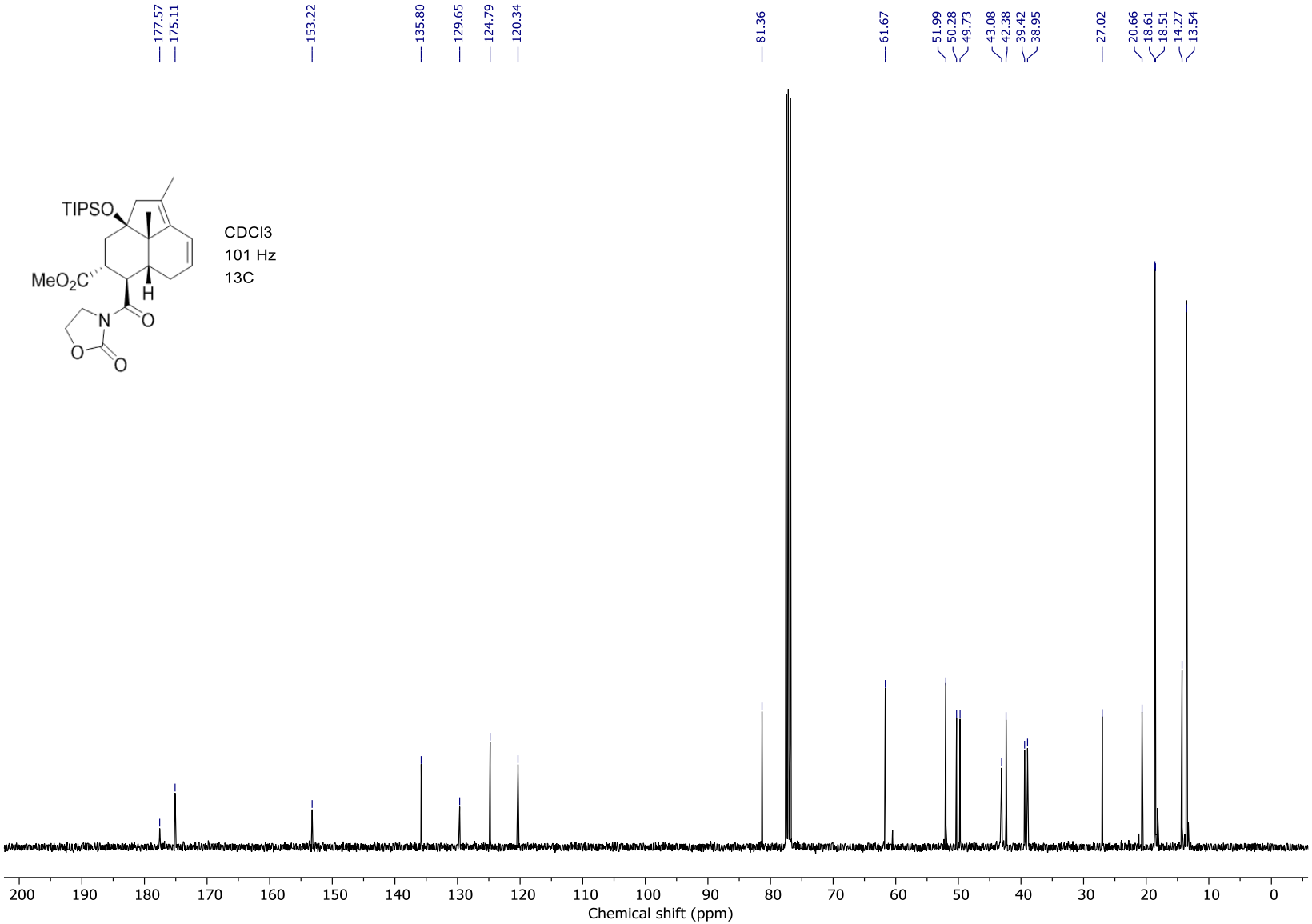
177.57
175.11
153.22
135.80
129.65
124.79
120.34
81.36
61.67
51.99
50.28
49.73
43.08
42.38
39.42
38.95
27.02
20.66
18.61
18.51
14.27
13.54
TIPSO
MeO2C
H
N
O
O
O
CDCl3
101 Hz
13C
200
190
180
170
160
150
140
130
120
110
100
90
80
70
60
50
40
30
20
10
0
Chemical shift (ppm)

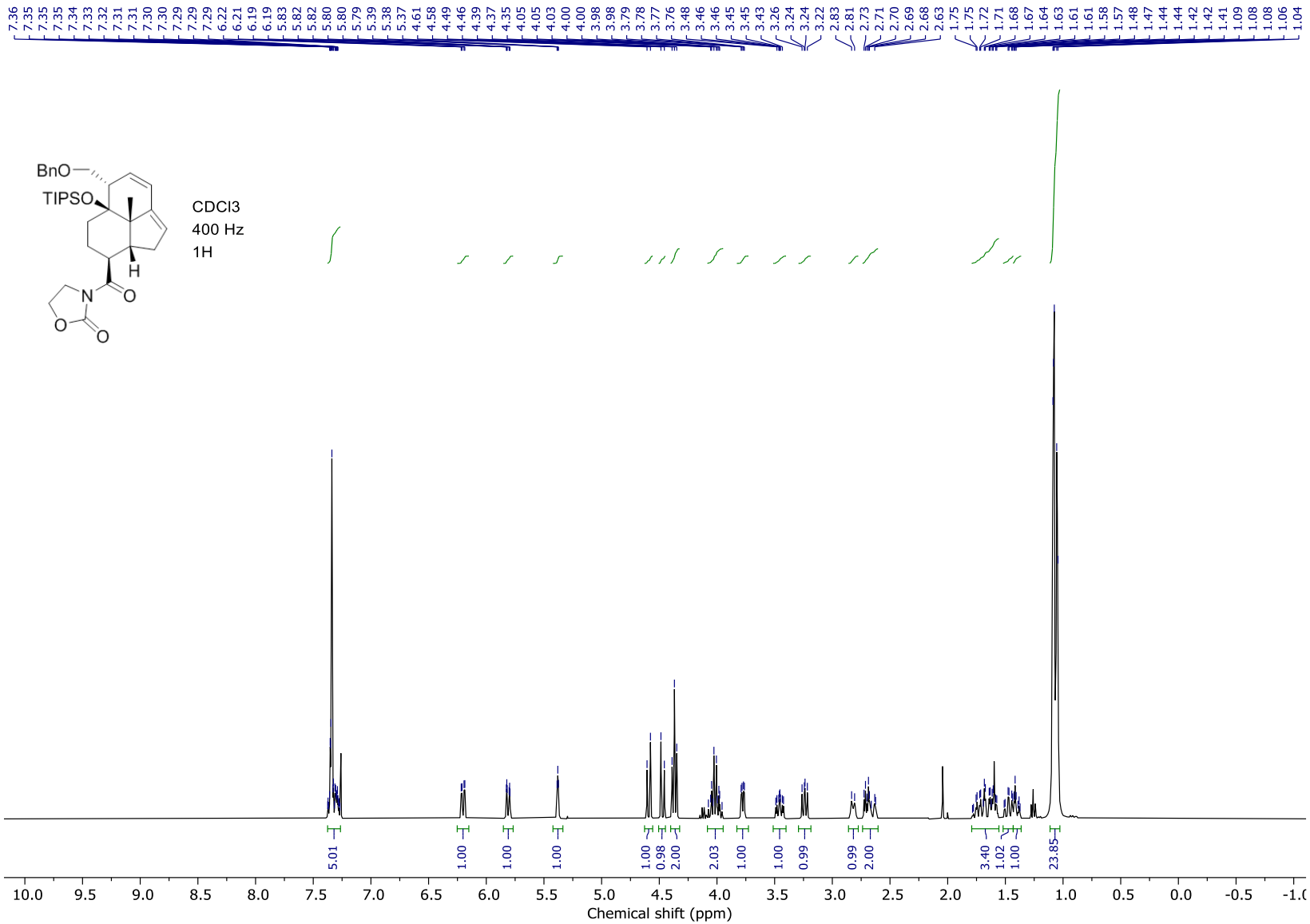
BnO
TIPSO
H
N
O
O
O
CDCl3
400 Hz
1H
Chemical shift (ppm)

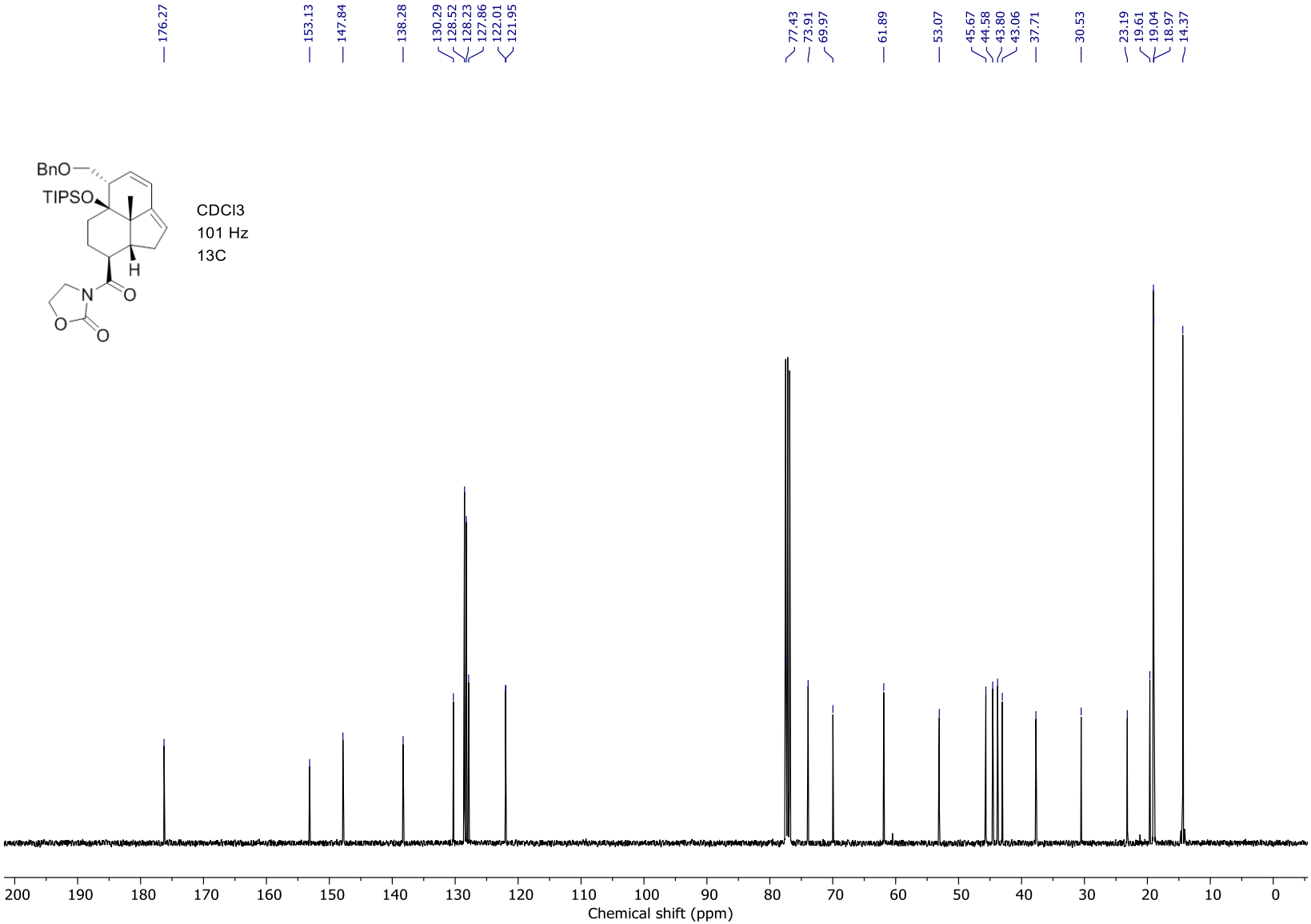
176.27
153.13
147.84
138.28
130.29
128.52
128.23
127.86
122.01
121.95
77.43
73.91
69.97
61.89
53.07
45.67
44.58
43.80
43.06
37.71
30.53
23.19
19.61
19.04
18.97
14.37
BnO
TIPSO
H
N
O
O
O
CDCl3
101 Hz
13C
200
190
180
170
160
150
140
130
120
110
100
90
80
70
60
50
40
30
20
10
0
Chemical shift (ppm)

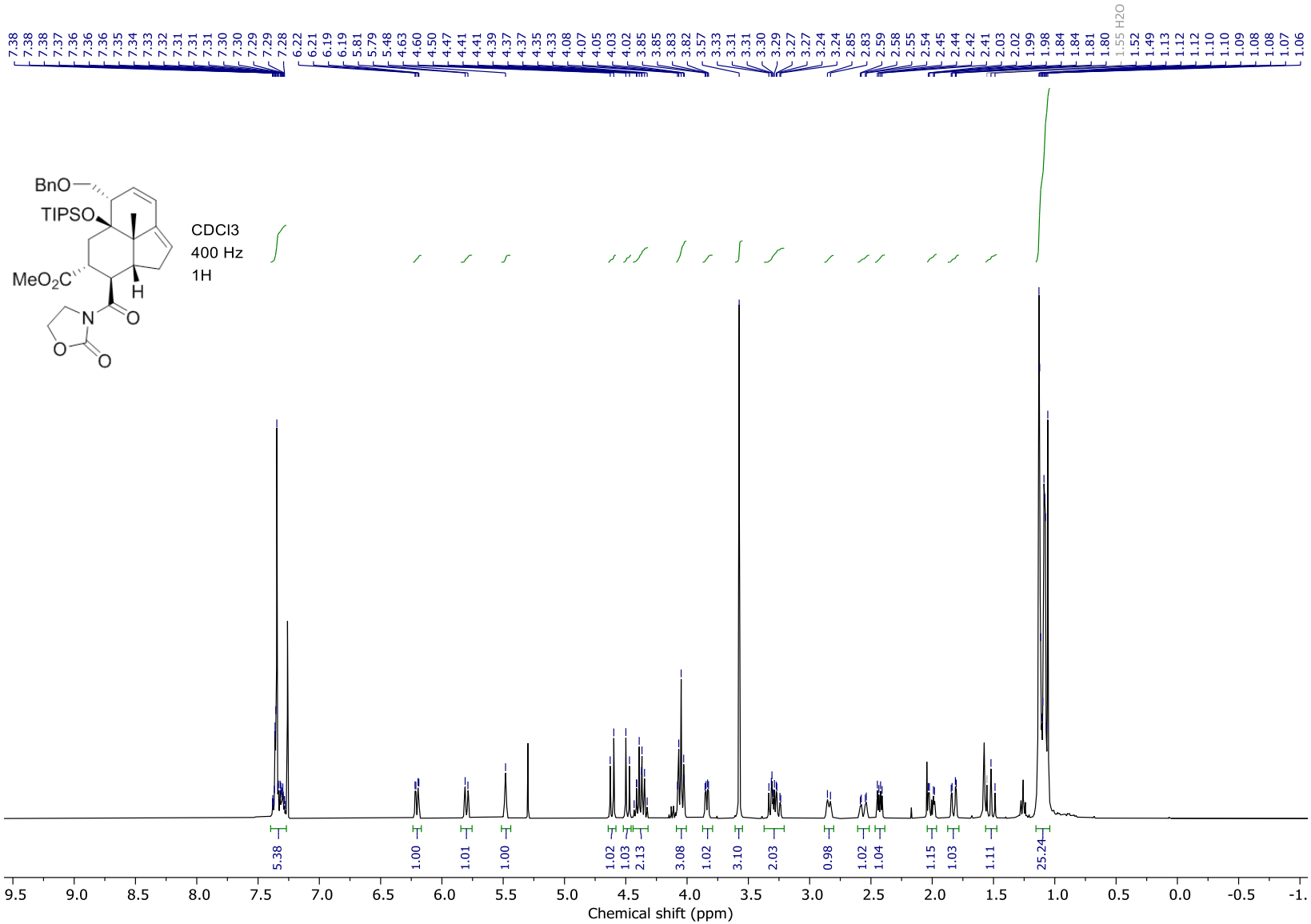
BnO
TIPSO
MeO2C
H
N
O
O
O
CDCl3
400 Hz
1H
H2O
5.38
1.00
1.01
1.00
1.02
1.03
2.13
3.08
1.02
3.10
2.03
0.98
1.02
1.04
1.15
1.03
1.11
25.24
Chemical shift (ppm)

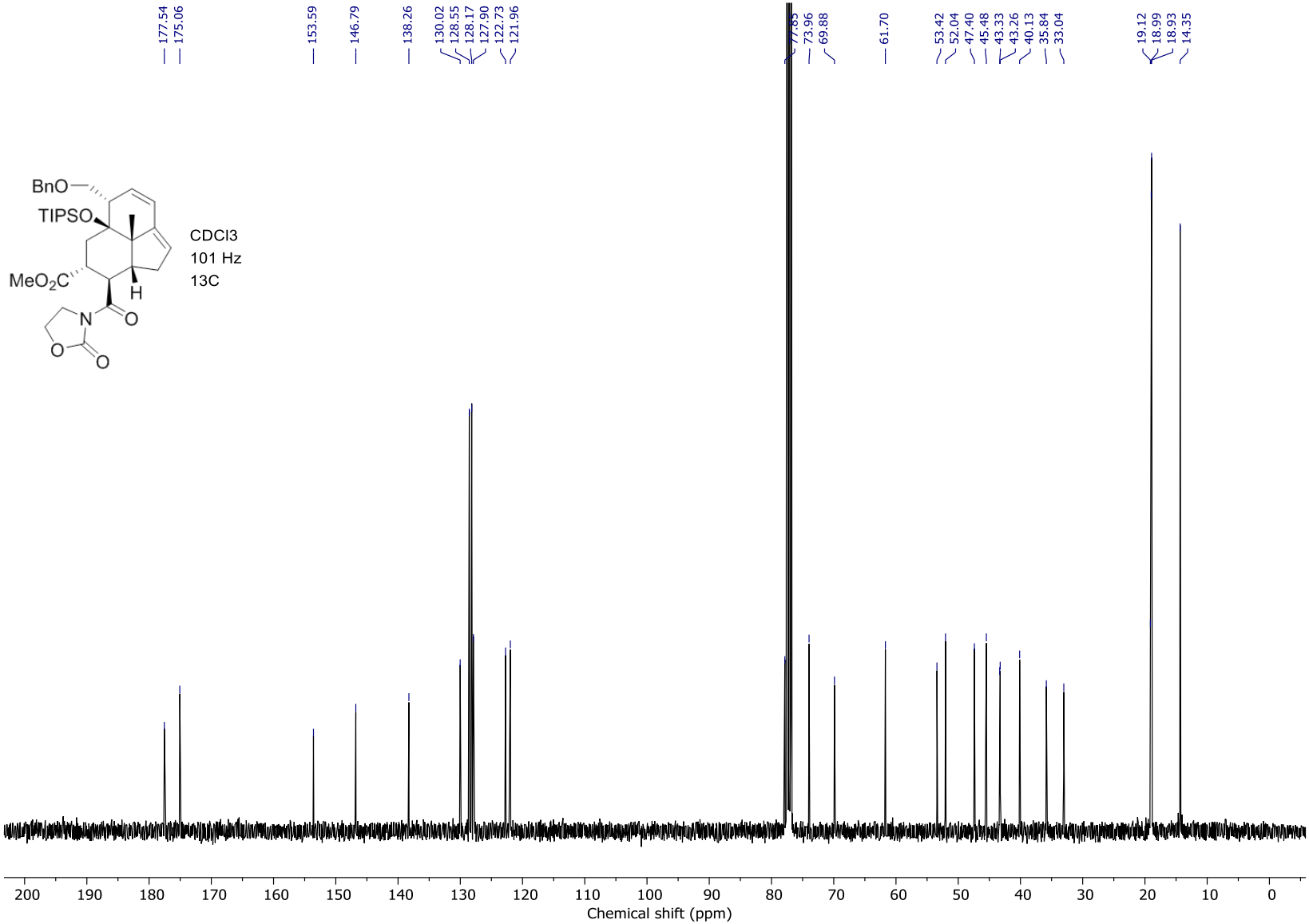
177.54
175.06
153.59
146.79
138.26
130.02
128.55
128.17
127.90
122.73
121.96
77.85
73.96
69.88
61.70
53.42
52.04
47.40
45.48
43.33
43.26
40.13
35.84
33.04
19.12
18.99
18.93
14.35
BnO
TIPSO
MeO2C
H
N
O
O
O
O
CDCl3
101 Hz
13C
200
190
180
170
160
150
140
130
120
110
100
90
80
70
60
50
40
30
20
10
0
Chemical shift (ppm)

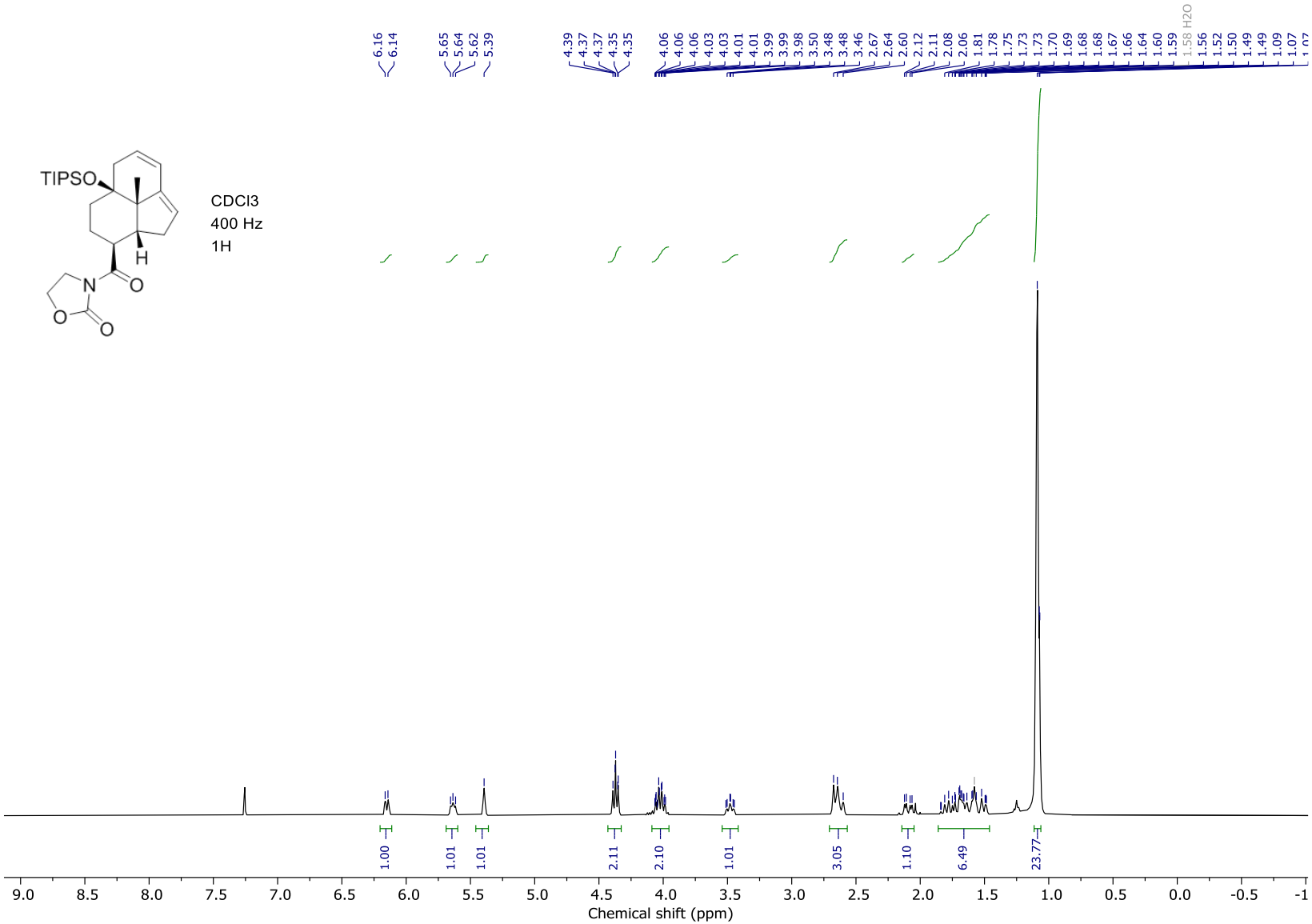
TIPSO
H
N
O
O
O
CDCl3
400 Hz
1H
6.16
6.14
5.65
5.64
5.62
5.39
4.39
4.37
4.37
4.35
4.35
4.06
4.06
4.06
4.03
4.03
4.01
4.01
3.99
3.99
3.98
3.50
3.48
3.48
3.46
2.67
2.64
2.60
2.12
2.11
2.08
2.06
1.81
1.78
1.75
1.73
1.73
1.70
1.69
1.68
1.68
1.67
1.66
1.64
1.60
1.59
1.58 H2O
1.56
1.52
1.50
1.49
1.49
1.09
1.07
1.00
1.01
1.01
2.11
2.10
1.01
3.05
1.10
6.49
23.77
9.0
8.5
8.0
7.5
7.0
6.5
6.0
5.5
5.0
4.5
4.0
3.5
3.0
2.5
2.0
1.5
1.0
0.5
0.0
-0.5
-1
Chemical shift (ppm)

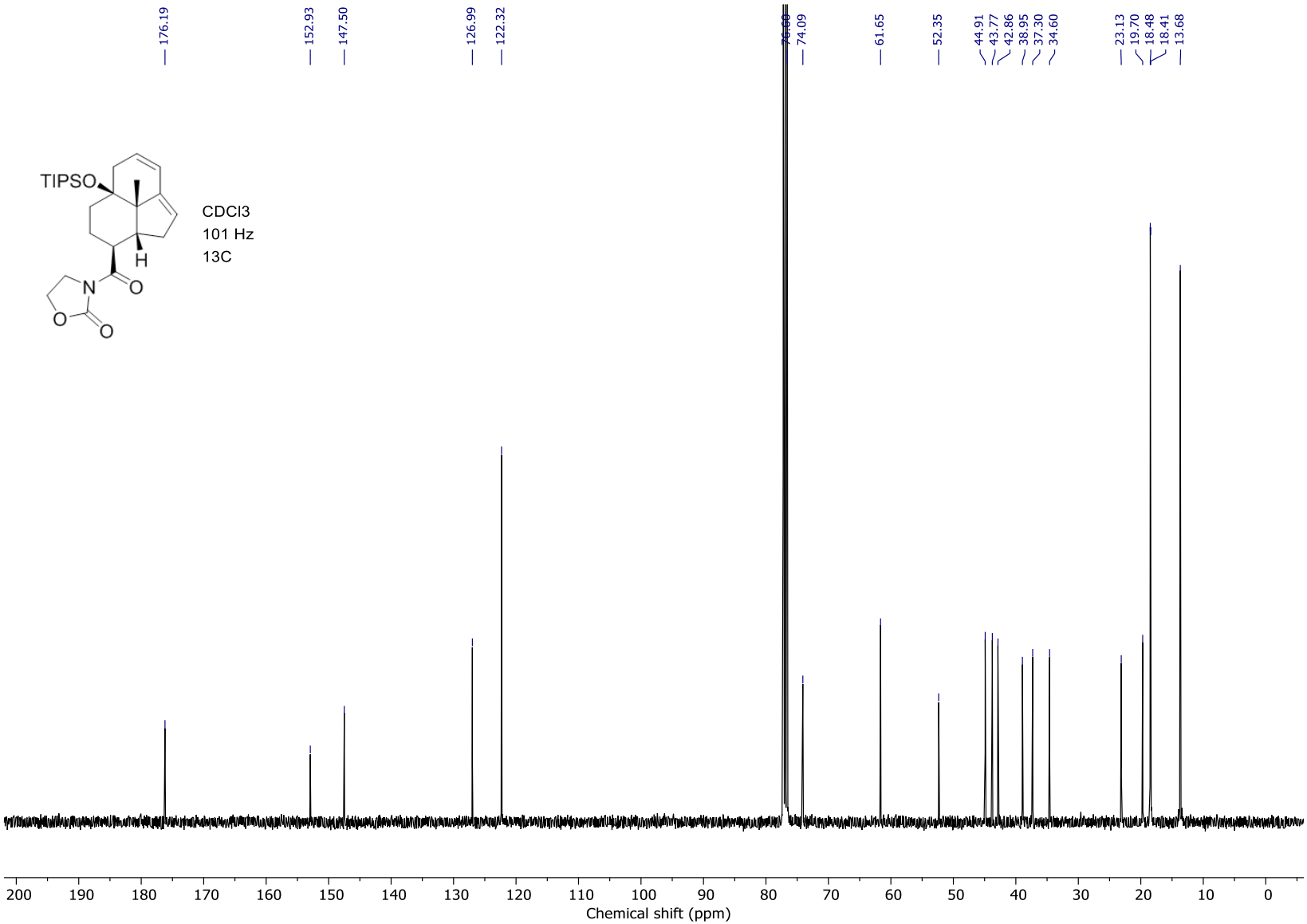
176.19
152.93
147.50
126.99
122.32
74.09
61.65
52.35
44.91
43.77
42.86
38.95
37.30
34.60
23.13
19.70
18.48
18.41
13.68
TIPSO
H
N
O
O
O
CDCl3
101 Hz
13C
200
190
180
170
160
150
140
130
120
110
100
90
80
70
60
50
40
30
20
10
0
Chemical shift (ppm)

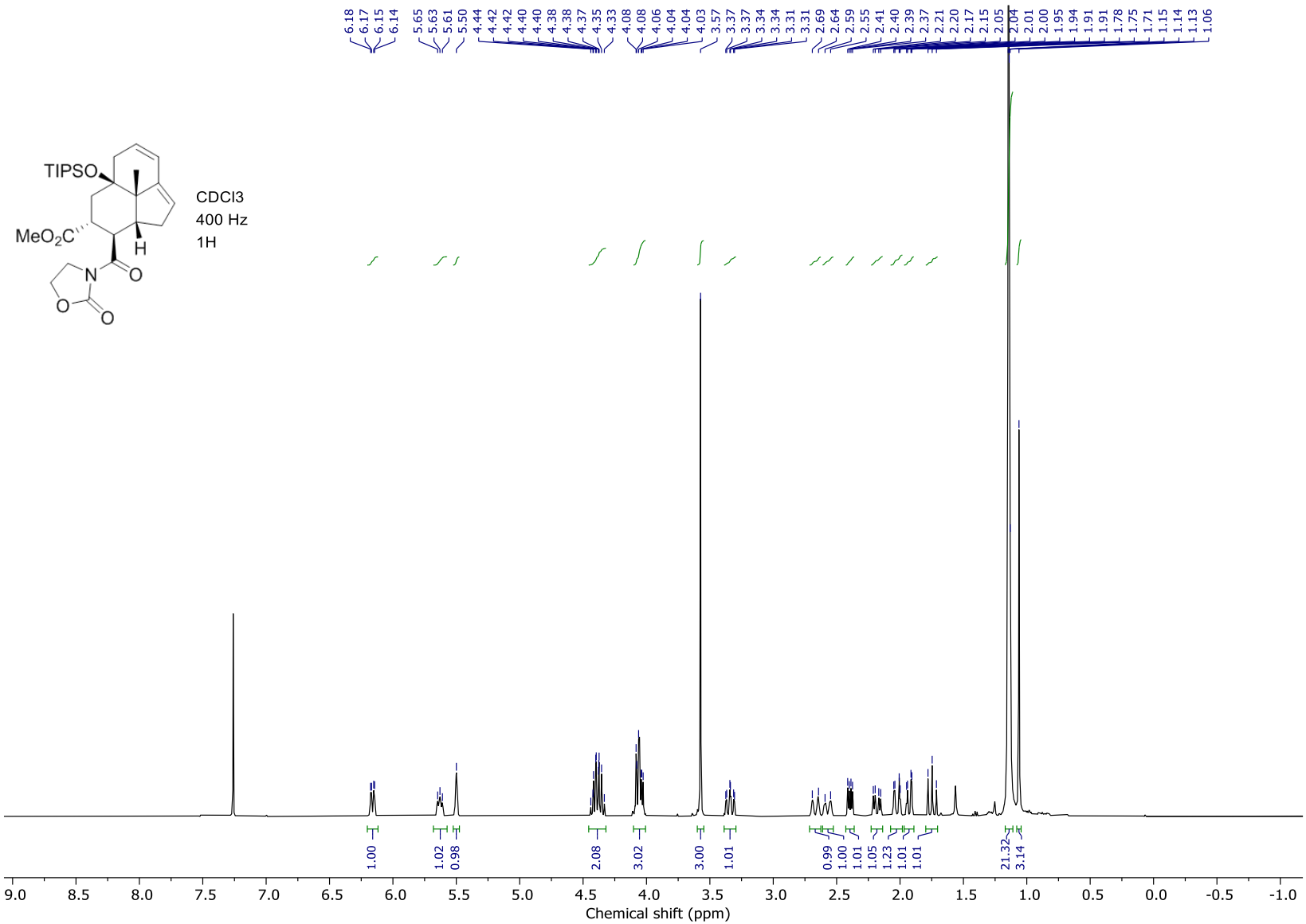
TIPSO
MeO2C
H
N
O
O
O
CDCl3
400 Hz
1H
6.18 6.17 6.15 6.14 5.65 5.63 5.61 5.50 4.44 4.42 4.42 4.40 4.40 4.38 4.38 4.37 4.35 4.33 4.08 4.08 4.06 4.04 4.04 4.03 3.57 3.37 3.37 3.34 3.34 3.31 3.31 2.69 2.64 2.59 2.55 2.41 2.40 2.39 2.37 2.21 2.20 2.17 2.15 2.05 2.04 2.01 2.00 1.95 1.94 1.91 1.91 1.78 1.75 1.71 1.15 1.14 1.13 1.06
1.00 1.02 0.98 2.08 3.02 3.00 1.01 0.99 1.00 1.01 1.05 1.23 1.01 1.01 21.32 3.14
9.0 8.5 8.0 7.5 7.0 6.5 6.0 5.5 5.0 4.5 4.0 3.5 3.0 2.5 2.0 1.5 1.0 0.5 0.0 -0.5 -1.0
Chemical shift (ppm)

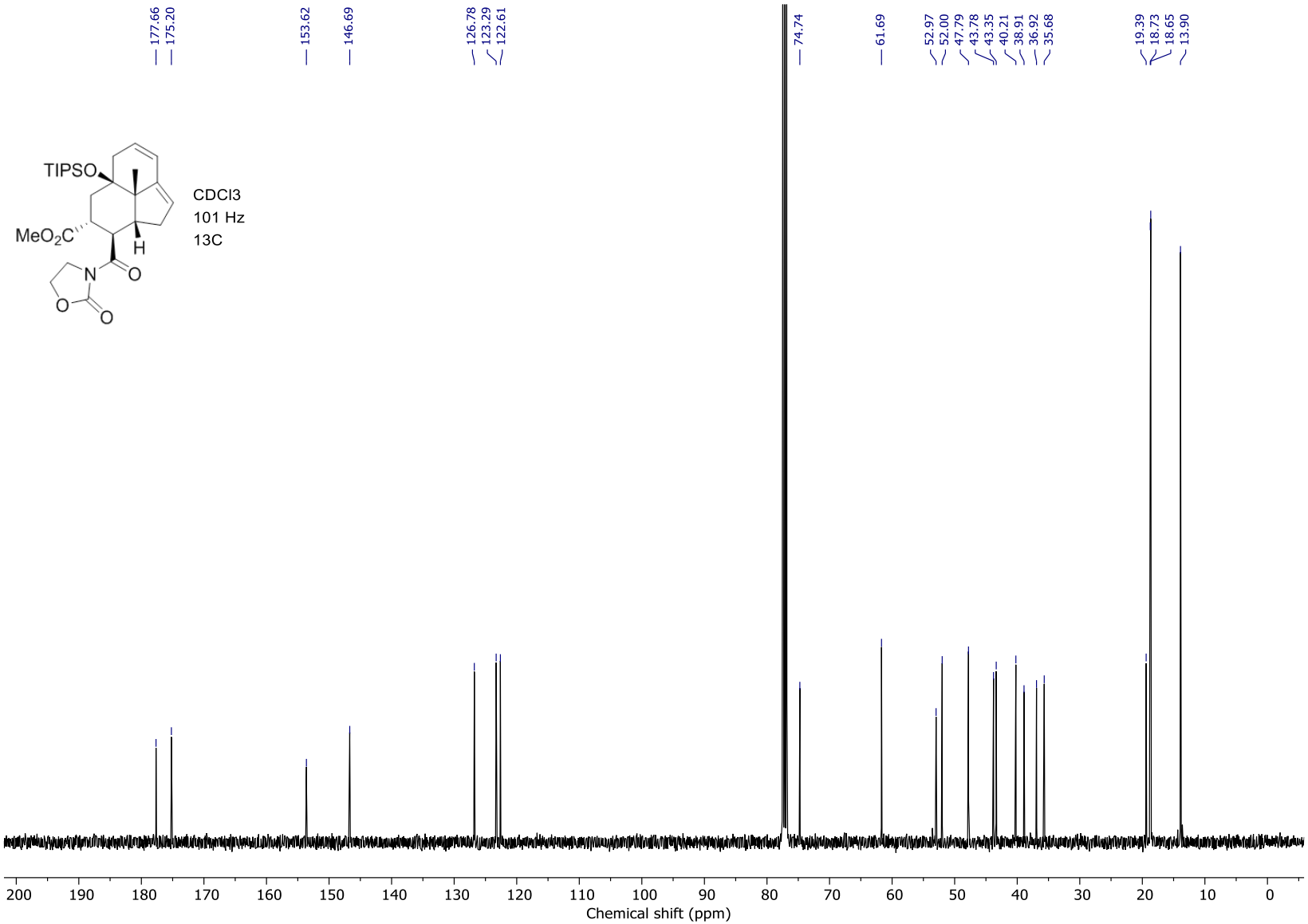
177.66
175.20
153.62
146.69
126.78
123.29
122.61
74.74
61.69
52.97
52.00
47.79
43.78
43.35
40.21
38.91
36.92
35.68
19.39
18.73
18.65
13.90
TIPSO
MeO2C
H
N
O
O
O
CDCl3
101 Hz
13C
200
190
180
170
160
150
140
130
120
110
100
90
80
70
60
50
40
30
20
10
0
Chemical shift (ppm)

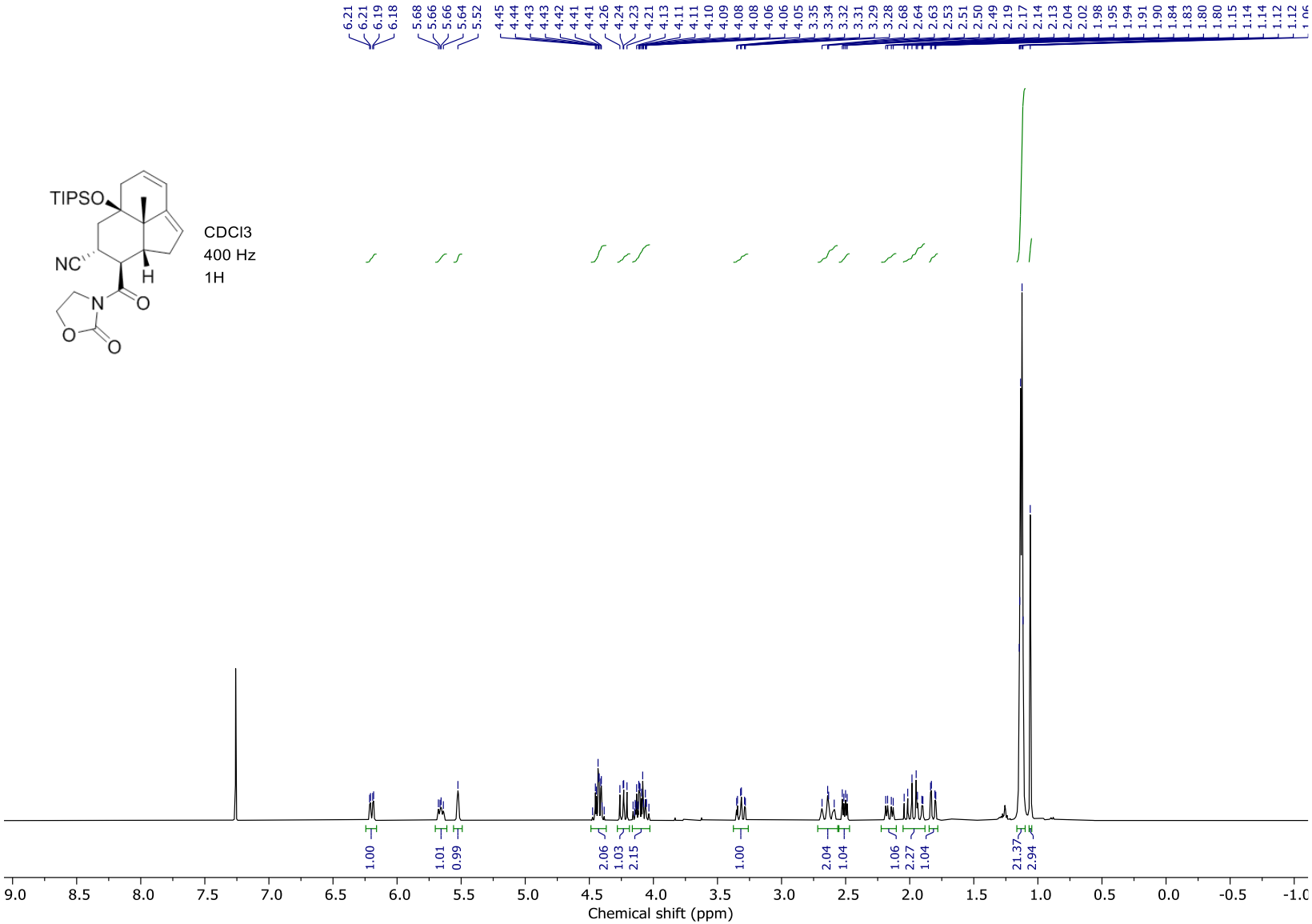
TIPSO
NC
H
N
O
O
O
CDCl3
400 Hz
1H
6.21 6.21 6.19 6.18 5.68 5.66 5.66 5.64 5.52 4.45 4.44 4.43 4.43 4.42 4.41 4.41 4.26 4.24 4.23 4.21 4.13 4.11 4.11 4.10 4.09 4.08 4.08 4.06 4.06 4.05 3.35 3.34 3.32 3.31 3.29 3.28 2.68 2.64 2.63 2.53 2.51 2.50 2.49 2.19 2.17 2.14 2.13 2.04 2.02 1.98 1.95 1.94 1.91 1.90 1.84 1.83 1.80 1.80 1.15 1.14 1.14 1.12 1.12
1.00 1.01 0.99 2.06 1.03 2.15 1.00 2.04 1.04 1.06 2.27 1.04 21.37 2.94
9.0 8.5 8.0 7.5 7.0 6.5 6.0 5.5 5.0 4.5 4.0 3.5 3.0 2.5 2.0 1.5 1.0 0.5 0.0 -0.5 -1.0
Chemical shift (ppm)

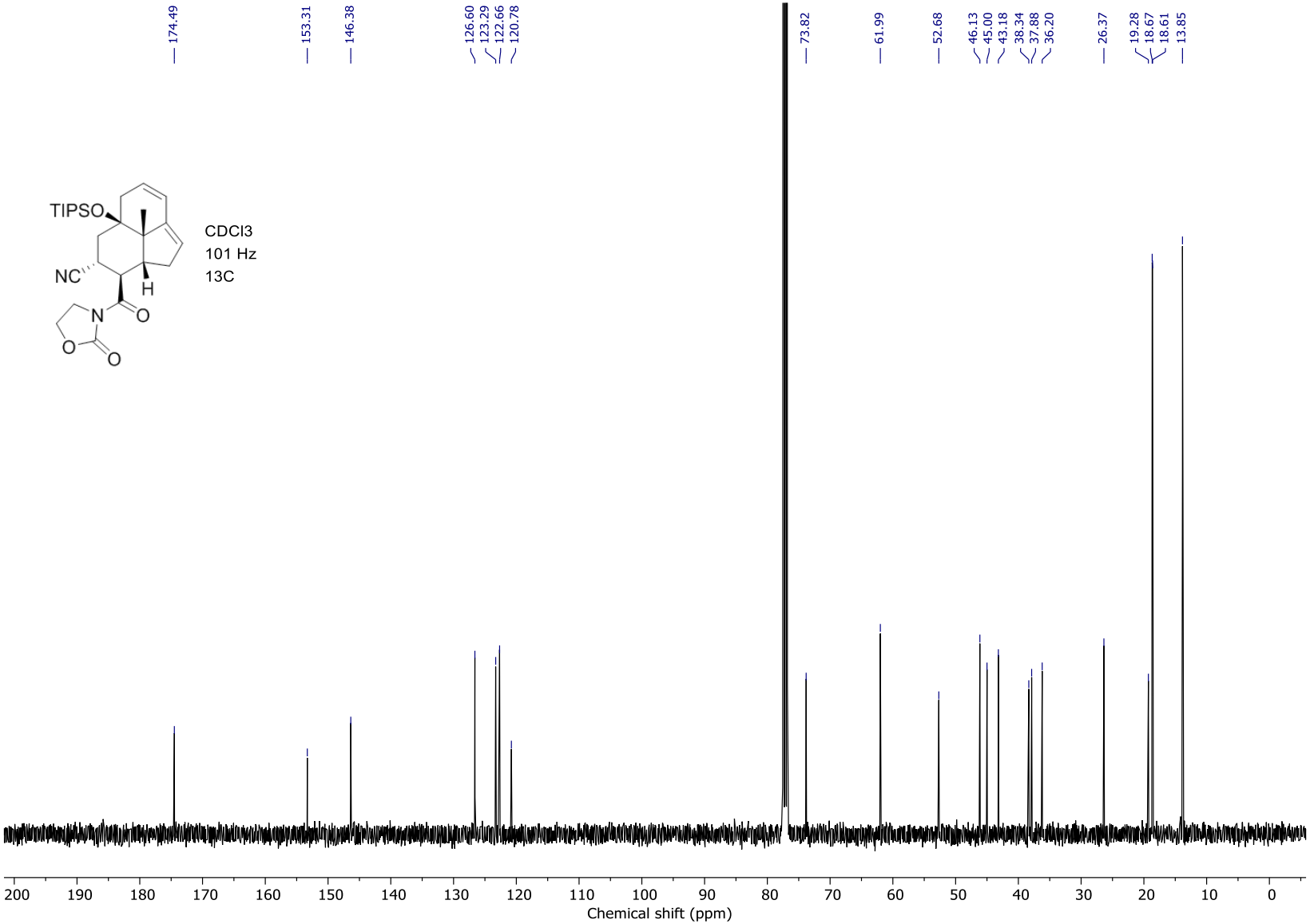
174.49
153.31
146.38
126.60
123.29
122.66
120.78
73.82
61.99
52.68
46.13
45.00
43.18
38.34
37.88
36.20
26.37
19.28
18.67
18.61
13.85
TIPSO
NC
H
N
O
O
O
CDCl3
101 Hz
13C
200
190
180
170
160
150
140
130
120
110
100
90
80
70
60
50
40
30
20
10
0
Chemical shift (ppm)

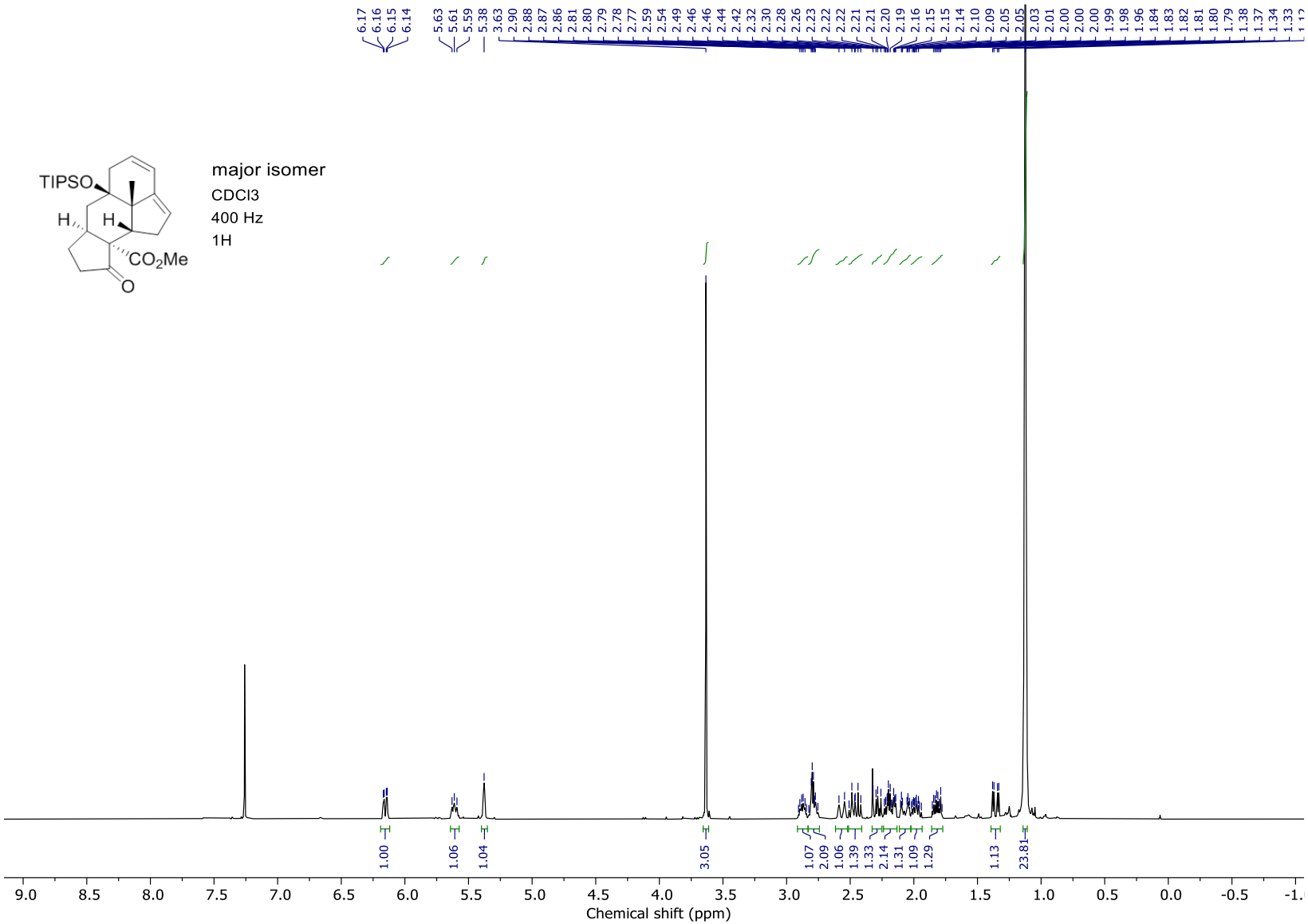
TIPSO
H
H
CO2Me
O
major isomer
CDCl3
400 Hz
1H
Chemical shift (ppm)

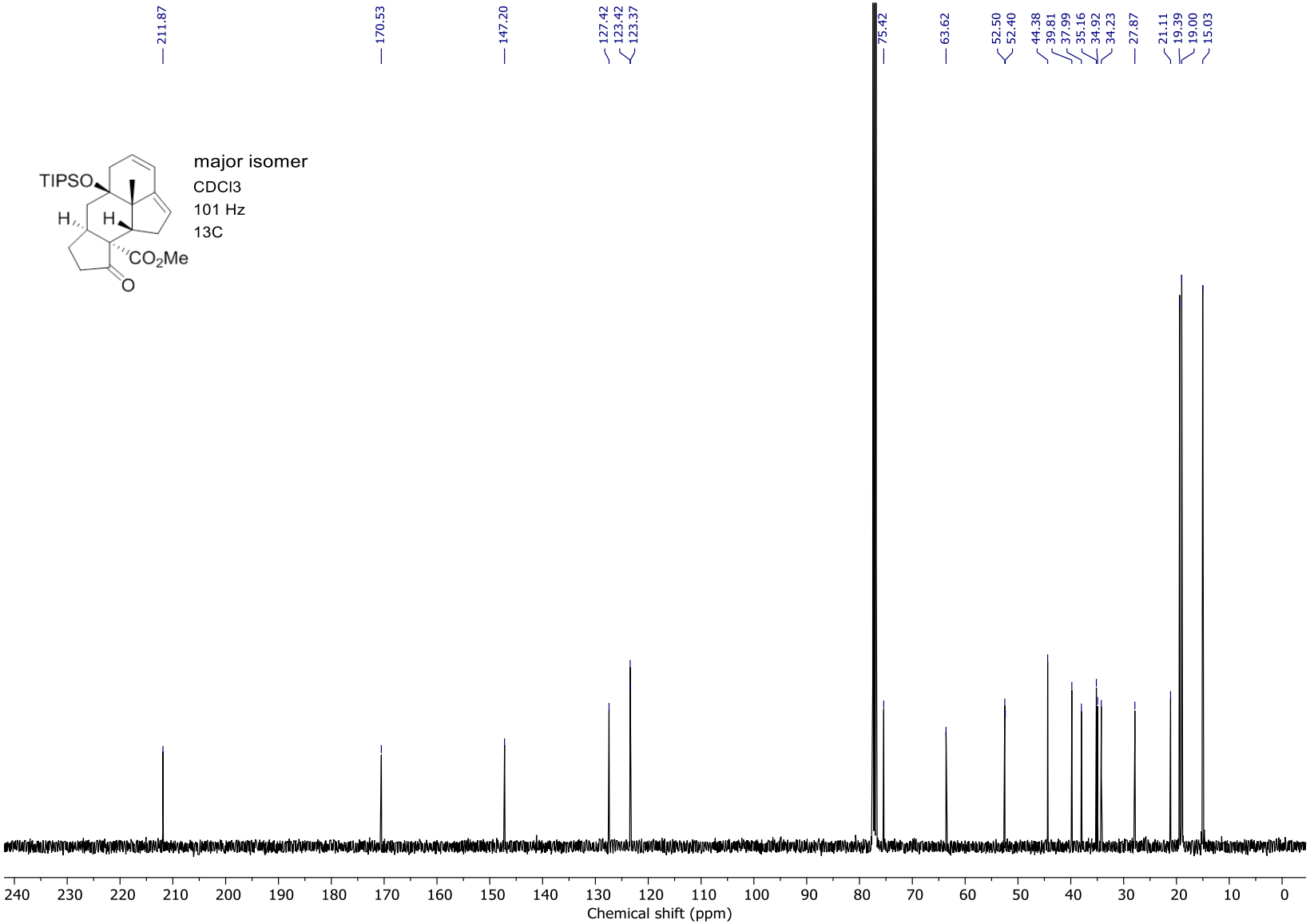
211.87
170.53
147.20
127.42
123.42
123.37
75.42
63.62
52.50
52.40
44.38
39.81
37.99
35.16
34.92
34.23
27.87
21.11
19.39
19.00
15.03
TIPSO
H
H
CO2Me
O
major isomer
CDCl3
101 Hz
13C
240 230 220 210 200 190 180 170 160 150 140 130 120 110 100 90 80 70 60 50 40 30 20 10 0
Chemical shift (ppm)

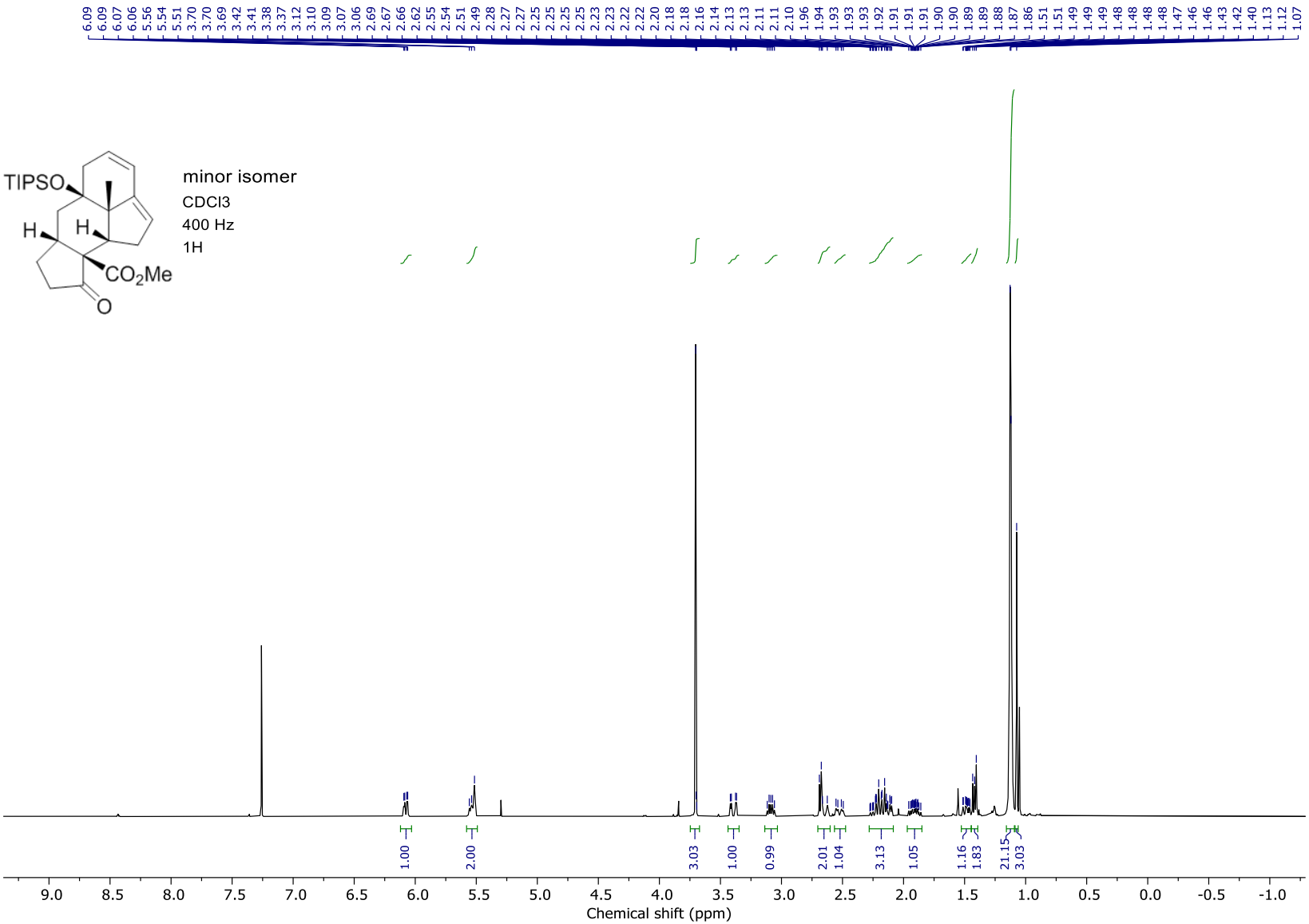
TIPSO
H
H
CO2Me
O
minor isomer
CDCl3
400 Hz
1H
Chemical shift (ppm)

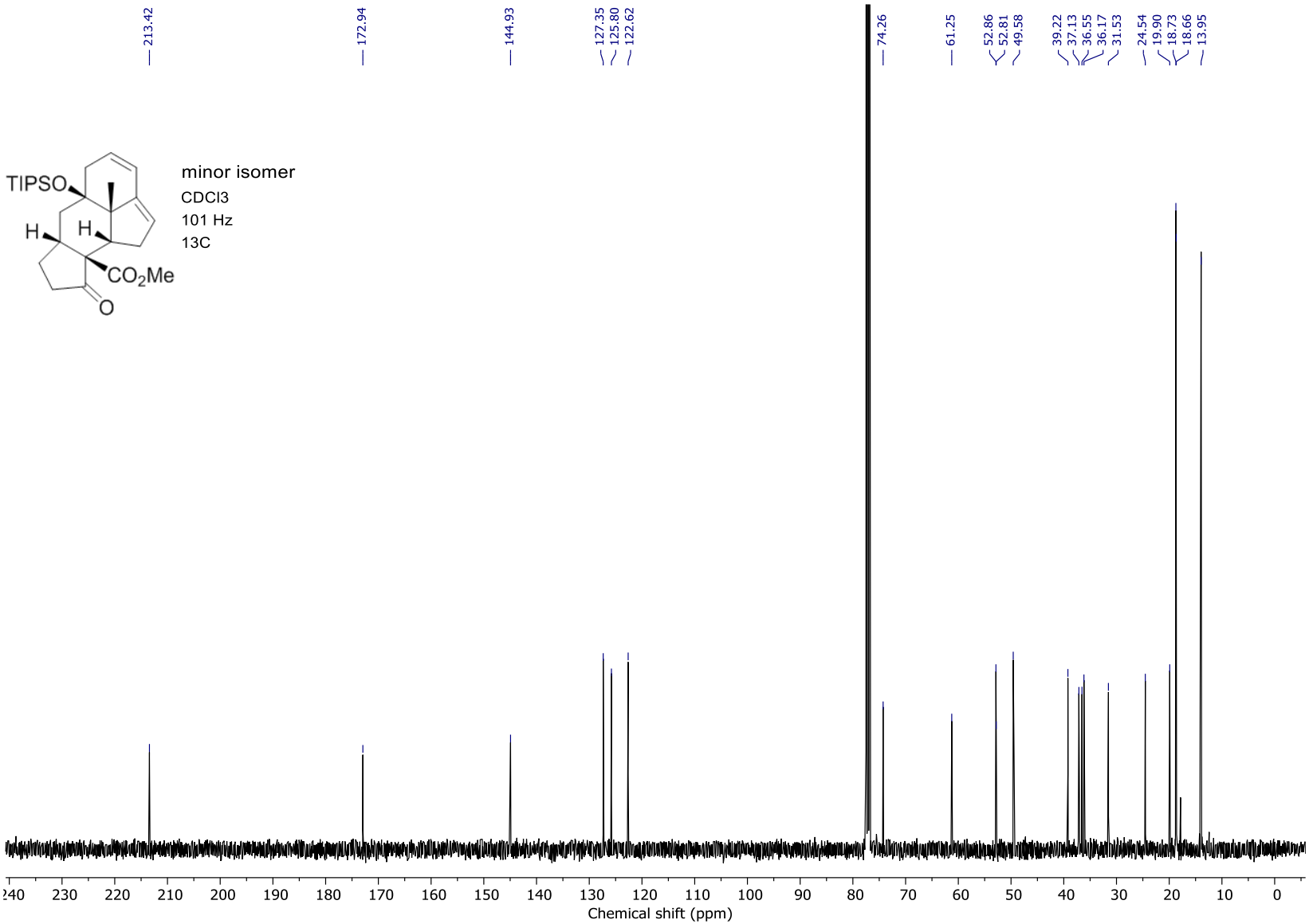
213.42
172.94
144.93
127.35
125.80
122.62
74.26
61.25
52.86
52.81
49.58
39.22
37.13
36.55
36.17
31.53
24.54
19.90
18.73
18.66
13.95
TIPSO
H
H
CO2Me
O
minor isomer
CDCl3
101 Hz
13C
240 230 220 210 200 190 180 170 160 150 140 130 120 110 100 90 80 70 60 50 40 30 20 10 0
Chemical shift (ppm)

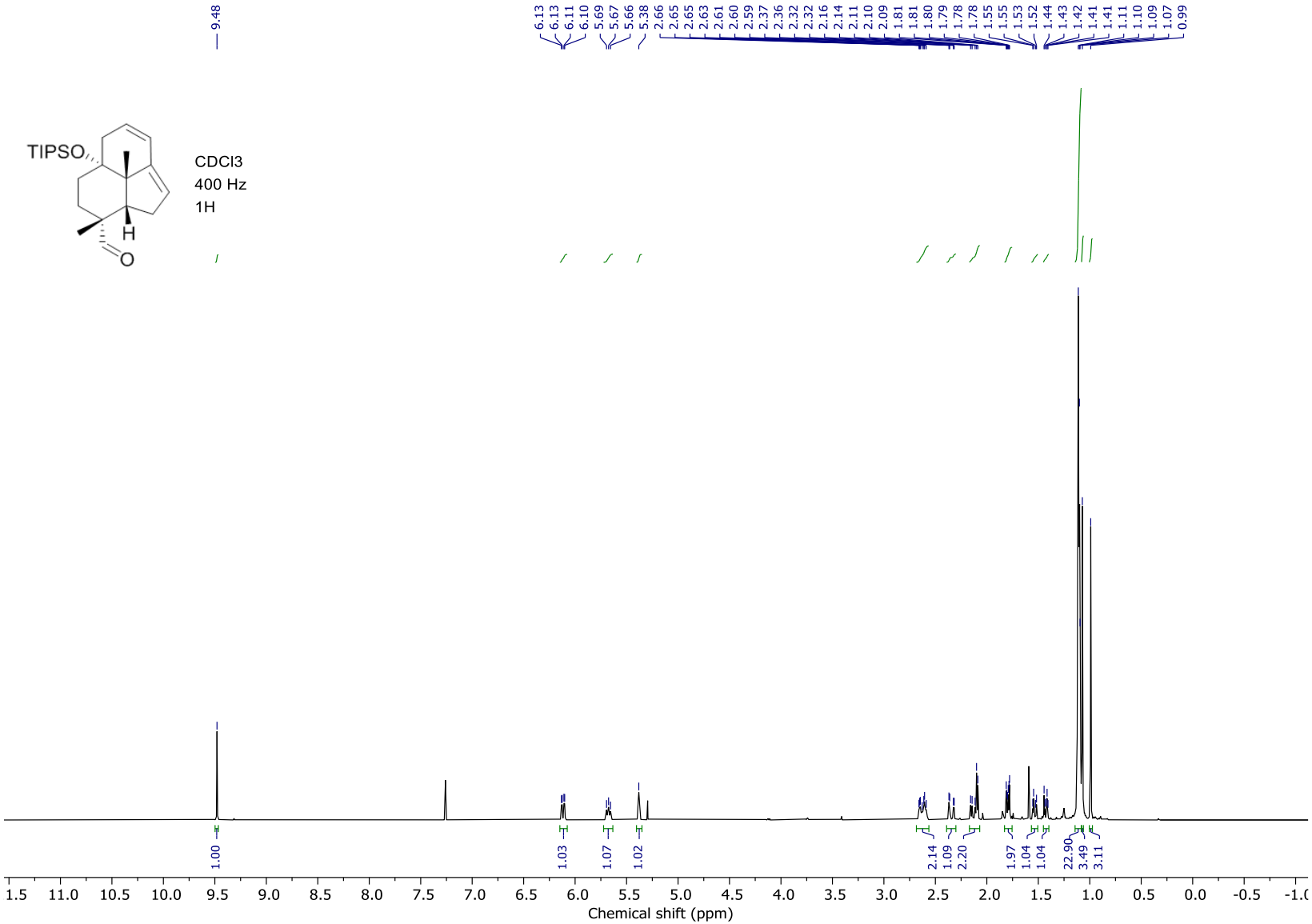
TIPSO
H
O
CDCl3
400 Hz
1H
9.48
6.13
6.13
6.11
6.10
5.69
5.67
5.66
5.38
2.66
2.65
2.65
2.63
2.61
2.60
2.59
2.37
2.36
2.32
2.32
2.16
2.14
2.11
2.10
2.09
1.81
1.81
1.80
1.79
1.78
1.78
1.55
1.55
1.53
1.52
1.44
1.43
1.42
1.41
1.41
1.11
1.10
1.09
1.07
0.99
1.00
1.03
1.07
1.02
2.14
1.09
2.20
1.97
1.04
1.04
22.90
3.49
3.11
1.5 11.0 10.5 10.0 9.5 9.0 8.5 8.0 7.5 7.0 6.5 6.0 5.5 5.0 4.5 4.0 3.5 3.0 2.5 2.0 1.5 1.0 0.5 0.0 -0.5 -1.0
Chemical shift (ppm)

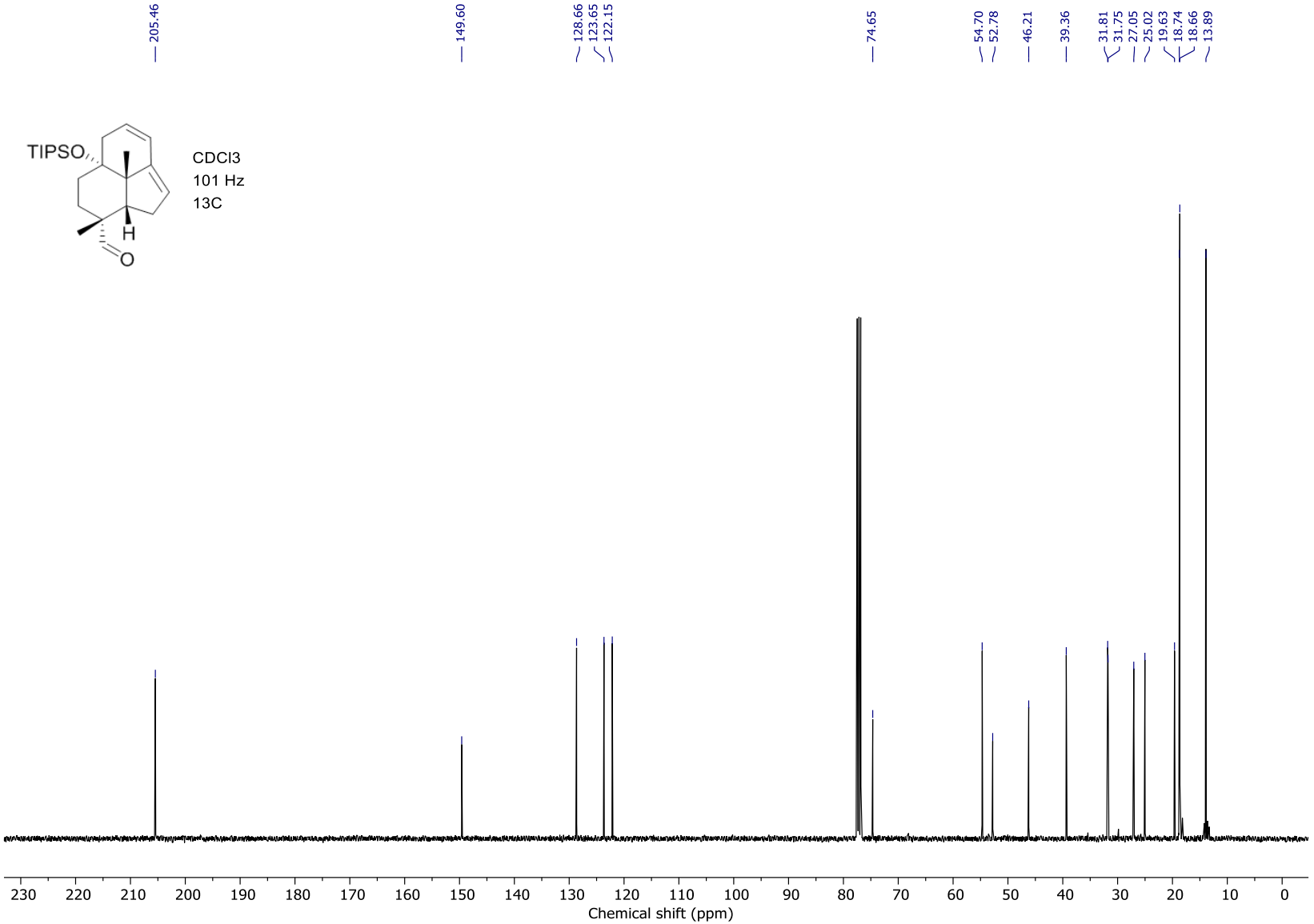
205.46
149.60
128.66
123.65
122.15
74.65
54.70
52.78
46.21
39.36
31.81
31.75
27.05
25.02
19.63
18.74
18.66
13.89
TIPSO
H
O
CDCl3
101 Hz
13C
230 220 210 200 190 180 170 160 150 140 130 120 110 100 90 80 70 60 50 40 30 20 10 0
Chemical shift (ppm)

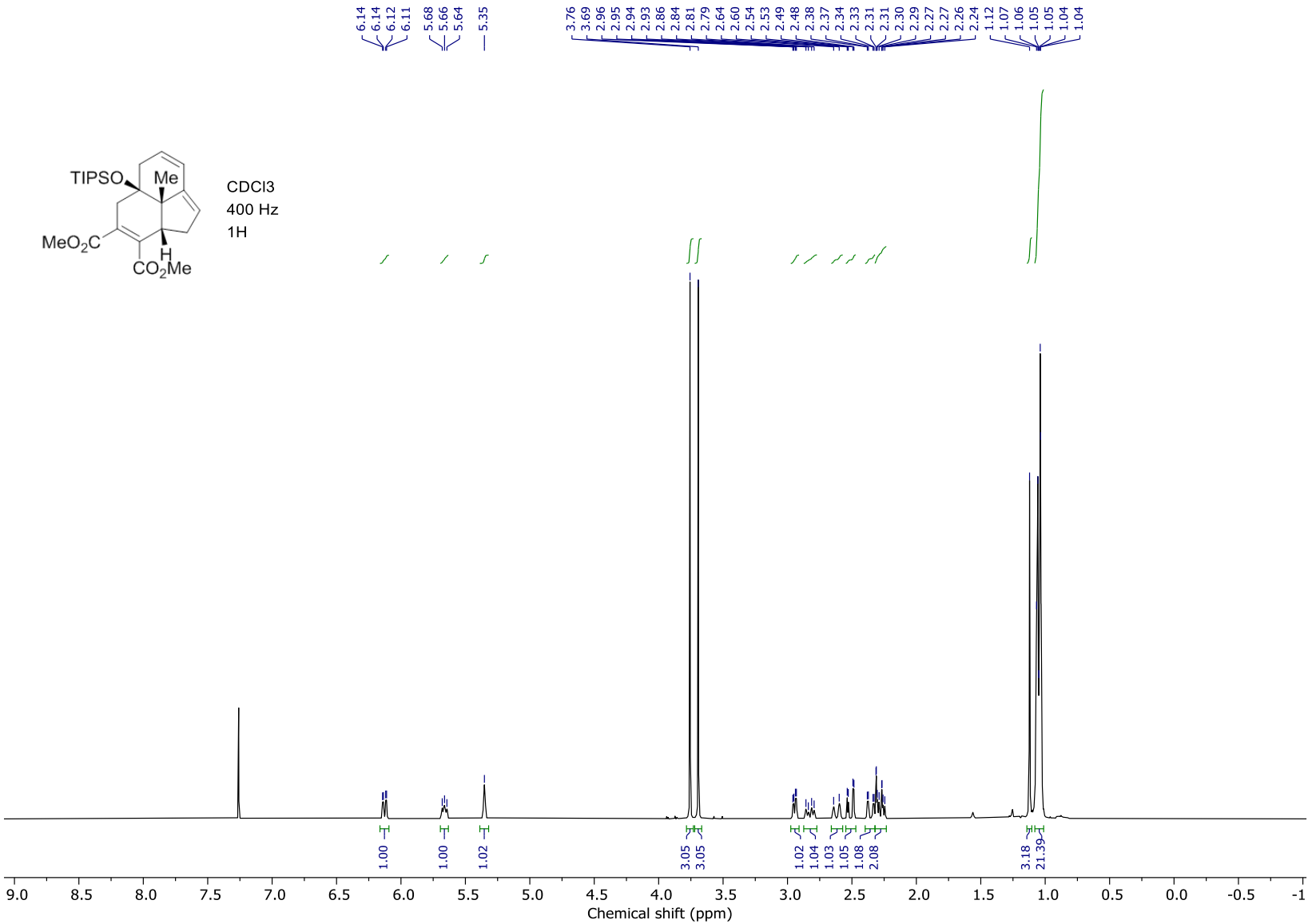
TIPSO
Me
MeO2C
H
CO2Me
CDCl3
400 Hz
1H
6.14
6.14
6.12
6.11
5.68
5.66
5.64
5.35
3.76
3.69
2.96
2.95
2.94
2.93
2.86
2.84
2.81
2.79
2.64
2.60
2.54
2.53
2.49
2.48
2.38
2.37
2.34
2.33
2.31
2.31
2.30
2.29
2.27
2.27
2.26
2.24
1.12
1.07
1.06
1.05
1.05
1.04
1.04
1.00
1.00
1.02
3.05
3.05
1.02
1.04
1.03
1.05
1.08
2.08
3.18
21.39
9.0
8.5
8.0
7.5
7.0
6.5
6.0
5.5
5.0
4.5
4.0
3.5
3.0
2.5
2.0
1.5
1.0
0.5
0.0
-0.5
-1
Chemical shift (ppm)

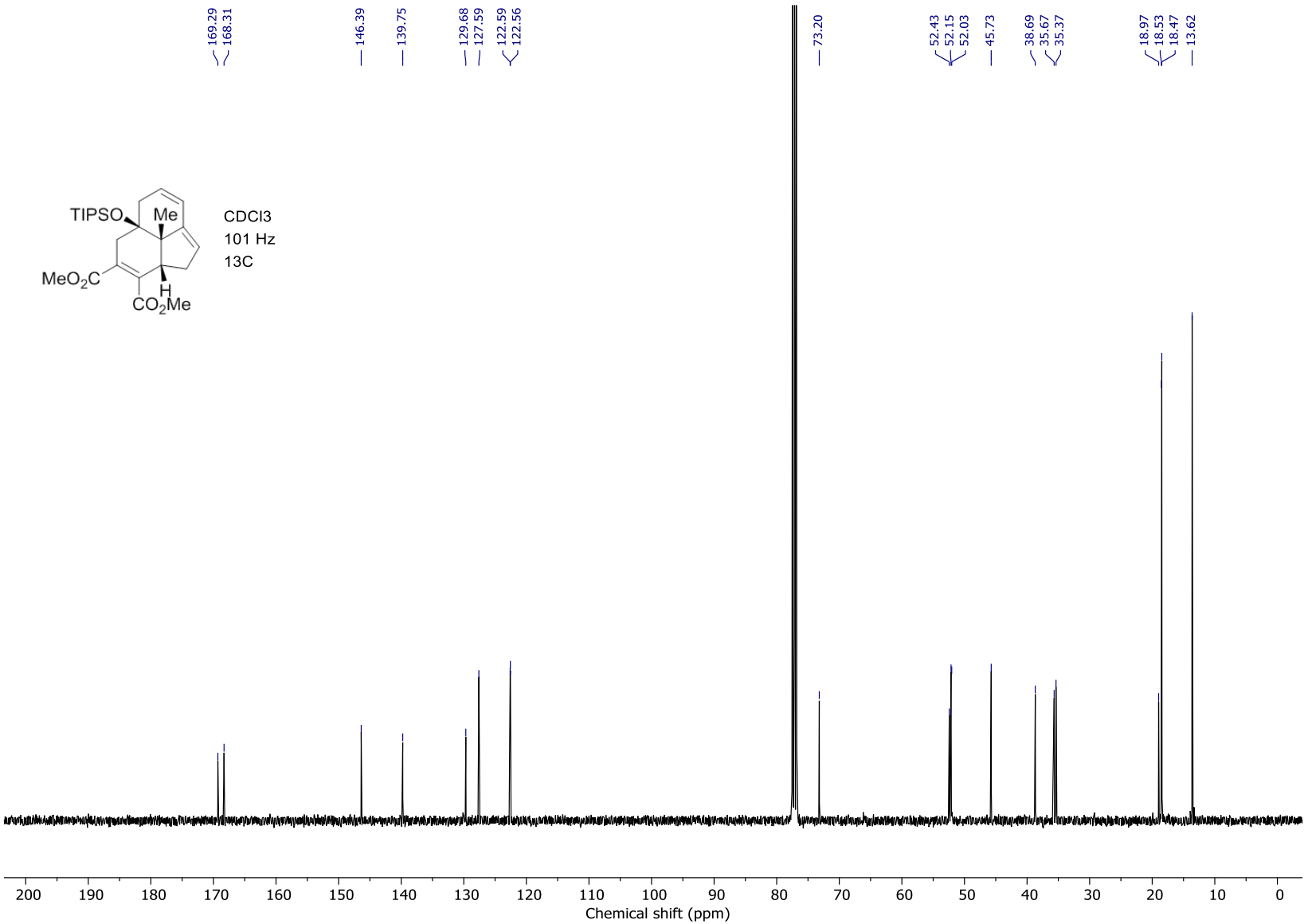
169.29
168.31
146.39
139.75
129.68
127.59
122.59
122.56
73.20
52.43
52.15
52.03
45.73
38.69
35.67
35.37
18.97
18.53
18.47
13.62
TIPSO
Me
MeO2C
H
CO2Me
CDCl3
101 Hz
13C
200
190
180
170
160
150
140
130
120
110
100
90
80
70
60
50
40
30
20
10
0
Chemical shift (ppm)

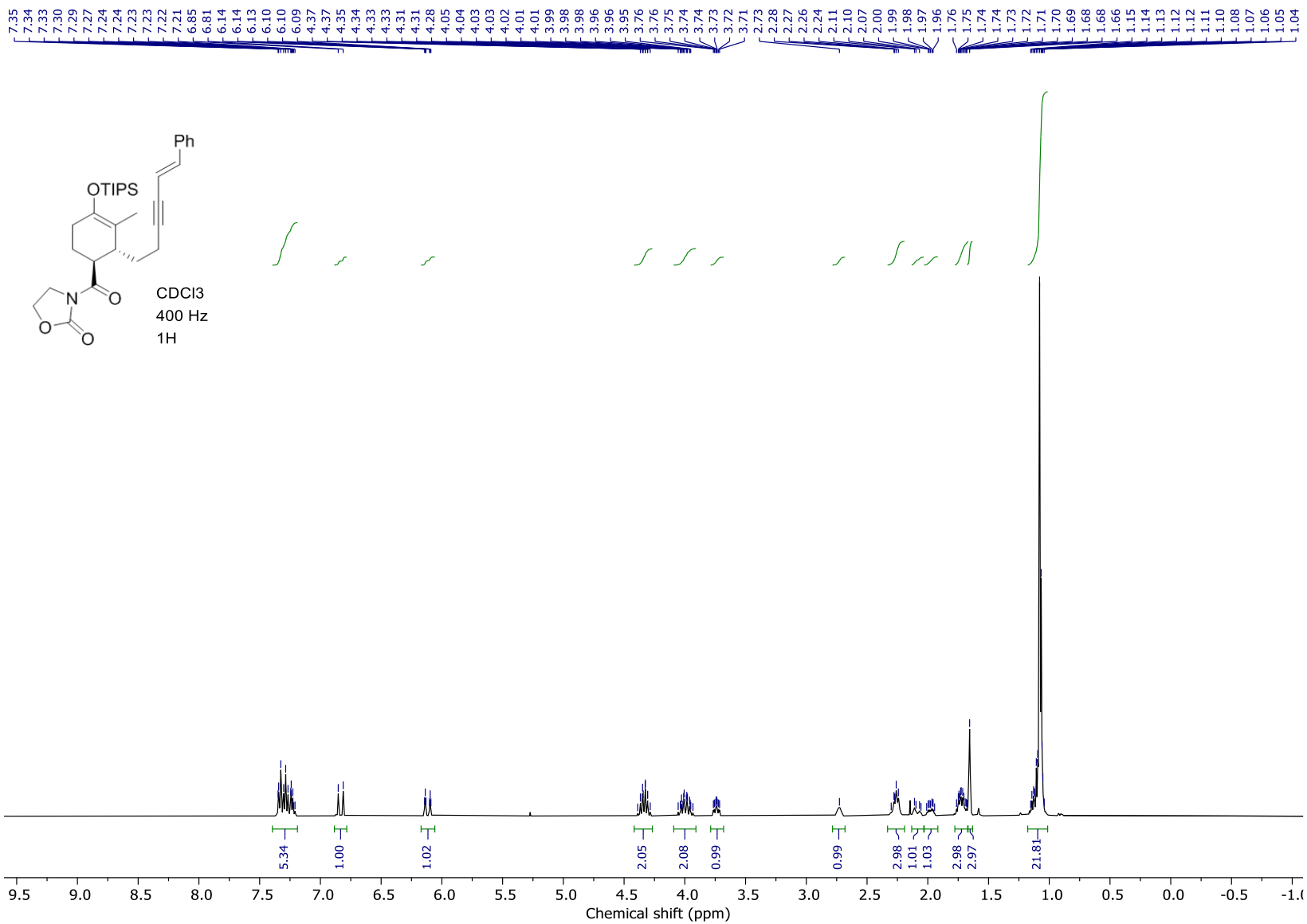
Ph
OTIPS
N
O
O
O
CDCl3
400 Hz
1H
5.34
1.00
1.02
2.05
2.08
0.99
0.99
2.98
1.01
1.03
2.98
2.97
21.81
Chemical shift (ppm)

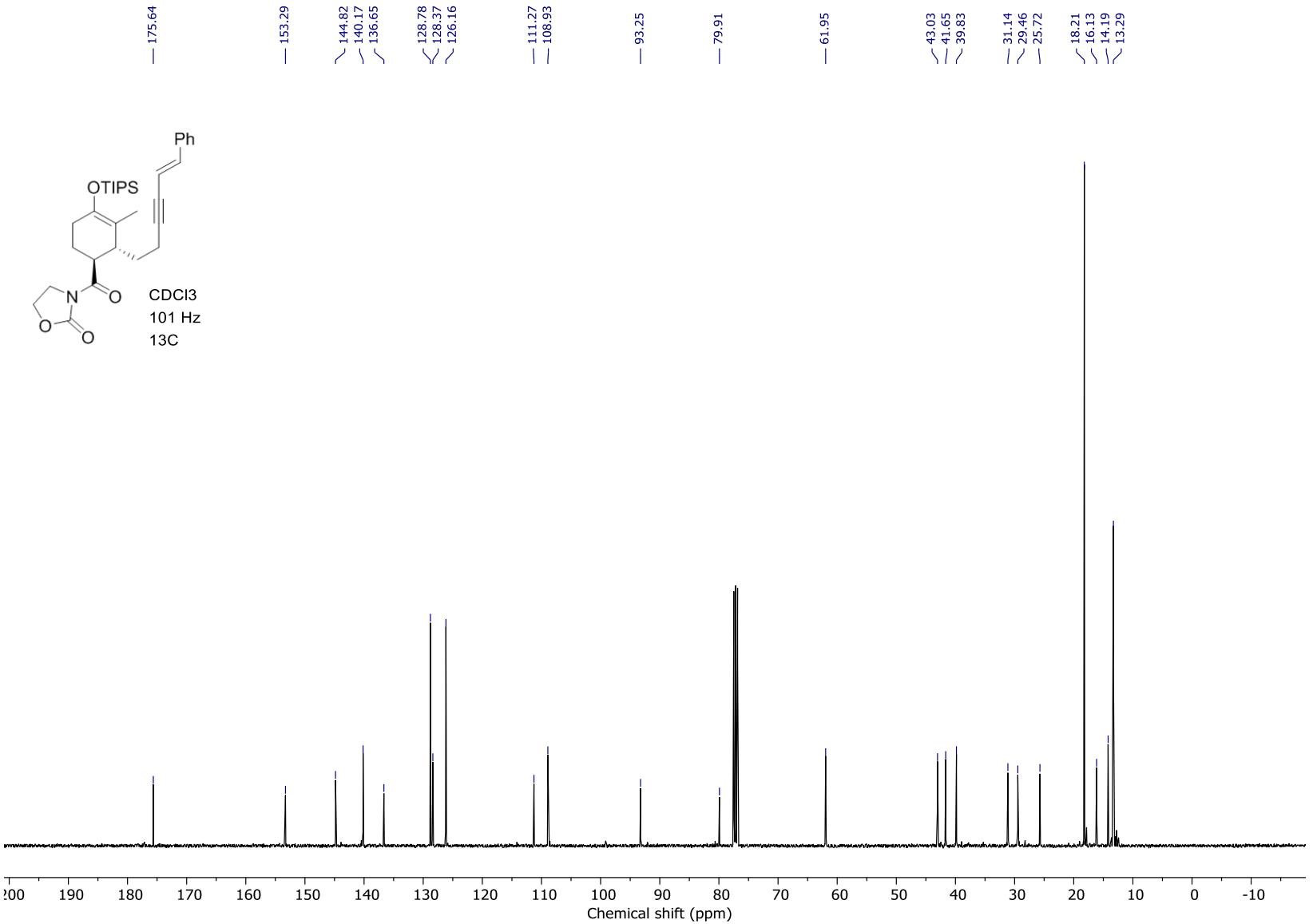
175.64
153.29
144.82
140.17
136.65
128.78
128.37
126.16
111.27
108.93
93.25
79.91
61.95
43.03
41.65
39.83
31.14
29.46
25.72
18.21
16.13
14.19
13.29
Ph
OTIPS
N
O
O
O
CDCl3
101 Hz
13C
200
190
180
170
160
150
140
130
120
110
100
90
80
70
60
50
40
30
20
10
0
-10
Chemical shift (ppm)

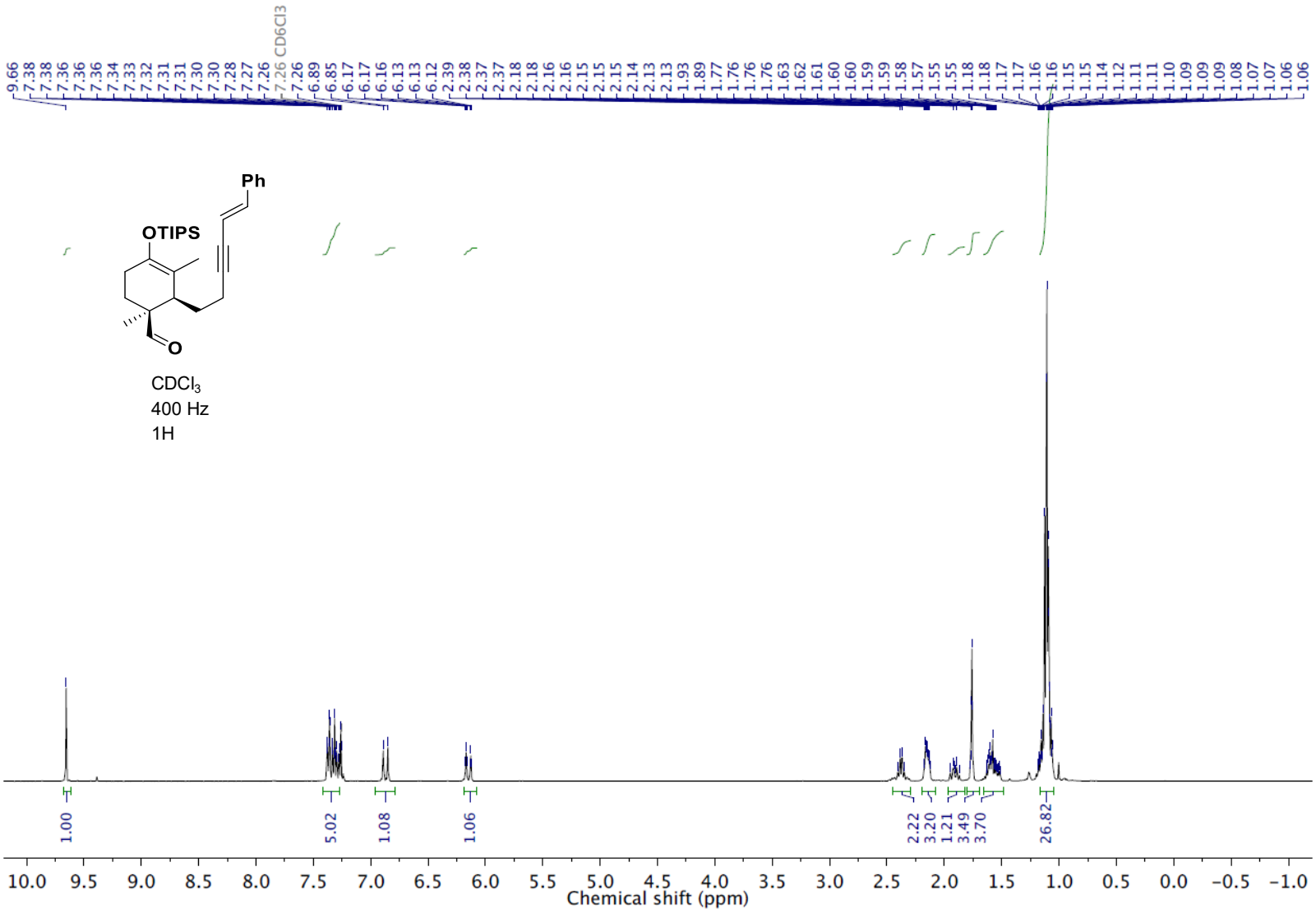

Spectra from Alyson Poyser's MSc thesis

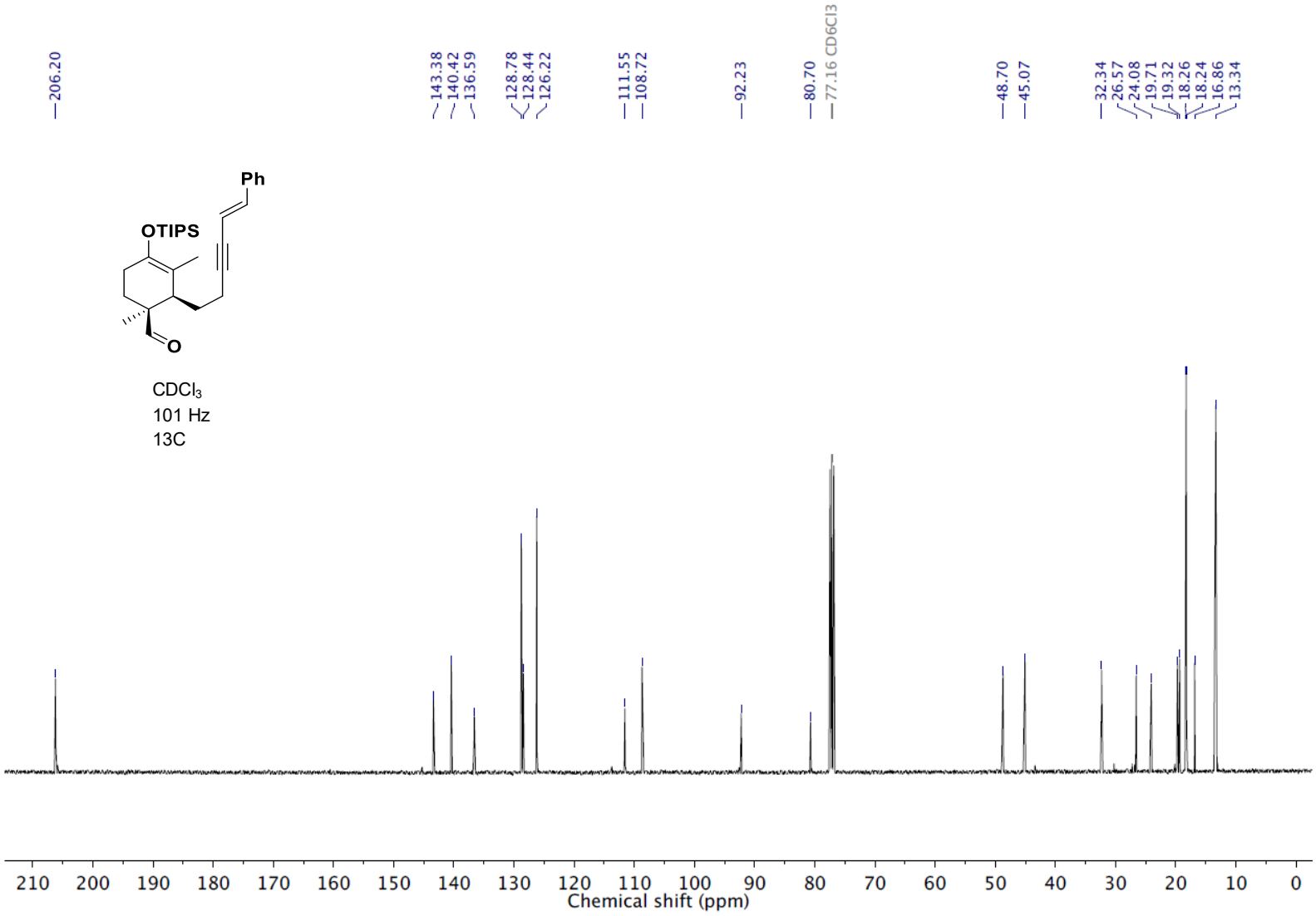

Spectra from Alyson Poyser's MSc thesis

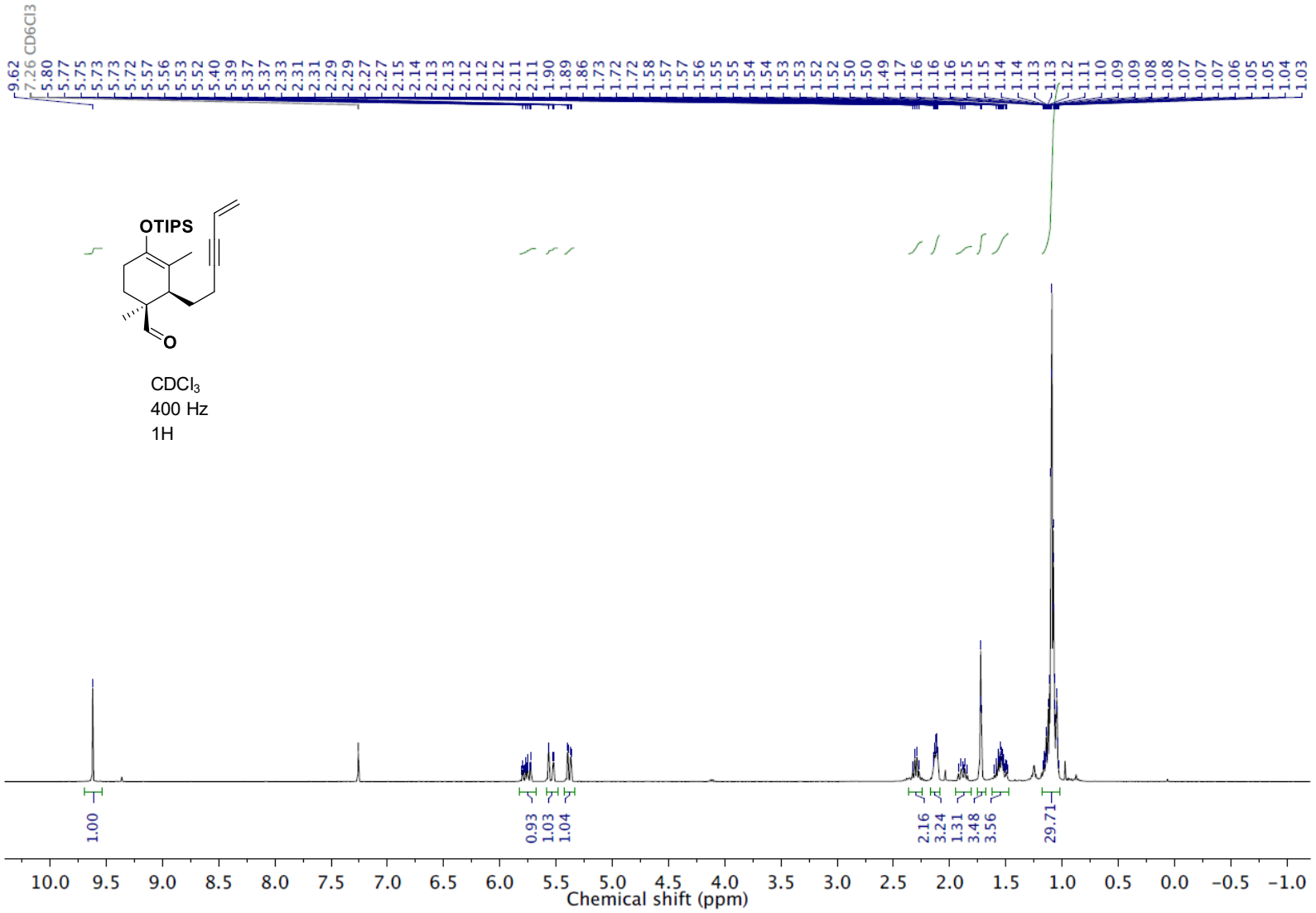

Spectra from Alyson Poyser's MSc thesis

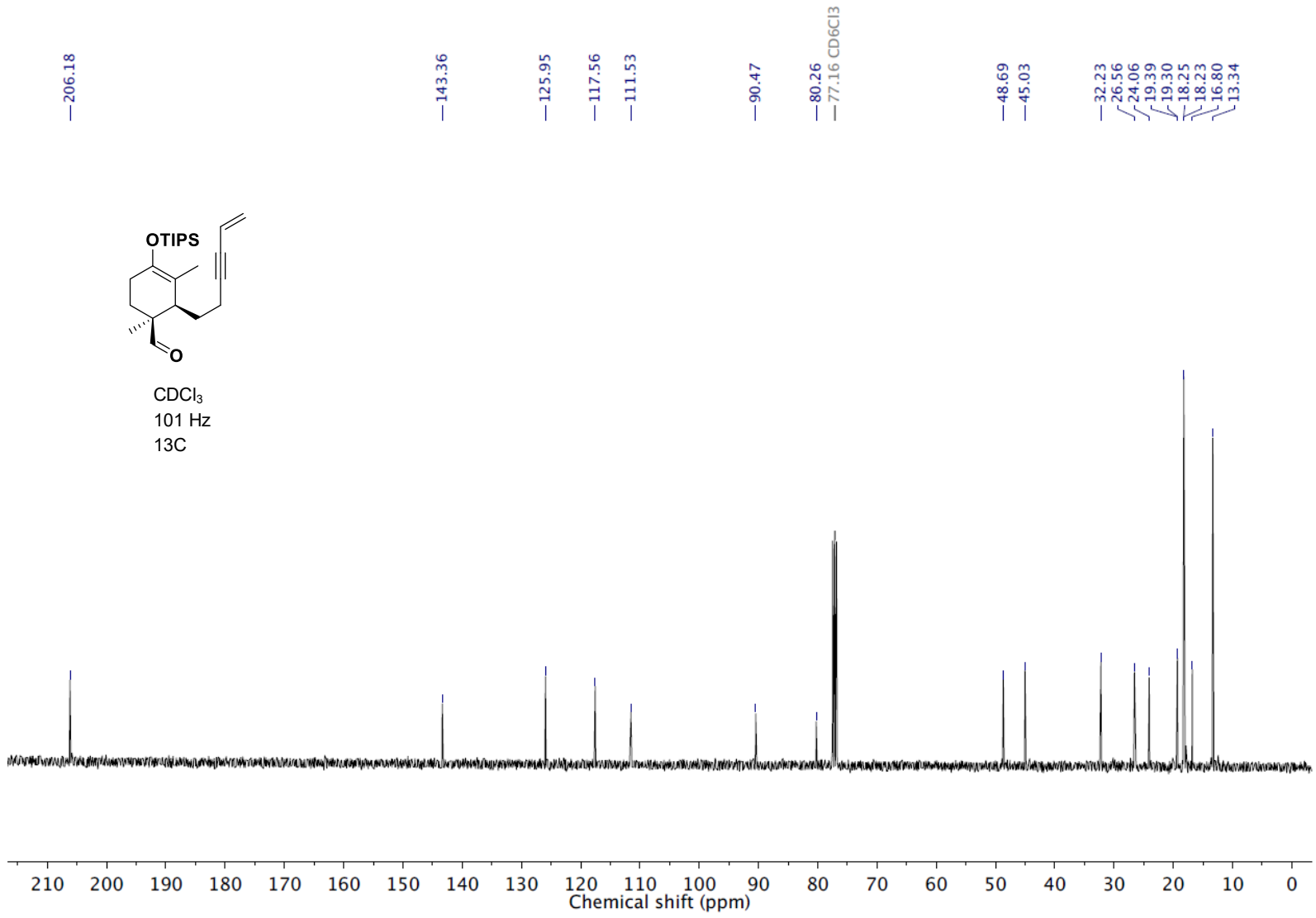

Spectra from Alyson Poyser's MSc thesis

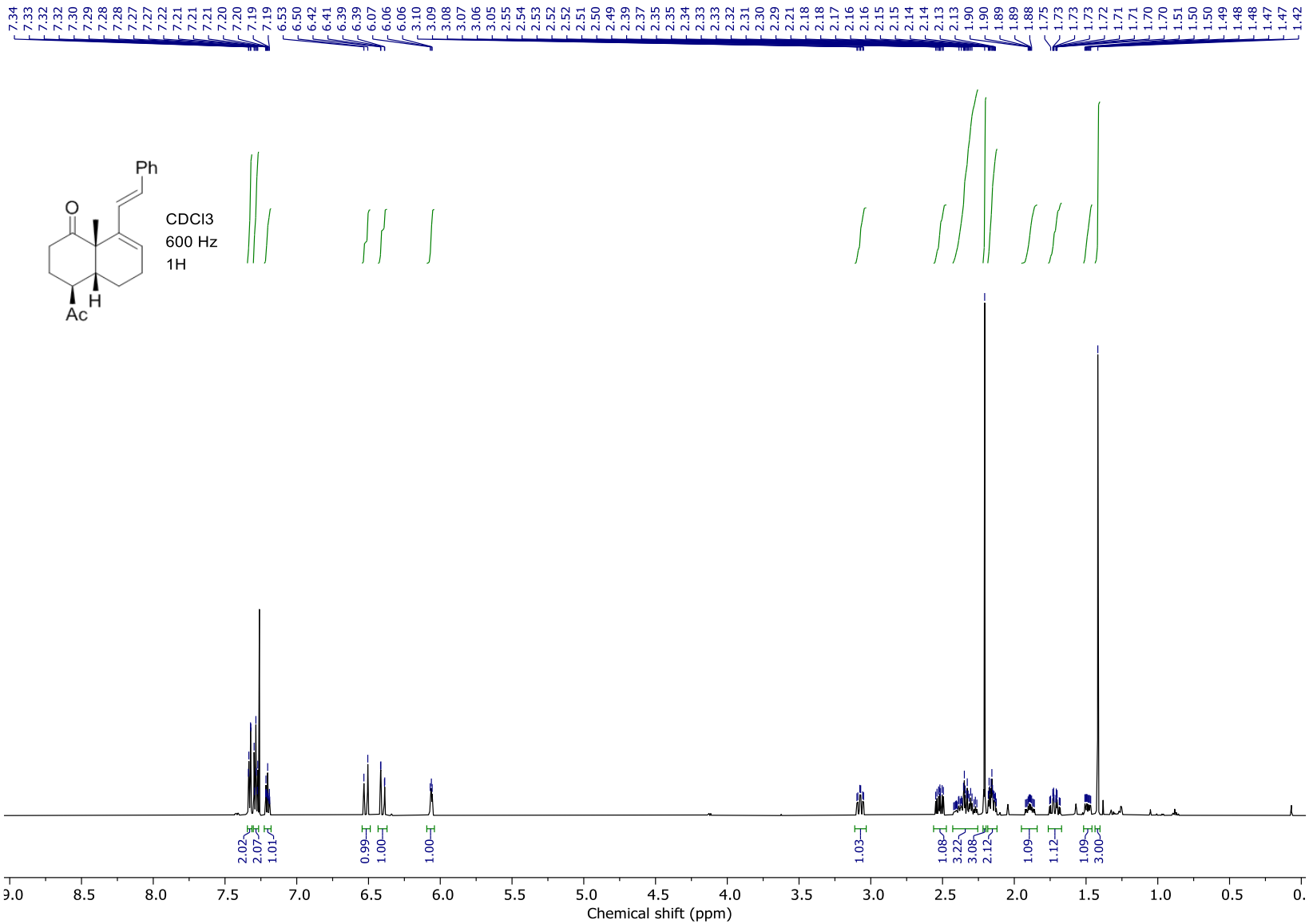
Ph
O
Ac
H
CDCl3
600 Hz
1H
Chemical shift (ppm)

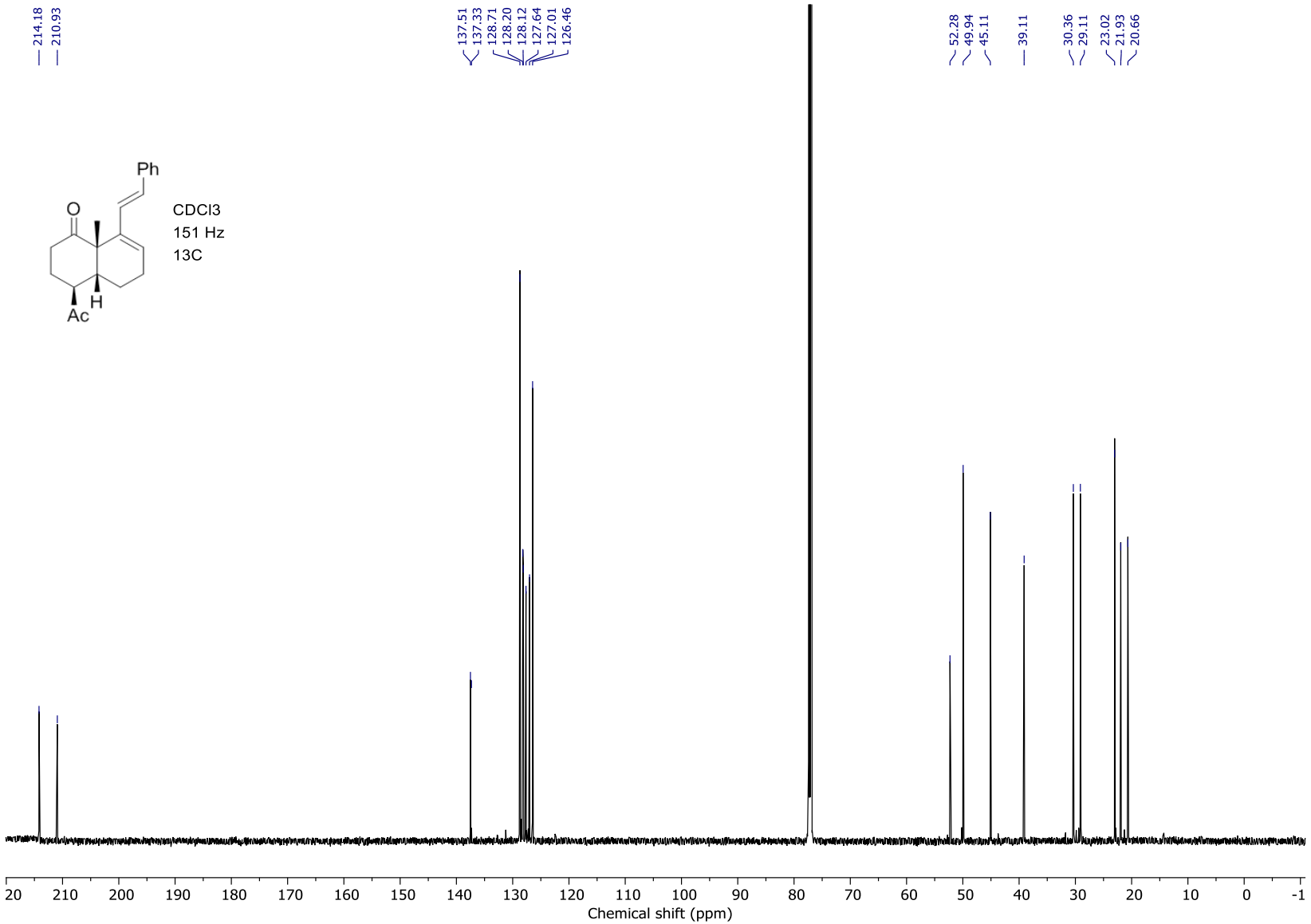
214.18
210.93
137.51
137.33
128.71
128.20
128.12
127.64
127.01
126.46
52.28
49.94
45.11
39.11
30.36
29.11
23.02
21.93
20.66
Ph
O
Ac
H
CDCl3
151 Hz
13C
20
210
200
190
180
170
160
150
140
130
120
110
100
90
80
70
60
50
40
30
20
10
0
-1
Chemical shift (ppm)

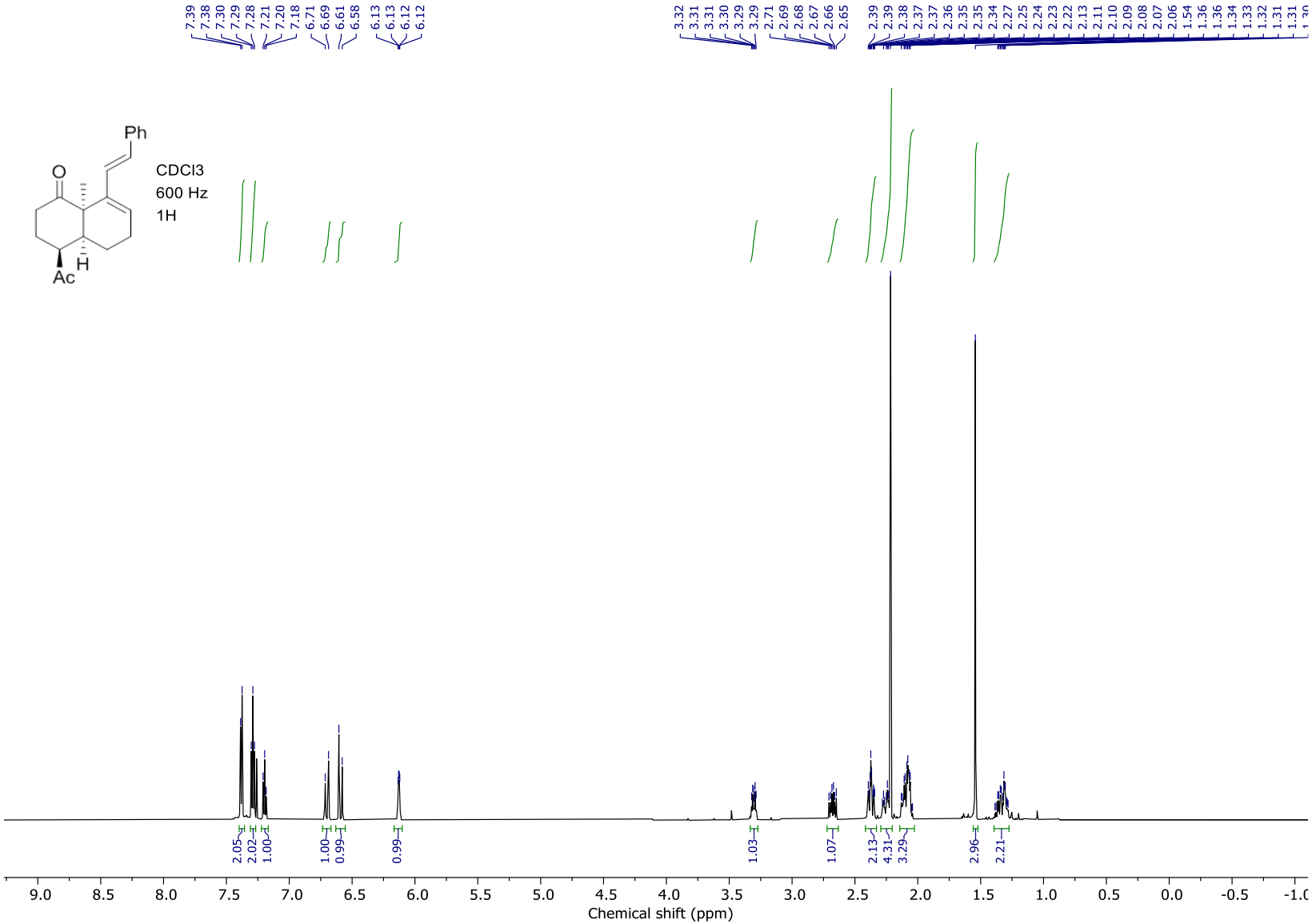
Ph
O
Ac
H
CDCl3
600 Hz
1H
Chemical shift (ppm)

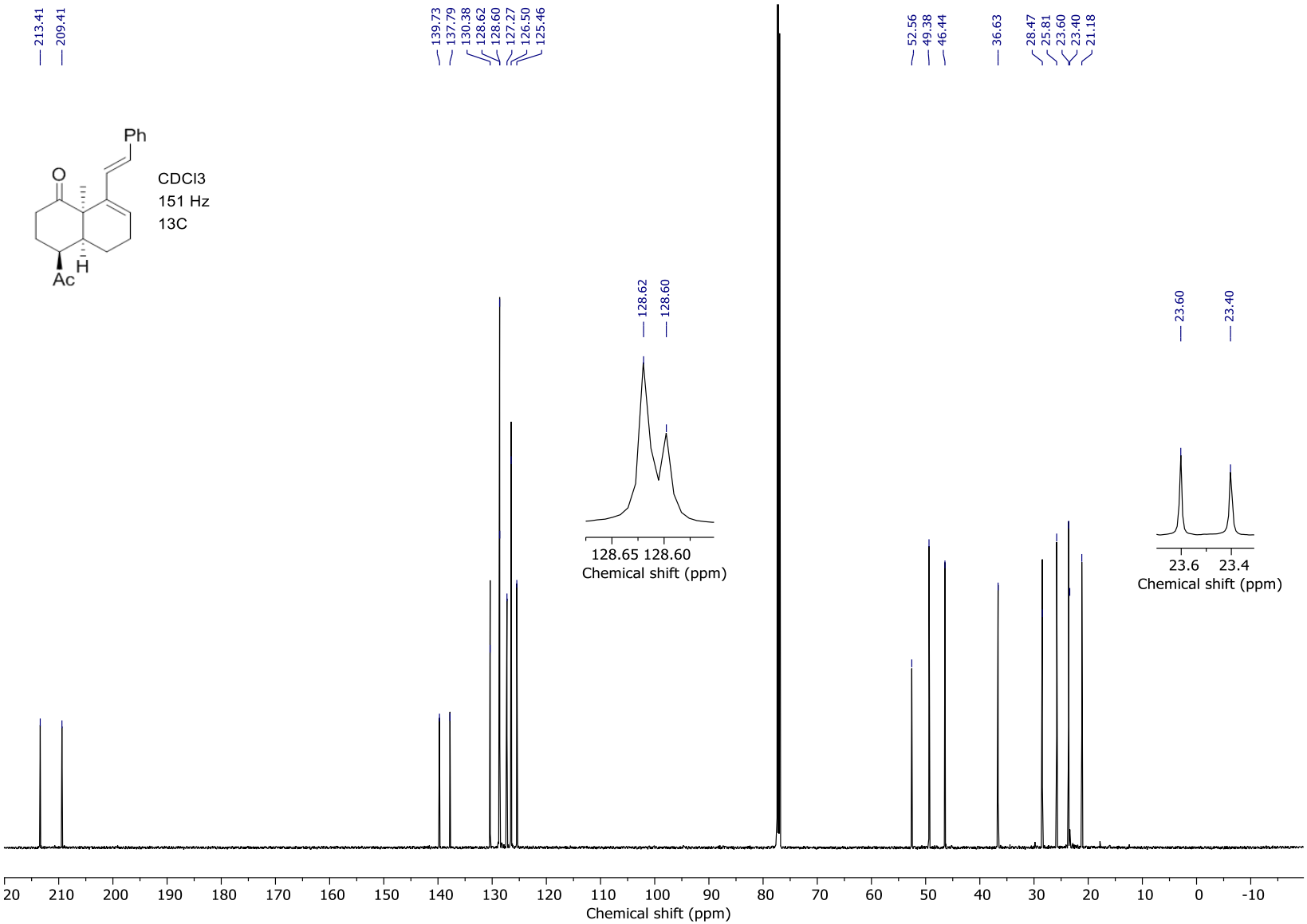
213.41
209.41
139.73
137.79
130.38
128.62
128.60
127.27
126.50
125.46
52.56
49.38
46.44
36.63
28.47
25.81
23.60
23.40
21.18
Ph
O
Ac
H
CDCl3
151 Hz
13C
128.62
128.60
128.65 128.60
Chemical shift (ppm)
23.60
23.40
23.6 23.4
Chemical shift (ppm)
20 210 200 190 180 170 160 150 140 130 120 110 100 90 80 70 60 50 40 30 20 10 0 -10
Chemical shift (ppm)

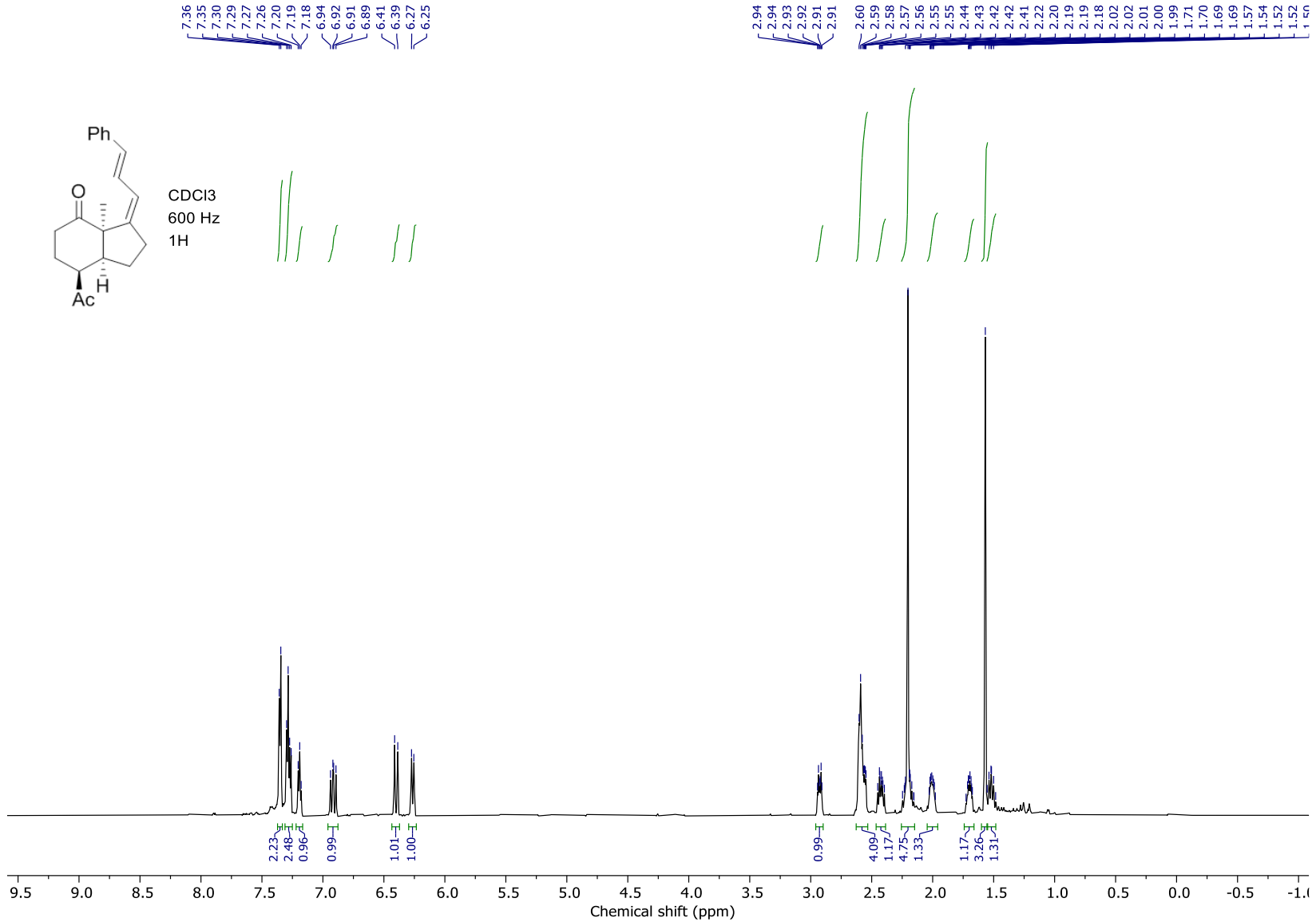
Ph
O
Ac
H
CDCl3
600 Hz
1H
7.36 7.35 7.30 7.29 7.27 7.26 7.20 7.19 7.18 6.94 6.92 6.91 6.89 6.41 6.39 6.27 6.25
2.94 2.94 2.93 2.92 2.91 2.91 2.60 2.59 2.58 2.57 2.56 2.55 2.55 2.44 2.43 2.42 2.42 2.41 2.22 2.20 2.19 2.19 2.18 2.02 2.02 2.01 2.00 1.99 1.71 1.70 1.69 1.69 1.57 1.54 1.52 1.52
2.23 2.48 0.96 0.99 1.01 1.00 0.99 4.09 1.17 4.75 1.33 1.17 3.26 1.31
9.5 9.0 8.5 8.0 7.5 7.0 6.5 6.0 5.5 5.0 4.5 4.0 3.5 3.0 2.5 2.0 1.5 1.0 0.5 0.0 -0.5
Chemical shift (ppm)

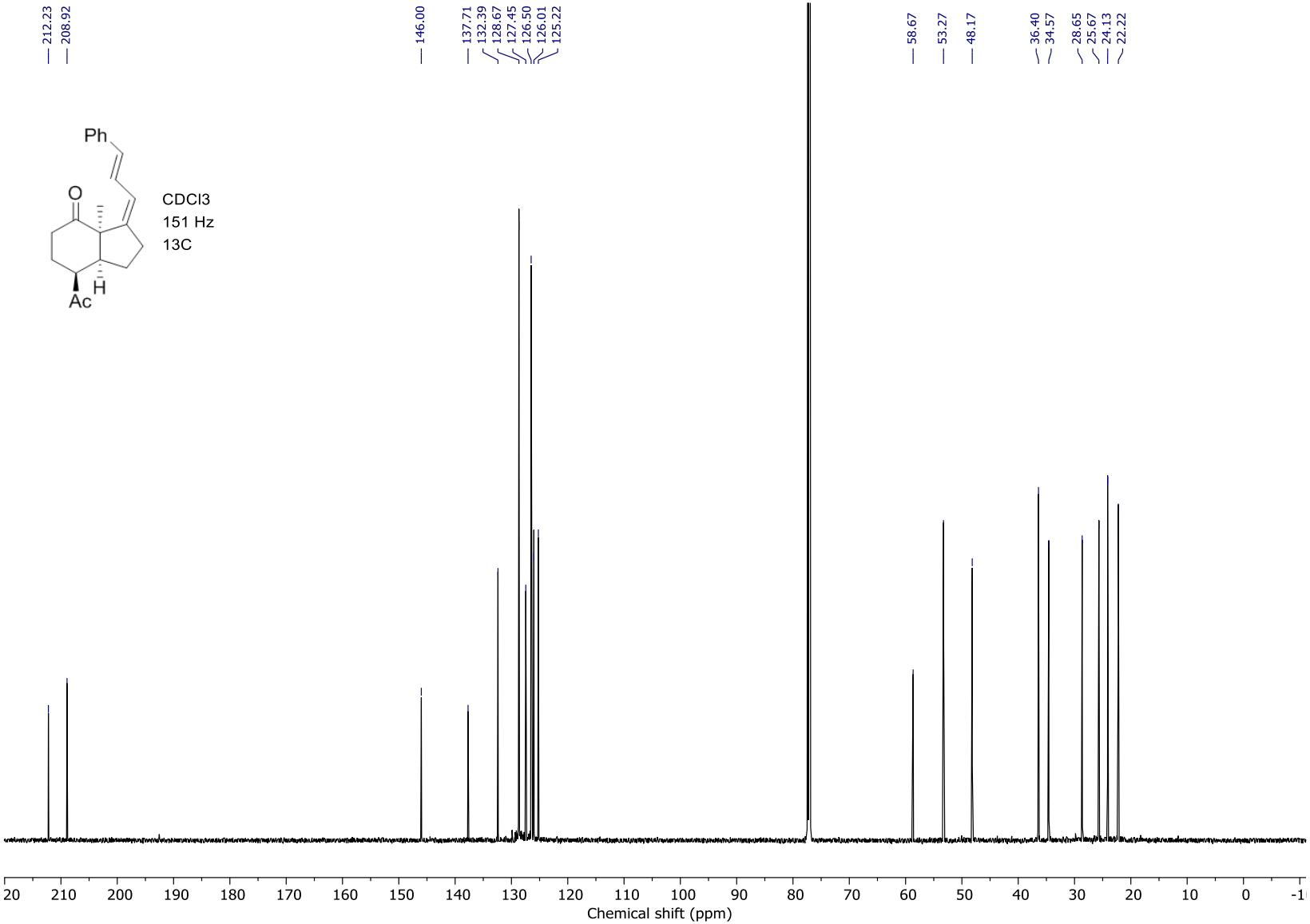
212.23
208.92
146.00
137.71
132.39
128.67
127.45
126.50
126.01
125.22
58.67
53.27
48.17
36.40
34.57
28.65
25.67
24.13
22.22
Ph
O
Ac
H
CDCl3
151 Hz
13C
20
210
200
190
180
170
160
150
140
130
120
110
100
90
80
70
60
50
40
30
20
10
0
Chemical shift (ppm)

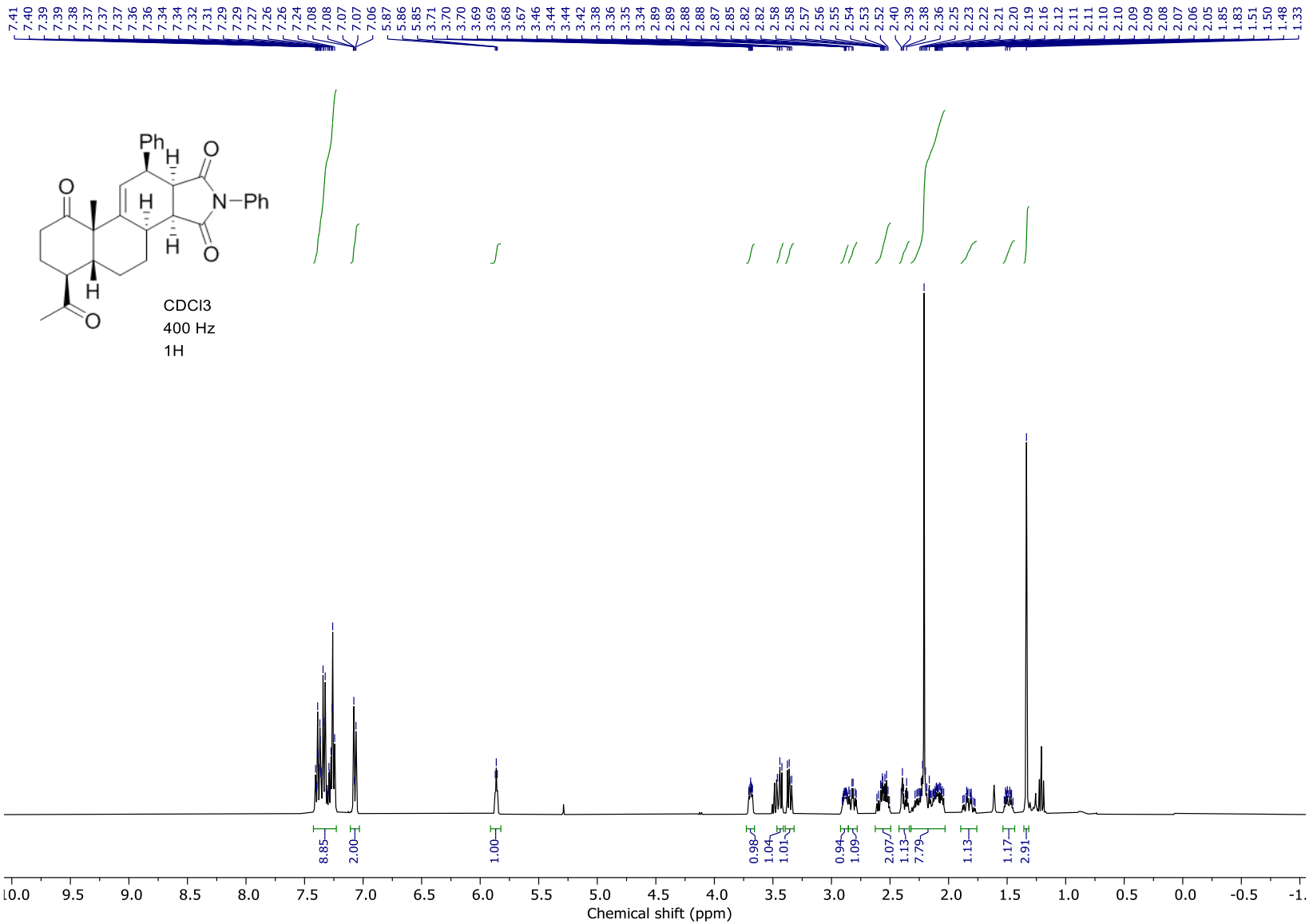
CDCl3
400 Hz
1H
Chemical shift (ppm)

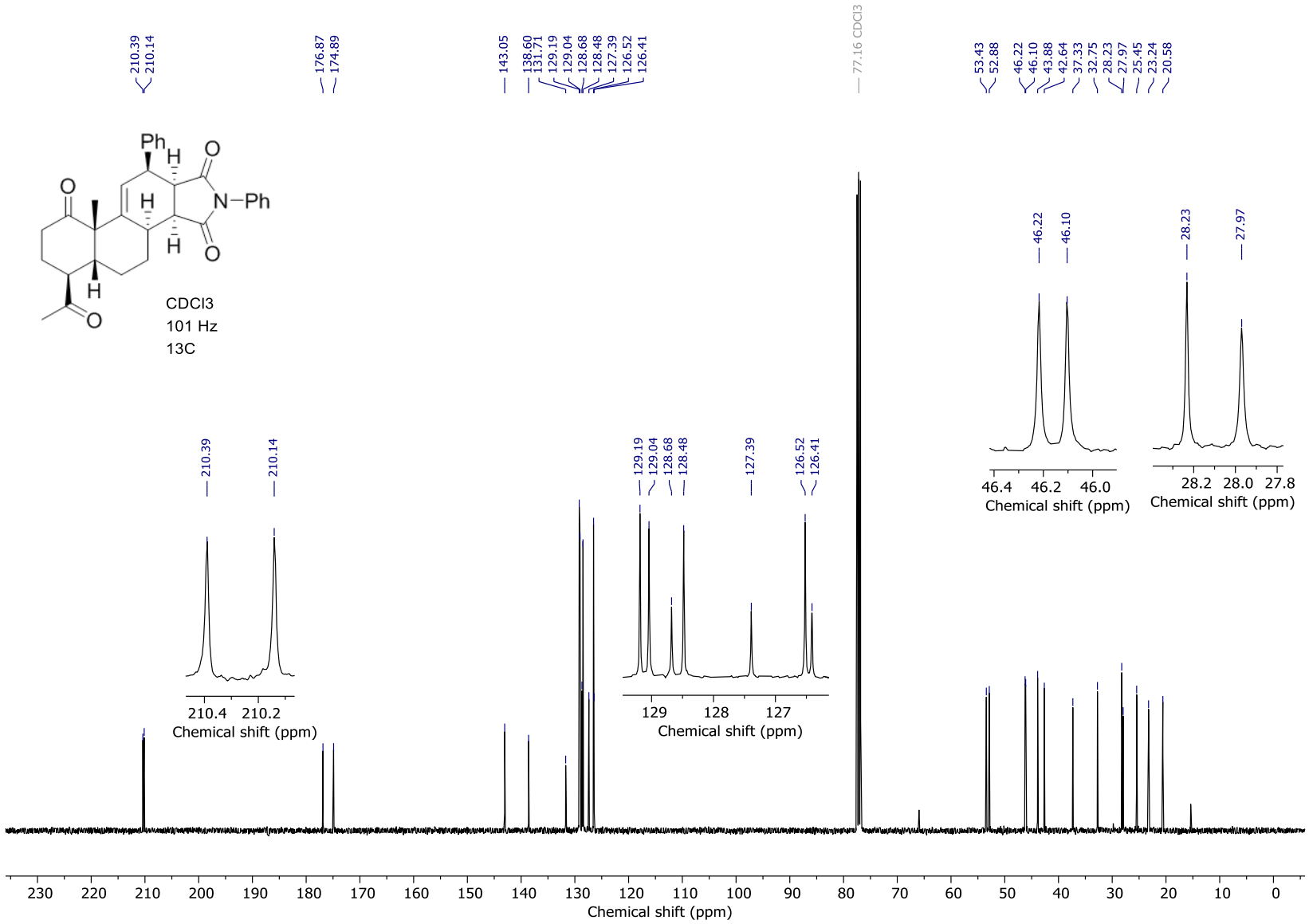
210.39
210.14
176.87
174.89
143.05
138.60
131.71
129.19
129.04
128.68
128.48
127.39
126.52
126.41
77.16 CDCl3
53.43
52.88
46.22
46.10
43.88
42.64
37.33
32.75
28.23
27.97
25.45
23.24
20.58
Ph
H
O
N–Ph
CDCl3
101 Hz
13C
210.4 210.2
Chemical shift (ppm)
129 128 127
Chemical shift (ppm)
46.4 46.2 46.0
Chemical shift (ppm)
28.2 28.0 27.8
Chemical shift (ppm)
230 220 210 200 190 180 170 160 150 140 130 120 110 100 90 80 70 60 50 40 30 20 10 0
Chemical shift (ppm)

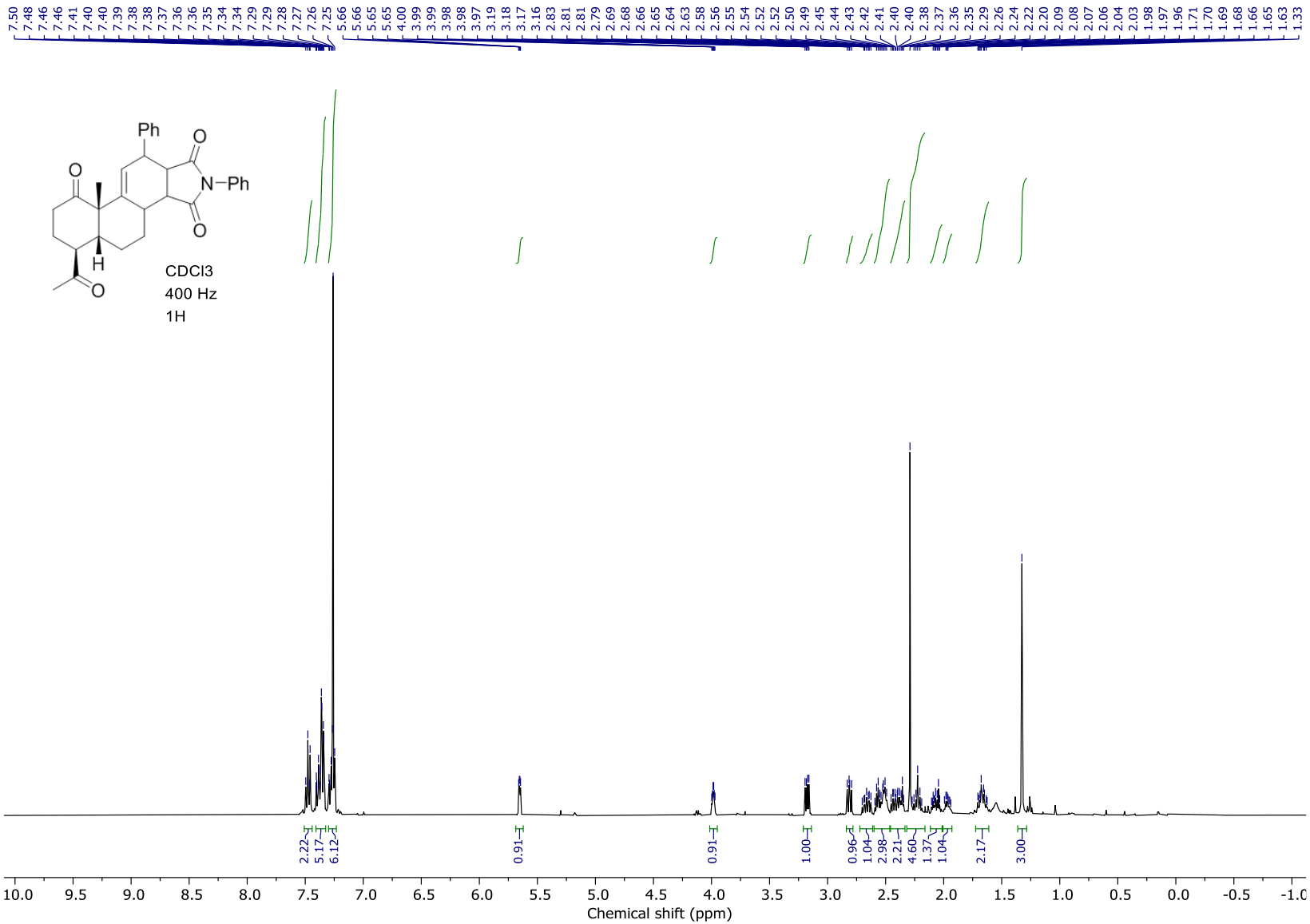
Ph
O
O
N–Ph
O
O
H
O
CDCl3
400 Hz
1H
Chemical shift (ppm)

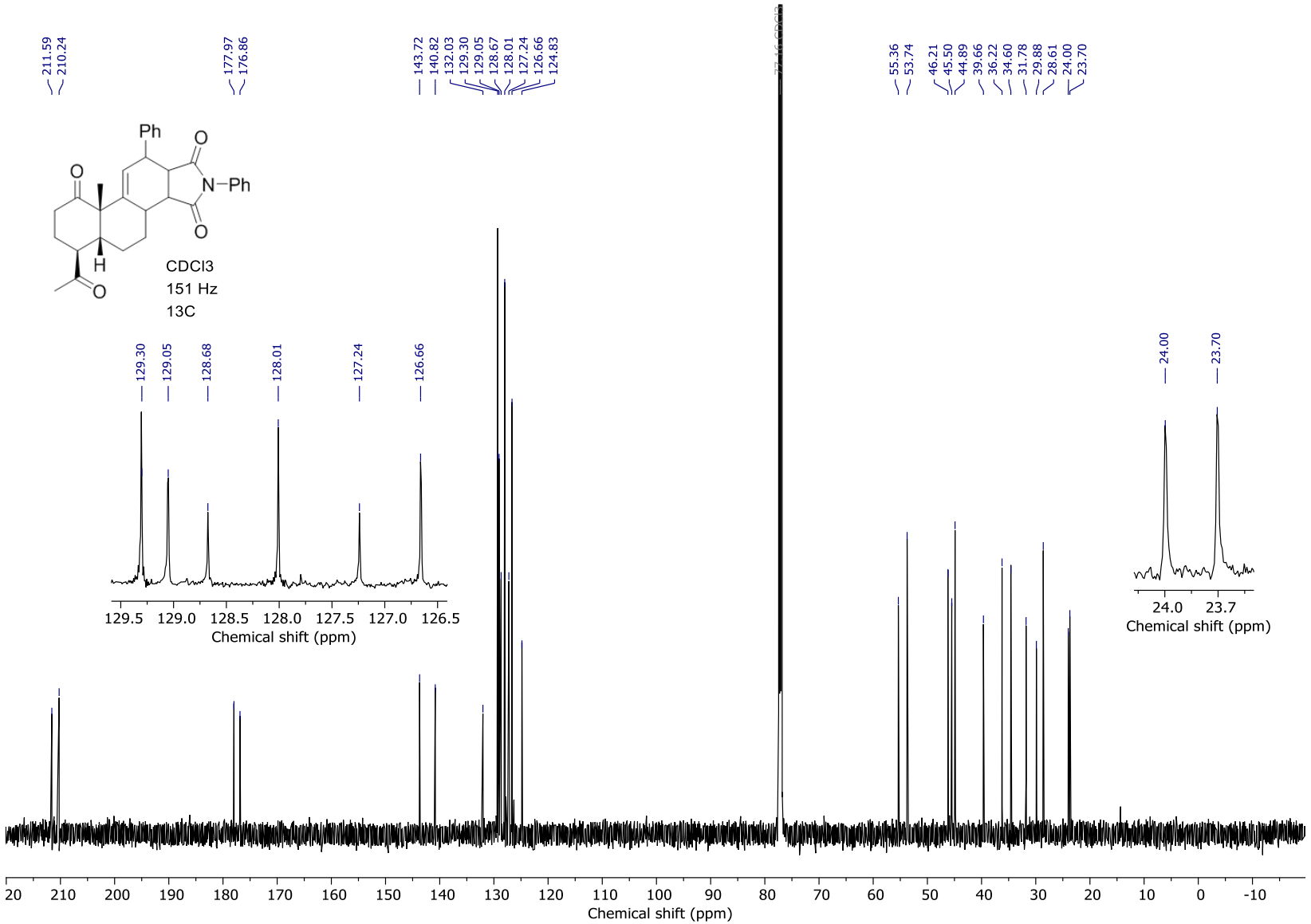
211.59
210.24
177.97
176.86
143.72
140.82
132.03
129.30
129.05
128.67
128.01
127.24
126.66
124.83
55.36
53.74
46.21
45.50
44.89
39.66
36.22
34.60
31.78
29.88
28.61
24.00
23.70
Ph
O
O
N–Ph
O
H
O
CDCl3
151 Hz
13C
129.30
129.05
128.68
128.01
127.24
126.66
129.5 129.0 128.5 128.0 127.5 127.0 126.5
Chemical shift (ppm)
24.00
23.70
24.0 23.7
Chemical shift (ppm)
20 210 200 190 180 170 160 150 140 130 120 110 100 90 80 70 60 50 40 30 20 10 0 -10
Chemical shift (ppm)

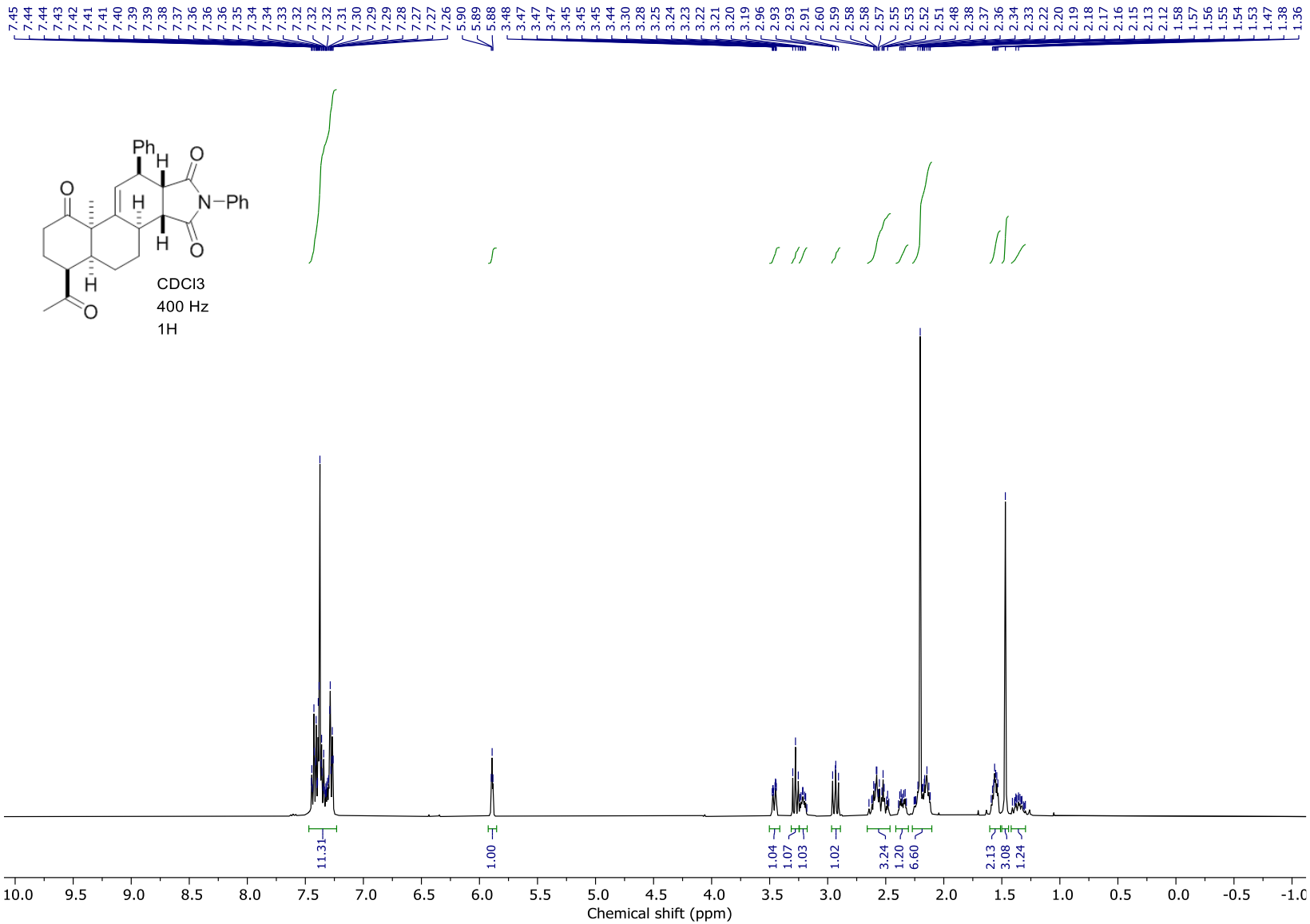
CDCl3
400 Hz
1H
11.31
1.00
1.04
1.07
1.03
1.02
3.24
1.20
6.60
2.13
3.08
1.24
Chemical shift (ppm)

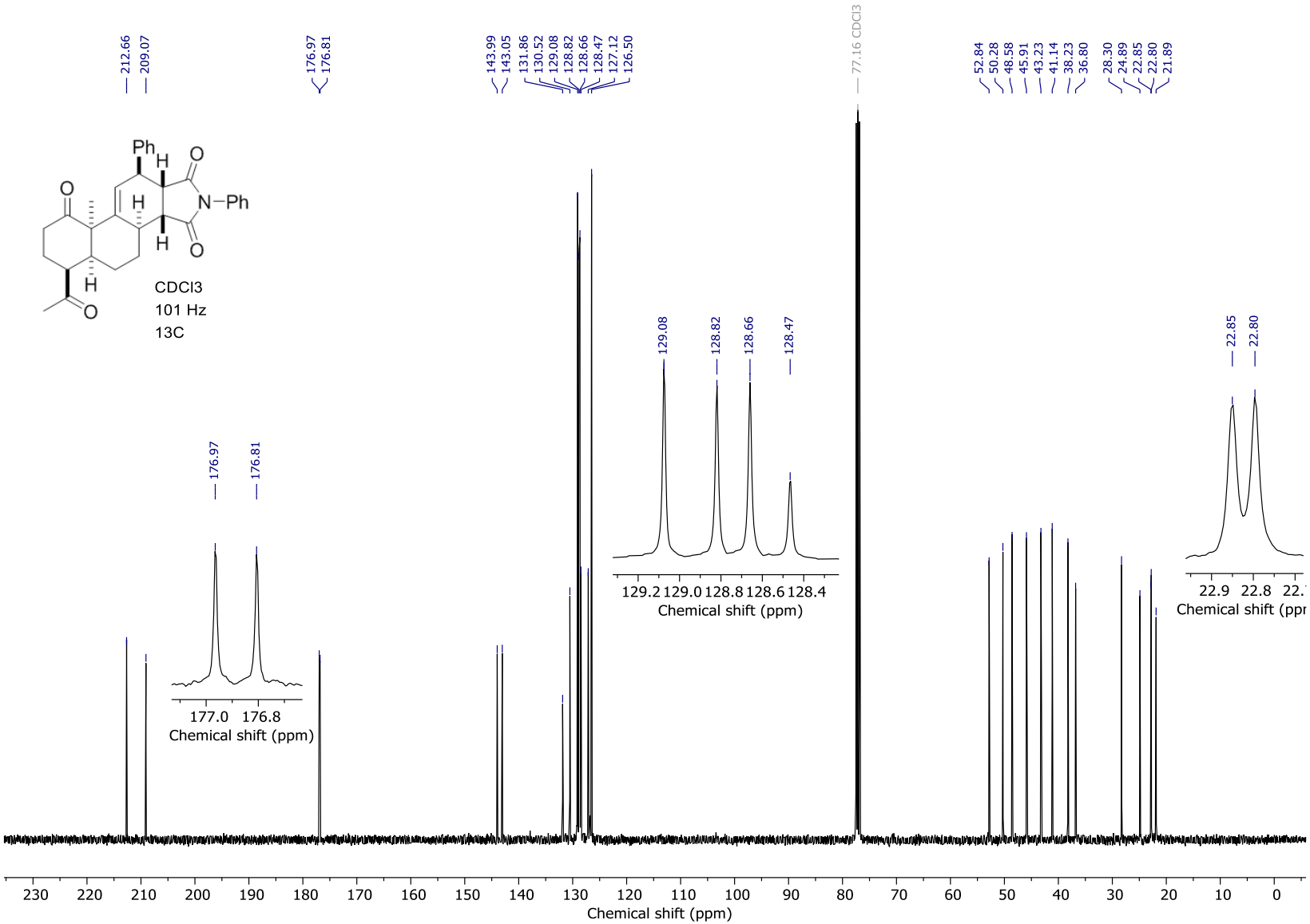
212.66
209.07
176.97
176.81
143.99
143.05
131.86
130.52
129.08
128.82
128.66
128.47
127.12
126.50
77.16 CDCl3
52.84
50.28
48.58
45.91
43.23
41.14
38.23
36.80
28.30
24.89
22.85
22.80
21.89
Ph
H
O
N–Ph
CDCl3
101 Hz
13C
177.0 176.8
Chemical shift (ppm)
129.2 129.0 128.8 128.6 128.4
Chemical shift (ppm)
22.9 22.8
Chemical shift (ppm)
230 220 210 200 190 180 170 160 150 140 130 120 110 100 90 80 70 60 50 40 30 20 10 0
Chemical shift (ppm)

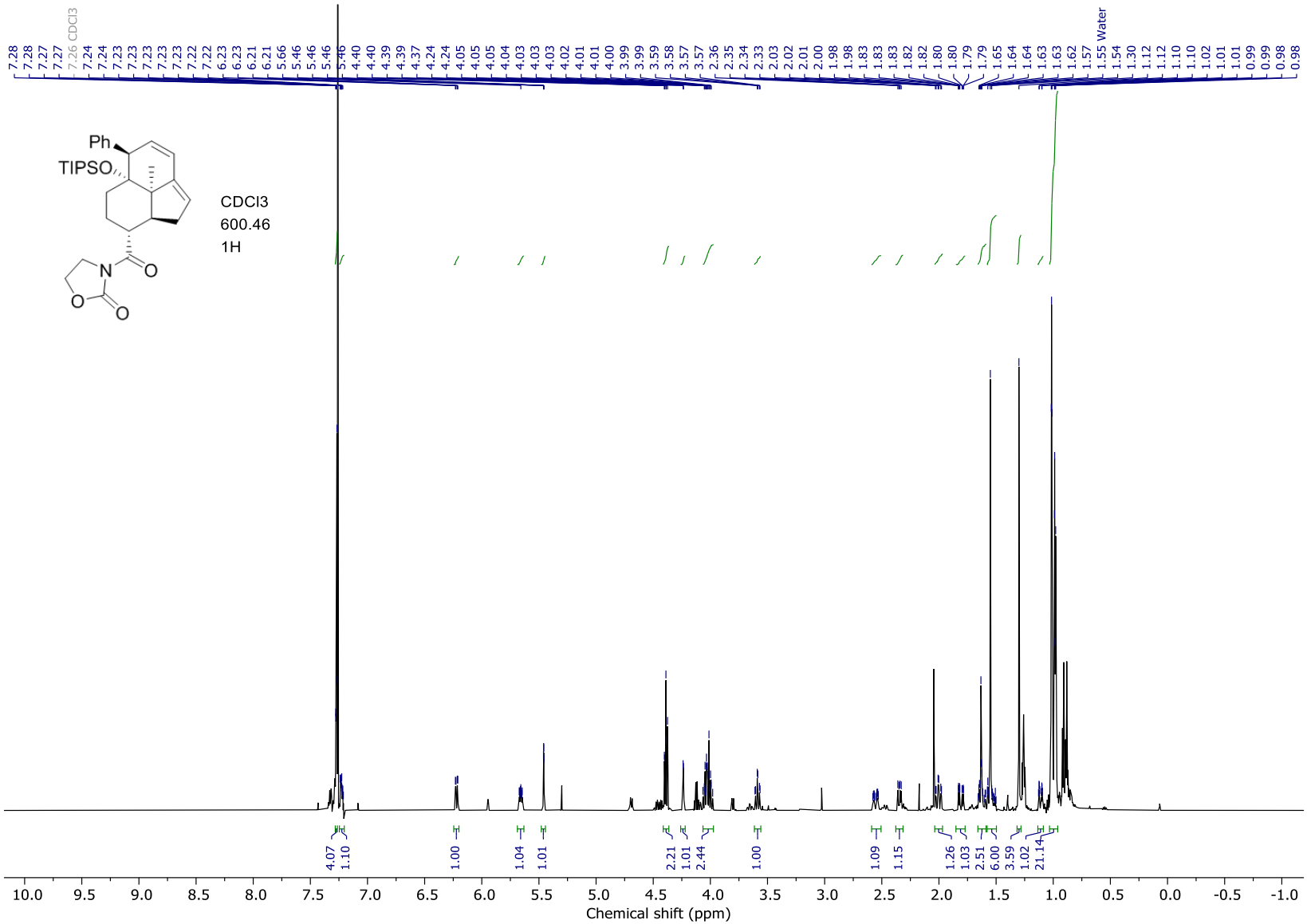
Ph
TIPSO
N
O
O
O
CDCl3
600.46
1H
Water
Chemical shift (ppm)

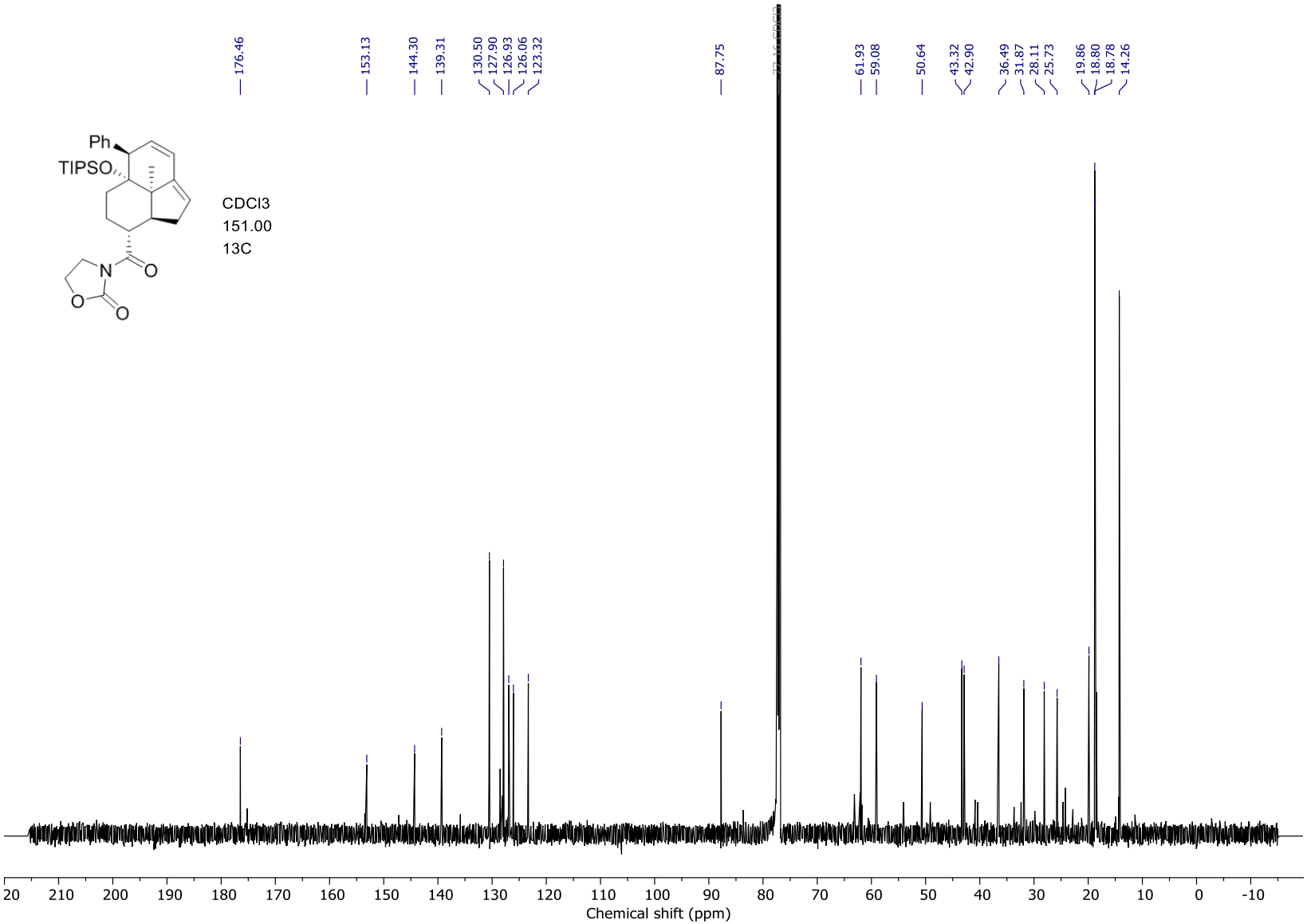
176.46
153.13
144.30
139.31
130.50
127.90
126.93
126.06
123.32
87.75
61.93
59.08
50.64
43.32
42.90
36.49
31.87
28.11
25.73
19.86
18.80
18.78
14.26
Ph
TIPSO
N
O
O
O
CDCl3
151.00
13C
20 210 200 190 180 170 160 150 140 130 120 110 100 90 80 70 60 50 40 30 20 10 0 -10
Chemical shift (ppm)

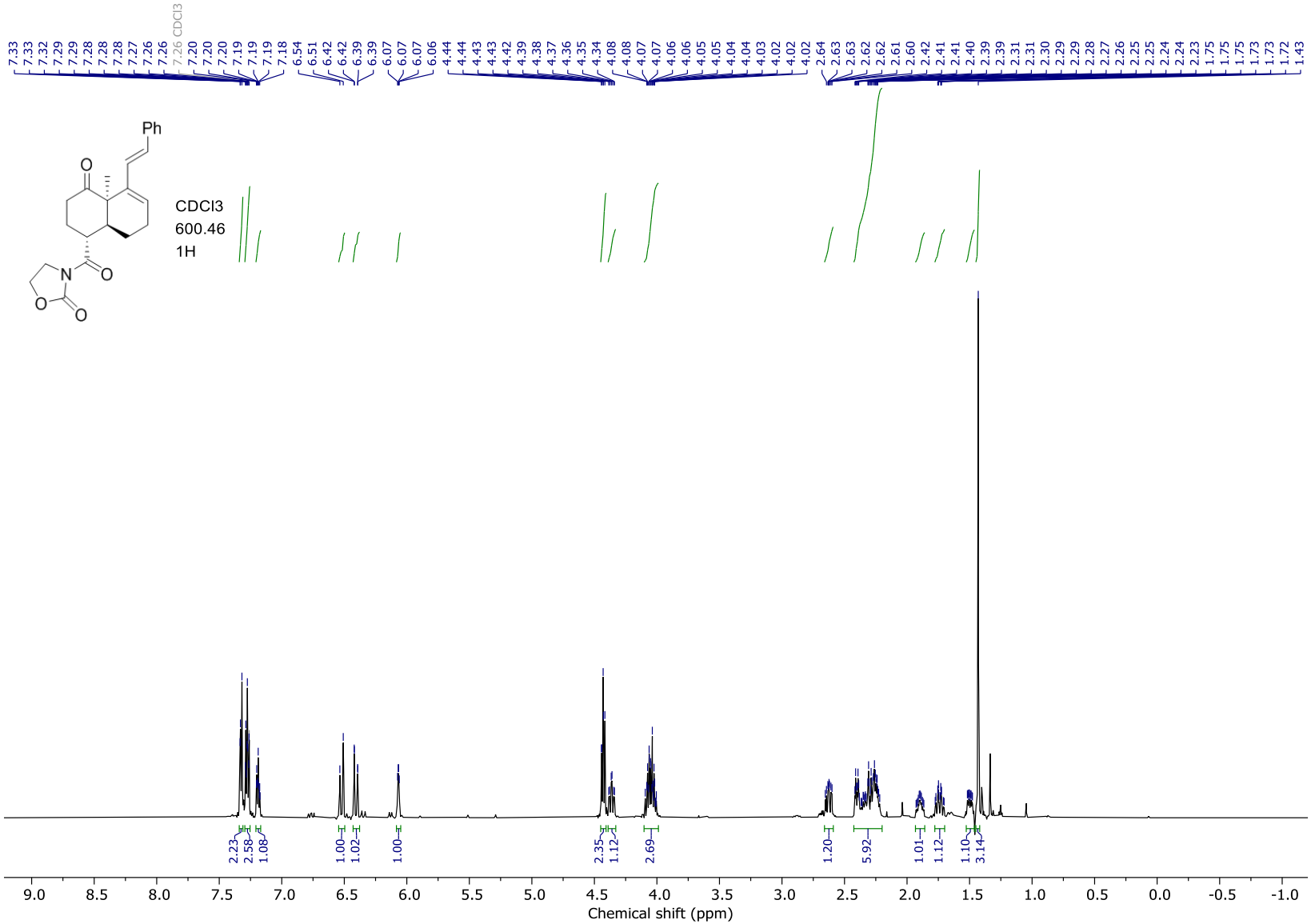
Ph
O
O
N
O
O
O
CDCl3
600.46
1H
7.33 7.33 7.32 7.29 7.29 7.28 7.28 7.28 7.27 7.26 7.26 7.26 CDCl3 7.20 7.20 7.20 7.19 7.19 7.19 7.18 6.54 6.51 6.42 6.42 6.39 6.39 6.07 6.07 6.07 6.06 4.44 4.44 4.43 4.43 4.42 4.39 4.38 4.37 4.36 4.35 4.34 4.08 4.08 4.07 4.07 4.06 4.06 4.05 4.05 4.04 4.04 4.03 4.02 4.02 4.02 2.64 2.63 2.63 2.62 2.62 2.61 2.60 2.42 2.41 2.41 2.40 2.39 2.39 2.31 2.31 2.30 2.29 2.29 2.28 2.27 2.26 2.25 2.25 2.24 2.24 2.23 1.75 1.75 1.75 1.73 1.73 1.72 1.43
2.23 2.58 1.08 1.00 1.02 1.00 2.35 1.12 2.69 1.20 5.92 1.01 1.12 1.10 3.14
9.0 8.5 8.0 7.5 7.0 6.5 6.0 5.5 5.0 4.5 4.0 3.5 3.0 2.5 2.0 1.5 1.0 0.5 0.0 -0.5 -1.0
Chemical shift (ppm)

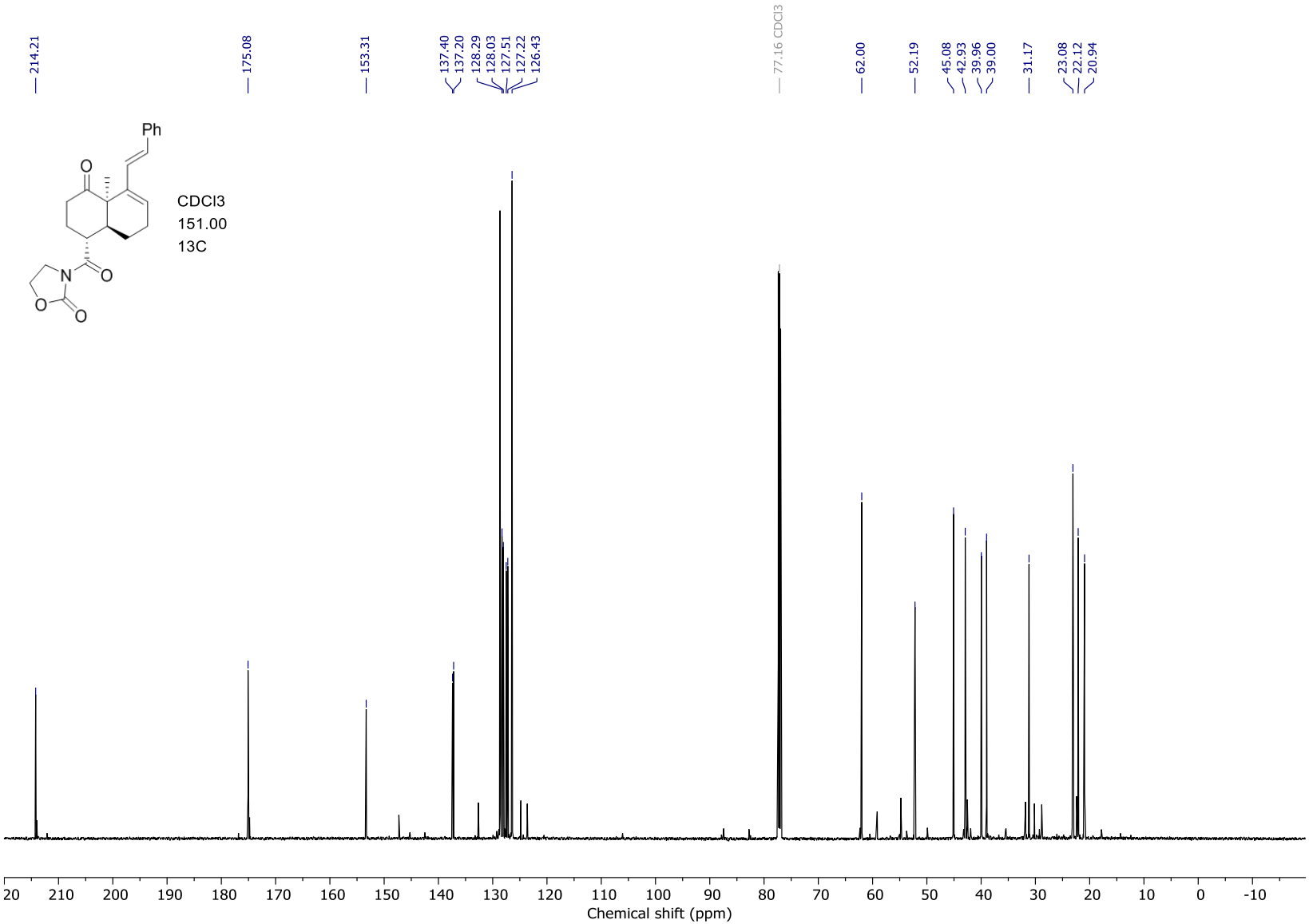
214.21
175.08
153.31
137.40
137.20
128.29
128.03
127.51
127.22
126.43
77.16 CDCl3
62.00
52.19
45.08
42.93
39.96
39.00
31.17
23.08
22.12
20.94
Ph
O
N
O
O
O
CDCl3
151.00
13C
20 210 200 190 180 170 160 150 140 130 120 110 100 90 80 70 60 50 40 30 20 10 0 -10
Chemical shift (ppm)

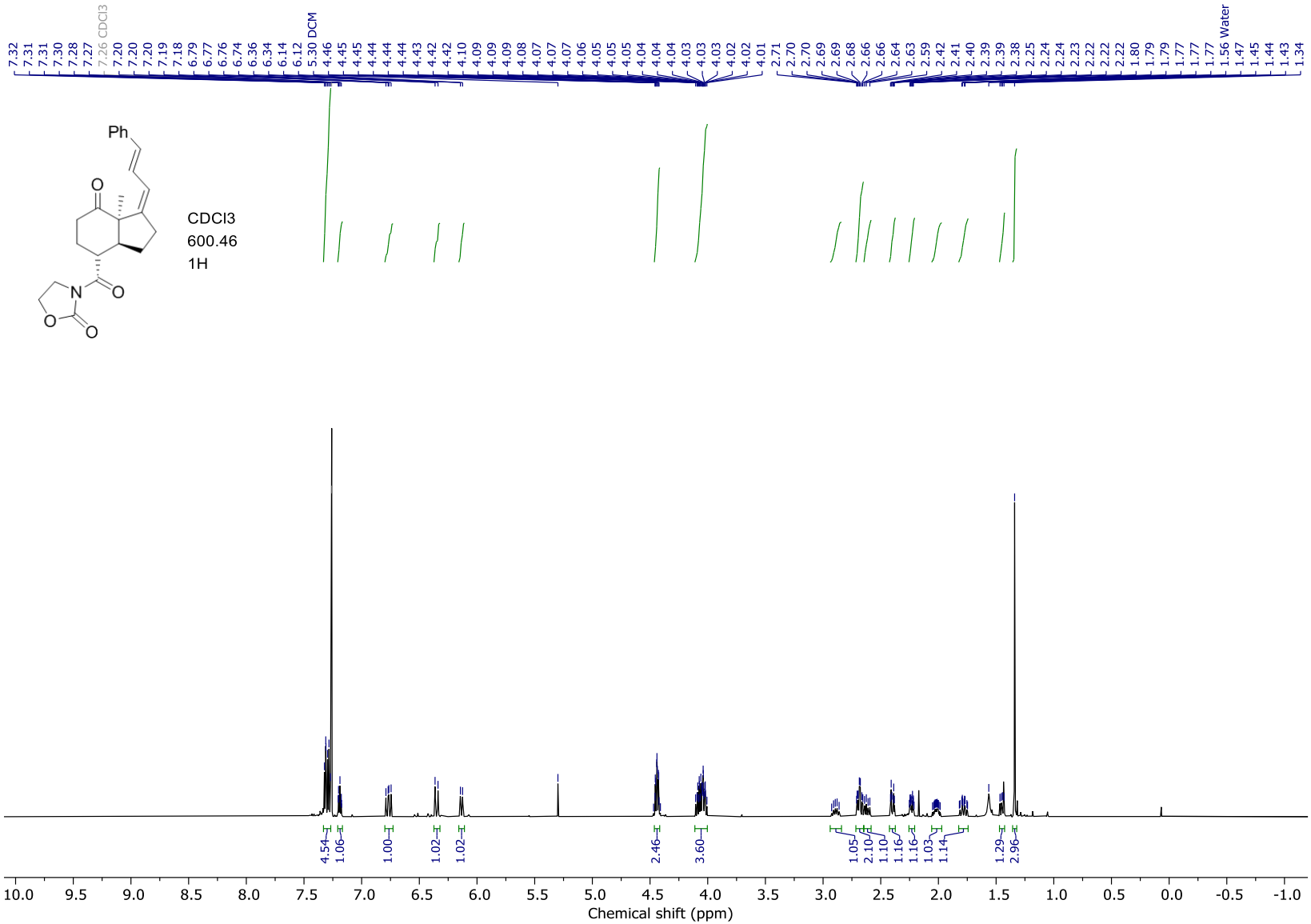
7.32 7.31 7.31 7.30 7.28 7.27 7.26 CDCl3 7.20 7.20 7.20 7.19 7.18 6.79 6.77 6.76 6.74 6.36 6.34 6.14 6.12 5.30 DCM 4.46 4.45 4.45 4.44 4.44 4.43 4.42 4.42 4.10 4.09 4.09 4.09 4.08 4.07 4.07 4.07 4.06 4.05 4.05 4.05 4.04 4.04 4.04 4.03 4.03 4.03 4.02 4.02 4.01 2.71 2.70 2.70 2.69 2.69 2.68 2.66 2.66 2.64 2.63 2.59 2.42 2.41 2.40 2.39 2.39 2.38 2.25 2.24 2.24 2.23 2.22 2.22 1.80 1.79 1.79 1.77 1.77 1.77 1.56 Water 1.47 1.45 1.44 1.43 1.34
Ph
O
N
O
O
O
CDCl3
600.46
1H
4.54
1.06
1.00
1.02
1.02
2.46
3.60
1.05
2.10
1.10
1.16
1.03
1.14
1.29
2.96
10.0 9.5 9.0 8.5 8.0 7.5 7.0 6.5 6.0 5.5 5.0 4.5 4.0 3.5 3.0 2.5 2.0 1.5 1.0 0.5 0.0 -0.5 -1.0
Chemical shift (ppm)

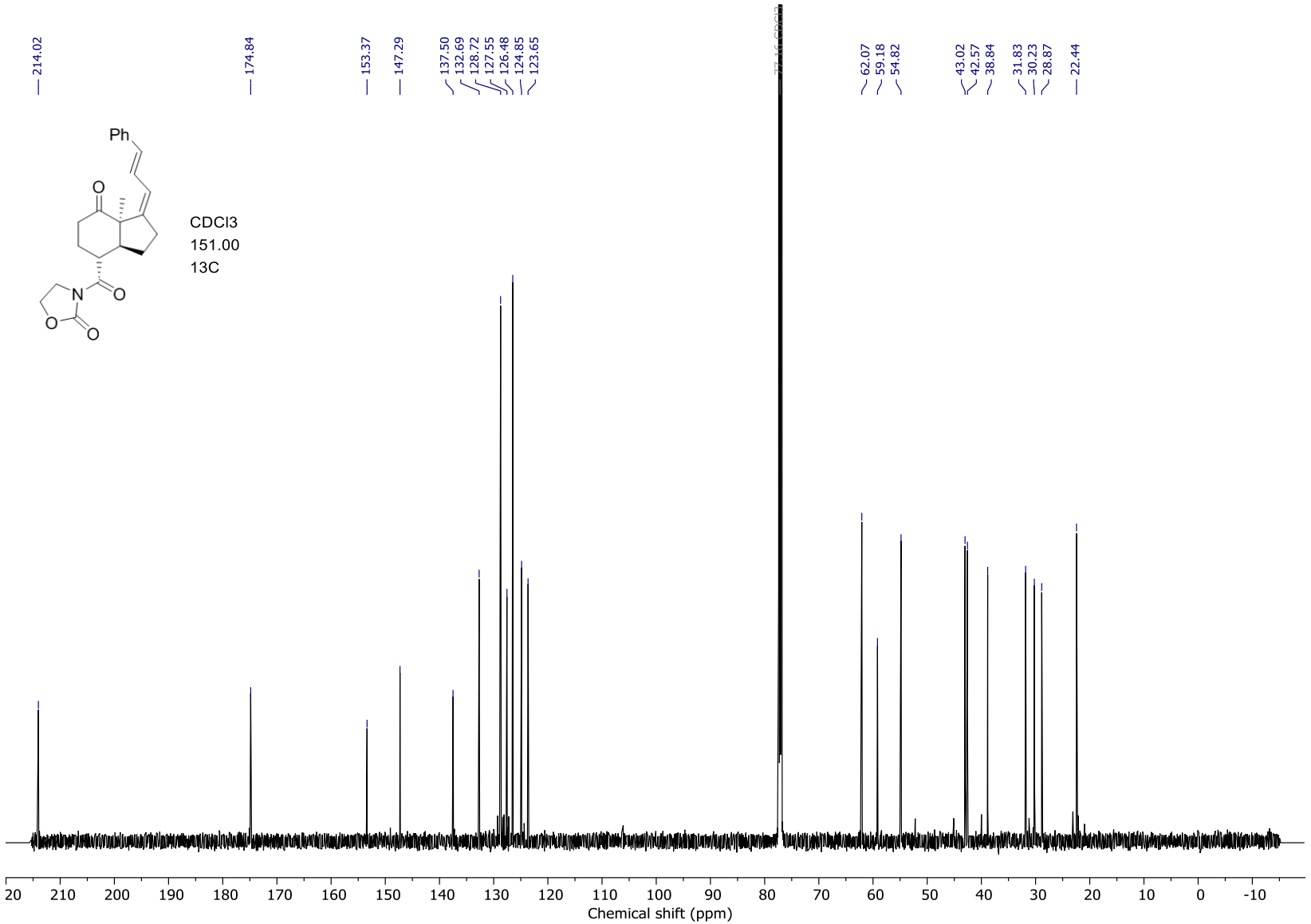
214.02
174.84
153.37
147.29
137.50
132.69
128.72
127.55
126.48
124.85
123.65
77.16
62.07
59.18
54.82
43.02
42.57
38.84
31.83
30.23
28.87
22.44
Ph
O
N
O
O
O
CDCl3
151.00
13C
20 210 200 190 180 170 160 150 140 130 120 110 100 90 80 70 60 50 40 30 20 10 0 -10
Chemical shift (ppm)

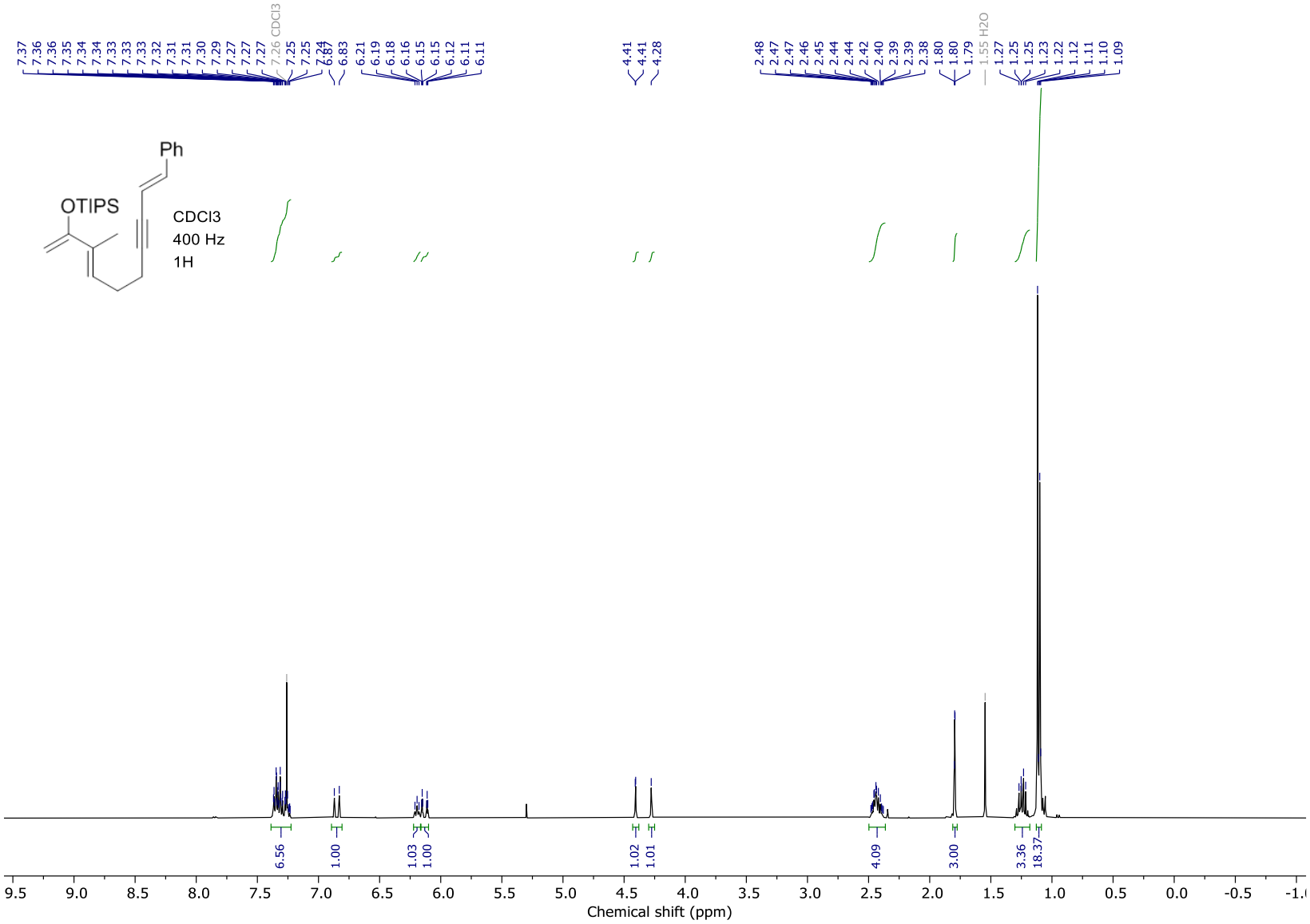
Ph
OTIPS
CDCl3
400 Hz
1H
7.26 CDCl3
1.55 H2O
6.56
1.00
1.03
1.00
1.02
1.01
4.09
3.00
3.36
18.37
Chemical shift (ppm)

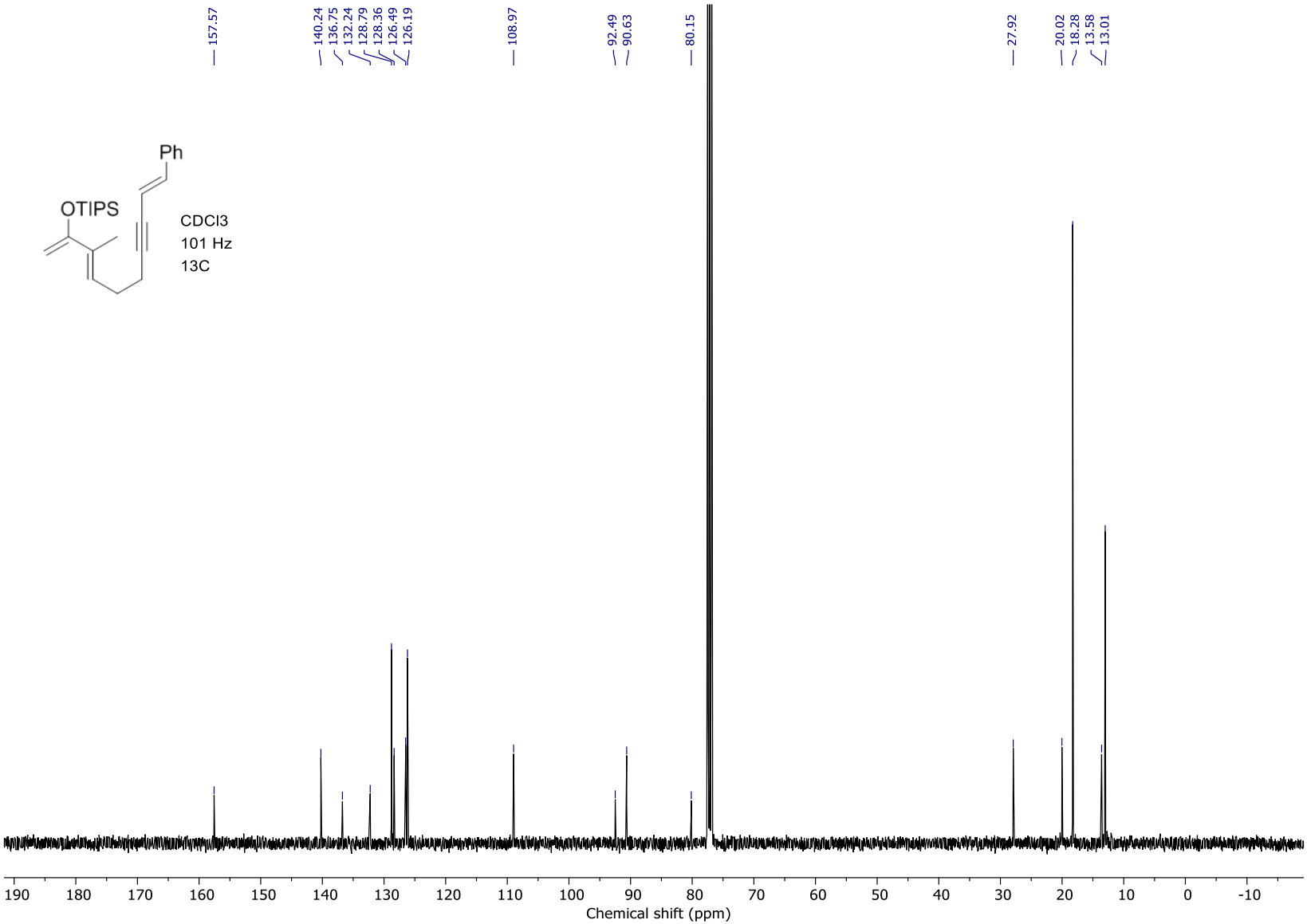
157.57
140.24
136.75
132.24
128.79
128.36
126.49
126.19
108.97
92.49
90.63
80.15
27.92
20.02
18.28
13.58
13.01
Ph
OTIPS
CDCl3
101 Hz
13C
190
180
170
160
150
140
130
120
110
100
90
80
70
60
50
40
30
20
10
0
-10
Chemical shift (ppm)

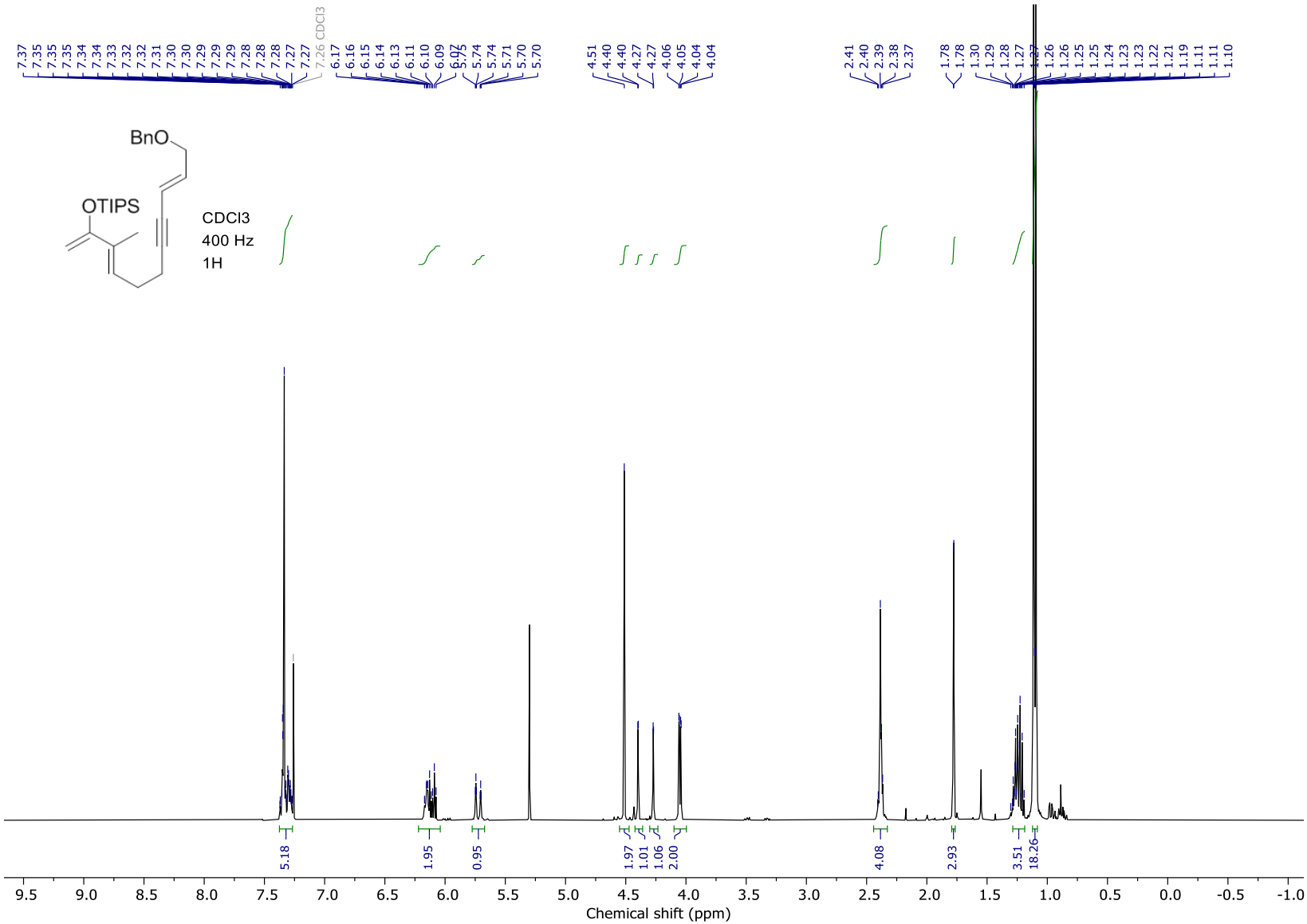
BnO
OTIPS
CDCl3
400 Hz
1H
7.37 7.35 7.35 7.35 7.34 7.34 7.33 7.32 7.32 7.31 7.30 7.30 7.29 7.29 7.29 7.28 7.28 7.28 7.27 7.26 CDCl3
6.17 6.16 6.15 6.14 6.13 6.11 6.10 6.09 6.07 5.75 5.74 5.74 5.71 5.70 5.70
4.51 4.40 4.40 4.27 4.27 4.06 4.05 4.04 4.04
2.41 2.40 2.39 2.38 2.37
1.78 1.78 1.30 1.29 1.28 1.27 1.26 1.26 1.25 1.25 1.24 1.23 1.23 1.22 1.21 1.19 1.11 1.11 1.10
5.18
1.95
0.95
1.97
1.01
1.06
2.00
4.08
2.93
3.51
18.26
9.5 9.0 8.5 8.0 7.5 7.0 6.5 6.0 5.5 5.0 4.5 4.0 3.5 3.0 2.5 2.0 1.5 1.0 0.5 0.0 -0.5 -1.0
Chemical shift (ppm)

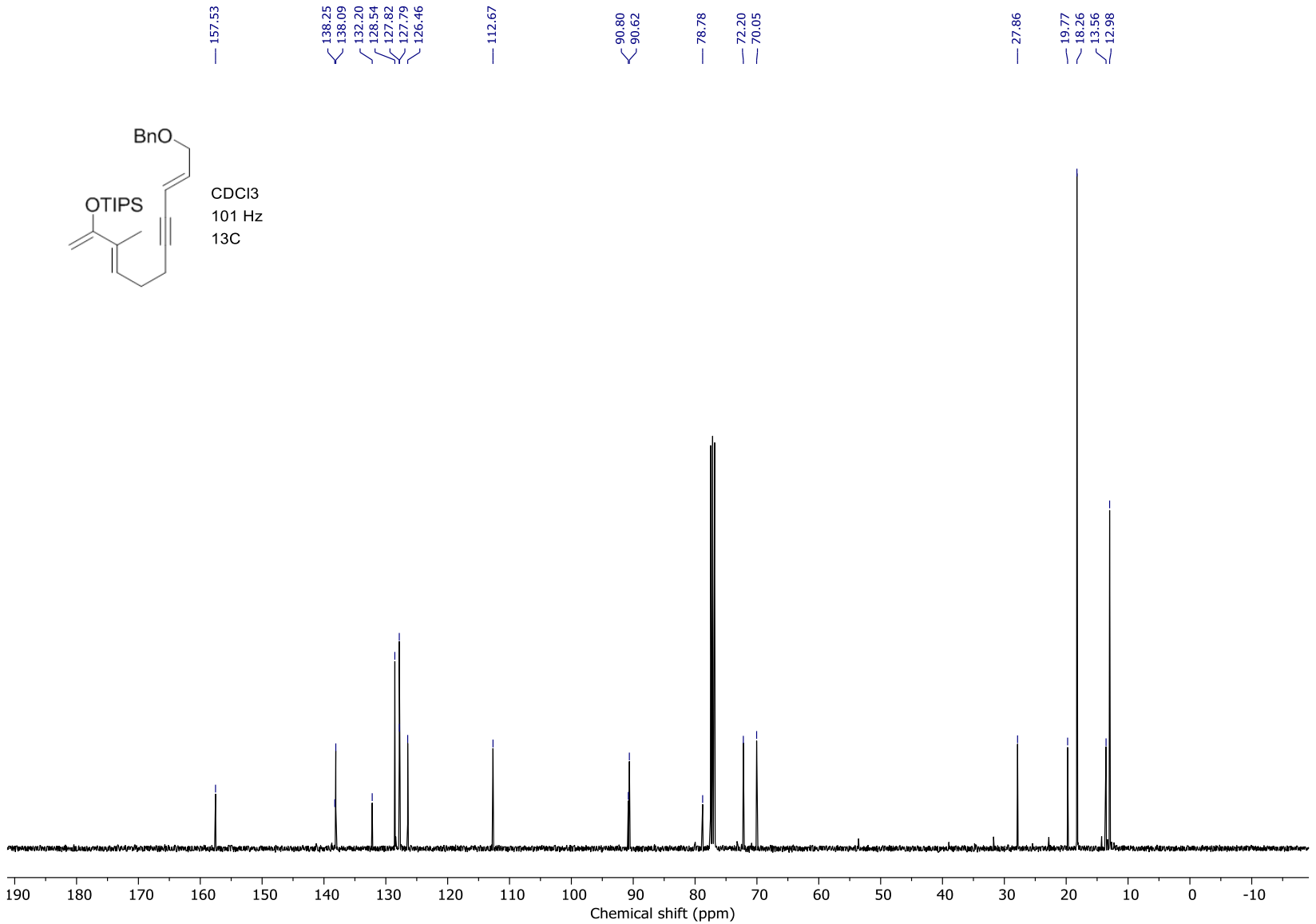
157.53
138.25
138.09
132.20
128.54
127.82
127.79
126.46
112.67
90.80
90.62
78.78
72.20
70.05
27.86
19.77
18.26
13.56
12.98
BnO
OTIPS
CDCl3
101 Hz
13C
190 180 170 160 150 140 130 120 110 100 90 80 70 60 50 40 30 20 10 0 -10
Chemical shift (ppm)

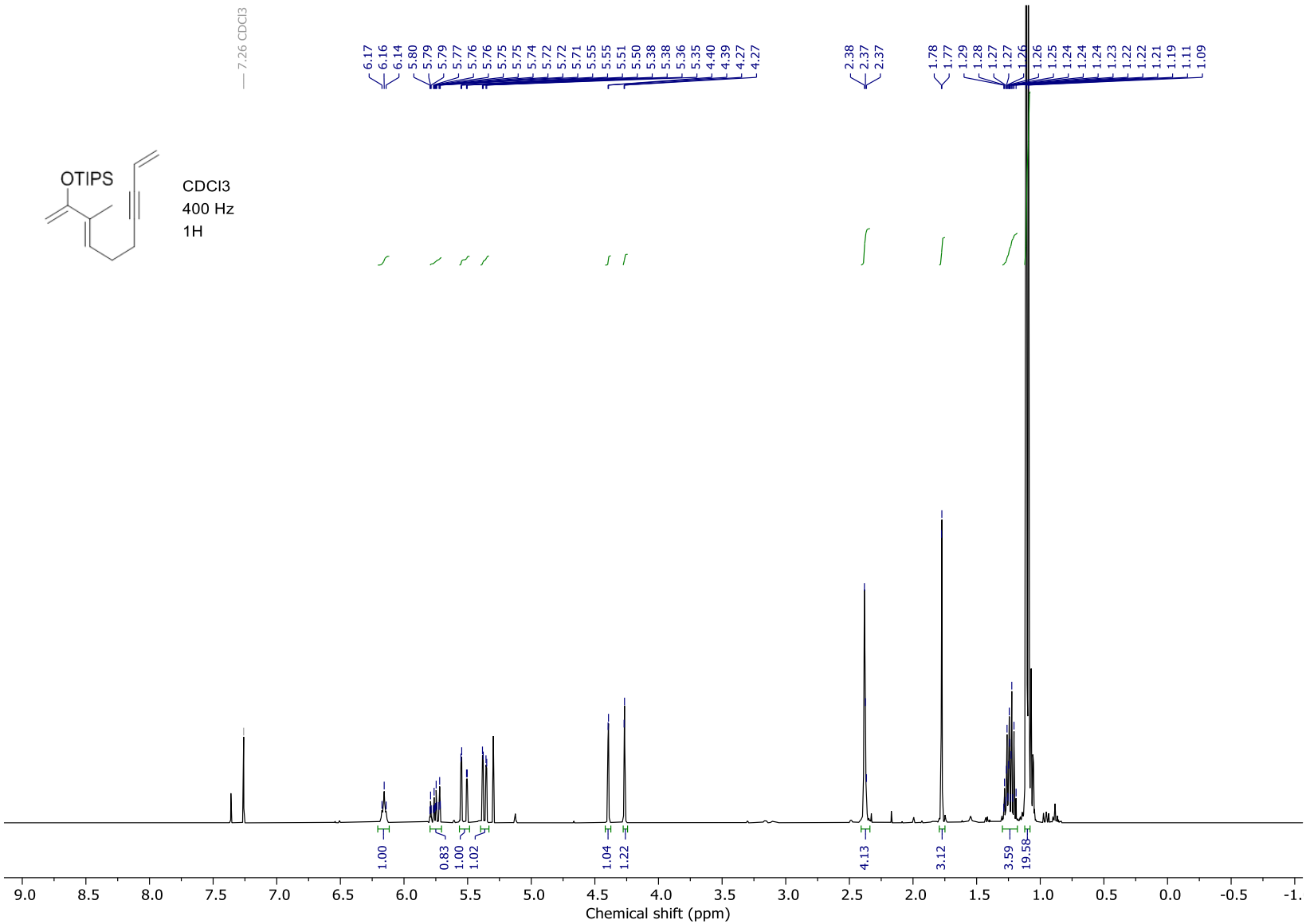
7.26 CDCl3
6.17
6.16
6.14
5.80
5.79
5.79
5.77
5.76
5.76
5.75
5.75
5.74
5.72
5.72
5.71
5.55
5.55
5.51
5.50
5.38
5.38
5.36
5.35
4.40
4.39
4.27
4.27
2.38
2.37
2.37
1.78
1.77
1.29
1.28
1.27
1.27
1.26
1.26
1.25
1.24
1.24
1.24
1.23
1.22
1.22
1.21
1.19
1.11
1.09
OTIPS
CDCl3
400 Hz
1H
1.00
0.83
1.00
1.02
1.04
1.22
4.13
3.12
3.59
19.58
9.0
8.5
8.0
7.5
7.0
6.5
6.0
5.5
5.0
4.5
4.0
3.5
3.0
2.5
2.0
1.5
1.0
0.5
0.0
-0.5
-1.
Chemical shift (ppm)

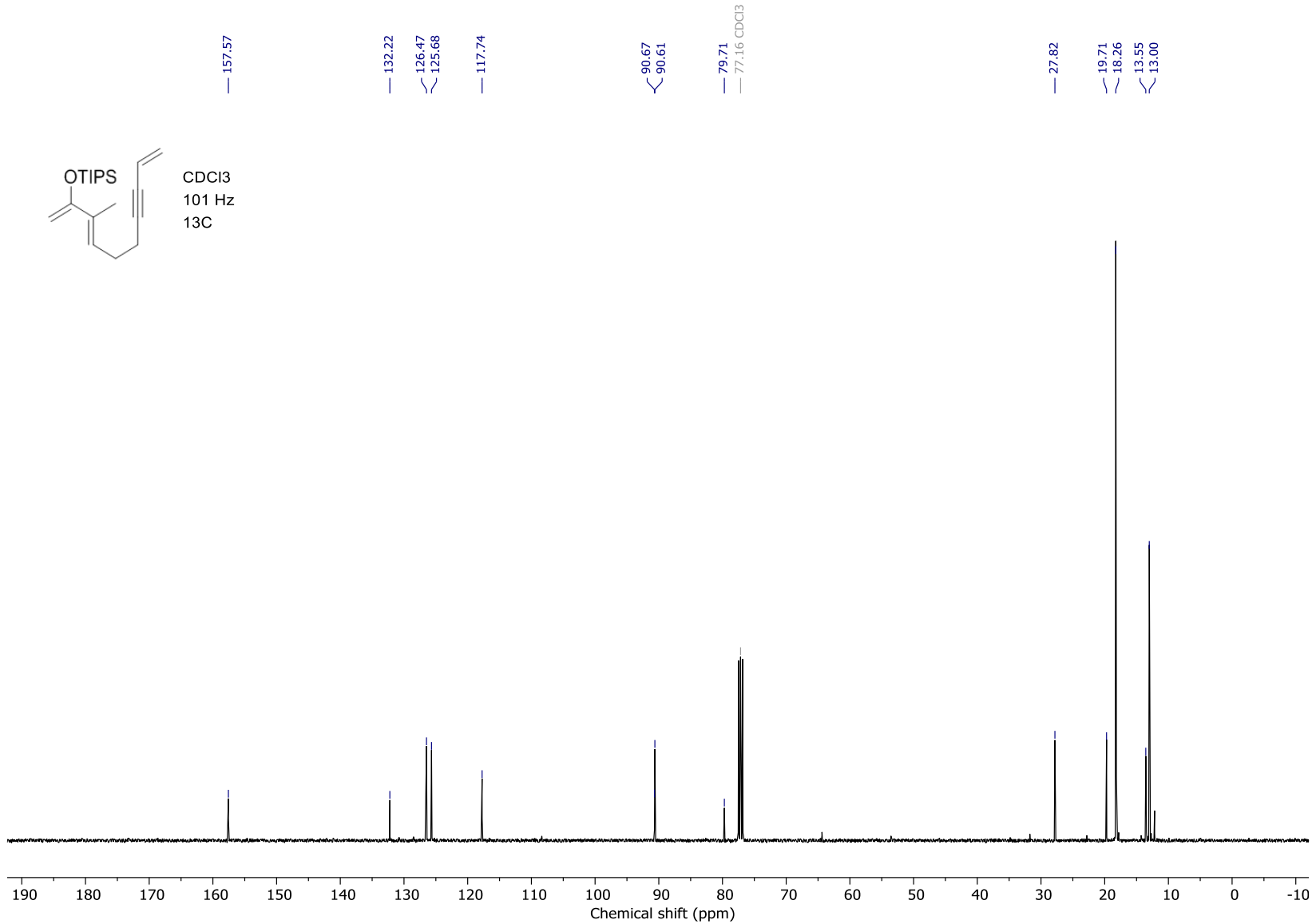
157.57
132.22
126.47
125.68
117.74
90.67
90.61
79.71
77.16 CDCl3
27.82
19.71
18.26
13.55
13.00
OTIPS
CDCl3
101 Hz
13C
190 180 170 160 150 140 130 120 110 100 90 80 70 60 50 40 30 20 10 0 -10
Chemical shift (ppm)

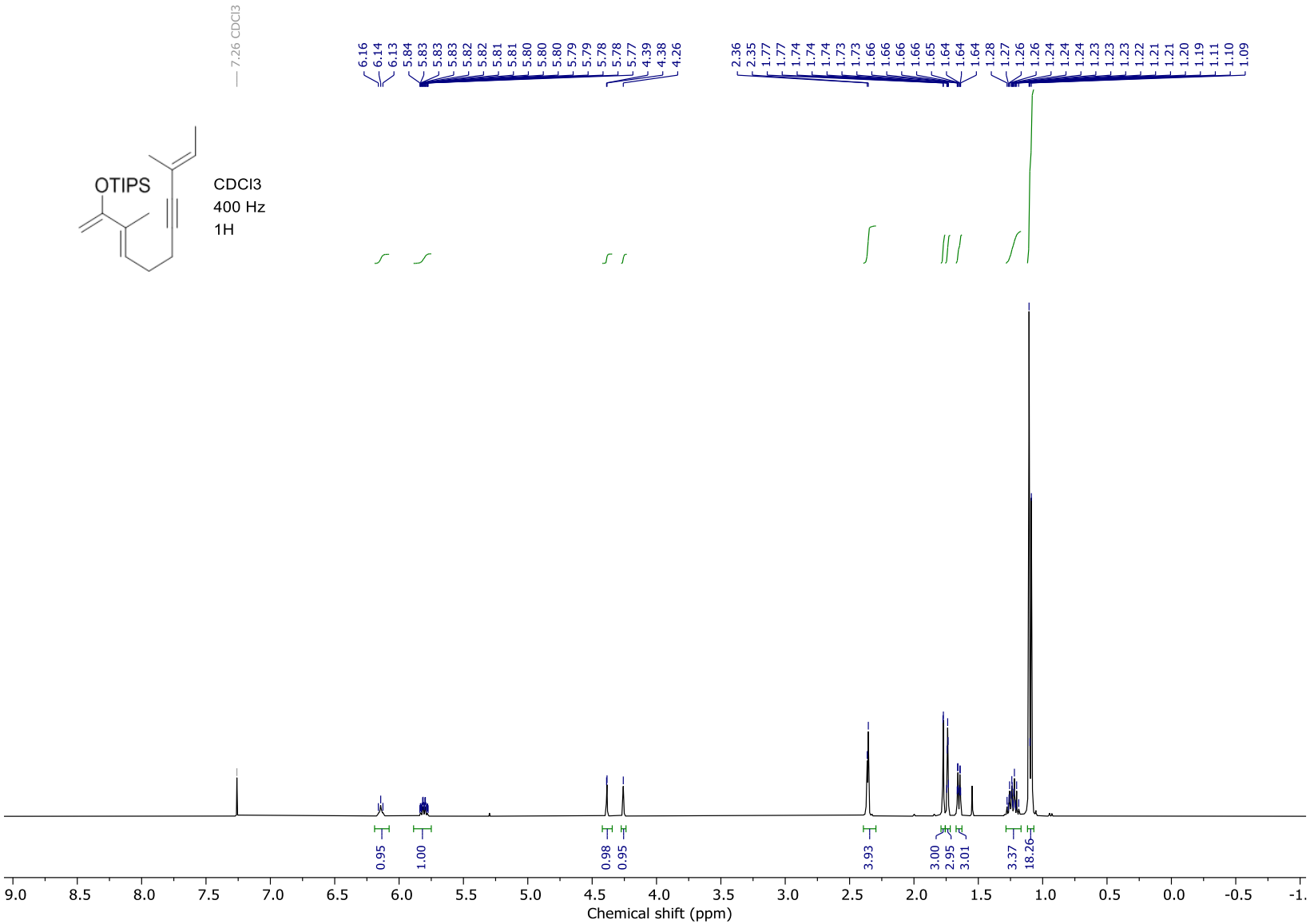
7.26 CDCl3
6.16
6.14
6.13
5.84
5.83
5.83
5.83
5.82
5.82
5.81
5.81
5.80
5.80
5.80
5.79
5.79
5.78
5.78
5.77
4.39
4.38
4.26
2.36
2.35
1.77
1.77
1.74
1.74
1.74
1.73
1.73
1.66
1.66
1.66
1.66
1.65
1.64
1.64
1.64
1.28
1.27
1.26
1.26
1.24
1.24
1.24
1.23
1.23
1.22
1.21
1.21
1.20
1.19
1.11
1.10
1.09
OTIPS
CDCl3
400 Hz
1H
0.95
1.00
0.98
0.95
3.93
3.00
2.95
3.01
3.37
18.26
9.0
8.5
8.0
7.5
7.0
6.5
6.0
5.5
5.0
4.5
4.0
3.5
3.0
2.5
2.0
1.5
1.0
0.5
0.0
-0.5
Chemical shift (ppm)

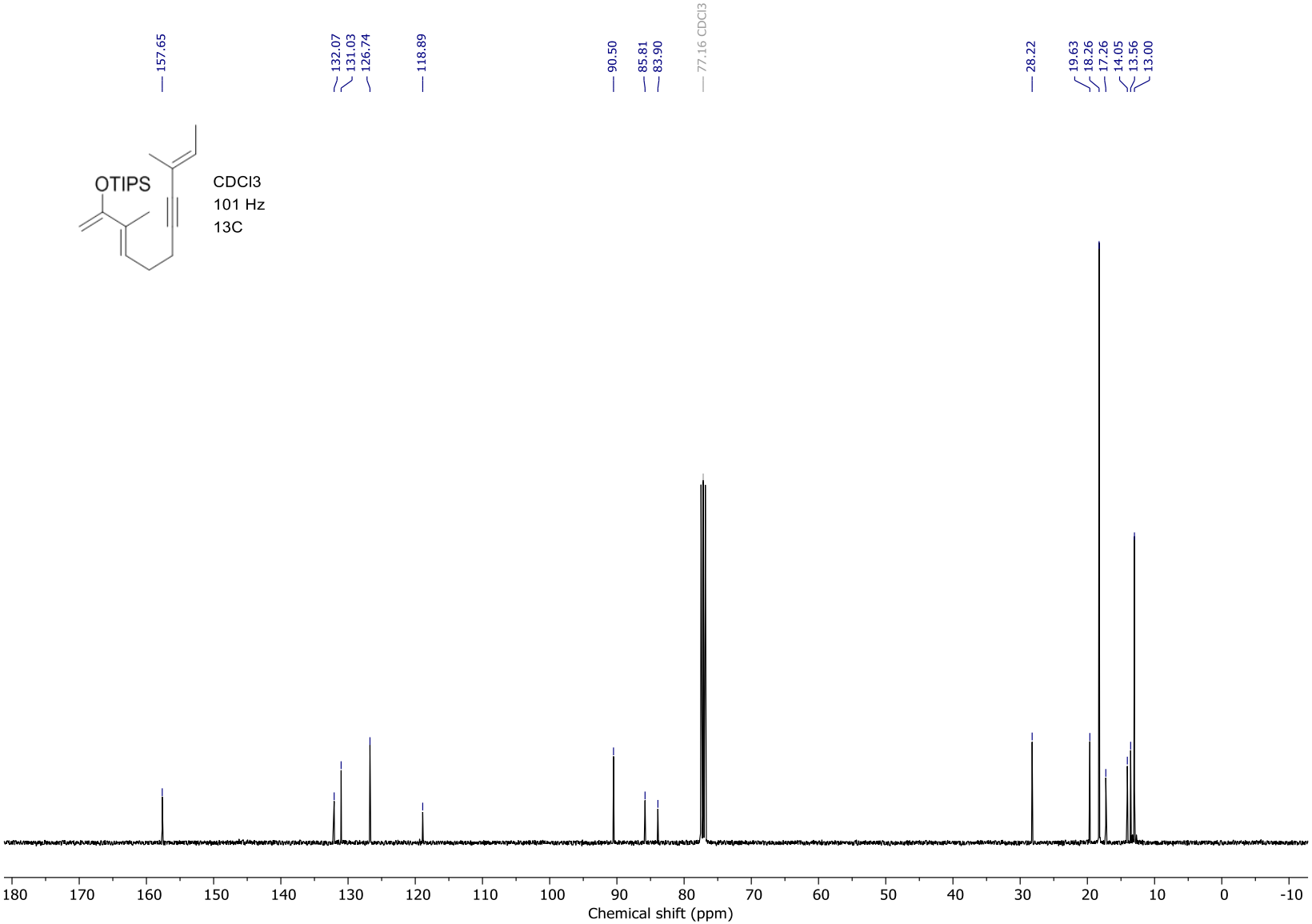
157.65
132.07
131.03
126.74
118.89
90.50
85.81
83.90
77.16 CDCl3
28.22
19.63
18.26
17.26
14.05
13.56
13.00
OTIPS
CDCl3
101 Hz
13C
180
170
160
150
140
130
120
110
100
90
80
70
60
50
40
30
20
10
0
-10
Chemical shift (ppm)

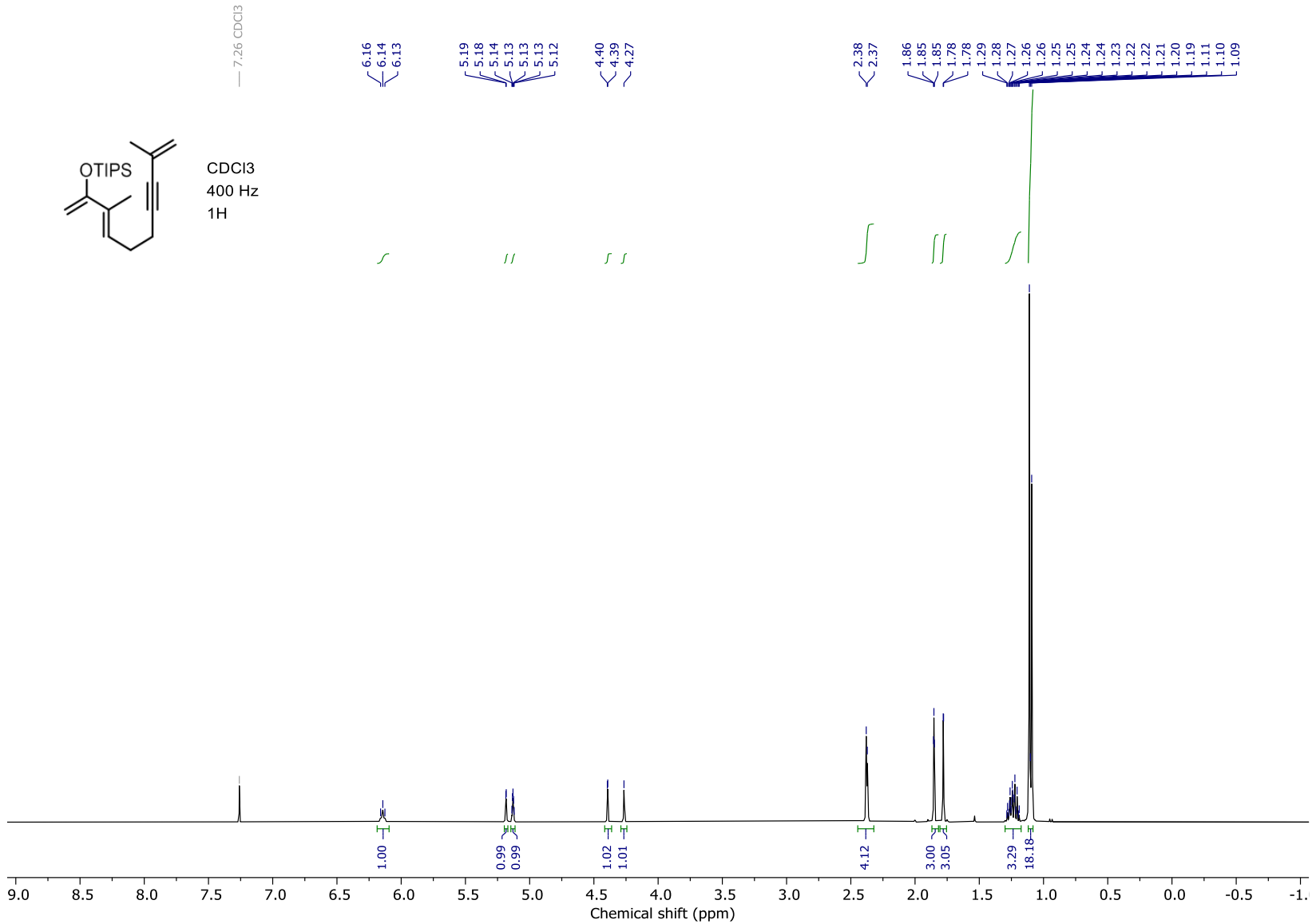
OTIPS
CDCl3
400 Hz
1H
7.26 CDCl3
6.16
6.14
6.13
5.19
5.18
5.14
5.13
5.13
5.13
5.12
4.40
4.39
4.27
2.38
2.37
1.86
1.85
1.85
1.78
1.78
1.29
1.28
1.27
1.26
1.26
1.25
1.24
1.24
1.23
1.22
1.22
1.21
1.20
1.19
1.11
1.10
1.09
1.00
0.99
0.99
1.02
1.01
4.12
3.00
3.05
3.29
18.18
9.0
8.5
8.0
7.5
7.0
6.5
6.0
5.5
5.0
4.5
4.0
3.5
3.0
2.5
2.0
1.5
1.0
0.5
0.0
-0.5
Chemical shift (ppm)

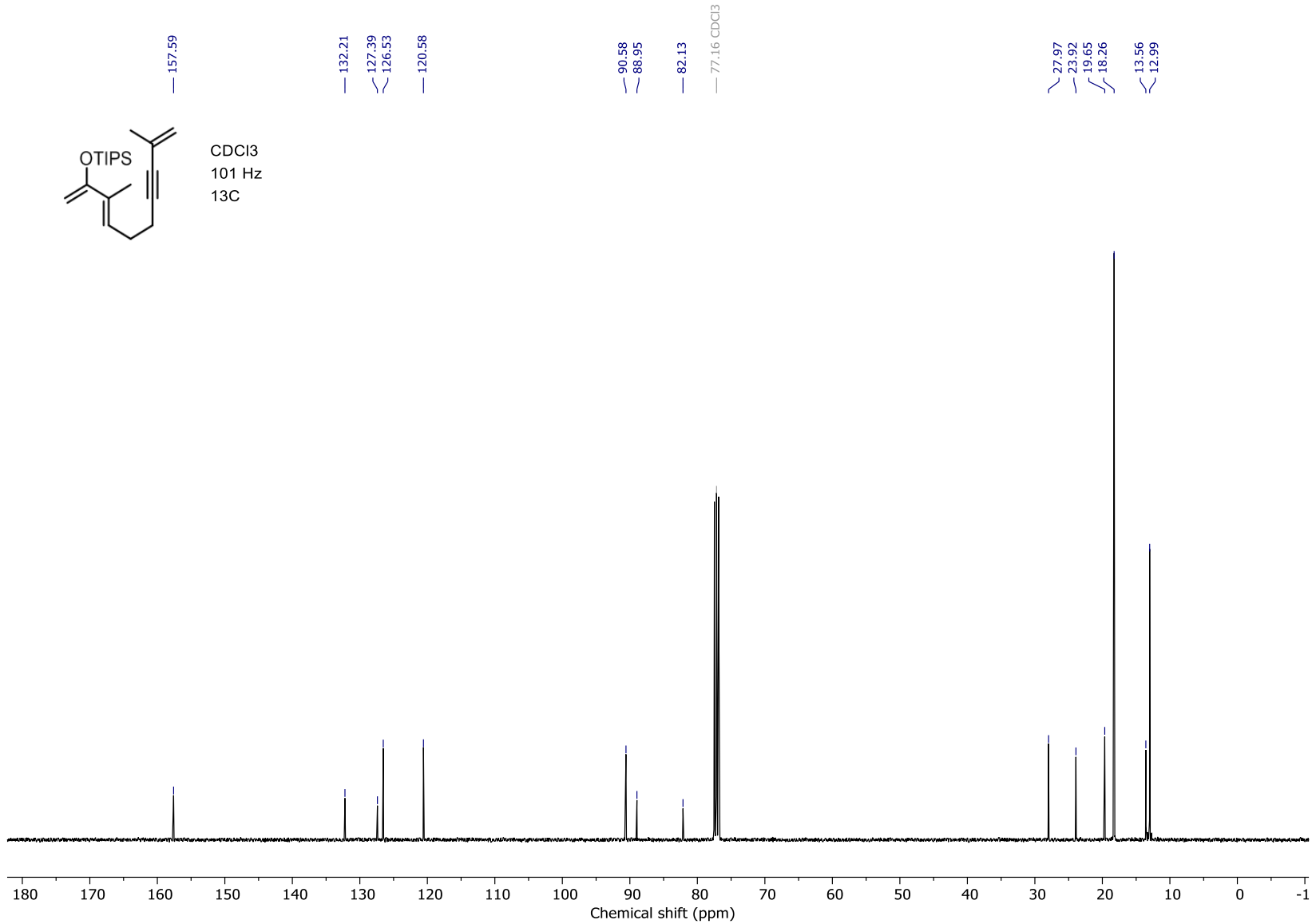
157.59
132.21
127.39
126.53
120.58
90.58
88.95
82.13
77.16 CDCl3
27.97
23.92
19.65
18.26
13.56
12.99
OTIPS
CDCl3
101 Hz
13C
180 170 160 150 140 130 120 110 100 90 80 70 60 50 40 30 20 10 0 -1
Chemical shift (ppm)

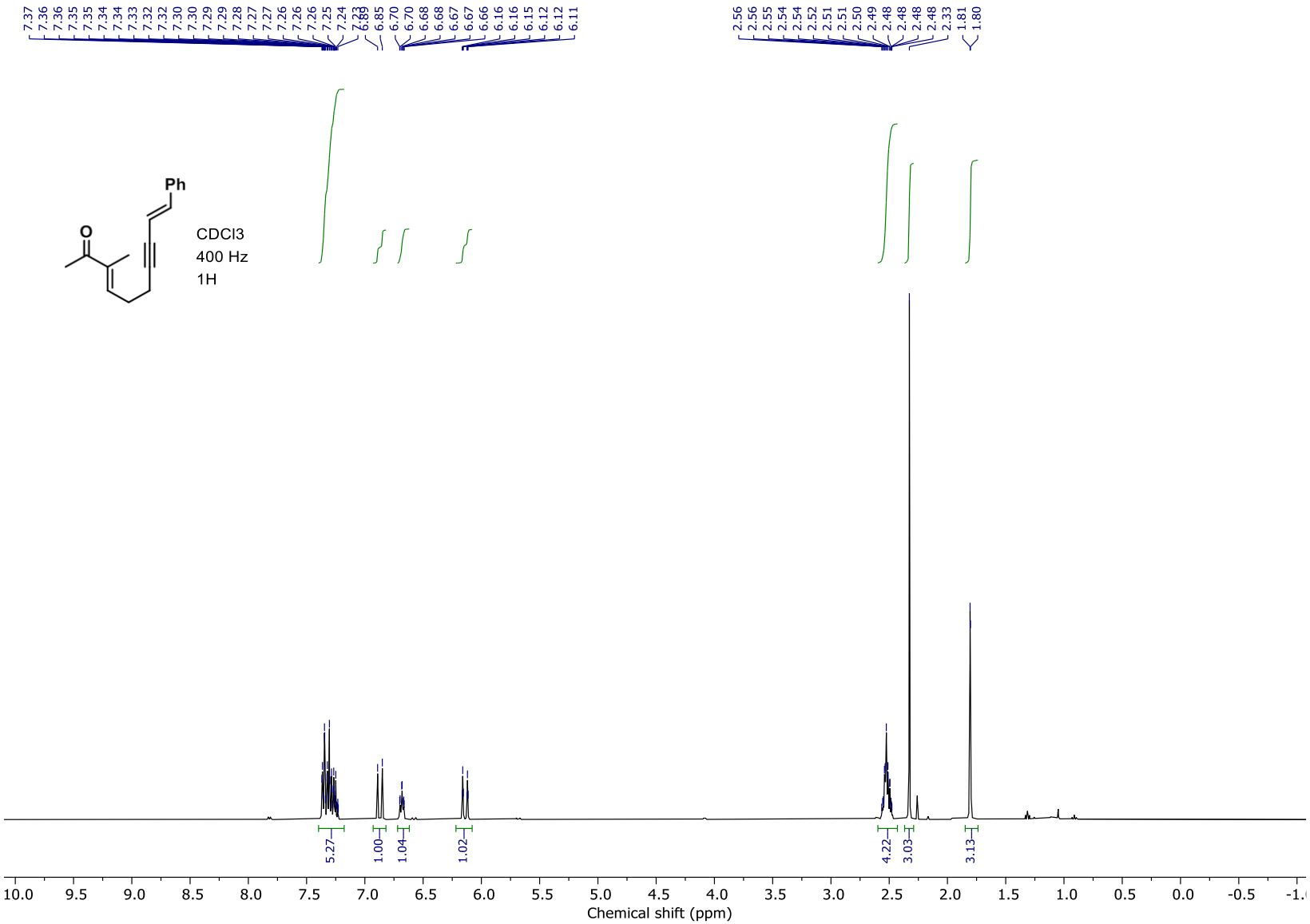
Ph
O
CDCl3
400 Hz
1H
7.37 7.36 7.36 7.35 7.35 7.34 7.34 7.33 7.32 7.32 7.30 7.30 7.29 7.29 7.28 7.27 7.27 7.26 7.26 7.26 7.25 7.24 6.85 6.70 6.70 6.68 6.68 6.67 6.67 6.66 6.16 6.16 6.15 6.12 6.12 6.11
2.56 2.56 2.55 2.54 2.54 2.52 2.51 2.51 2.50 2.49 2.48 2.48 2.48 2.33 1.81 1.80
5.27
1.00
1.04
1.02
4.22
3.03
3.13
10.0 9.5 9.0 8.5 8.0 7.5 7.0 6.5 6.0 5.5 5.0 4.5 4.0 3.5 3.0 2.5 2.0 1.5 1.0 0.5 0.0 -0.5
Chemical shift (ppm)

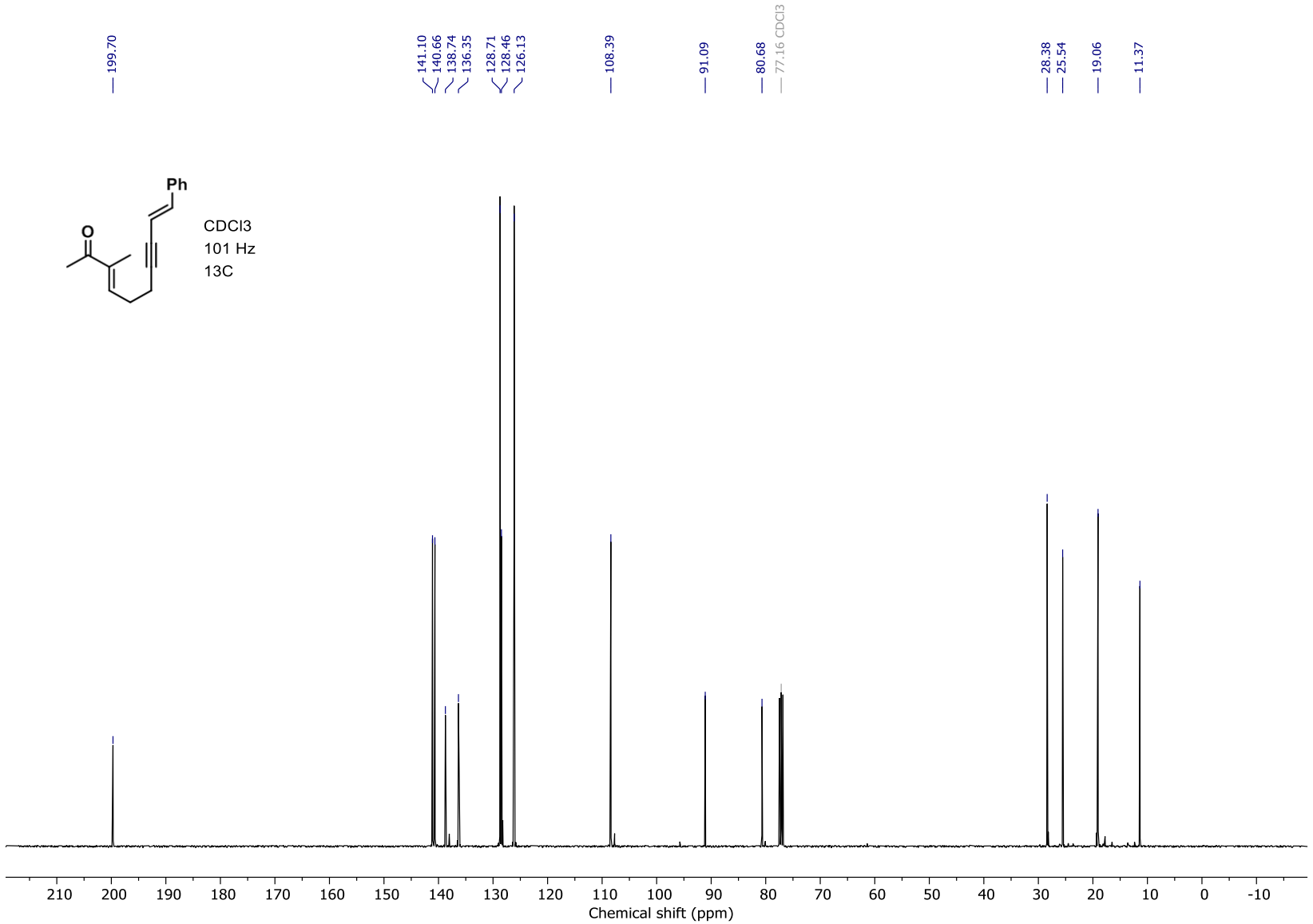
199.70
141.10
140.66
138.74
136.35
128.71
128.46
126.13
108.39
91.09
80.68
77.16 CDCl3
28.38
25.54
19.06
11.37
Ph
O
CDCl3
101 Hz
13C
210 200 190 180 170 160 150 140 130 120 110 100 90 80 70 60 50 40 30 20 10 0 -10
Chemical shift (ppm)

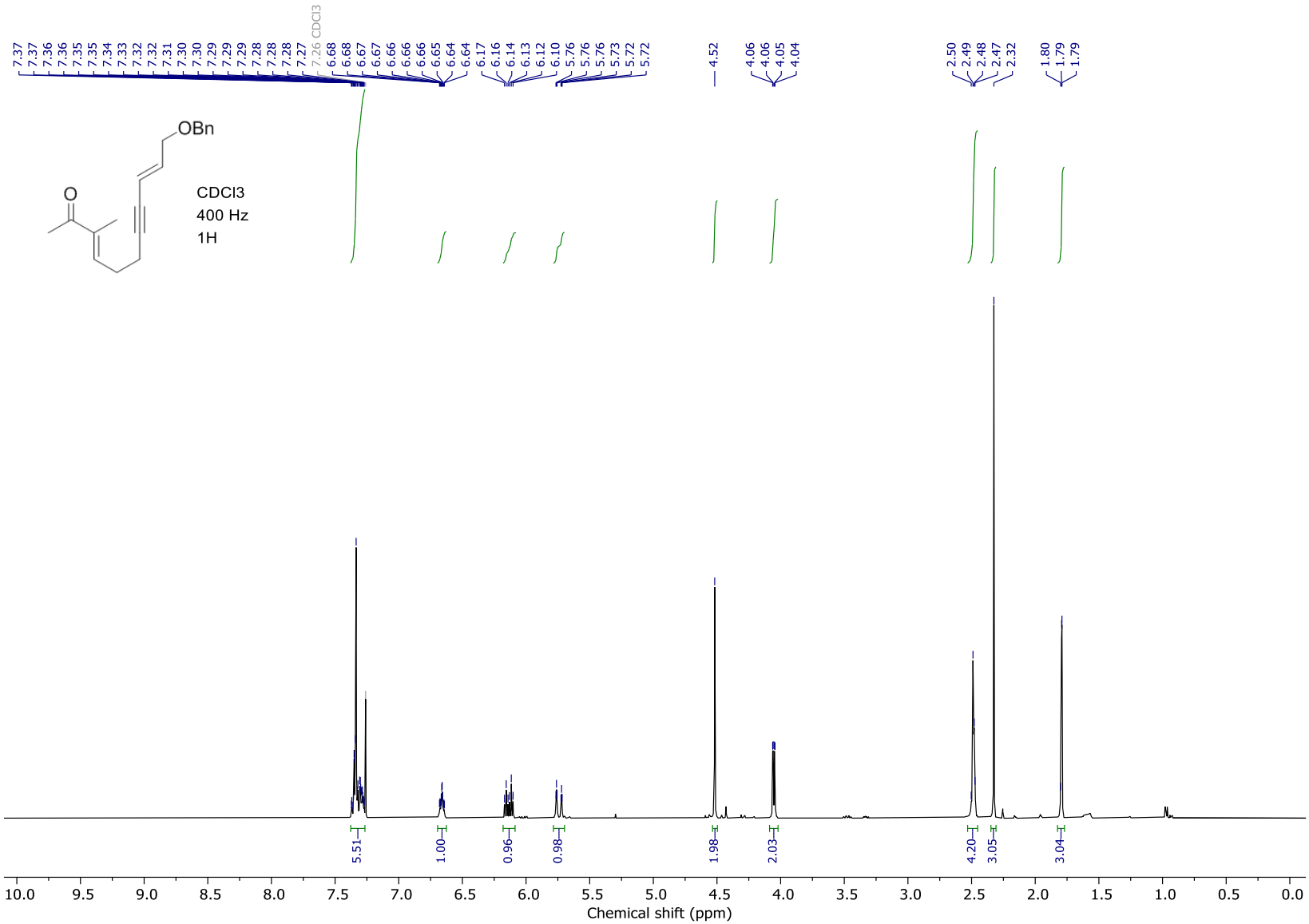
OBn
O
CDCl3
400 Hz
1H
7.37 7.37 7.36 7.36 7.35 7.35 7.34 7.33 7.32 7.32 7.31 7.30 7.30 7.29 7.29 7.29 7.28 7.28 7.28 7.27 7.26 CDCl3 6.68 6.68 6.67 6.67 6.66 6.66 6.66 6.65 6.64 6.64 6.17 6.16 6.14 6.13 6.12 6.10 5.76 5.76 5.76 5.73 5.72 5.72
4.52
4.06 4.06 4.05 4.04
2.50 2.49 2.48 2.47 2.32
1.80 1.79 1.79
5.51
1.00
0.96
0.98
1.98
2.03
4.20
3.05
3.04
10.0 9.5 9.0 8.5 8.0 7.5 7.0 6.5 6.0 5.5 5.0 4.5 4.0 3.5 3.0 2.5 2.0 1.5 1.0 0.5 0.0
Chemical shift (ppm)

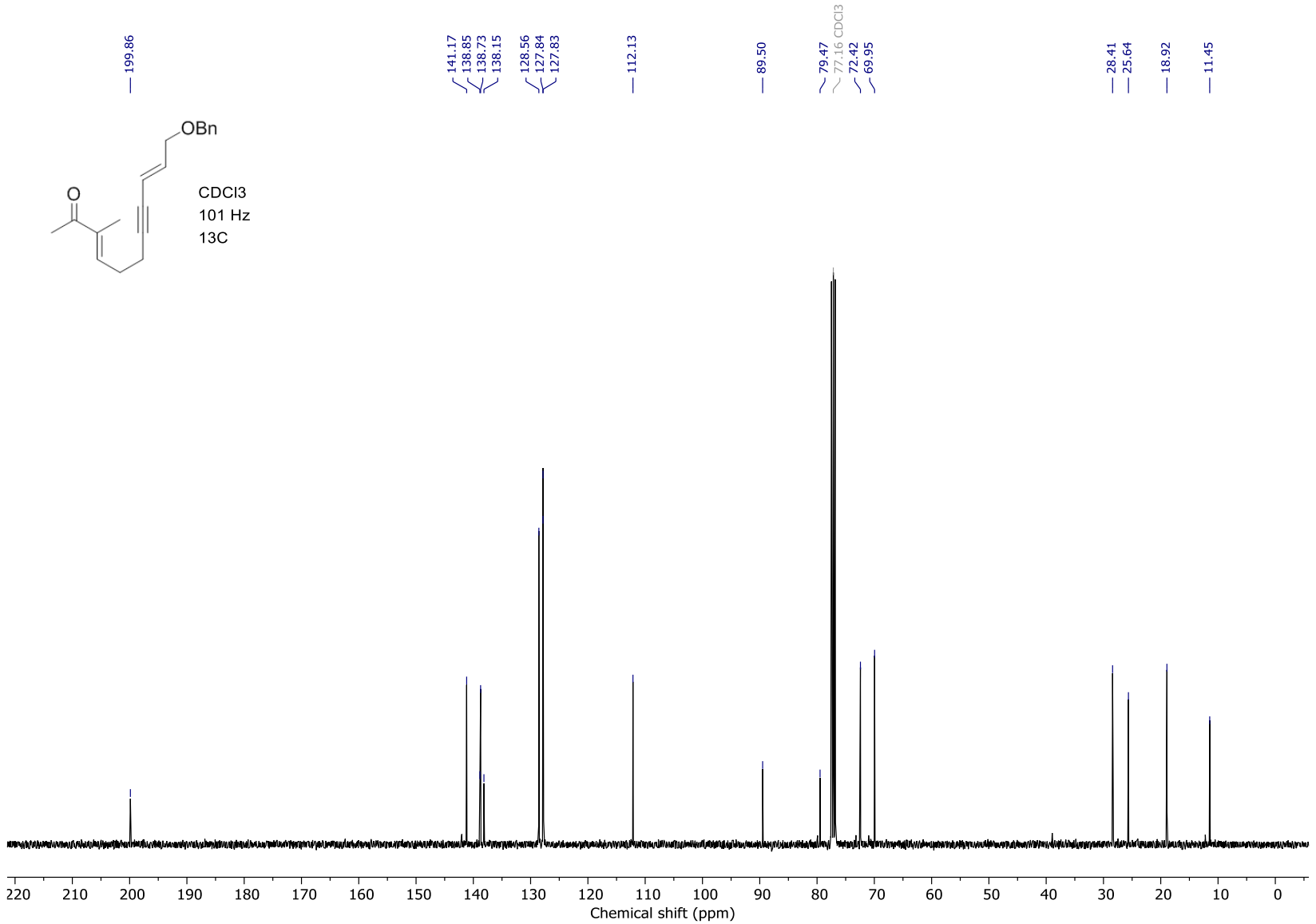
199.86
141.17
138.85
138.73
138.15
128.56
127.84
127.83
112.13
89.50
79.47
77.16 CDCl3
72.42
69.95
28.41
25.64
18.92
11.45
OBn
O
CDCl3
101 Hz
13C
220 210 200 190 180 170 160 150 140 130 120 110 100 90 80 70 60 50 40 30 20 10 0
Chemical shift (ppm)

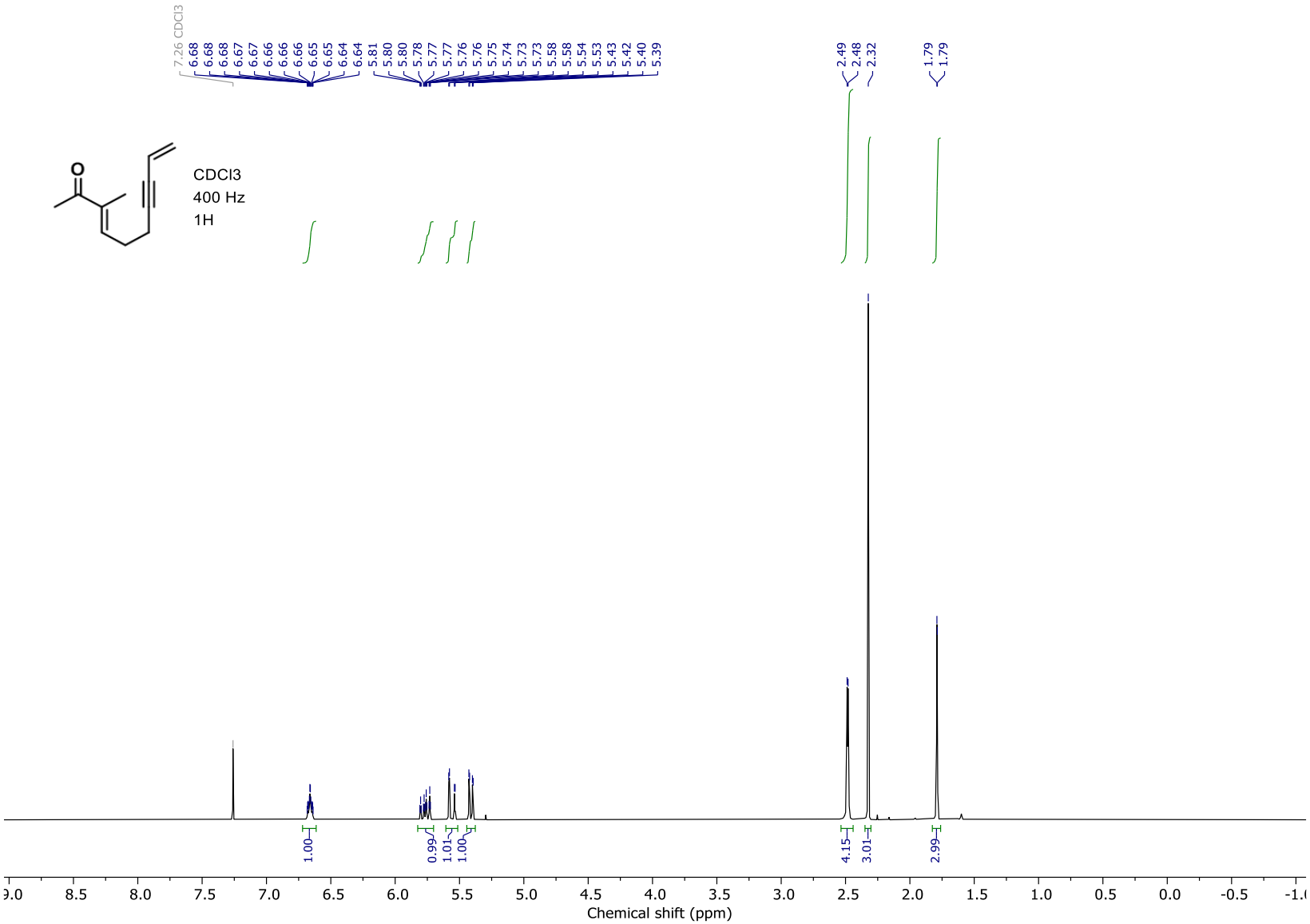
7.26 CDCl3
6.68
6.68
6.68
6.67
6.67
6.66
6.66
6.66
6.65
6.65
6.64
6.64
5.81
5.80
5.80
5.78
5.77
5.77
5.76
5.76
5.75
5.74
5.73
5.73
5.58
5.58
5.54
5.53
5.43
5.42
5.40
5.39
2.49
2.48
2.32
1.79
1.79
CDCl3
400 Hz
1H
1.00
0.99
1.01
1.00
4.15
3.01
2.99
Chemical shift (ppm)

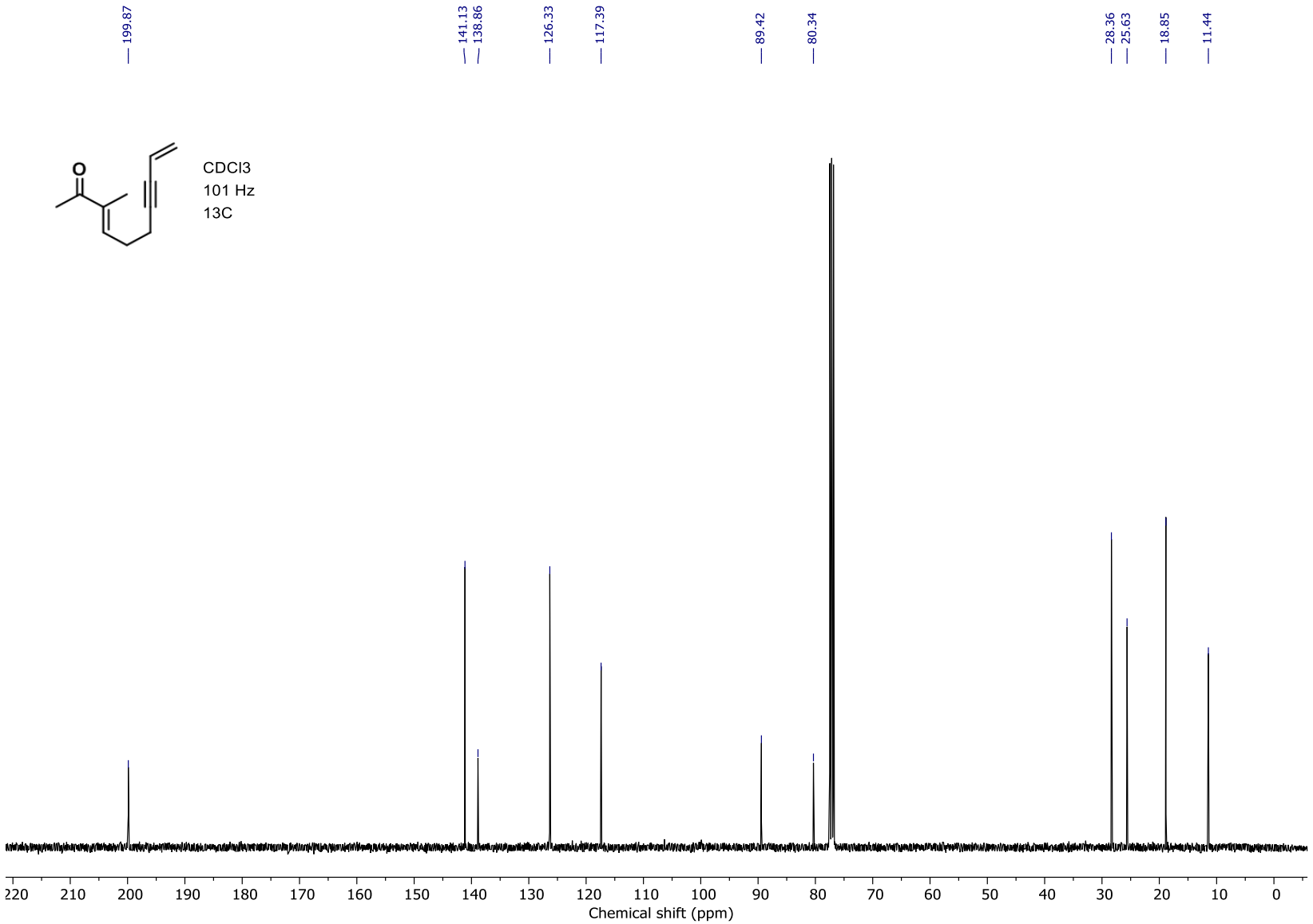
199.87
141.13
138.86
126.33
117.39
89.42
80.34
28.36
25.63
18.85
11.44
CDCl3
101 Hz
13C
220 210 200 190 180 170 160 150 140 130 120 110 100 90 80 70 60 50 40 30 20 10 0
Chemical shift (ppm)

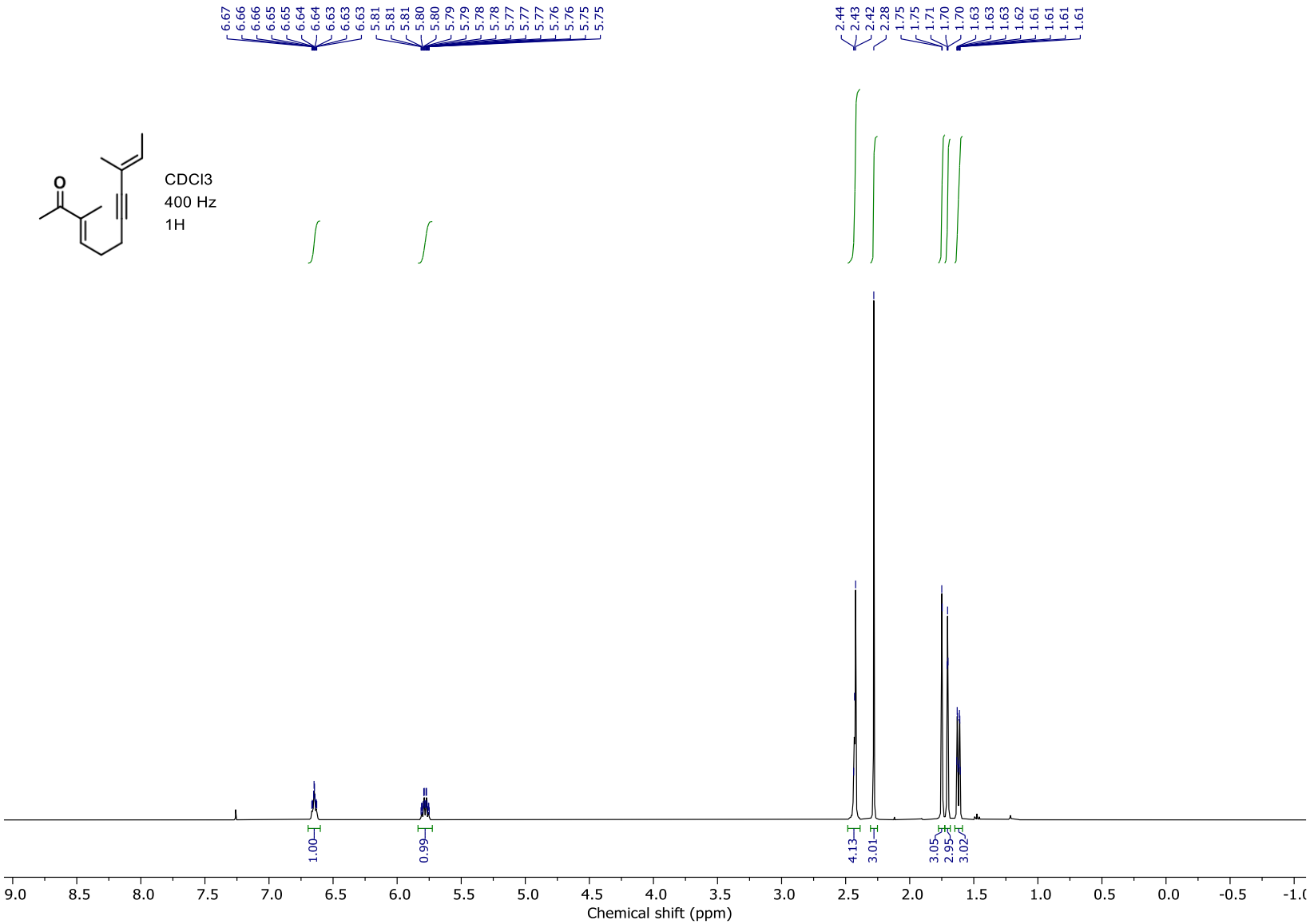
CDCl3
400 Hz
1H
6.67 6.66 6.66 6.65 6.65 6.64 6.64 6.63 6.63 6.63
5.81 5.81 5.81 5.80 5.80 5.79 5.79 5.78 5.78 5.77 5.77 5.77 5.76 5.76 5.75 5.75
2.44 2.43 2.42 2.28 1.75 1.75 1.71 1.70 1.70 1.63 1.63 1.63 1.62 1.61 1.61 1.61 1.61
1.00 0.99 4.13 3.01 3.05 2.95 3.02
9.0 8.5 8.0 7.5 7.0 6.5 6.0 5.5 5.0 4.5 4.0 3.5 3.0 2.5 2.0 1.5 1.0 0.5 0.0 -0.5
Chemical shift (ppm)

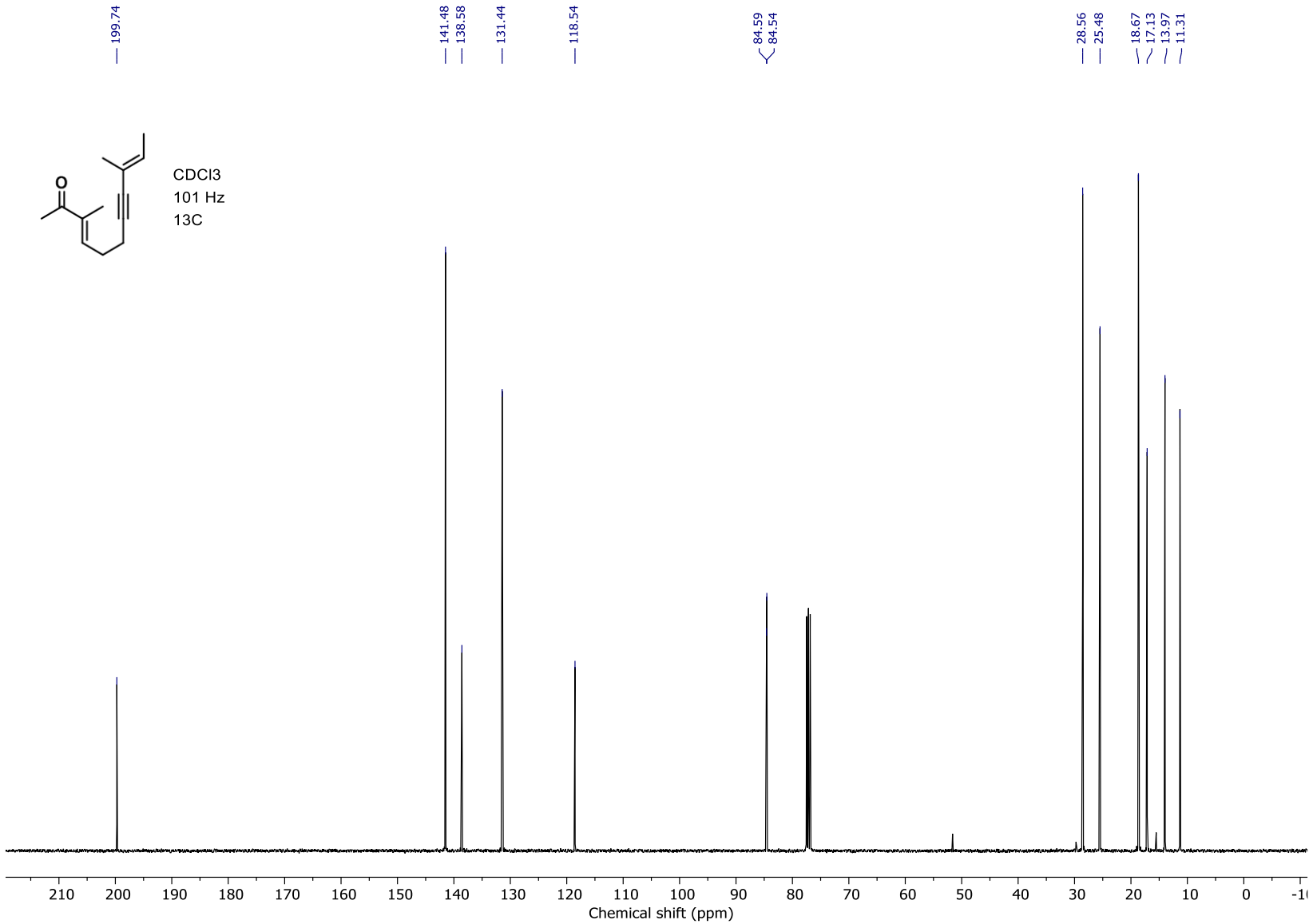
199.74
141.48
138.58
131.44
118.54
84.59
84.54
28.56
25.48
18.67
17.13
13.97
11.31
CDCl3
101 Hz
13C
210 200 190 180 170 160 150 140 130 120 110 100 90 80 70 60 50 40 30 20 10 0
Chemical shift (ppm)

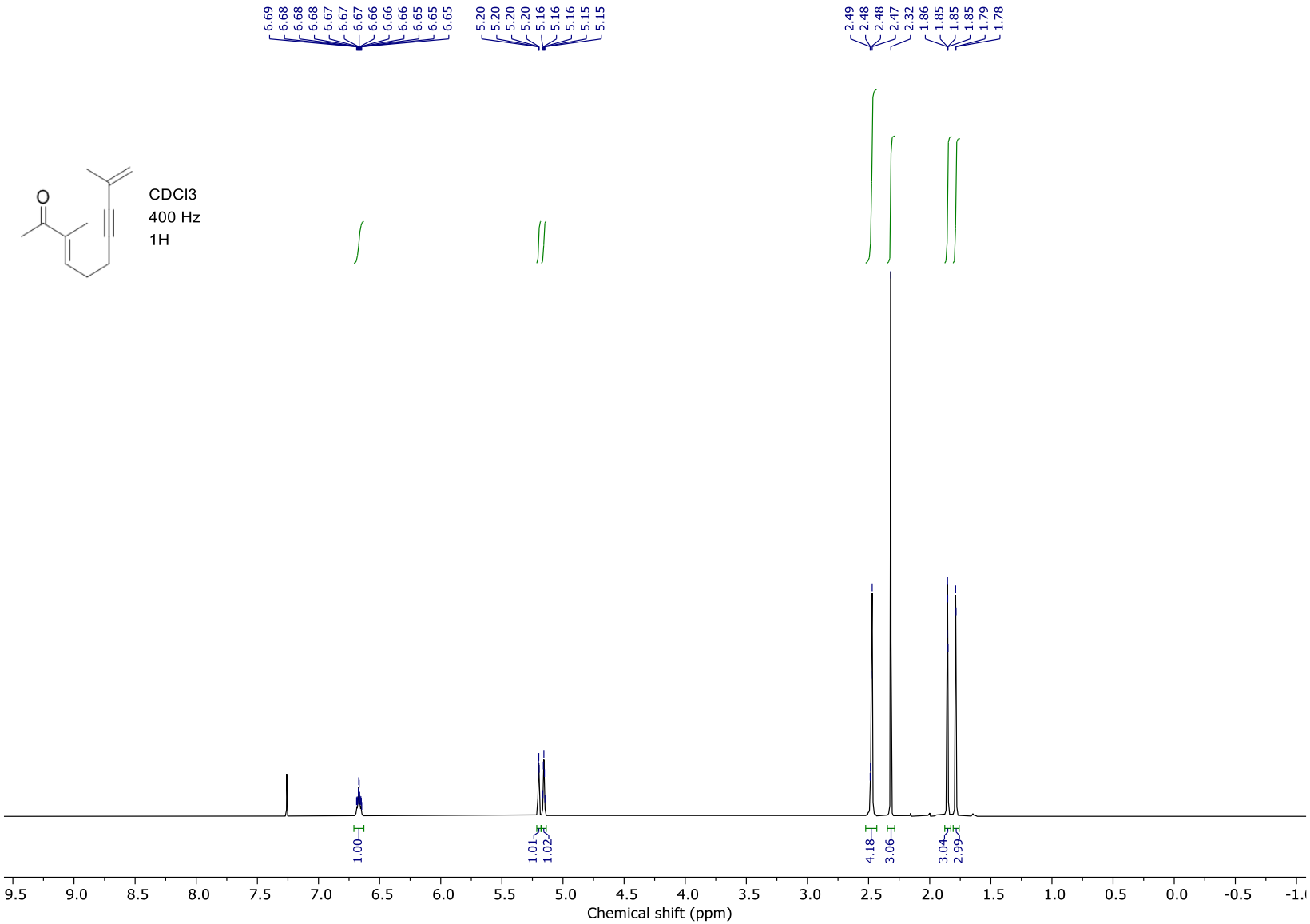
6.69
6.68
6.68
6.68
6.67
6.67
6.67
6.66
6.66
6.66
6.65
6.65
6.65
5.20
5.20
5.20
5.20
5.16
5.16
5.16
5.15
5.15
2.49
2.48
2.48
2.47
2.32
1.86
1.85
1.85
1.85
1.79
1.78
O
CDCl3
400 Hz
1H
1.00
1.01
1.02
4.18
3.06
3.04
2.99
9.5
9.0
8.5
8.0
7.5
7.0
6.5
6.0
5.5
5.0
4.5
4.0
3.5
3.0
2.5
2.0
1.5
1.0
0.5
0.0
-0.5
Chemical shift (ppm)

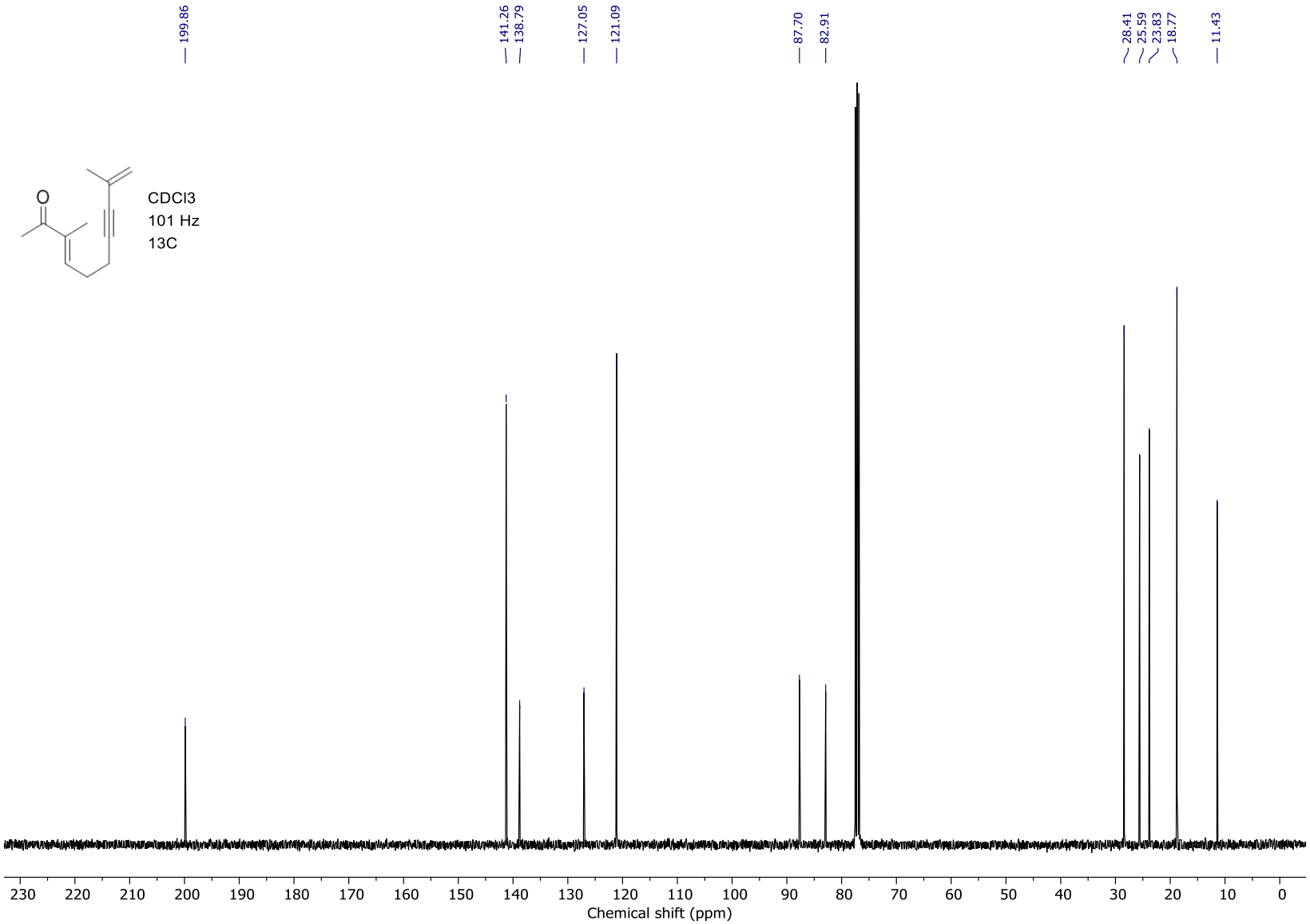
199.86
141.26
138.79
127.05
121.09
87.70
82.91
28.41
25.59
23.83
18.77
11.43
O
CDCl3
101 Hz
13C
230 220 210 200 190 180 170 160 150 140 130 120 110 100 90 80 70 60 50 40 30 20 10 0
Chemical shift (ppm)

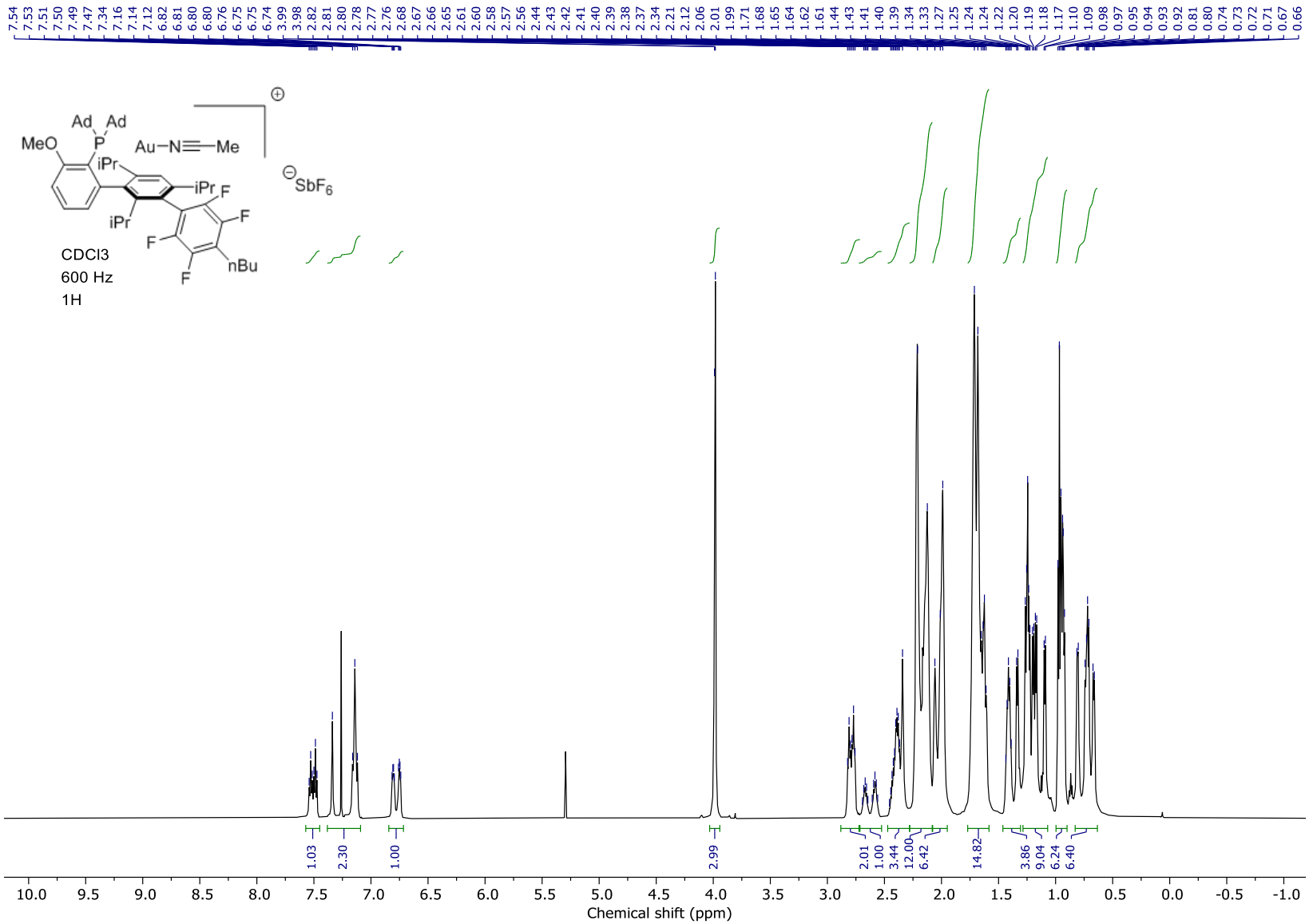
CDCl3
600 Hz
1H
Chemical shift (ppm)

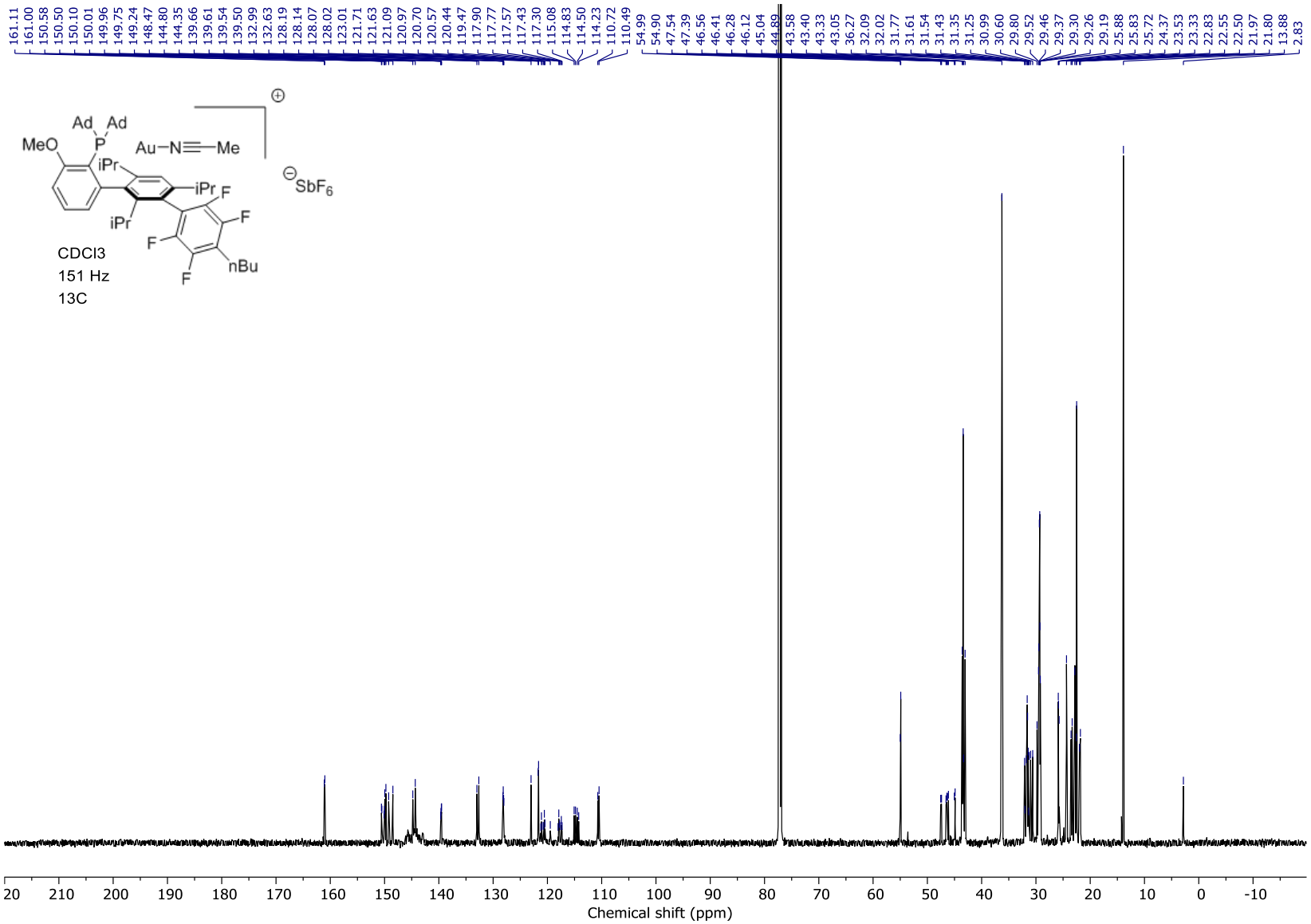
161.11
161.00
150.58
150.50
150.10
150.01
149.96
149.75
149.24
148.47
144.80
144.35
139.66
139.61
139.54
139.50
132.99
132.63
128.19
128.14
128.07
128.02
123.01
121.71
121.63
121.09
120.97
120.70
120.57
120.44
119.47
117.90
117.77
117.57
117.43
117.30
115.08
114.83
114.50
114.23
110.72
110.49
54.99
54.90
47.54
47.39
46.56
46.41
46.28
46.12
45.04
44.89
43.58
43.40
43.33
43.05
36.27
32.09
32.02
31.77
31.61
31.54
31.43
31.35
31.25
30.99
30.60
29.80
29.52
29.46
29.37
29.30
29.26
29.19
25.88
25.83
25.72
24.37
23.53
23.33
22.83
22.55
22.50
21.97
21.80
13.88
2.83
Ad
Ad
P
MeO
iPr
Au–N≡Me
iPr
iPr
F
F
F
F
nBu
⊖SbF6
CDCl3
151 Hz
13C
20
210
200
190
180
170
160
150
140
130
120
110
100
90
80
70
60
50
40
30
20
10
0
-10
Chemical shift (ppm)

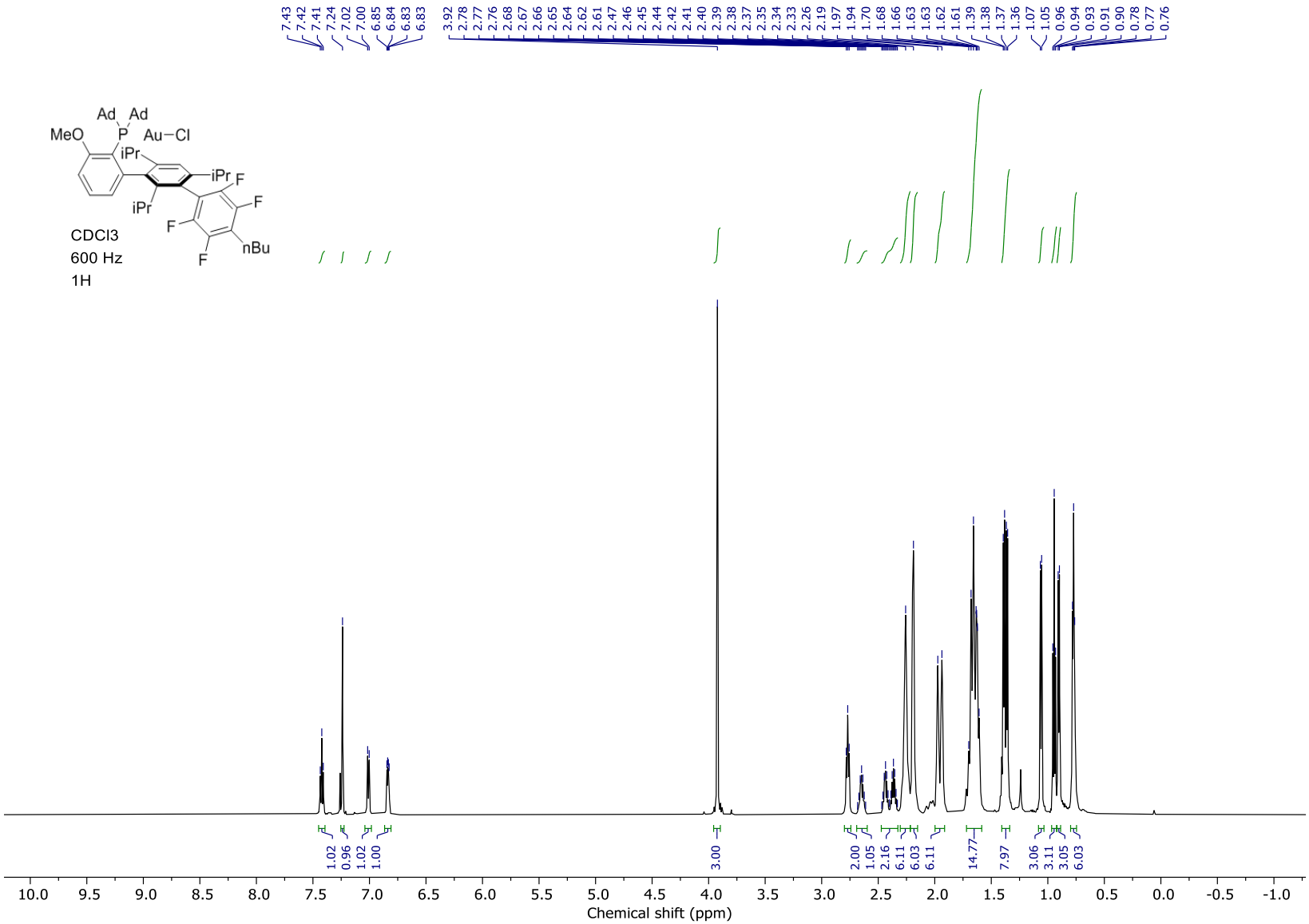
7.43 7.42 7.41 7.24 7.02 7.00 6.85 6.84 6.83 6.83
3.92 2.78 2.77 2.76 2.68 2.67 2.66 2.65 2.64 2.62 2.61 2.47 2.46 2.45 2.44 2.42 2.41 2.40 2.39 2.38 2.37 2.35 2.34 2.33 2.26 2.19 1.97 1.94 1.70 1.68 1.66 1.63 1.63 1.62 1.61 1.39 1.38 1.37 1.36 1.07 1.05 0.96 0.94 0.93 0.91 0.90 0.78 0.77 0.76
Ad Ad
MeO P Au−Cl
iPr
iPr
iPr
F
F
F
F
nBu
CDCl3
600 Hz
1H
1.02 0.96 1.02 1.00
3.00
2.00 1.05 2.16 6.11 6.03 6.11
14.77
7.97
3.06 3.11 3.05 6.03
10.0 9.5 9.0 8.5 8.0 7.5 7.0 6.5 6.0 5.5 5.0 4.5 4.0 3.5 3.0 2.5 2.0 1.5 1.0 0.5 0.0 -0.5 -1.0
Chemical shift (ppm)

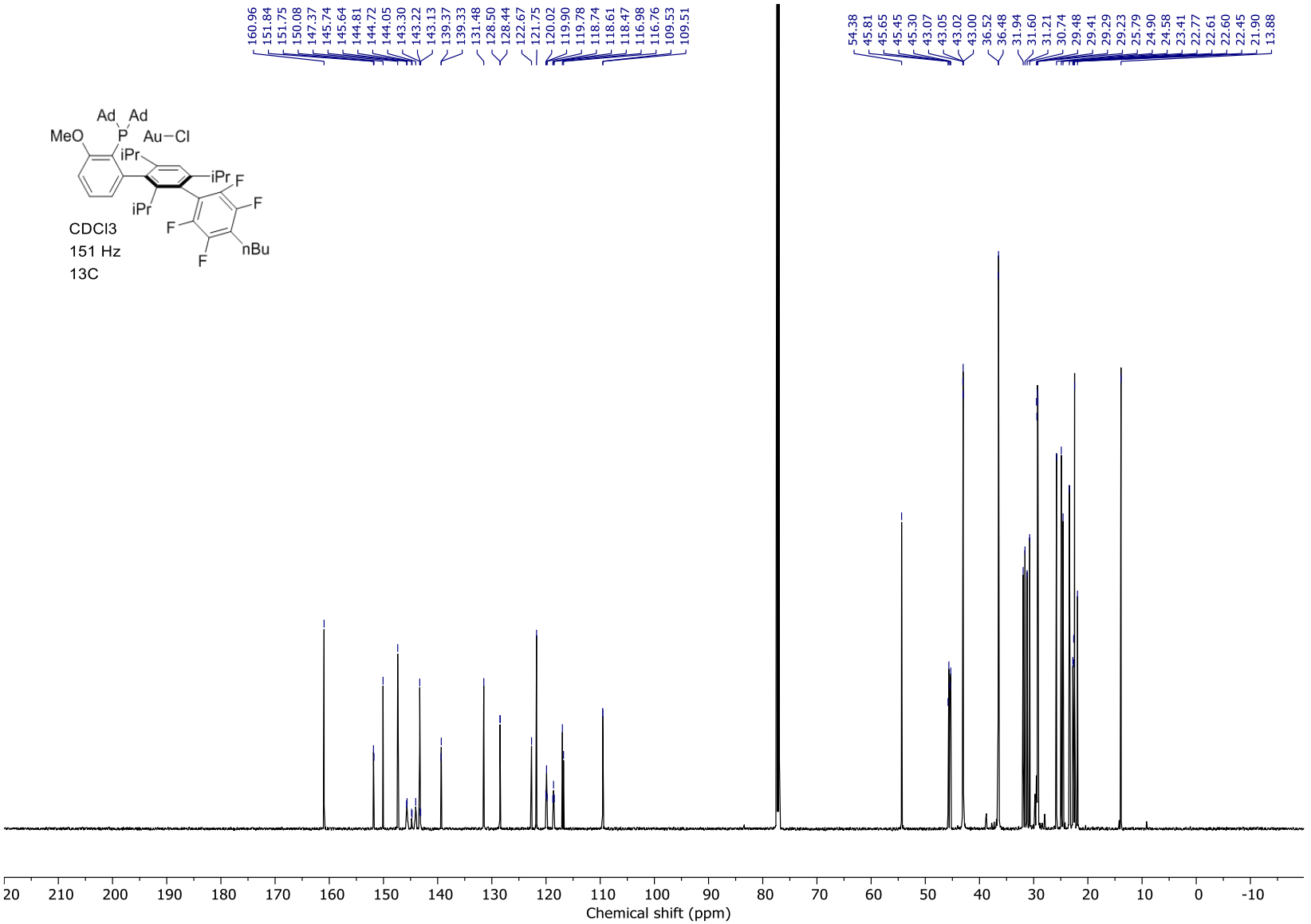
160.96
151.84
151.75
150.08
147.37
145.74
145.64
144.81
144.72
144.05
143.30
143.22
143.13
139.37
139.33
131.48
128.50
128.44
122.67
121.75
120.02
119.90
119.78
118.74
118.61
118.47
116.98
116.76
109.53
109.51
54.38
45.81
45.65
45.45
45.30
43.07
43.05
43.02
43.00
36.52
36.48
31.94
31.60
31.21
30.74
29.48
29.41
29.29
29.23
25.79
24.90
24.58
23.41
22.77
22.61
22.60
22.45
21.90
13.88
Ad
Ad
MeO
P
Au−Cl
iPr
iPr
iPr
F
F
F
F
nBu
CDCl3
151 Hz
13C
20
210
200
190
180
170
160
150
140
130
120
110
100
90
80
70
60
50
40
30
20
10
0
-10
Chemical shift (ppm)

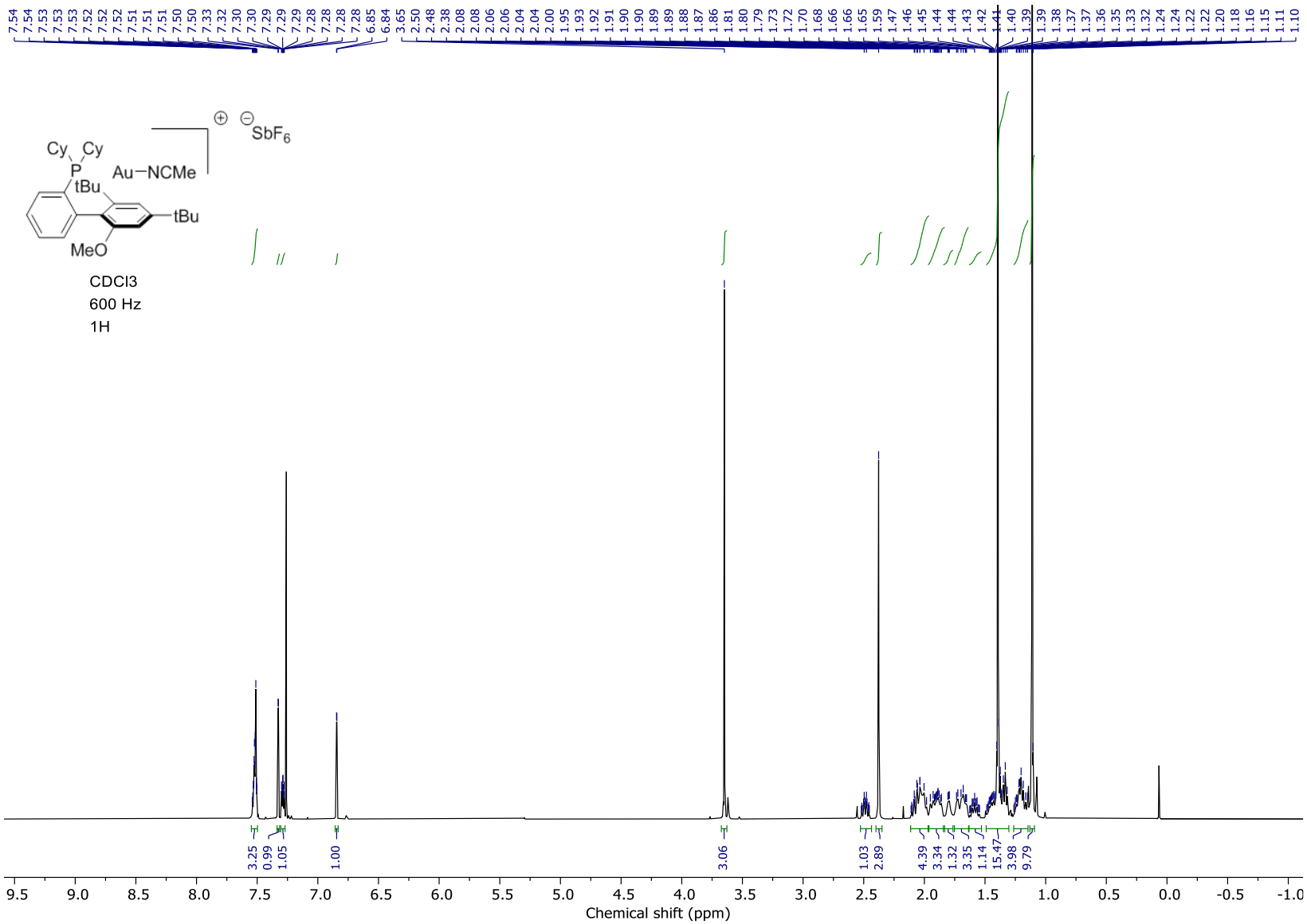
Cy
Cy
P
tBu
Au—NCMe
tBu
MeO
SbF6
CDCl3
600 Hz
1H
Chemical shift (ppm)

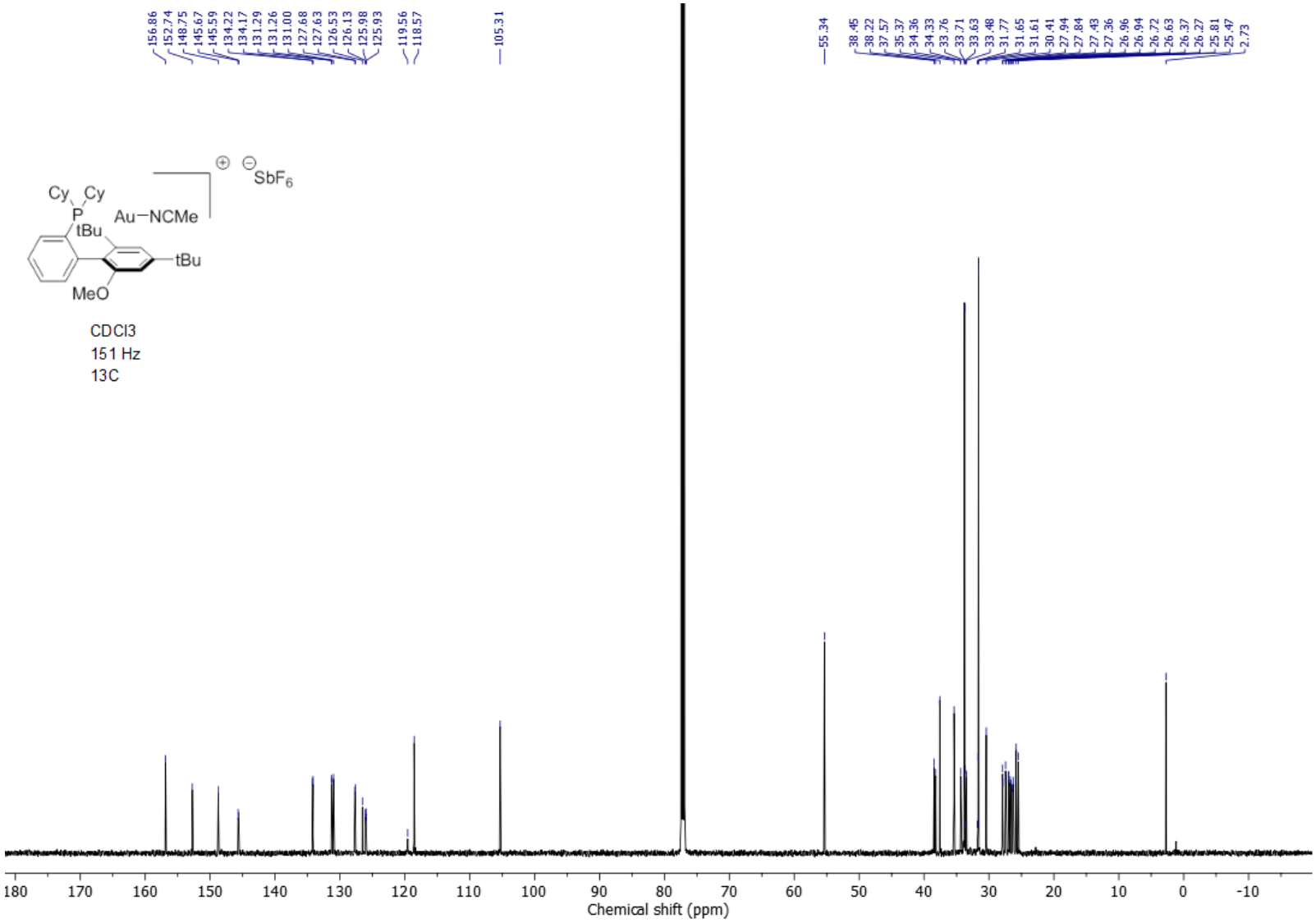
156.86
152.74
148.75
145.67
145.59
134.22
134.17
131.29
131.26
131.00
127.68
127.63
126.53
126.13
125.98
125.93
119.56
118.57
105.31
55.34
38.45
38.22
37.57
35.37
34.36
34.33
33.76
33.71
33.63
33.48
31.77
31.65
31.61
30.41
27.94
27.84
27.43
27.36
26.96
26.94
26.72
26.63
26.37
26.27
25.81
25.47
2.73
Cy
Cy
P
tBu
Au—NCMe
tBu
MeO
SbF6
CDCl3
151 Hz
13C
180
170
160
150
140
130
120
110
100
90
80
70
60
50
40
30
20
10
0
-10
Chemical shift (ppm)

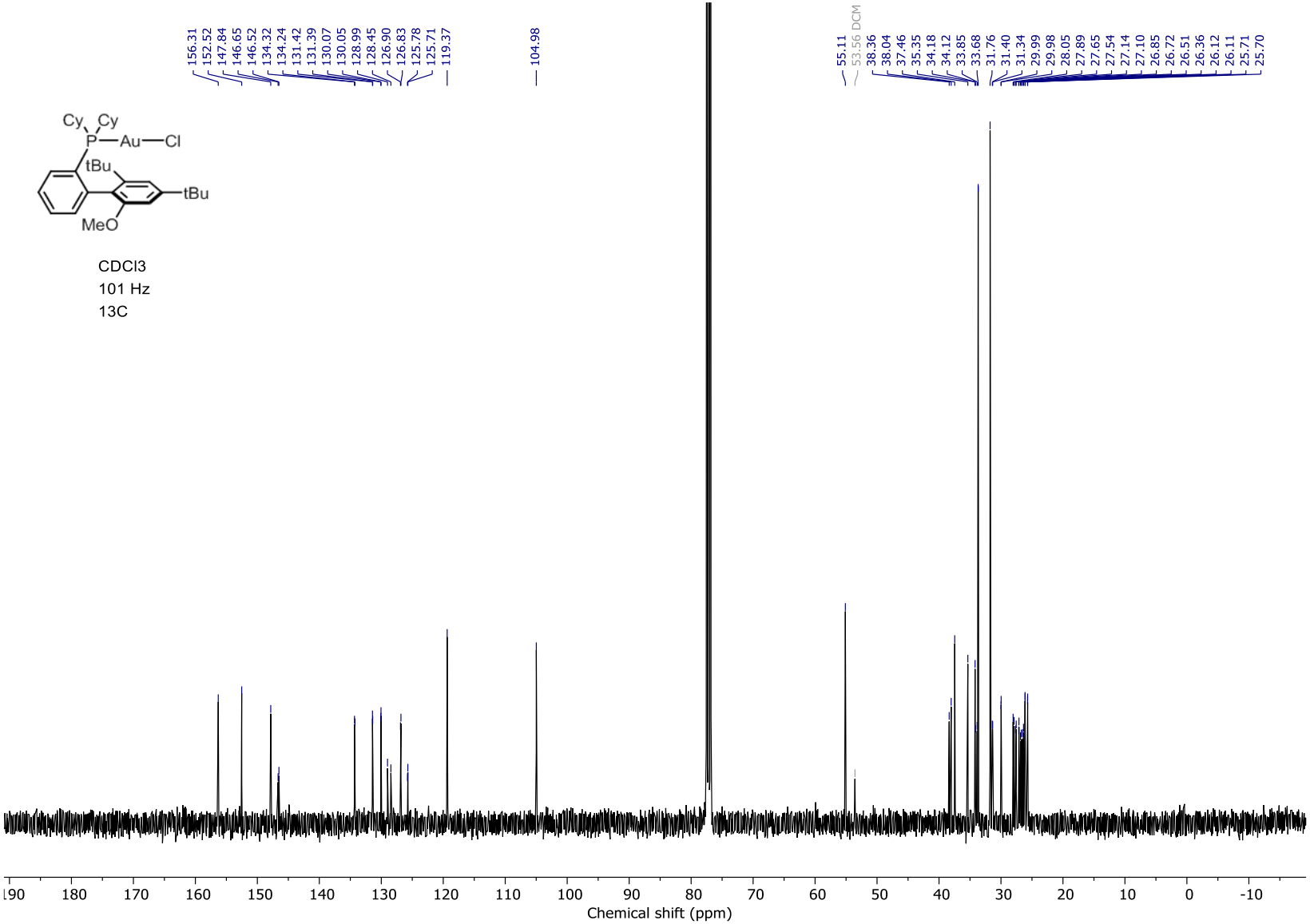
156.31
152.52
147.84
146.65
146.52
134.32
134.24
131.42
131.39
130.07
130.05
128.99
128.45
126.90
126.83
125.78
125.71
119.37
104.98
55.11
53.56 DCM
38.36
38.04
37.46
35.35
34.18
34.12
33.85
33.68
31.76
31.40
31.34
29.99
29.98
28.05
27.89
27.65
27.54
27.14
27.10
26.85
26.72
26.51
26.36
26.12
26.11
25.71
25.70
Cy
Cy
P
Au
Cl
tBu
tBu
MeO
CDCl3
101 Hz
13C
190
180
170
160
150
140
130
120
110
100
90
80
70
60
50
40
30
20
10
0
-10
Chemical shift (ppm)

6.2 Chapter 3 NMR Spectra (Salvinorin A)

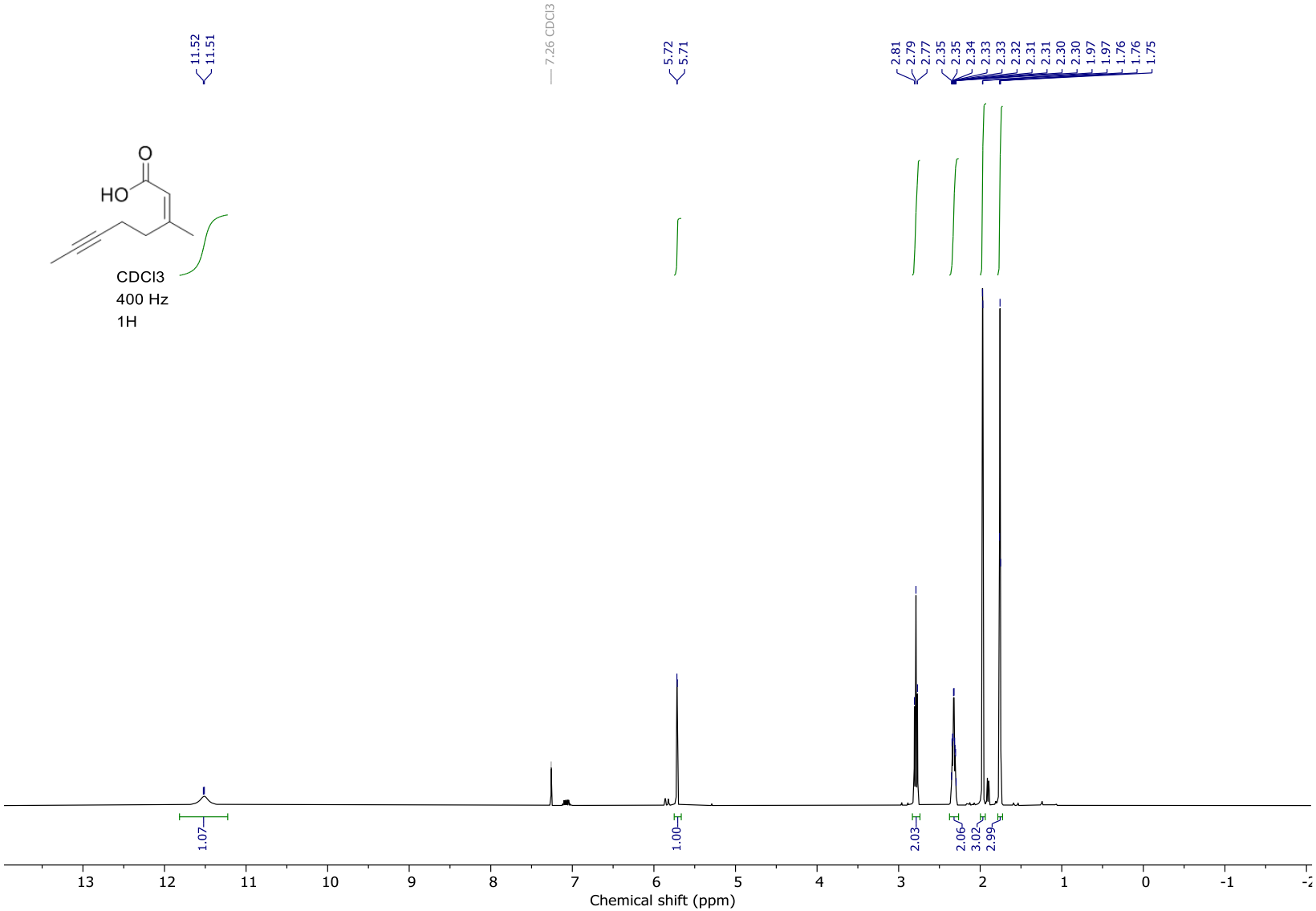

Spectra from Philippe McGee's Ph.D. thesis

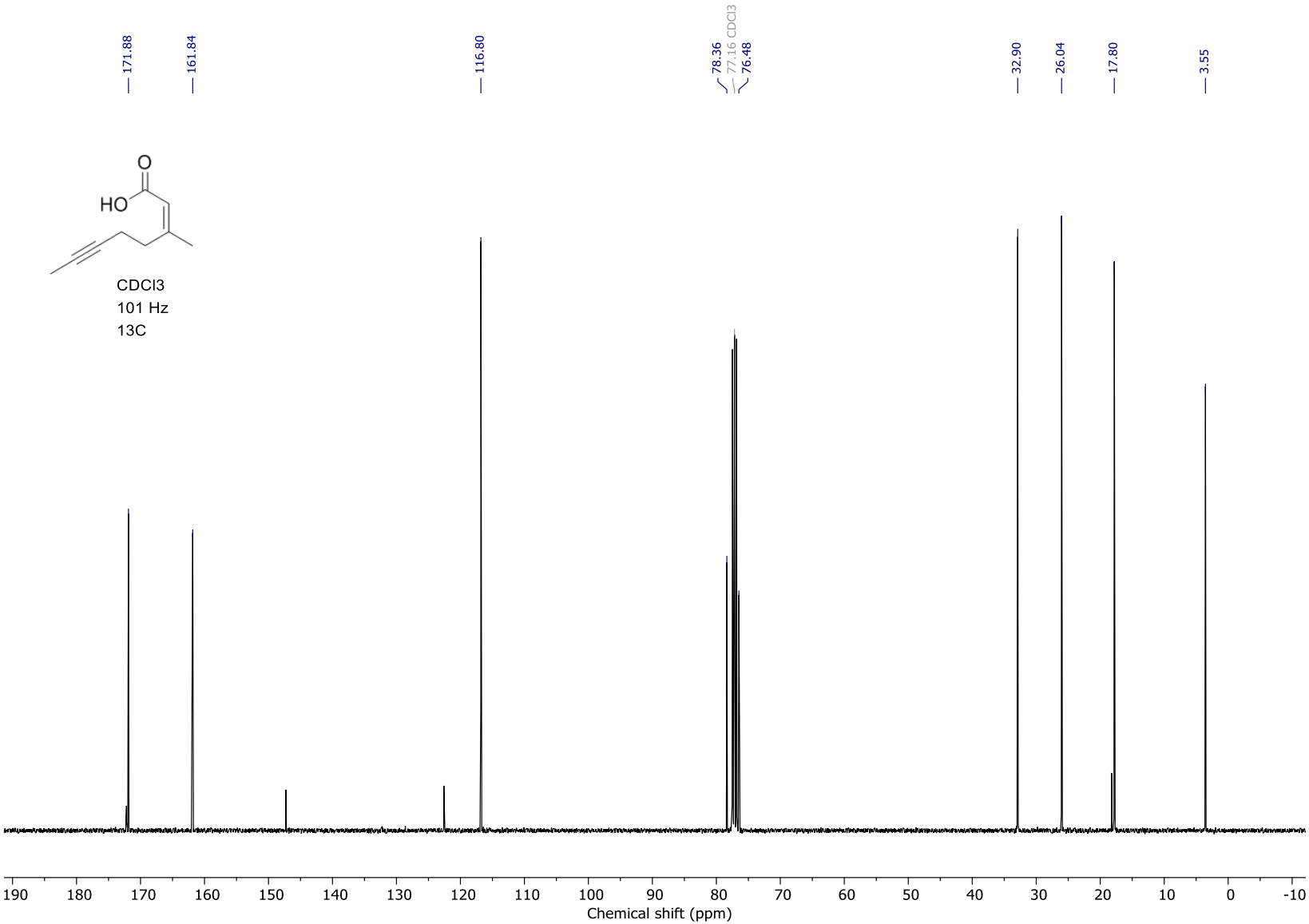

Spectra from Philippe McGee's Ph.D. thesis

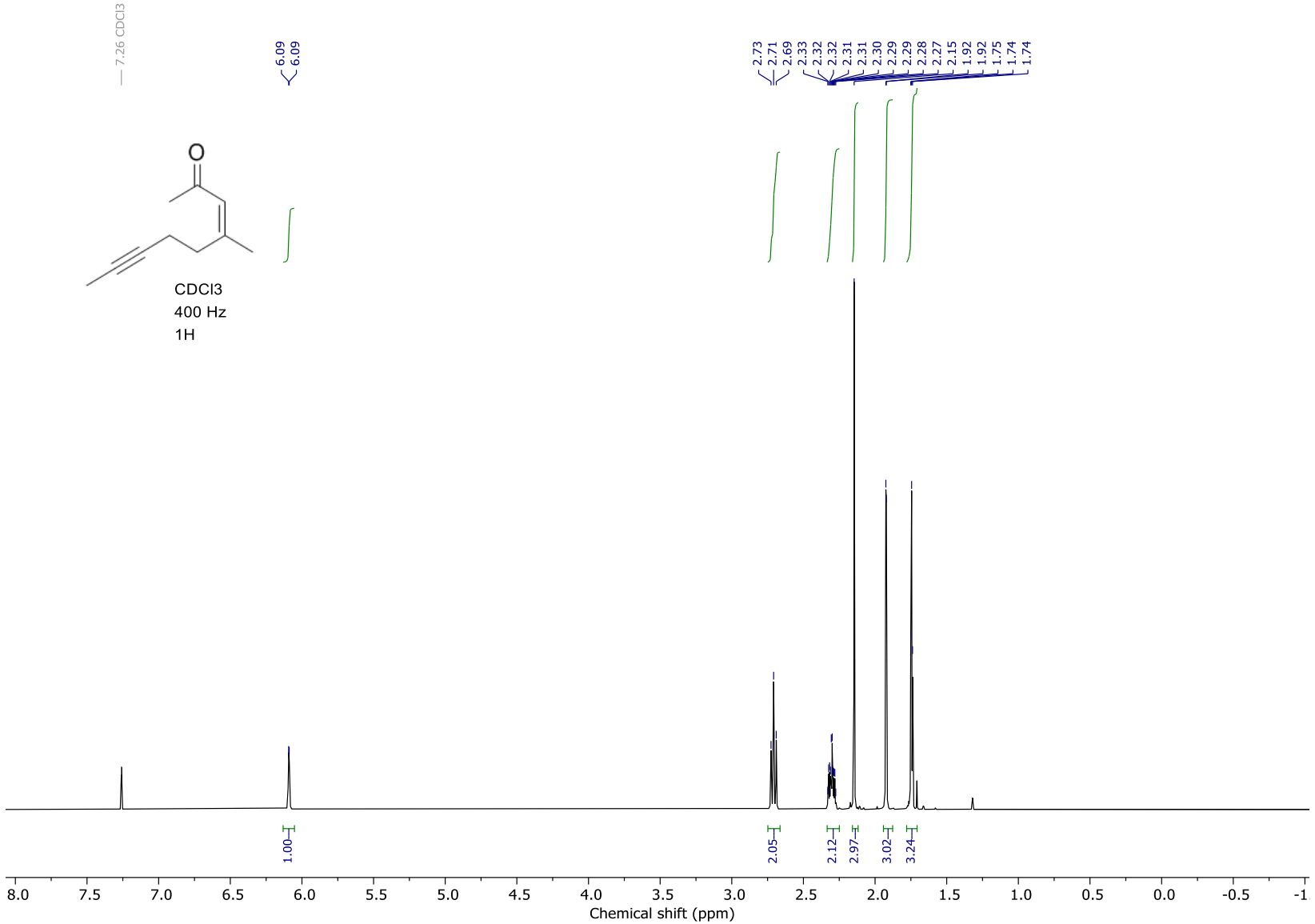

Spectra from Philippe McGee's Ph.D. thesis

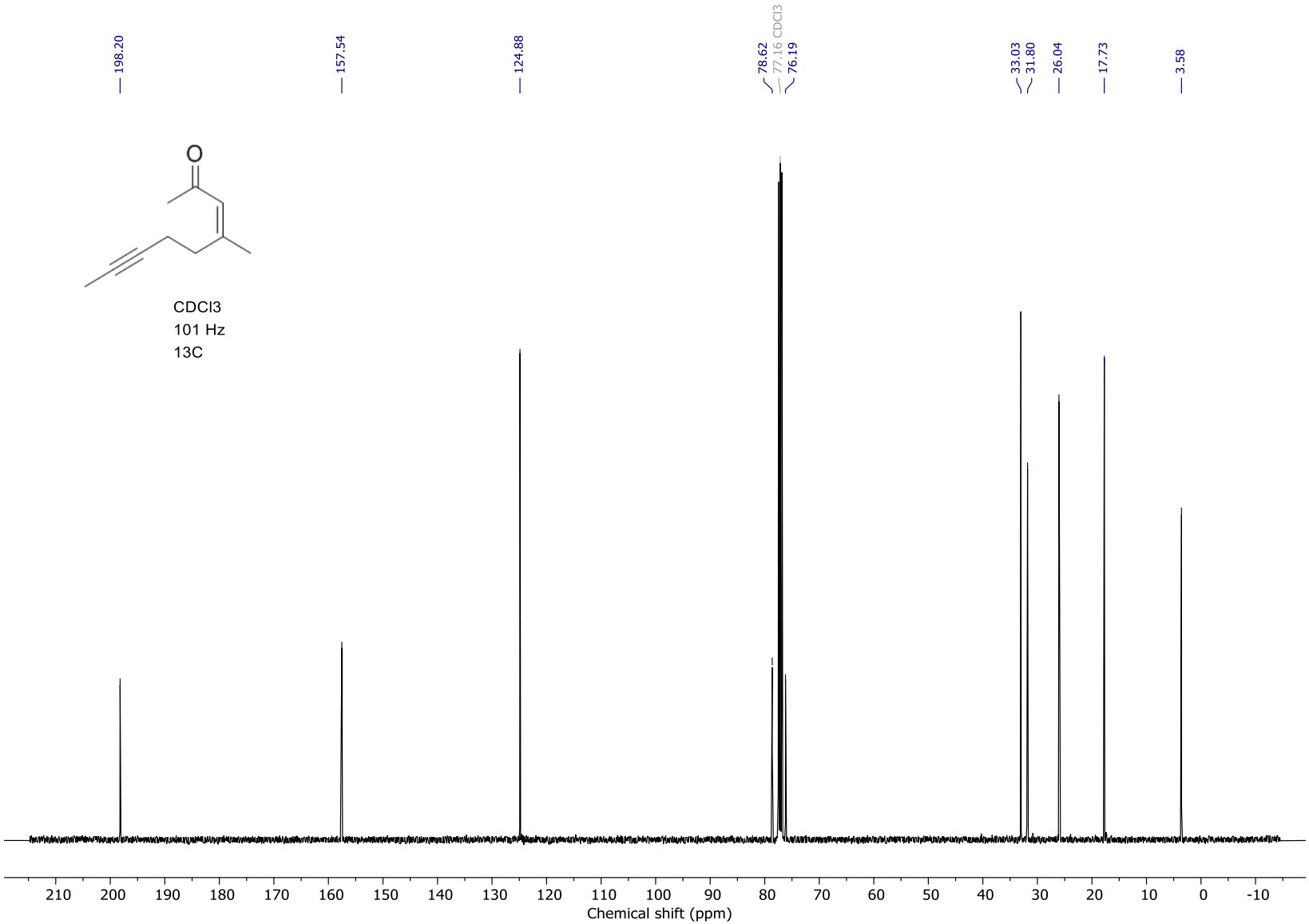

Spectra from Philippe McGee's Ph.D. thesis

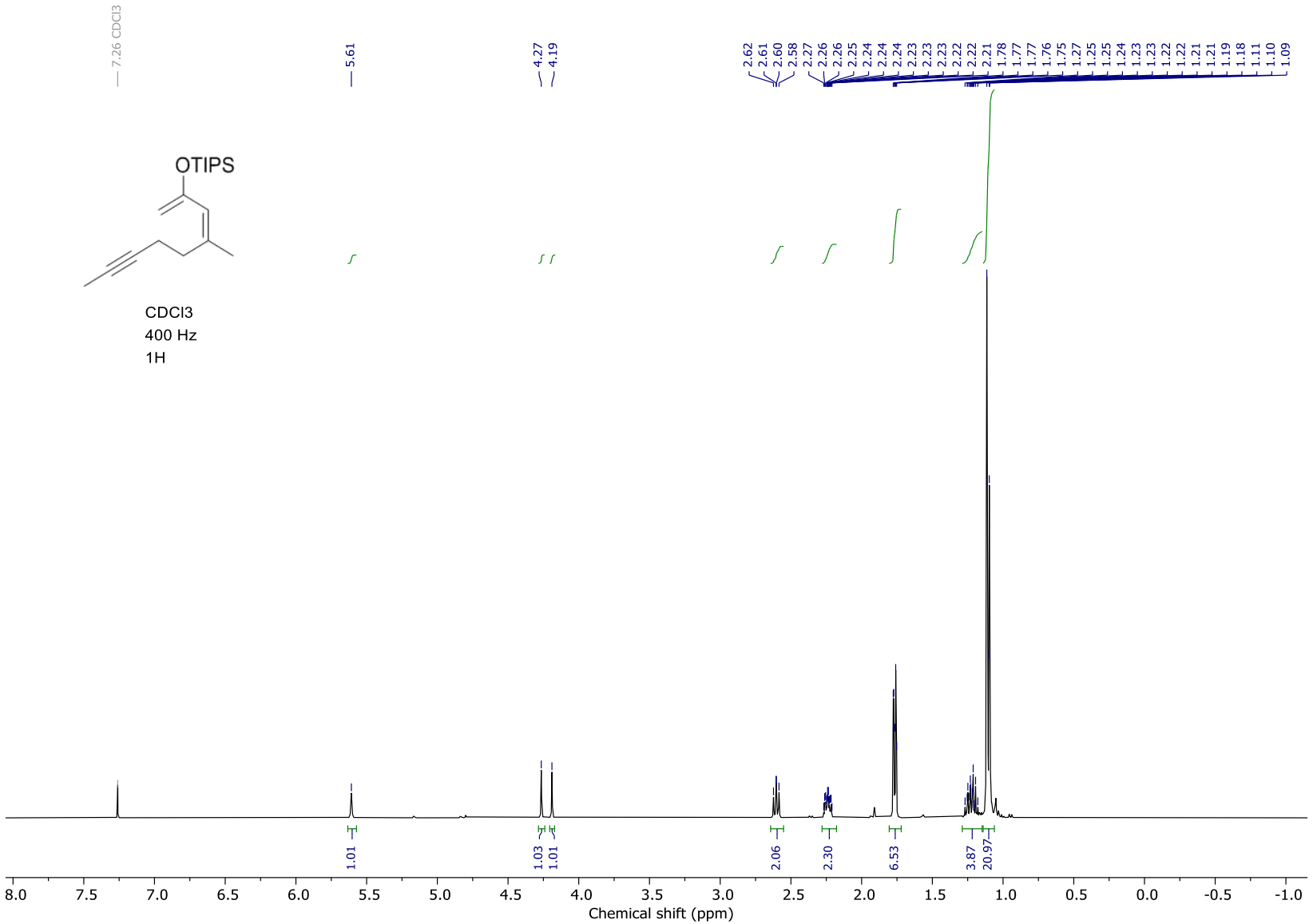

Spectra from Philippe McGee's Ph.D. thesis

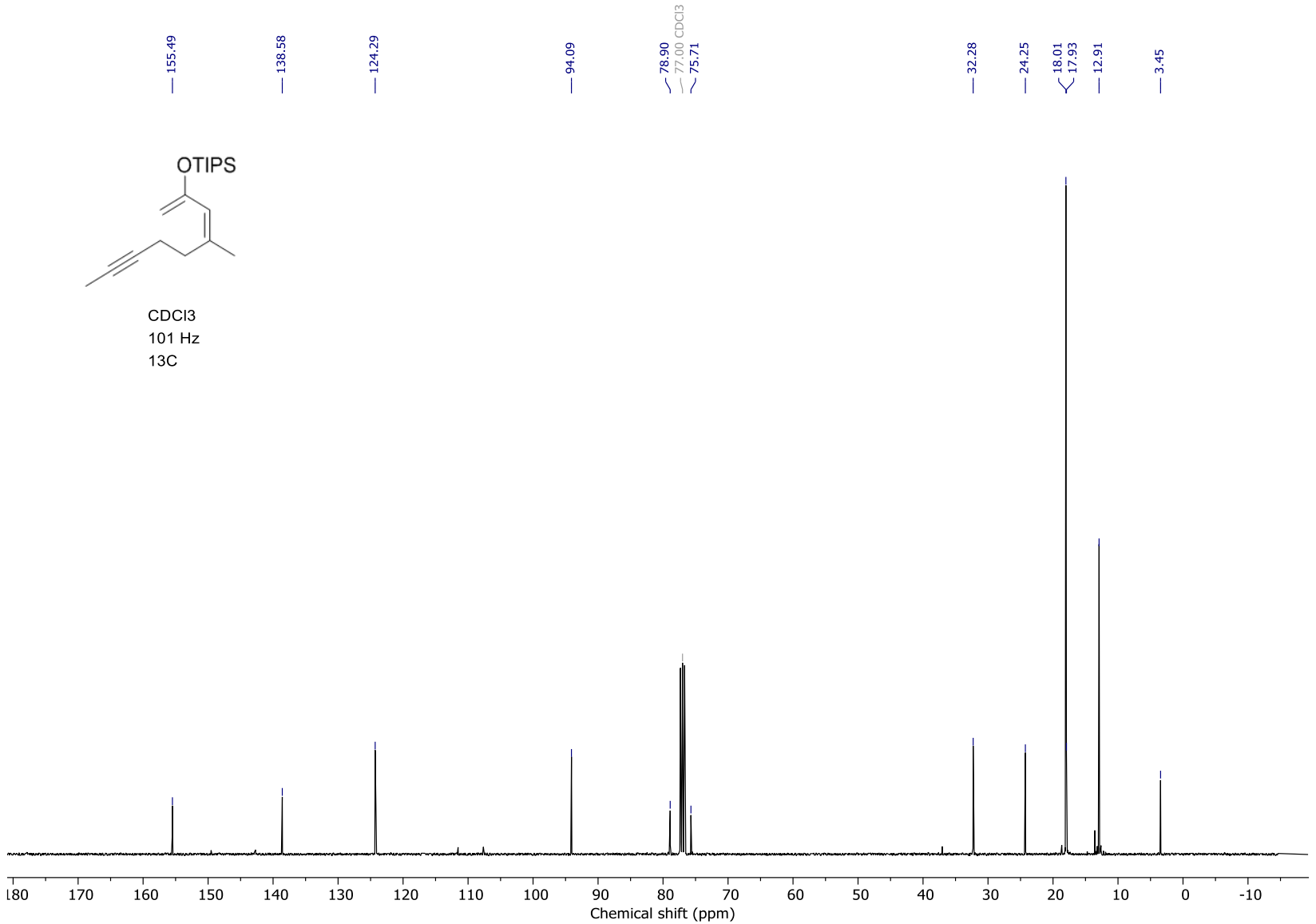

Spectra from Philippe McGee's Ph.D. thesis

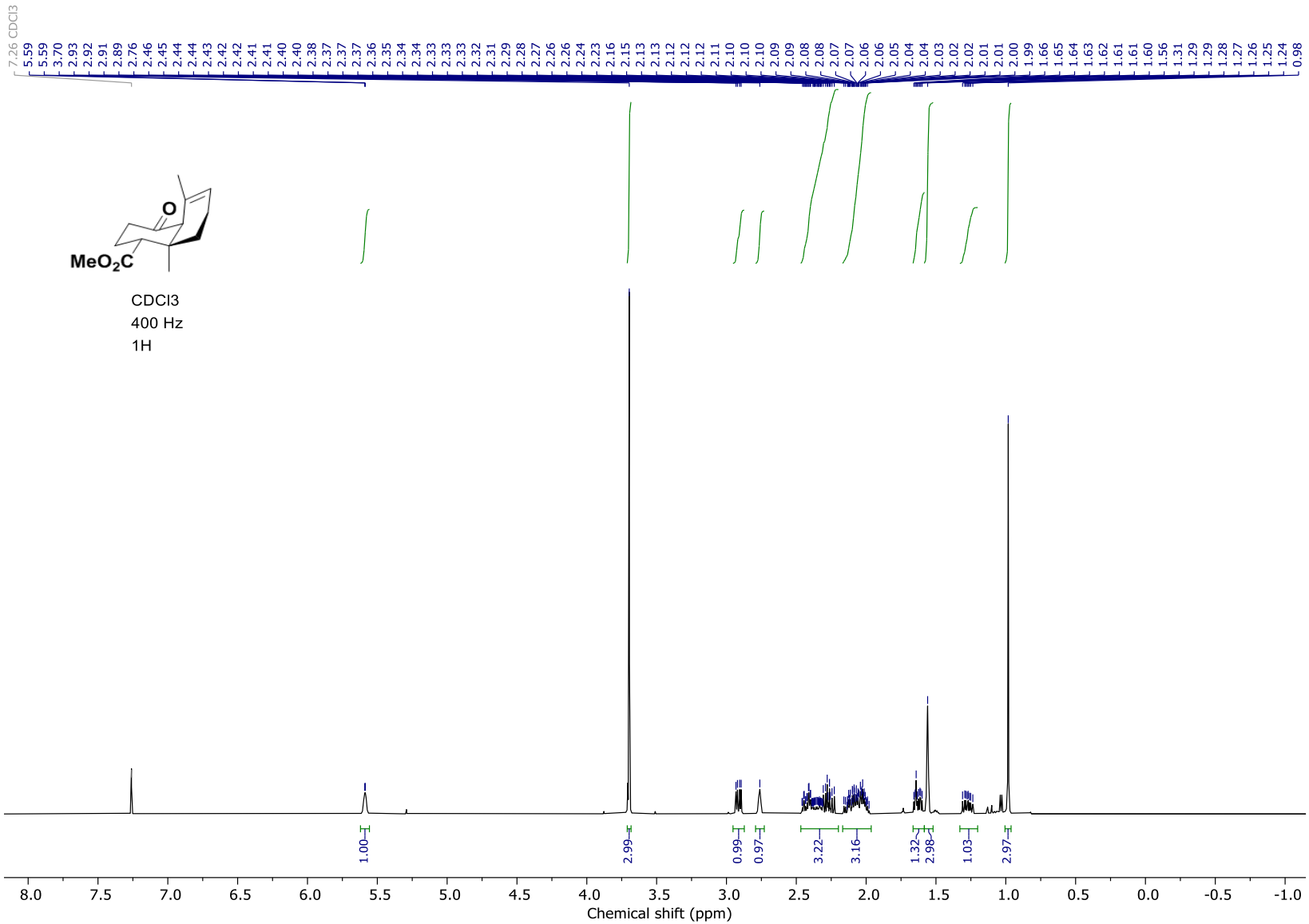

Spectra from Philippe McGee's Ph.D. thesis

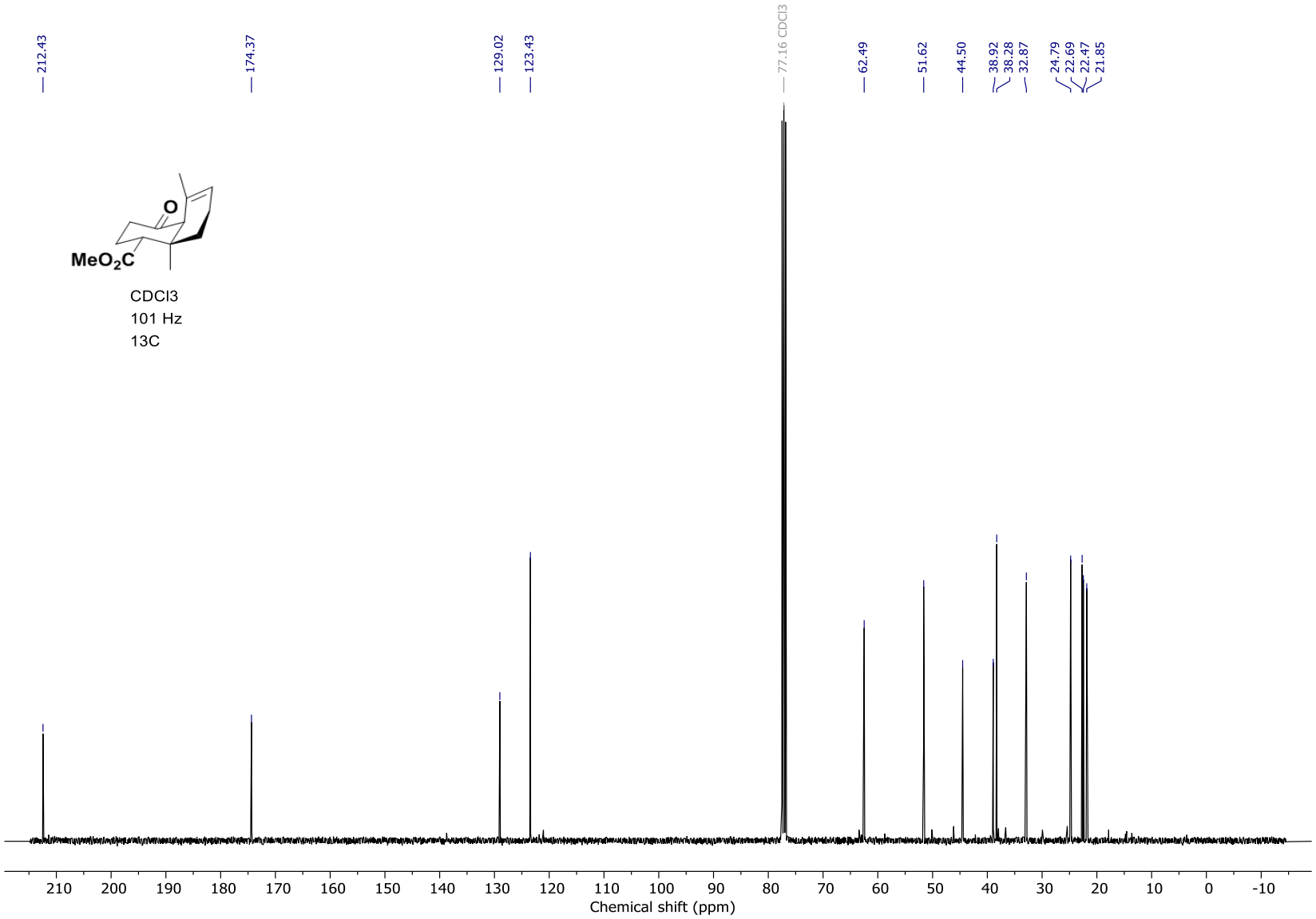

Spectra from Philippe McGee's Ph.D. thesis

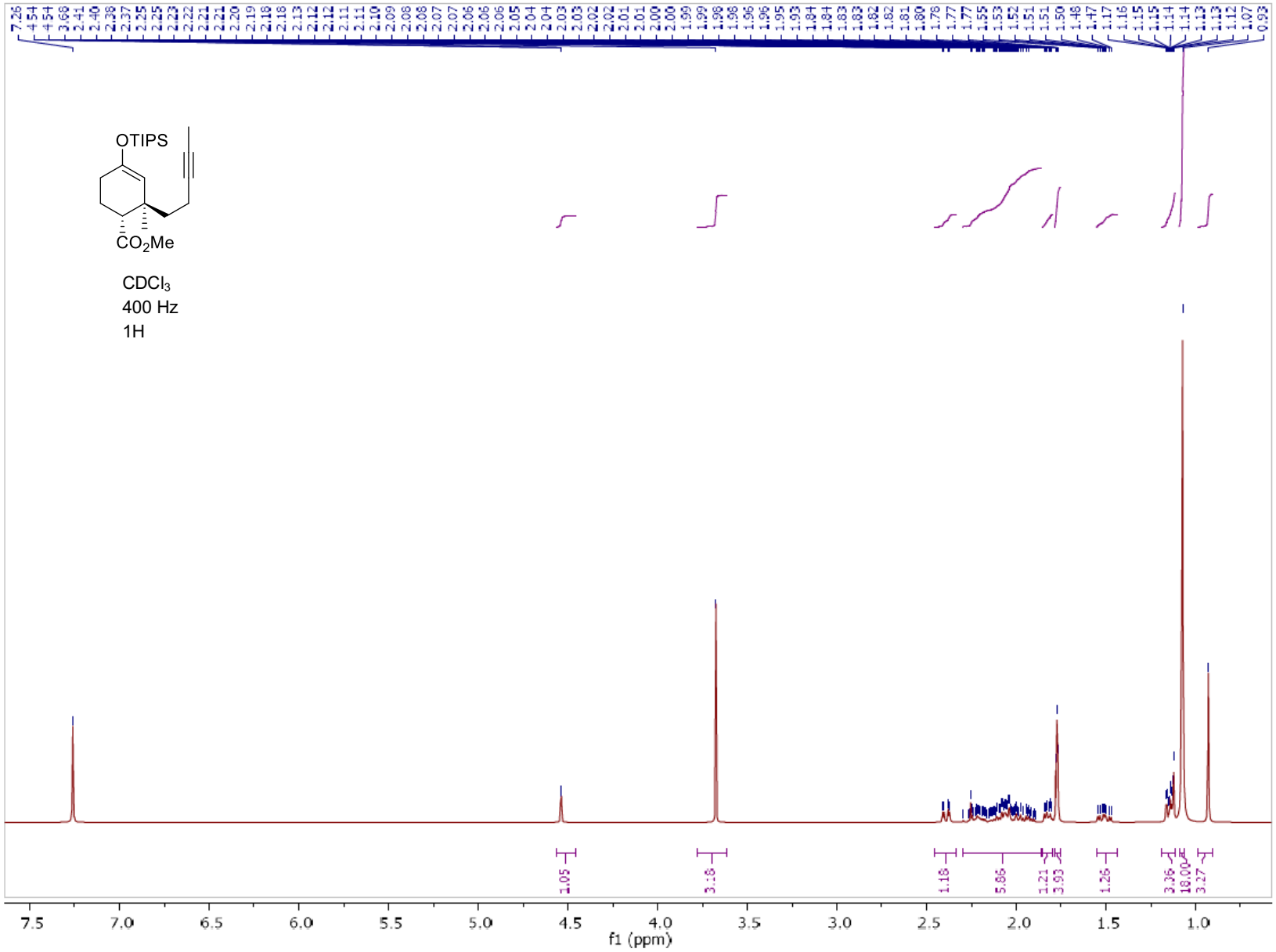

Spectra from Philippe McGee's Ph.D. thesis

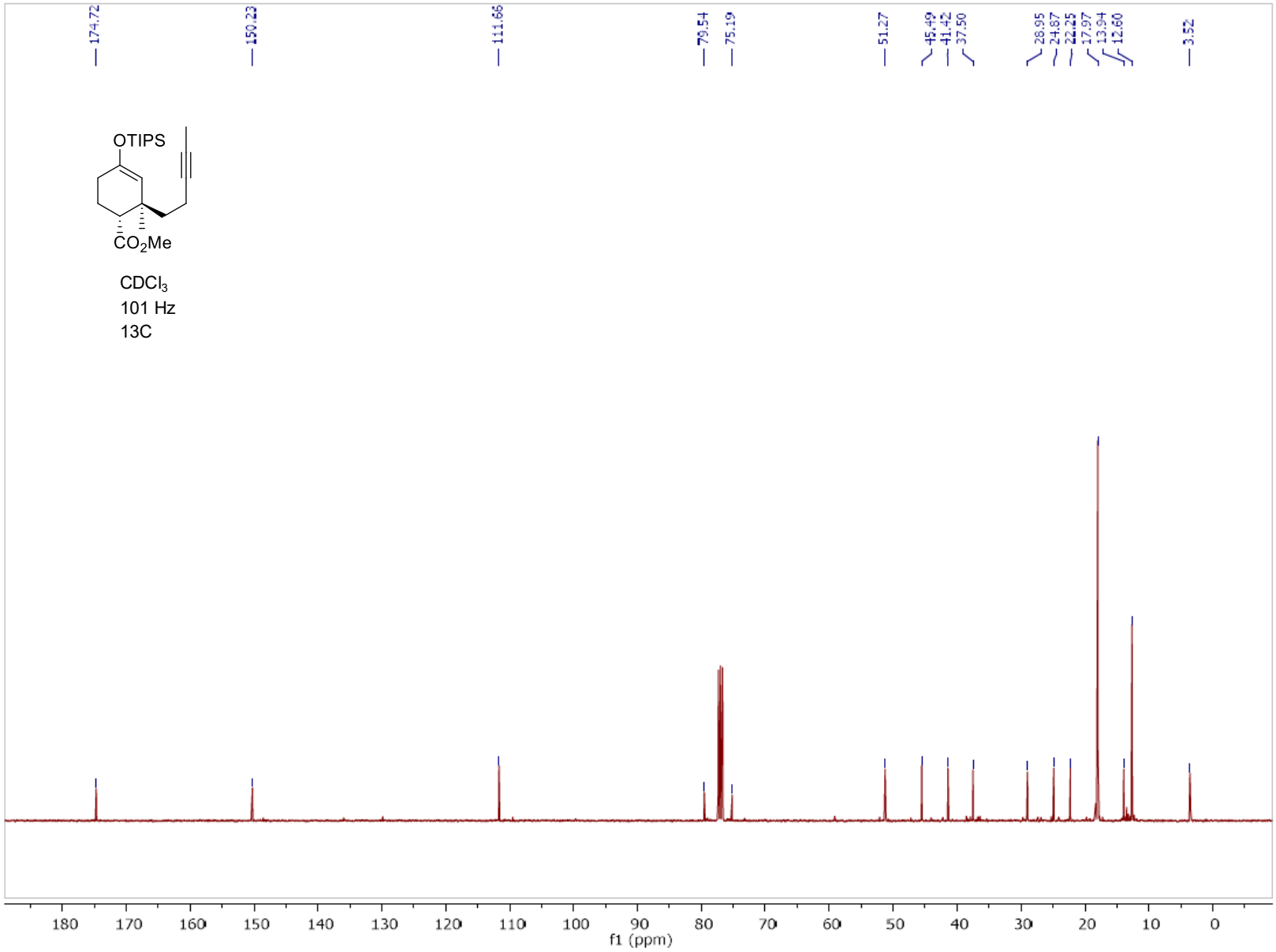

Spectra from Philippe McGee's Ph.D. thesis

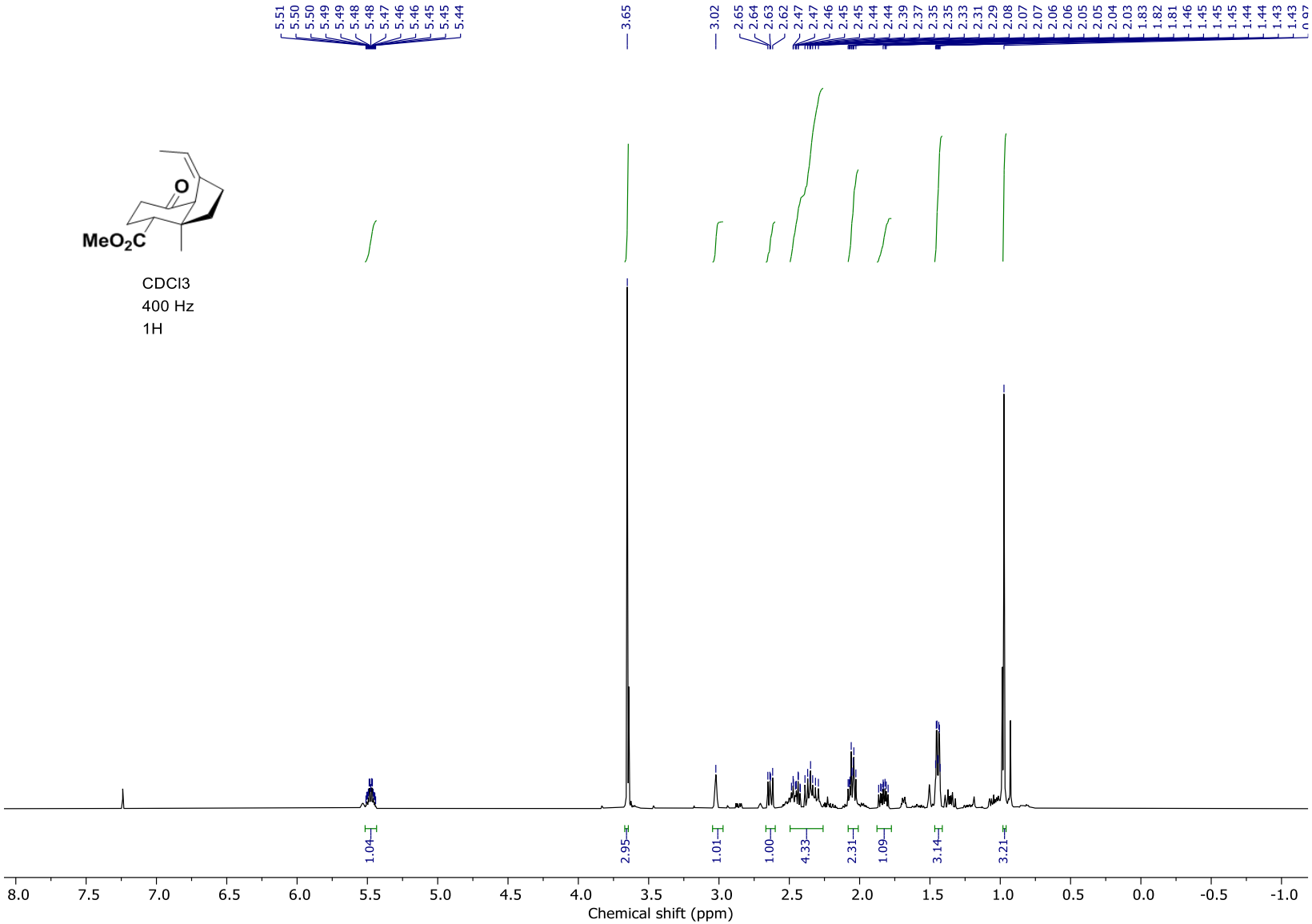

Spectra from Philippe McGee's Ph.D. thesis

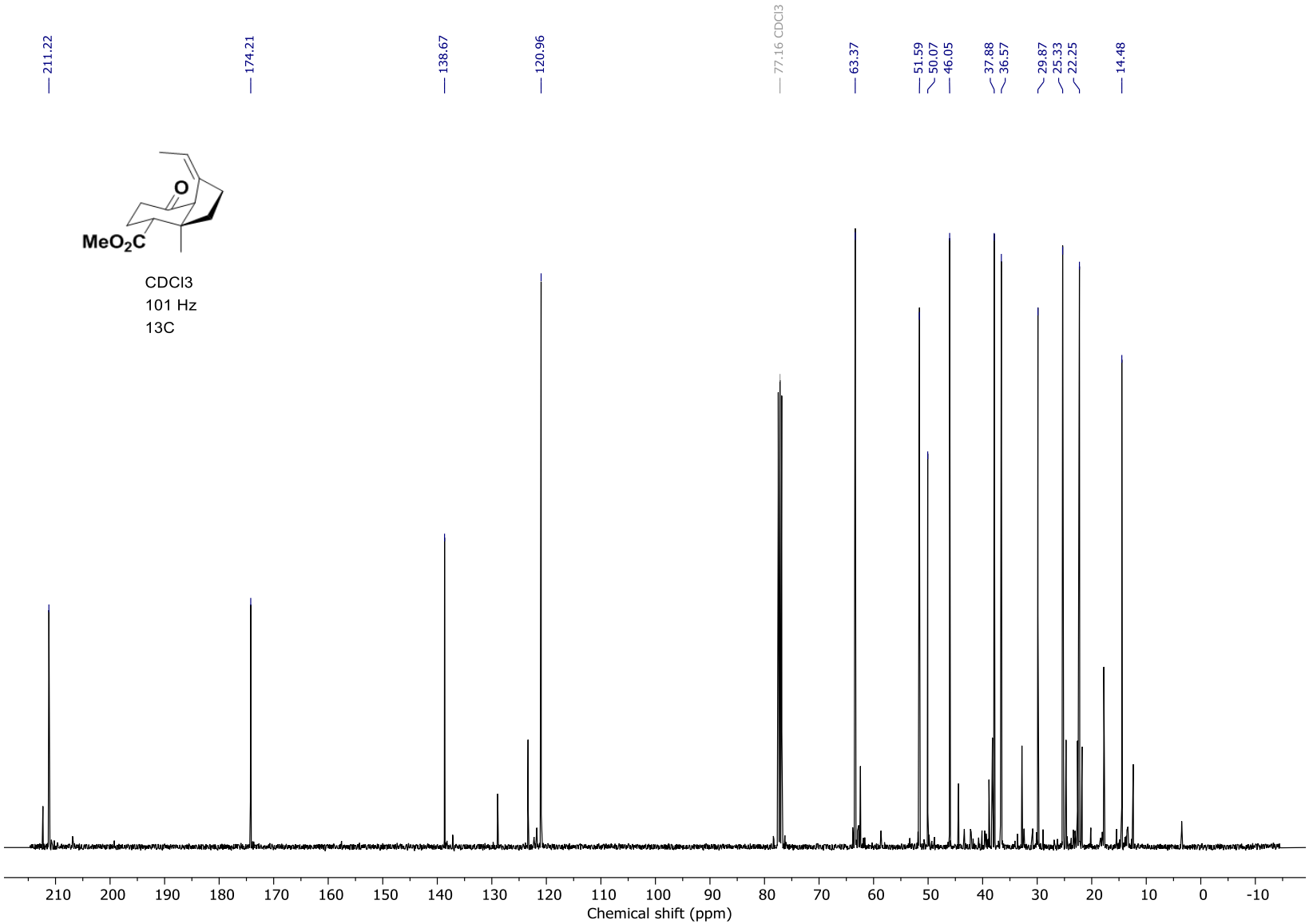

Spectra from Philippe McGee's Ph.D. thesis

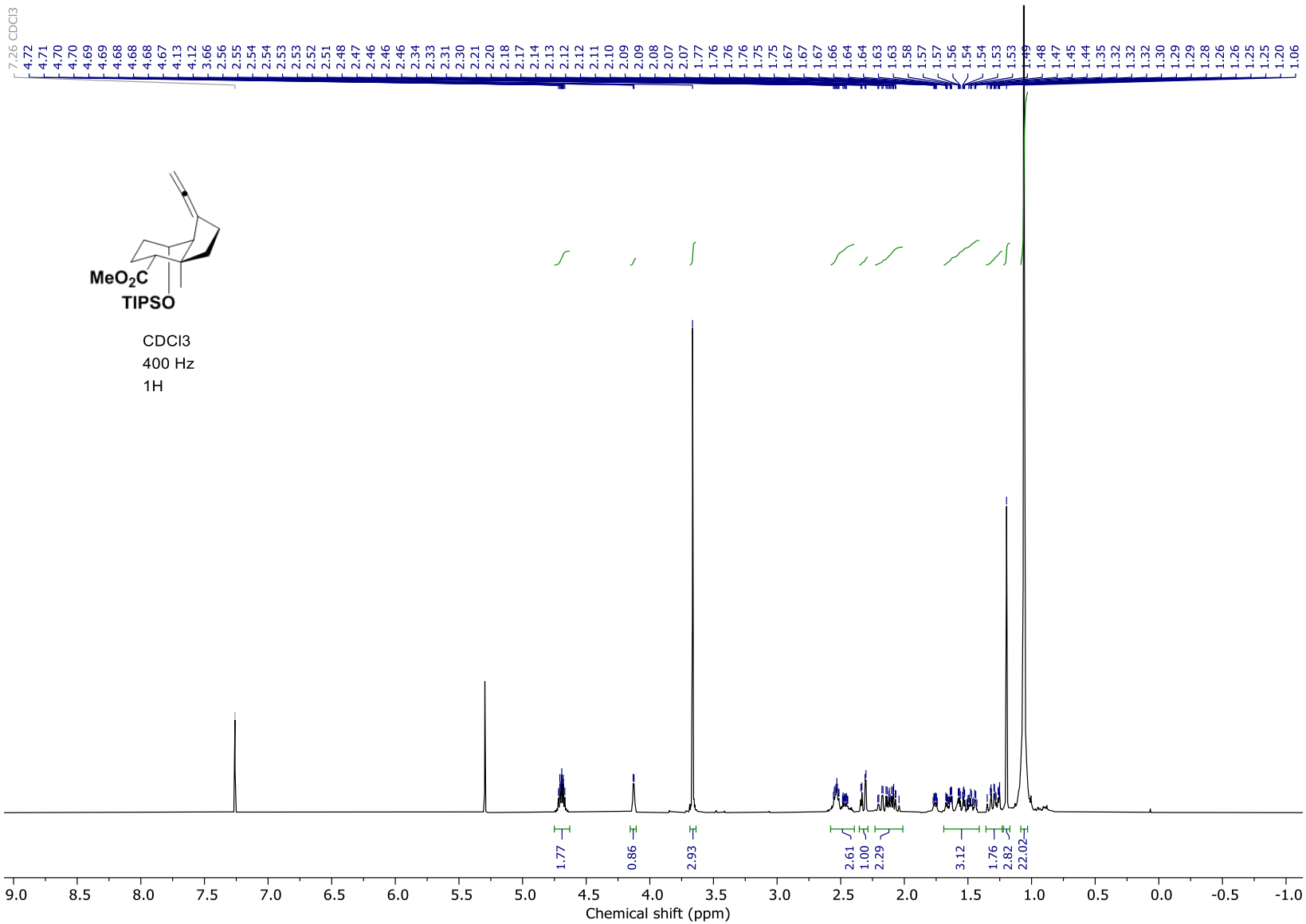

Spectra from Philippe McGee's Ph.D. thesis

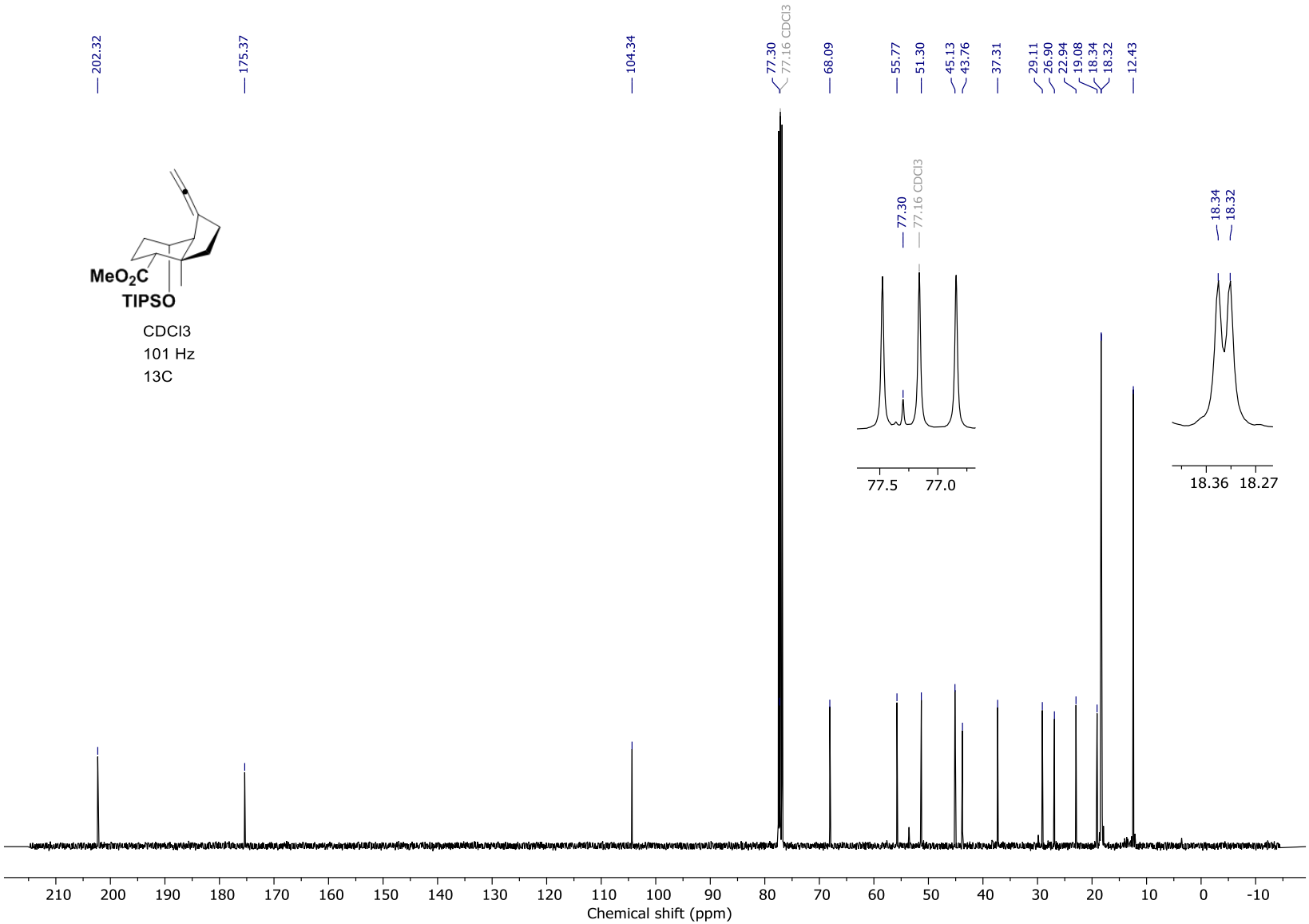

Spectra from Philippe McGee's Ph.D. thesis

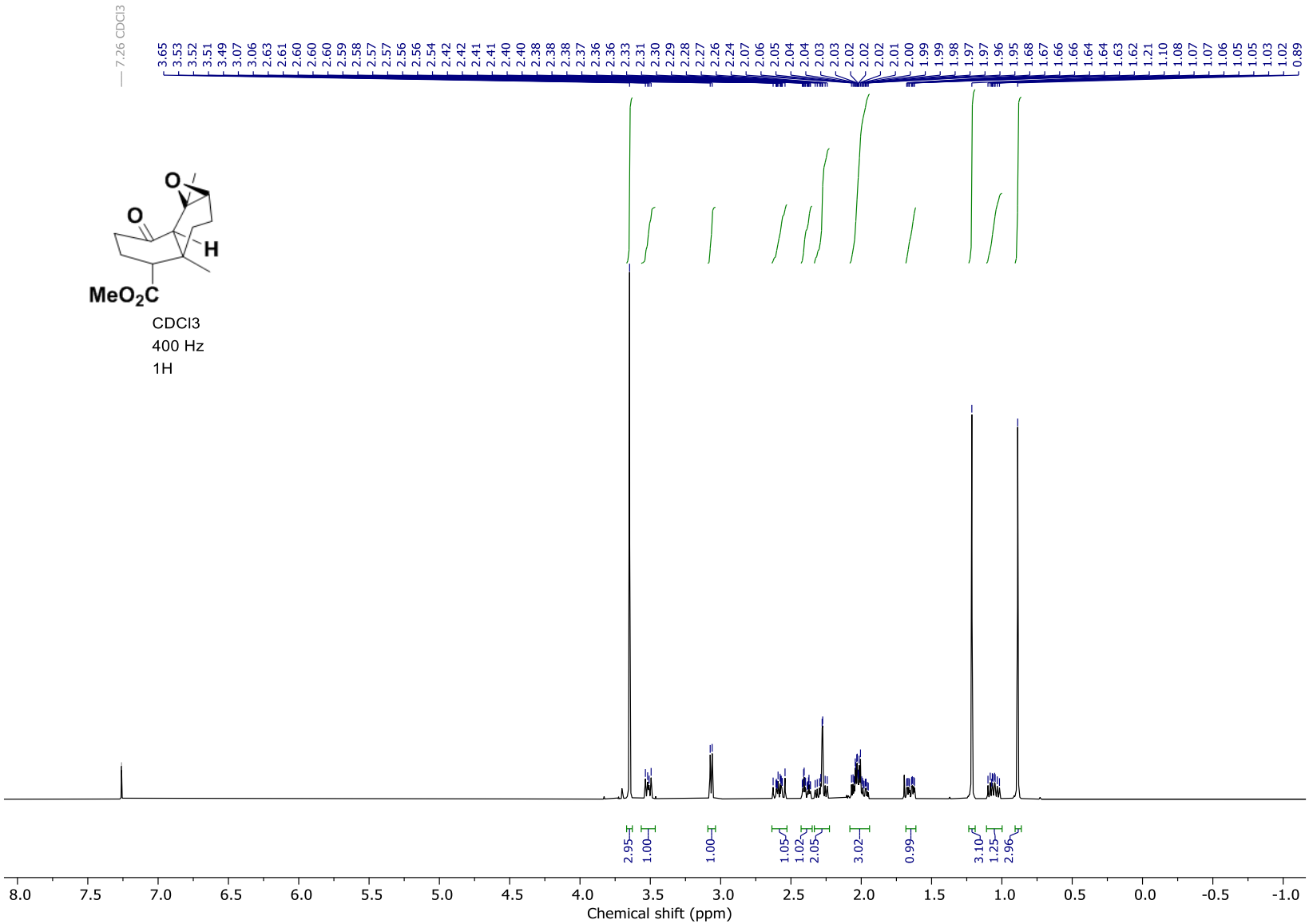

Spectra from Philippe McGee's Ph.D. thesis

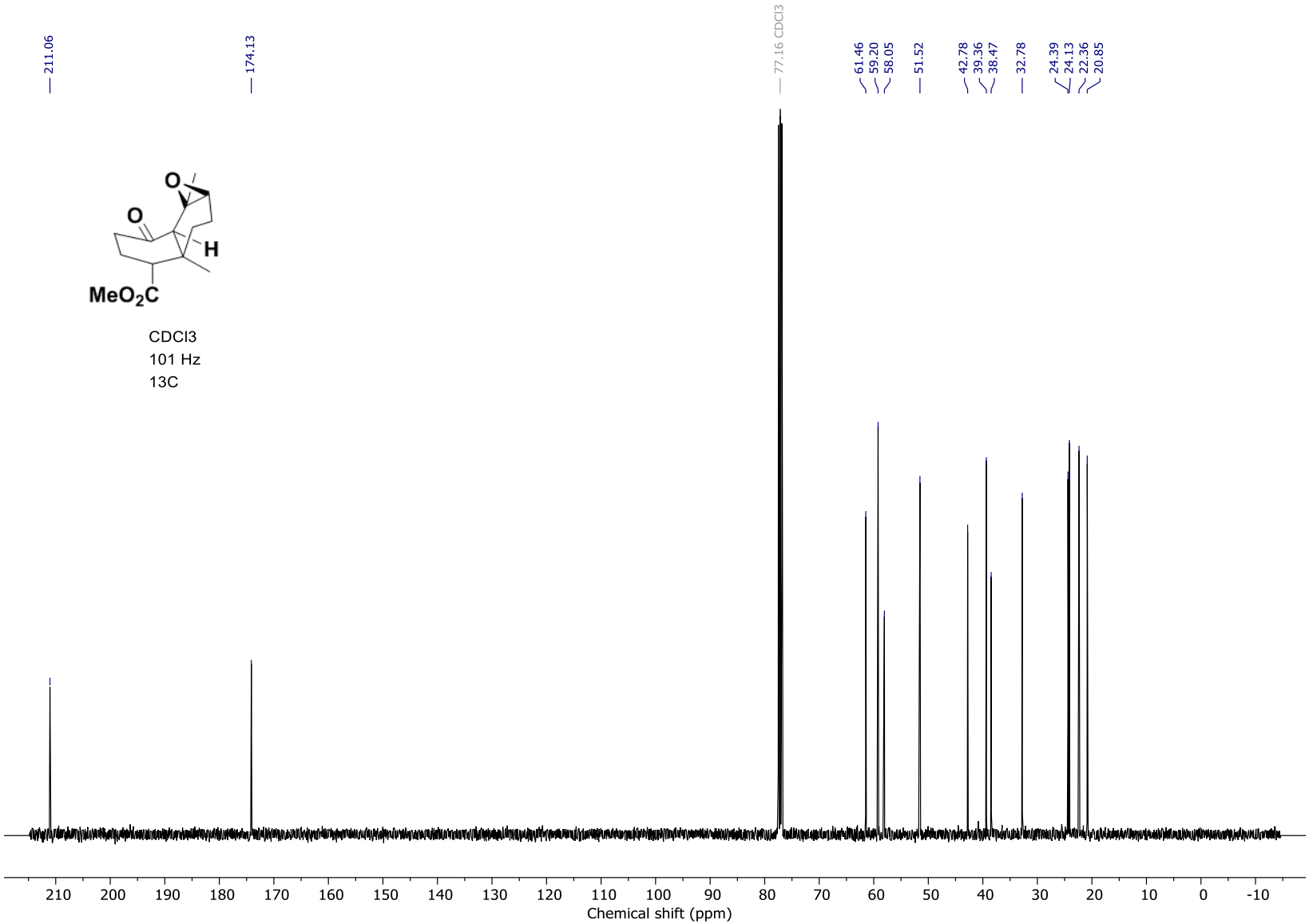

Spectra from Philippe McGee's Ph.D. thesis

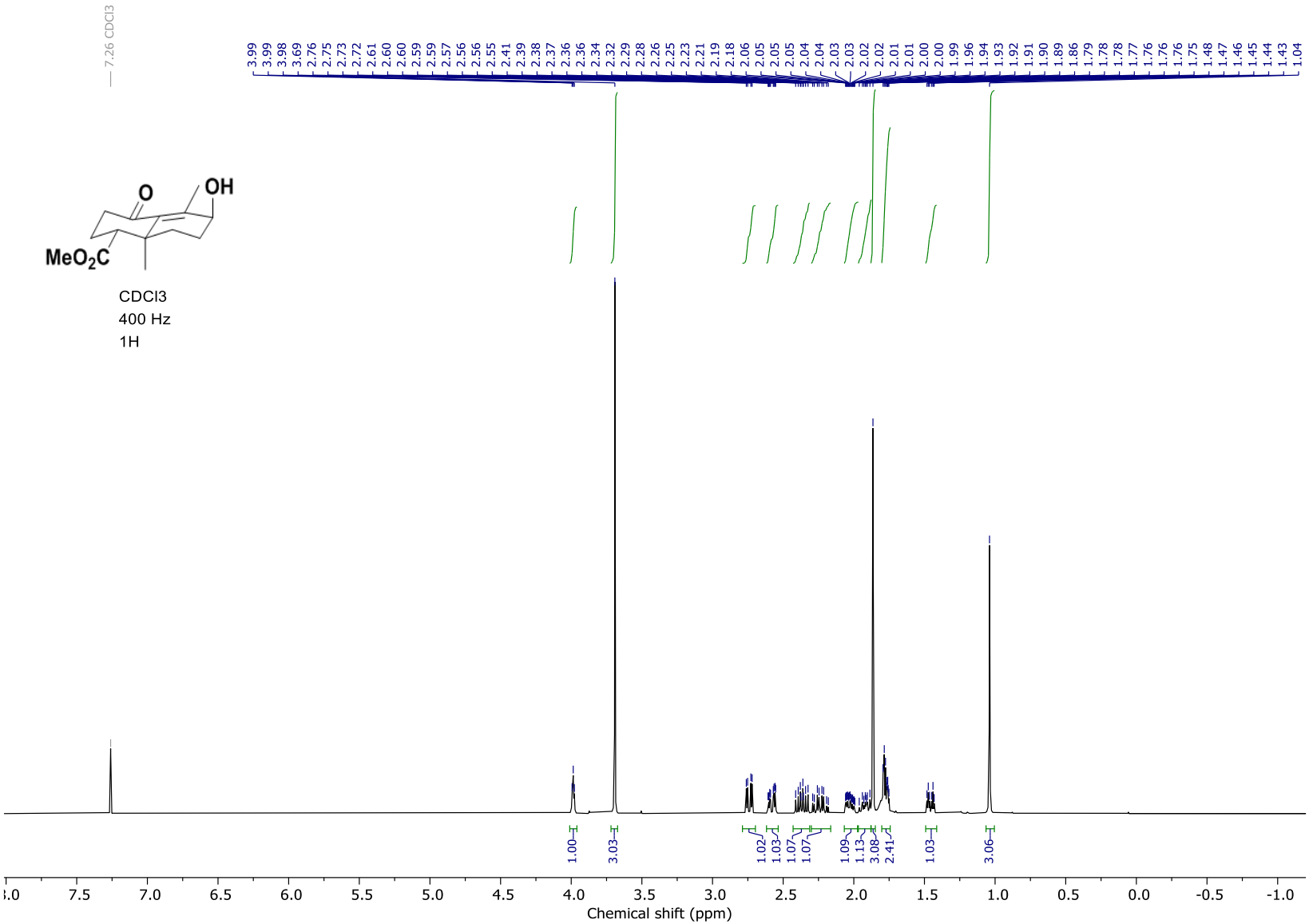

Spectra from Philippe McGee's Ph.D. thesis

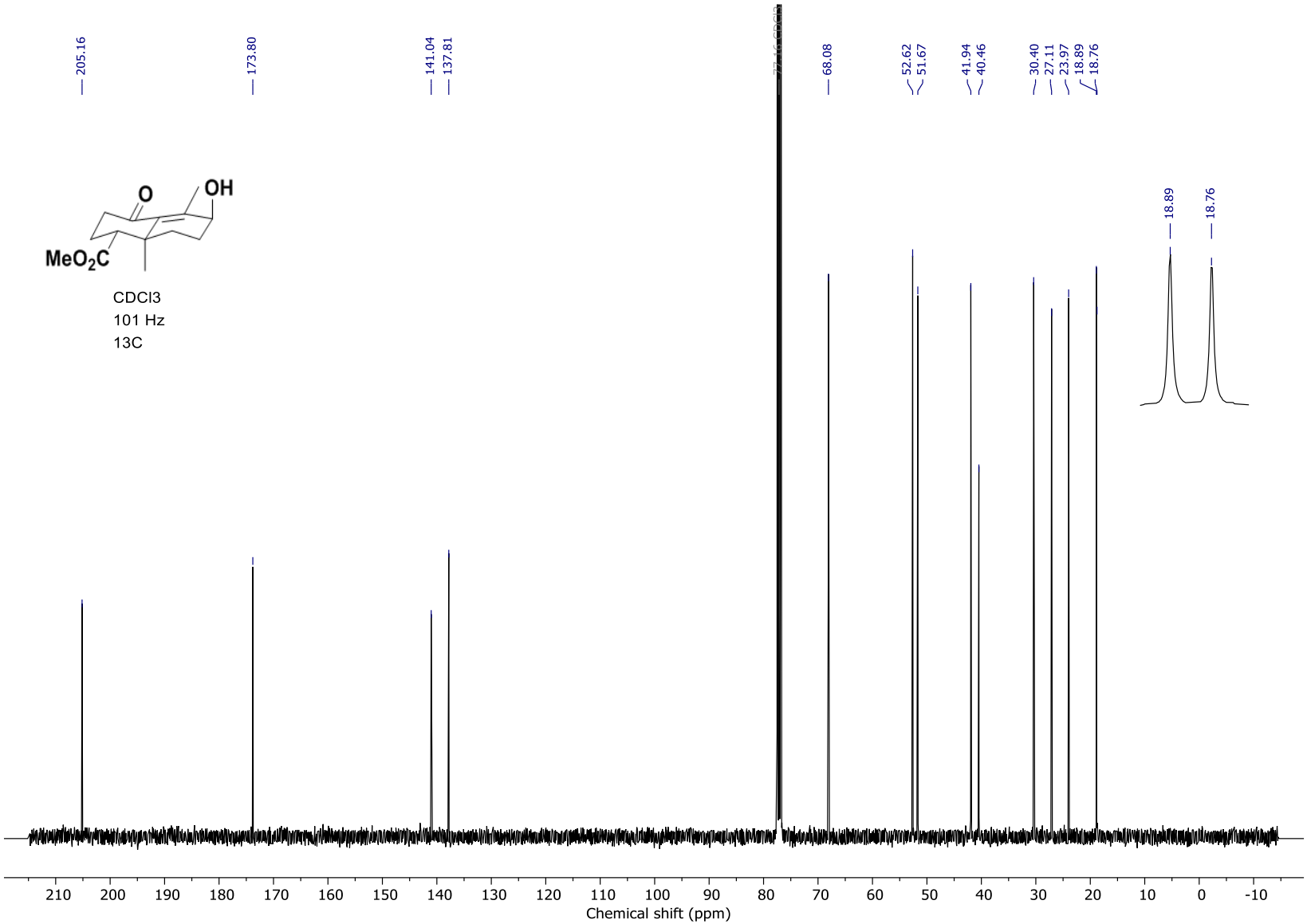

Spectra from Philippe McGee's Ph.D. thesis

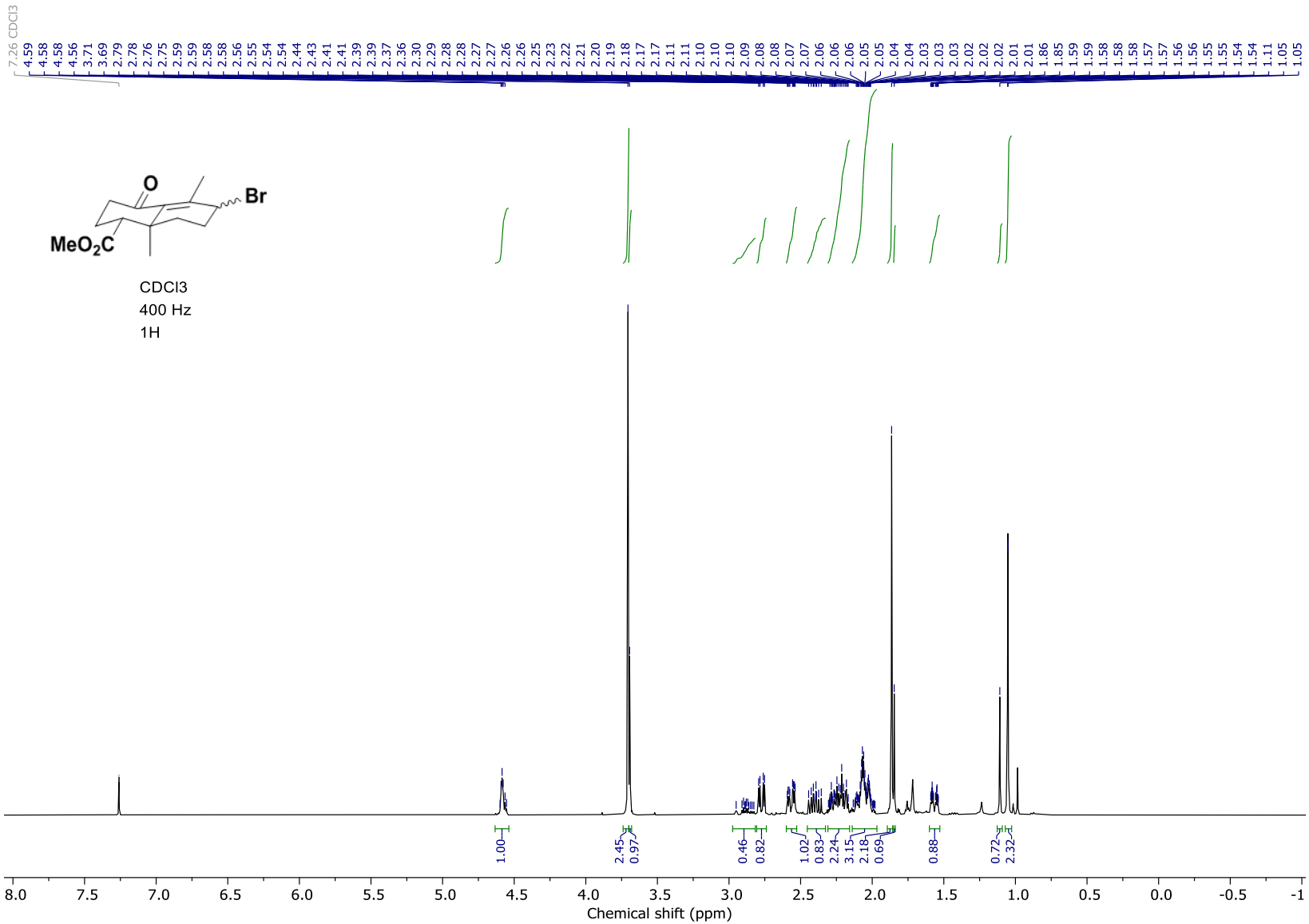

Spectra from Philippe McGee's Ph.D. thesis

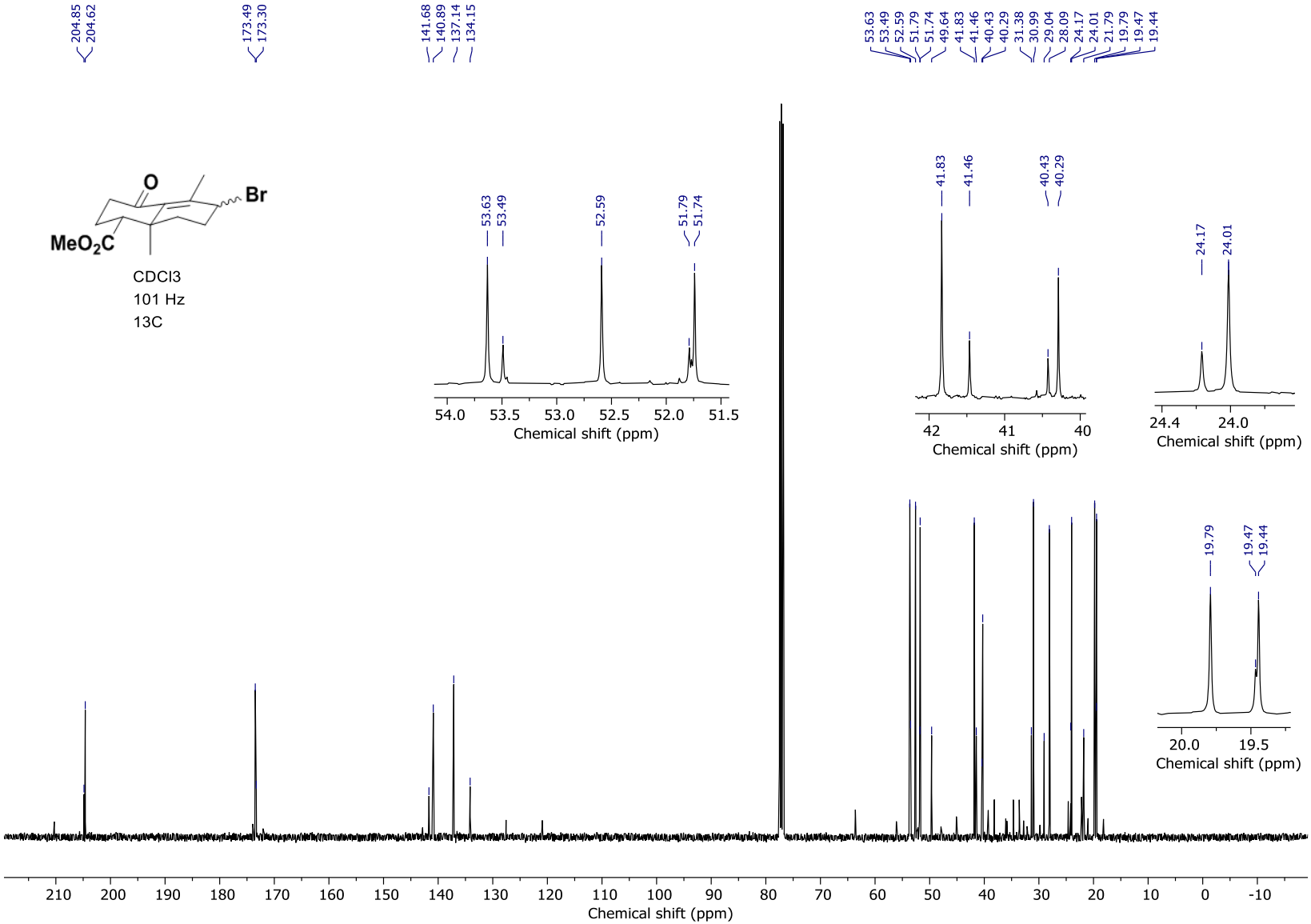

Spectra from Philippe McGee's Ph.D. thesis

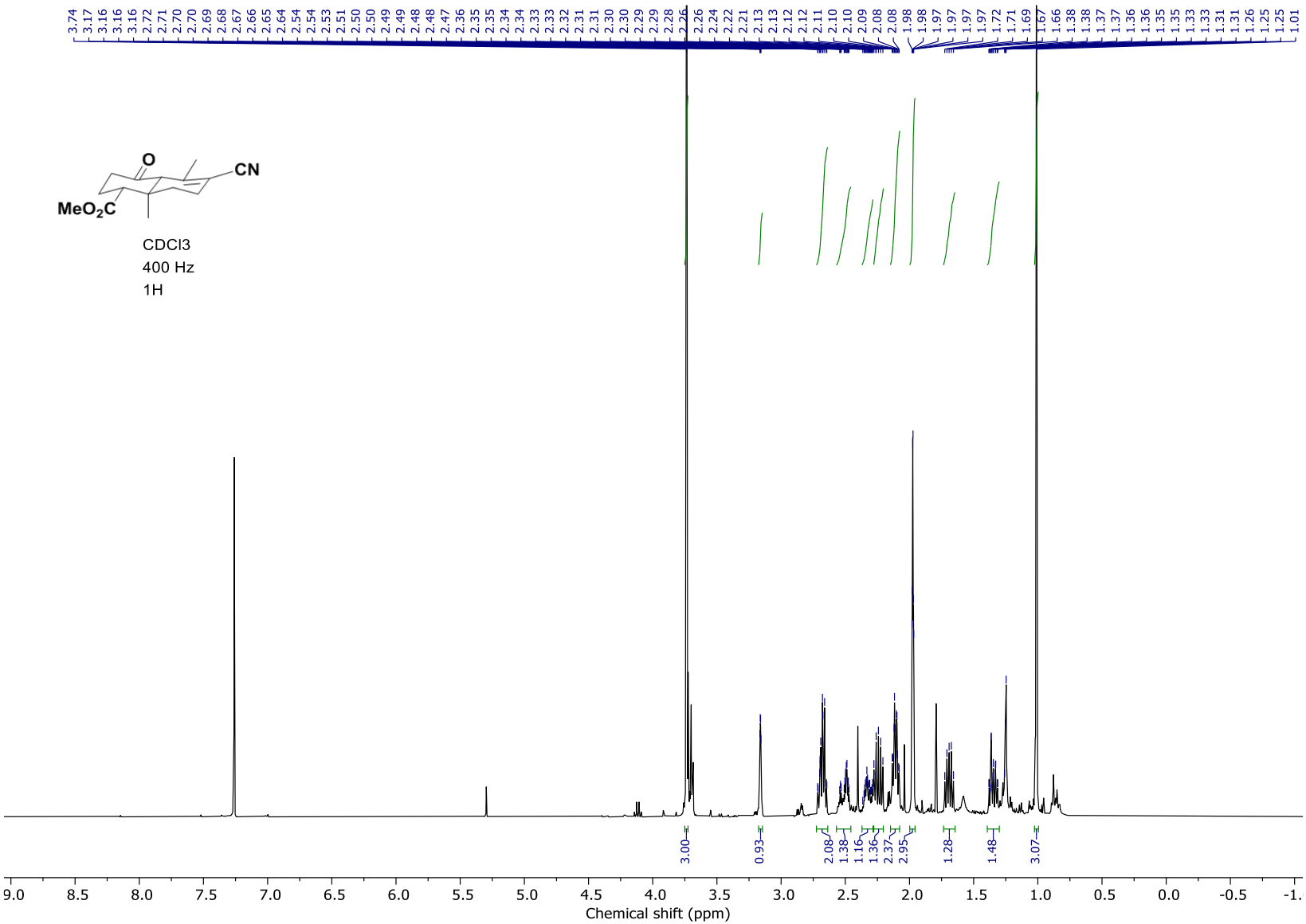

Spectra from Philippe McGee's Ph.D. thesis

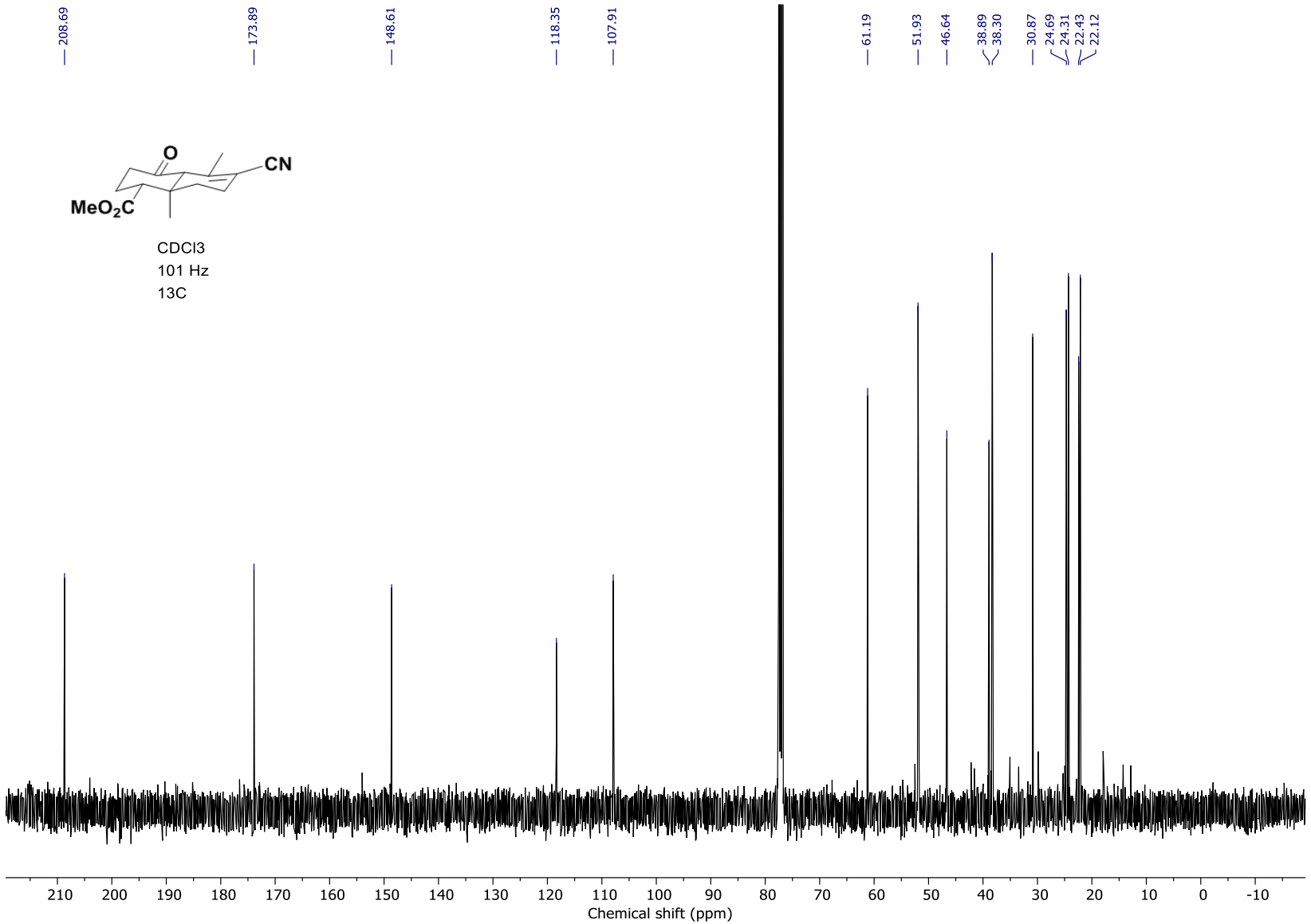

Spectra from Philippe McGee's Ph.D. thesis

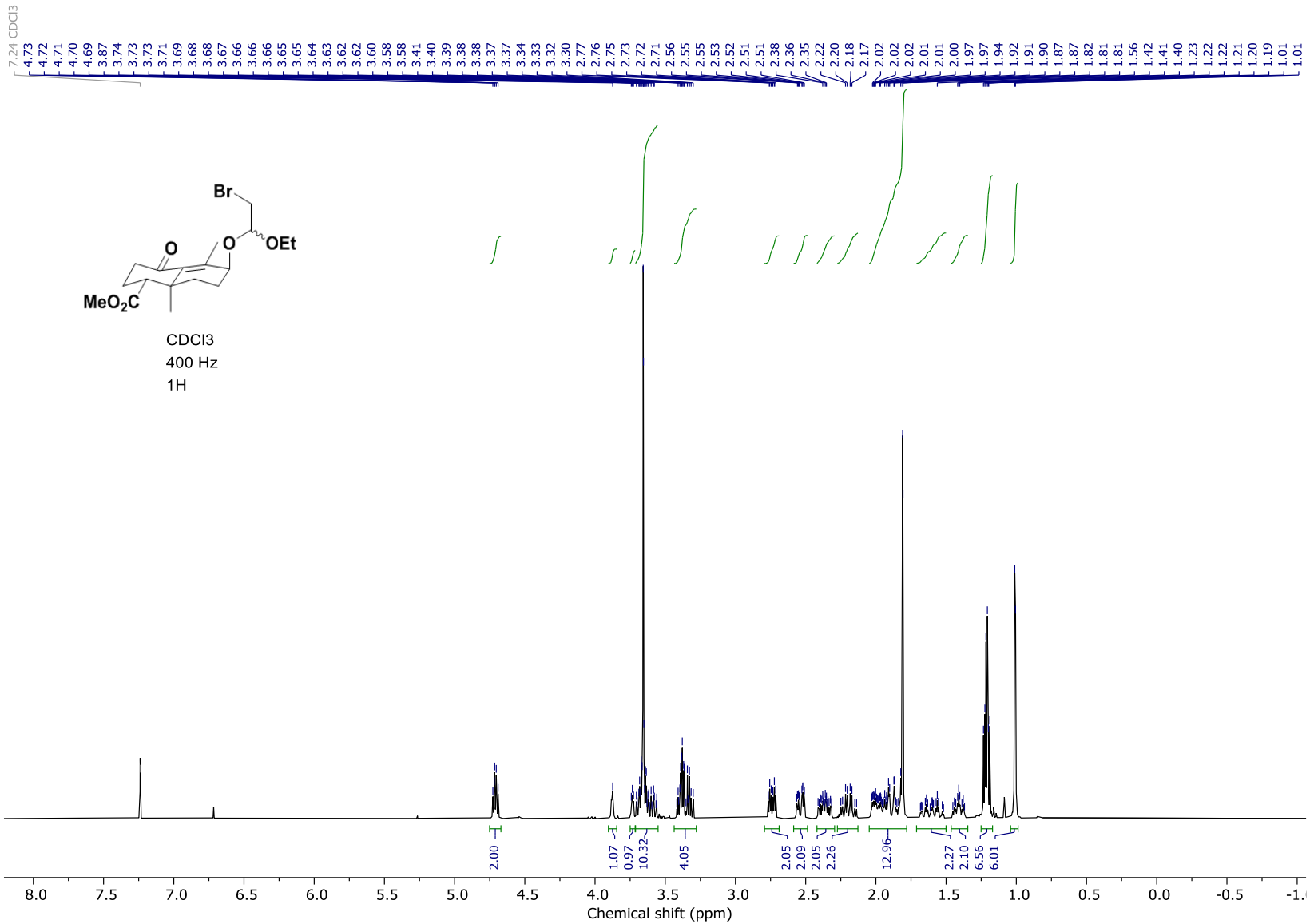

Spectra from Philippe McGee's Ph.D. thesis

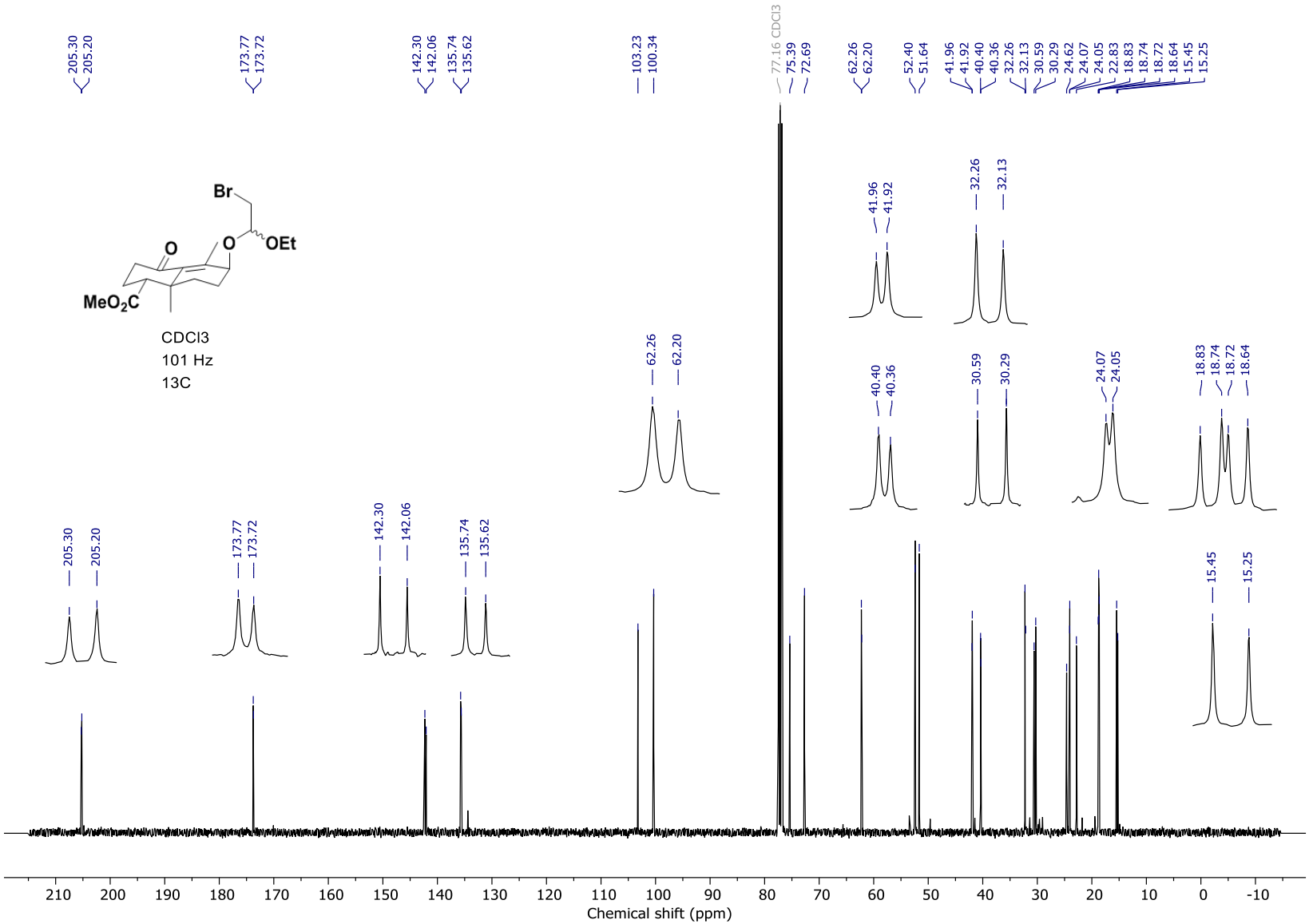

Spectra from Philippe McGee's Ph.D. thesis

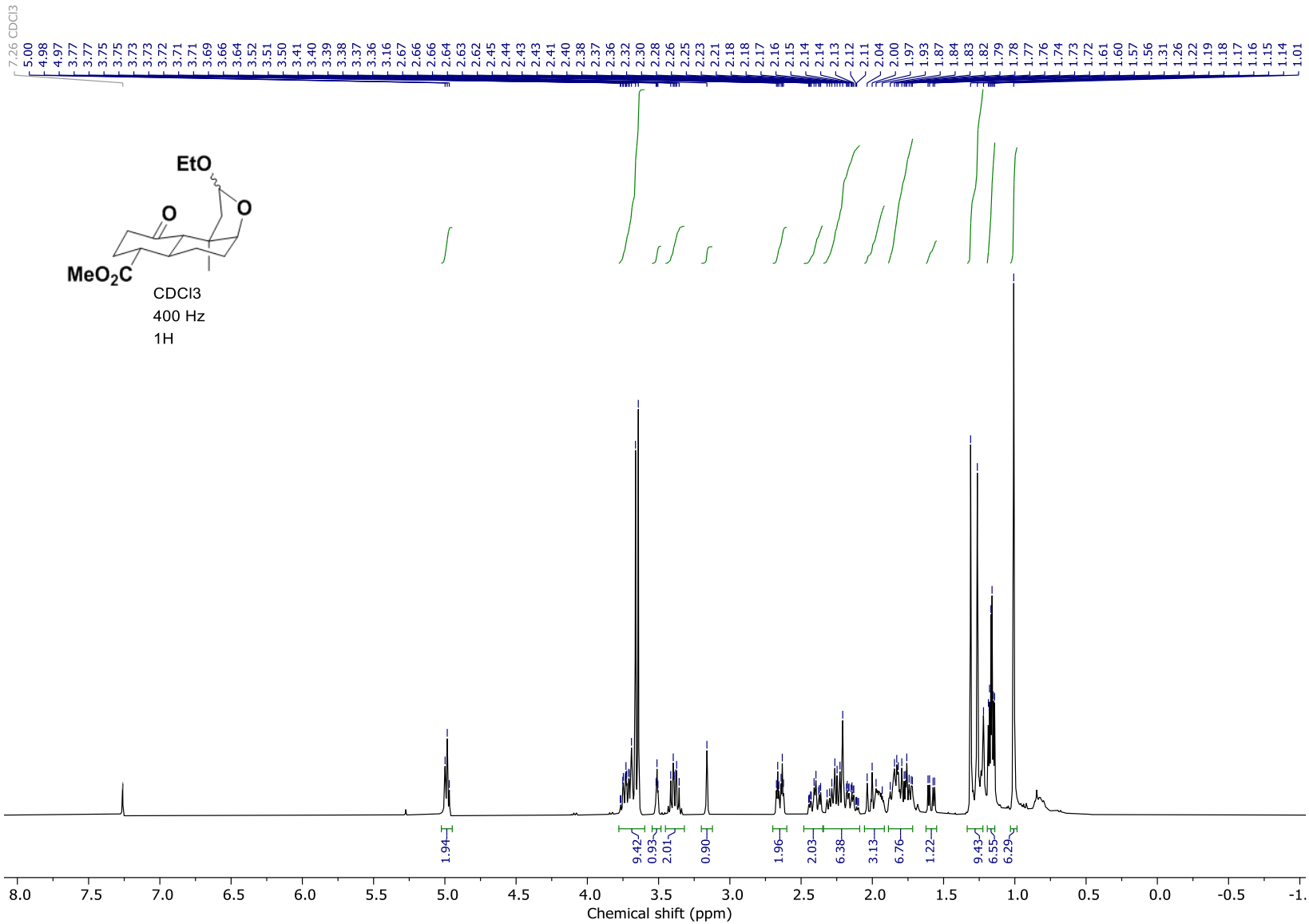

Spectra from Philippe McGee's Ph.D. thesis

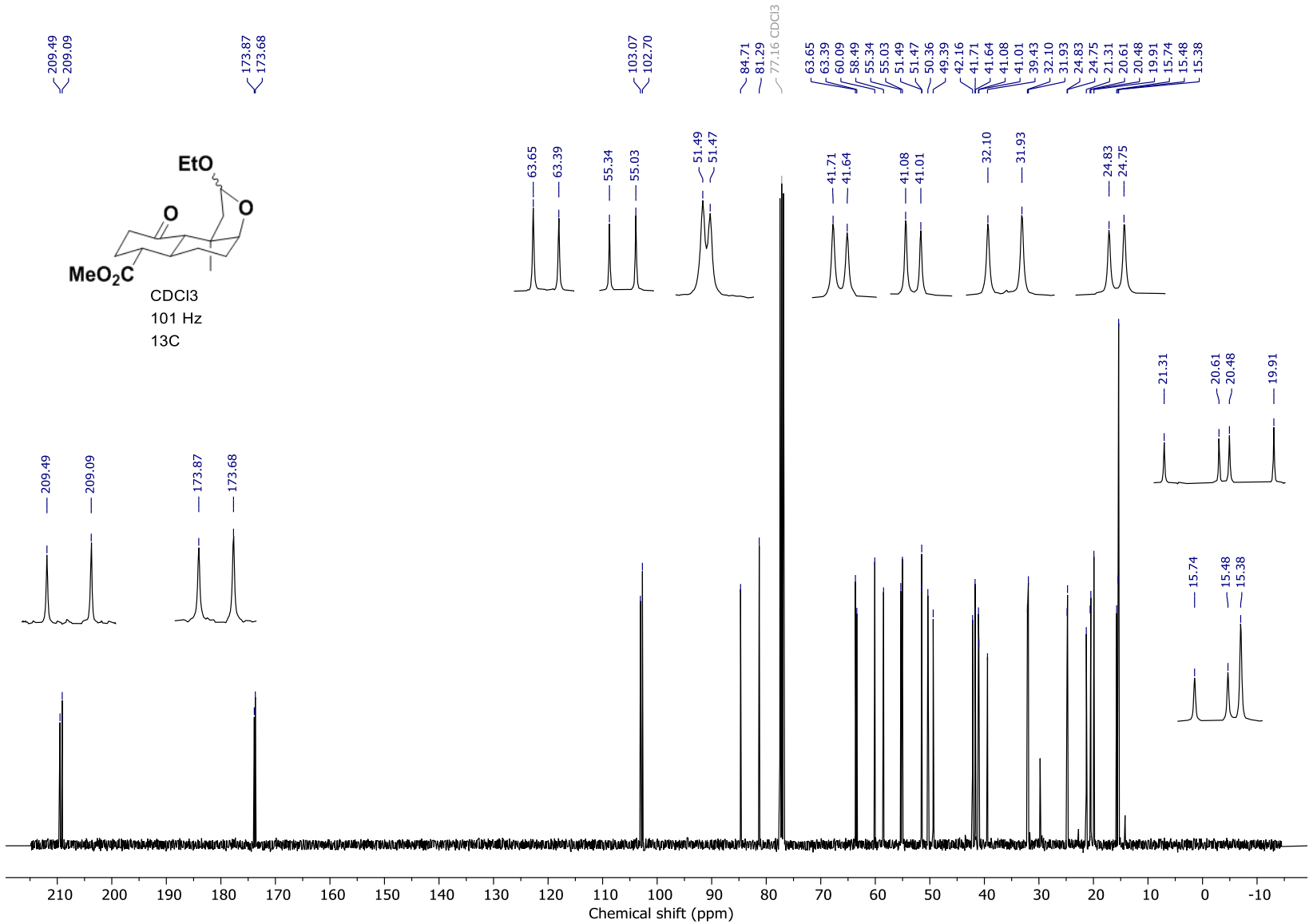

Spectra from Philippe McGee's Ph.D. thesis

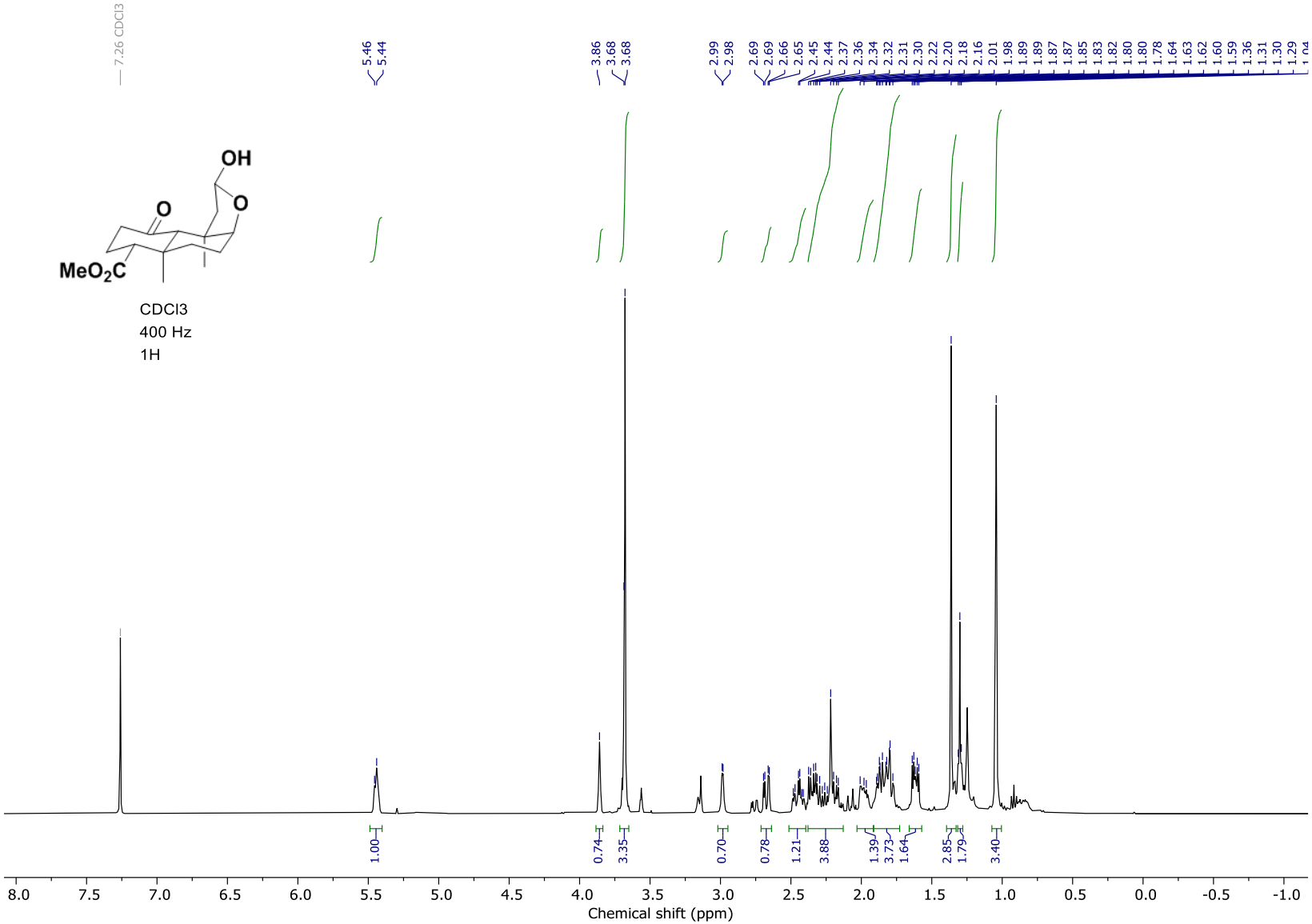

Spectra from Philippe McGee's Ph.D. thesis

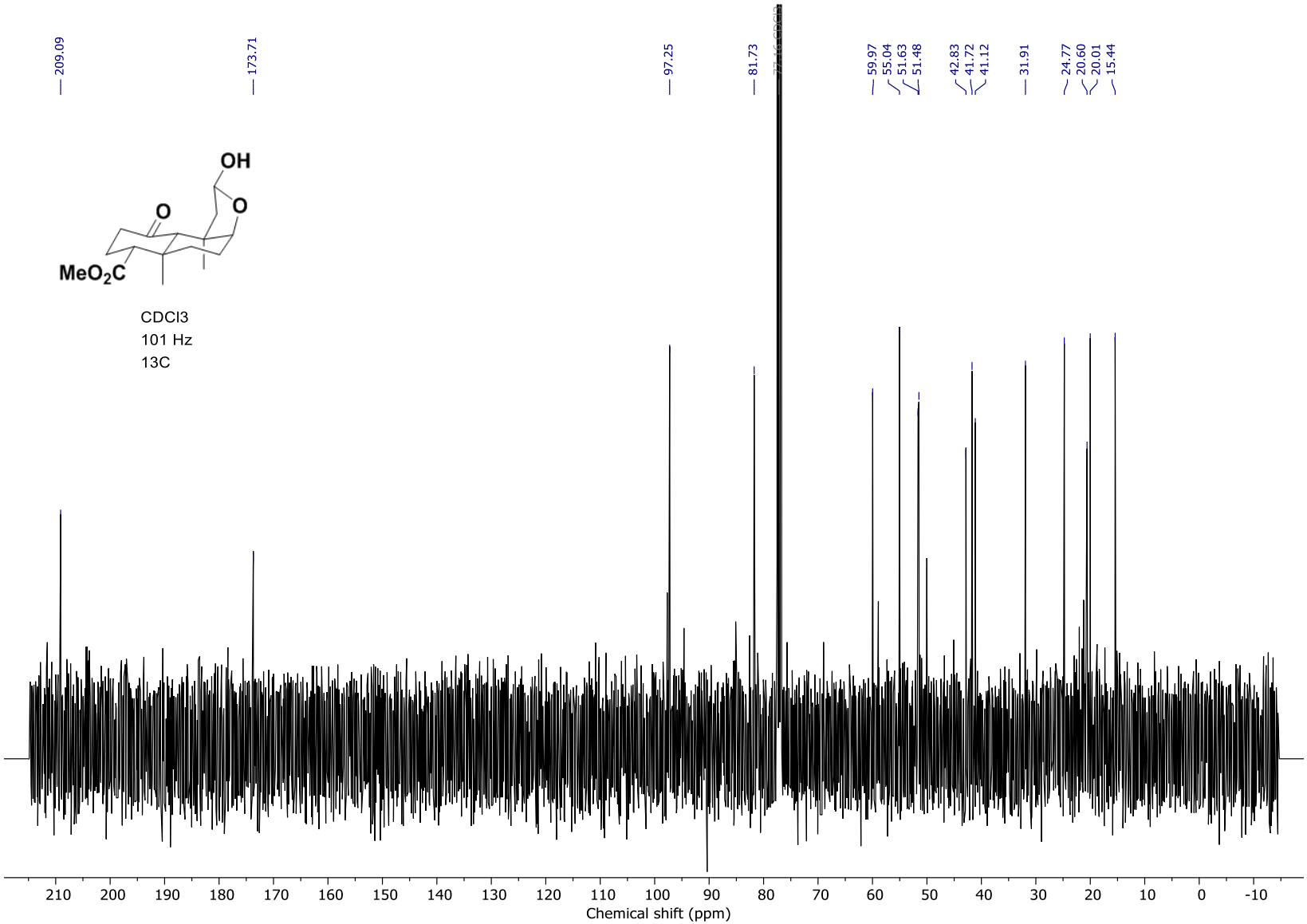

Spectra from Philippe McGee's Ph.D. thesis

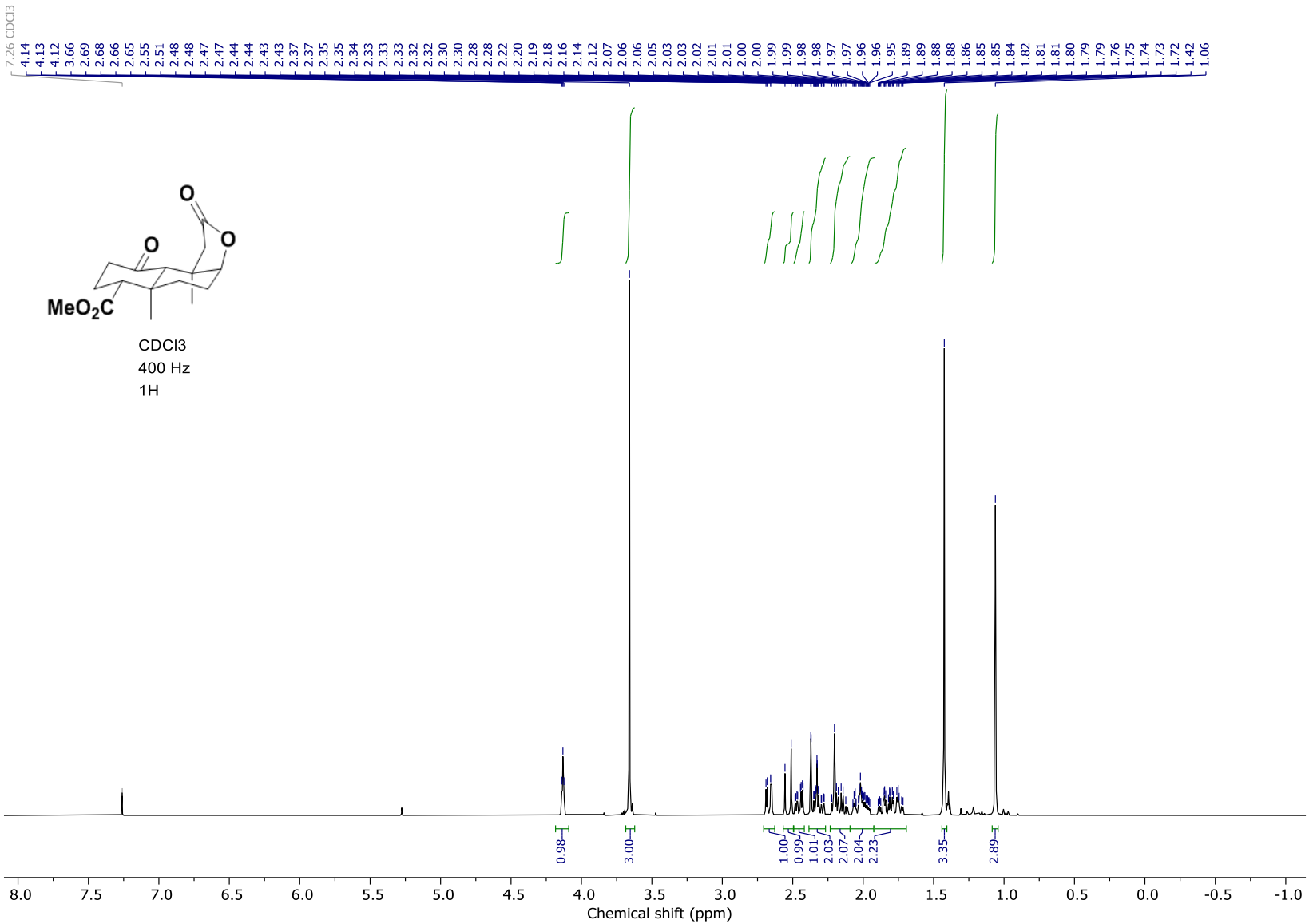

Spectra from Philippe McGee's Ph.D. thesis

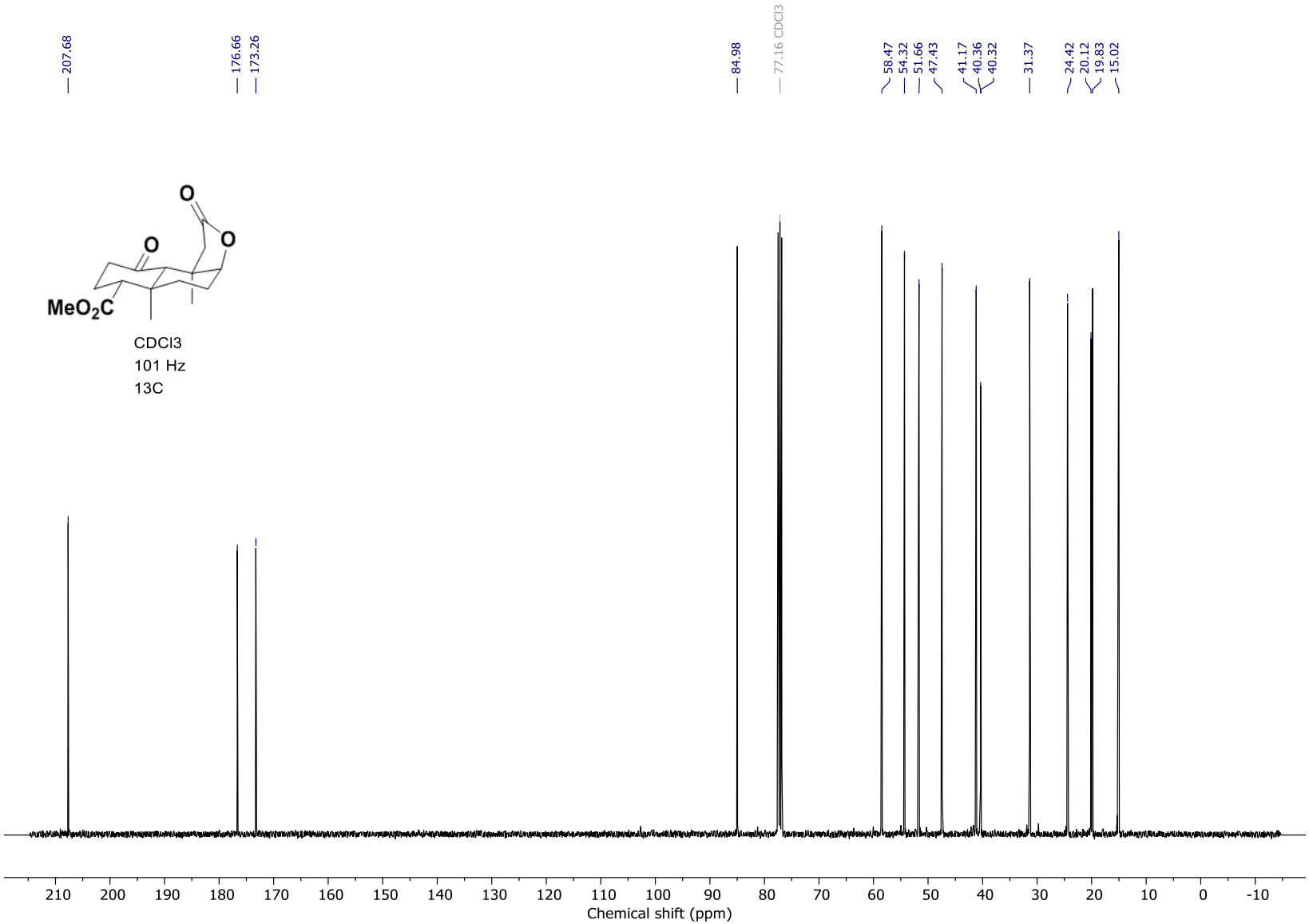

Spectra from Philippe McGee's Ph.D. thesis

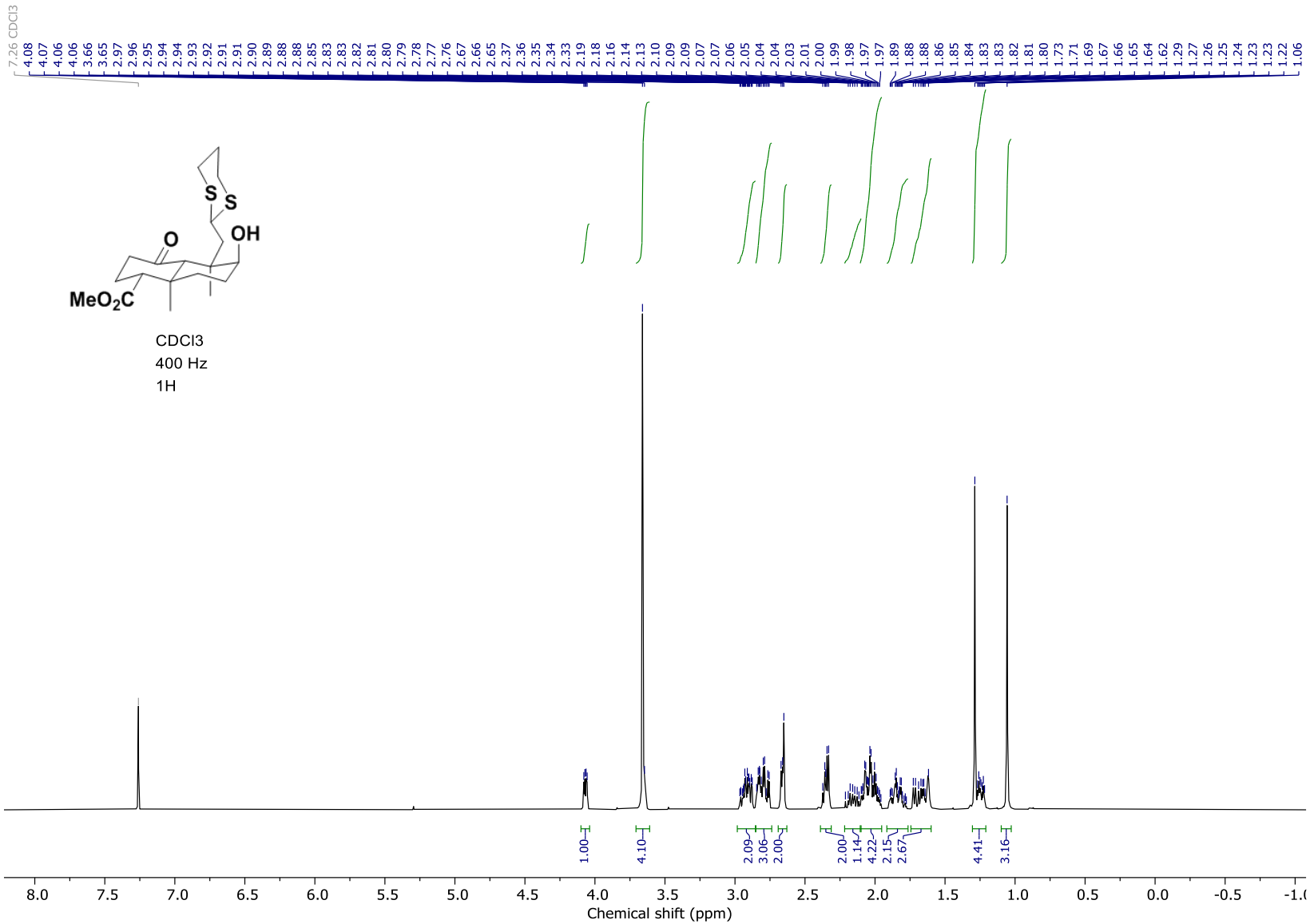

Spectra from Philippe McGee's Ph.D. thesis

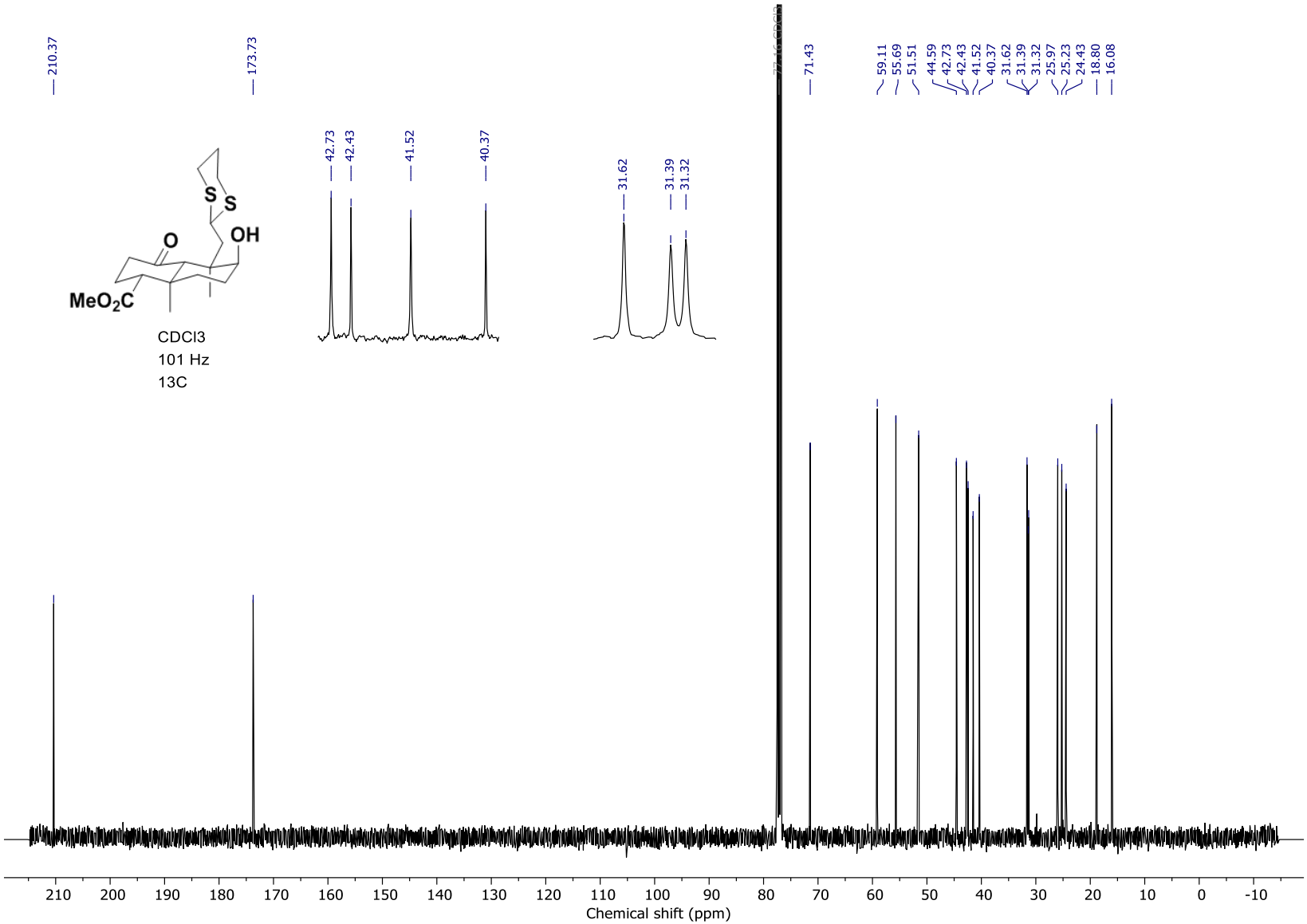

Spectra from Philippe McGee's Ph.D. thesis

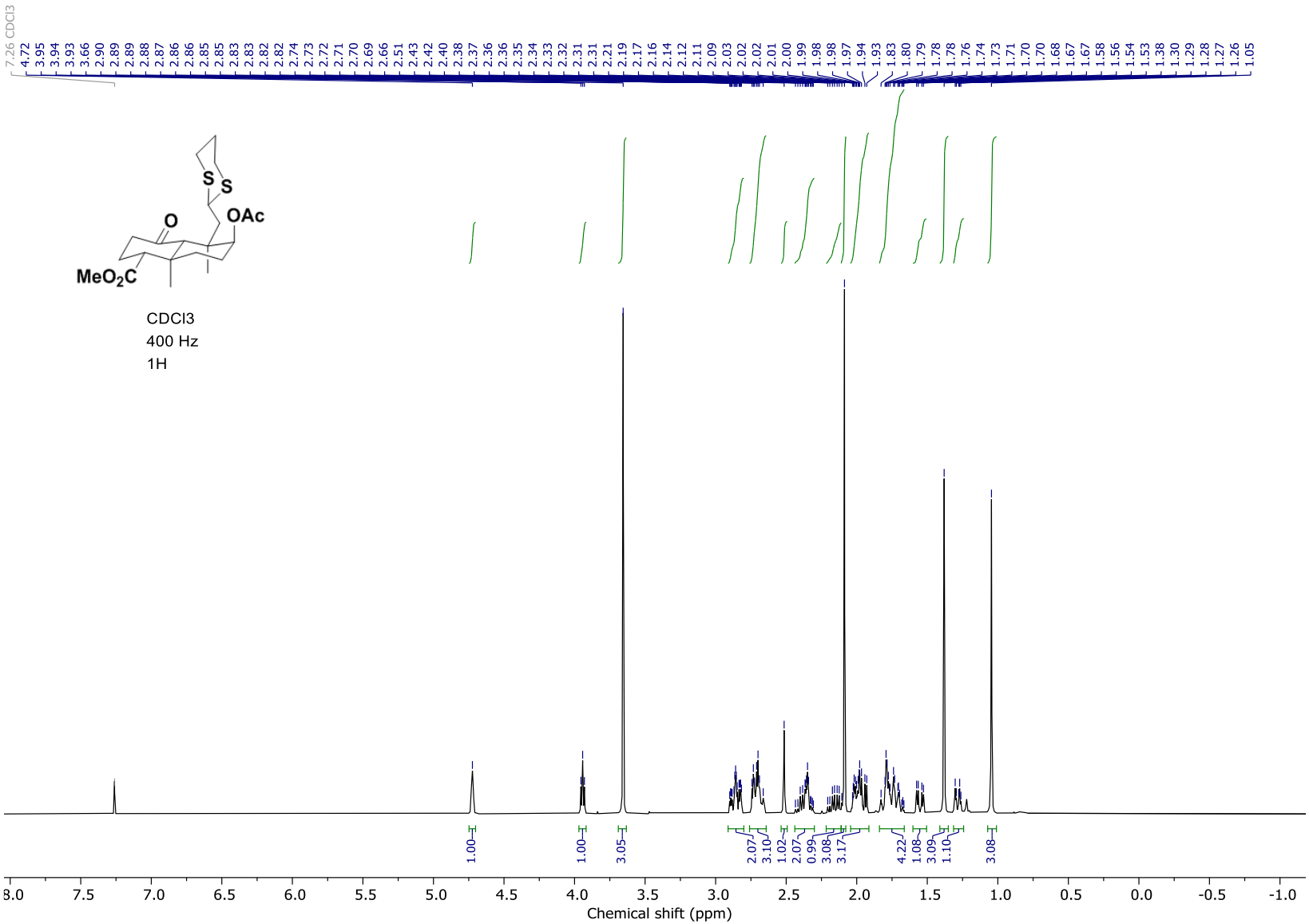

Spectra from Philippe McGee's Ph.D. thesis

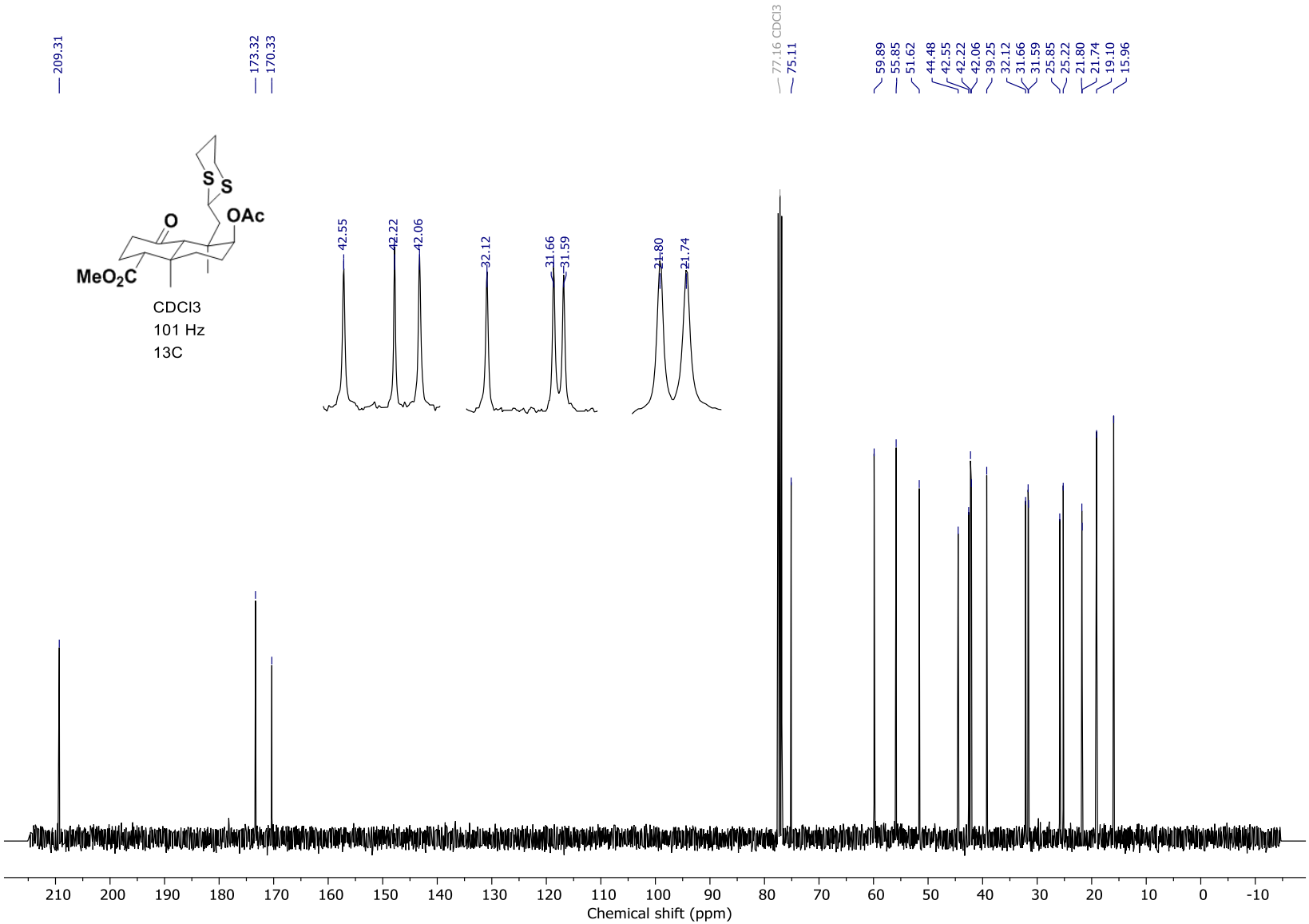

Spectra from Philippe McGee's Ph.D. thesis

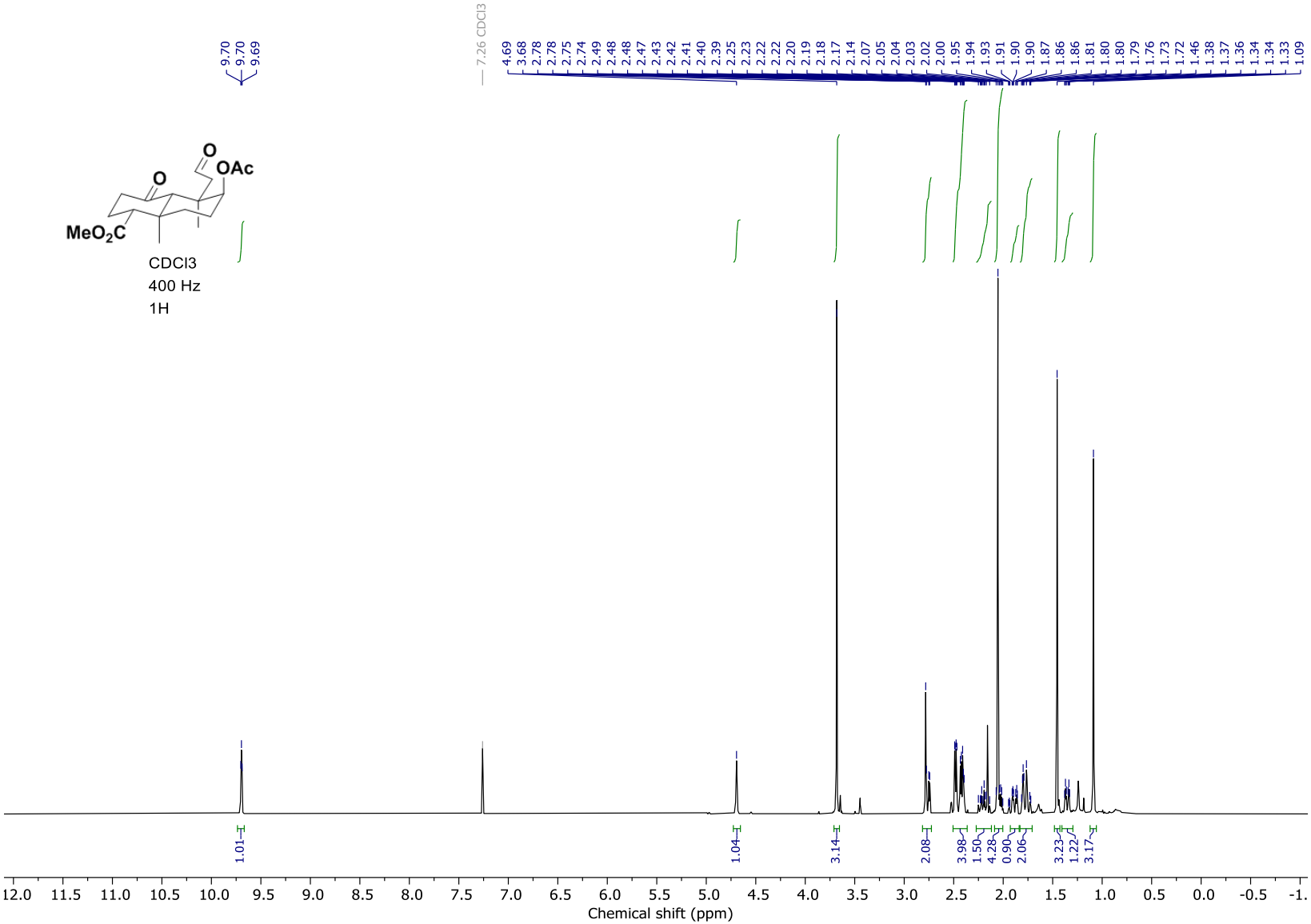

Spectra from Philippe McGee's Ph.D. thesis

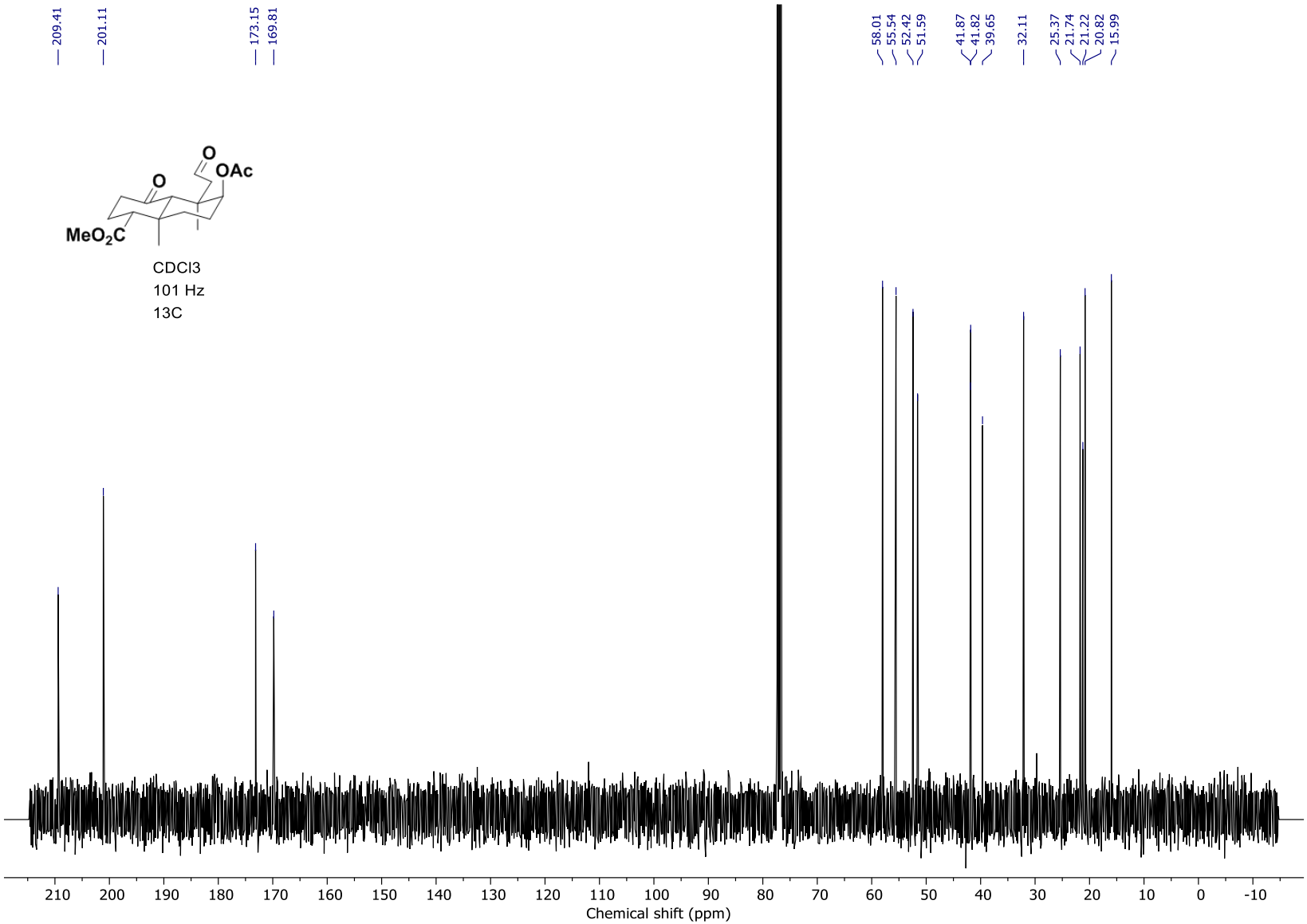

Spectra from Philippe McGee's Ph.D. thesis

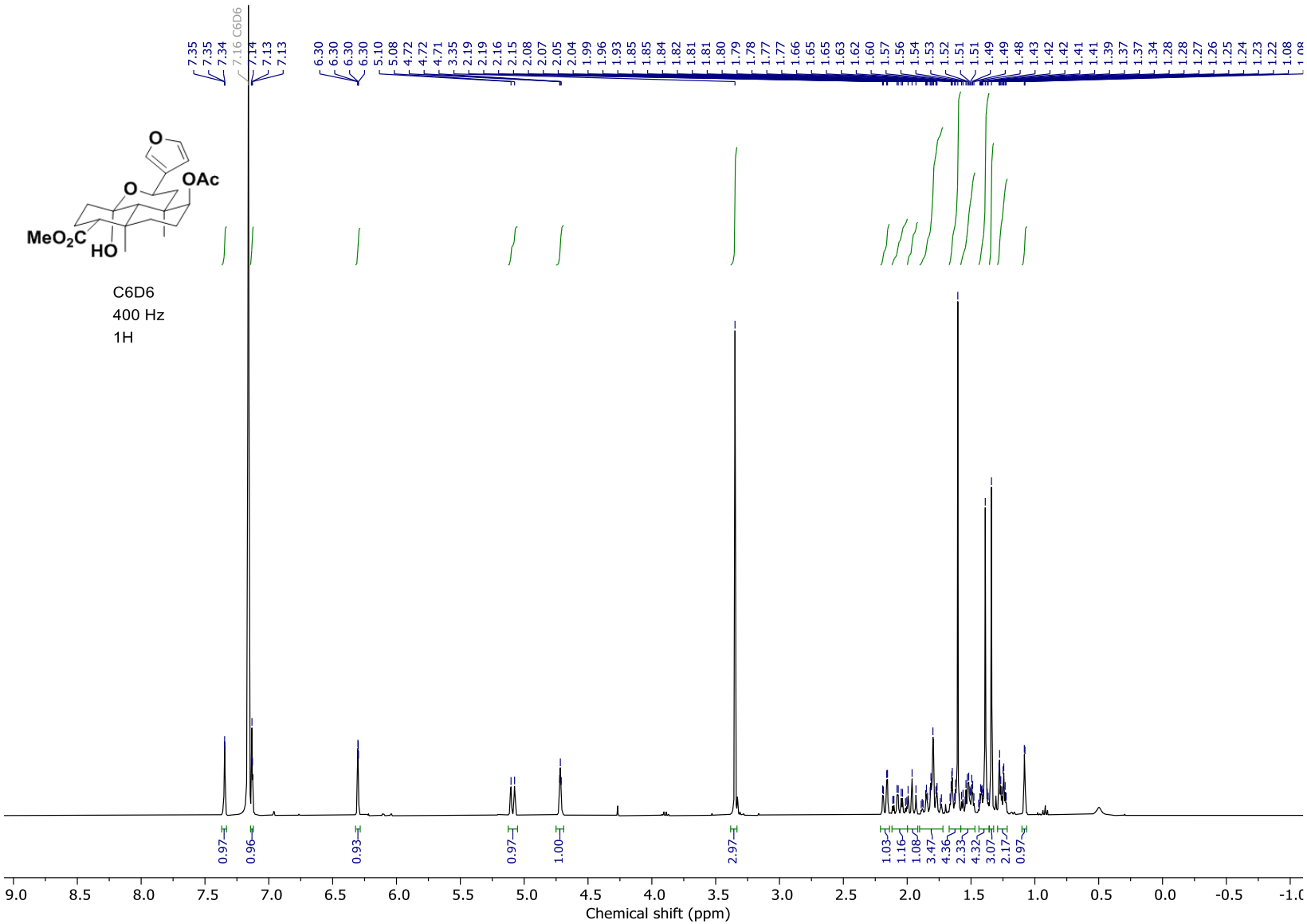
O
OAc
O
MeO2C
HO
C6D6
400 Hz
1H
Chemical shift (ppm)

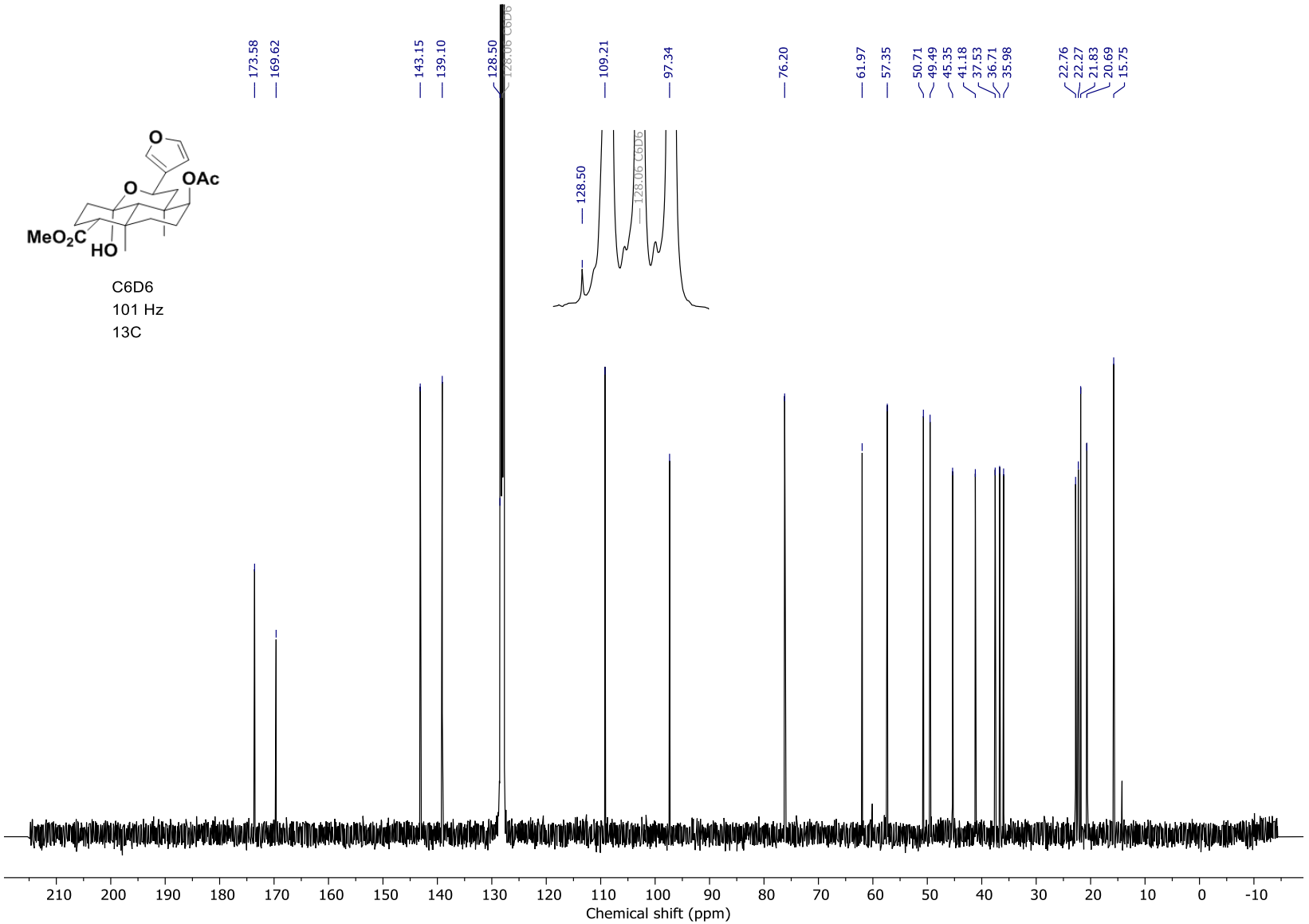
173.58
169.62
143.15
139.10
128.50
128.06 C6D6
109.21
97.34
76.20
61.97
57.35
50.71
49.49
45.35
41.18
37.53
36.71
35.98
22.76
22.27
21.83
20.69
15.75
O
O
OAc
MeO2C
HO
C6D6
101 Hz
13C
210 200 190 180 170 160 150 140 130 120 110 100 90 80 70 60 50 40 30 20 10 0 -10
Chemical shift (ppm)

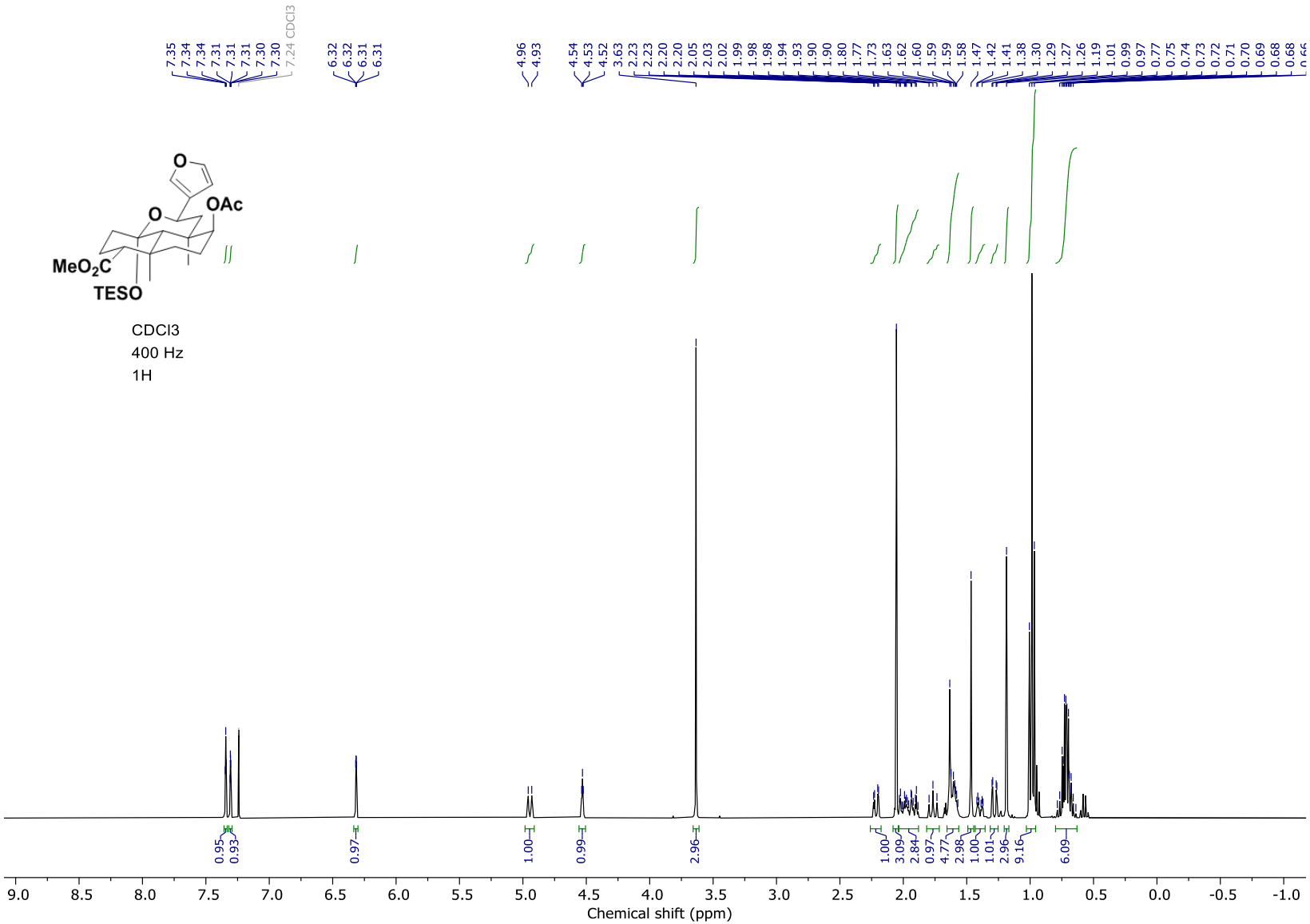

Spectra from Philippe McGee's Ph.D. thesis

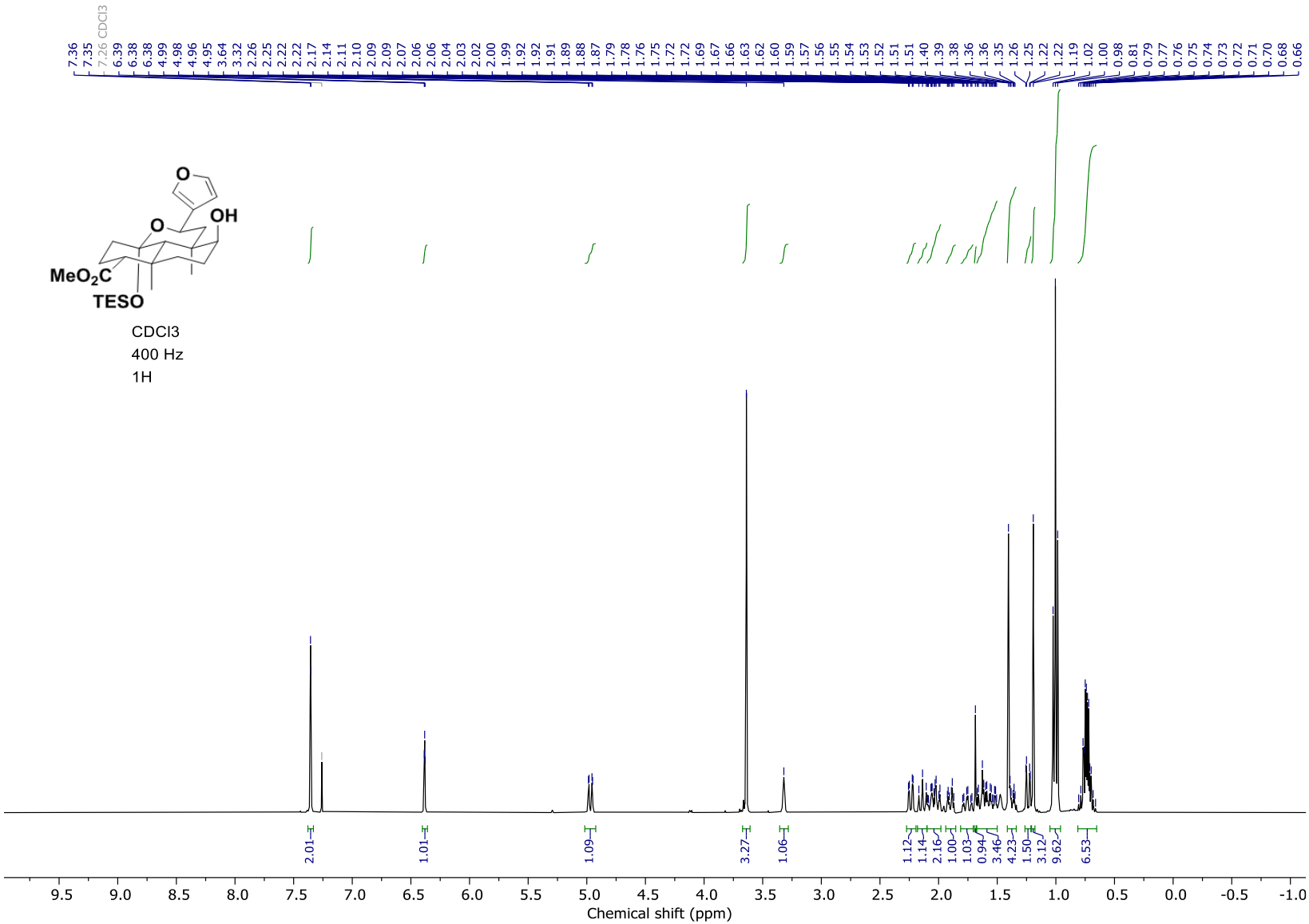

Spectra from Philippe McGee's Ph.D. thesis

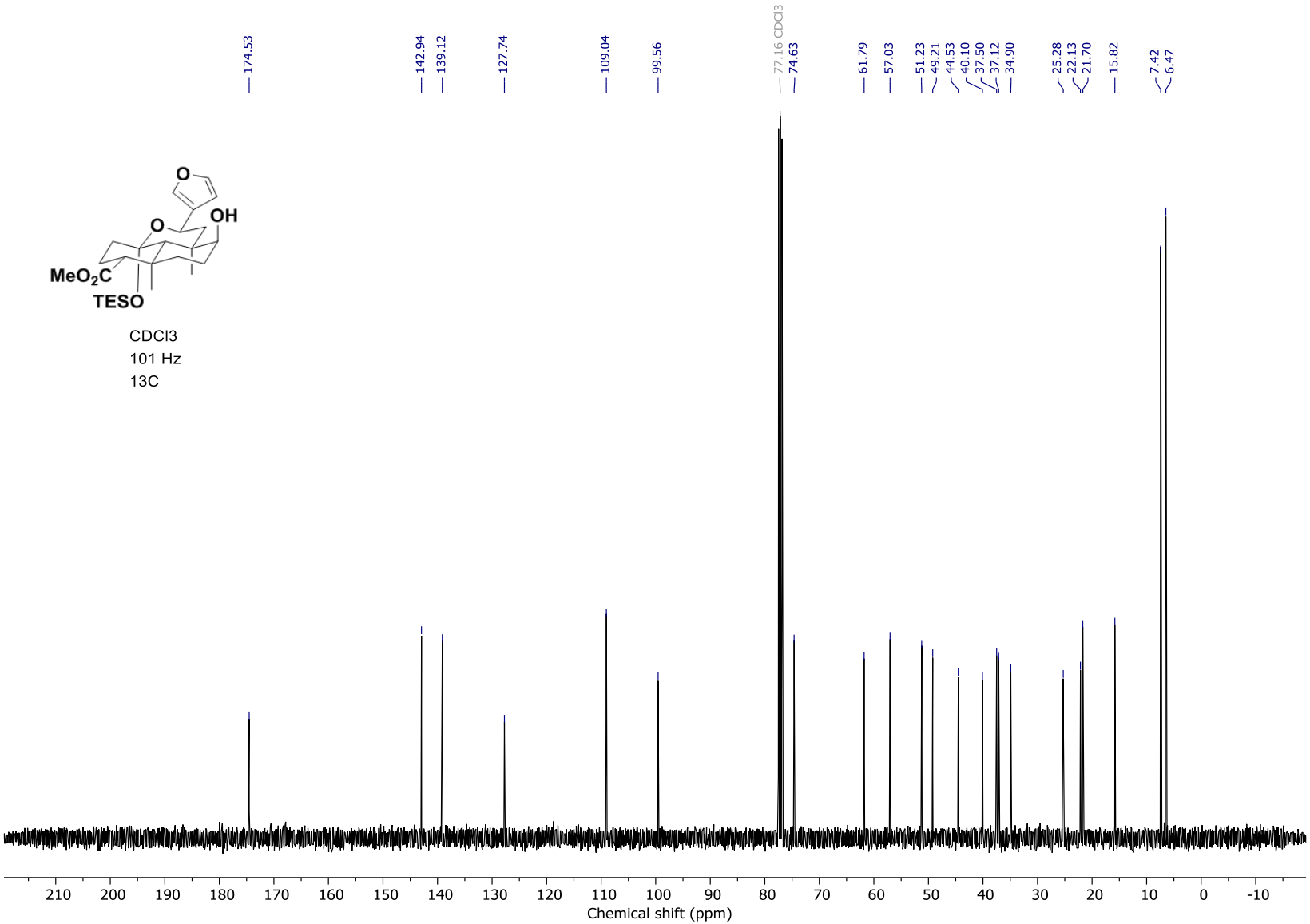

Spectra from Philippe McGee's Ph.D. thesis

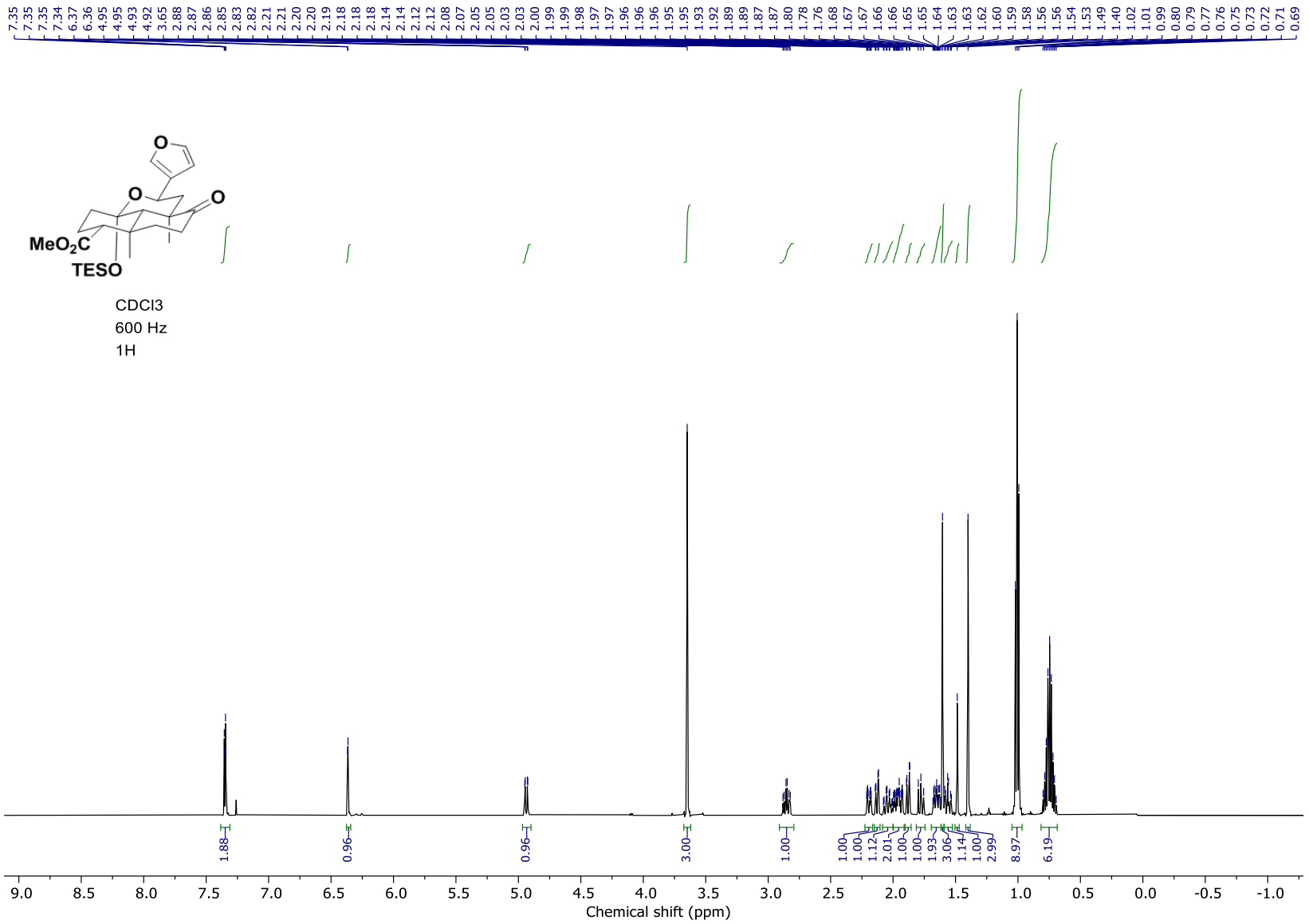
7.35 7.35 7.34 6.37 6.36 4.95 4.95 4.93 4.92 3.65 2.88 2.87 2.86 2.85 2.83 2.82 2.21 2.20 2.20 2.19 2.18 2.18 2.14 2.14 2.12 2.12 2.08 2.07 2.05 2.05 2.03 2.03 2.00 1.99 1.99 1.98 1.97 1.97 1.96 1.96 1.96 1.95 1.95 1.93 1.92 1.89 1.89 1.87 1.87 1.80 1.78 1.76 1.68 1.67 1.67 1.66 1.66 1.65 1.65 1.64 1.63 1.63 1.62 1.60 1.59 1.58 1.56 1.56 1.54 1.53 1.49 1.40 1.02 1.01 0.99 0.80 0.79 0.77 0.76 0.75 0.73 0.72 0.71 0.69
O
O
O
MeO2C
TESO
CDCl3
600 Hz
1H
1.88
0.96
0.96
3.00
1.00
1.00
1.00
1.12
2.01
1.00
1.00
1.93
3.06
1.14
1.00
2.99
8.97
6.19
9.0 8.5 8.0 7.5 7.0 6.5 6.0 5.5 5.0 4.5 4.0 3.5 3.0 2.5 2.0 1.5 1.0 0.5 0.0 -0.5 -1.0
Chemical shift (ppm)

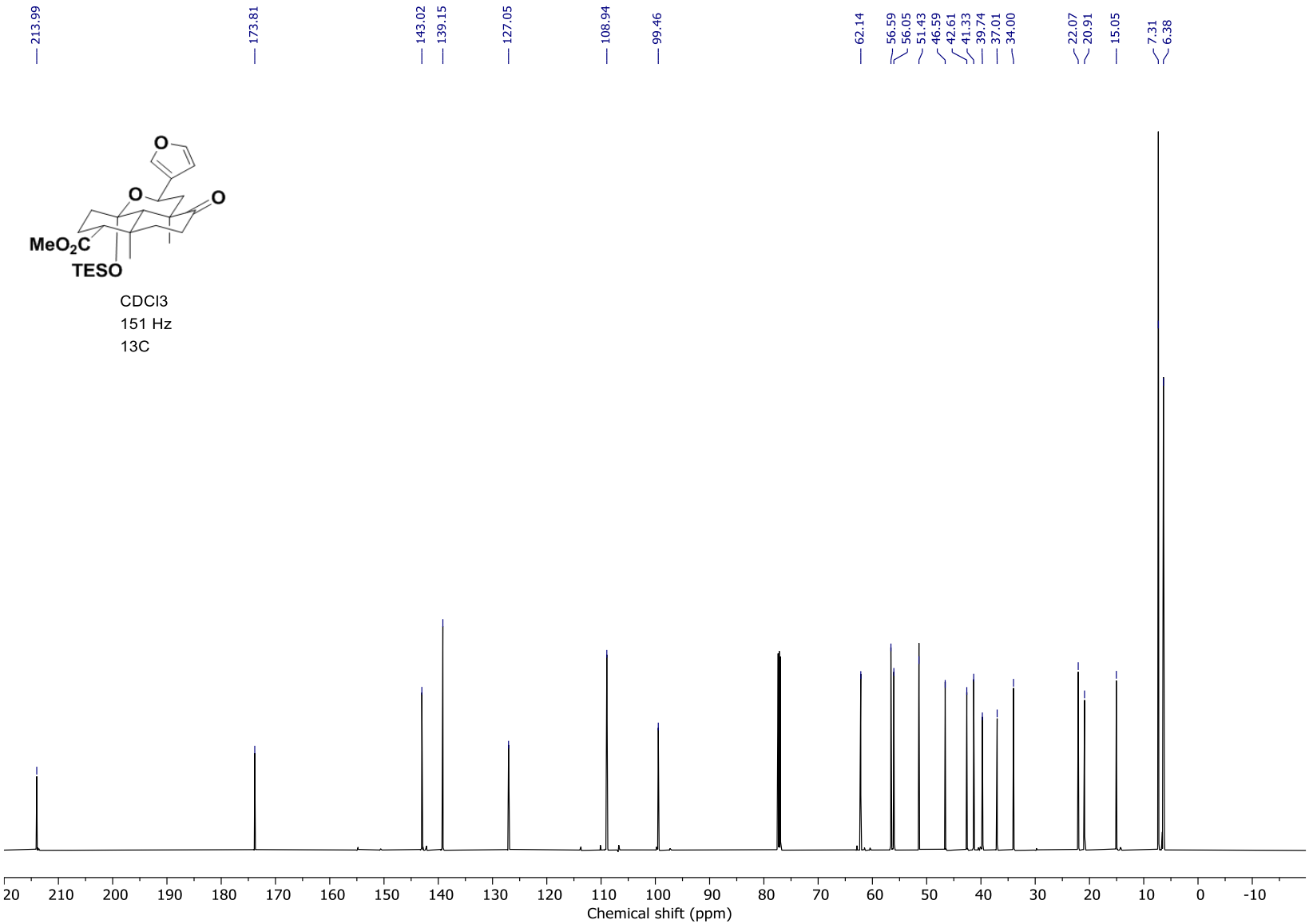
213.99
173.81
143.02
139.15
127.05
108.94
99.46
62.14
56.59
56.05
51.43
46.59
42.61
41.33
39.74
37.01
34.00
22.07
20.91
15.05
7.31
6.38
O
O
O
MeO2C
TESO
CDCl3
151 Hz
13C
20 210 200 190 180 170 160 150 140 130 120 110 100 90 80 70 60 50 40 30 20 10 0 -10
Chemical shift (ppm)

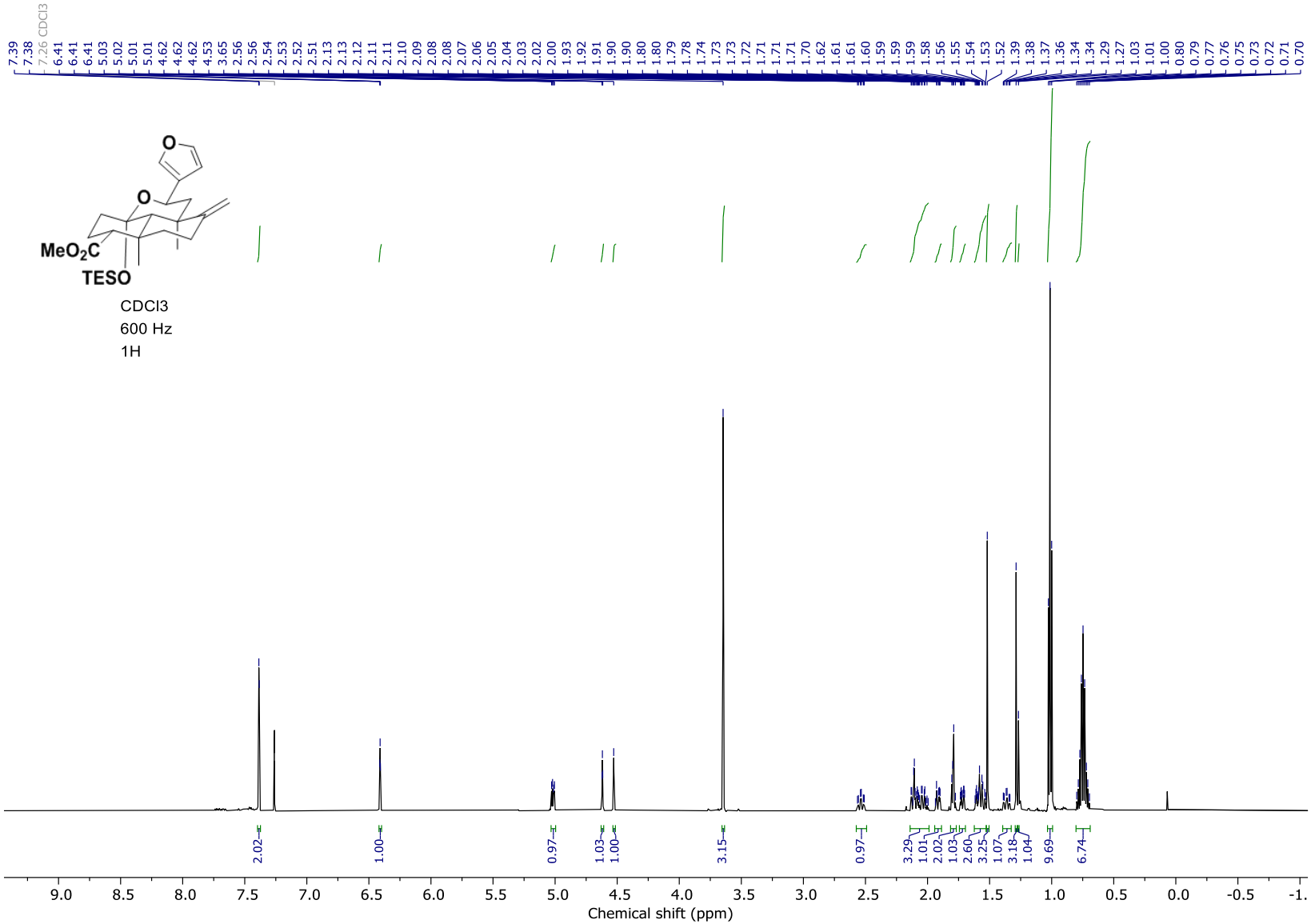
MeO2C
TESO
CDCl3
600 Hz
1H
Chemical shift (ppm)

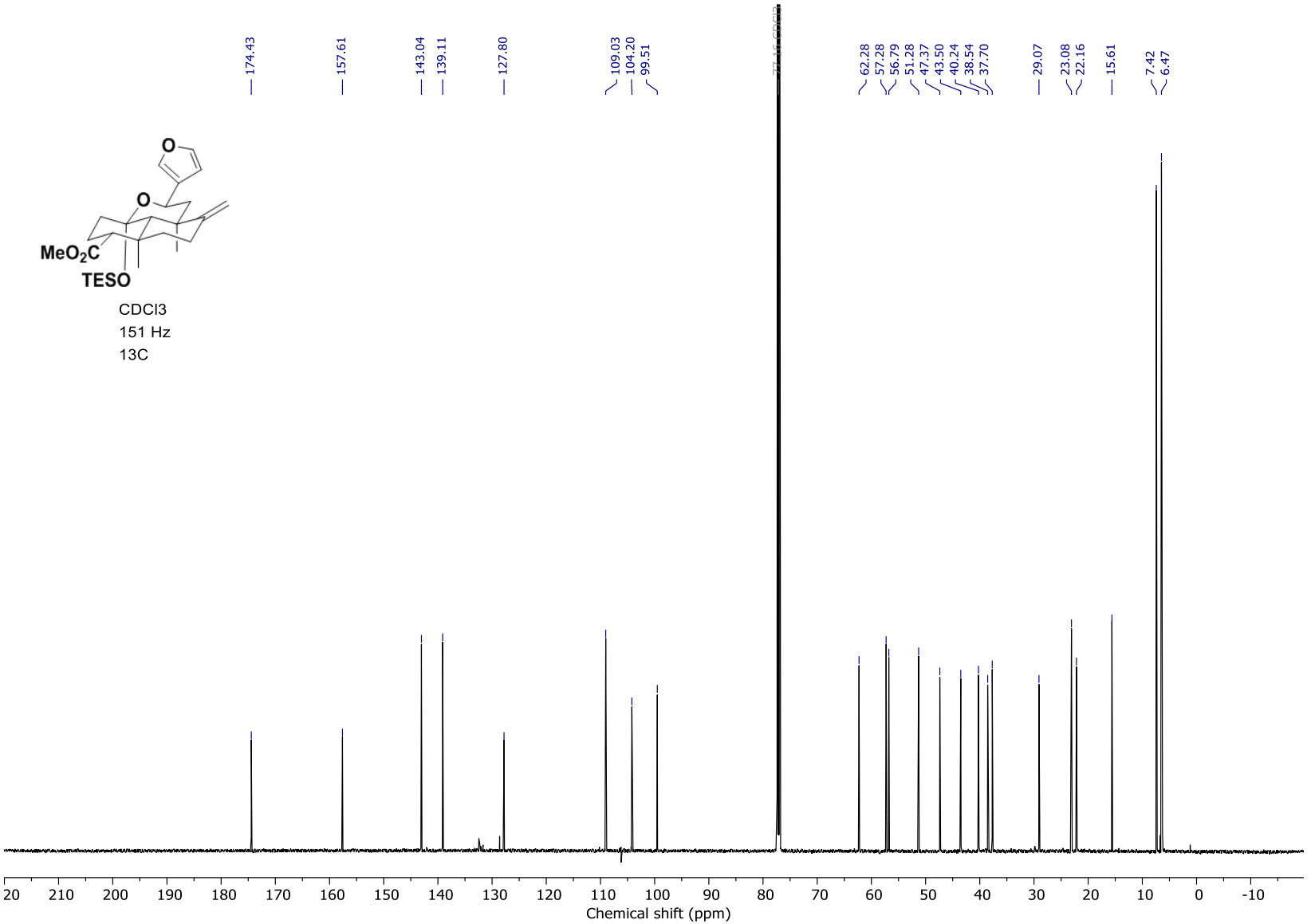
174.43
157.61
143.04
139.11
127.80
109.03
104.20
99.51
77.16
62.28
57.28
56.79
51.28
47.37
43.50
40.24
38.54
37.70
29.07
23.08
22.16
15.61
7.42
6.47
O
O
MeO2C
TESO
CDCl3
151 Hz
13C
20 210 200 190 180 170 160 150 140 130 120 110 100 90 80 70 60 50 40 30 20 10 0 -10
Chemical shift (ppm)

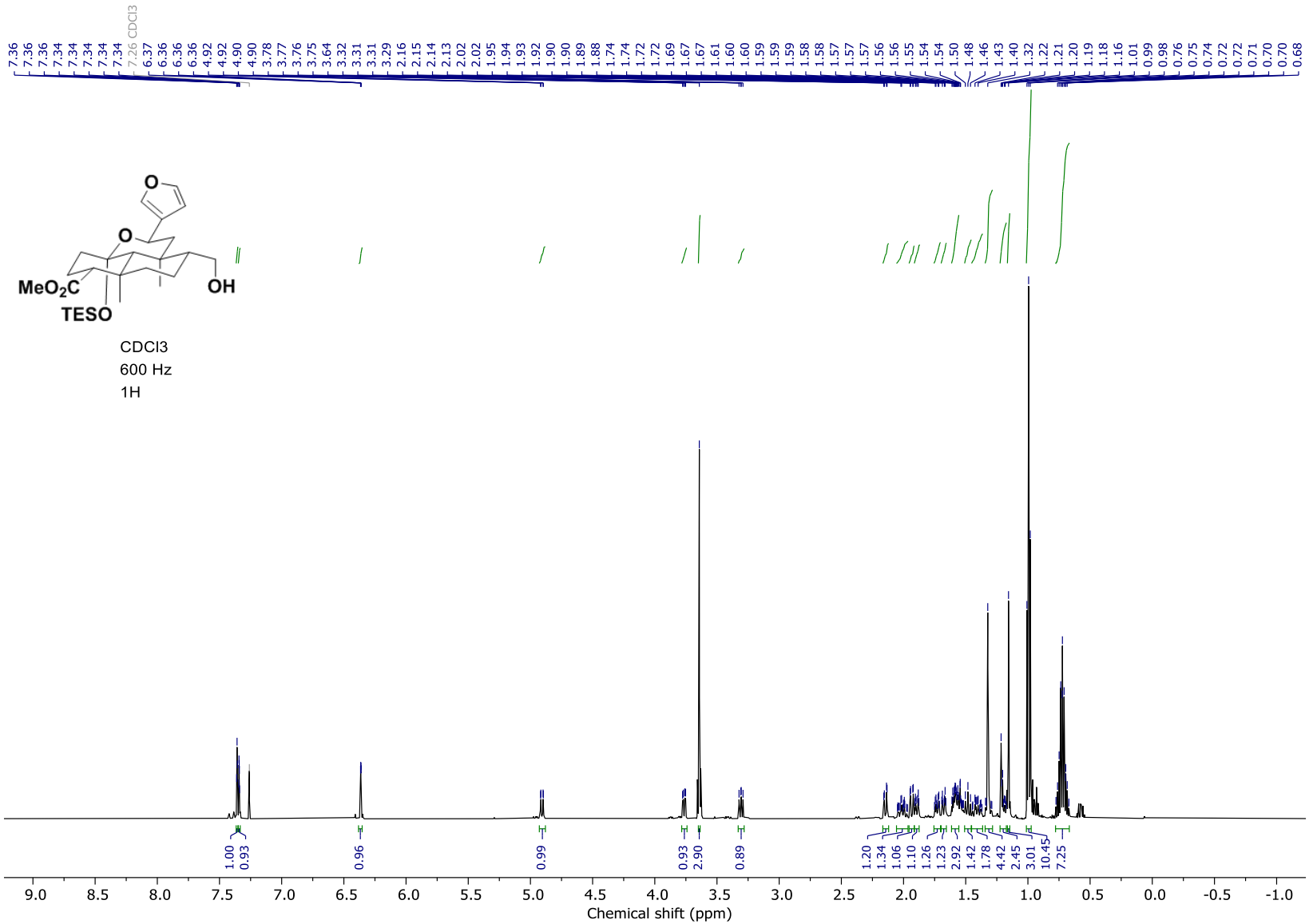
MeO2C
TESO
OH
O
O
CDCl3
600 Hz
1H
Chemical shift (ppm)

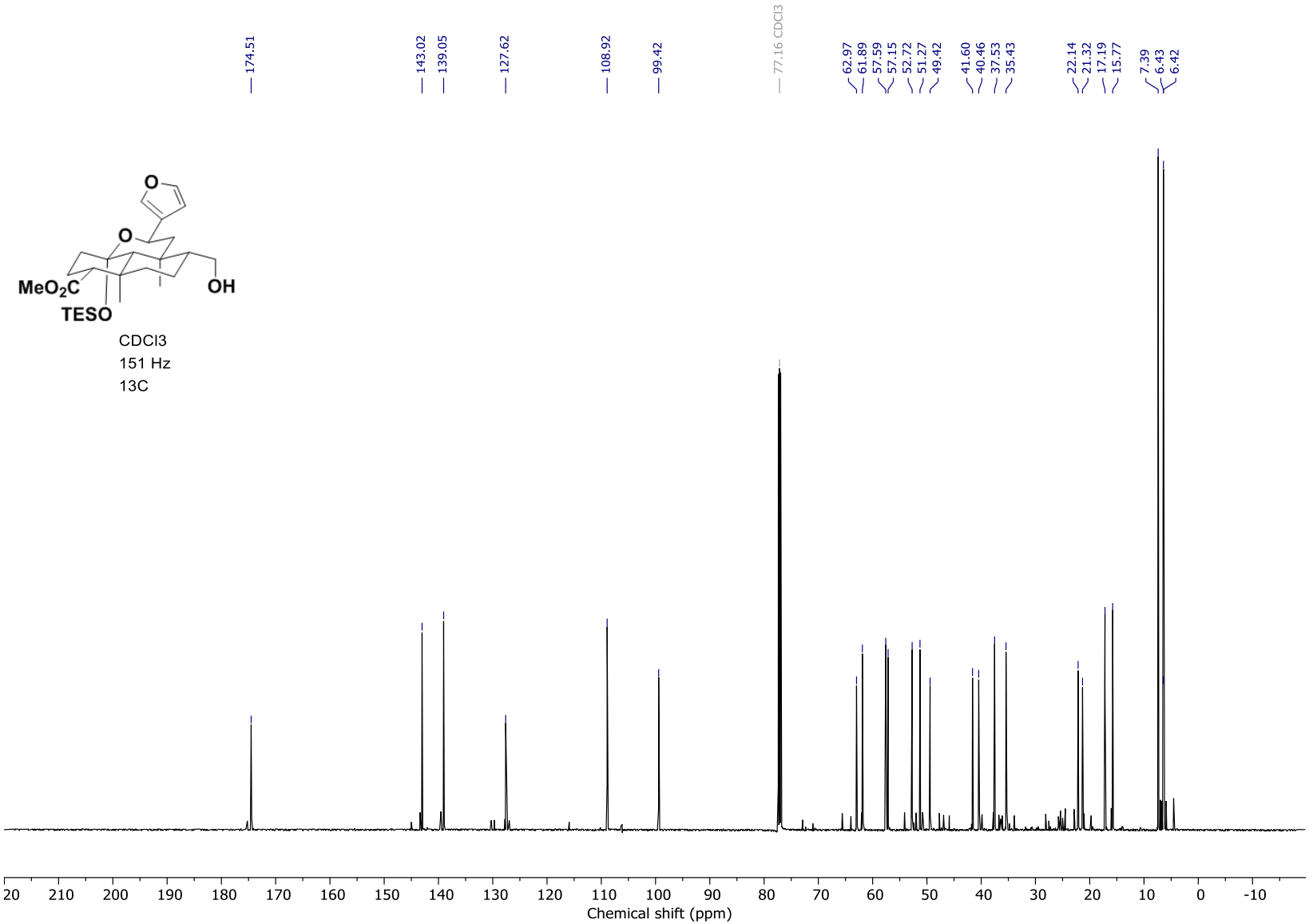
174.51
143.02
139.05
127.62
108.92
99.42
77.16 CDCl3
62.97
61.89
57.59
57.15
52.72
51.27
49.42
41.60
40.46
37.53
35.43
22.14
21.32
17.19
15.77
7.39
6.43
6.42
O
O
MeO2C
OH
TESO
CDCl3
151 Hz
13C
20 210 200 190 180 170 160 150 140 130 120 110 100 90 80 70 60 50 40 30 20 10 0 -10
Chemical shift (ppm)

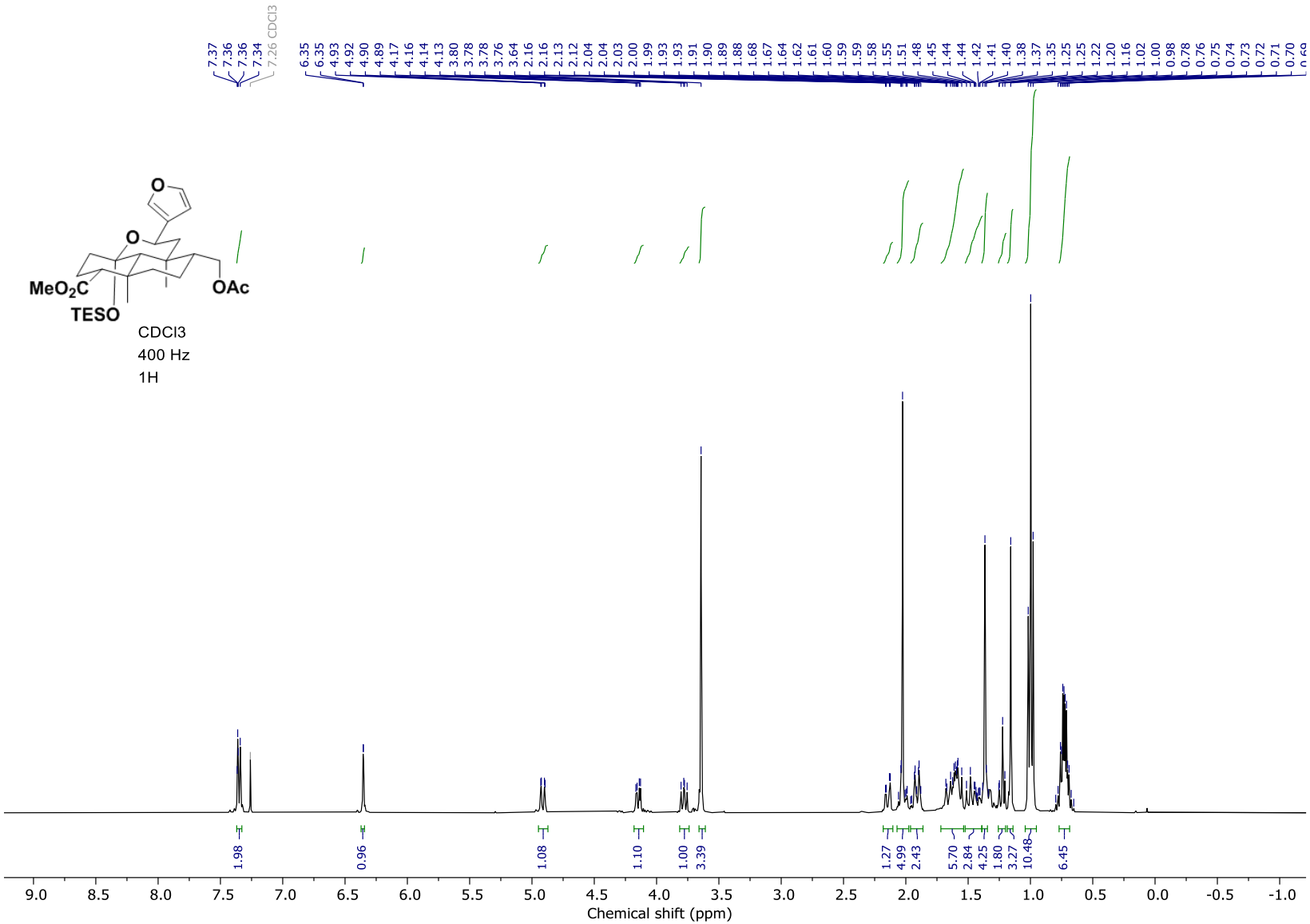
MeO2C
TESO
OAc
CDCl3
400 Hz
1H
Chemical shift (ppm)

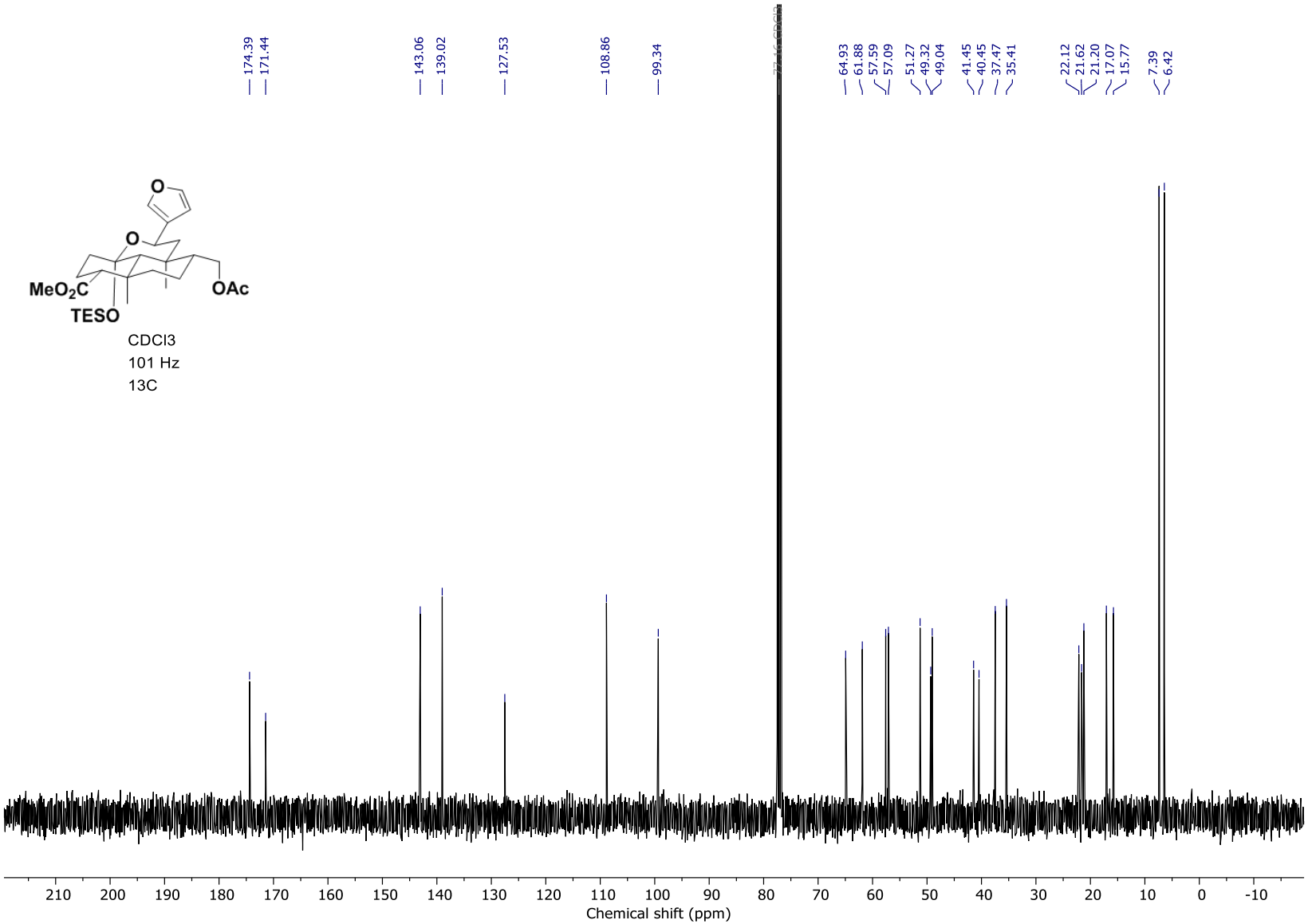
174.39
171.44
143.06
139.02
127.53
108.86
99.34
64.93
61.88
57.59
57.09
51.27
49.32
49.04
41.45
40.45
37.47
35.41
22.12
21.62
21.20
17.07
15.77
7.39
6.42
O
O
MeO2C
OAc
TESO
CDCl3
101 Hz
13C
210 200 190 180 170 160 150 140 130 120 110 100 90 80 70 60 50 40 30 20 10 0 -10
Chemical shift (ppm)

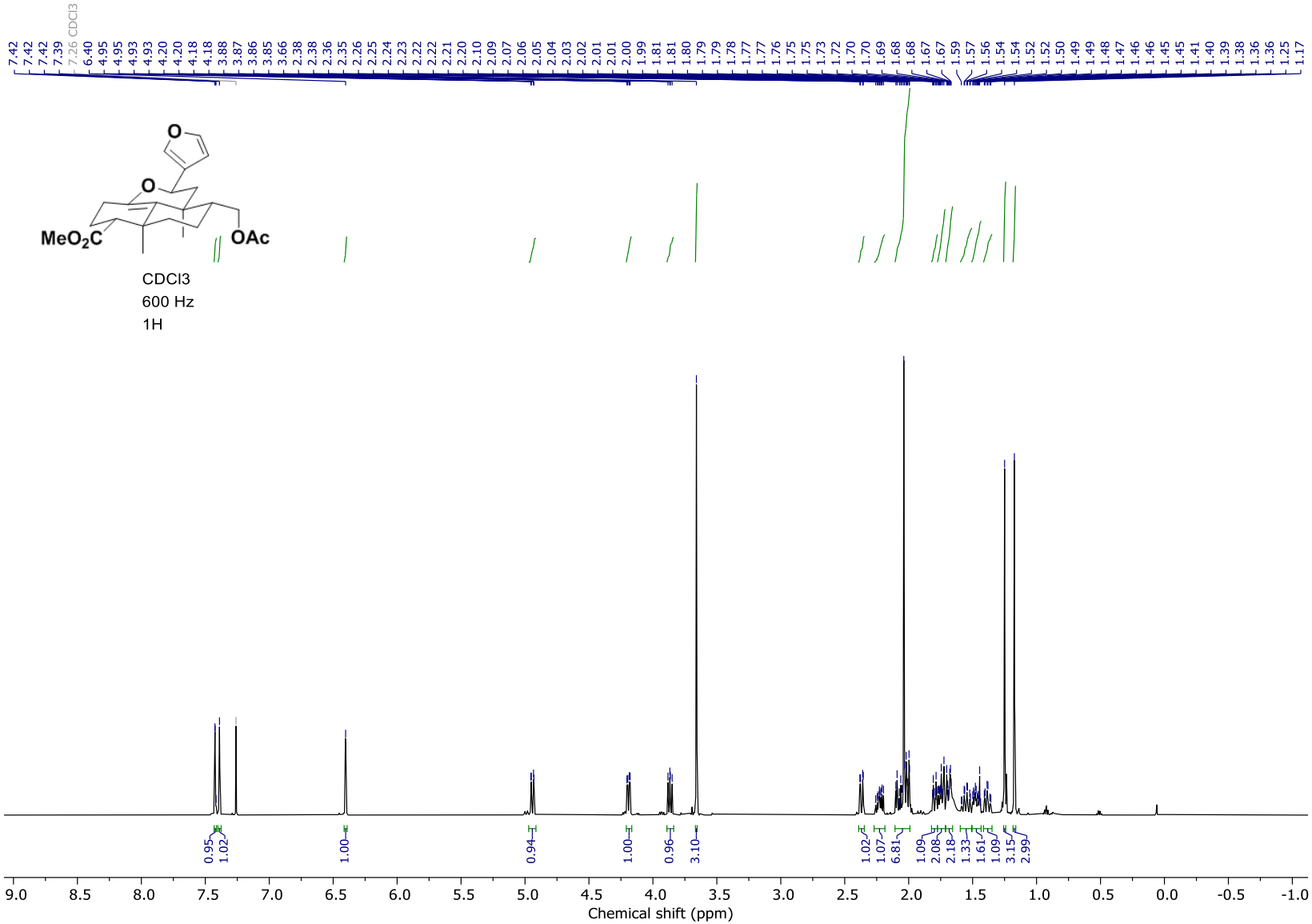
7.42 7.42 7.42 7.39 7.26 CDCl3 6.40 4.95 4.95 4.93 4.93 4.20 4.20 4.18 4.18 3.88 3.87 3.86 3.85 3.66 2.38 2.38 2.36 2.35 2.26 2.25 2.24 2.23 2.22 2.22 2.21 2.20 2.10 2.09 2.07 2.06 2.05 2.04 2.03 2.02 2.01 2.01 2.00 1.99 1.81 1.81 1.80 1.79 1.79 1.78 1.77 1.77 1.76 1.75 1.75 1.73 1.72 1.70 1.70 1.69 1.68 1.68 1.67 1.67 1.59 1.57 1.56 1.54 1.54 1.52 1.52 1.50 1.49 1.49 1.48 1.47 1.46 1.46 1.45 1.45 1.41 1.40 1.39 1.38 1.36 1.36 1.25 1.17
O
O
MeO2C
OAc
CDCl3
600 Hz
1H
0.95 1.02 1.00 0.94 1.00 0.96 3.10 1.02 1.07 6.81 1.09 2.08 2.18 1.33 1.61 1.09 3.15 2.99
9.0 8.5 8.0 7.5 7.0 6.5 6.0 5.5 5.0 4.5 4.0 3.5 3.0 2.5 2.0 1.5 1.0 0.5 0.0 -0.5 -1.0
Chemical shift (ppm)

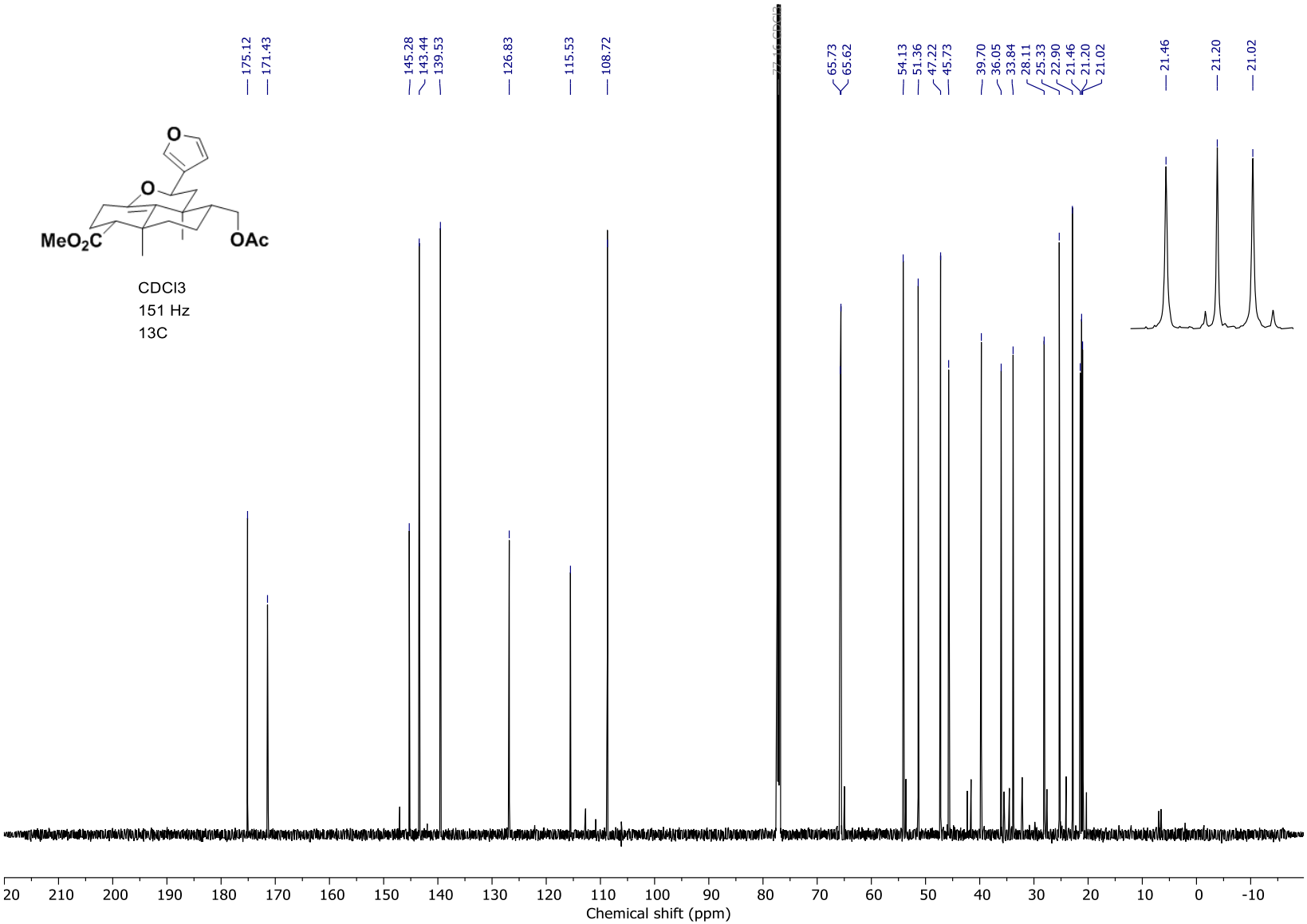
175.12
171.43
145.28
143.44
139.53
126.83
115.53
108.72
77.16
65.73
65.62
54.13
51.36
47.22
45.73
39.70
36.05
33.84
28.11
25.33
22.90
21.46
21.20
21.02
21.46
21.20
21.02
O
O
MeO2C
OAc
CDCl3
151 Hz
13C
20 210 200 190 180 170 160 150 140 130 120 110 100 90 80 70 60 50 40 30 20 10 0 -10
Chemical shift (ppm)

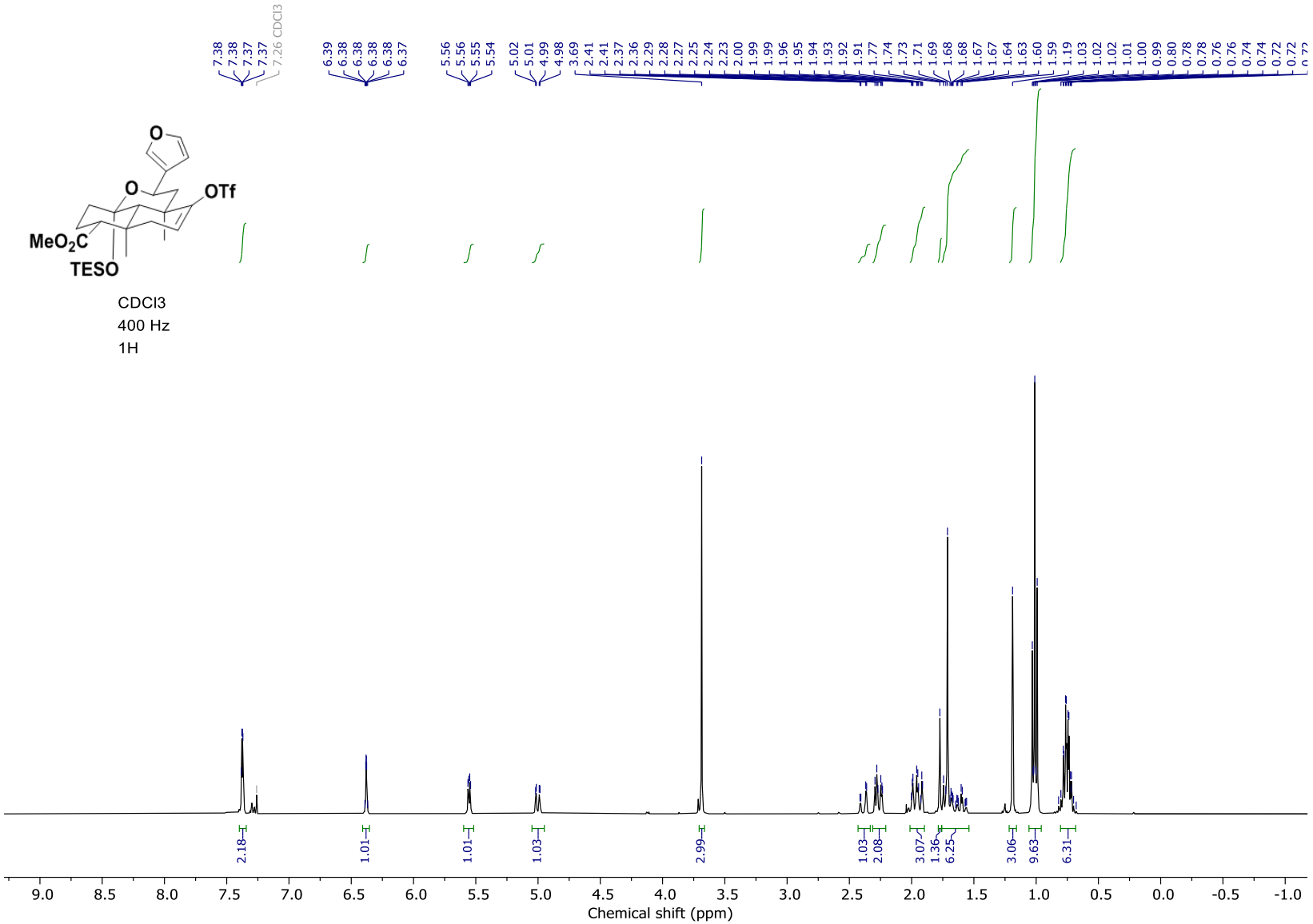
O
O
OTf
MeO2C
TESO
CDCl3
400 Hz
1H
7.38 7.38 7.37 7.37 7.26 CDCl3
6.39 6.38 6.38 6.38 6.37
5.56 5.56 5.55 5.54
5.02 5.01 4.99 4.98
3.69
2.41 2.41 2.37 2.36 2.29 2.28 2.27 2.25 2.24 2.23 2.00 1.99 1.99 1.96 1.95 1.94 1.93 1.92 1.91 1.77 1.74 1.73 1.71 1.69 1.68 1.68 1.67 1.67 1.64 1.63 1.60 1.59 1.19 1.03 1.02 1.02 1.01 1.00 0.99 0.80 0.78 0.78 0.76 0.76 0.74 0.74 0.72 0.72
2.18 1.01 1.01 1.03 2.99 1.03 2.08 3.07 1.36 6.25 3.06 9.63 6.31
9.0 8.5 8.0 7.5 7.0 6.5 6.0 5.5 5.0 4.5 4.0 3.5 3.0 2.5 2.0 1.5 1.0 0.5 0.0 -0.5 -1.0
Chemical shift (ppm)

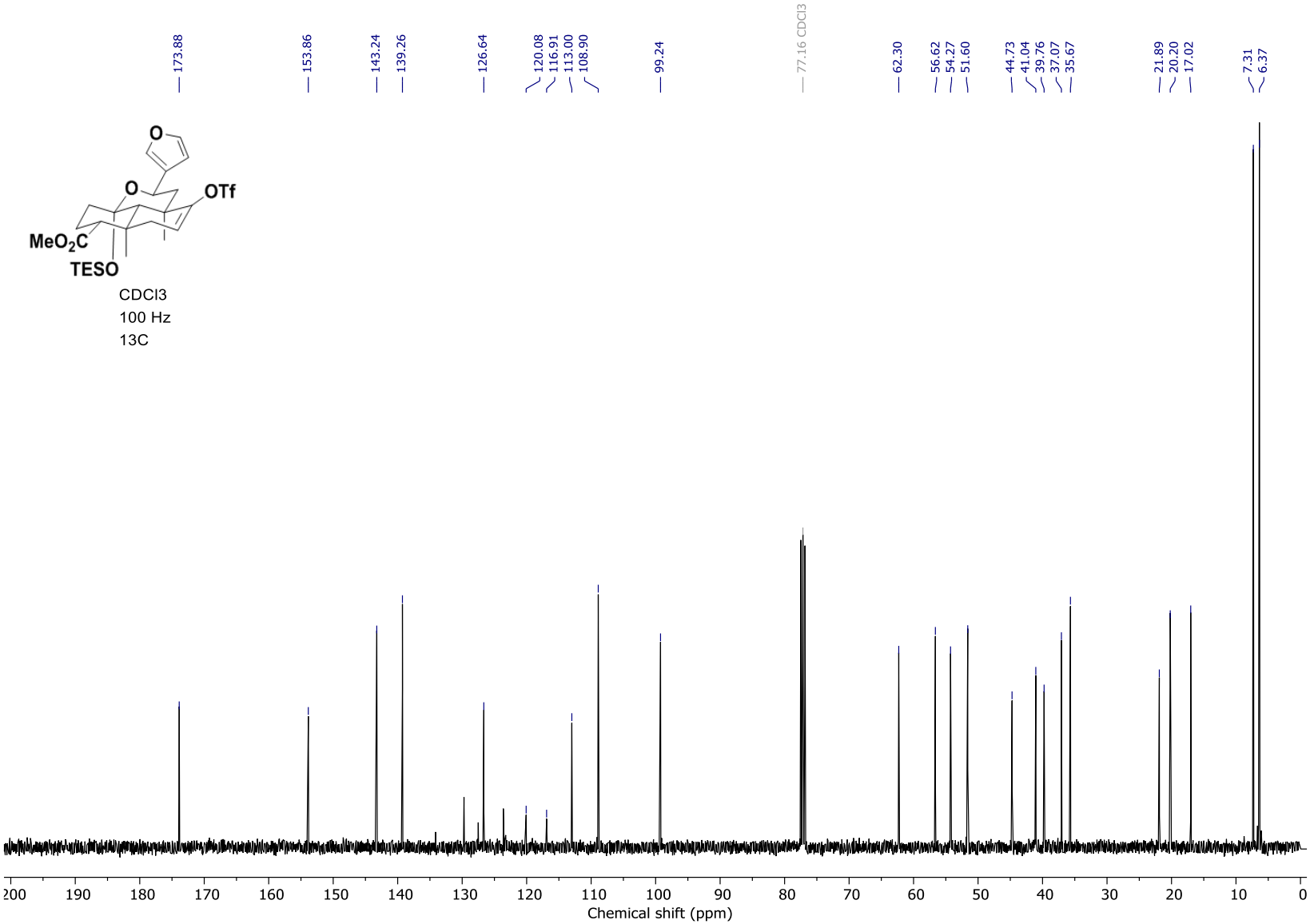
173.88
153.86
143.24
139.26
126.64
120.08
116.91
113.00
108.90
99.24
77.16 CDCl3
62.30
56.62
54.27
51.60
44.73
41.04
39.76
37.07
35.67
21.89
20.20
17.02
7.31
6.37
O
O
OTf
MeO2C
TESO
CDCl3
100 Hz
13C
200
190
180
170
160
150
140
130
120
110
100
90
80
70
60
50
40
30
20
10
0
Chemical shift (ppm)

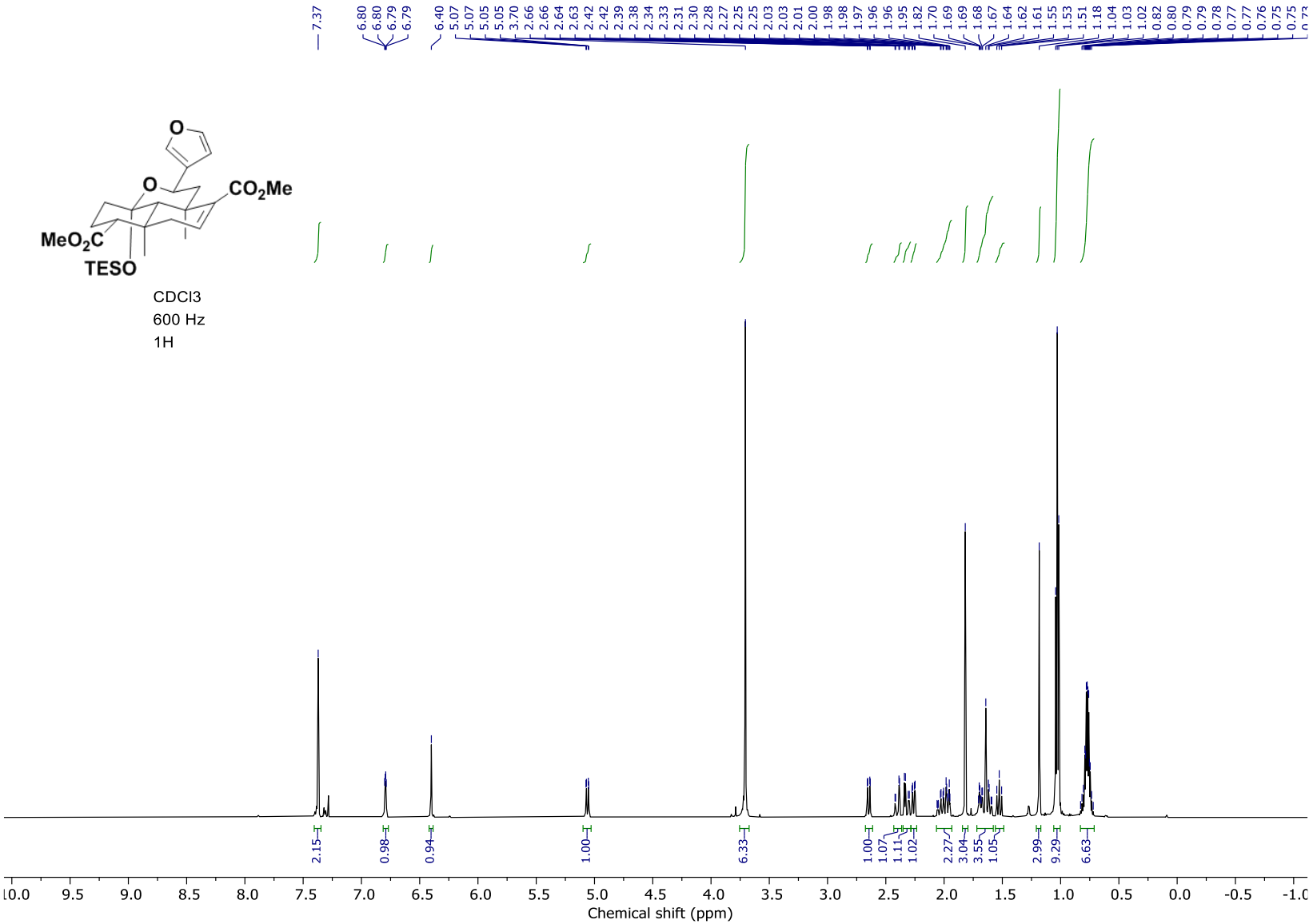
O
O
CO2Me
MeO2C
TESO
CDCl3
600 Hz
1H
Chemical shift (ppm)

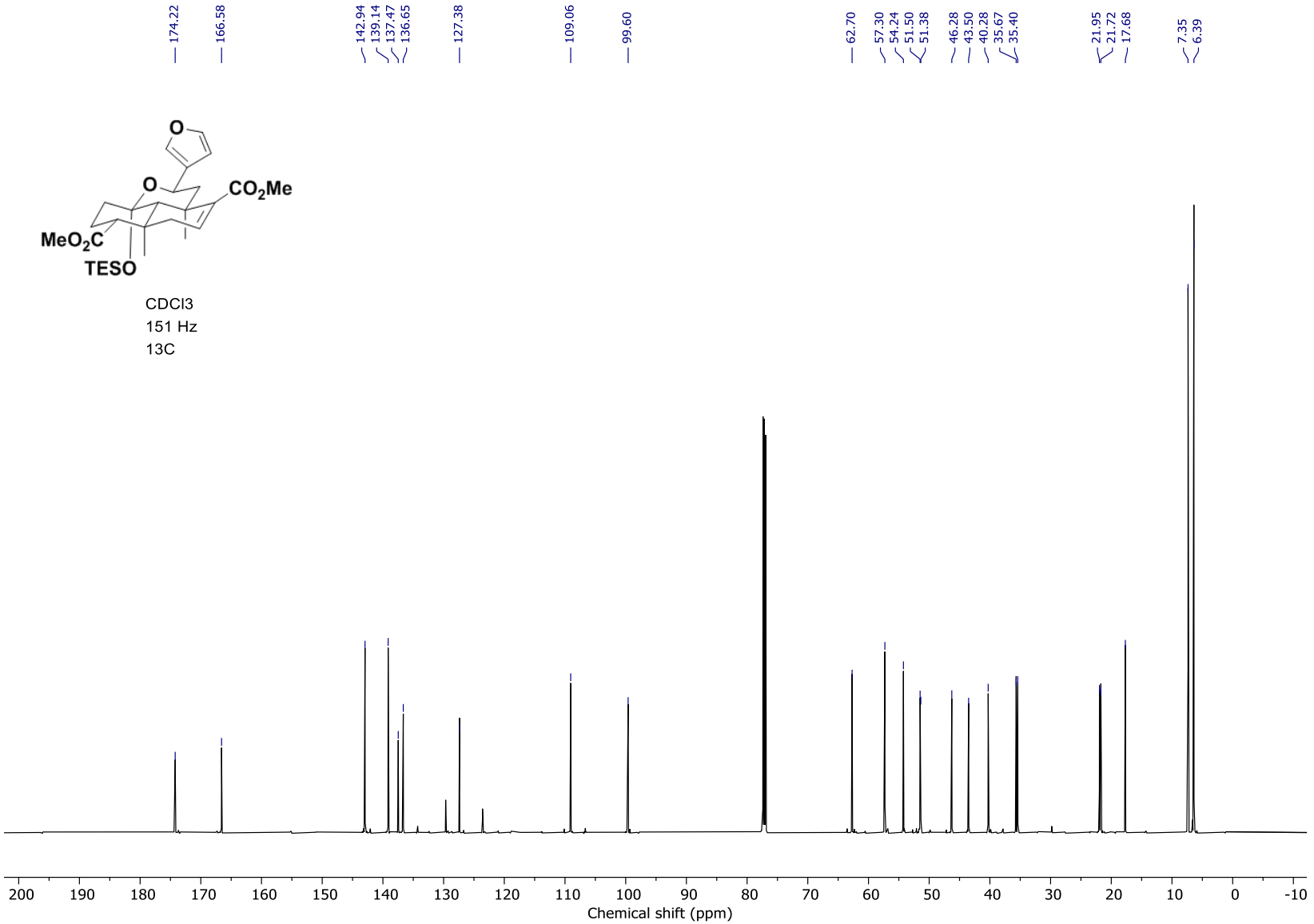
174.22
166.58
142.94
139.14
137.47
136.65
127.38
109.06
99.60
62.70
57.30
54.24
51.50
51.38
46.28
43.50
40.28
35.67
35.40
21.95
21.72
17.68
7.35
6.39
O
O
CO2Me
MeO2C
TESO
CDCl3
151 Hz
13C
200 190 180 170 160 150 140 130 120 110 100 90 80 70 60 50 40 30 20 10 0 -10
Chemical shift (ppm)

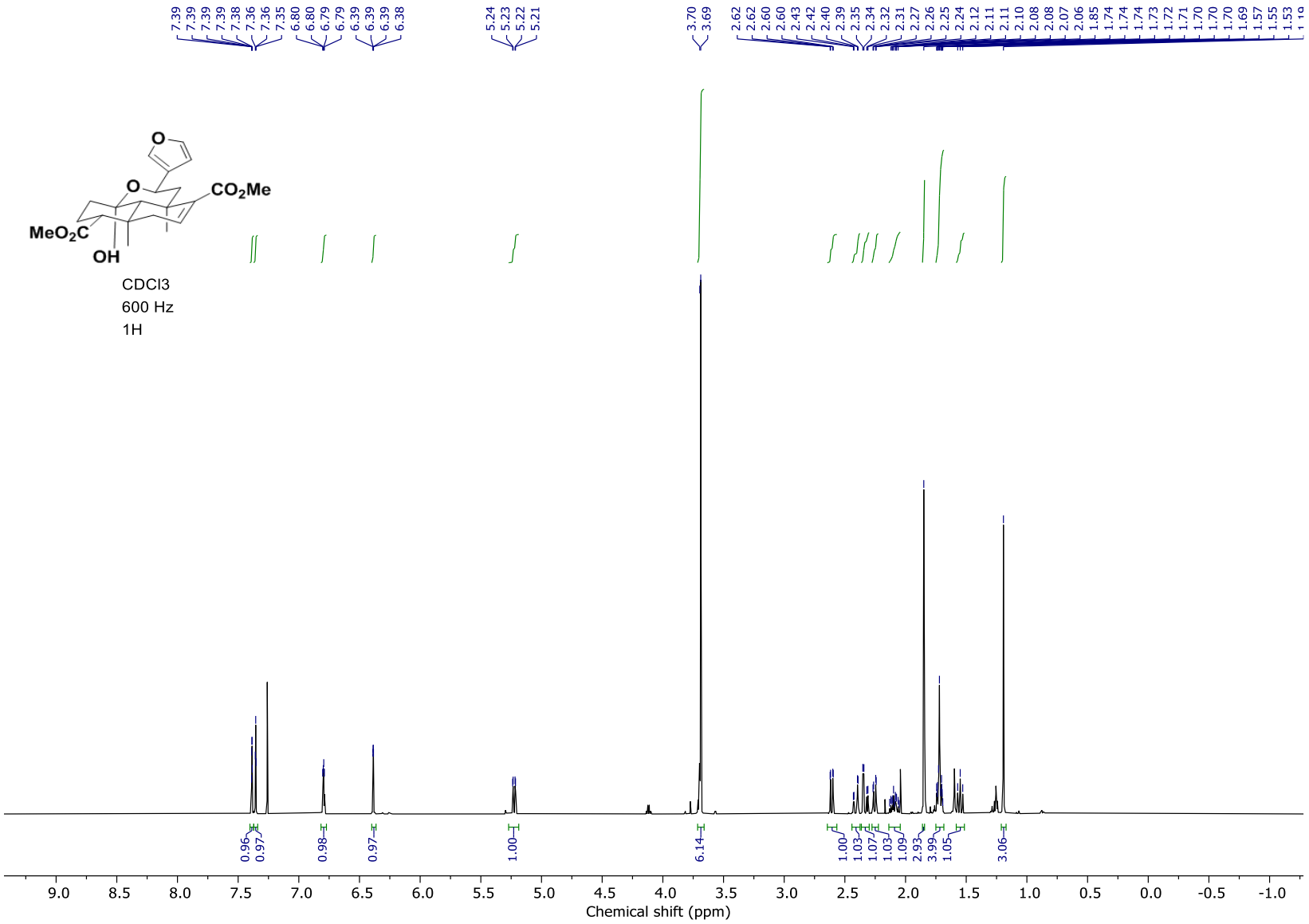
O
O
CO2Me
MeO2C
OH
CDCl3
600 Hz
1H
Chemical shift (ppm)

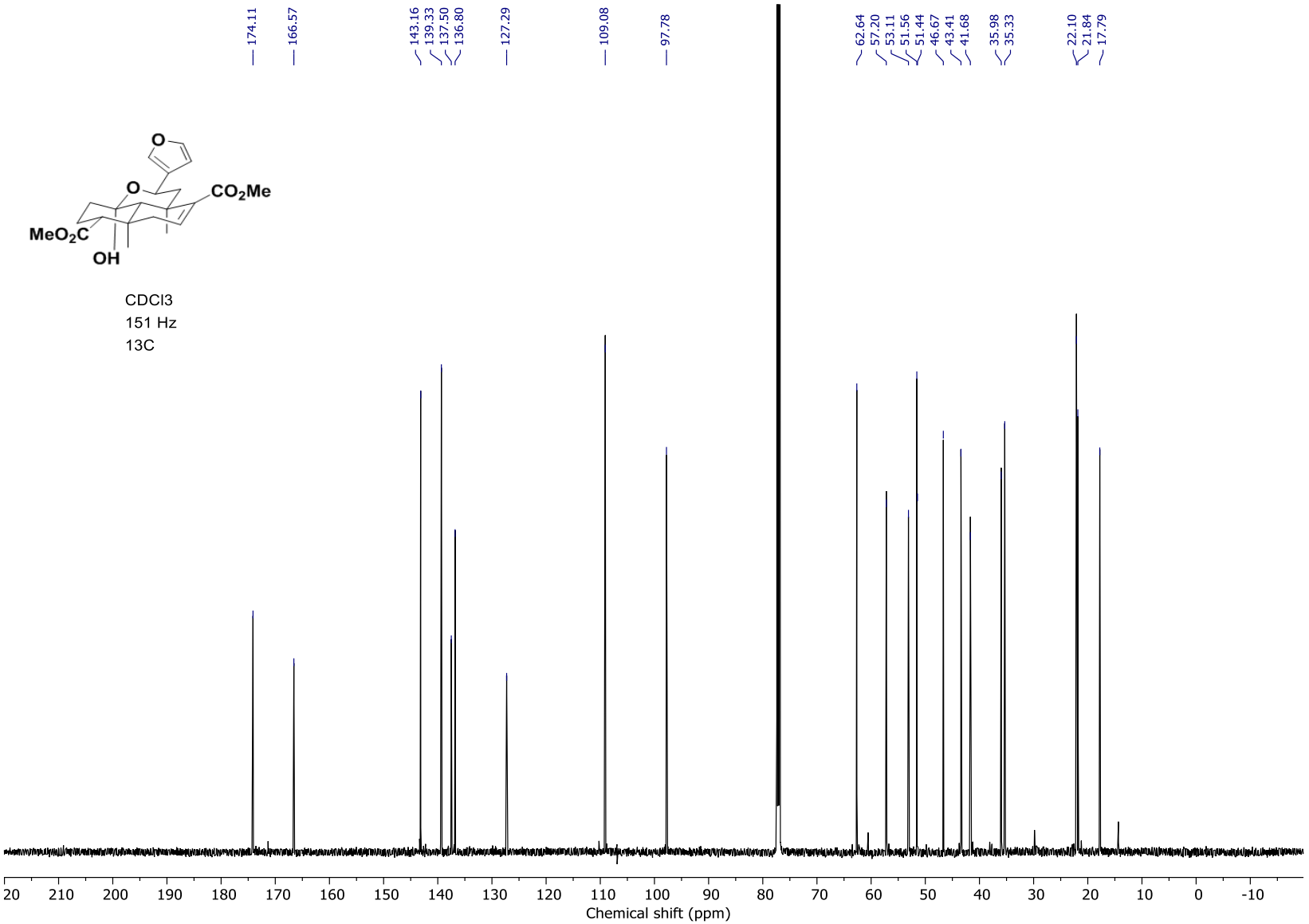
174.11
166.57
143.16
139.33
137.50
136.80
127.29
109.08
97.78
62.64
57.20
53.11
51.56
51.44
46.67
43.41
41.68
35.98
35.33
22.10
21.84
17.79
O
O
CO2Me
MeO2C
OH
CDCl3
151 Hz
13C
20 210 200 190 180 170 160 150 140 130 120 110 100 90 80 70 60 50 40 30 20 10 0 -10
Chemical shift (ppm)

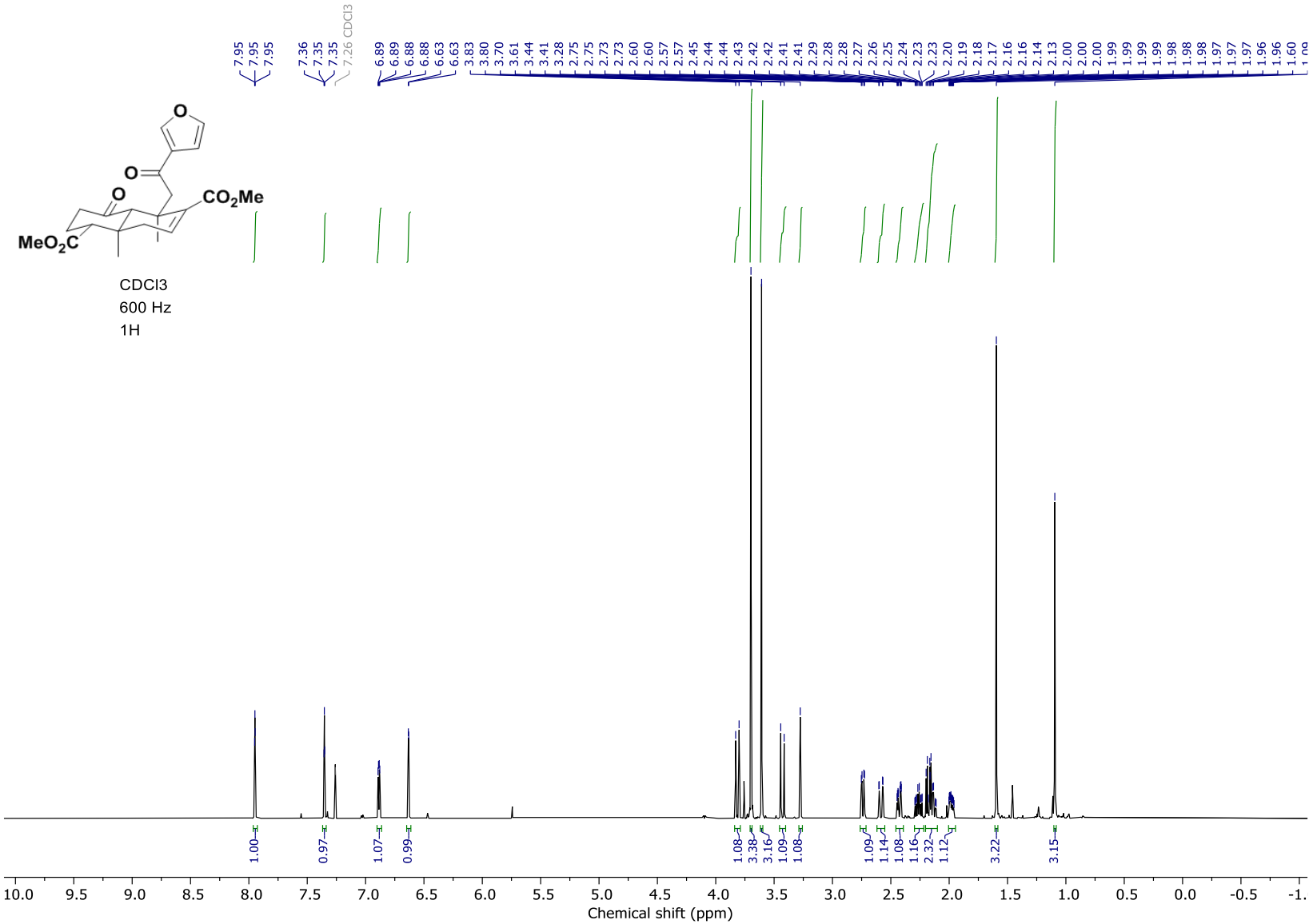
CDCl3
600 Hz
1H
Chemical shift (ppm)

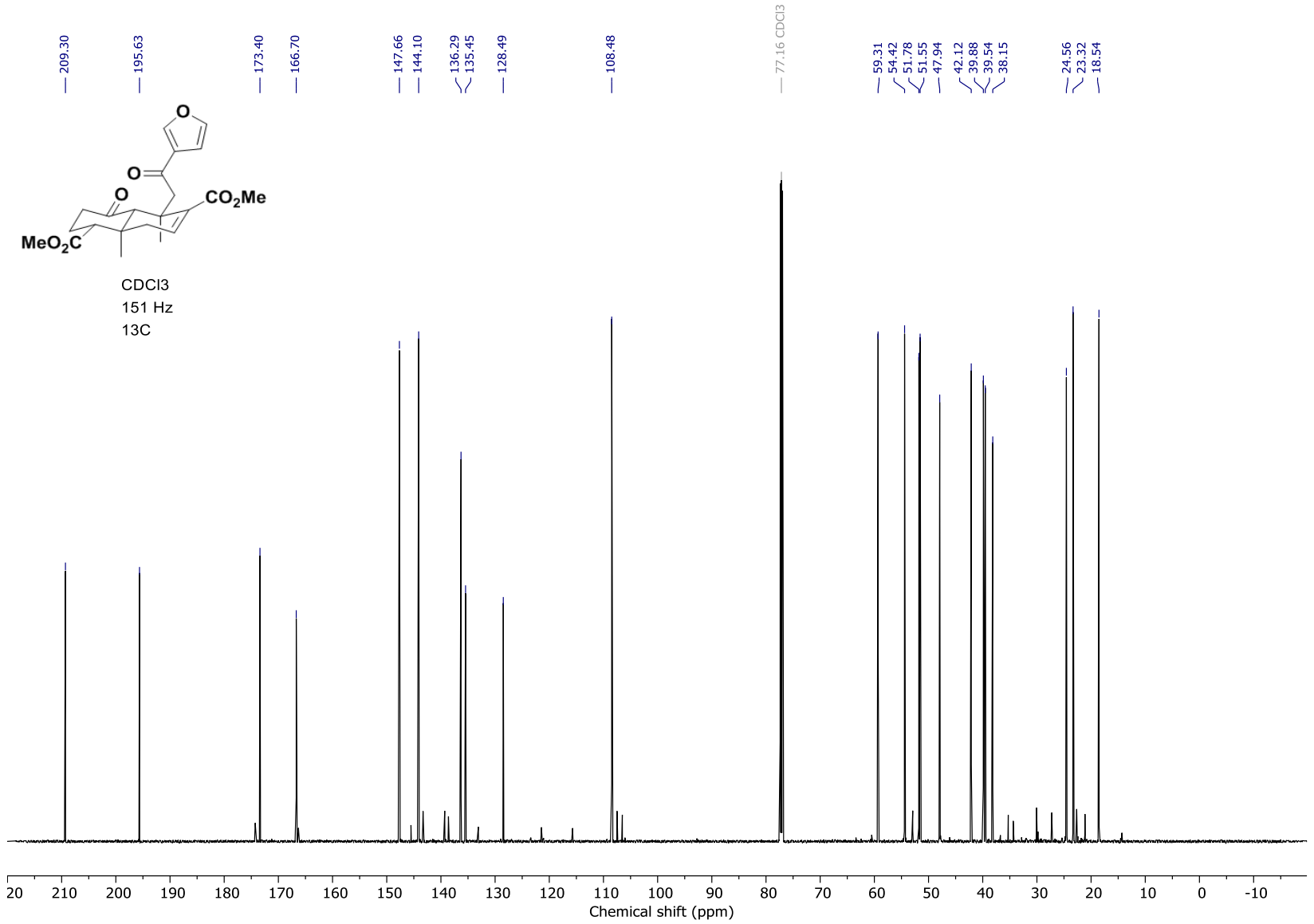
209.30
195.63
173.40
166.70
147.66
144.10
136.29
135.45
128.49
108.48
77.16 CDCl3
59.31
54.42
51.78
51.55
47.94
42.12
39.88
39.54
38.15
24.56
23.32
18.54
O
O
O
CO2Me
MeO2C
CDCl3
151 Hz
13C
20 210 200 190 180 170 160 150 140 130 120 110 100 90 80 70 60 50 40 30 20 10 0 -10
Chemical shift (ppm)

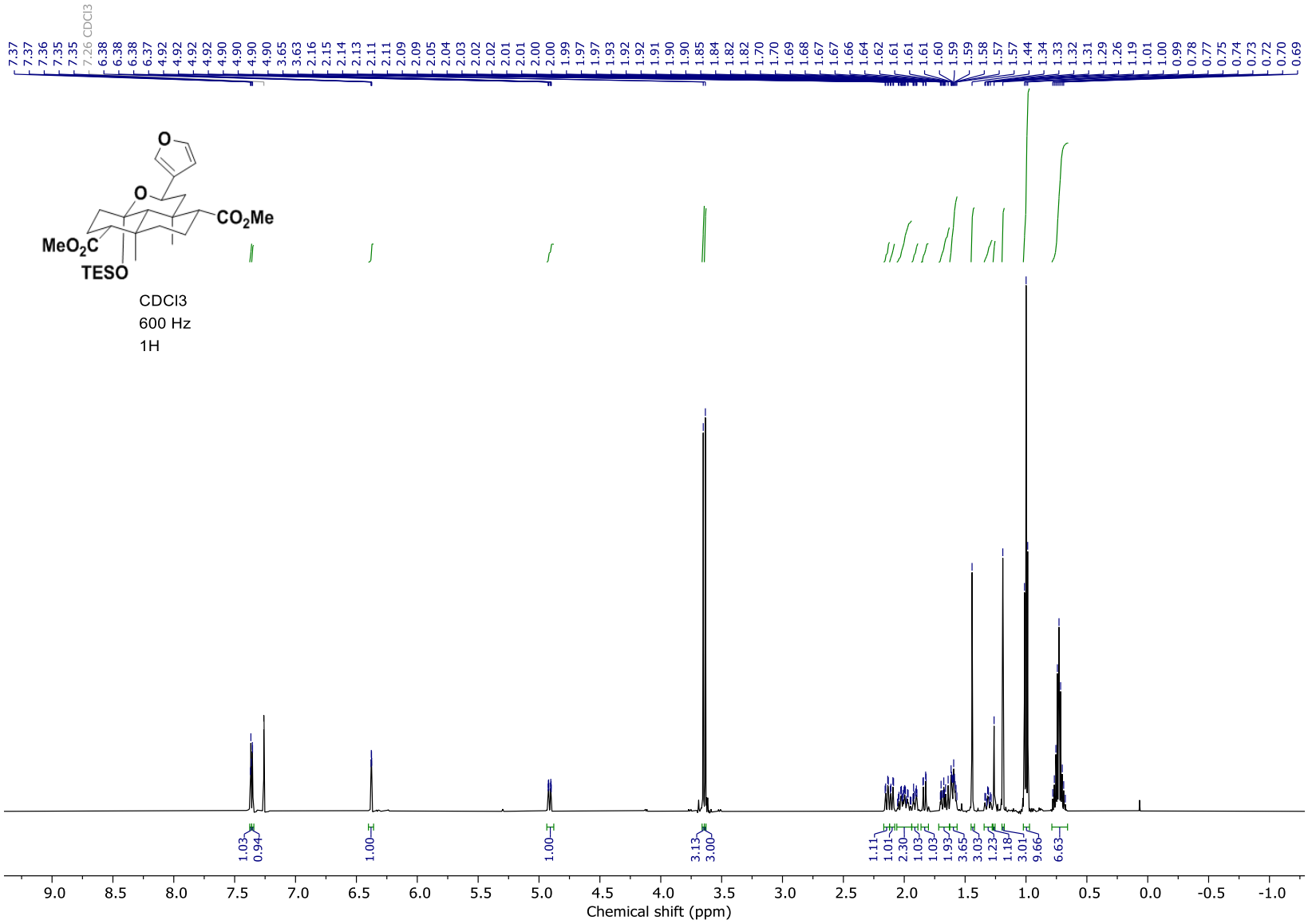
7.37 7.37 7.36 7.35 7.35 7.26 CDCl3 6.38 6.38 6.37 4.92 4.92 4.92 4.90 4.90 4.90 4.90 3.65 3.63 2.16 2.15 2.14 2.13 2.11 2.11 2.09 2.09 2.05 2.04 2.03 2.02 2.02 2.01 2.01 2.00 2.00 1.99 1.97 1.97 1.93 1.92 1.91 1.90 1.90 1.85 1.84 1.82 1.82 1.70 1.70 1.69 1.68 1.67 1.67 1.66 1.64 1.62 1.61 1.61 1.61 1.60 1.59 1.59 1.58 1.57 1.57 1.44 1.34 1.33 1.32 1.31 1.29 1.26 1.19 1.01 1.00 0.99 0.78 0.77 0.75 0.74 0.73 0.72 0.70 0.69
O
O
CO2Me
MeO2C
TESO
CDCl3
600 Hz
1H
1.03 0.94 1.00 1.00 3.13 3.00 1.11 1.01 2.30 1.03 1.93 3.65 3.03 1.23 1.18 3.01 9.66 6.63
9.0 8.5 8.0 7.5 7.0 6.5 6.0 5.5 5.0 4.5 4.0 3.5 3.0 2.5 2.0 1.5 1.0 0.5 0.0 -0.5 -1.0
Chemical shift (ppm)

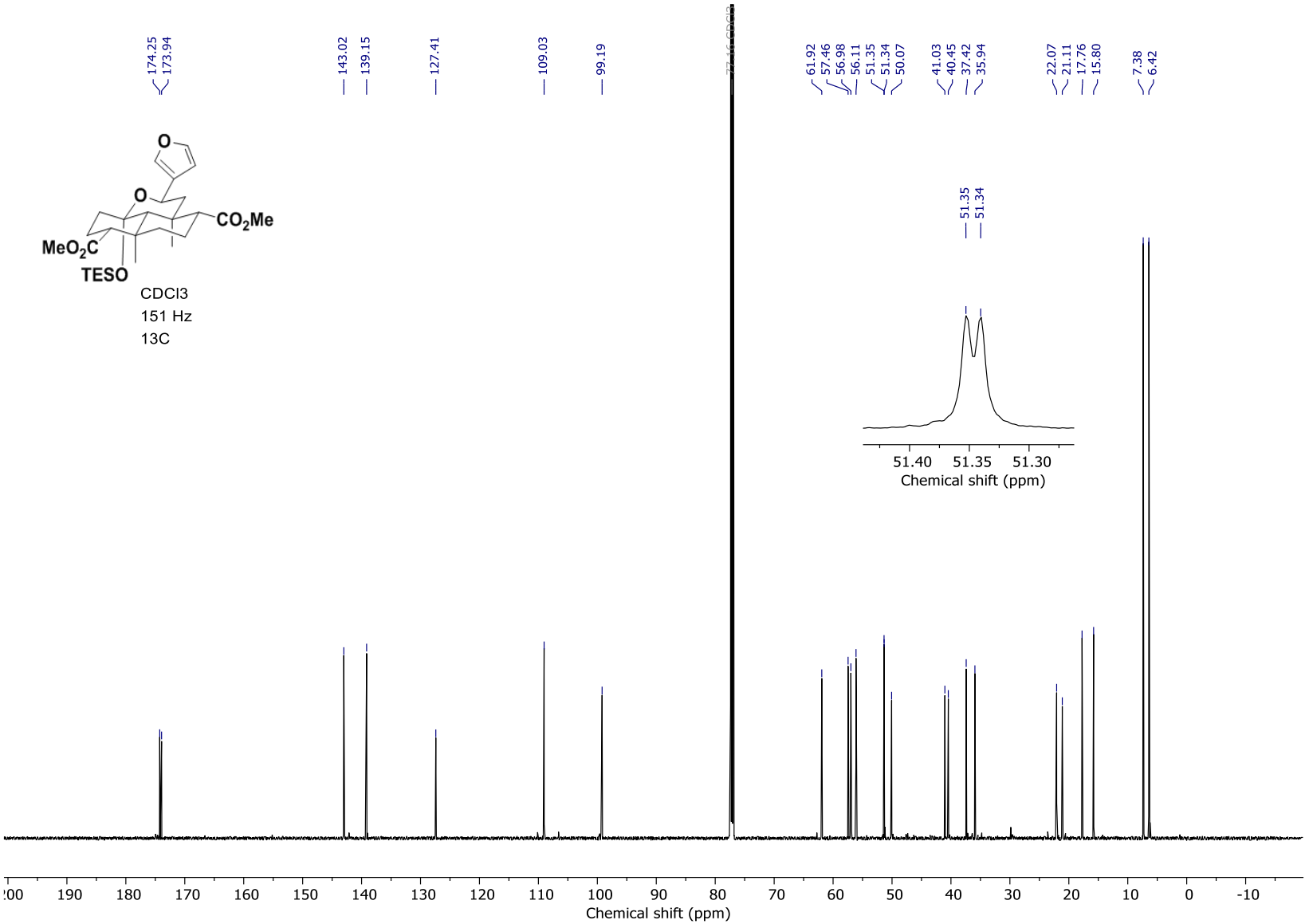
174.25
173.94
143.02
139.15
127.41
109.03
99.19
77.16
61.92
57.46
56.98
56.11
51.35
51.34
50.07
41.03
40.45
37.42
35.94
22.07
21.11
17.76
15.80
7.38
6.42
O
O
CO2Me
MeO2C
TESO
CDCl3
151 Hz
13C
51.40
51.35
51.30
Chemical shift (ppm)
Chemical shift (ppm)

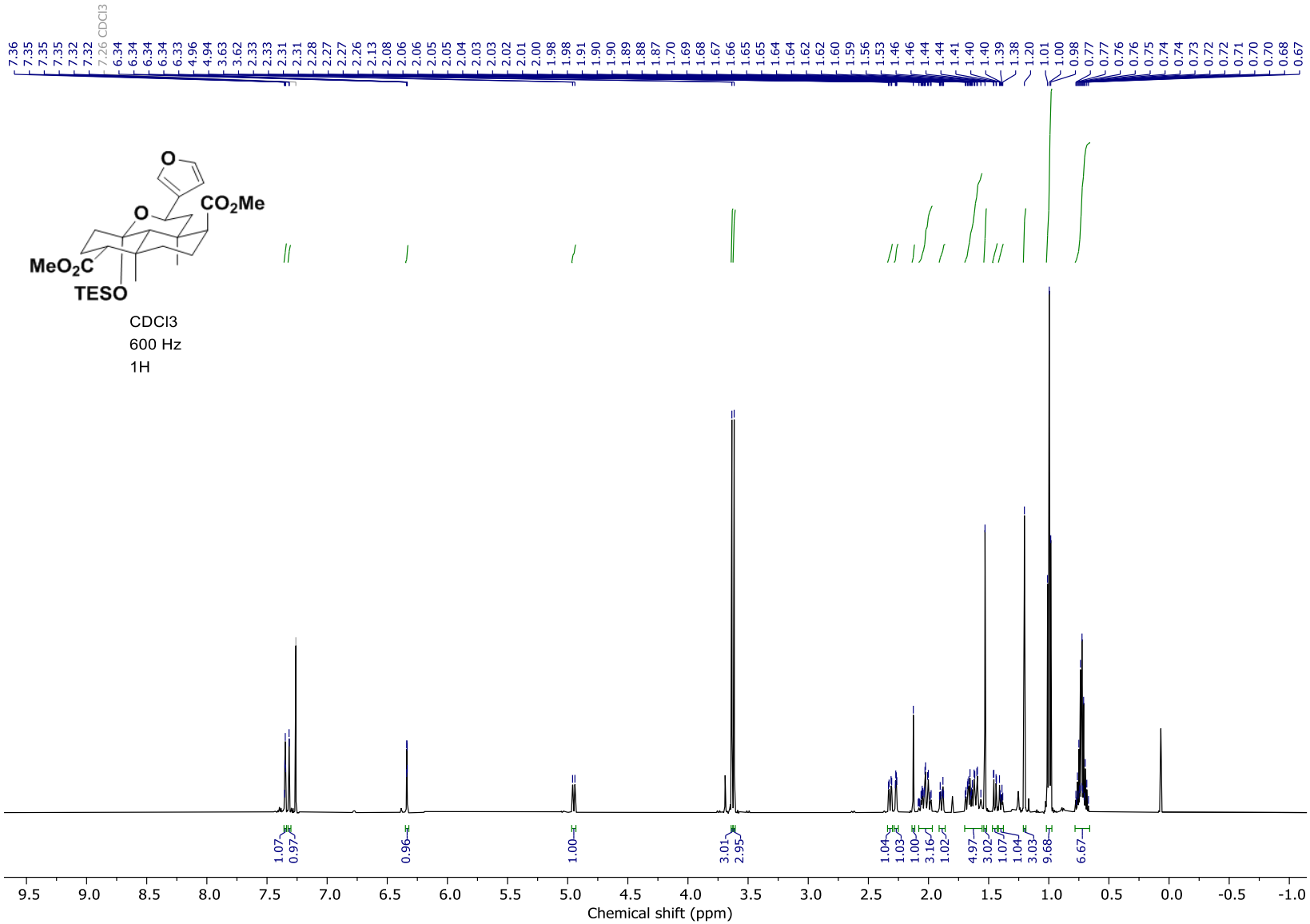
O
O
CO2Me
MeO2C
TESO
CDCl3
600 Hz
1H
Chemical shift (ppm)

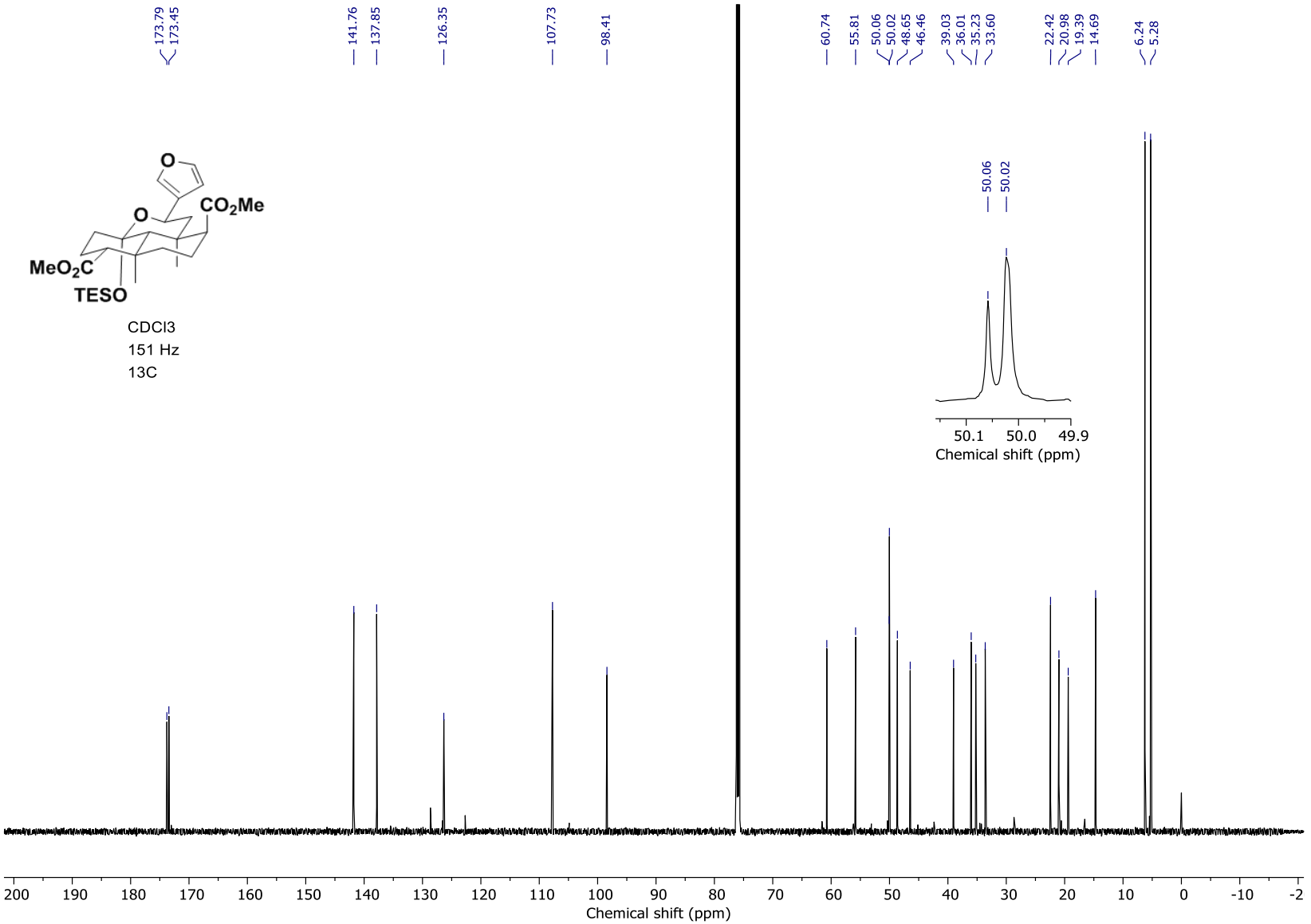
173.79
173.45
141.76
137.85
126.35
107.73
98.41
60.74
55.81
50.06
50.02
48.65
46.46
39.03
36.01
35.23
33.60
22.42
20.98
19.39
14.69
6.24
5.28
O
O
CO2Me
MeO2C
TESO
CDCl3
151 Hz
13C
50.06
50.02
50.1
50.0
49.9
Chemical shift (ppm)
200 190 180 170 160 150 140 130 120 110 100 90 80 70 60 50 40 30 20 10 0 -10 -2
Chemical shift (ppm)

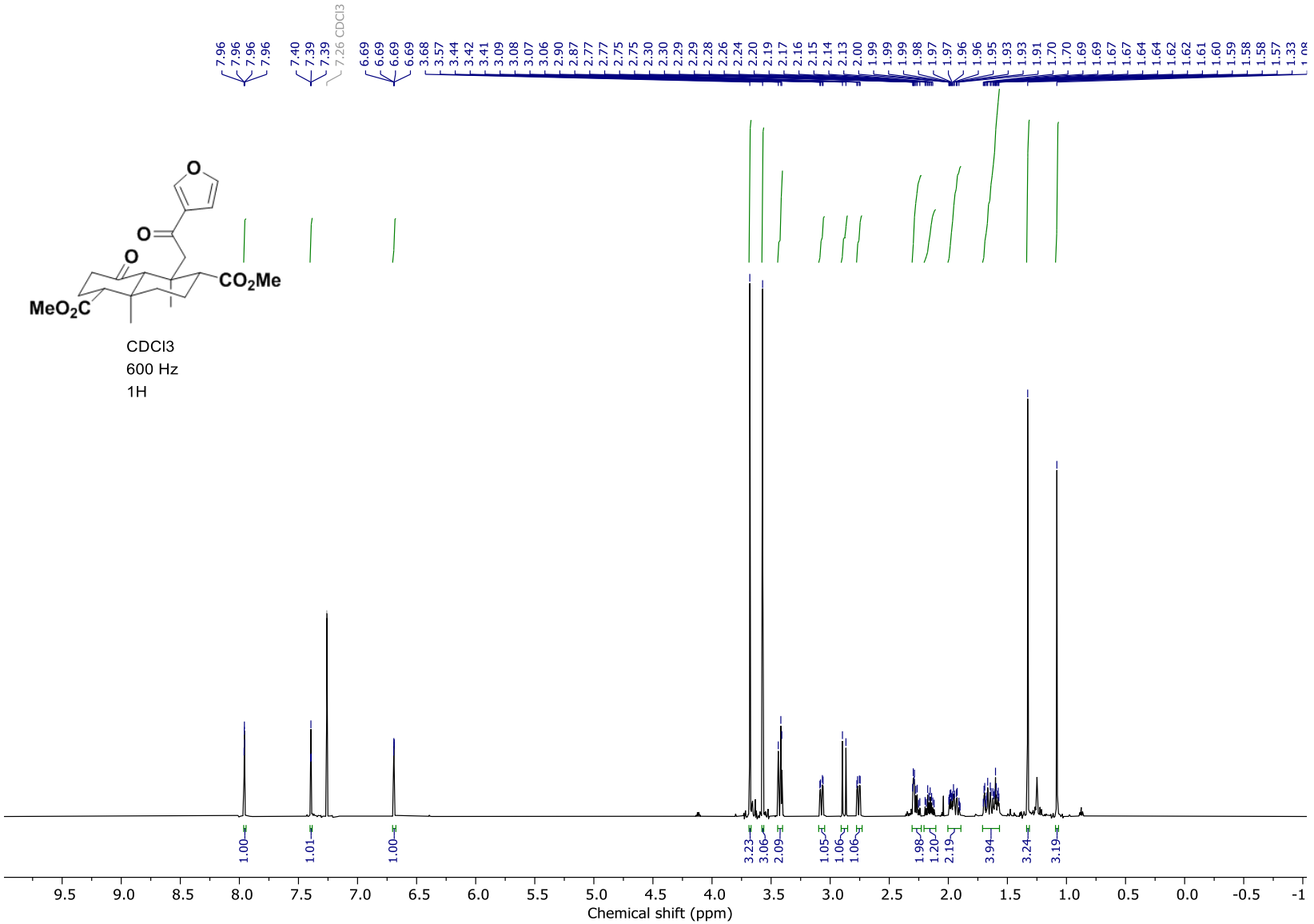
CDCl3
600 Hz
1H
Chemical shift (ppm)

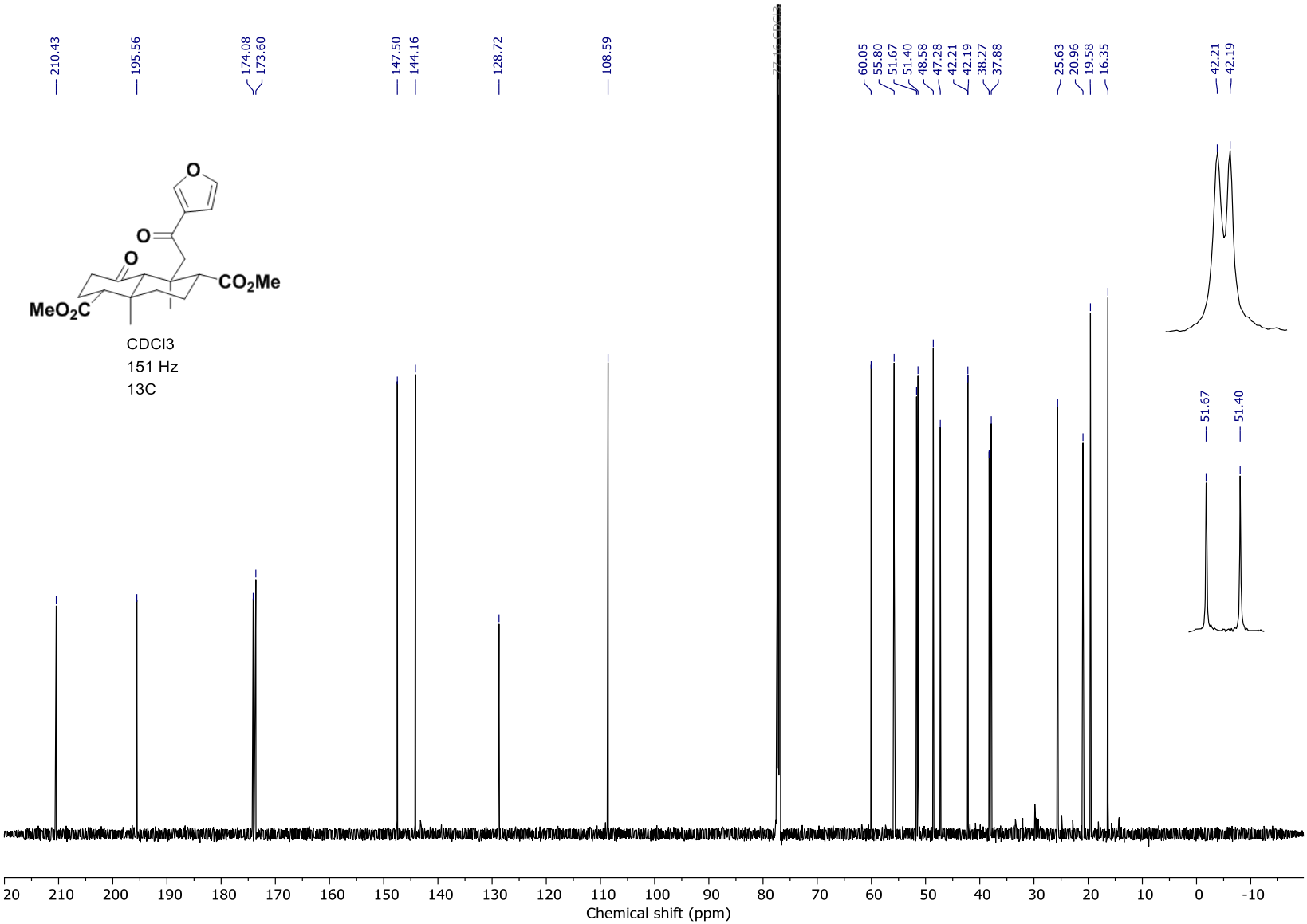
210.43
195.56
174.08
173.60
147.50
144.16
128.72
108.59
77.16 CDCl3
60.05
55.80
51.67
51.40
48.58
47.28
42.21
42.19
38.27
37.88
25.63
20.96
19.58
16.35
42.21
42.19
51.67
51.40
O
O
O
CO2Me
MeO2C
CDCl3
151 Hz
13C
20 210 200 190 180 170 160 150 140 130 120 110 100 90 80 70 60 50 40 30 20 10 0 -10
Chemical shift (ppm)

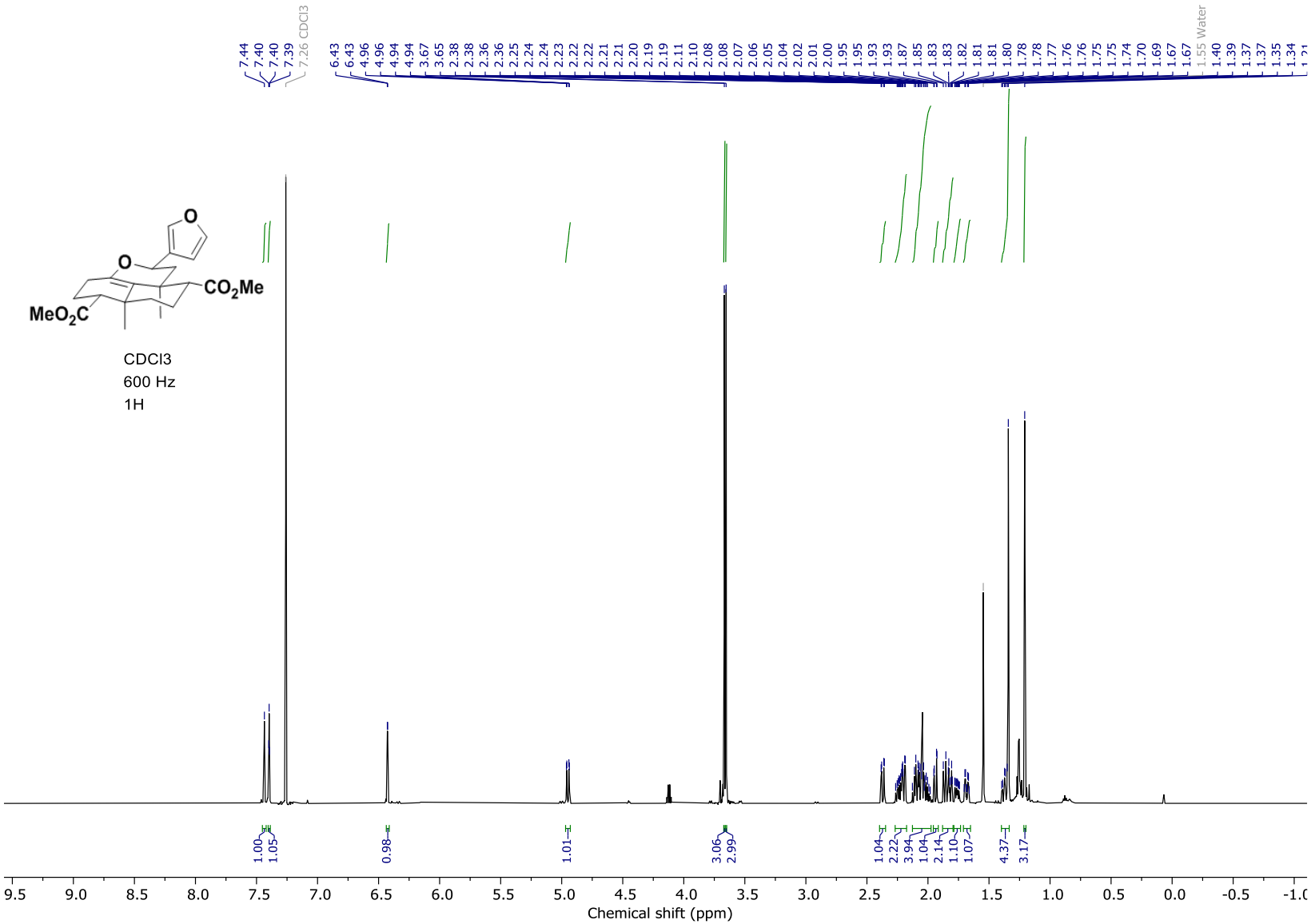
CDCl3
600 Hz
1H
Chemical shift (ppm)

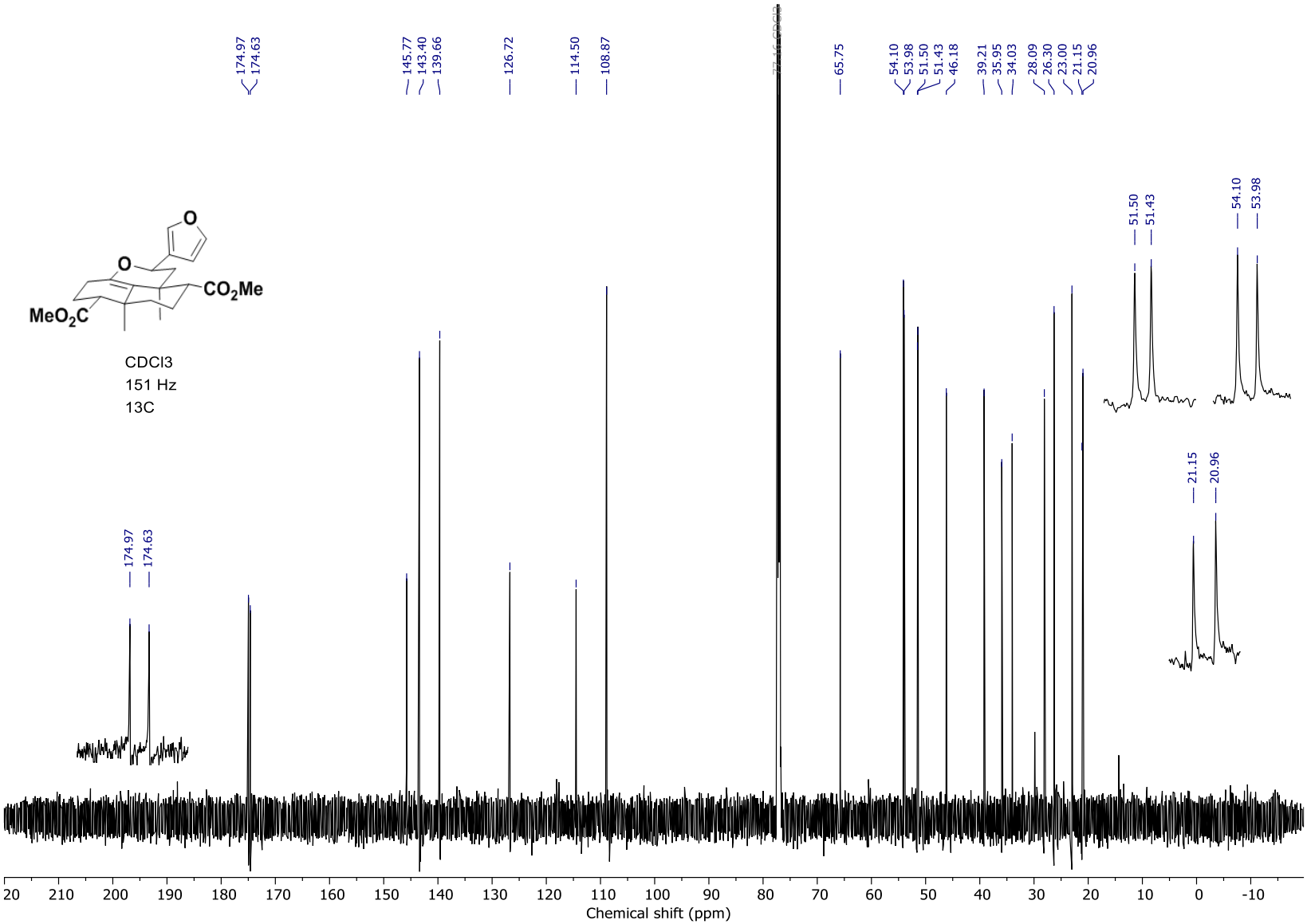
174.97
174.63
145.77
143.40
139.66
126.72
114.50
108.87
77.16
65.75
54.10
53.98
51.50
51.43
46.18
39.21
35.95
34.03
28.09
26.30
23.00
21.15
20.96
O
O
CO2Me
MeO2C
CDCl3
151 Hz
13C
Chemical shift (ppm)

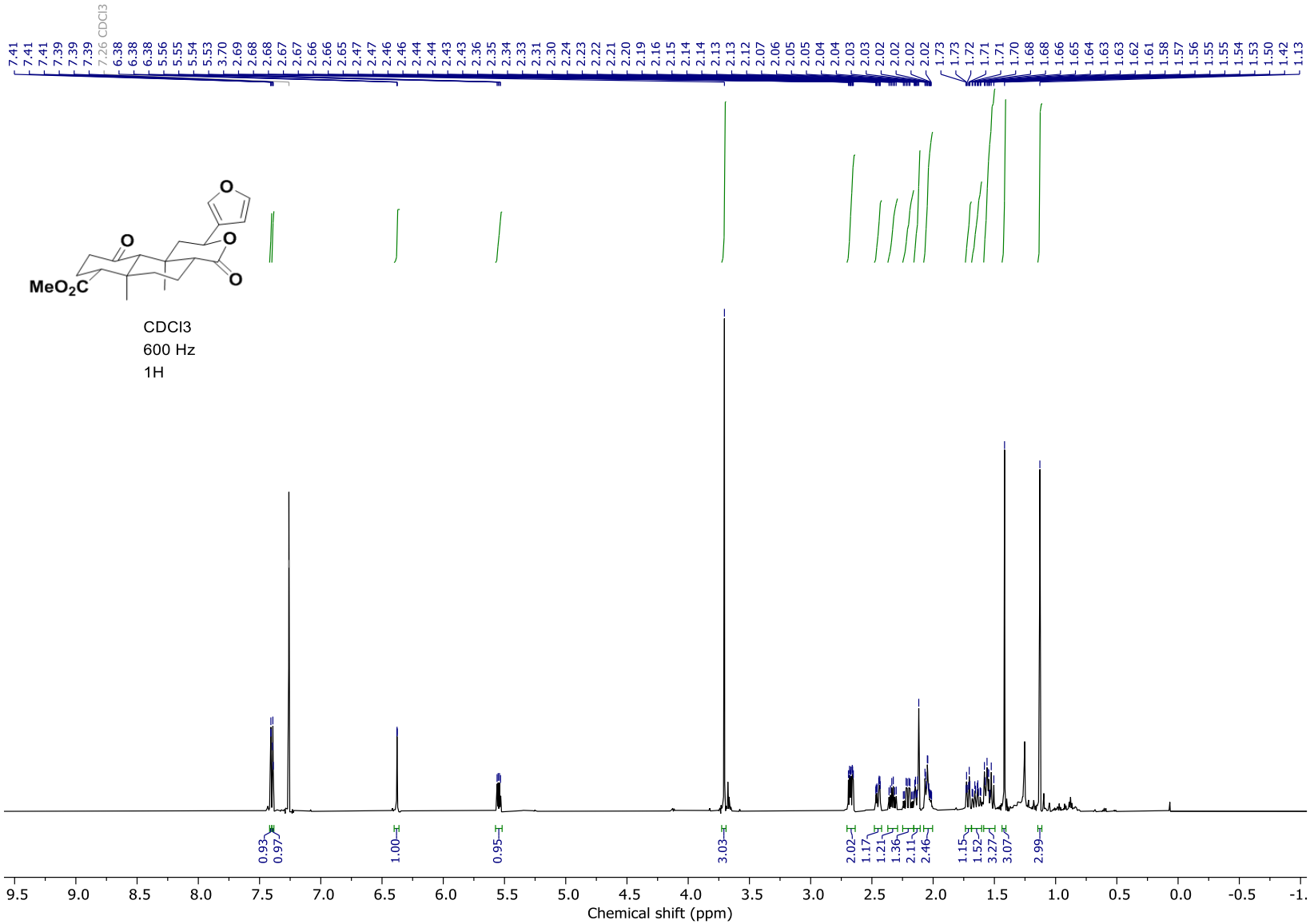
MeO2C
CDCl3
600 Hz
1H
Chemical shift (ppm)

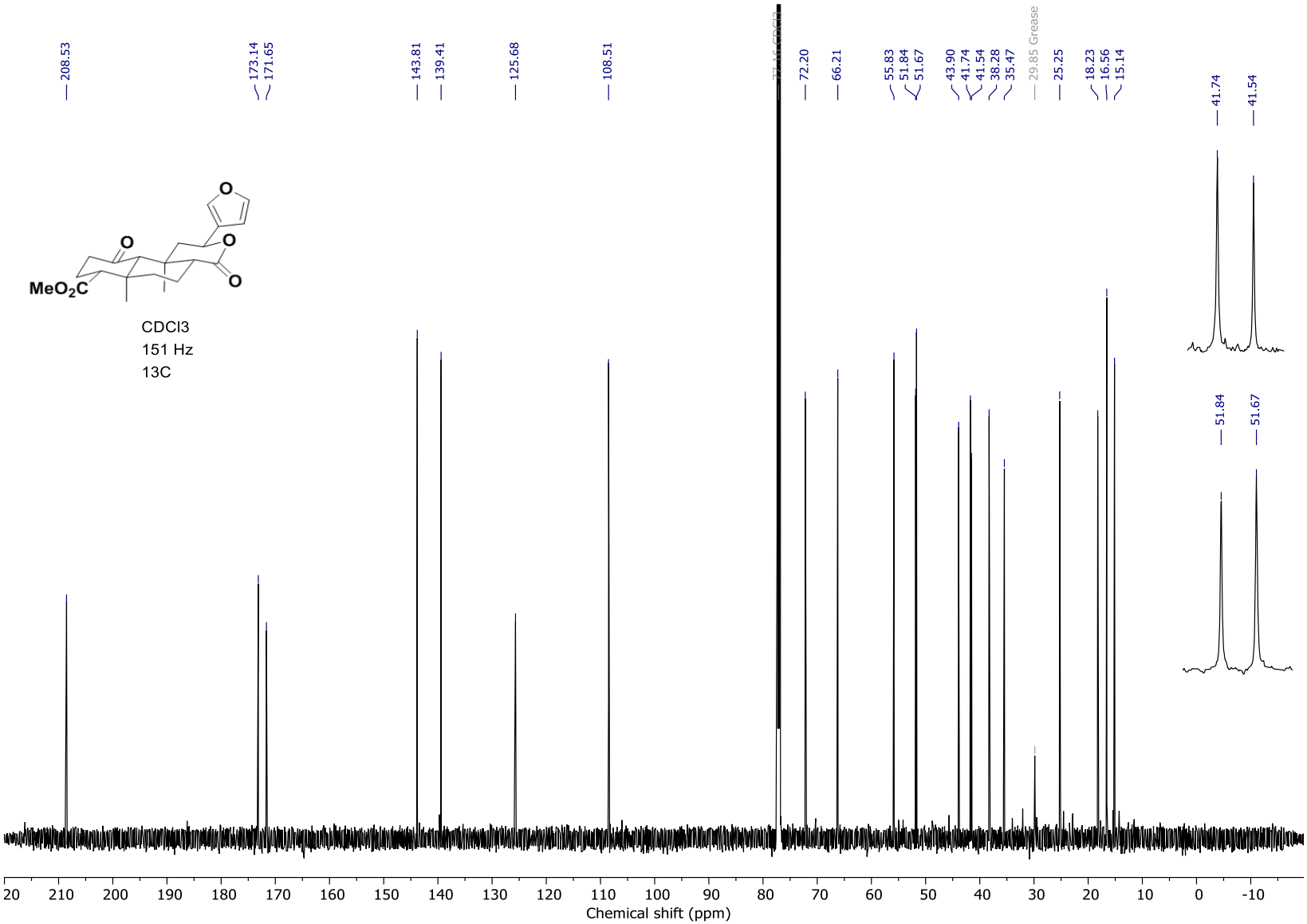
208.53
173.14
171.65
143.81
139.41
125.68
108.51
77.16 CDCl3
72.20
66.21
55.83
51.84
51.67
43.90
41.74
41.54
38.28
35.47
29.85 Grease
25.25
18.23
16.56
15.14
41.74
41.54
51.84
51.67
MeO2C
CDCl3
151 Hz
13C
Chemical shift (ppm)

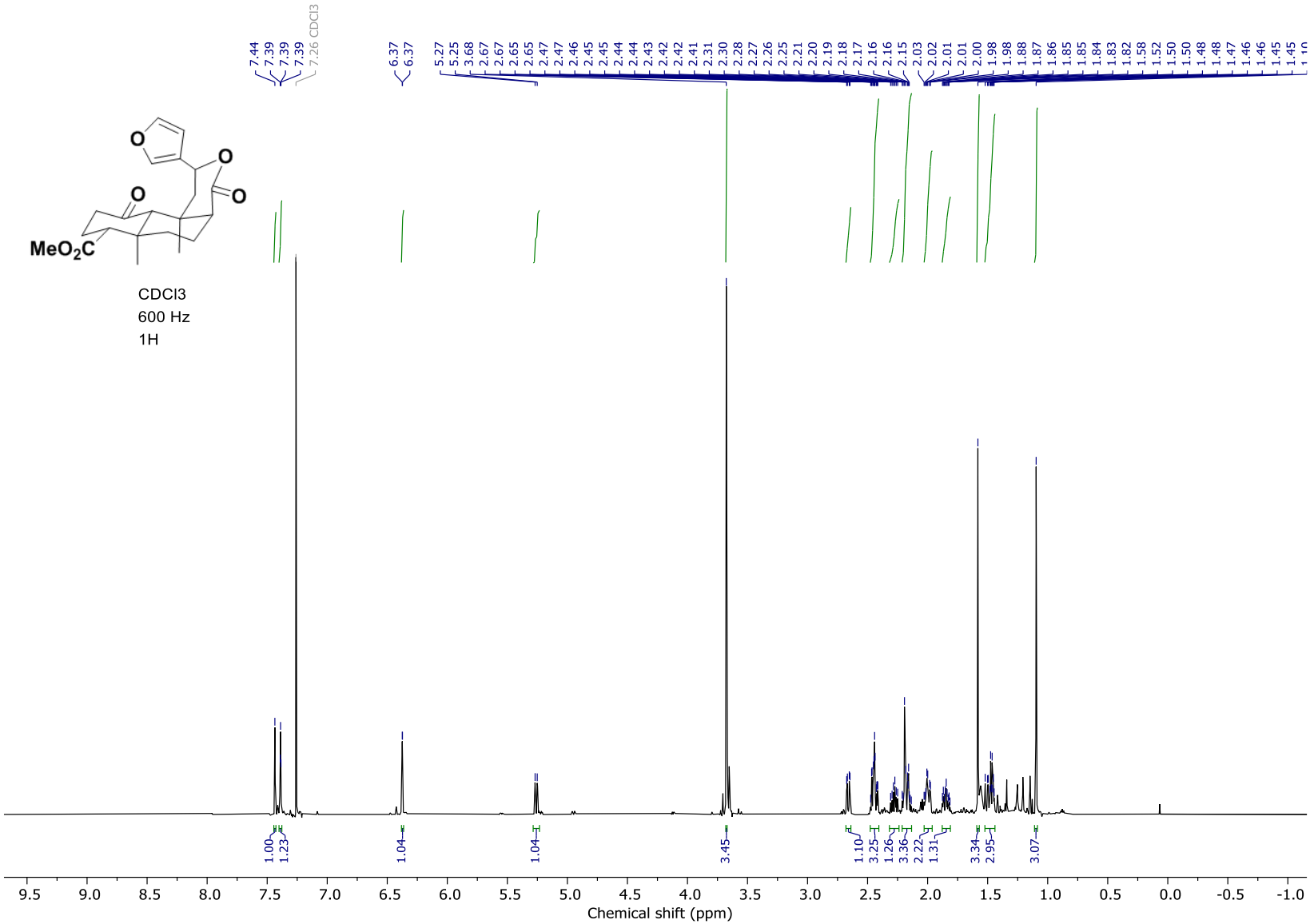
CDCl3
600 Hz
1H
Chemical shift (ppm)

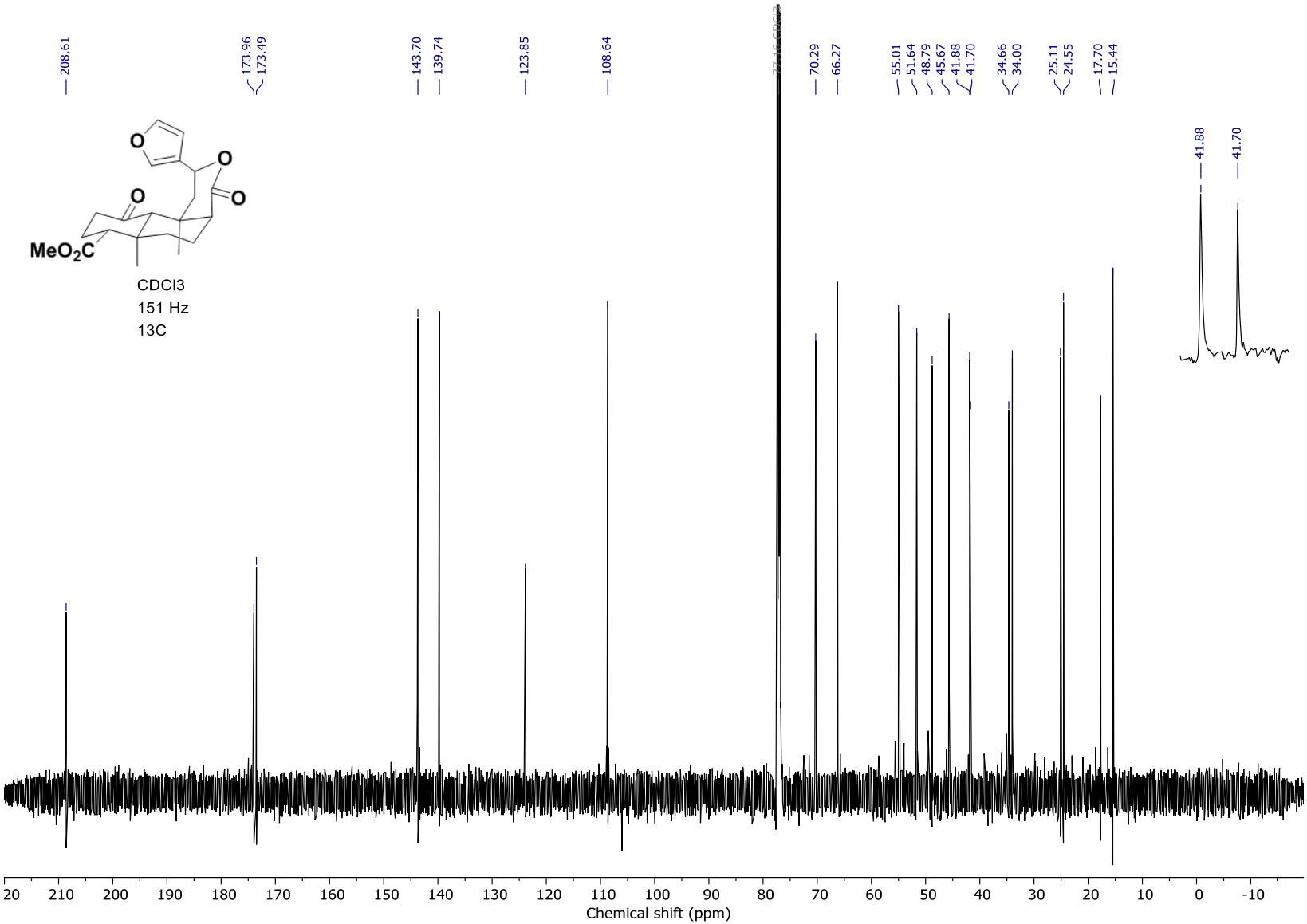
208.61
173.96
173.49
143.70
139.74
123.85
108.64
77.16
70.29
66.27
55.01
51.64
48.79
45.67
41.88
41.70
34.66
34.00
25.11
24.55
17.70
15.44
MeO2C
CDCl3
151 Hz
13C
Chemical shift (ppm)